JAN 2 8 1946

VOLUME 102 NUMBER 3

THE ASTROPHYSICAL JOURNAL

NOVEMBER 1945

A STUDY OF GENERAL AND SELECTIVE ABSORPTION IN FOUR SMALL DARK NEBULAE . . . . . *Lawrence Garnett Stoddard* 267
THE CAPE MAGNITUDES AND THE INTERNATIONAL SYSTEM . . . . . *Frederick H. Seares and Mary C. Joyner* 281
B CASSIOPEIAE AS A SUPERNOVA OF TYPE I . . . . . *W. Baade* 309
SIX-COLOR PHOTOMETRY OF STARS. III. THE COLORS OF 238 STARS OF DIFFERENT SPECTRAL TYPES . . . . . *Joel Stebbins and A. E. Whitford* 318
MEASUREMENTS IN THE SPECTRA OF U ORIONIS, R SERPENTIS, R AQUILAE, AND R CASSIOPEIAE . . . . . *Paul W. Merrill* 347
IDENTIFICATION OF THE POST-MAXIMUM LINES IN THE SPECTRUM OF NOVA (RS) OPHIUCHI . . . . . *A. H. Joy and P. Swings* 353
THE SPECTRUM OF NOVA PUPPIS 1942 . . . . . *Reeves F. Sanford* 367
REGRESSION LINES AND THE FUNCTIONAL RELATION. II. CHARLIER'S FORMULAE FOR A MOVING CLUSTER . . . . . *Frederick H. Seares* 366
NEBULOUS OBJECTS IN THE ANDROMEDA NEBULA . . *C. K. Seyfert and J. J. Nassau* 377
RADIAL VELOCITIES AND SPECTRAL CLASSES FOR SOME STARS OF LARGE PROPER MOTION . . . . . *W. J. Luyten* 382
A THEORETICAL DICUSSION OF THE CONTINUOUS SPECTRUM OF THE SUN . . . . . *Guido Münch* 385
ON THE CONTINUOUS ABSORPTION COEFFICIENT OF THE NEGATIVE HYDROGEN ION. II . . . . . *S. Chandrasekhar* 395
THE RADIATIVE EQUILIBRIUM OF AN EXPANDING PLANETARY NEBULA. I. RADIATION PRESSURE IN LYMAN-α . . . . . *S. Chandrasekhar* 402
CURVE OF GROWTH FOR β CANIS MAJORIS . . . . . *Helen R. Steel* 429
THE SPECTROSCOPIC ORBIT OF TU MONOCEROTIS . . . . . *Armin J. Deutsch* 433
THE SPECTRUM OF β CORONAE BOREALIS . . . . . *W. A. Hiltner* 438
SPECTROGRAPHIC OBSERVATIONS OF THE ECLIPSING VARIABLES W URSAE MINORIS, XZ SAGITTARII, AND KO AQUILAE . . . . . *Jorge Sahade* 470
THE PROBLEM OF U CORONAE BOREALIS, RS VULPECULAE, AND TV CASSIOPEIAE . . . . . *J. Sahade and O. Struve* 480
THE WOLF-RAYET SPECTROSCOPIC BINARY HD 168206 . . . . . *W. A. Hiltner* 492
THE SPECTROSCOPIC ORBIT OF THE ECLIPSING VARIABLE BD+55°616 . . . . . *Armin J. Deutsch* 496
A SPECTROGRAPHIC STUDY OF 68 υ HERCULIS . . . . . *Burke Smith* 500
REVIEWS 511
INDEX 513

THE UNIVERSITY OF CHICAGO PRESS
CHICAGO, ILLINOIS, U.S.A.

November 1945 Vol. 102, No. 3

THE ASTROPHYSICAL JOURNAL

AN INTERNATIONAL REVIEW OF SPECTROSCOPY AND ASTRONOMICAL PHYSICS

Edited by

OTTO STRUVE
Managing Editor

S. CHANDRASEKHAR
Associate Managing Editor

Yerkes Observatory of the University of Chicago

PAUL W. MERRILL
Mount Wilson Observatory of the Carnegie Institution of Washington

HARLOW SHAPLEY
Harvard College Observatory
Cambridge, Massachusetts

J. H. MOORE
Lick Observatory
University of California

With the Collaboration of the American Astronomical Society

Collaborating Editors:

1943-45	1944-46	1945-47
S. B. NICHOLSON Mount Wilson Observatory	JOEL STEBBINS Washburn Observatory	CECILIA H. PAYNE-GAPOSCHKIN Harvard College Observatory
D. B. McLAUGHLIN University of Michigan	A. N. VYSSOTSKY Leander McCormick Observatory	H. N. RUSSELL Princeton University
J. A. PEARCE Dominion Astrophysical Observatory, Victoria	W. W. MORGAN Yerkes Observatory	R. H. BAKER University of Illinois

The Astrophysical Journal is published bimonthly by the University of Chicago at the University of Chicago Press, 5750 Ellis Avenue, Chicago, Illinois, during July, September, November, January, March, and May. ¶The subscription price is $10.00 a year; the price of single copies is $2.00. Orders for service of less than a full year will be charged at the single-copy rate. ¶Postage is prepaid by the publishers on all orders from the United States and its possessions, Argentina, Bolivia, Brazil, Chile, Colombia, Costa Rica, Cuba, Dominican Republic, Ecuador, Guatemala, Haiti, Republic of Honduras, Mexico, Morocco (Spanish Zone), Nicaragua, Panama, Paraguay, Peru, Rio de Oro, El Salvador, Spain (including Balearic Islands, Canary Islands, and the Spanish Offices in Northern Africa; Andorra), Spanish Guinea, Uruguay, and Venezuela. ¶Postage is charged extra as follows: for Canada and Newfoundland, 42 cents on annual subscriptions (total $10.42); on single copies, 7 cents (total $2.07); for all other countries in the Postal Union, 96 cents on annual subscriptions (total $10.96), on single copies 16 cents (total $2.16). ¶Patrons are requested to make all remittances payable to The University of Chicago Press, in United States currency or its equivalent by postal or express money orders or bank drafts.

The following are authorized agents:

For the British Empire, except North America, India, and Australasia: The Cambridge University Press, Bentley House, 200 Euston Road, London, N.W. 1, England. Prices of yearly subscriptions and of single copies may be had on application.

Claims for missing numbers should be made within the month following the regular month of publication. The publishers expect to supply missing numbers free only when losses have been sustained in transit, and when the reserve stock will permit.

Business correspondence should be addressed to The University of Chicago Press, Chicago 37, Illinois.

Communications for the editors and manuscripts should be addressed to: Otto Struve, Editor of THE ASTROPHYSICAL JOURNAL, Yerkes Observatory, Williams Bay, Wisconsin.

Line drawings and photographs should be made by the author, and all marginal notes such as co-ordinates, wave lengths, etc., should be included in the cuts. It will not be possible to set up such material in type.

One copy of the corrected galley proof should be returned as soon as possible to the editor, Yerkes Observatory, Williams Bay, Wisconsin. Authors should take notice that the manuscript will not be sent to them with the proof.

The cable address is "Observatory, Williamsbay, Wisconsin."

The articles in this journal are indexed in the *International Index to Periodicals*, New York, N.Y.

Applications for permission to quote from this journal should be addressed to The University of Chicago Press, and will be freely granted.

Entered as second-class matter, July 31, 1940, at the Post-Office at Chicago, Ill., under the act of March 3, 1879.
Acceptance for mailing at special rate of postage provided for in United States Postal Act of October 3, 1917, Section 1103, amended February 28, 1925.

[PRINTED IN U.S.A.]

THE ASTROPHYSICAL JOURNAL

AN INTERNATIONAL REVIEW OF SPECTROSCOPY AND ASTRONOMICAL PHYSICS

VOLUME 102 NOVEMBER 1945 NUMBER 3

A STUDY OF GENERAL AND SELECTIVE ABSORPTION IN FOUR SMALL DARK NEBULAE

LAURENCE GARNETT STODDARD
University of California
Received August 26, 1945

ABSTRACT

Four small dark clouds of Barnard's list were studied by star counts according to photographic and photovisual magnitudes in the obscured regions and the surrounding star fields. Magnitude sequences were set up by comparisons with selected areas and extended by long-exposure objective-grating plates. Attempts were made to find the star density and general interstellar absorption in the comparison regions surrounding the dark clouds, but no unique solutions could be found. The total absorptions by each cloud were determined directly from the Wolf diagrams. All four clouds showed a selective absorption; and the mean ratio of photographic to photovisual absorption is 1.31. The distances of the clouds could not be determined accurately, only an upper limit of the distance (1000 parsecs) could be ascertained. The angular diameters then indicate that these objects may be comparable in size with the Orion nebula and that the absorption coefficients in the clouds themselves are at least of the order of 0.2 per parsec.

I. INTRODUCTION

Most of the obscuring regions so far investigated are extended regions of obscuration. E. E. Barnard's list[1] includes many small objects about which little is known. I have attempted to study the absorption as affecting photovisual and photographic light in the four Barnard areas shown in Table 1, by means of star counts in the dark nebula and in the surrounding normal regions.

TABLE 1

CO-ORDINATES AND SIZES OF THE BARNARD AREAS

Barnard Area	α(1938)	δ(1938)	Diameter	l	b
B 34	$5^h39^m.5$	+32° 37′	20′	144°.3	+2°.9
B 201	2 08.6	+56 42	10	101.7	−3.5
B 226	5 32.5	+33 39	17	142.6	+2.2
B 227	6 03.2	+19 40	12	158.2	+1.1

The study of the absorption in the four dark nebulae was made as follows:

1. Comparisons with selected areas were made in both photographic and photovisual light in order to establish magnitude sequences in each area.
2. These sequences were extended to fainter stars by plates of longer exposure taken with a parallel-wire grating before the objective.

[1] *A Photographic Atlas of Selected Regions of the Milky Way*, I, 18, 1927.

3. On long-exposure photographs taken without the grating, star counts were made in the Barnard areas and also in the areas immediately surrounding them. The results were plotted as Wolf diagrams. This was done for both wave-length regions.

4. By trial and error, values of the general photographic and photovisual absorption coefficients and the star density were found for the unobscured areas. They had to represent both photographic and photovisual star counts simultaneously within the statistical uncertainty.

5. For small dark clouds, like those here considered, the thickness can be neglected, and the cloud can be treated like an absorbing screen. Assuming that the density law and general interstellar absorption are the same in the obscured field as in its surroundings, the total visual and photographic absorption by the nebula and an estimate of its distance were obtained by trial and error.

II. OBSERVATIONAL EQUIPMENT

The observations were made during the academic year 1937–38 with the 36-inch reflecting telescope of the Steward Observatory of the University of Arizona. This telescope has a silvered primary mirror with aluminized secondaries. The plates were exposed at the Newtonian focus, which gives a plate scale of 1 mm = 45″, corresponding to a focal length of 180 inches. This telescope has a Ross coma corrector, and all the plates were taken with the corrector in place. This gives a photometric field slightly over 0°.8 in diameter, over which there is no appreciable distance correction ($<0^m.02$).

TABLE 2

GRATING CONSTANTS

	Theoretical	Empirical	No. of Determinations	Adopted
g_{1-0}*	1.92 mag.	1.906±0.025 mag.	53	1.91 mag.
g_{2-0}	3.42	3.363±0.041	14	3.39

* The subscripts refer to the spectral order.

The photographic magnitudes were obtained from Imperial Eclipse Soft HD 850 plates, which were exposed without a filter. The effective wave length of this combination is approximately λ 4450.

The photovisual magnitudes were obtained with Eastman I-G and I-G Special plates used with a Wratten Minus Blue (No. 12) filter. This combination has a wave length of approximately λ 5600. These effective wave lengths were obtained from objective-grating plates.

In order to extend the magnitude sequences in the neighborhood of the Barnard areas to fainter stars, it was necessary to construct an objective grating for the 36-inch reflector. The rods, made of $\frac{1}{8}$-inch drill rod, are spaced $\frac{3}{8}$ inch apart, center to center. The grating constants are shown in Table 2.

III. MAGNITUDE SEQUENCES

Since the Polar Sequence is only 32° above the horizon in Tucson and rather awkward to observe (as it is necessary to swing the reflector under the observing platform), and also because of city lights, it was decided to establish the magnitude sequences in the Barnard areas by comparison with selected areas instead of the Polar Sequence. For the

standards in the photographic region, the magnitudes were taken from the *Mount Wilson Catalogue*.[2] In the photovisual region some of Seares's unpublished values were used.[3]

For each Barnard area in both photographic and photovisual wave-length regions, six comparisons were made without the grating. The exposure times were 5 minutes in the photographic and 8 minutes in the photovisual region. All comparisons were made when the two areas were at nearly the same zenith distance. The atmospheric extinctions in the Tucson region have been investigated by Pettit.[4] In the photographic and photovisual regions these are, respectively, $0^m.40$ and $0^m.32$ per atmosphere. The average differential extinction corrections are $0^m.03$ (photographic) and $0^m.05$ (photovisual).

The plates were measured with a Stetson-type photometer in which the thermopile was replaced by a photoelectric cell. The method of reduction follows that of Stetson[5] with some modifications. For various reasons not all the comparisons could be used. Table 3 gives a list of those actually used. The brighter stars in each area are designated

TABLE 3

COMPARISONS BETWEEN BARNARD AND SELECTED AREAS

Barnard Area	Pg	Pv	Comparison Area	Barnard Area	Pg	Pv	Comparison Area
B 34.....	5	5	S.A. 49	B 226.....	5	4	S.A. 49
B 201.....	5	6	S.A. 45	B 227.....	5	5	S.A. 73

TABLE 4

MAGNITUDE SEQUENCE EXTENSION PLATES

	B 34	B 201	B 226	B 227		B 34	B 201	B 226	B 227
Pg.....	2	2	2	2	Pv.....	1	2	2	1

by letters. Their adopted magnitudes, listed in Tables 5–8, are the means of the various direct comparisons with selected areas. The internal agreement (neglecting systematic errors) indicates the following probable errors for the adopted magnitudes of these stars:

$$\text{Pg}, \pm 0^m.04; \qquad \text{Pv}, \pm 0^m.06.$$

To extend the magnitude sequences to fainter stars, exposures of 1–1½ hours were taken with the grating. The number of grating plates used for each area is given in Table 4.

The diffraction images of different orders were not widely enough separated for the use of the Stetson photometer. These plates were, therefore, measured by comparison with a graduated series of star images. The first-order (or first- and second-order) images of the brighter stars were measured, together with the zero-order images of the fainter stars. By applying these grating constants to the known magnitudes of the brighter stars, a curve was plotted relating scale reading and magnitude. From this curve the magnitudes of the fainter stars were read off.

In the cases where only one satisfactory plate was available, it was measured three times independently; all other plates were measured twice.

[2] *Mount Wilson Catalogue of Photographic Magnitudes in Selected Areas 1–139*, 1930.

[3] Private communication to Dr. E. F. Carpenter.

[4] *Ap. J.*, **75**, 185, 1932; *Mt. W. Contr.*, No. 445.

[5] *Ap. J.*, **43**, 253 and 325, 1916.

In Tables 5–8 the stars designated by numbers are those for which the magnitudes were obtained from the long-exposure grating plates. The probable errors of these magnitudes are shown in the accompanying tabulation.

	1 Observation	2 Observations		1 Observation	2 Observations
Pg.	±0.09 mag.	±0.05 mag.	Pv.	±0.12 mag.	±0.06 mag.

TABLE 5

MAGNITUDE SEQUENCES B 34

Star	Pg. Mag.	No. of Deter.	Pv. Mag.	No. of Deter.	Star	Pg. Mag.	No. of Deter.	Pv. Mag.	No. of Deter.
a	13.90	5	13.29	1	1	16.11	2	14.88	1
b	12.32	5	12.03	5	2	16.03	2	.....	.....
c	13.79	5	13.43	5	3	15.92	2	15.43	1
d	11.29	5	11.22	5	4	14.53	1	13.80	1
e	12.56	5	12.53	5	5	15.56	2	15.37	1
f	12.81	5	12.23	5	6	15.76	2	15.58	1
g	13.82	5	13.31	5	7	14.68	2	14.51	1
h	14.16	1	13.80	4	8	15.32	2	14.82	1
i	11.20	5	11.00	5	9	14.56	2	13.67	1
j	14.48	5	14.15	3	10	15.99	2	.....	.....
k	12.10	4	10.39	5	11	14.82	2	14.54	1
l	14.18	3	12.67	1	12	16.04	2	14.71	1
m	13.81	5	12.20	5	13	15.56	2	15.55	1
n	13.83	5	13.18	5	14	15.45	2	15.00	1
o	.....	.....	13.41	2					

TABLE 6

MAGNITUDE SEQUENCES B 201

Star	Pg. Mag.	No. of Deter.	Pv. Mag.	No. of Deter.	Star	Pg. Mag.	No. of Deter.	Pv. Mag.	No. of Deter.
a	10.35	5	10.68	5	5	16.86	2	.....	.....
b	14.44	4	13.56	2	6	16.94	2	.....	.....
c	14.07	5	13.85	3	7	15.30	2	14.88	2
d	13.58	5	13.27	6					
e	14.77	5	14.23	2	8	15.61	2	14.46	2
					9	14.50	2	13.41	2
f	14.54	5	13.38	2	10	14.68	2	14.42	2
h	13.95	5	13.48	4	11	14.55	2	14.26	2
i	13.41	5	13.00	6	12	14.62	2	14.24	2
j	13.78	5	13.14	6					
k	13.50	5	13.21	6	13	14.61	2	14.12	2
					14	15.81	2	14.30	2
l	13.91	5	13.51	4	15	14.28	2	14.23	2
m	13.05	5	12.70	6	16	15.05	2	14.56	2
o	14.23	5	13.48	2	17	15.37	2	14.42	2
p	14.80	5	.....	.....					
1	15.71	2	14.96	2	18	14.78	2	.....	.....
					19	15.75	2	.....	.....
2	14.76	2	14.95	2	20	16.52	2	14.82	1
3	16.52	2	.....	.....	21	16.83	2	.....	.....

TABLE 7

MAGNITUDE SEQUENCES B 226

Star	Pg. Mag.	No. of Deter.	Pv. Mag.	No. of Deter.	Star	Pg. Mag.	No. of Deter.	Pv. Mag.	No. of Deter.
a	12.91	5	12.48	4	2	16.13	2	14.93	1
b	14.08	3	13.50	3	3	14.48	2	14.41	2
c	13.10	5	12.86	4	4	14.27	2	13.97	2
d	13.89	3	13.61	4	5	16.15	2	.....	.....
e	11.76	5	12.00	4					
					6	15.44	2	14.98	1
f	12.99	5	13.02	4	7	16.38	1	15.50	1
g	13.98	3	13.52	2	8	15.84	2	14.95	2
h	14.05	3	13.68	1	9	16.48	1	14.93	1
i	12.65	5	12.61	2	10	14.63	2	14.57	1
j	12.22	5	12.47	3					
					11	15.33	2	15.13	1
k	12.24	5	12.55	3	12	15.32	2	15.07	1
l	13.95	3	13.72	4	13	15.95	2	15.02	1
m	10.90	1	10.87	4	14	15.20	2	15.03	2
n	13.70	3	13.31	1	15	16.63	2	.....	.....
o	13.59	3	13.16	1					
					16	16.73	1	.....	.....
1	16.29	1	.....	.....					

TABLE 8

MAGNITUDE SEQUENCES B 227

Star	Pg. Mag.	No. of Deter.	Pv. Mag.	No. of Deter.	Star	Pg. Mag.	No. of Deter.	Pv. Mag.	No.of Deter.
a	14.71	3	13.80	2	1	14.45	2	13.77	1
b	14.70	2	13.79	2	2	15.68	2	14.90	1
c	13.83	3	13.70	5	3	15.56	2	14.81	1
d	12.81	5	12.75	5	4	16.55	2	.....	.....
e	14.37	3	.....	.....	5	16.80	1	.....	.....
f	14.16	3	13.88	2	6	16.09	2	15.79	1
g	14.19	3	13.85	3	7	16.38	2	15.85	1
h	14.80	3	.....	.....	8	16.58	2	15.05	1
i	14.43	3	14.01	3	9	16.70	1	.....	.....
j	14.30	3	13.80	4	11	17.04	1	.....	.....
k	14.37	3	13.97	3	12	16.64	2	15.53	1
l	14.56	3	13.51	3	13	16.22	2	15.81	1
m	11.44	5	11.56	5	14	15.92	2	15.17	1
n	14.93	2	.....	.....	15	15.76	2	15.11	1
o	14.38	2	13.84	2					

The color equation between the Steward and the Mount Wilson magnitudes was determined from 42 stars of the selected areas, with a total of 220 photographic and 230 photovisual observations. The following relations between the Steward magnitudes, m_S, and the Mount Wilson magnitudes, m_W, were found:

$$\text{Pg.: } m_W - m_S = -(0.02 \pm 0.01)\,CI_W + (0.02 \pm 0.01)\,.$$

$$\text{Pv.: } m_W - m_S = +(0.01 \pm 0.01)\,CI_W - (0.02 \pm 0.01)\,.$$

where CI_W is the Mount Wilson color index. Since the coefficients are small, it was concluded that the Steward magnitudes are essentially the same as the Mount Wilson magnitudes. The positions of the stars are indicated on the charts of the areas in Plates XX-XXIII.

IV. THE STAR COUNTS

The plates used for counting the stars were all made without the grating. They are 90-minute exposures in the photographic region and $2\frac{1}{2}$-hour exposures in the photovisual. While it was planned to have duplicate plates in all cases, a few plates had to be rejected because of unsatisfactory qualities. The plates actually used are listed in Table 9.

TABLE 9

PLATES FOR STAR COUNTING

	B 34	B 201	B 226	B 227		B 34	B 201	B 226	B 227
Pg.....	2	1	1	2	Pv.....	2	2	1	2

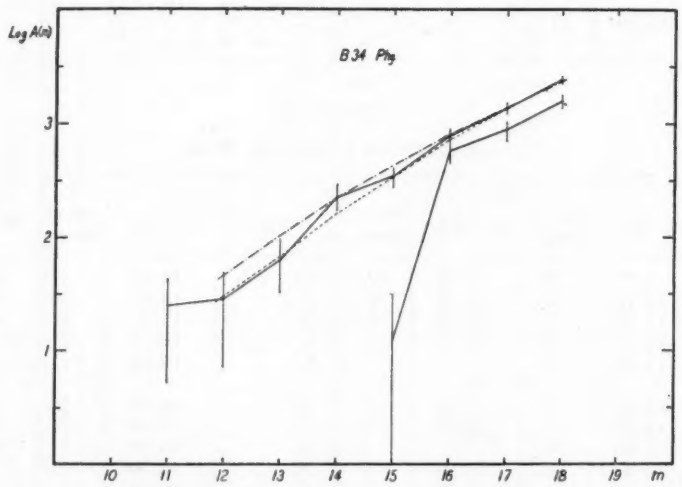

FIG. 1.—B 34. Photographic. Wolf diagram

The star counts were made by placing the plate, emulsion side down, on a glass reticle and counting the stars falling between successive images of a graduated set of images. The stars of the known magnitude sequences were compared individually with the scale, and their position in the sequence was estimated to tenths of an interval. The reticle used had squares with 4-mm sides which correspond to 0.00251 square degree. Stars were counted in all the squares that fell within the boundary of the nebula and also in the region surrounding it but definitely not in it. The surrounding comparison region comprised, on the average, approximately three times the area of the dark cloud. A plot of the scale readings of the sequence stars against their magnitude was made, and from this curve the magnitudes corresponding to the various scale images were found. The total number of stars counted in each scale interval was reduced to an area of 1 square degree.

PLATE XX

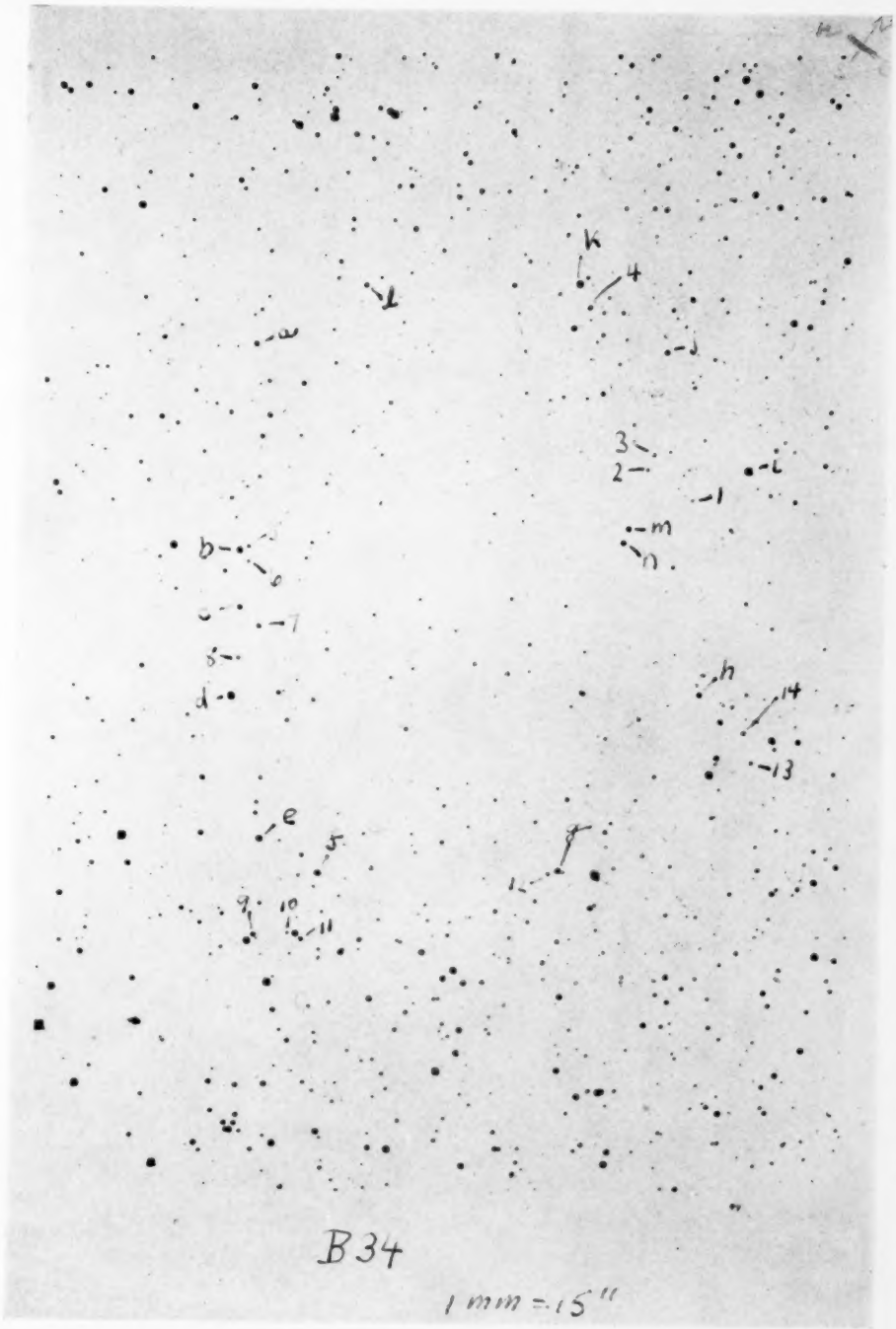

PLATE XXI

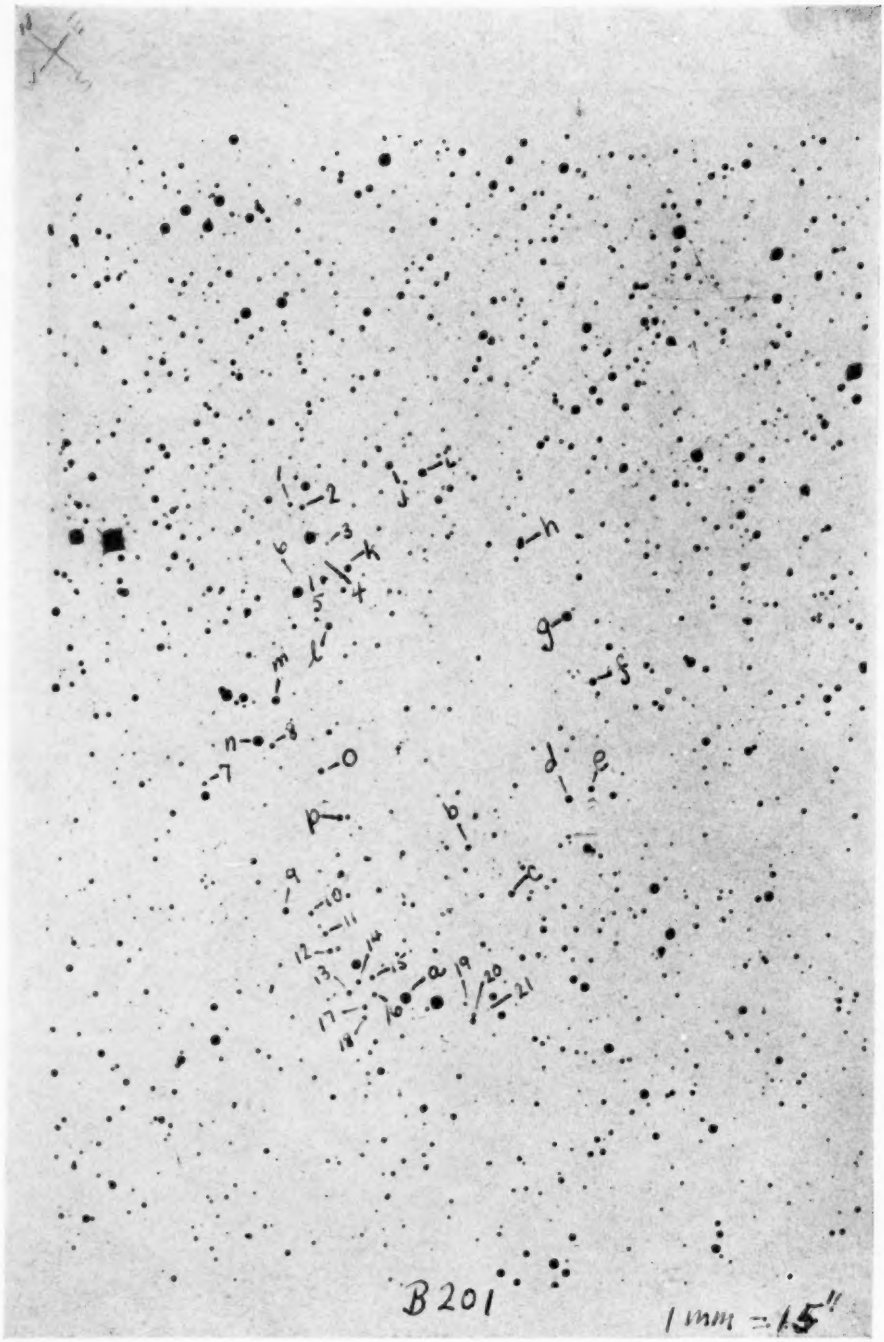

PLATE XXII

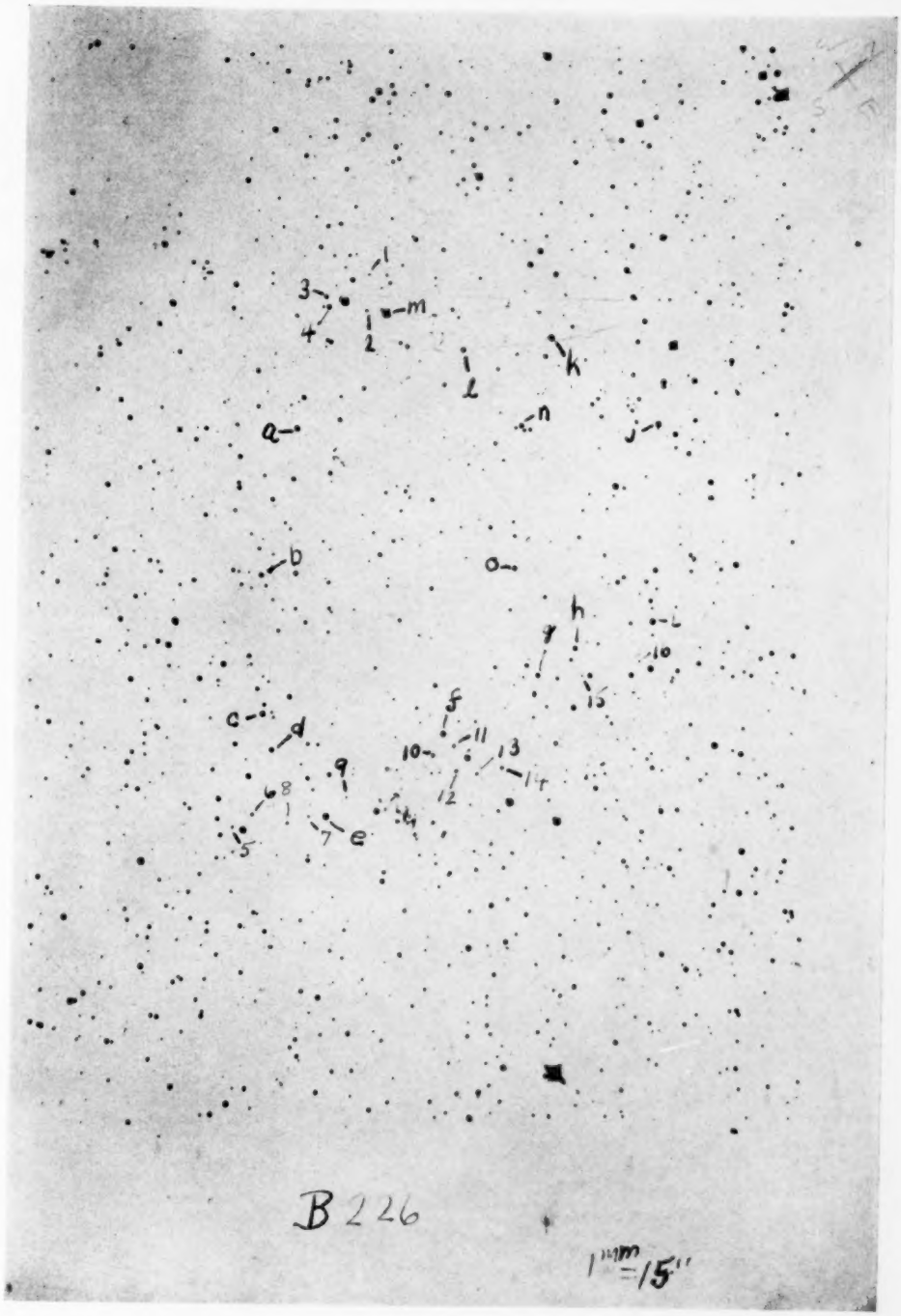

PLATE XXIII

The number of stars per square degree equal to and brighter than each scale image, $N(m)$, was then plotted against the magnitude of the scale image. A separate curve was made for both the obscured and the unobscured areas. In general, the stars were counted

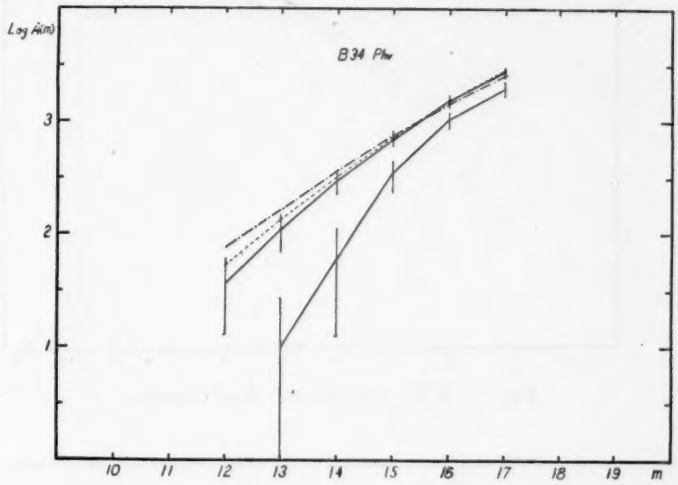

FIG. 2.—B 34. Photovisual. Wolf diagram

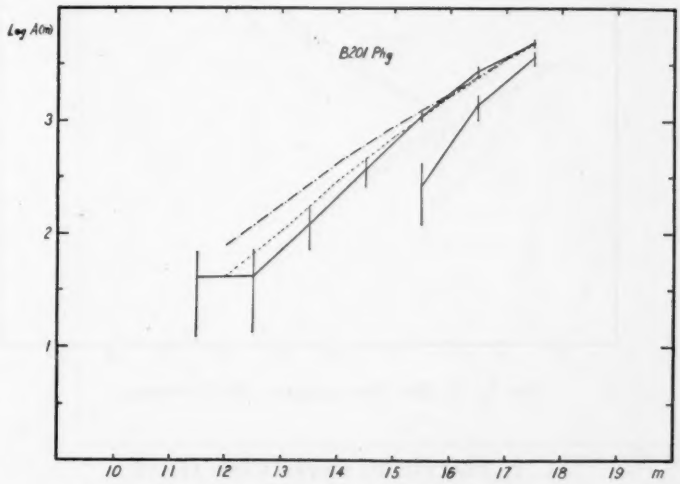

FIG. 3.—B 201. Photographic. Wolf diagram

on two separate plates, and the results of both counts were plotted together. A smooth curve was passed through the points thus determined. The values of $N(m)$, at intervals of 1 mag., were read from this curve; and the number of stars per 1-mag. interval,

$$A\,(m) = N\,(m+\tfrac{1}{2}) - N\,(m-\tfrac{1}{2})\,,$$

was plotted against the magnitude. This gave the observed Wolf diagrams in their final form (Figs. 1–8). The vertical lines indicate the statistical uncertainty of the counts.

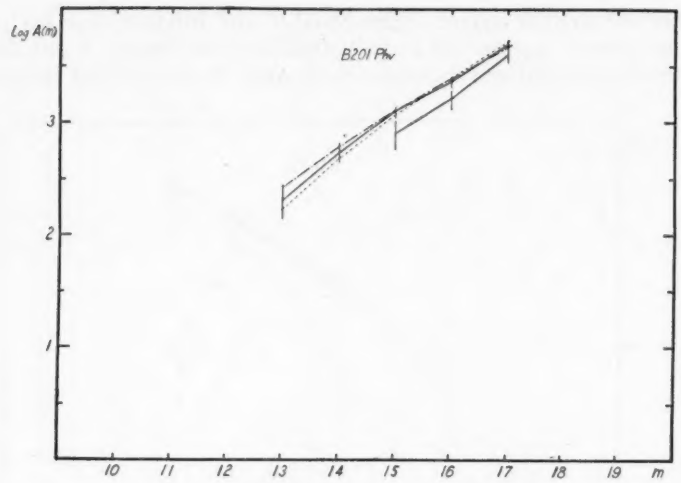

FIG. 4.—B 201. Photovisual. Wolf diagram

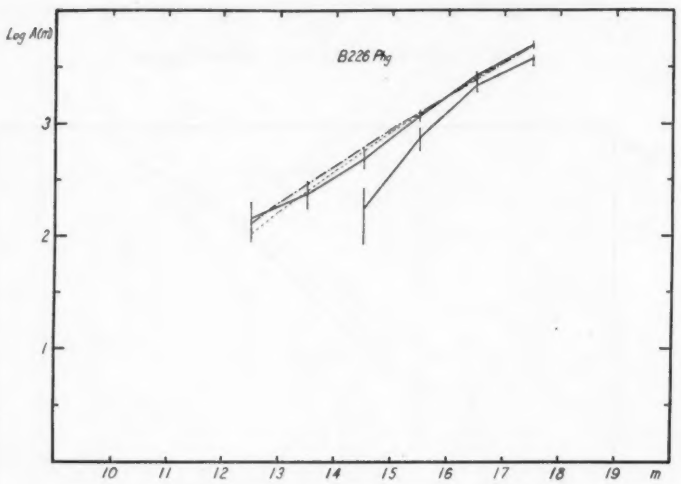

FIG. 5.—B 226. Photographic. Wolf diagram

V. ANALYSIS OF UNOBSCURED AREAS

The fundamental equation of statistical astronomy, expressed in terms of the distance modulus y, is[6]

$$A(m) = 0.1402 D_0 \int_{-\infty}^{+\infty} D(y) \Phi(M) 10^{0.6y} dy , \qquad (1)$$

where $A(m)$ is the number of stars per square degree in the magnitude interval $m \pm \frac{1}{2}$; $D(y)$ is the density function expressed in terms of the density in the neighborhood of the

[6]Von der Pahlen, *Lehrbuch der Stellarstatistik*, p. 420.

sun as unity; $\Phi(M)$ is the relative luminosity function, which is the fraction of stars in a given volume with absolute magnitudes in the interval $M \pm \frac{1}{2}$. It is assumed to be independent of the distance. D_0 is the number of stars per cubic parsec in the vicinity of the sun, and y is the distance modulus $y = m - M$.

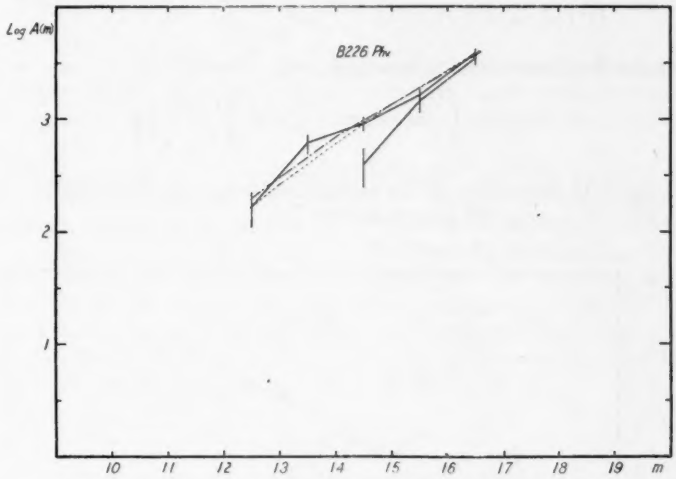

FIG. 6.—B 226. Photovisual. Wolf diagram

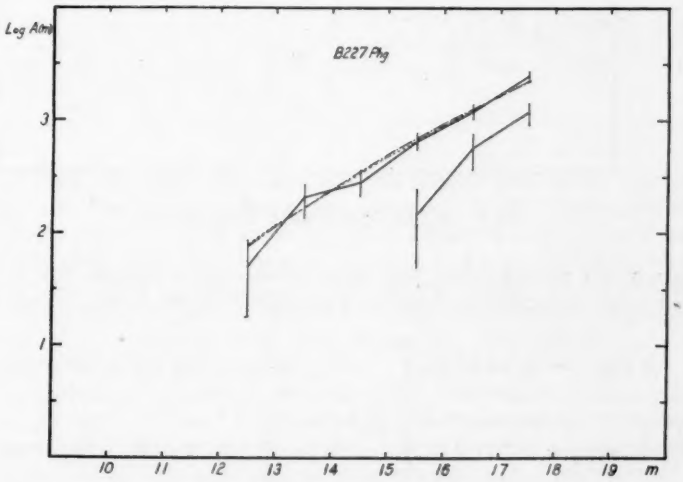

FIG. 7.—B 227. Photographic. Wolf diagram

When we introduce a general space absorption which is assumed to be a function of the distance, the distance modulus becomes

$$y = m - M = 5 \log r - 5 + a(r), \qquad (2)$$

where $a(r)$ is the absorption between the observer and a star at distance r (in parsecs). It should be borne in mind that the distance modulus corresponding to a given distance is different for photographic and photovisual wave-length regions.

Equation (1) now takes the form

$$A(m) = 0.1402 D_0 \int_{-\infty}^{+\infty} D'(y)\,\Phi(M)\,10^{0.6y} dy\,, \tag{3}$$

where

$$D'(y) = D(y)\,P(y) \tag{4}$$

may be called the fictitious density function and

$$P(y) = \left[e^{3a(r)/5 \log e} \left(1 + r\,\frac{a^1(r)}{5 \log e} \right) \right], \tag{5}$$

where $a^1(r)$ is the first derivative of the absorption law $a(r)$, and where r is to be considered as a function of y, according to equation (2).

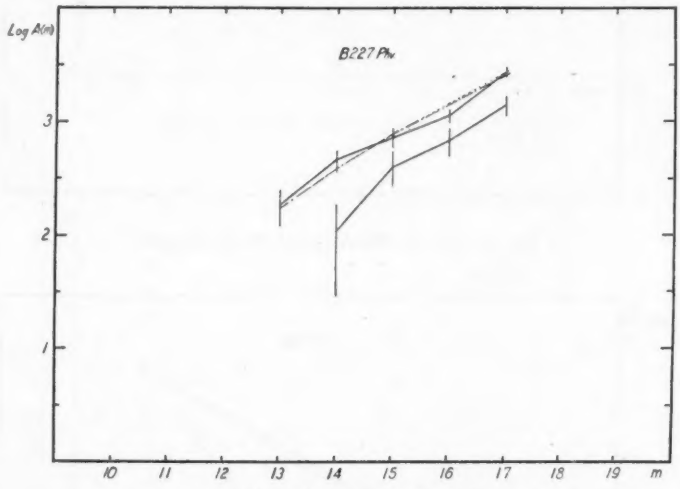

FIG. 8.—B 227. Photovisual. Wolf diagram

The counts in the photographic and photovisual region provide one with $A(m)_p$ and $A(m)_v$. If one tries to represent them with equations of the form (3), one has

$$A(m)_p = 0.1402 D_0 \int_{-\infty}^{+\infty} D(y_p)\,P_p(y_p)\,\Phi_p(M_p)\,10^{0.6y_p} dy_p$$

and

$$A(m)_v = 0.1402 D_0 \int_{-\infty}^{+\infty} D(y_v)\,P_v(y_v)\,\Phi_v(M_v)\,10^{0.6y_v} dy_v\,,$$

where the p subscript refers to the photographic and v to the photovisual region. Here $D(y_p)$, $D(y_v)$, $P_p(y_p)$, and $P_v(y_v)$ are unknown functions, the last two related to the photographic and visual absorption laws.

It is assumed that the luminosity functions, $\Phi_p(M_p)$ and $\Phi_v(M_v)$, are the same as in the vicinity of the sun, and Van Rhijn's[7] values of these were adopted. The two density functions must fulfil the condition that they give the same values for distance moduli y_p and y_v, which correspond to the same distance. This introduces a third equation with

[7] *Groningen Pub.*, No. 47, 1936.

no additional unknown quantities. In order to have a unique solution, it is necessary to have a fourth equation which is furnished by the assumption of a constant ratio between photographic and photovisual absorption:

$$\frac{a_p}{a_v} = 1.5 .$$

Attempts were made by trial and error to find the solutions for the four unobscured areas, but without success. It is believed that errors in the magnitude scales, in the assumption that $a_p/a_v = 1.5$, and possibly also in the luminosity functions were responsible for the difficulty.

The assumption that $a_p/a_v = 1.5$ was then dropped, and an attempt was made to represent the two star counts of each area under the assumption of constant density and uniform absorption, determining the absorption coefficients for each area and each wave length so as to obtain the best fit. B 226 and B 227 could be satisfactorily represented with these assumptions, but B 201 and B 34 could not. In all cases, the greater the galactic latitude, the greater the discrepancy. The thinning-out of the absorbing material with increasing distance from the central plane of the galaxy would explain the discrepancy. The values of the absorption coefficients in magnitudes per kiloparsec that hold best for constant densities and absorption are given in Table 10.

TABLE 10

ABSORPTION COEFFICIENTS IN UNOBSCURED AREAS
(Constant Densities and Absorptions)

	B 34	B 201	B 226	B 227		B 34	B 201	B 226	B 227
a_p	1.70	1.05	1.05	1.50	a_p/a_v	1.26	1.05	1.14	1.11
a_v	1.35	1.00	0.92	1.35					

The star numbers computed with these data are represented on the Wolf diagrams by a dot-and-dash line. The photographic absorption coefficients obtained are rather large, compared with the average value given by other methods (e.g., galactic star clusters, cepheid variables, etc.); and the mean ratio $a_p/a_v = 1.14$ is rather small, compared with other determinations. Both would indicate that the star density is probably not constant but decreases with distance. The possibility of systematic errors in the magnitude scales should, however, also be considered in this connection. The ratio a_p/a_v is particularly sensitive to such errors.

Bok[8] has found that in this part of the galaxy the star density decreases rapidly with increasing distance from the sun. An attempt was therefore made to represent the unobscured areas with uniform absorption for each region, but with the star density varying with the distance. While such solutions are not determinate, the values of absorption coefficients and star densities in Table 11 give a good representation of the star counts and may be accepted as a possible interpretation.

The star numbers computed with these data are represented on the Wolf diagrams by a dashed line. Here, in general, the greater the galactic latitude, the more rapidly the density decreases, which is in agreement with our knowledge of the galaxy.

Thus both B 226 and B 227 have two solutions which satisfy the observed curves equally well. From the above data it is impossible to tell which of the two more nearly represents the true conditions.

[8] Bok, *Distribution of the Stars in Space*, p. 105, University of Chicago Press, 1937.

VI. ANALYSIS OF THE DARK AREAS

When, by trial and error, values of $a(r)$ and $D(y)$ are found such that the observed star counts in the unobscured regions are well represented, the absorbing power and distance of the cloud are found by the following method:

The assumption is made here that the dark clouds are so small that their depths can be neglected. It is also assumed that the true star density is the same in the direction of the nebula as in the surrounding star field.

TABLE 11

ABSORPTION COEFFICIENTS IN UNOBSCURED AREAS

(Variable Densities and Constant Absorptions)

	B 34	B 201	B 226	B 227
a_p	0.80	0.50	0.62	0.77
a_v	0.58	0.45	0.54	0.65
a_p/a_v	1.38	1.11	1.15	1.18
	Mean $a_p/a_v = 1.20$			

DENSITIES

r (Parsecs)	B 34	B 201	B 226	B 227
100	1.00	1.00	1.00	1.00
200	0.70	0.90	0.75	0.83
500	0.25	0.20	0.50	0.63
1000	0.25	0.20	0.50	0.43
2000	0.25	0.28	0.45	0.30
5000	0.25	0.30	0.42	0.25
10,000	0.25	0.15	0.40	0.25

If one designates with

$$\left.\begin{aligned} F_1(y_1)\,dy &= 10^{0.6y_1} D_0 D'(y_1)\,dy \quad \text{in the unobscured region}, \\ F_2(y_2)\,dy &= 10^{0.6y_2} D_0 D'(y_2)\,dy \quad \text{in the obscured region}, \end{aligned}\right\} \tag{6}$$

then $0.1402\,F(y)dy$ represents the number of stars per square degree situated between the distance limits corresponding to the distance moduli $y \pm (dy/2)$.

When $D'(y_1)$ has been determined, $F_1(y_1)$ can be plotted. Designating with y_0 the distance modulus of the dark nebula, one has for $y_1 \leqq y_0$, $y_2 = y_1$, since up to that distance the absorption is the same in both regions. For $y_1 > y_0$, one has $y_2 = y_1 + a$, where a is the absorption by the cloud in magnitudes. Then $F_2(y_2)$ is found in the following way:

$$\text{for } y_2 < y_0: \qquad F_2(y_2) = F_1(y_1),$$

$$\text{for } y_2 < y_0 + a: \qquad F_2(y_2) = F_1(y_2 - a)$$

(between y_0 and $y_0 + a$, one has $F_2(y_2) = 0$).

By trial and error, values of a and y_0 can be found which satisfy the equation

$$A'(m) = 0.1402 \int_{-\infty}^{+\infty} F_2(y_2)\, \Phi(m - y_2)\, dy_2, \qquad (7)$$

where $A'(m)$ is the observed frequency function of apparent magnitudes in the obscured area.

As can be seen from the observed Wolf diagrams, these areas will not give a good determination of the distance of the cloud, since there are too few stars in front of such small objects. It is further to be noted that the curves for the unobscured and obscured regions have a tendency to converge for fainter magnitudes. This is contrary to the theory and must be due to some systematic error affecting the star counts. It might to some extent result from errors in the magnitude scales, or it might be due to the fact that counts are generally more complete in a poor region than in a rich field.

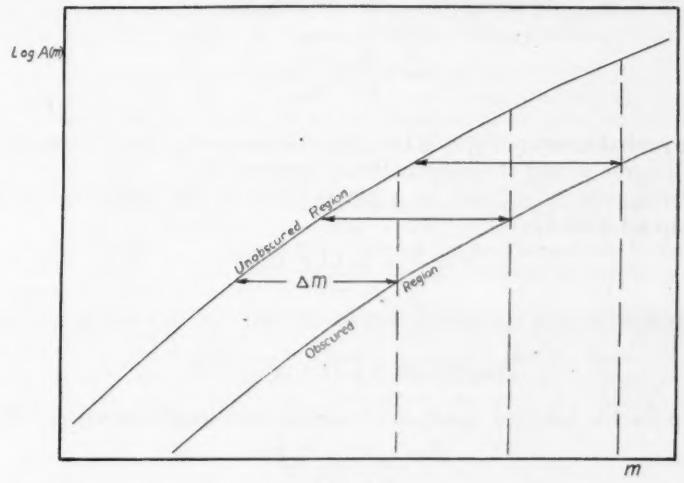

FIG. 9

The values of the total absorption of each cloud were taken directly from the Wolf diagrams, and various values of the clouds' distances were tried. The solutions of the equations do not give very definite values of the distances but do offer some idea as to the maximum probable distances, which in all cases is of the order of 1000 parsecs.

Since the chief object of this investigation was to determine the total photographic and photovisual absorption of these clouds and their ratios, the adopted values of these quantities were obtained as follows:

From the observed curves, the quantities Δm were formed for the last three magnitudes as shown in Figure 9. These three determinations were given equal weight, since the greater statistical accuracy of the last points was considered to be compensated for by the greater uncertainty of the magnitude scale. The results of this method are rather uncertain when the curves show considerable irregularities.

It is noted that both obscured and unobscured areas often show peaks or depressions at the same magnitudes (example, B 227 pv.). Some of these irregularities are thus probably due to errors in the magnitude limits adopted. A second determination of the $A(m)$ was made by drawing a smooth curve through the points of the unobscured region. The magnitude corrections thus determined for the unobscured curve were applied to the obscured curve. This method smoothed out both curves. The absorption of the cloud was determined in the same manner as in the original curve.

The adopted values of the cloud absorptions given in Table 12 are the means of the two determinations.

TABLE 12

TOTAL ABSORPTIONS FOR THE BARNARD AREAS

	B 34	B 201	B 226	B 227
a_p	$0^m.80 \pm 0^m.06$	$0^m.94 \pm 0^m.11$	$0^m.48 \pm 0^m.04$	$1^m.36 \pm 0^m.13$
a_v	$0^m.69 \pm {}^m.05$	$0^m.58 \pm {}^m.05$	$0^m.32 \pm {}^m.05$	$1^m.02 \pm {}^m.05$
$\eta = a_p/a_v$	1.16 ± 0.09	1.62 ± 0.13	1.50 ± 0.23	1.33 ± 0.07

The probable errors of a_p and a_v are computed from the agreement of the Δm's as taken from both the rough and the smoothed curves. The probable errors of each of the four ratios $\eta = a_p/a_v$ were computed from the relation

$$\epsilon_\eta^2 = \frac{\epsilon_p^2}{a_v^2} + \frac{a_p^2}{a_v^4}\epsilon_v^2 ,$$

where ϵ is the probable error of η, ϵ_p is the probable error of a_p, and ϵ_v that of a_v. The four values of η all agree within the observational uncertainty.

Each determination of η based on n plates received the weight $p = n/\epsilon^2_\eta$, and the weighted mean adopted is

$$\eta = \frac{a_p}{a_v} = 1.31 \pm 0.03 .$$

On the assumption that the absorption varies with the wave length according to the formula

$$\text{Absorption} = \text{Constant} \times \lambda^{-\beta} ,$$

the value of β for the adopted value of η and for wave lengths 5600 and 4450 is

$$\beta = 1.17 \pm 0.10 .$$

The value of the ratio of photographic to color absorption as given by the above results is

$$\chi = \frac{a_p}{a_p - a_v} = 4.24 \pm 0.40 .$$

If one assumes that these dark nebulae are roughly spherical, with a distance of 1000 parsecs and an average apparent diameter of 15′, the true diameter is of the order of 5 parsecs. These objects are apparently of the same order of size as the Orion nebula and other luminous diffuse nebulae. The absorption coefficients in the clouds in the photographic region would range from approximately $0^m.1$ per parsec for B 226 to about $0^m.25$ per parsec for B 227. If these clouds are nearer than 1000 parsecs, as is very probable, their true dimensions are reduced, and the absorption coefficients correspondingly increased. In these small clouds the absorption coefficient is thus a few hundred times larger than the generally accepted values of the general interstellar absorption coefficient.

I am indebted to Dr. R. J. Trumpler, who suggested the problem, for his advice and suggestions throughout; to the Regents of the University of Arizona for the award of the Steward Observatory Fellowship for the year 1937–38; and to Dr. E. F. Carpenter, director of the Steward Observatory, for many valuable suggestions as to observational technique. I am also indebted to Dr. Jesse L. Greenstein and Dr. Lawrence H. Aller for several valuable suggestions.

THE CAPE MAGNITUDES AND THE INTERNATIONAL SYSTEM*

FREDERICK H. SEARES[1] AND MARY C. JOYNER

Mount Wilson Observatory

Received July 6, 1945

ABSTRACT

The Cape magnitudes and colors derived by Stoy and Menzies for the southern Comparison Stars for Eros and by Stoy for stars in the Harvard Standard Regions at declination −45° have been reduced to the International system with the aid of Mount Wilson observations of the Eros stars based directly on the North Polar Standards.

Local irregularities in the Mount Wilson Pg scale and in the zero points for both Pg and Pv magnitudes have been eliminated without changing either the general scale relations or the mean zero points. Yerkes observations, similarly revised for local zero-point error, confirm the Mount Wilson results within narrow limits of error.

For the Eros stars both the Mount Wilson and the reduced Cape color indices are, in the mean, independent of magnitude; hence, for both series the Pg and Pv scales are sensibly parallel. The zero-point corrections to the spectrum-color relation are +0.03 and +0.02 mag., respectively; the zero points for Pg and Pv magnitudes are therefore consistent within quantities of the same order.

The reduction formulae for Eros stars, equations (10), lead to equations (16)–(18), which apply to the Cape basic magnitudes in the Standard Regions at −45°. These formulae agree with Stoy's provisional reduction to about the eighth magnitude. Below this limit, divergences of 11 per cent are found for both Pg and Pv scales. Tests similar to those used for the Eros stars, applied to the reduced basic magnitudes, give similarly accordant results and show that the transfer of the basic magnitudes to the Eros fields has been highly successful. Moreover, the scale reductions are confirmed approximately by the known behavior of the Harvard Pg standards in these same fields.

Stoy's comparisons with the Hyades, Praesepe, and the Pleiades are examined in detail. What at first seemed a conflict between his provisional reduction and that from the Eros stars is explained. The reduced zero points for the Hyades and Praesepe appear to be correct, since the color indices thus defined are normal for the spectral types concerned, as they should be. Field stars for the Hyades beyond 200 parsecs show, however, a color excess of 0.3 mag., in general agreement with Ramberg's conclusion that an obscuring cloud behind the cluster begins at about 140 parsecs.

I. INTRODUCTION

A recent investigation by R. H. Stoy[2] has given us basic Pg and Pv magnitudes of high internal accuracy for each of the nine Harvard Standard Regions at declination −45° (E zone). Comparisons with the Hyades, Praesepe, and the Pleiades led to a provisional connection of these magnitudes with the International system. Owing to inherent difficulties in the cluster observations, Stoy and Menzies[3] also transferred the basic scales at −45° to the southern Eros stars for comparison with Mount Wilson and Yerkes magnitudes that had been referred directly to the International standards. Difficulties again appeared, which led to the conclusion (p. 313): "In view of the large systematic errors that affect both the Mt. Wilson and Yerkes magnitudes of the Eros Comparison Stars it would appear that neither series can be regarded as an accurate representation of the International Scale as embodied in the North Polar Sequence."

In a third article[4] Stoy reports additional comparisons with the Pleiades, discusses the zero-point and scale relations, and, summarizing, says (p. 317): ". . . . the Cape photographic magnitudes probably need a zero-point correction of −0^m.13, though no satis-

* *Contributions from the Mount Wilson Observatory, Carnegie Institution of Washington*, No. 710.

[1] Research Associate, Carnegie Institution of Washington.

[2] *M.N.*, **103**, 288, 1944. Hereafter designated as "Stoy I."

[3] *M.N.*, **104**, 298, 1944. Hereafter designated as "Stoy and Menzies."

[4] *M.N.*, **104**, 317, 1944. Hereafter designated as "Stoy II."

factory reduction to the International System is possible until further work has been done in the Northern Hemisphere."

Through the kindness of Mr. Stoy we were able to study in detail the last two of these three articles in advance of publication, an opportunity for which he has our grateful thanks.

The accidental errors of the Mount Wilson[5] observations of the Eros stars are certainly large, and there are clearly important irregularities in zero point relative to the Yerkes[6] data. As Stoy remarks, all this appears in our original discussion. Nevertheless, the foregoing citations seem to us to present much too gloomy an outlook. We agree that further work in the northern hemisphere is needed. The Eros stars should be recompared with the Polar Standards, but chiefly as a check on and a refinement of results that may be obtained by continuing the discussion beyond the point at which Stoy has left it.

The justification for further discussion at this stage lies in two general considerations: first, since the Mount Wilson observations of the Eros stars include 30 polar comparisons for Pg magnitudes and 30 for Pv, the mean zero points for all fields together should be correct within 0.01 or 0.02 mag.; and, second, owing to the accuracy of the Cape measurements, it should be possible to use these observations to correct the Mount Wilson magnitudes for any field-to-field change in zero point. These local corrections conceivably may change the Mount Wilson scales; but that is a detail open to direct test—and correction. In any event, we may thus obtain revised magnitudes, at least partially freed from zero-point errors, for a comparison with the Cape results and a revision of Stoy's provisional reduction formulae. With minor reservations, these remarks also apply to the Yerkes observations of Eros stars. Agreement between Yerkes and Mount Wilson results for these stars—should agreement be found—will of course give added weight to any revision of the reduction formulae for the Cape magnitudes. Further, the residuals in color index should provide a test of the constancy of the Cape zero points, assumed as a means of correcting locally the Mount Wilson and the Yerkes zero points. Finally, the standard spectrum-color relation may be used effectively to test the zero-point consistency of each of the Pg and Pv series of magnitudes—Eros stars, both Mount Wilson and Cape, Harvard Standard Regions, and the clusters.

The procedure thus outlined leads to formulae (16) and (17) for the reduction of the Cape magnitudes. Except for the zero-point correction of -0.15 mag., instead of the -0.13 mag. suggested by Stoy, the first of equations (16) and the first of (17) are identical with Stoy's formulae, reprinted here as equations (14). For stars brighter than about the eighth magnitude we therefore substantially confirm Stoy's results. For fainter stars, however, we find divergences in scale from his formulae amounting to 11 per cent.

At first sight these scale differences for the fainter stars seem to conflict with the generally accordant scale factors found by Stoy from the cluster comparisons. It turns out on analysis, however, that the Cape Pg magnitudes for the Pleiades present the only certain discordance. These magnitudes apparently are not representative of the basic Cape results; certainly they are inconsistent with the Cape Pv results for the Pleiades. Generally speaking, however, the Cape data are highly accordant and of fine precision, and in working with them one gains the impression that Stoy and Menzies have provided a sound basis for a photometric connection of the northern and the southern hemispheres that will meet modern requirements.

[5] Seares, Sitterly, and Joyner, *Mt. W. Contr.*, No. 415; *Ap. J.*, **72**, 311, 1930. A decentered objective, discovered when it was too late to repeat the observations, introduced large asymmetrical plate errors which could not be completely removed. The zero-point error relative to Yerkes, progressive from field to field for the stars observed in common, was also a matter of concern. The results, though disappointing, were sufficiently accurate for the reduction of the measurements of position of Eros, for which they were intended, and on that account were finally printed.

[6] Ross and Zug, *A.N.*, **239**, 289, 1930.

II. NOTATION

The Cape results for the Harvard Standard Regions at $-45°$ declination[2] include three series of magnitudes: (1) Pg, Pv, from intercomparisons of the 9 fields; on the mean scale and the mean zero point of the Harvard standards in these fields. (2) Pg′, Pv′, from diffraction-grating plates; scale and zero point the same as for system (1), the grating being used to extrapolate the scale beyond the limits of the Harvard standards. (3) IPg, IPv, a weighted combination of (1) and (2) reduced to the International system by Stoy's provisional formulae, equations (14) of this paper.

Later we shall use Pg′ and Pv′ as Cape "basic" magnitudes, a designation introduced here for convenience. From the standpoint of accidental error, the term "basic" would apply more appropriately to the weighted mean of systems (1) and (2) used to obtain system (3); but weighting factors were lacking, and, moreover, we wished to use certain comparisons made by Stoy which involve Pg′ and Pv′ and not the weighted means. For the present purpose the difference in procedure is otherwise unimportant.

For uniformity and for simplicity later on, it is desirable to modify the foregoing notation. We write

$\mathrm{Pg_C}$, $\mathrm{Pv_C}$ for the Cape basic magnitudes Pg′, Pv′,

$\mathrm{Pg_I}$, $\mathrm{Pv_I}$ for the Cape IPg, IPv.

Further, for the Eros comparison stars we use

$\mathrm{Pg_W}$, $\mathrm{Pv_W}$ for the Mount Wilson magnitudes,[5]

$\mathrm{Pg_Y}$, $\mathrm{Pv_Y}$ for the Yerkes magnitudes.[6]

The letter C with any one of the foregoing subscript symbols indicates the corresponding color index. Finally, a prime or double prime attached to any magnitude or color symbol indicates a corrected value, reduced, or partially reduced at least, to the International system.

III. EROS STARS—CAPE AND MOUNT WILSON OBSERVATIONS

In this section we derive formulae for the reduction of the Cape magnitudes of Eros stars to the system of the Mount Wilson results for these stars. We correct the Mount Wilson magnitudes locally for zero-point error, also for local errors of scale (Pg only) which make their appearance during the comparisons, taking care, however, that the scale corrections used do not change either the mean zero point or the general scale relations. The mean zero point for all fields together and the smoothed scale we accept provisionally as representative of the International system, as originally they were intended to be.

The published Cape magnitudes are IPg, IPv values, that is, $\mathrm{Pg_I}$, $\mathrm{Pv_I}$ in the notation used here. Grouped according to magnitude, the differences $\mathrm{Pg_W} - \mathrm{Pg_I}$ and $\mathrm{Pv_W} - \mathrm{Pv_I}$ give a provisional reduction of the Cape results to the Mount Wilson system. The reduced Cape values $\mathrm{Pg_I'}$ and $\mathrm{Pv_I'}$ we suppose to be free from any zero-point error depending on the individual field, or, more conveniently, simply on the declination—an assumption to be justified later. The differences $\mathrm{Pg_I'} - \mathrm{Pg_W}$ and $\mathrm{Pv_I'} - \mathrm{Pv_W}$, grouped according to declination, should then reveal any declination error in the Mount Wilson zero points.

The results thus found, including the group means, the numbers of stars (in parentheses), and the adopted, smoothed corrections, are in Table 2, columns 4 and 5. For declination we use simply the zone portion of the *Durchmusterung* number of the star. The maximum correction to $\mathrm{Pv_W}$ is 0.06 mag., but for $\mathrm{Pg_W}$, in zones $-9°$ to $-11°$, it rises to 0.2 mag. For all stars together, the weighted mean correction is zero, as it should be.

Denoting the corrected Mount Wilson magnitudes by $\mathrm{Pg_W'}$ and $\mathrm{Pv_W'}$, we revise the comparison with the Cape data by grouping the differences $\mathrm{Pg_W'} - \mathrm{Pg_I}$ and $\mathrm{Pv_W'} - \mathrm{Pv_I}$

according to their respective Cape magnitudes. The group means are in Table 1, columns 2 and 8, the results for the Bright Extra Stars (hereafter simply Bright Stars) and the Comparison Stars proper being listed separately. The numbers of stars, as usual, are given in parentheses.

The change in each group mean produced by correcting the Mount Wilson zero points is shown in columns 3 and 9 of Table 1; the differences Column 2 *minus* Column 3 and Column 8 *minus* Column 9 thus reproduce the original Mount Wilson-Cape comparison. It is obvious that the local zero-point corrections have not appreciably affected the Mount Wilson scales.

Plots of the differences in Table 1, columns 2 and 8, show for Pv only slight disturbances by accidental errors. For Pg, however, such errors are obviously important. Most

TABLE 1

SCALE COMPARISON: CAPE AND MOUNT WILSON

(Unit, 0.01 Mag.)

Pg_I (1)	$Pg'_W - Pg_I$ (2)	Dec. Corr. (3)	δPg_W (4)	$Pg''_W - Pg_I$ (5)	v^*_{Pg} (6)	Pv_I (7)	$Pv'_W - Pv_I$ (8)	Dec. Corr. (9)	v^*_{Pv} (10)
5.70..	− 2(7)	+3	−13	−15	+2	5.35...	−3(12)	−2	−4
6.25..	−20(11)	0	+ 6	−14	+3	6.12...	+1(8)	+1	0
6.75..	−26(11)	−3	+ 6	−20	−3	6.38...	+2(8)	0	+1
7.25..	−20(11)	+2	+ 3	−17	0	6.62...	0(9)	+4	−1
7.75..	−23(11)	+2	− 1	−20†	−3	6.88...	+2(9)	−1	+1
8.25..	−14(5) − 9(20)	−3 0	− 6	−16	0	7.25...	+3(17) − 1(7)	+1 +2	+1
8.75..	− 1(7) − 8(22)	−1 +2	− 4	−10	+1	7.75...	..... − 6(17)	 0	−7
9.12..	..... −11(18)	..... −1	+ 3	− 8	−1	8.12...	..... − 1(15)	..... +1	−2
9.38..	..... −12(26)	..... +1	+ 4⁵	− 7⁵	−3	8.38...	..... 0(20)	 0	−1
9.62..	..... − 6(34)	..... +1	+ 3⁵	− 2⁵	−1	8.62...	..... + 3(21)	 0	0
9.88..	..... − 1(45)	..... −1	+ 2	+ 1	0	8.88...	..... + 8(31)	..... +1	+2
10.12..	..... + 3(22)	 0	− 1	+ 2	−2	9.12...	..... +10(47)	 0	+1
10.38..	..... +14(30)	..... −2	− 3	+11	+4	9.38...	..... +10(43)	 0	−2
10.66..	..... +22(11)	..... +1	− 6	+16	+6	9.62...	..... +14(26)	..... −1	0
						9.88...	..... +17(15)	 0	0
All..	−18.6(63)‡ (228)	+0.2 0.0	0.0	−17.3‡	+0.1	All..	+0.9(63) (242)	+0.4 +0.1	−0.5

* Observation *minus* Formula.

† Three discordant stars omitted.

‡ Weighted mean of first six groups.

of them undoubtedly are in the Mount Wilson data. For example, the first difference, −0.02, is algebraically much too large, because Pg_W, as shown by C_W and the spectral types of the stars, is certainly too large. In general, the differences suggest oscillations superimposed on an underlying trend similar to the trend for Pv shown in column 8. The appearance of these local irregularities was not unexpected. Their occurrence was, in fact, predicted in *Mt. W. Contr.* No. 415, pages 5 and 6.[5] To smooth them out, we apply to Pg'_W the local corrections of scale listed in column 4 and obtain

$$Pg''_W = Pg'_W + \delta Pg_W .$$

These local scale corrections, like the declination corrections, affect neither the general trend of the scale nor the mean zero point.

The adopted MW-Cape Pg scale reduction is therefore defined by the differences in column 5 of Table 1, which, in general, are satisfactorily represented by the formula

$$Pg''_W - Pg_I = -0.17 + 0.11\,(Pg_I - 8.2) \quad (= -0.17 \text{ for } Pg_I < 8.2) . \quad (1)$$

Similarly, from column 8,

$$Pv'_W - Pv_I = +0.01 + 0.11\,(Pv_I - 8.4) \quad (= +0.01 \text{ for } Pv_I < 8.4) . \quad (2)$$

TABLE 2

LOCAL ERRORS IN ZERO POINT

(Unit, 0.01 Mag.)

DEC. (1)	YERKES STARS		COMPARISON STARS			BRIGHT STARS			RESIDUALS IN C	
	$Pg_W - Pg_Y^*$ (2)	$Pv_W - Pv_Y$ (3)	$Pg_I' - Pg_W$ (4)	$Pv_I' - Pv_W$ (5)	$C_I' - C_W$ (6)	$Pg_I' - Pg_W$ (7)	$Pv_I' - Pv_W$ (8)	$C_I' - C_W$ (9)	v_W (10)	v_I (11)
0°	+ 1(8), + 1	− 1(8), − 1	....., − 5	0(8), 0	− 5					
− 1	− 3(6), − 5	− 2(6), − 4	− 4(4), − 2	+ 2(6), +2	− 4				−5(12)	−4(15)
2	−28(6), −11	− 6(6), − 7	+ 4(6), + 2	+ 5(6), +4	− 2	−10(2), − 5	+ 6(2), + 6	−11	−8(11)	−5(11)
3	−27(5), −18	−14(5), −10	+ 1(5), + 3	+ 5(5), +5	− 2	+ 4(4), + 4	+10(4), +10	− 6	−5(12)	−3(15)
4	−12(7), −20	−11(7), −10	+ 6(7), + 5	+ 7(7), +6	− 1	+22(2), +15	+11(2), +10	+ 5	−5(10)	−1(16)
5	−15(5), −20	−19(5), − 8	+ 8(5), + 6	+ 3(5), +3	+ 3	+17(2), +17	+ 8(2), + 8	+ 9	−1(9)	−2(16)
6	−20(7), −20	+ 7(7), − 3	− 1(6), + 1	−10(6), −4	+ 5	+14(2), +16	0(2), 0	+16	0(8)	−2(13)
7	−16(6), −20	− 3(5), + 1	+ 2(5), + 3	− 1(5), −3	+ 6	+15(3), +15	− 6(3), − 2	+17	0(7)	−4(9)
8	−25(6), −18	+ 3(4), + 3	+13(5), +11	+ 1(6), −3	+14	+ 8(1), +12	+ 7(1), − 1	+13	−4(8)	−4(8)
9	− 8(6), −12	+ 2(2), + 7	+17(3), +17	− 7(3), −3	+20				−1(9)	−2(10)
10	−12(7), − 7	+18(7), +10	+21(7), +20	− 2(7), −2	+22	+16(2), + 4	− 2(2), 0	+ 4	+2(13)	0(15)
11	− 3(6), 0	+12(6), +12	+20(5), +19	− 2(5), 0	+19	− 8(2), − 4	0(2), 0	− 4	+8(16)	0(17)
12	+ 9(6), + 8	+10(4), +10	− 2(4), +10	+ 7(4), +4	+ 6	− 6(4), − 6	+ 4(4), + 3	− 9	+9(13)	−1(12)
13	− 2(7), +15	+ 4(6), + 7	+ 4(7), − 2	+ 4(7), +4	− 6	−15(1), − 6	+12(1), + 3	− 9	+4(16)	−2(12)
14	+27(11), +22	+ 6(9), + 7	−13(10), − 8	+ 5(10), +5	−13	− 3(3), − 4	− 1(3), − 1	− 3	−4(13)	−2(11)
15	+28(5), +28	+12(5), +10	− 9(5), −10	+ 7(5), +5	−15	+20(1), − 4	−16(1), − 6	+ 2	−7(17)	−3(15)
16	+32(7), +32	+ 7(7), +10	− 5(7), −11	− 1(7), 0	−11	− 4(4), − 4	− 8(4), − 6	+ 2	−8(13)	−4(13)
17	.....	.....	−13(8), −12	0(8), 0	−12				−7(12)	−4(12)
18	.....	.....	−12(4), −11	+ 6(4), +5	−16	+10(1), 0	+14(1), +10	−10	−3(12)	0(11)
19	.....	.....	− 9(7), − 9	+ 5(7), +5	−14	−10(2), 0	+11(2), +12	−12	−2(15)	+2(16)
20	.....	.....	− 2(15), − 4	+ 2(16), +2	− 6	−43(1), 0	+16(1), +12	−12	+1(22)	+2(25)
21	.....	.....	− 3(23), − 2	0(23), 0	− 2	+ 3(6), 0	+ 1(6), + 6	− 6	−1(37)	+1(37)
22	.....	.....	+ 2(32), 0	− 4(33), −4	+ 4	− 8(3), − 2	+15(3), 0	− 2	0(48)	0(39)
23	.....	.....	− 3(23), 0	− 2(23), −2	+ 2	+ 2(9), − 3	−11(9), − 6	+ 3	0(53)	0(37)
24	.....	.....	+ 2(17), 0	− 2(17), −2	+ 2	−13(3), − 7	− 4(3), − 6	− 1	+2(41)	0(26)
25	.....	.....	− 1(8), 0	− 3(9), −2	+ 2	− 6(3), −10	− 6(3), − 7	− 3	+3(28)	+1(16)
−26	.....	.....	.....	.....	.....	−14(2), −14	− 8(2), − 7	− 7	+2(16)	.....
All	− 2.8(111), −1.3	+ 1.8(99), +1.8	− 0.2(228), −0.2	+ 0.1(242), +0.1	.....	− 0.1(63), +0.2	+ 0.3(63), −0.6	.....	−0.5(164)	−0.8(151)

* Observed difference, number of stars (in parentheses), and adopted difference.

The corresponding residuals (observation − formula) are in columns 6 and 10. The v_{Pg} series still shows some clustering of signs, and the systematic trend below $Pg_I = 10.0$ may be significant; but in general the individual residuals are within their respective uncertainties. The discontinuities in the formulae at $Pg_I = 8.2$ and $Pv_I = 8.4$ doubtless are oversimplifications; but in view of the errors involved, there is no point in a more complicated formulation.

No color corrections have been applied. For Pg and Pv separately (Table 3, cols. 3 and 4) the effect is negligible. Only in the differences $C'_W - C'_I$ (Table 3, col. 5) is there definite evidence of a systematic trend.

TABLE 3

COLOR EQUATION

(Unit, 0.01 Mag.)

C_I (1)	$Pg_W - Pg'_Y$ (2)	$Pg'_W - Pg'_I$ (3)	$Pv'_W - Pv'_I$ (4)	$C'_W - C'_I$ (5)
−0.15	− 8(1)	− 1.8(6)	− 3.7(7)	+ 2
−0.05	+17(2)	− 1.4(16)	− 0.2(16)	− 1
+0.05	− 7(3)	+ 1.4(9)	− 1.6(9)	+ 3
+0.15	+ 3(4)	+ 2.7(14)	− 0.2(14)	+ 3
+0.25	+ 3(13)	+ 0.4(29)	− 2.2(31)	+ 3
+0.35	0(18)	+ 0.5(33)	− 0.4(36)	+ 1
+0.45	+ 4(9)	− 1.9(25)	+ 0.5(26)	− 2
+0.55	+ 1(5)	− 0.8(13)	− 2.5(13)	+ 2
+0.65	0(4)	− 8.8(6)	− 2.9(8)	− 6
+0.75	+ 8(12)	+ 6.3(18)	+ 0.4(20)	+ 6
+0.85	− 1(5)	+ 1.1(24)	+ 1.2(23)	0
+0.95	− 2(9)	− 2.1(26)	+ 2.7(27)	− 5
+1.05	− 7(9)	− 1.5(22)	− 1.2(22)	0
+1.15	− 4(5)	− 3.6(7)	− 0.2(9)	− 3
+1.25	−13(1)	+ 6.5(6)	− 2.0(6)	+ 8
+1.35	− 9(3)	+ 1.1(8)	− 0.6(8)	+ 2
+1.45	− 7(5)	+ 2.8(10)	+ 3.5(11)	− 1
+1.55	− 7(1)	+ 0.3(7)	+ 2.4(8)	− 2
+1.65	− 4(2)	− 1.8(6)	+ 4.2(5)	− 6
+1.75	.....	− 5.7(3)	+ 2.3(3)	− 8
+1.85	.....	− 7.0(2)	− 2.0(2)	− 5
+2.05	.....	−12 (1)	+30 (1)	−42
All	0.0(111)	0.0(291)	0.0(305)	0

IV. TESTS BASED ON COLOR INDEX

Consider now the color indices

$$C''_W = Pg''_W - Pv'_W , \qquad C'_I = Pg'_I - Pv'_I , \tag{3}$$

where, it will be recalled,

$$\left.\begin{aligned} Pg''_W &= Pg_W + \text{dec. corr.} + \text{local scale corr.} , \\ Pv'_W &= Pv_W + \text{dec. corr.} , \end{aligned}\right\} \tag{4}$$

and where, reduced to the corrected MW system,

$$\left.\begin{aligned} Pg'_I &= Pg_I + \text{right-hand member of eq. (1)} , \\ Pv'_I &= Pv_I + \text{right-hand member of eq. (2)} . \end{aligned}\right\} \tag{5}$$

For each subtype, B9, A0, ... G0, we form mean colors and then the residuals (later types are not used because they include undefined mixtures of giants and dwarfs)

$$v_W = C'_W - \overline{C'_W}, \qquad v_I = \overline{C'_I} - C'_I. \tag{6}$$

If the Cape magnitudes are free from local zero-point errors, as was assumed in deriving the zero-point corrections for Mount Wilson, the residuals v_I should show no systematic change with declination. Even if such errors are present, the mean color for a group of stars will be little affected, since the stars will generally be scattered over a considerable range in declination. C'_I for a single star, however, and v_I to nearly the same degree, will include the difference in the zero-point errors for the corresponding values of Pg'_I and Pv'_I. Further, any such errors will have been carried over by the correction process into v_W.

To test these possibilities, we group the residuals according to declination, form means for each 1° zone, and then overlapping means for successive groups of three zones. These smoothed mean values, Table 2, columns 10 and 11, are definitely systematic, but so small as to be of no significance for the present purpose. The general parallelism of columns 10 and 11 shows that the correction formulae (4) have worked well except for zones −11° to −13°, where there still remains a small irregularity in the values of $v_W - v_I$.

It will be noted that the constancy test does not reach the Pg and Pv zero points directly, for we can deal only with color indices; but since any fluctuations in the zero point of Pg are independent of those in Pv, the zero-point range in C may be expected to exceed the corresponding changes for the magnitudes. The progressive change in v_I with declination shows that the Cape zero points can still be improved, but for the number of plates used the agreement is exceptionally good. The weighted mean v_I, Table 2, column 11, is −0.01 mag. That it is not zero is due to the omission of two discordant stars, Nos. 543 and 698, for which v_I = +0.46 and +0.34 mag., respectively.

For a test of another kind we group the residuals v_W and v_I according to magnitude. The results, in Table 4, sometimes rather ragged because of the small numbers of stars in many of the groups, show for types B9–A5, for both the Cape and Mount Wilson, a small but definite increase in color index with increasing magnitude—about 0.1 mag. for the 4.5-mag. interval. The F0–F5 stars, in the mean, show no certain change, while for F8–G0 there is just a suggestion of a decrease in color with increasing magnitude. We shall return to these results in considering similar data in Table 10. Here we note only that for all types together (Table 4, cols. 11–13) the residual progressive effect in the means is scarcely to be detected. The inference, therefore, is that, aside from any effect of luminosity on color, which for the types concerned is not likely to be important, the Pg and Pv scales for both the Cape and the Mount Wilson magnitudes stand in the proper relation to each other; the respective scales are parallel, and the magnitudes themselves internally consistent. Finally, it follows that, if either of the reduction formulae (1) and (2) is in error, the other must also be in error by an equal amount.

V. EROS STARS—YERKES AND MOUNT WILSON OBSERVATIONS

The next step, a check of the Mount Wilson results against the Yerkes observations of Eros stars, involves a revision of the comparison given in *Mt. W. Contr.* No. 415, Table VII.[5] The magnitude differences in this table are affected by local zero-point (declination) errors in all four series of magnitudes. Moreover, they are regression differences and show the characteristic regression effect. Since we now require the functional relationship of the Yerkes and the Mount Wilson scales, this effect must be removed or, preferably, avoided altogether by grouping the MW-Y differences (after correction for declination error) according to a neutral argument, say the Cape Pg_I and Pv_I magnitudes.

TABLE 4

RESIDUALS IN COLOR INDEX

P_{GI} or P_{GW}	B9–A5			F0–F5			F8–G0			B9–G0		
(1)	Cape (2)	MW (3)	All (4)	Cape (5)	MW (6)	All (7)	Cape (8)	MW (9)	All (10)	Cape (11)	MW (12)	All (13)
5.5–.....	+ 4(3)	−10(4)	− 4(7)	− 2(2)	+ 8(3)	+ 4(5)	+15(1)	+26(1)	+20(2)	+4(6)	+1(8)	+2(14)
6.0–.....	− 4(5)	− 6(6)	− 5(11)	−12(2)	+10(3)	+ 1(5)	.....	.....	.....	−6(7)	0(9)	−3(16)
6.5–.....	0(8)	− 3(7)	− 1(15)	− 4(4)	−19(3)	−10(7)	.....	+ 4(2)	+ 4(2)	−1(12)	−6(12)	−4(24)
7.0–.....	− 2(7)	.....	− 2 (7)	0(4)	0(4)	0(8)	+ 5(3)	− 7(2)	0(5)	0(14)	−2(6)	−1(20)
7.5–.....	− 3(5)	− 5(2)	− 3(7)	− 5(3)	+14(1)	0(4)	+ 1(3)	− 3(1)	0(4)	−3(11)	0(4)	−2(15)
8.0–.....	− 4(7)	+ 5(6)	0(13)	− 1(4)	0(5)	0(9)	− 7(1)	.....	− 7(1)	−3(12)	+3(11)	0(23)
8.5–.....	− 1(3)	+ 1(6)	0(9)	+ 2(6)	0(6)	+ 1(12)	+ 1(5)	0(7)	+ 1(12)	+1(14)	0(19)	+1(33)
9.0–.....	+ 4(9)	+ 5(7)	+ 4(16)	+ 1(13)	− 2(13)	0(26)	− 6(8)	− 5(8)	− 5(16)	0(30)	−1(28)	−1(58)
9.5–.....	+ 6(3)	+ 2(6)	+ 3(9)	0(12)	− 4(9)	− 2(21)	− 4(19)	+ 1(17)	− 2(36)	−2(34)	−1(32)	−1(66)
10.0–.....	+16(1)	+21(2)	+19(3)	+ 3(5)	− 2(13)	0(18)	+ 3(5)	− 2(13)	0(18)	+4(11)	0(28)	+1(39)
⩾10.5....	.....	.....	.....	.....	+16(2)	+16(2)	.....	− 5(5)	− 5(5)	.....	+1(7)	+1(7)
All....	+ 0.1(51)	+ 0.3(46)	+ 0.2(97)	− 0.3(55)	− 0.8(62)	− 0.6(117)	− 2.0(45)	− 1.0(56)	− 1.5(101)	−0.7(151)	−0.6(164)	−0.6(315)

Such a grouping involves no selection of Mount Wilson or Yerkes errors; hence it introduces no systematic error into the group means and thus gives directly the required functional relation.

Since the MW-Y scale differences are certainly small, we find the declination correction at once by grouping the values of $Pg_W - Pg_Y$ and $Pv_W - Pv_Y$ according to declination (Table 2, cols. 2 and 3). The smoothed correction-curves reduce Y to the zero point of MW. Relative declination errors are thus eliminated from the magnitude differences, but the mean zero point for the corrected Y magnitudes is that of MW for the 111 stars of the Y list. This, however, is not quite the same as the MW mean for the entire list (228 Pg_W, 242 Pv_Y; none of the Bright Stars was observed at Yerkes), which is our reference standard. Additional corrections reducing Pg_W to $\overline{Pg'_W}$ and Pv_W to $\overline{Pv'_W}$ are therefore required. These may be applied either to the individual stars or as a single correction to the mean zero points of Pg_W and Pv_W for the restricted list of 111 stars. Since the accidental errors enter differently in the two reductions, both methods are used.

TABLE 5

SCALE COMPARISON: YERKES AND MOUNT WILSON

(Unit, 0.01 Mag.)

Pg_I	$Pg_W - Pg'_Y$	$Pg'_W - Pg'_Y$	δPg_W	$Pg''_W - Pg'_Y$		ϵ	No.	Pv_I	$Pv_W - Pv'_Y$	$Pv'_W - Pv'_Y$	$Pv'_W - Pv'_Y$ (Scale Only)		ϵ	Color Coeff.	No.
(1)	(2)	(3)	(4)	(5)	(6)	(7)	(8)	(9)	(10)	(11)	(12)	(13)	(14)	(15)	(16)
8.20..	+9	+10	−6	+6	+4	±12.3	12	7.27..	0	+3	− 1	+ 1	± 7.4	0.00	6
8.85..	0	+ 6	−3	0	+3	10.3	8	7.89..	−1	−1	− 2	− 3	6.4	.00	7
9.10..	−8	− 6	+3	−2	−3	14.3	5	8.12..	+2	+7	+ 1	+ 5	3.9	.00	6
9.38..	−5	− 4	+4	+2	0	15.2	16	8.38..	0	+2	− 1	0	3.6	.00	7
9.62..	−8	− 3	+4	−1	+1	15.9	14	8.62..	+4	+4	+ 3	+ 2	4.6	.00	12
9.88..	−4	− 1	+2	+1	+1	11.9	21	8.88..	+4	+6	+ 3	+ 4	6.1	.00	13
10.11..	−1	+ 6	−1	+1	+5	10.2	10	9.12..	+5	+7	+ 4	+ 5	7.0	− .04	15
10.34..	−1	− 2	−3	−1	−5	11.3	16	9.38..	+1	+2	0	0	7.0	− .08	20
10.76..	−2	+ 4	−6	−5	−2	±15.9	9	9.62..	0	+1	− 1	− 1	11.1	− .12	11
								9.88..	−9	−9	−10	−11	13.3	− .16	8
								10.19..	0	−2	− 1	− 4	± 8.0	−0.20	6
All...	−2.2*	+ 0.8	−0.3	+0.5	+0.4	±13.0	111	All..	+1.2†	+2.4	+ 0.2	+ 0.4	± 7.2	.....	111

* Reduction to $\overline{Pg'_W}$ for 228 stars, +2.9.

† Reduction to $\overline{Pv'_W}$ for 242 stars, +1.4.

Discordant differences in Table 2 cause minor disagreements. For example, those in column 2, chiefly in zones −2°, −3°, and −13°, account largely for the discrepancy of 0.015 mag. between the actual weighted mean difference and the weighted mean of the corrections given in the last line of the table. Again, in column 3 the means for the 99 stars used are both +0.018 mag.; but had 12 omitted stars been retained, the weighted mean of the actual differences would have been +0.005 mag. The omitted stars, mostly faint and perhaps affected by color equation, are retained, however, for the scale comparison in Table 5.

Writing

$$Pg'_Y = Pg_Y + \text{dec. corr., Table 2, col. 2},$$

$$Pv'_Y = Pv_Y + \text{dec. corr., Table 2, col. 3},$$

we find the mean differences $Pg_W - Pg'_Y$ and $Pv_W - Pv'_Y$ in Table 5, columns 2 and 10. Correcting the individual differences (first method of reduction) with the aid of Table 2, columns 4 and 5, to eliminate the local zero-point errors in Pg_W and in Pv_W, we obtain columns 3 and 11 of Table 5. Columns 2 and 3 are still affected by local scale errors in Pg_W. The corrections, taken from Table 1, column 3, are in column 4 of Table 5. Applied

to column 3, they give the final results in column 6, Table 5. It is worth noting that these corrections here smooth out local irregularities in the differences, as they did in the comparison with the Cape. In correcting column 2 for local scale error, we apply at the same time the mean zero-point correction (second method) that reduces $\overline{Pg_W}$ for the 111 Yerkes stars to $\overline{Pg'_W}$. This quantity, the weighted mean of the values in Table 2, column 4, for the numbers of stars shown in column 2 of the same table, is +0.029 mag. The final result is column 5.

For the Pv differences, column 11, Table 5, is final. To reduce column 10 to comparability with column 11, the correction +0.014 mag. must be applied (from Table 2, cols. 3 and 5, as for Pg). To show the Pv scale relations more clearly, the zero-point differences are removed altogether, giving the values in columns 12 and 13. A comparison of these two columns and also of columns 5 and 6 shows that the final scale differences for the two methods of reduction are practically the same.

All the results in Table 5 have been corrected for color equation. A smoothed curve, based on the differences in Table 3, column 2, has been used for Pg_Y, the same for all magnitudes. For $Pv_I < 9.0$, the Pv_Y color correction is zero. For fainter stars, cC_I has been used, where the coefficient c is given in Table 5, column 15. The last two or three of these coefficients are not well determined, but the number of stars affected is small.

In judging the Mount Wilson–Yerkes scale agreement shown by columns 5 and 6 and columns 12 and 13 of Table 5, the average error for a single difference, columns 7 and 14, and the numbers of stars, columns 8 and 16, must be taken into account. The systematic differences are slight and chiefly in the direction of small negative values for a few of the fainter stars. On the whole, however, the Yerkes results give a good general confirmation of both the Mount Wilson scales. Certainly they present no evidence that would lead us to question the scale factors appearing in the reduction formulae for the Cape magnitudes in equations (1) and (2).[7]

For an easier comparison of the scales the Yerkes results have been reduced to the mean Mount Wilson zero points defined by all the Mount Wilson stars—not merely the 111 stars included in the comparison with Yerkes. The means of the reduced differences should therefore be zero. The actual values from Table 5, columns 5–6 and 10–11, are

$$Pg''_W - Pg'_Y = +0.005\,, \qquad Pv'_W - Pv'_Y = +0.025 \text{ mag}\,.$$

The discrepancy for Pv arises mostly from the 12 rather discordant stars included in Table 5 but omitted from Table 2, column 3.

There still remains an important point, namely, the agreement between the observed mean Yerkes zero points and the mean zero points for all the Mount Wilson stars. Since all four zero points have been fixed by polar comparisons, the numerical relations between them indicate the success attained in transferring the International zero points to the Eros stars.

[7] Stoy and Menzies, pp. 312–313, recalling that Yerkes magnitudes were used in determining the Mount Wilson plate corrections, suggest that the progressive zero-point error in Yerkes might have influenced the Mount Wilson scales. Any direct influence from this source on the magnitudes of Eros stars should have been eliminated by the averaging of results from overlapping plates—and has been, otherwise the field-to-field differences in *Mt. W. Contr.* No. 415, Table III, would not show a proper alternation in sign. There is, therefore, nothing forced in the agreement shown in Table 5.

The effect of an asymmetrical error in the plate corrections—from any source—upon the reduction-curves derived from the polar standards would be serious if the standards of different magnitudes were not more or less uniformly distributed over the plate. Actually, the distribution was such that there can have been no appreciable disturbance from this cause. In fact, there would have been none even if the plate corrections had been disregarded altogether in drawing the reduction-curves. The scatter in the plotted points would have been greater and the individual curves less certain, but the mean scales would not have been appreciably changed.

From Table 2, columns 2 and 3, we have

$$\text{Mean } Pg_W - Pg_Y = -0.028 \text{ (111 stars)},$$
$$\text{Mean } Pv_W - Pv_Y = +0.018 \text{ (99 stars)}.$$

For all 111 stars the second value becomes +0.005 mag. The reductions to the reference points defined by all the Mount Wilson stars (the standards for the discussion), as already explained, are +0.029 and +0.014 mag., respectively. Hence, corrected for local zero-point errors, we have

$$\left.\begin{array}{l}\text{Observed zero-point difference, MW} - \text{Y}: \\ \text{Pg, } +0.001; \text{ Pv, } +0.032 \text{ (99 stars) or } +0.019 \text{ (111 stars)}.\end{array}\right\} \quad (7)$$

The uncertainty in these quantities is obviously rather large; but at least they present no contradiction, and to this extent the evidence favoring equations (1) and (2) is strengthened.

TABLE 6

SPECTRUM-COLOR RELATION: EROS STARS

(Unit, 0.01 Mag.)

HD	C_S	$C_S - C_W$	$C_S - C'_W$			AD		$C_S - C'_I$			AD
			Bright	Comp.	All	C_W	C'_W	Bright	Comp.	All	C'_I
(1)	(2)	(3)	(4)	(5)	(6)	(7)		(8)	(9)	(10)	(11)
B5	−39	− 5(1)	+ 5(1)	.....	+ 5(1)	.....	.....	−9(1)	.....	− 9(1)	.....
B8	−29	− 3(2)	− 1(1)	+20(1)	+ 9(2)	±20	±10.5	.....	−10(1)	−10(1)	.....
B9	−23	− 6(5)*	+ 5(4)	−18(1)	0(5)	20	15.6	+6(5)	+15(1)	+ 8(6)	±5.3
A0	−15	− 1(21)	+17(10)	− 8(11)	+ 3(21)	21‡	18.9‡	+6(13)	+ 7(7)	+ 7(20)	7.6
A2	− 5	+ 3(13)	+15(6)	− 2(7)	+ 5(13)	17	13.7	+5(7)	− 7(7)	− 1(14)	9.3
A3	− 2	+ 1(3)	0(1)	− 6(2)	− 4(3)	6	3	−8(1)	− 9(2)	− 9(3)	5.7
A5	0	+ 2(9)	.....	− 2(9)	− 2(9)	7	6.7	−1(1)	− 6(7)	− 6(8)	5.8
A7	+ 5	+23(1)	.....	+23(1)	+23(1)	.....	.....	.....	+19(1)	+19(1)	.....
F0	+12	+ 2(26)	0(9)	+ 1(17)	+ 1(26)	16	14.7	+3(8)	− 6(15)	− 3(23)	7.8
F2	+16	+ 5(13)	− 7(4)	+ 8(9)	+ 4(13)	17§	14.5§	+ 2(5)	− 5(5)	− 2(10)	3.4
F5	+26	− 3(27)	−23(2)	− 1(25)	− 3(27)	14.5	10.4	−5(2)	+ 5(20)	+ 3(22)	5.6
F8	+35	+ 9(34)†	+ 6(4)	+ 7(30)	+ 7(34)	11.5‖	10.9‖	+4(5)	+ 6(22)	+ 5(27)	8.7
G0	+42	+ 5(27)	+ 1(2)	+ 6(25)	+ 6(27)	±15**	±15.4**	0(3)	+ 7(17)	+ 6(20)	±8.2
All	.....	+ 2.7	+ 5.4	+ 2.3	+ 3.0	.....	.....	+3.3	+ 1.9	+ 2.1	.....
M.E.	.....	.....	± 2.1	± 1.2	± 1.0	.....	±13.6	±1.0	± 0.7	± 0.6	±6.1

* The value of C_W for B9 in *Mt. W. Contr.* No. 415 should have been −0.17, not −0.19.

† One star was accidentally omitted from *Mt. W. Contr.* No. 415. C_W is not changed.

‡ Omission of 4 discordant stars would reduce the deviations to ± 16 and ± 13.5 without changing C'_W.

§ Omission of 2 discordant stars would reduce the deviations to ± 10 and ± 6.8 without changing C'_W.

‖ Omission of 2 discordant stars would reduce the deviations to ± 9 and ± 7.7 without changing C'_W.

** The large AD is due to 2 low-weight observations. Their omission would reduce C'_W from 0.36 to 0.32 mag. and the deviations to about ± 13 and ± 12.

VI. CONSISTENCY OF Pg AND Pv ZERO POINTS TESTED BY THE SPECTRUM-COLOR RELATION

Having checked the Mount Wilson Pg and Pv zero points against the Yerkes results, we now check them against each other with the aid of the spectrum-color relation. A similar test will also be applied to the reduced Cape magnitudes. Since the minimum galactic latitude for the Eros stars is about 25°, complications from space absorption are scarcely to be feared. The spectrum-color relation should therefore be normal, and hence comparable with the standard relation obtained from polar stars by freeing their colors from color excess.

In Table 6 the normal colors C_S for HD subtypes taken from *Mt. W. Contr.* No. 684,

Table 7,[8] are in column 2. Column 3 gives the differences $C_S - C_W$ for the original, uncorrected mean values of C_W as printed in *Mt. W. Contr.* No. 415, Table XI,[5] while columns 4–6 are based on the means of the corrected Mount Wilson colors for the Bright Stars, for the Comparison Stars proper, and for both together. Similar differences for the Cape colors, corrected for scale by formulae (1) and (2) and for color equation by Table 3, column 5, are in columns 8–10. Finally, columns 7 and 11 give the average deviations of C_W, C'_W, and C'_I from their respective means for each subtype.

The slight run in the differences in Table 6, column 3, has mostly been removed by the revision of the Mount Wilson data (Fig. 1, plot 1). The results for the Cape in column 10 show, however (disregarding differences depending on a single star), an irregularity (Fig. 1, plot 2) which, in view of the precision of the Cape measures, should be real; it is, in fact, confirmed by other data (Table 9, and Fig. 1, plots 3 and 4) and represents a residual color equation, presumably arising from hydrogen absorption. This irregularity,

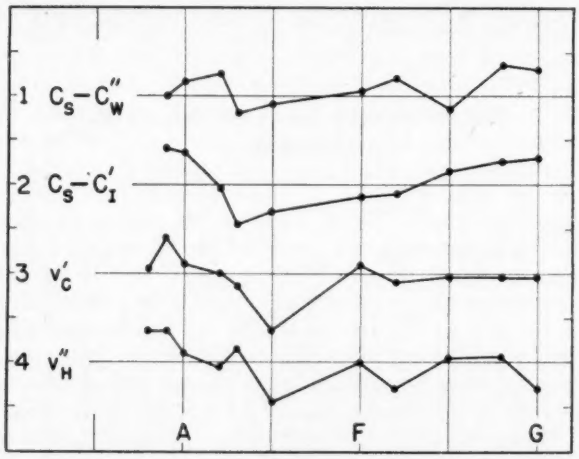

FIG. 1.—Deviations from International color index. Plots 1 and 2, Eros stars; 3 and 4, Harvard Standard Regions. Instruments: 1, Mount Wilson Cooke triplet; 2 and 3, the Cape cameras; 4, various telescopes used for the Harvard standards. Plots 2–4 reveal residual color equations affecting early A stars. Vertical scale: distance between plots = 0.2 mag.

a "fine structure" effect, escapes the corrections taken from the last column of Table 3 because they have been obtained by grouping the magnitude differences according to color; it is revealed only when the grouping argument is spectral type.

On the whole, though, color differences between Mount Wilson and the Cape have been well eliminated. Table 1, columns 6 and 10, shows that for all types together the mean colors should agree within 0.01 mag. For types B5–G0 (about one-half the material) we have from Table 6, columns 6 and 10, a similar degree of accordance. Hence, for the late-type stars there can be no great disparity in color.

The weighted means of the differences $C_S - C_W$, etc., in the next to the last line of Table 6 are the zero-point corrections required to reduce the several spectrum-color relations to the normal relation defined by C_S. The results for the Bright and the Comparison Stars, for both Mount Wilson and the Cape (cols. 4–5 and 8–9) agree within their respective mean errors. Nevertheless, the similarity in algebraic sign for Bright *minus* Comparison Stars suggests a real differential effect of 0.01 or 0.02 mag. The agreement here is a fairly satisfactory check on the Mount Wilson Pg zero point for the Bright Stars relative to that for Pv, which is not controlled by the comparison with Yerkes.

[8] *Ap. J.*, **98**, 261, 1943.

A similar result may be obtained from the last two columns of Table III of *Mt. W. Contr.* No. 415,[5] which are, in effect, comparisons of bright and faint stars.

The result for the revised Mount Wilson data as a whole, +0.03 mag. (col. 6), is the same as for the uncorrected observations (col. 3). For the reduced Cape colors (col. 10) the correction is +0.02 mag.

We adopt the Mount Wilson value

$$\overline{C_S - C''_W} = +0.03 \pm 0.010 \text{ (m.e.)}, \tag{8}$$

rather than that from the Cape data, which may still be slightly affected by the residual color equation. This discrepancy may originate either in the spectral types—a systematic difference of one classification unit between polar and Eros stars would account for it—or in the magnitudes. Provisionally we suppose the types to be correct, and because of the higher weight of the Pv observations, distribute the difference between the Pg and Pv magnitudes as follows:

$$\text{IPg} = \text{Pg}''_W + 0.02\,, \qquad \text{IPv} = \text{Pv}'_W - 0.01\,. \tag{9}$$

Then, from equations (1) and (2) we obtain for the reduction of the Cape Pg_I and Pv_I magnitudes to the International system,

$$\left.\begin{aligned} \text{IPg} - \text{Pg}_I &= -0.15 + 0.11\,(\text{Pg}_I - 8.2) \quad (= -0.15 \text{ for } \text{Pg}_I < 8.2)\,, \\ \text{IPv} - \text{Pv}_I &= \quad\; + 0.11\,(\text{Pv}_I - 8.4) \quad (= 0 \quad\;\; \text{for } \text{Pv}_I < 8.4)\,. \end{aligned}\right\} \tag{10}$$

These small adjustments are chiefly a matter of internal consistency; the changes are of the same order as the uncertainty affecting them.

The zero-point correction to the spectrum-color relation is closely related to the much-discussed value of C for A0 stars in unobscured regions. Stoy and Menzies are right in attributing a considerable accidental element to the agreement within 0.01 mag. indicated by the difference for A0 in Table 6, column 3. The re-reduction of Mount Wilson has, in fact, changed this difference by 0.04 mag., just about the probable error of the original value. The significant detail, however, is the zero-point difference between the two spectrum-color relations expressed by equation (8). The corresponding value for A0 indicated by all the Mount Wilson observations of Eros stars of types G0 and earlier —not merely those of type A0—is

$$C''_W = C_S - 0.03 = -0.18 \pm 0.010\,.$$

For the present it seems best to attribute the discrepancy of 0.03 mag. to zero-point errors in the magnitudes of the Eros stars as indicated by formulae (9).

In this connection it may be added that F. E. Carr's[9] color index for A0 stars from the Eros plates mentioned in Stoy II, page 315, cannot be interpreted without further knowledge of the zero-point errors of the Eros plates used by him. The stars are in declinations +42° to +49°, far from the fields used here. If the zero points are correct, as in the mean they may well be, then Carr's value $C = -0.05$ mag. for A0 would indicate a mean color excess of +0.1 mag.—a not unreasonable result, since the galactic latitudes of the stars are all less than about 15°. The majority of the Eros stars, however, are in higher latitudes; and Carr's result, therefore, is not necessarily inconsistent with the value found here.

VII. ERRORS

To compute the mean errors in the last line of Table 6, the accidental errors of spectral classification, which are included in the residuals of the color indices (cols. 7 and 11), were removed with the aid of Tables 14 and 14*a* of *Mt. W. Contr.* No. 684[8] (see, however,

[9] *Ap. J.*, **76**, 70, 1932.

the discussion based on Table 15 of the same *Contribution*). In addition, allowance was made for the dispersion in color for stars of the same type, about ± 0.035 mag. (*Mt. W. Contr.* No. 684, eq. [25]). The resulting mean errors for catalogue values of C'_W and C'_I are ± 0.136 and ± 0.061 mag., respectively.

If we suppose the errors for Yerkes and Mount Wilson to be the same, then columns 7 and 14 of Table 5 give for Pg'_W and Pv'_W mean errors of ± 0.115 and ± 0.064 mag., respectively, or ± 0.132 mag. for C'_W, which agrees with the value from Table 6.

Further, with Stoy and Menzies' (p. 308) probable errors for single Pg and Pv observations, namely, ± 0.069 and ± 0.043 mag., and with 4.7 and 3.2 as the respective average numbers of observations, we find ± 0.059 mag. for the average mean error of a catalogue C_I. For all but the Bright Stars, however, the error in C'_I is necessarily a little larger. Since C'_I differs from the International color C only by accidental errors, equations (10) give

$$C'_I = \text{const.} + 1.11\, C_I ,$$

whence

$$C'_I - \overline{C'_I} = 1.11\,(C_I - \overline{C_I}) \qquad (Pg_I > 8.3, \text{approx.}) .$$

For the Bright Stars, however, the scale factors in equations (10) are generally zero, and the coefficient in the foregoing equation is unity.

In Table 6 we are concerned with a mixture of one-third Bright Stars and two-thirds Comparison Stars. Altogether, we should expect an increase of about 7 per cent; actually, we find 11 per cent, the excess being due apparently to the systematic differences between the colors of Bright and Comparison Stars of the same type (Table 6, cols. 8 and 9). The mean error ± 0.059 mag. computed from the Stoy-Menzies data thus becomes ± 0.065 mag. The agreement with that in Table 6, column 11, is well within the uncertainty of the comparison. The agreement is also of interest because it indicates that in computing catalogue errors the division of the listed numbers of Cape observations by 2 or 3, as Stoy and Menzies have suggested, is unnecessary. On the other hand, it appears that the errors for Mount Wilson given in *Mt. W. Contr.* No. 415,[5] are, in part at least, internal errors. To reproduce the mean error of Table 6, column 7, the tabular numbers of observations must be divided by 2.

The values of AD in Table 6, column 7, show that the corrections applied to C_W have generally decreased the accidental errors, but not by any large amount. This is entirely reasonable. The local scale corrections are small, and only one-fourth of the stars are affected by zero-point errors greater than 0.1 mag. (see Table 2).

VIII. REDUCTION FORMULAE FOR CAPE BASIC MAGNITUDES AND THE HARVARD STANDARDS

As already noted in Section II, we use as Cape basic magnitudes Stoy's Pg′, Pv′ values (Pg_C, Pv_C in the present notation) for stars in the Harvard Standard Regions at $-45°$ declination (E zone). The basic magnitudes were transferred to the Eros fields by Stoy and Menzies and transformed into the Pg_I, Pv_I system by the provisional reduction formulae

$$\left.\begin{aligned} Pg_I &= Pg_C - 0.11\, Pv_C + 0.88 \\ Pv_I &= Pv_C + 0.14\, C_C , \qquad C_C = Pg_C - Pv_C . \end{aligned}\right\} \tag{11}$$

Further, Stoy himself has compared Pg_C and Pv_C for the Standard Regions with the corresponding Harvard magnitudes Pg_H and Pv_H, for which he uses the notation Pg(H) and Pv(H). From Stoy I, Tables IX and XIII and Tables XVI and XX, respectively, we obtain the relations

$$\left.\begin{aligned} Pg_H &= Pg_C + 0.01\ (Pg_C - 8.8) + 0.06\ (C_C - 0.5) - 0.020 , \\ Pv_H &= Pv_C + 0.045\,(Pv_C - 8.2) + 0.18\ (C_C - 0.5) + 0.028 , \end{aligned}\right\} \tag{12}$$

where the constant terms are the means of Stoy's zero-point differences for all the E1 . . . . E9 Regions.[10]

For the reduction of Pg_I and Pv_I to the International system, we have obtained equations (10). For the further discussion equations (10) to (12) may be written

$$\left.\begin{aligned} IPg &= Pg_I + 0.110\,(Pg_I - 8.0) - 0.172 \quad (= Pg_I - 0.150 \text{ for } Pg_I < 8.2)\,, \\ IPv &= Pv_I + 0.110\,(Pv_I - 8.0) - 0.044 \quad (= Pv_I \text{ for } Pv_I < 8.4)\,. \end{aligned}\right\} \tag{13}$$

$$\left.\begin{aligned} Pg_I &= Pg_C - 0.110\,(Pg_C - 8.0) + 0.110C_C\,, \\ Pv_I &= Pv_C \qquad\qquad\qquad\quad + 0.140C_C\,. \end{aligned}\right\} \tag{14}$$

$$\left.\begin{aligned} Pg_H &= Pg_C + 0.010\,(Pg_C - 8.0) + 0.060C_C - 0.058\,, \\ Pv_H &= Pv_C + 0.045\,(Pv_C - 8.0) + 0.180C_C - 0.071\,. \end{aligned}\right\} \tag{15}$$

The substitution of equations (14) into (13) gives

$$\left.\begin{aligned} IPg &= Pg_C - 0.110\,(Pg_C - 8.0) + 0.110C_C - 0.150 \quad (Pg_C < 8.22 - 0.12C_C) \\ &= Pg_C - 0.012\,(Pg_C - 8.0) + 0.122C_C - 0.172 \quad (Pg_C \geqslant 8.22 - 0.12C_C)\,. \end{aligned}\right\} \tag{16}$$

$$\left.\begin{aligned} IPv &= Pv_C \qquad\qquad\qquad + 0.140C_C \qquad\quad (Pv_C < 8.40 - 0.14C_C) \\ &= Pv_C + 0.110\,(Pv_C - 8.0) + 0.155C_C - 0.044 \quad (Pv_C \geqslant 8.40 - 0.14C_C)\,. \end{aligned}\right\} \tag{17}$$

Noting that $C = IPg - IPv$ and $Pv_C = Pg_C - C_C$, we obtain for the color indices

$$\left.\begin{aligned} C &= C_C - 0.110\,(Pg_C - 8.0) - 0.030C_C - 0.150 \quad (Pg_C < 8.22 - 0.12C_C) \\ &= C_C - 0.122\,(Pg_C - 8.0) + 0.077C_C - 0.128 \quad (Pg_C \geqslant 8.40 + 0.86C_C)\,. \end{aligned}\right\} \tag{18}$$

For values of Pg_C lying between the limits of equations (18), C may be found by combining the second of equations (16) with the first of (17).

Formulae (16)-(18) represent, provisionally at least, the reduction of the Cape Pg_C and Pv_C magnitudes to the International system. At the moment, strictly speaking, they define the reduction only for the Pg_C and Pv_C magnitudes of the Eros stars. We assume, however, that formulae (16)-(18) also apply to the basic magnitudes in the Harvard Standard Regions—in other words, that there has been no disturbance of scales and zero points in transferring the basic system to the Eros fields. The validity of this assumption will be tested in the following section.

Formulae (15), on the other hand, apply specifically to the Standard E Regions; Pg_C and Pv_C here represent the actual basic magnitudes. But since we have just assumed the systematic identity of these magnitudes with the corresponding values for the Eros stars, we may combine equations (15) with (16) and (17). Subtracting the former from the latter, we obtain, in succession,

$$\left.\begin{aligned} IPg &= Pg_H - 0.120\,(Pg_C - 8.0) + 0.050C_C - 0.092 \quad (Pg_C < 8.22 - 0.12C_C) \\ &= Pg_H - 0.022\,(Pg_C - 8.0) + 0.062C_C - 0.114 \quad (Pg_C \geqslant 8.22 - 0.12C_C)\,, \end{aligned}\right\} \tag{19}$$

$$\left.\begin{aligned} IPv &= Pv_H - 0.045\,(Pv_C - 8.0) - 0.040C_C + 0.071 \quad (Pv_C < 8.40 - 0.14C_C) \\ &= Pv_H + 0.065\,(Pv_C - 8.0) - 0.025C_C + 0.027 \quad (Pv_C \geqslant 8.40 - 0.14C_C)\,. \end{aligned}\right\} \tag{20}$$

[10] Reprinted here in Table 7, cols. 2 and 3. Note that the Pg difference for E5 in Stoy I, Table XIII should be −0.29, not +0.29.

Then, in analogy with equations (18),

$$\left.\begin{aligned} C &= C_H - 0.075\,(Pg_C - 8.0) + 0.045C_C - 0.163 \quad (Pg_C < 8.22 - 0.12C_C) \\ &= C_H - 0.087\,(Pg_C - 8.0) + 0.152C_C - 0.141 \quad (Pg_C \geqslant 8.40 + 0.86C_C)\,. \end{aligned}\right\} \quad (21)$$

Further substitutions based on formulae (15) give

$$\left.\begin{aligned} IPg &= Pg_H - 0.117\,(Pg_H - 8.0) + 0.062C_H - 0.100 \quad (Pg_H < 8.16 - 0.07C_H) \\ &= Pg_H - 0.019\,(Pg_H - 8.0) + 0.068C_H - 0.116 \quad (Pg_H \geqslant 8.16 - 0.07C_H)\,. \end{aligned}\right\} \quad (22)$$

$$\left.\begin{aligned} IPv &= Pv_H - 0.044\,(Pv_H - 8.0) - 0.036C_H + 0.068 \quad (Pv_H < 8.35 + 0.04C_H) \\ &= Pv_H + 0.061\,(Pv_H - 8.0) - 0.040C_H + 0.032 \quad (Pv_H \geqslant 8.35 + 0.04C_H)\,. \end{aligned}\right\} \quad (23)$$

$$\left.\begin{aligned} C &= C_H - 0.072\,(Pg_H - 8.0) + 0.054C_H - 0.168 \quad (Pg_H < 8.16 - 0.07C_H) \\ &= C_H - 0.080\,(Pg_H - 8.0) + 0.170C_H - 0.148 \quad (Pg_H \geqslant 8.35 + 1.04C_H)\,. \end{aligned}\right\} \quad (24)$$

Equations (19)–(21) and (22)–(24) are alternative formulae for reducing the Harvard magnitudes in the Standard E Regions to the International system. The first group, involving Cape data, answers our present requirements; the second, in the conventional form, is added for completeness. Since only second-order changes are involved in passing from one group to the other, the coefficients and constants are nearly the same.

The third decimal occurring in the formulae of this section is not to be taken as an indication of reliability. It is retained only to secure computational accuracy in the second decimal of the reduced magnitudes and colors.

IX. TESTS OF THE CAPE BASIC MAGNITUDES AND THE HARVARD STANDARDS

Since transfers of scale and zero point from the Harvard Standard Regions to the Eros fields underlie the last three groups of equations, it is important to check the consistency of the reduced magnitudes obtained with these formulae. To this end we use the reduced colors C'_C and C'_H given by equations (18) and (21) and the spectrum-color relation, much as in the discussion of the Eros stars.

TABLE 7

SPECTRUM-COLOR RELATION: HARVARD STANDARD REGIONS

(Unit, 0.01 Mag.)

HSR	$Pg_H - Pg_C$	$Pv_H - Pv_C$	$C_C - C_H$	$C_S - C'_C$		$C_S - C'_H$		No. of Stars	$C'_C - C'_H$		(10) − (11)	Color Excess	Galactic Long. Lat.
				Mean	*AD*	Mean	*AD*		(7) − (5)	(4) − (5)			
(1)	(2)	(3)	(4)	(5)	(6)	(7)	(8)	(9)	(10)	(11)	(12)	(13)	(14)
E1....	+ 6	+ 4	− 2	0	±10.5	+ 1	±16.6	8	+ 1	− 7	+ 8	+ 2	248° −71°
E2....	−13	+ 6	+19	− 1	6.9	+ 6	8.6	12	+ 7	+14	− 7	+ 1	158 −35
E3....	+13	− 5	−18	+ 6	5.4	−12	12.4	8	−18	−23	+ 5	+ 1	221 −19
E4....	+21	+15	− 6	+ 8	6.0	− 4	14.4	12	−12	−11	− 1	− 3	237 + 4
E5....	−29†	−17	+12	− 1	6.4	+ 4	16.3	11‡	+ 5	+ 7	− 2	+ 2	263 +16
E6....	− 5	+ 2	+ 7	− 7	7.8	−10	12.8	17	− 3	+ 2	− 5	+10	291 +12
E7....	−12	− 5	+ 7	−11	8.4	−20	11.4	12	− 9	+ 2	−11	+15	312 − 7
E8....	+ 7	+11	+ 4	+ 3	5.4	+ 2	12.1	11‡	− 1	− 1	0	− 1	322 −33
E9....	− 6	+14	+20	+ 1	± 6.4	+13	± 8.5	12	+12	+15	− 3	− 2	316 −61
All..	− 2.0	+ 2.8	+ 4.8	− 0.2	± 7.0	− 2.2	±12.4	103	− 2.0	− 0.2	± 4.7	+ 2.8	.....
e^*..	±12.9	± 8.5	.....	± 4.5	.....	± 8.7	.....	.....	± 8.0	± 9.7	.....	.....	.....

* For one Standard Region.

† The algebraic sign in Stoy I, Table XIII, is reversed.

‡ Ten stars for Harvard.

For each star we form the differences $C_S - C'_C$ and $C_S - C'_H$, where C_S is the normal color (Table 6, col. 2) corresponding to the HD type of the star. Since the late-type giants and dwarfs are not segregated, only types G0 and earlier can be used, as before. The respective means of these differences for each E Region are in Table 7, columns 5 and 7. Relative to these means, we form the residuals

$$v_C = C_S - C'_C - \overline{C_S - C'_C}, \qquad v_H = C_S - C'_H - \overline{C_S - C'_H}. \tag{25}$$

The values of v_C and v_H, usually in the order of Pg_C, are in Table 8. Means of these residuals, grouped according to type, are in Table 9, and according to magnitude, in Table

TABLE 8

RESIDUALS IN $C_S - C'_C$ AND IN $C_S - C'_H$

(Unit, 0.01 Mag.)

HSR	Star	Pg_C	HD	v_C	v_H	HSR	Star	Pg_C	HD	v_C	v_H	HSR	Star	Pg_C	HD	v_C	v_H
E1...	A	7.32	F0	−14	−28	E4...	B	7.47	A0	− 3	−37	E7...	A	6.93	F0	− 2	+26
	B	7.70	B9	+ 7	+24		C	7.98	A0	− 1	+ 1		C	7.47	B8	+ 8	+21
	E	7.74	F0	− 6	−15		F	8.13	A2	− 3	− 9		D	7.84	B8	+ 7	+15
	F	8.20	F2	− 2	− 6		G	8.19	A2	+ 8	+17		H	8.31	A3	+16	− 7
	G	8.81	F5	− 7	+23		H	8.76	A2	− 6	−16		I	8.64	B8	−14	− 8
	I	8.54	F2	+ 6	−18		I	9.44	A3	− 8	−12		L	9.11	B8	+ 3	−14
	K	9.04	F2	−14	+ 5		K	9.49	A0	− 1	+28		M	8.94	A0	−13	−25
	M	9.67	A2	+28	+14		L	9.70	A0	+ 4	+29		O	9.37	A0	+ 9	− 8
							M	9.79	A2	− 7	− 5		P	9.55	A0	+ 5	+ 6
E2...	A	7.26	G0	+ 2	− 3		P	9.93	A0	− 9	− 7		Q	9.58	A0	−11	− 7
	B	7.74	A5	+10	− 2		Q	10.26	A3	+ 9	+ 8		R	9.72	A5	− 7	0
	C	7.75	A0	−15	−28		R	10.48	G0	+13	+ 4		S	10.23	B8	− 6	0
	F	8.26	A2	+13	+ 8												
	G	8.64	F8	+ 6	+18	E5...	A	7.25	A0	+ 3	−10	E8...	A	8.07	A3	− 6	+10
	I	8.67	G0	+ 4	+ 2		B	7.21	F8	−14	(−54)		B	7.88	A0	+10	+26
	K	8.86	B9	−11	0		D	7.77	B9	+16	+11		D	7.91	F0	+ 3	+ 9
	L	8.90	F8	− 6	+15		E	7.98	A0	+11	− 2		F	8.10	A5	− 2	0
	M	8.86	G0	+ 3	+ 4		F	8.08	G0	+ 4	−25		G	8.52	F5	− 9	+13
	N	9.16	G0	−21	− 7		G	8.31	F8	+ 1	−40		H	8.57	A2	−12	−21
	O	9.43	G0	+12	(+52)		H	8.71	A2	− 1	− 6		I	8.75	A0	− 2	− 7
	R	9.83	G0	(−38)	− 9		I	9.02	F0	− 4	+12		K	8.85	F5	0	− 6
	S	9.95	G0	0	+ 7		K	9.15	A3	− 3	+23		P	9.72	F5	+ 4	−10
							N	10.16	A0	− 9	+23		Q	9.92	F5	+ 3	−19
E3...	A	7.56	A3	− 4	+13		O	10.32	A2	− 4	+11		T	10.63:	F8	+ 8	(−51)
	C	7.52	A0	+ 5	− 1												
	D	7.64	A0	+ 5	+ 1	E6...	A	6.43	F8	− 2	− 5	E9...	A	7.35	A0	− 9	− 4
	E	7.96	B9	0	− 7		C	6.83	B9	− 7	−29		B	7.25	F8	− 1	+ 6
	F	8.19	B9	− 3	+14		D	7.26	A0	+15	+22		D	7.81	G0	− 8	− 2
	G	8.35	A0	−13	+22		F	7.71	G0	+ 4	+12		E	8.01	F0	− 7	+ 4
	H	8.96	A3	+ 1	−22		G	8.01	B9	+ 5	−13:		F	8.09	A0	+ 6	−22
	I	9.25	F0	+12	−19		H	8.55	A0	+16	−13		G	8.61	F2	+ 1	+ 9
							I	8.63	F5	−14	−19		H	8.58	F5	+12	+13
							K	8.62	F8	+ 5	− 4		I	9.16	G0	− 6	− 7
							L	9.17	G0	−11	+ 6		K	9.21	F0	+16	+11
							M	9.27	A0	+10	+12		L	9.29	A5	− 3	− 1
							N	9.28	A0	− 3	−14		M	9.62	F2	+ 5	+ 9
							O	9.65	A2	+ 8	+ 7		N	9.59	A2	− 3	−14
							P	9.75	A2	−11	+ 6						
							R	10.08	A2	−11	− 4						
							S	10.23	B5	− 4	+16						
							T	10.25	A0	+ 3	+24						
							U	10.43	F2	+ 3	−12						

10. By using residuals, instead of the differences themselves, the relative zero-point errors for the different regions are eliminated from the discussion.

Actually, most of the tabulated results represent a second approximation. The original residuals, grouped according to type (v'_C, v'_H, Table 9, cols. 2 and 3), were found to be systematic. Figure 1, plots 3 and 4, illustrates the irregularity and shows its close similarity to that already described for the Cape colors of Eros stars (plot 2). Plots 2 and 3 relate to results obtained with the Cape telescopes; plot 4, to the Harvard instrument. Plot 1, on the other hand, for $C_S - C''_W$ from Table 6, column 6, refers to the Mount Wilson Cooke triplet. The larger accidental errors are here a complication, but obviously

the deviations differ from those of the other plots. For the Cape and Harvard we therefore have residual color equations, supplementary to those expressed by the linear terms in equations (18) and (21). Their removal leads to the residuals in Table 9, columns 4 and 5, and to all those given in Tables 7, 8, and 10. Portions of Tables 4 and 6 should also have been revised; but these tables were finished before the reality of the correction was

TABLE 9

RESIDUAL COLOR EQUATION

(Unit, 0.01 Mag.)

HD (1)	v_C' (2)	v_H' (3)	v_C (4)	v_H (5)	No. (6)
B5	−13	+9	−4	+16	1
B8	+ 1	+7	0	+ 3	5
B9	+ 8	+7	+1	0	7
A0	+ 2	+2	0	0	25
A2	0	−1	0	− 1	13
A3	− 3	+3	+1	+ 2	7
A5	−13	−9	0	− 1	4
F0	+ 2	0	0	0	8
F2	− 2	−6	0	− 2	6
F5	− 1	+1	−2	− 1	7
F8	− 1	+1	0	− 2	8*
G0	− 1	−6	0	− 1	12

* Six stars for Harvard.

TABLE 10

RESIDUALS IN COLOR INDEX

(Unit, 0.01 Mag.)

P_{GC} (1)	$-v_C$ (CAPE)				$-v_H$ (HARVARD)		
	B5–A5 (2)	F0–F5 (3)	F8–G0 (4)	B5–G0 (5)	B5–A5 (6)	F0–G0 (7)	B5–G0 (8)
7.17	−1(6)	+8(2)	+4(4)	+2(12)	+ 6(6)	+ 1(5)	+4(11)
7.75	−4(12)	+2(2)	+2(2)	−3(16)	− 4(12)	− 1(4)	−3(16)
8.25	−2(10)	+1(2)	−2(2)	−1(14)	− 2(10)	+ 17(4)	+3(14)
8.75	+5(9)	+2(7)	−2(5)	+2(21)	+13(9)	− 4(12)	+3(21)
9.25	0(8)	−2(4)	+6(4)	+1(16)	− 2(8)	0(7)	−1(15)
9.75	0(10)	−4(3)	0(1)	−1(14)	− 3(10)	+ 4(5)	0(15)
10.31	+3(7)	−3(1)	0(2)	0(10)	−11(7)	+ 4(2)	−8(9)
All	−0.3(62)	+0.7(21)	+0.3(20)	0.0(103)	− 0.5(62)	+ 1.2(39)	+0.1(101)

established and have been allowed to stand, since the general conclusions are not affected.

Consider now the implications of these results. First, in Table 7, each mean difference in columns 5 and 7 includes the zero-point correction to the spectrum-color relation for the region in question, as defined by the reduced Cape and Harvard magnitudes, respectively. Further, since half the regions are in low galactic latitudes (Table 7, col. 14) and since E7 in particular is within about 16° of the direction of the galactic center, some in-

fluence of space absorption is to be expected. Each mean difference thus becomes a combination of zero-point correction, z, and color excess, E, of the form

$$\overline{C_S - C'_C} = z_C - E, \qquad \overline{C_S - C'_H} = z_H - E. \tag{26}$$

For all regions together,

$$z_C - E = -0.002 \pm 0.015, \qquad z_H - E = -0.022 \pm 0.029, \tag{27}$$

where the appended quantities are average errors based on the fluctuations from field to field. Similarly, from the high-latitude regions E1, 2, and E8, 9, for which the color excess should be insensible,

$$z_C = +0.008 \pm 0.022, \qquad z_H = +0.055 \pm 0.044. \tag{28}$$

Only the last of the four quantities in equations (27) and (28) exceeds the uncertainty affecting it. The various average errors, however, should be larger than those properly belonging to z_C and z_H, because they include not only the dispersion arising from the z's but also that from the color excess and the classification errors. The differences between columns 5 and 7 of Table 7, which appear in column 10, are values of $z_H - z_C$ free from color excess and classification errors, which have been eliminated in forming the differences.

Theoretically, the zero-point corrections can be separated by combining the data in columns 5, 7, and 10; but if, instead of column 10, we use column 11, which is merely another series of values for $C'_C - C'_H$ based on the differences $C_C - C_H$ in column 4, derived, in turn, from Stoy's zero-point differences[11] in columns 2 and 3, we obtain a quite different result. The difficulty, of course, is that the regions are too few in number to admit of statistical combinations of this kind. We can therefore only let the errors of relations (27) and (28) stand as a rough indication of the uncertainty in z_C and z_H.

Equations (28) give a relative zero-point error in the Cape and the Harvard colors of $z_C - z_H = -0.047$ mag. A much more reliable value from relations (27), based on all the regions, is +0.020 mag. Hence we infer that at least one of the values (28) is considerably in error. To improve the result we may obtain an average value of E for substitution into equations (27), as follows: We form the means of columns 5 and 7 of Table 7, with weights of 3 and 1, respectively. At the same time, we adjust the zero point to give a zero mean difference for the four high-latitude regions. The results are the values of the color excess in Table 7, column 13, with $E = 0$, in the mean, for regions E1, 2 and E8, 9.

The values +0.10 and +0.15 mag., respectively, for E6 and E7 are probably significant. That nothing shows for E4 and E5, where, on the basis of latitude, an appreciable color excess might also be expected, may be only a result of zero-point error. For all 9 regions the average E is +0.028 mag., whence, from equations (27),

$$z_C = +0.026, \qquad z_H = +0.006, \tag{29}$$

with uncertainties of, say, 0.02 and 0.03 mag., respectively. The relative error $z_C - z_H = +0.02$ mag., of course, remains unchanged.

Thus far we have two important conclusions: first, for types B5–G0 the color terms of the reduction formulae require only minor supplementary corrections (Table 9); second, the mean zero-point corrections to the spectrum-color relations indicated by the values (29) do not exceed their respective uncertainties. More specifically, this means that the average relative error in the zero points of the Pg and Pv scales in the nine Standard E Regions, for both Cape and Harvard, probably does not exceed 0.02 or 0.03 mag. For individual fields the relative error, of course, may be larger, especially for Harvard.

[11] Stoy I, Tables XIII and XX.

Several other conclusions also follow from Tables 7–10. First, the residuals v_C and v_H in Table 8 test for each region the parallelism of the Pg and Pv scales. The subdivision of the stars into small groups and the influence of classification errors obscure, to some extent, the underlying relations. The behavior of the residuals must therefore be judged in the light of the average deviations in Table 7, columns 6 and 8. For v_C, that is, for C'_C, progressive effects of perhaps 4 or 5 per cent occur in E5 and E7, but there is little else that cannot be explained as accidental error. For C'_H the agreement is less satisfactory, and conspicuous progressions appear in E7 and E8. The significant result from Table 8 is that the differential Pg-Pv scale error for the Cape magnitudes is so small that for most of the regions it is masked by the accidental fluctuations in v_C. The latter, which include the classification uncertainty, have an average value of ± 0.07 mag. per star.

Second, columns 5 and 8 of Table 10 give the equivalent of Table 8 for all regions combined. In addition, columns 2–4, 6, and 7 show a partial segregation of the results according to spectrum. For easier comparison with Table 4, which gives similar results for the Eros stars, the signs of v_C and v_H in Table 10 have been reversed. The residuals are therefore values of $C'_C - C_S$ and $C'_H - C_S$ freed from the systematic differences affecting the various regions. Hence, in both Tables 4 and 10 a positive residual indicates an excess of color—relative to the mean C of the stars available (Table 4) or to the normal C_S for the type in question (Table 10). That the reference values differ in the two tables was only a matter of convenience.

For all types together, Table 10 shows no appreciable dependence of the reduced colors on magnitude, either for the Cape or for Harvard. Table 4 has already given a similar result for the Cape and the Mount Wilson colors of Eros stars, and again we conclude that there is no serious relative error in the respective Pg and Pv scales. It should be noted, however, that here the range is only 2 mag., as against 4.5 mag., and the number of stars a third that available for Table 4.

Third, consider now the results for different spectral types. Any progressive change in $-v_H$ is obscured by the accidental errors. These residuals are therefore omitted. Further, the low-weight final values in Table 4, columns 4 and 7, and the initial value in column 10 of the same table are also omitted. The remaining data give the following coefficients of change (unit, 0.01 mag.) in color per unit of magnitude (numbers of stars in parentheses):

	B9–A5	F0–F5	F8–G0
Table 4.....	$+2.1 \pm 0.37$ (94),	-0.1 ± 0.62 (115),	-0.4 ± 0.37 (99),
Table 10....	$+1.8 \pm 1.04$ (62),	-3.7 ± 0.84 (21),	-2.4 ± 1.76 (20).

(30)

Judged by the mean errors, the only discrepancy between the two tables occurs for the F0–F5 stars; the value for Table 10, however, is deceptive in its precision. The coefficient for B9–A5 stars seems to be definitely positive. That for F8–G0 is probably negative; it is at least different from that for B9–A5. These small differential effects between the types may be only uncompensated color equation, for it would not be surprising to find that the coefficients of the color terms in the reduction formulae depend slightly on magnitude. But since apparently faint stars are of lower average luminosity than bright stars, a luminosity effect may be involved. If so, then the suggested negative trend for F8–G0 is in harmony with the known relation for late-type stars, while an opposed change holds for B9–A5; that is, the color for these types increases with decreasing luminosity.

The various inferences drawn from Tables 7–10 may be summed up in a single phrase—the close comparability of the Cape basic standards with the Pg_C and Pv_C magnitudes for the Eros stars. Scale factors, zero points, and color indices are all closely accordant. Stoy and Menzies have therefore been successful to a high degree in transferring the Cape system to the Eros stars. The reduction formulae (16)–(18) derived from the Eros stars should therefore be equally applicable to the basic standards. The assumption underlying the transformations of Section VIII therefore appears to be fully justified.

X. COMPARISONS WITH CLUSTERS

Stoy's provisional reduction of the Cape basic magnitudes to the International system was found from comparisons with the Hyades, Praesepe, and the Pleiades. The result was equations (14). For bright stars, as already noted, the reduction derived here from the Eros stars, equations (16) and (17), is the same as Stoy's, except for a zero-point correction. Below magnitudes 8.2–8.4, however, there is a difference of 11 per cent in scale for the two sets of formulae.

In an attempt to locate the source of this discrepancy we have examined most of the comparisons with Stoy's cluster data. Here, as elsewhere, we use the notation Pg'_C and Pv'_C for the reduced magnitudes computed from formulae (16) and (17). The corrections to these reduced magnitudes indicated by the several series of cluster magnitudes, which, for the moment, are regarded as standards, are shown in Figure 2, plotted against the reduced magnitude, either Pg'_C or Pv'_C. Since the accidental errors of the Cape magnitudes are small, the regression effect may be neglected.

It is important to note that the exact relation of none of these "standards" to the International system is known. The zero points are all uncertain, and there are obvious inconsistencies in scale. Nevertheless, if we may suppose the scale factors for the different series of standards—whether correct or not—to be merely constant throughout the interval of about three magnitudes covered by them, we shall have a basis for differentiation between the two sets of reduction formulae. In general, a linear trend in the plotted points favors equations (16) and (17), whereas equations (14) require a downward divergence in the plotted points, relative to the general trend for the brighter stars, beginning at about 8.2 for Pg'_C and 8.4 for Pv'_C. The numbers of the following paragraphs refer to the corresponding plots of Figure 2.

1. *Hyades*, $Pg_R - Pg'_C$.—The values of Pg_R are from J. Ramberg's "Catalogue I*A*."[12] For $Pg'_C < 9.0$ the magnitudes are by Hertzsprung, for fainter stars by Ramberg himself, connected with polar standards by six comparisons on four plates. The mean error of the zero point, magnitudes 9–10, is about ± 0.04 mag. There is no evidence of color equation. The run in the differences beginning near $Pg'_C = 8.0$ is of the kind just described as favoring the reduction given by equations (14). Other comparisons, however, indicate that the progression originates in Pg_R.

2. *Hyades*, $Pv_G - Pv'_C$.—A comparison with K. Graff's[13] visual magnitudes after correction for a linear scale divergence, where

$$Pv_G = \text{Graff vis. } m + 0.15\,(m - 8.0) - 0.07\,. \tag{31}$$

There is no change in the trend of the differences at $Pv'_C = 8.4$. The second of equations (17) therefore applies, rather than the second of (14).

3. *Hyades*, $Pv_{RC} - Pv'_C$.—The color index $C_{RC} = Pg_R - Pv'_C$ is used to reduce Pg_R to the photovisual system for comparison with Pv'_C. For a single star the difference $Pv_{RC} - Pv'_C$ vanishes; but if we use for the reduction the mean C_{RC} for all stars of the same spectral type; that is, if we form

$$Pv_{RC} - Pv'_C = Pg_R - \overline{C_{RC}} - Pv'_C\,, \tag{32}$$

we obtain a useful result.

Plot 2 shows that the scale factor for Pv'_C is in all probability constant. Hence the irregularities in plot 3 must originate in Pg_R. With allowance for the fact that the differences are plotted against Pv'_C, the trend is very similar to that in plot 1. Consequently, the progression in plot 1 is to be attributed, mostly if not wholly, to Pg_R.

4. *Hyades*, $Pv'_C + \overline{C'_C} - Pg'_C$.—Here, as for plot 3, we use mean color indices for stars of the same type—in this instance, the mean of the reduced Cape colors—the dif-

[12] *Stockholms Observatoriums Annaler*, **13**, No. 9, 1941. [13] *A.N.*, **220**, 135, 1924.

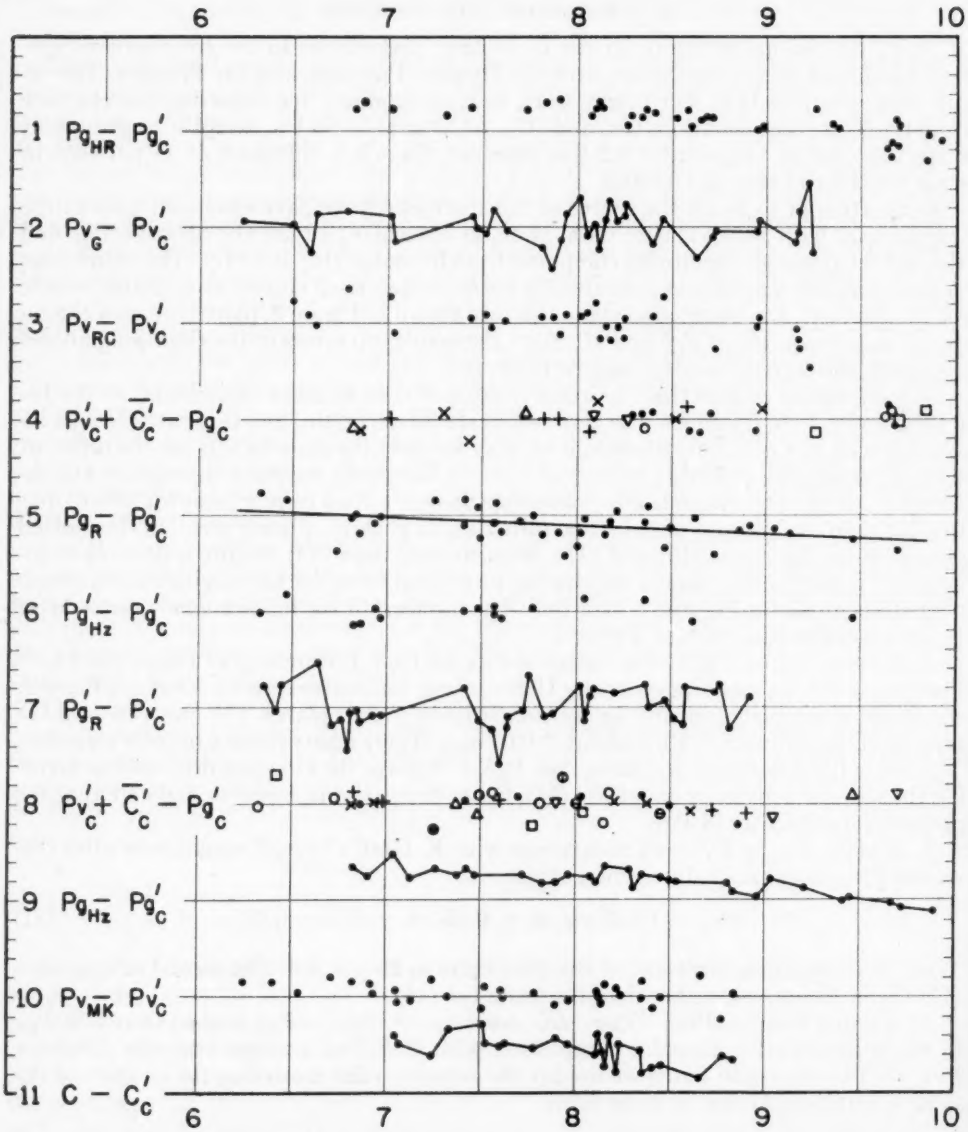

FIG. 2.—Comparisons of Cape magnitudes, reduced to International system, with results by other observers. Plots 1–4, Hyades stars; 5–8, Praesepe; 9–11, Pleiades. Details for individual plots are given in the text paragraphs headed by the corresponding number. Vertical scale: distance between plots = 0.5 mag.

ferent types being distinguished by special symbols. Seven of the 37 stars listed by Stoy have not been included. Five are isolated examples of different subtypes[14] and cannot be used, since mean observed colors are not available; two others of the same type, residuals +0.02 and −0.02 mag., are not included because their magnitudes, 9.68 and

[14] Star No. 97 is erroneously listed by Stoy as dG5. It should be gG5, as given by Ramberg.

9.92, are so nearly the same that they contribute nothing and would only confuse the diagram.

The overlap in magnitude for the stars of different types is such as to leave no doubt as to the high degree of consistency between the Pg'_C and the Pv'_C magnitudes. This circumstance by itself does not establish the correctness of formulae (16) and (17). The differences in plot 4 have the form $\overline{C'_C} - C'_C$; hence they may also be regarded as residuals in color index. But the colors given by the two sets of reduction formulae are nearly the same, as may be seen by comparing the respective differences of equations (14) with equations (18). What plot 4 shows is a parallelism of scales. A change in scale factor near the eighth magnitude is excluded only when we consider plot 3 (unless we suppose that Graff also has a similar change at the same magnitude). In brief, therefore, Pg'_C, Pv'_C, and Graff with the linear correction all run parallel; Pg_R alone is outstanding.

The average deviations in the data used for plot 4 give for a single star a mean error of ± 0.055 mag. Since the stars are selected and grouped according to spectral type, this value includes the influence of classification error, which is probably of the order of ± 0.03 mag. For C'_C itself, therefore, $\epsilon(C) = \pm 0.046$ mag., and for the reduced Cape magnitudes, assumed to be equal in precision, $\epsilon(Pg) = \epsilon(Pv) = \pm 0.033$ mag.

5. *Praesepe*, $Pg_R - Pg'_C$.—The magnitudes Pg_R given by Ramberg, "Catalogue II,"[12] are referred to the scale and zero point of Haffner[15] and to the International color system. Their relation to the reduced Cape magnitudes is expressed by

$$Pg_R - Pg'_C = -0.043\,(Pg'_C - 8.0) - 0.06\,, \tag{33}$$

with an average deviation of ± 0.058 mag. Ramberg's monochromatic magnitudes, reduced to the International color system, give exactly the same relation. Neither series of residuals shows any evidence of a change in trend near the eighth magnitude.

6. *Praesepe*, $Pg'_{Hz} - Pg'_C$.—From magnitudes for 16 stars by Hertzsprung[16]

$$Pg'_{Hz} - Pg'_C = -0.03\,(Pg'_C - 7.4) - 0.13\,. \tag{34}$$

Ramberg, in his Table 18,[12] gives corrections that reduce Vanderlinden's results, which are on the scale and zero point of Hertzsprung, to the system of Haffner. These corrections may also be used to refer Hertzsprung to Haffner. Denoting the reduced values by Pg'_{Hz}, we find

$$Pg'_{Hz} - Pg'_C = -0.01\,(Pg'_C - 8.0)\,, \tag{35}$$

with an average deviation of ± 0.038 mag. The residuals are shown in plot 6. Theoretically, this equation should be the same as equation (33). Notwithstanding the discrepancy, the relation appears to be linear.

7. *Praesepe*, $Pv'_R - Pv'_C$.—We correct the values of Pg_R for the linear divergence shown in plot 5, giving Pg'_R; then form $Pv'_R = Pg'_R - \overline{C'_C}$, where the mean color includes only stars of the same type. Finally, comparison with Pv'_C gives plot 7. The average difference, ± 0.085 mag., is large, but there seems to be no change in trend near the eighth magnitude.

The photovisual standards based on Vanderlinden's effective wave lengths,[17] unfortunately, are unreliable and are not used here. The corresponding color indices, which may be found by forming $Pg(S) - Pv(S)$ from the data in Stoy I, Table XXIII, are practically constant and equal to -0.05 mag. from A0 to F8 for which the normal increase in color is 0.50 mag. The peculiarity is observational and extends to field stars as well as to members of the cluster. Vanderlinden's linear reduction formula for the polar stars, which

[15] *Veröff. d. U. Sternwarte zu Göttingen*, No. 54, 1937.

[16] *A.N.*, **205**, 71, 1917.

[17] *Etude de l'amas de Praesepe*, Gembloux, 1933.

we have tested and used for another purpose,[18] obviously does not apply to his measures of Praesepe.

8. *Praesepe*, $Pv'_C + \overline{C'_C} - Pg'_C$.—The procedure here is the same as for plot 4 of the Hyades, special symbols again indicating stars of the same type. The scales of the reduced Cape magnitudes show no inconsistency. As before, the plotted differences may be regarded as residuals in C'_C. With allowance for classification error the mean error in the color is ± 0.058 mag. The omission of three abnormal residuals, $+0.16$, $+0.14$, and -0.14 mag., reduces the error to ± 0.032 mag. The corresponding mean errors in the reduced Cape magnitudes (assumed to be the same for Pg and Pv) are ± 0.041 and ± 0.023 mag., respectively.

9. *Pleiades*, $Pg'_C - Pg_{Hz}$.—The values of Pg_{Hz} are the Hertzsprung standards listed by Stoy. They are given without any statement as to origin in *Memoirs of the Royal Danish Academy*, Ser. 8, Vol. **4**, No. 4, 1923, but clearly they are the results of Hertzsprung's two investigations in *Astronomische Nachrichten*, Nos. 4452 and 4785.[19] The zero point is that of the *Göttingen Aktinometrie*. The measures were made with a UV Zeiss triplet, and hence require a large negative color correction, apparently about $-0.3C$. This uncertain correction has not been applied. It would affect the scale factor but not the change in the trend occurring at about $Pg'_C = 8.3$, similar to that shown in plot 1.

This change in trend is also shown by Hellerich's magnitudes of the Pleiades[20] (not plotted), which supposedly are already reduced to the International system.

To utilize the Pg_C measures for faint stars for which there are no corresponding values of Pv_C, and hence no C_C, and likewise the Pv_C measures for bright stars for which values of Pg_C are lacking, all the Cape data for the Pleiades have been reduced with an unpublished series of colors based on the effective wave lengths of Hertzsprung and a series of exposure-ratio observations made at Mount Wilson. Relative to the International zero point, the adopted values of C may be too large by 0.05 or 0.06 mag., but any dependence on magnitude should be negligible. To obtain suitable formulae for the reduction of Pg_C and Pv_C, C_C in equations (16) and (17) must be replaced by C with the aid of equation (18).

As it stands, plot 9 favors Stoy's formula, the first of equations (14), rather than the formulae derived here. There is evidence, however, that the Pg_C magnitudes for the fainter Pleiades, are not representative of the Cape basic magnitudes in the Harvard Standard E Regions.

10. *Pleiades*, $Pv_{MK} - Pv'_C$.—For this comparison the visual magnitudes of Müller and Kempf,[21] which are on the system of the *Potsdam Durchmusterung*, have been reduced to the International system by the corrections given in Table 36 of *Magnitudes and Colors of Stars North of +80°*.[22] The results are nearly the same as those given by

$$IPv - PD = -0.20 + 0.09C\,, \tag{36}$$

the formula used by Stoy. In the critical region $Pv'_C = 7.0$–9.0 the agreement shown by the plot in both scale and zero point is close.

An interpretation of plots 9 and 10 is complicated by the fact that the magnitude scales of Müller and Kempf and of Hertzsprung are not consistent. The differences $Pg_{MK} - Pg_{Hz}$, where $Pg_{MK} = Pv_{MK} + C$, should be independent of magnitude. Actually they run approximately as follows (unit, 0.01 mag.):

Pg_{Hz}	3–4	5	6–7	8	9
$Pg_{MK} - Pg_{Hz}$	-5	$+5$	$+15$	$+13$	$+10$

[18] *Mt. W. Contr.*, No. 699; *Ap. J.*, **100**, 264, 1944.

[19] **186**, 177, 1910; **200**, 137, 1915.

[20] *A.N.*, **262**, 49, 1937.

[21] *A.N.*, **150**, 193, 1899.

[22] *Carnegie Inst. Washington Pub.*, No. 532, 1941.

with rather ragged values in the interval 8.5–9.5. A dependence of the Hertzsprung-Mount Wilson color index C on magnitude to the extent required to account for these differences is inadmissible. The divergence of Pg'_C from Pg_{MK} is more nearly linear than that shown in plot 9, but the scale factor is even larger. The inference therefore seems to be an error in Pg'_C. Hence, we proceed to a test of the consistency of Pg'_C and Pv'_C for the Pleiades.

Conditions in the Pleiades are not suited to comparisons of the kind illustrated by plots 4 and 8, in which the colors of stars of the same spectral type are studied in relation to apparent magnitude. Of the types listed by Stoy, A0 is the only one covering any considerable range in magnitude. The values of C'_C for these stars do, in fact, show a large progressive change with magnitude. By itself this circumstance does not necessarily indicate a lack of parallelism in the Pg'_C and Pv'_C scales, for there is still the unsettled question of a luminosity effect for early-type stars. Moreover, for stars in which colors and magnitudes are closely correlated, as in the Pleiades, classification errors introduce a progression in color of the kind actually observed.

11. *Pleiades*, $C - C'_C$.—This comparison of the reduced Cape colors with the Hertzsprung-Mount Wilson data at once puts the question beyond doubt. Since any magnitude error in C is certainly small, there is clearly a large progressive error in C'_C, that is, an inconsistency in the Pg'_C and Pv'_C scales. Since the Pv'_C scale agrees well with Pv_{MK} (plot 10) for the interval 7–9, probabilities seem to locate the difficulty in Pg'_C.

A review of the foregoing evidence shows that the photographic magnitudes for the fainter Pleiades present the only real conflict with the reduction formulae (16) and (17). There seems little doubt that the values of Pg'_C are abnormal and, as already suggested, not representative of the Cape basic magnitudes when reduced by these formulae. Stoy has explained the difficulties met in obtaining the Pg comparison plates for the Pleiades. If a suggestion may be ventured, it would be that under the atmospheric and topographical conditions described a satisfactory transfer of the Cape Pg scale to the Pleiades would be nearly impossible.

Although the Pleiades present the only conflict with the reduction formulae for faint stars found here from the Eros stars, it is also true that Stoy's comparisons with the clusters could scarcely lead to these formulae. Here it is to be remembered that the two sets of reduction formulae disagree only for stars fainter than magnitudes 8.2–8.4. Usually the brighter stars dominate the situation; and, even when there are stars extending well below the critical limit, defective magnitudes point toward an erroneous conclusion for two of the important comparisons (plots 1 and 9). With the data as they are, the scale relations indicated by the second of equations (16) and the second of (17) would not be detected. Altogether, these circumstances explain what at first seemed to be a serious conflict between Stoy's results and those indicated by the Eros stars.

XI. ZERO POINTS IN THE CLUSTERS

In attempting to fix zero points with the aid of the cluster comparisons, Stoy has experienced the difficulties met by everyone who tries to bring order into the miscellaneous and chaotic results on the brightness of cluster stars. Scale errors, unknown color equations, and other uncertainties nearly always lead to contradictory or inconclusive results. Of the data used here, Ramberg's Pg_R magnitudes between 9 and 11, as already mentioned, are on the International system, with a mean error of about 0.04 mag. The mean of the $Pg_R - Pg'_C$ differences for the 14 stars between 8.9 and 10.0 (plot 1) is -0.03 mag. The agreement is within the uncertainty, but obviously the result is of low weight. Again, the 25 Pleiades stars between magnitudes 7 and 9 (plot 10) give the mean difference $Pv_{MK} - Pv'_C = +0.005$ mag. Doubtless there is something of accident in this agreement, but at least it is an agreement. Otherwise, the cluster comparisons yield nothing of any weight on zero points. Faced by this impasse, Stoy in his last article has turned to other evidence and finds a correction of —0.13 mag. to Pg_C, nearly the same, as already stated, as the -0.15 mag. derived here (first of eqs. [16]).

As matters stand at present, one will fare better to reverse the procedure—to follow the long route: Pole to Eros stars to Standard Regions at $-45°$ to clusters, and then use the resulting Cape magnitudes to standardize zero points in the clusters. In justification of this suggestion it may be noted that the mean zero points for the Eros stars found from the Mount Wilson and the Yerkes observations are accordant and well checked by the small correction to the zero point of the spectrum-color relation (eqs. [7]-[10]). A similar control checks the connection of the Eros stars with the Harvard Standard Regions (first of eqs. [29]). Finally, the transfers to the cluster fields, with the exception of Pg'_C for the Pleiades, seem to be of unusual accordance. An average residual of 0.03 mag.[23] implies a zero-point mean error of ± 0.017 mag. in the average for 6 comparison plates. We cannot check this result directly, but we may test the consistency of the resulting Pg'_C and Pv'_C zero points for cluster stars by again computing the zero-point correction to the observed spectrum-color relation.

Details for the Hyades and Praesepe are in Table 11. Owing to the abnormality in C'_C

TABLE 11

ZERO-POINT CORRECTION AND COLOR EXCESS

(Unit, 0.01 Mag.)

HYADES						PRAESEPE							
Ramberg Sp. (1)	Cluster $C_S-C'_C$ (2)	Cluster No. (3)	Field $C_S-C'_C$ (4)	Field No. (5)	Field ρ (6)	Ramberg Sp. (7)	Cluster $C_S-C'_C$ (8)	Cluster No. (9)	Field $C_S-C'_C$ (10)	Field No. (11)	Field ρ (12)	MW Sp. (13)	Cluster $C_S-C'_C$ (14)	Cluster No. (15)
A0	.....	....	−25	2	260†	A0	− 6	3‡	.....	....	.....	A2s	+ 2	1
A3	.....	....	−15	1	322†	A2	0	4‡	− 6	2	154	A3n	− 3	3
F2	− 8	1	− 2	1	81	A3	− 3	6	− 4	1	226	A4n	− 2	3
F5	− 9	3	0	3	96	A5	− 2	5	.....	....	.....	A5n	+ 2	2
F8	− 6	4	+ 2	1	81	F0	− 1	5	.....	....	.....	A6n	+ 3	8
dG0	− 7	6	− 7	3	98	F2	.....	....	− 5	1	153	A7n	+11	1
dG5	+ 2	1	.....	....	.....	F8	.....	....	− 1	3	68	cF0	+10	1
dG8	+ 5	2	.....	....	.....	dG0	(−19)	(1)	+ 9	1	53	F2p	(+22)	(1)
dK0	+15	3	.....	....	.....	gG5	− 4	2	−16	1	350	F3p	(+27)	(1)
gG5	.....	....	−44	1	215†	gG8	− 7	1	.....	....	.....	F5	(−33)	(1)
gG8	.....	....	−31	1	406†	gK0	+12	1	+10	2	408	gG6	− 7	1
gK0	.....	....	−47	3	299†	.....	.....	....	.....	....	.....	gG7	− 9	3
gM	.....	....	−40	1	222†	.....	.....	....	.....	....	.....	.....	.....	....
All..	− 2	20	− 3*	17	.....	All..	− 3	25	− 1	11	.....	.....	− 1	23

* Eight stars, $\rho<100$ parsecs.

† Distance not corrected for absorption.

‡ Only two A0 and three A2 stars were used. The three stars rejected from column 9 are the same as those rejected from column 15.

shown by plot 11, the Pleiades cannot be included. Values of $C_S - C'_C$ for Praesepe stars are given for both Ramberg and Mount Wilson classifications, columns 8 and 14. Harvard spectra might also have been used for both clusters, but those listed are sufficient for our purpose. Mount Wilson spectra are also available for the Hyades, but mainly for stars brighter than those observed at the Cape, and with two exceptions there are no corresponding values of C'_C. Cluster members and field stars are treated separately. For Mount Wilson, however, there is no column of Praesepe field stars because only two of these objects have been observed.

[23] Stoy II, p. 318.

The galactic latitude of Praesepe, +34°, indicates that space absorption is not to be feared. For the Hyades, however, the lower galactic latitude, −20°, and the proximity of the Taurus cloud at once raise a question. The photometric distances[24] of the clusters are: Hyades, 53 parsecs; Praesepe, 139 parsecs. Distances for the field stars are given in Table 11, columns 6 and 12.

Since the normal spectrum-color relation is defined for HD types, allowance must be made for deviations from the Harvard system. The Mount Wilson classifications have been reduced to this system by Tables 2 and 3 of *Mt. W. Contr.* No. 683.[25] The systematic relations for Ramberg are not known in detail, and we can only apply a small average correction, which will be introduced later. Accidental errors of classification, of course, enter to their full amount into $C_S - C'_C$.

For the Hyades, the cluster members and the field stars within 100 parsecs show, in general, only small fluctuations in $C_S - C'_C$. Their means, Table 11, columns 2 and 4, are −0.02 and −0.03 mag., respectively, with an average deviation per star of ±0.070 mag. On the other hand, the 9 field stars with $\rho > 200$ parsecs give a mean $C_S - C'_C$ of −0.36 mag. Remembering that, in general, $C_S - C'_C = z - E$, a combination of zero-point error and color excess, we find for the 9 stars, $E = +0.3$ mag. This result is in general agreement with Ramberg's[12] conclusion from star counts that an obscuring cloud behind the central Hyades begins at about 140 parsecs.

TABLE 11*a*

ADOPTED ZERO-POINT CORRECTIONS

Cluster	Sp.	$C_S - C'_C$	*AD*	Cluster	Field	Total No.
Hyades.....	Ramberg	−1.4	±7.0	20	8 ($\rho<100$)	28
Praesepe.....	Ramberg	1.4	5.9	25	11 (all)	36
Praesepe.....	MW	−0.7	±6.4	23	2	25

Three of the Praesepe members, Ramberg Nos. 57, 193, and 457, have been omitted from the final results because of discordances, mostly in the classifications. It happens, however, that the mean values of $C_S - C'_C$ are scarcely affected. Columns 8, 10, and 14 of Table 11 give no evidence of color excess, even for the more remote field stars, in harmony with what was to be expected for the region of Praesepe.

Combining values of $C_S - C'_C$ for cluster members and for the field stars that appear to be absorption free, we have the results summarized in Table 11*a*. On the average, Ramberg's spectra require a correction of +0.35 of a classification unit to reduce them to the Harvard system. The mean values of $C_S - C'_C$ from Table 11 have accordingly been increased by 0.01 mag. for entry in Table 11*a*. This table also includes the two Praesepe field stars having Mount Wilson classifications that do not appear in Table 11. The average deviations in $C_S - C'_C$ for individual stars, ±0.064 mag. in the mean, are practically the same as those for the Eros stars (Table 6, col. 11) and for the basic standards (Table 7, col. 6).

[24] The distances given here are based on Mount Wilson spectroscopic absolute magnitudes and include the systematic corrections by Russell and Moore (*Mt. W. Contr.*, No. 636, Table 12, and eq. [36]; *Ap. J.*, **92**, 354, 1940). When possible, Pv'_C magnitudes have been used. Values based on Ramberg's spectra and the corresponding mean absolute magnitudes are: Hyades, 56 parsecs; Praesepe, 141 parsecs, practically the same as those cited in the text. In striking contrast are the smaller distances derived from proper motions. For example, Smart's solution for the Hyades (*M.N.*, **99**, 168, 1939) gives 35 parsecs. Distances of Praesepe based indirectly on the motions of the Hyades are also discordant, and a similar discrepancy occurs for the Pleiades. Part of this systematic difference, at least, is a hidden regression effect introduced by an improper use of Charlier's formulae for the convergent of a moving cluster. The matter will be discussed in *Contribution* No. 716.

[25] Seares and Joyner, *Ap. J.*, **98**, 244, 1943.

For both clusters the zero-point correction to the spectrum-color relation is -0.01 mag. This value, which expresses the consistency of the Pg'_C and Pv'_C zero points, is unexpectedly small, for it includes the classification error, as well as that from the comparisons with the Standard Regions; whereas the comparison plates themselves contribute to the zero point of C'_C a mean error of ± 0.024 mag.

XII. EVIDENCE FROM THE HARVARD STANDARDS

The evidence on the reduction of the Cape magnitudes supplied by the Eros stars has already been discussed at length and appears to be conclusive. There remains, however, a detail not yet mentioned that should not be overlooked, for it directly concerns the Pg magnitudes of the fainter stars. The basic Cape Pg_C magnitudes agree very closely in scale and zero point with the Harvard Pg_H magnitudes of the Standard Regions, as may be seen from Stoy I, Table IX, or again by forming the difference between formulae (16) and (22), in which the respective scale factors are practically identical. The Harvard standards cover the interval 7–11 (approximately); but, on the average, only 5 Pg_H standards per region are brighter than 8.0. Hence, the relation of Pg_H to the International system (found from the Eros stars) is, in the main, that expressed by the second of equations (22); the first equation, covering an interval of only a magnitude, scarcely counts and, so far as the Harvard standards themselves are concerned, may be, to some extent, a computational result. In any event, for the fainter stars we find a scale correction to Pg_H of only 2 per cent.

This result is perfectly consistent with what we know of the Harvard photographic standards. Based originally on the old Polar Standards, they were later reduced to the International system by corrections which should insure close, but not necessarily exact, agreement with that system. This independent evidence supporting the second of equations (22) is of considerable weight. It is, of course, equally strong in support of the second of equations (16).

Since the relation of the Pv_H standards to the International system is unknown, no similar argument holds for the second of equations (17). The parallelism of the Pg'_C and Pv'_C scales is well established, however, by the behavior of the color indices. Hence, indirectly, the second of equations (22) also confirms the connection of the Pv_H magnitudes with the International standards expressed by the second of equations (23).

As a closing word, we may repeat what in substance was said at the beginning. We do not regard the present discussion as final. Formulae (16)–(18), judged by all the tests that can now be applied, seem to be close to the true reduction. Nevertheless, the actual relation of the Cape basic magnitudes to the International system is probably not so simple as that expressed by the linear formulae. The zero-point corrections required by the Mount Wilson magnitudes to reduce the spectrum-color relation to the standard relation are only $+0.02$ and -0.01 mag., respectively; and yet there remains here a small uncertainty that should be removed for a definitive solution. Finally, the Cape zero points for the Eros stars, although probably very close to their true values relative to the basic standards at $-45°$, show a small drift in declination (Table 2, col. 11) that should also be removed.

Beginning anew, one would not select the Eros stars for a connection of the two hemispheres; but with so much work done on them already, the simplest procedure now is to utilize them to the full. It is doubtful, however, if their recomparison with the Polar Standards, which thus becomes desirable, should be undertaken at Mount Wilson; the meridian altitudes of about half the stars are only 30°–36°, and the increasing illumination of the southern sky from valley lights in recent years might introduce a new factor of uncertainty. Observations from Palomar Mountain, with similar terrain north and south and no valley lights at all, would be safer. And, besides, there would be the advantage of one degree less in latitude.

B CASSIOPEIAE AS A SUPERNOVA OF TYPE I*

W. BAADE
Mount Wilson Observatory
Received June 13, 1945

ABSTRACT

The light-curve of the nova of 1572, derived from Tycho's observations, shows that the star was a supernova of type I which reached at maximum the apparent magnitude −4.0.

The fact that no expanding shell can be detected at the place where the supernova flared up indicates that the excitation provided by the stellar remnant is insufficient. This, in turn, suggests that the star is much more advanced toward the final white-dwarf state than are the stellar remnants of the supernovae of A.D. 1054 and 1604.

It has been pointed out in a previous paper[1] that B Cassiopeiae, the bright nova of 1572, was undoubtedly a supernova because of its amplitude, which exceeded 22 mag. The recent recognition of two types of supernovae makes it desirable to decide whether the star was a supernova of type I or type II. The light-curve of the nova, derived in the present paper, clearly indicates a supernova of type I. Because it throws new light on the final state of a supernova, B Cas is of particular interest.

I. THE LIGHT-CURVE OF B CAS

Our main sources of information about the nova are Tycho's preliminary report of 1573 (*De stella nova*) and the extensive discussion of the whole material, including the observations of others, in his *Progymnasmata*, published in 1602.

The data collected by Tycho leave little doubt that the nova flared up in the first days of November, 1572.[2] The earliest reliable date of discovery is the morning of November 6, when the nova was noticed by W. Schuler at Wittenberg. From then on, the discoveries follow one another rapidly. On November 7, it was noticed by P. Haintzel at Augsburg and observers at Winterthur; on November 8, by Maurolycus at Messina, Thurneysser at Berlin, and D. Chytraeus at Rostock. Tycho himself discovered the nova on the evening of November 11.

Although the new star caused great excitement among the contemporary scholars, Tycho seems to have been the only observer who deemed it worth while to describe the light-changes of the nova from its appearance in November, 1572, until it became invisible to the naked eye in March, 1574. To make the reader familiar with the data available for the construction of the light-curve, we reproduce here Tycho's short description. Important observations by other observers will be mentioned later in the discussion. Tycho's report in the *Progymnasmata*,[3] freely translated, is as follows:

> When first seen, the nova outshone all fixed stars, Vega and Sirius included. It was even a little brighter than Jupiter, then rising at sunset, so that it equalled Venus when this planet shines in its maximum brightness. . . . . The nova stayed at nearly this same brightness through almost the whole of November. On clear days it was seen by many observers in full daylight, even at noontime, a distinction otherwise reserved to Venus only. At night it often shone through clouds which blotted out all other stars.
>
> However, the nova did not retain this extraordinary brightness throughout its whole apparition but faded gradually until it finally disappeared. The successive steps were as follows:
>
> As already stated, the nova was as bright as Venus in November [1572]. In December it was

* *Contributions from the Mount Wilson Observatory, Carnegie Institution of Washington*, No. 711.

[1] W. Baade, *Mt. W. Contr.*, No. 600; *Ap. J.*, **88**, 285, 1938.

[2] All dates given in the present paper are Julian style.

[3] Tycho Brahe, *Opera omnia*, ed. J. L. E. Dreyer, **2**, 309, 1915.

about equal to Jupiter. In January [1573] it was a little fainter than Jupiter and surpassed considerably the brighter stars of the first class. In February and March it was as bright as the last-named group of stars. In April and May it was equal to the stars of the second magnitude. After a further decrease in June it reached the third magnitude in July and August, when it was closely equal to the brighter stars of Cassiopeia, which are assigned to this magnitude. Continuing its decrease in September, it became equal to the stars of the fourth magnitude in October and November. During the month of November, in particular, it was so similar in brightness to the near-by eleventh star of Cassiopeia that it was difficult to decide which of the two was the brighter. At the end of 1573 and in January, 1574, the nova hardly exceeded the stars of the fifth magnitude. In February it reached the stars of the sixth and faintest class. Finally in March it became so faint that it could not be seen any more.

The following discussion, in which we shall try to transform Tycho's description of the light-changes into modern magnitudes, naturally falls into two parts: the maximum phase of the nova when it was compared with Venus and Jupiter and the later decline, when stars served as reference objects.

A. THE MAXIMUM PHASE

In Table 1 are given the positions and magnitudes of Venus and Jupiter when the nova was near its maximum. The positions were computed with the help of P. V. Neugebauer's tables.[4] The adopted light-elements are those of G. Müller,[5] with the exception

TABLE 1

POSITIONS AND MAGNITUDES OF VENUS AND JUPITER (1572–73)

Planet	Jul. Date, G.M.T.	$\lambda_{geoc.}$	$\beta_{geoc.}$	$\lambda_{\odot}$	log Δ	log r	Phase Angle	m_v
Venus.....	1572 Nov. 10.0	196°.2	+1°.0	238°.3	9.6530	9.8570	113°	−4.35
	20.0	203.4	+2.1	248.5	9.7167	9.8565	104	−4.29
	30.0	212.2	+2.8	258.6	9.7746	9.8562	96	−4.19
	Dec. 10.0	222.0	+3.1	268.8	9.8277	9.8563	90	−4.09
Jupiter.....	1572 Nov. 15.0	20.8	−1.5	243.4	0.6223	0.6957	.....	−2.61
	Dec. 15.0	20.3	−1.3	273.9	0.6629	0.6963	.....	−2.40
	1573 Jan. 15.0	22.9	−1.1	305.5	0.7072	0.6967	.....	−2.18

of the constant term for Jupiter, for which the value recently derived by W. Becker[6] was used.

Table 1 settles the question as to whether Tycho's statement that the nova "equalled Venus when this planet shines in its maximum brightness" refers to actual observations or not. In November, 1572, Venus was, indeed, near its maximum brightness, approaching greatest western elongation from the sun on its way from inferior conjunction. Since the nova was circumpolar in northern Europe, it could easily be compared with Venus in the early morning hours.

Tycho's statement that the nova at its maximum equaled Venus would indicate that its apparent magnitude was $m_v = -4.3$. It seems, however, that Tycho was inclined to overstate the maximum brightness of the nova. In his preliminary report of 1573 he makes it even brighter than Venus. Although in the *Progymnasmata* his estimate is more conservative, it still appears somewhat too high, since most of the other observers seem to agree that the nova at maximum was distinctly fainter than Venus. Considerable weight in this respect should be given to the estimates of three observers, who, we know, saw the nova at its maximum. One was the well-known astronomer C. Peucer, who ob-

[4] *Tafeln zur astronomischen Chronologie*, Vol. 2, Leipzig, 1914.

[5] *Photometrie der Gestirne*, Leipzig, 1897.

[6] *Sitz.-Ber. Preuss. Akad. d. Wiss., Phys.-math. Kl.*, 1933, p. 839.

served the nova first on November 16 and noted[7] that "it surpassed in brightness all stars and planets with the exception of Venus." Even more definite is the statement of J. Praetorius, who likewise saw the nova first on November 16. According to his estimate,[8] the nova was "brighter than Jupiter but easily fainter than Venus." The third observer who probably saw the nova before November 17 was M. Maestlin. He states[9] that it "almost equalled Venus." Since Venus in November, 1572, had the visual magnitude $m_v = -4.3$, we cannot be far from the truth if we ascribe to the estimates of both Praetorius and Maestlin the apparent magnitude $m_v = -3.8$. The mean of the estimates of Tycho, Praetorius, and Maestlin is then $m_v = -4.0$, a value which probably represents the true maximum brightness of the nova within ± 0.3 mag.[10] It was high enough, as the later light-curve will show, to make the nova a daylight object for about 2 weeks around the maximum,[11] in agreement with the statements of Tycho and Maestlin that "in the beginning" the nova could be seen in daytime. The exact date of the maximum cannot be determined from the existing observations. Probably it took place near the middle of November, since the nova seems to have remained more or less constant from its discovery until the later part of November.

In December, 1572, the nova had become perceptibly fainter. Tycho's estimate that it was then about as bright as Jupiter corresponds to $m_v = -2.4$ (see Table 1).

B. THE FURTHER DECLINE OF THE NOVA

In order to describe the further decline of the nova, Tycho resorted to magnitudes. Since the investigation of the nova of 1572 was his first original work in the field of astronomy, it is reasonable to assume that in referring to the stars of a given magnitude he adhered strictly to the authoritative source of that time—Ptolemy's Almagest. Occasional remarks in his report support this view, for instance, when he amplifies the statement that in July and August, 1573, the nova was of the third magnitude by adding: "It was closely equal to the brighter stars in Cassiopeia which are assigned to this magnitude." The following conversion of Tycho's estimates is based on this assumption.

1573 January.—Nova a little fainter than Jupiter; considerably brighter than the brighter stars of the first class.

The stars of magnitude 1, according to Ptolemy,[12] which were visible together with the nova in January and February for an observer in northern Europe, are shown in the accompanying tabulation. Obviously, the description, "the brighter stars of the first class,"

Star	Ptolemy's Mag.	Harv. R.P.	Star	Ptolemy's Mag.	Harv. R.P.
α Lyr*	1	0.14	α C Mi*	1	0.48
α Aur*	1	0.21	α C Ma	1	−1.58
α Tau	1	1.06	α Boo*	1	0.24
α Ori	1–2	0.5–1.1 (var)	α Vir	1	1.21
β Ori*	1	0.34			

[7] Brahe, *op. cit.*, **3**, 120, 1916. [8] *Ibid.*, pp. 154–55. [9] *Ibid.*, p. 158.

[10] It should be mentioned here that a Korean record of the nova contains a statement about its brightness at maximum. According to R. Segikuchi, the nova is described in *Bunken Bikoh* as follows: "In the 11th moon, 5th year of Senso [November–December, 1572], a strange star was observed by the side of Sakusei [γ Cas] with magnitude as bright as Venus" (Y. Iba, *Pop. Astr.*, **46**, 142, 1938). This estimate agrees well with those of the European observers.

[11] For a discussion of the conditions of daylight visibility see N.U. Mayall and J. H. Oort, *Pub. A.S.P.*, **54**, 98, 1942.

[12] See Ptolemy's *Catalogue of Stars*, ed. Peters and Knobel, Table VIII, Carnegie Institution of Washington, 1915.

refers to the group of nearly equally bright stars marked by asterisks. Sirius, which in a literal sense is the most outstanding example of a bright star of Ptolemy's class 1, has been excluded because it deviates from the group which Tycho obviously meant as much in one direction as the fainter stars of Ptolemy's class 1 deviate in the other. It is rather remarkable that Sirius, which would have provided a convenient intermediary step between Jupiter and what we today call the "zero magnitude," was not used as a comparison star in the estimates. One can only suspect that a comparison with Sirius appeared meaningless to Tycho, who tried to describe the later light-curve of the nova in the conventional system of the Almagest.

The mean magnitude of the stars marked with asterisks, which we identify with Tycho's brighter stars of the first class, is $m_v = +0.28$ on the Harvard system. Jupiter's brightness in January, 1573, was $m_v = -2.18$ (see Table 1). Tycho's interpolation of the nova into this large interval of 2.46 mag. must have been a crude affair. I have assumed that his estimate is roughly equivalent to

$$m_{\text{Nova}} = m_{\text{Jupiter}} + \frac{1}{3} \cdot 2.46 ,$$

which gives $m_{\text{Nova}} = -1.4$.

1573 February–March.—Tycho's estimate that the nova was as bright as the brighter stars of the first class corresponds to the Harvard magnitude $m_v = +0.3$ (see above).

1573 April–May.—Nova equal to the stars of the second magnitude.

Almagest stars of the second magnitude, which in April and May (lower culmination of Cassiopeia) were conveniently located for comparisons with the nova, are given in the following tabulation. Their mean magnitude on the Harvard system is $m_v = +1.60$.

Star	Ptolemy's Mag.	Harv. R.P.	Star	Ptolemy's Mag.	Harv. R.P.
α Gem	2	1.58	β Per	2	2.2 (var)
β Gem	2	1.21	α Cyg	2	1.33
β Aur	2	2.07	α Aql	2–1	0.89
α Per	2	1.90			

1573 July–August.—Nova closely equal to the brighter stars of Cassiopeia, which are assigned to the third class.

According to the Almagest, the third-magnitude stars in Cassiopeia are as given in the next tabulation. Their mean magnitude is $m_v = +2.49$.

Star	Ptolemy's Mag.	Harv. R.P.	Star	Ptolemy's Mag.	Harv. R.P.
α Cas	3	2.47	γ Cas	3–2	2.25
β Cas	3	2.42	δ Cas	3	2.80

1573 October–November.—Nova equal to stars of fourth magnitude; in November very similar to the near-by eleventh star of Cassiopeia.

Since Tycho states explicitly that his estimate for July–August, 1573, when he assigned the nova to the third magnitude, was based on comparisons with third-magnitude stars in Cassiopeia, it is reasonable to assume that his fourth magnitude is similarly defined by those stars of Cassiopeia which belong to Ptolemy's class 4, if for no other reason than that they were the nearest and most convenient comparison stars. Cassiopeia stars

of the fourth magnitude, according to Ptolemy, are shown in the accompanying tabulation. Their mean magnitude is $m_v = +4.03$. Since the eleventh star of Cassiopeia is κ, the magnitude of the nova in November was $m_v = +4.24$.

Star	Ptolemy's Mag.	Harv. R.P.	Star	Ptolemy's Mag.	Harv. R.P.
ζ Cas.	4–3	3.72	ι Cas.	4	4.59
η Cas.	4	3.64	ϑ Cas.	4	4.52
ϵ Cas.	4	3.44	κ Cas.	4–5	4.24

1573 December–1574 January.—Nova hardly exceeded the stars of the fifth magnitude. It is impossible to tell which stars of the fifth magnitude Tycho may have used for his estimate. Of the Cassiopeia stars, only φ is assigned in the Almagest to class 5, and Tycho would hardly have based his estimate on a single star, being aware that each class covered a considerable interval in brightness. Under these circumstances it seems best to use the mean relation between Ptolemy's classes and the Harvard magnitudes. According to K. Lundmark,[13] we have the values shown in the following tabulation. For

Ptolemy's Mag.	Harv. R.P.	Tycho's Mag.	Harv. R.P.
5–4.	4.78	5.	4.68
5.	4.91	5.	4.87
5–6.	. . . . .	5:.	4.51
6–5.	. . . . .	6.	5.22
6.	5.29	6.	5.20
		6:.	5.21

comparison we give also the relation between Tycho's magnitudes in his catalogue of 777 stars[14] and the Harvard system. Since between December, 1573, and January, 1574, the nova hardly exceeded the stars of the fifth magnitude, it was probably close to $m_v = +4.7$.

1574 February.—The nova reached the sixth and faintest class. The tables given above show that the nova was about $m_v = +5.3$.

C. THE LIGHT-CURVE

The data derived in the preceding discussion are summarized in Table 2.

The resulting light-curve of the nova is shown in Figure 1. It is very much better than would have been expected in view of the estimates, which at first sight appear to be extremely crude. If we consider that half of the estimates refer to 60-day intervals and that the corresponding magnitudes follow a smooth light-curve with residuals generally not exceeding 0.25 mag., the accuracy of Tycho's estimates may indeed appear remarkable. There seems to be only one explanation. When Tycho attempted to describe the later light-changes of the nova on the system of Ptolemy's magnitudes, he must have faced the difficulty that stars assigned to the same class actually covered quite a range in brightness. To overcome this difficulty he seems to have adopted—consciously or unconsciously—the obvious device of noting the approximate dates between which the nova stayed within a given magnitude class. His statement: "The nova was equal to the

[13] *Handb. d. Ap.*, **5**, Part I, 231, 1932.

[14] *Op. cit.*, **2**, 258, 1915.

stars of the fourth magnitude in October and November" should therefore be read: "The nova entered Ptolemy's class 4 in October and left it in November." With such a procedure the mean magnitude of the nova for a given time interval is easily obtained with an accuracy of a quarter of a magnitude, particularly if the light-changes are linear, as in the present case.

The light-curve itself is typical of a supernova of type I as shown by comparison with the visual light-curves of two other supernovae of this class, SN Oph (1604) and SN in I.C. 4182 (see Fig. 1). As will be pointed out in a later paper, a very characteristic feature of supernovae of type I is the linear decrease in brightness which sets in at about 120 days after maximum and is characterized by a gradient of $+0.0137 \pm 0.0012$ mag. per day. With a gradient of $+0.014$ mag. per day for the phase interval 120^d–460^d B Cas conforms to this pattern perfectly. The descent from the maximum is less steep in B Cas than in the recent SN in I.C. 4182, but it is quite evident from the data now available

TABLE 2

MAGNITUDES OF B CAS (1572)

Date (Tycho)	Adopted Mean Date (Julian)	Description	m_v	Phase
1572 Nov.	1572 Nov. 15	Almost as bright as Venus	−4.0	0^d
Dec.	Dec. 15	About as bright as Jupiter	−2.4	30
1573 Jan.	1573 Jan. 15	A little fainter than Jupiter; considerably brighter than the brighter stars of first mag.	−1.4	61
Feb.–Mar.	Mar. 2	Equal to brighter stars of first mag.	+0.3	107
Apr.–May	May 1	Equal to stars of second mag.	+1.6	167
July–Aug.	Aug. 1	Equal to α, β, γ, δ Cas	+2.5	259
Oct.–Nov.	Nov. 1	Equal to stars of fourth mag.	+4.0	351
Nov.	Nov. 15	Equal to κ Cas	+4.2	365
1573 Dec.–1574 Jan.	1574 Jan. 1	Hardly exceeding stars of fifth mag.	+4.7	412
1574 Feb.	Feb. 15	Equal to stars of sixth mag.	+5.3	457
Mar.	Mar. 15	Invisible	.....	485

that there is some variation in the form of maxima of supernovae of type I, especially in their heights and widths.

The color changes of B Cas, too, were apparently those of a typical supernova of type I. All observers agree that at maximum the star had a color like Venus and Jupiter; that, as it decreased, it began to redden until it reached a color similar to that of Mars and Aldebaran; and that, later on, it returned to a whitish color like that of Saturn. But there are some discrepancies in the dating of the different phases, especially the third one. According to Maestlin and Peucer, the reddening of the nova became perceptible in December (Peucer gives December 14 as the date when the reddening became pronounced). Tycho states that after maximum the nova assumed a yellowish color and became red like Aldebaran shortly after the beginning of 1573. Praetorius finally remarks that the nova became red like Mars about two months after its appearance, i.e., in the first half of January, 1573. From all the evidence it seems that the reddening became noticeable in December and reached its full development early in January. There is disagreement, however, as to how long this red phase lasted. Maestlin states that by the end of February, 1573, the nova had returned to its original whitish color. On the other hand, Tycho claims that the nova retained its red color through February and March and returned to a color somewhat like the original one only in May. Probably this divergence of opinion is less serious than it seems, since color estimates, particularly in the range of low intensi-

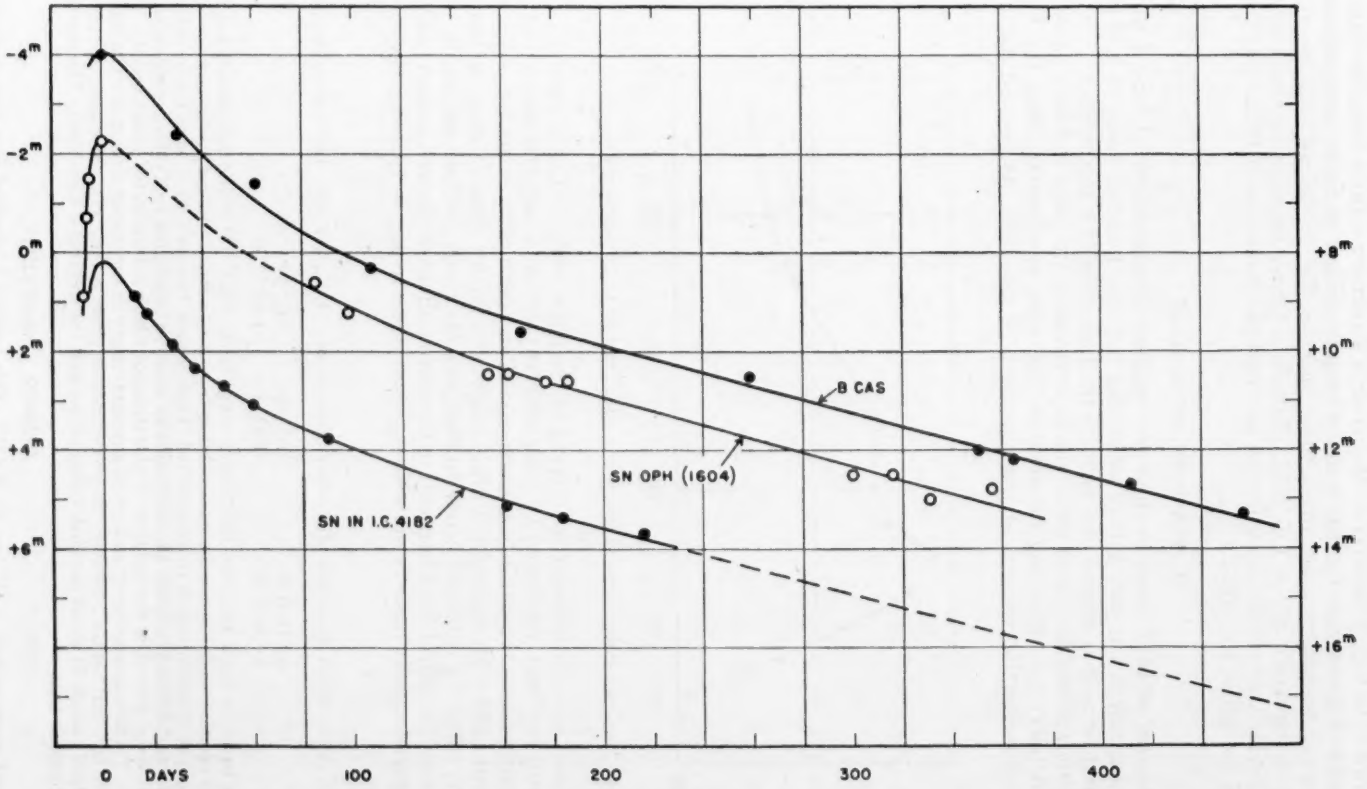

FIG. 1.—Visual light-curves of B Cas, SN Oph (1604), and SN in I.C. 4182. Magnitudes on the left refer to B Cas and SN Oph (1604); on the right, to SN in I.C. 4182. The extrapolated (*dotted*) part of the light-curve of SN in I.C. 4182 has been taken from the photographic light-curve, after an adjustment in zero point.

ties, are known to be highly subjective. Moreover, a supernova returns from the stage of maximum reddening so gradually that it would be quite difficult to fix by mere estimates the date on which the star returned to a whitish color (see Fig. 2). Judged from the color-index curve of the recent SN in I.C. 4182, Maestlin's figures seem to be closer to the truth than Tycho's, even if we allow for the fact that the maximum of B Cas was wider than that of the SN in I.C. 4182.

II. THE REMNANT OF B CAS

The supernova of 1572 raises to three the number of supernovae of type I which have been observed in our own galaxy within the last nine hundred years. It is of particular interest because it throws new light on the final state of a supernova.

It is well known that the places where the supernovae of A.D. 1054 and 1604 flared up are occupied today by expanding nebulosities, the most spectacular being the Crab nebula, which forms the remnant of the supernova of A.D. 1054. As pointed out in a

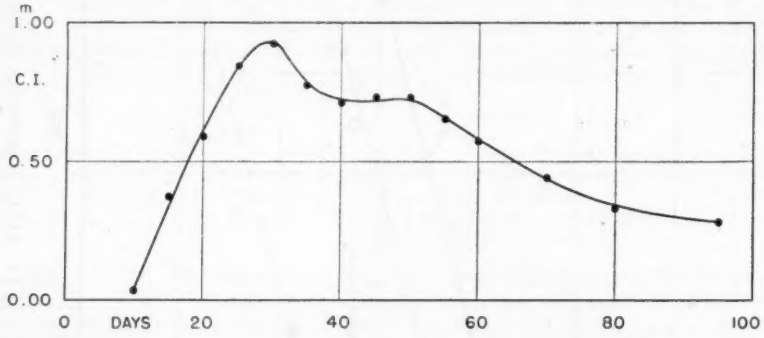

FIG. 2.—Color-index curve of SN in I.C. 4182 from 0^d to 100^d after maximum

previous paper,[1] no such remnant is observed in the place where B Cas appeared. This negative result has been confirmed by later observations, in which the search was extended to fainter limits. To put it quantitatively: If any nebulosity exists in the place of B Cas, it must have a photographic surface brightness fainter than 25 mag. per square second of arc, which for extended nebulosities represents about the limit attainable with an $f/5$ reflector. The search for a blue star in the surroundings of the well-known position of B Cas[15] proved equally unsuccessful. No such star down to $m_{pg} = 19.0$ could be found on the plates.

[15] S. Böhme, in the latest discussion of Tycho's observations (*A.N.*, **262**, 497, 1937) gives two solutions:

a) 1950.0.....$0^h22^m1^s1$ $+63°52'1''$
b) 1950.0.....$0^h22^m4^s6$ $+63°52'30''$

Solution (*a*) is based on the 7 reference stars which occur in the FK3; (*b*) includes in addition η and ι Cas, for which positions and proper motions were taken from Boss's *P.G.C.* Böhme leaves open the question of which of the two solutions is to be preferred. There seems, however, to be little doubt that the unexpectedly large difference between the two solutions must be attributed to Tycho's measure of the distance ι Cas–Nova, since it is the inclusion of this distance which influences the result unduly. That the error lies in Tycho's measurement and not in any uncertainty of the proper motion of ι Cas follows at once from the fact that the *G.C.* confirms the proper motion given in the *P.G.C.* Moroever, the proper motion is negligibly small. It seems justified, therefore, to omit the distance ι Cas–Nova. The resulting position of the nova is then

1950.0.....$0^h22^m0^s2$ $+63°52'12''$,

with a computed mean error of $\pm 23''$ (see Pl. XXIV). This position is identical with that derived by Argelander (*A.N.*, **62**, 273, 1864), who also excluded ι Cas because its proper motion was not known at

PLATE XXIV
North

PLATE XXIV

North

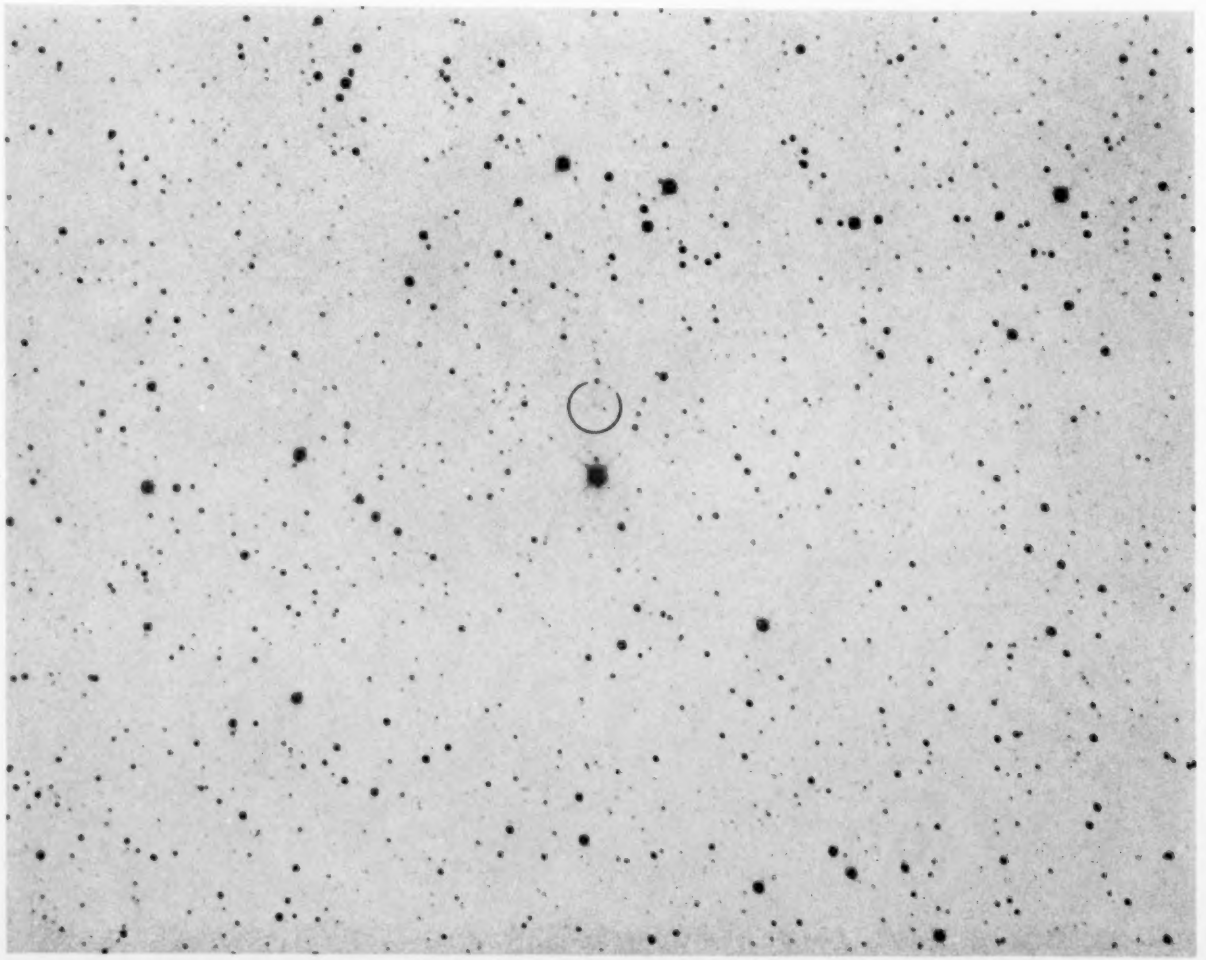

Prec.

FIELD OF B CASSIOPEIAE

Four-hour red exposure at 60-inch telescope, 1941, October 18; computed position of supernova and its mean error are marked by the circle. (Scale, 1 mm = 5".32.)

UNIV. OF MICH.

Now there is every reason to believe that masses comparable to those of the Crab nebula were ejected during the outburst of B Cas; the astonishing uniformity of supernovae of type I as regards both light-curves and spectral development leaves hardly any doubt about that. There can also be no doubt that since the outburst the ejected masses have expanded into a sizable disk, about 2′ in diameter, because the distance of B Cas must be roughly the same as that of the Crab nebula. Therefore, if the shell is unobservable today, the reason must be that the excitation provided by the stellar remnant is insufficient. Such a state of affairs is not unexpected. It will be recalled that the recent investigation of the Crab nebula[16] has led to some remarkable results regarding the stellar remnant which excites the shell. This star has all the earmarks of a white dwarf in so far as its diameter and its density are concerned; but instead of having a luminosity of about $+10^{M}$, it has the bolometric luminosity -1^{M}, the determining factor being the abnormal surface temperature of 5.10^{5} degrees. S. Chandrasekhar, whose theory of the supernova process predicts a white dwarf as the stellar remnant of the cataclysm, has explained this anomaly by pointing out that degeneracy throughout the star—the fully developed white-dwarf state—will be attained only after some finite time. The abnormal luminosity of the central star of the Crab nebula and that of the nebula itself are thus attributed to the fact that the transition into the white-dwarf stage is still under way. The same argument would indicate that the transition of the stellar remnant of B Cas into a white dwarf is much more advanced. As mentioned previously, the photographic surface brightness of the shell of B Cas is fainter than 25 mag. per square second of arc. On the assumption that the distance ($m-M = 10$) and linear rate of expansion ($V = 1000$ km/sec) are about the same as those of the Crab nebula, the present shell of B Cas should have a diameter of the order of 2 minutes of arc and hence an integrated apparent magnitude $m_{pg} \geqq +15$. The corresponding absolute magnitude, which may be taken as the bolometric magnitude of the central star, is $M_{bol} \geqq +5^{M}$, compared with $M_{bol} = -1^{M}$ for the central star of the Crab nebula. This would indicate that the surface temperature of the stellar remnant of B Cas is, at best, only one-fourth of that of the central star of the Crab, or $\sim 1.10^{5}$ degrees. Although our reasoning has admittedly been crude, the result obtained should be of the right order. It strongly suggests that the stellar remnant of B Cas is probably not far from the final white-dwarf state. The low absolute magnitude of the star, $M_{pg} \geqq +9$, points in the same direction.

It is impossible at present to press the search for the stellar remnant of B Cas to still fainter limits, since the nova, on account of its high declination, cannot be reached with the 100-inch telescope. However, there is every prospect that it will be found when the 200-inch telescope comes into operation.

---

that time. The position computed by Hind (*M.N.*, **21**, 233, 1861), which has been frequently used by recent observers, deviates from this position by 1′.8 and is obviously wrong, as Argelander has already pointed out.

[16] R. Minkowski, *Mt. W. Contr.*, No. 666; *Ap. J.*, **96**, 199, 1942.

SIX-COLOR PHOTOMETRY OF STARS

III. THE COLORS OF 238 STARS OF DIFFERENT SPECTRAL TYPES*

JOEL STEBBINS[1] AND A. E. WHITFORD[2]
Mount Wilson Observatory and Washburn Observatory
Received June 8, 1945

ABSTRACT

Colors have been obtained for 238 stars of all spectral types from O to M by measuring intensities in six spectral regions from λ 3530 to λ 10,300 A (Tables 2 and 3). The early-type stars from O to B3 show small dispersion in intrinsic color, but many are strongly affected by space reddening. A dozen late-type giants in low latitudes are likewise affected. The most marked effect of absolute magnitude is near spectrum K0, where the colors of dwarfs, ordinary giants, and supergiants are all different (Fig. 1).

The observed colors of the stars agree closely with the colors of a black body at suitable temperatures (Fig. 2). The derived relative color temperatures are based upon the mean of ten stars of spectrum dG6 with an assumed temperature of 5500°K. On this scale the values are 23,000° for O stars, 11,000° for A0, and 5950° for dG0. An alternative scale, with 6700° and spectrum dG2 for the sun, gives 140,000° for O stars, 16,000° for A0, and 6900° for dG0 (Table 7). A definitive zero point for the temperature scale has not been determined.

The bluest O and B stars agree very well with each other, but there is still the possibility that all are slightly affected by space reddening. A dozen bright stars of the Pleiades seem normal for their type. The colors of P Cygni are anomalous, as is the space reddening of the Trapezium cluster of Orion (Figs. 3 and 4).

Comparisons of the new colors with the International colors and our previous photoelectric colors C_1 of the North Polar Sequence give the ratios of the scales of color index. These ratios depend upon whether change of color is caused by change of spectral type or by change of space reddening (Table 11). Good agreement is found with the Greenwich gradients and especially with the results of the spectrophotometry by John S. Hall (Fig. 5).

I. THE OBSERVATIONS

The various kinds of stellar photometry may be classified as one-color, two-color, multicolor, and spectrophotometry, depending upon the number of spectral regions selected for measurement. Except in spectrophotometry the spectral regions are determined by the characteristics of the receiver, such as the eye, the photographic plate, the photoelectric cell, the thermocouple, etc., or by a combination of such a receiver with filters suitable for the desired result. Even with a black-body receiver like the thermocouple, equally receptive to all wave lengths, the measured responses to radiation are dependent upon the transmission of the atmosphere and of the optical system involved. When a dispersing agent like a prism or grating is used, it is possible to isolate a small range of wave lengths; and since the smaller the spectral range the less will be the total energy available, it follows that anything approaching monochromatic photometry of stars will need a large telescope. In fact, stellar spectroscopy with high dispersion may be looked upon as the natural application of stellar photometry to narrow regions of wave length.

The present six-color photometry of stars lies between one- and two-color photometry, on the one hand, and spectrophotometry, on the other. Obviously, measures in six spectral regions should give more information than measures in only two, while they should be easier to obtain than measures for the entire spectrum. The photocell gives a linear scale of response over a wide range of intensities and of wave lengths; also, freedom from many difficulties of photographic photometry. But, despite these advantages, there re-

* *Contributions from the Mount Wilson Observatory, Carnegie Institution of Washington*, No. 712.

[1] Research Associate of the Mount Wilson Observatory, Carnegie Institution of Washington.

[2] On leave at Massachusetts Institute of Technology.

main the limitations of any method where spectral regions extending over a thousand or more angstroms are integrated by the receiver into a single intensity. The effects of strong absorption lines or bands are buried in the results. In this respect the present work has the same drawback as ordinary photographic photometry; but even in spectrophotometry, where measures are limited to the continuous spectrum between spectral lines, there is always the possibility of a veil over the surface of a star which will modify the ideal black-body radiation, even if such were emitted in the first place. It remains to be seen what is the best method for deriving the color temperature of a star; up to the present there is much disagreement among the results from all methods.

Our photometer with a photocell and six filters was devised primarily for measures of extragalactic nebulae; but for the observations to be significant, such nebulae must be referred to standard stars of different spectral types. In the course of the work, so much

TABLE 1

OBSERVATIONS OF α URSAE MINORIS, AUGUST 18, 1944

	Color					
	U	V	B	G	R	I
λ (A)	3530	4220	4880	5700	7190	10,300
$1/\lambda$ (μ^{-1})	2.83	2.37	2.05	1.75	1.39	0.97
a	$0^m.530$	$0^m.292$	$0^m.180$	$0^m.136$	$0^m.058$	$0^m.030$
Deflection, d	27.8	50.1	74.4	65.8	58.4	60.8
log d	1.444	1.700	1.872	1.818	1.766	1.784
0.4 a sec z	0.382	0.210	0.130	0.098	0.042	0.022
log d_0	1.826	1.910	2.002	1.916	1.808	1.806
log (B, G, R) − log d_0	+ 0.083	− 0.001	− 0.093	− 0.007	+ 0.101	+ 0.103
Δ mag.	+ 0.21	0.00	− 0.23	− 0.02	+ 0.25	+ 0.26
Reduction to standard	− .06	− .14	+ .17	− .01	− .16	− .07
Final color	+ .15	− .14	− .06	− .03	+ .09	+ .19
Another set	+ .18	− .14	− .06	.00	+ .06	+ .17
Mean	$+ 0^m.165$	$- 0^m.14$	$- 0^m.06$	$- 0^m.015$	$+ 0^m.075$	$+ 0^m.18$
Av. deviation	± 0.015	± 0.00	± 0.00	± 0.015	± 0.015	± 0.010

of interest was found in the measures of various stars that this secondary program of calibration has perhaps grown to outweigh in emphasis the original program on the nebulae. We found that measures of normal and reddened B-type stars[3] gave a new determination of the law of space reddening by interstellar material, and other possibilities were opened up by the wide spectral range from 3530 A to 10,300 A.

The observations used in the present paper were made at Mount Wilson during the five summers of 1940–1944. Some measures were made with the 100-inch reflector, but most of them with the 60-inch, which, besides having the advantage of reaching the pole, is, in general, more readily manipulated than the larger telescope. A description of the installation and the methods of observation and reduction is given in our paper on B stars,[3] but a sample reduction is given here.

In Table 1, giving data for α Ursae Minoris, the designations of the different quantities under each color are mostly self-explanatory. The units used in Table 1 and throughout this paper are: angstroms for λ, microns $^{-1}$ for $1/\lambda$, and stellar magnitude for colors. In the next line below $1/\lambda$ in Table 1, is given a, the extinction in magnitude at the zenith. The deflection d, in millimeters, is the mean of two deflections, taken forward

[3] *Mt. W. Contr.*, No. 680; *Ap. J.*, **98**, 20, 1943.

and backward through the colors. For this bright star a 3-mag. absorbing screen over the large mirror was used; also, a shunt on the galvanometer giving one-third the full sensitivity. To log d is added 0.4 a sec z to obtain log d_0 for outside the atmosphere. The log d_0 is then subtracted from 1.909, the corresponding mean of blue, green, and red, to obtain Δ log; then Δ mag. $= 2.5\Delta$ log. The reduction to standard color, applied to the Δ mag., gives the final color referred to the mean of ten stars of average spectrum dG6. The results of a second set of observations, made the same night, are in the next line, and then the mean. The average deviation in all the colors from the mean of two sets is ± 0.009 mag., which is not particularly good for successive measures on the same night.

The use of a mean extinction coefficient for each color is justified by the accordance of the results for the same star at different zenith distances on different nights and in different seasons. A control on the extinction is given by measures of a polar star, usually NPS 4; this control also takes care of any variation in the color sensitivity of the photocell. Usually, in a run of several good nights the colors of the control star remain nearly enough the same, but occasionally an increased extinction will appear in the ultraviolet—say several hundredths, or even a tenth, of a magnitude. But there are also variations in the infrared, caused presumably by the strong water-vapor bands ρ and Φ on either side of the effective wave length at 10,300 A. Usually, for several nights we can assume constant reductions to standard for the other colors; but the infrared requires a "floating" correction for each run, or occasionally for a single night. For instance, the infrared correction in one season was determined as follows:

1944 July	12–13	$+0^m.03$
July	20–23	$-$ .03
Aug.	17–20	$-$ .07
Aug.	21	$-$ .04
Sept.	9–11	+0.02

Between the summers of 1940 and 1941 there were real changes in the photocell, amounting to more than 0.10 mag. between adjacent colors; but since 1941 the cell has been nearly constant. When a change in the cell is mixed up with a variation in the atmospheric extinction, the corrections on account of the cell are the same for all stars, while the corrections for the extinction vary with the air mass at different zenith distances. Moreover, in all strictness, for each filter the amount of the extinction depends upon the spectral type of the observed star; the redder the star, the longer the effective wave length and hence the smaller the extinction. For this reason it is impractical to determine the extinction thoroughly and accomplish anything else. We simply have to assume average conditions over several nights and be on the lookout for large discrepancies.

The net result of the outstanding errors is, for bright stars, to raise the probable error of a single determination to something like ± 0.02 mag. for the ultraviolet and infrared and to about half that amount for the other colors. For Polaris, in Table 1, the agreement between the two sets on the same night is only fair; there are many cases of better agreement for other stars even on different nights. We have in hand a study of the light and color variation of Polaris in the well-known period of 3.96 days. The approximate range is 0.16 mag. in U $-$ I, corresponding to a variation in the spectrum from cF7 to cF8.

In Table 2 the stars of the present work are listed in the order of the HD number, together with the right ascensions and declinations and the galactic co-ordinates l and b referred to the pole of the Lund tables, 12^h40^m, $+ 28^\circ.0$ (1900). The spectra in Table 2 are for index purposes only; they refer to the sections of Table 3 where the definite spectra and colors are arranged by types. The O and B stars previously published are included here, with additions, corrections, and revisions. The list of stars includes 75 O to B3 stars with different degrees of space reddening; 94 stars of the main sequence from B5 to M0; and 69 giant stars, mostly supergiants, from F3 to M7.

TABLE 2

LIST OF STARS OBSERVED

HD	Spec.	R.A. 1900	Dec. 1900	l	b	HD	Spec.	R.A. 1900	Dec. 1900	l	b
432	dF2	0h 3m8	+58° 36′	85°3	− 3°1	132813	gM5	14h56m0	+66° 20′	71°0	+46°4
571	cF2	0 5.1	+45 31	83.7	−16.1	133208	gG5	14 58.2	+40 47	33.5	+59.0
1064	B9	0 9.8	−10 7	66.9	−70.8	135722	gG4	15 11.5	+33 41	19.6	+57.2
1337	O8	0 12.5	+50 53	85.6	−10.9	136064	dF9	15 13.5	+67 44	70.8	+44.2
2905	B0	0 27.3	+62 23	88.5	+ 0.5	137422	A1	15 20.9	+72 11	74.9	+40.8
3651	dK1	0 34.2	+20 43	88.2	−41.3	142143	gM7	15 47.8	+48 47	43.3	+48.6
3765	dK5	0 35.3	+39 39	89.0	−22.3	142373	dF7	15 49.2	+42 44	34.1	+49.3
4406	dG3	0 41.3	+45 49	90.2	−16.2	143807	A1	15 57.4	+30 7	15.2	+47.2
4727	B5	0 44.3	+40 32	90.9	−21.5	144205	gM6	15 59.6	+47 31	40.9	+46.9
5394	B0	0 50.7	+60 11	91.3	− 1.8	144206	B8	15 59.6	+46 19	39.1	+47.1
5914	A5	0 55.6	+88 29	90.1	+26.5	145328	gK1	16 5.3	+36 45	25.1	+46.3
6920	dF7	1 4.6	+41 33	94.9	−20.2	147365	A9	16 16.5	+39 57	29.8	+44.3
8890	cF7	1 22.6	+88 46	90.3	+26.8	147379	dM0	16 16.5	+67 29	66.4	+39.2
9270	gG3	1 26.1	+14 50	106.1	−45.7	147394	B7	16 16.7	+46 33	39.0	+44.1
10204	A9	1 34.7	+42 47	100.5	−18.1	148478	gM1	16 23.3	−26 13	319.8	+13.7
10307	dG0	1 35.7	+42 7	100.9	−18.7	148783	gM6	16 25.4	+42 6	32.9	+42.7
10516	B0	1 37.4	+50 11	99.3	−10.8	151288	dM0	16 41.4	+33 41	22.3	+38.6
14622	dF2	2 16.6	+40 57	108.9	−17.5	152391	dG9	16 48.0	+ 0 11	346.1	+24.6
14633	O8	2 16.7	+41 2	108.9	−17.4	152601	gK3	16 49.2	− 5 59	340.7	+21.1
14662	cF8	2 16.9	+54 55	103.7	− 4.5	153344	dG4	16 53.8	+62 16	58.7	+36.8
15830	dG5	2 27.7	+42 21	110.3	−15.4	154345	dK0	16 59.8	+47 12	39.8	+36.8
16397	dG0	2 32.6	+30 24	116.9	−25.7	156729	A0	17 14.2	+37 24	28.4	+32.8
16901	cG0	2 37.6	+43 52	111.3	−18.3	157056	B2	17 15.9	−24 54	328.2	+ 5.1
19356	B9	3 1.7	+40 34	117.0	−14.0	157779	B9	17 20.2	+37 14	28.5	+31.6
20123	cG2	3 9.1	+50 34	112.7	− 4.8	157910	gG2	17 21.0	+37 2	28.3	+31.4
20902	cF4	3 17.2	+49 30	114.4	− 5.0	159181	cG2	17 28.2	+52 23	46.5	+32.5
23288	B7	3 38.9	+23 59	134.1	−22.5	163506	cF5	17 51.4	+26 4	18.8	+21.9
23302	B7	3 39.0	+23 48	134.2	−22.6	163770	cK1	17 52.8	+37 16	30.5	+25.3
23324	B8	3 39.2	+24 32	133.8	−22.0	164514	cA6	17 56.4	−22 54	334.8	− 1.7
23338	B7	3 39.3	+24 10	134.0	−22.3	166182	B2	18 4.4	+20 48	14.9	+17.1
23408	B9	3 39.9	+24 4	134.2	−22.3	166205	A2	18 4.5	+86 37	86.2	+28.5
23432	B8	3 40.0	+24 15	134.1	−22.1	166620	dK2	18 6.3	+38 27	32.5	+23.1
23441	B9	3 40.1	+24 13	134.1	−22.1	166734	B0	18 6.9	−10 46	346.6	+ 2.2
23480	B6	3 40.4	+23 39	134.6	−22.5	166926	A3	18 7.8	+87 0	86.6	+28.4
23630	B7	3 41.5	+23 48	134.7	−22.2	169034	B0	18 17.6	−13 39	345.3	− 1.6
23753	B8	3 42.5	+23 8	135.4	−22.6	169454	B1	18 19.6	−14 2	345.2	− 2.2
23850	B8	3 43.2	+23 45	135.0	−22.0	171635	cF8	18 30.8	+56 58	53.3	+24.4
23862	B8	3 43.3	+23 51	135.0	−21.9	171779	gG5	18 31.7	+52 16	48.4	+23.0
24398	B1	3 47.8	+31 35	130.3	−15.5	171871	B2	18 32.0	+51 2	47.1	+22.6
24504	B7	3 48.8	+47 35	119.7	− 3.3	172167	A1	18 33.6	+38 41	34.8	+18.2
24760	B2	3 51.1	+39 43	125.2	− 9.0	173638	cF4	18 41.2	−10 14	351.1	+ 5.0
24912	O7	3 52.5	+35 30	128.3	−12.0	173648	A9	18 41.3	+37 30	34.2	+16.4
29139	gK5	4 30.2	+16 18	148.9	−18.8	173649	A3	18 41.3	+37 30	34.2	+16.4
31964	cF2	4 54.8	+43 41	130.5	+ 2.4	174488	gM4	18 51.0	+36 46	34.3	+14 3
34085	B8	5 9.7	− 8 19	177.0	−23.7	175865	gM5	18 52.3	+43 49	41.2	+16.9
34759	B5	5 14.7	+41 43	134.2	+ 4.2	178770	gM6	19 4.8	+39 0	37.6	+12.8
36486	B0	5 26.9	− 0 22	171.5	−16.3	180163	B5	19 10.4	+38 58	38.1	+11.8
37022	(B0)	5 30.4	− 5 27	176.6	−17.9	182917	gM6	19 21.9	+50 3	49.2	+14.9
37128	B0	5 31.1	− 1 16	172.9	−15.8	183030	gM1	19 22.5	+88 59	88.9	+27.8
37742	B0	5 35.7	− 2 0	174.1	−15.1	183912	gK0	19 26.7	+27 45	29.7	+ 3.5
39801	gM2	5 49.8	+ 7 23	167.5	− 7.5	183914	B9	19 26.7	+27 45	29.7	+ 3.5
41074	A8	5 57.9	+42 59	137.3	+11.7	184279	B2	19 28.6	+ 3 34	8.9	− 9.0
51802	gM0	6 53.7	+87 12	93.2	+28.1	184915	B0	19 31.5	− 7 15	359.6	−14.7
66368	A3	7 58.0	+88 56	91.1	+28.4	186994	B0	19 42.5	+44 43	46.1	+ 9.3
103483	A0	11 49.9	+47 2	113.9	+68.6	187076	gM2	19 42.9	+18 17	23.5	− 4.6
107113	dF4	12 13.9	+86 59	90.4	+31.0	187138	gG9	19 43.3	+88 41	88.6	+27.6
107192	dF2	12 14.4	+88 15	90.2	+29.7	187642	A1	19 45.9	+ 8 36	15.6	−10.2
109358	dG0	12 29.0	+41 54	98.4	+75.9	188209	O8	19 49.0	+46 47	48.5	+ 9.4
111395	dG6	12 43.9	+25 23	286.4	+87.3	188252	B2	19 49.2	+47 41	49.3	+ 9.8
111812	dF5	12 46.8	+28 5	4.3	+88.5	188439	B2	19 50.1	+47 34	49.3	+ 9.6
112413	A1	12 51.4	+38 52	78.4	+78.9	188892	B5	19 52.3	+38 13	41.5	+ 4.3
112570	gK0	12 52.6	+46 44	83.3	+71.1	+35°3955	B0	20 2.2	+35 32	40.3	+ 1.2
113139	A6	12 56.5	+56 55	85.4	+60.9	190919	B1	20 2.2	+35 24	40.2	+ 1.1
113865	A3	13 1.5	+29 34	20.0	+85.0	191201	B0	20 3.6	+35 26	40.4	+ 0.9
114282	gK2	13 4.5	+88 11	89.8	+29.8	192107	gK5	20 8.1	− 1 19	9.5	−20.0
114710	dG0	13 7.2	+28 23	5.1	+84.0	192281	O5	20 9.0	+39 58	44.8	+ 2.6
115735	A0	13 14.0	+50 12	76.1	+66.9	192422	B0	20 9.7	+38 28	43.6	+ 1.6
118216	dF2	13 30.3	+37 42	45.9	+75.7	192639	O7	20 10.8	+37 3	42.6	+ 0.6
120315	B3	13 43.6	+49 49	65.2	+65.0	192640	A1	20 10.8	+36 30	42.1	+ 0.3
120933	gM2	13 47.4	+34 56	30.1	+74.1	192876	cG5	20 12.1	−12 49	358.9	−26.2
121409	A0	13 50.1	+54 13	68.8	+60.8	192947	gG8	20 12.5	−12 51	358.9	−26.3
125162	A0	14 12.6	+46 33	51.8	+64.0	193183	B2	20 13.8	+37 55	43.6	+ 0.5
125351	gK1	14 13.8	+35 58	47.9	+68.6	193237	B1	20 14.1	+37 43	43.5	+ 0.4
126327	gM7	14 19.7	+26 11	1.1	+67.8	193322	O8	20 14.6	+40 25	45.8	+ 2.0
127762	A5	14 28.1	+38 45	32.6	+65.1	193370	cF5	20 14.8	+34 40	41.1	− 1.4
128165	dK5	14 30.2	+53 20	59.0	+57.6	193443	O9	20 15.2	+37 57	43.8	+ 0.3
128998	A0	14 35.1	+54 27	59.7	+56.3	193514	O8	20 15.5	+38 57	44.7	+ 1.0

TABLE 2—*Continued*

HD	Spec.	R.A. 1900	Dec. 1900	l	b	HD	Spec.	R.A. 1900	Dec. 1900	l	b
193536	B2	20h15m6	+46° 0′	50°.4	+ 5°.1	209339	B0	21h57m6	+62° 0′	72°.1	+ 5°.7
194093	cF7	20 18.6	+39 56	45.8	+ 1.1	209750	cG1	22 0.6	− 0 48	28.5	−43.2
194279	B2	20 19.7	+40 26	46.3	+ 1.2	209772	gM5	22 0.9	+62 38	72.8	+ 6.0
194335	B3	20 20.0	+37 10	43.8	− 0.8	209975	O9	22 2.1	+61 48	72.4	+ 5.3
194839	B0	20 22.8	+41 3	47.2	+ 0.9	210745	cK5	22 7.4	+57 42	70.7	+ 1.5
195295	cF4	20 25.3	+30 2	38.7	− 6.0	210839	O6	22 8.1	+58 56	71.5	+ 2.5
195592	B0	20 27.2	+43 59	50.0	+ 2.3	211336	A6	22 11.4	+56 33	70.6	+ 0.2
195593	cF5	20 27.2	+36 36	44.2	− 2.3	212455	B3	22 19.3	+54 44	70.6	− 2.1
196321	gK5	20 31.5	− 2 54	11.2	−25.9	212710	B9	22 21.3	+85 36	87.3	+24.4
197345	A2	20 38.0	+44 55	51.9	+ 1.4	213087	B0	22 23.9	+64 37	76.1	+ 6.3
197770	B2	20 40.7	+56 46	61.4	+ 8.6	213306	cF4	22 25.4	+57 54	72.9	+ 0.4
198084	dF9	20 42.9	+57 13	61.9	+ 8.7	213310	gM0	22 25.4	+47 12	67.6	− 8.9
198478	B2	20 45.5	+45 45	53.4	+ 0.9	214168	B3	22 31.4	+39 7	64.5	−16.5
198781	B1	20 47.5	+63 40	67.3	+12.3	214665	gM4	22 34.7	+56 17	73.2	− 1.6
198846	O9	20 48.1	+34 17	45.1	− 7.0	214680	O9	22 34.8	+38 32	64.8	−17.3
199081	B3	20 49.7	+44 0	52.6	− 0.8	214868	gK2	22 36.1	+43 45	67.6	−12.8
199216	B1	20 50.7	+49 9	56.6	+ 2.3	214993	B1	22 37.0	+39 43	65.8	−16.5
199478	B8	20 52.4	+47 2	55.2	+ 0.9	215766	A0	22 42.4	−14 35	20.1	−59.6
199579	O6	20 53.1	+44 33	53.4	− 0.9	216411	B1	22 47.6	+58 28	75.7	− 0.4
200120	B3	20 56.4	+47 8	55.7	+ 0.4	216494	B9	22 48.2	−12 9	25.6	−59.5
200857	B2	21 1.0	+54 51	61.8	+ 5.2	217101	B2	22 53.1	+38 48	68.3	−18.7
200905	cK5	21 1.3	+43 32	53.7	− 2.7	217476	cG3	22 55.9	+56 25	75.9	− 2.7
201601	cF1	21 5.5	+ 9 44	28.1	−25.9	218173	B9	23 0.7	− 8 29	35.0	−59.5
201819	B1	21 7.0	+35 53	48.9	− 8.8	218342	B1	23 2.1	+62 41	79.0	+ 2.8
202751	dK6	21 12.9	− 0 15	20.0	−33.3	218356	cK0	23 2.2	+24 56	63.7	−32.1
203064	O8	21 14.8	+43 31	55.4	− 4.4	218376	B1	23 2.4	+58 53	77.7	− 0.8
203280	A3	21 16.2	+62 10	68.5	+ 8.9	218634	gM4	23 4.5	+ 8 8	53.9	−47.1
203374	B0	21 16.7	+61 25	68.0	+ 8.4	218639	A0	23 4.5	−15 3	25.4	−64.4
203938	B1	21 20.2	+46 44	58.3	− 2.7	218753	A9	23 5.5	+58 47	78.0	− 1.0
204075	cG4	21 21.0	−22 51	354.9	−45.1	219659	A0	23 12.4	−12 16	33.1	−64.2
204172	B0	21 21.7	+36 14	51.3	−10.6	219833	A0	23 13.8	−12 43	32.9	−64.7
204867	cG1	21 26.3	− 6 1	16.3	−39.2	220020	A0	23 15.4	− 9 28	38.9	−62.8
205021	B1	21 27.4	+70 7	74.9	+14.0	221525	gF0	23 27.8	+86 45	88.9	+24.9
205139	B1	21 28.3	+60 1	68.1	+ 6.4	222574	cG1	23 36.6	−18 22	30.1	−72.6
205196	B0	21 28.6	+57 4	66.2	+ 4.1	222661	B9	23 37.5	−15 6	38.5	−70.6
206165	B2	21 35.2	+61 38	69.8	+ 7.0	222847	B9	23 39.0	−18 50	30.0	−73.3
206773	B0	21 39.3	+57 17	67.4	+ 3.4	222935	dK2	23 40.0	+29 0	74.6	−31.2
206778	cK0	21 39.3	+ 9 25	33.9	−32.5	223640	B9	23 46.2	−19 28	31.9	−75.0
206859	cG3	21 39.8	+16 53	40.3	−27.4	224014	cG0	23 49.4	+56 57	83.1	− 4.4
206936	gM2	21 40.4	+58 19	68.2	+ 4.1	224572	B2	23 53.9	+55 12	83.4	− 6.2
207198	O9	21 42.2	+61 59	70.7	+ 6.9	225132	A0	23 58.6	−17 54	44.5	−76.1
207538	O9	21 44.6	+59 14	69.2	+ 4.5	225212	cK5	23 59.4	−11 4	58.7	−70.6

In Table 3 the first column gives the HD number; an asterisk (*) indicates a note at the end of the table. The second column gives the name of the star, if it has one. In the column headed "Z," an "i" denotes that the star is in E. P. Hubble's[4] zone of avoidance of the extragalactic nebulae; "o" indicates that the star is out of the zone; and "?" that it is near the border. The exact position may be found in Table 2.

The magnitude m is always visual. If given to hundredths, it is the Harvard photometric magnitude; if to tenths, it is usually a visual magnitude derived from photoelectric measures, with Harvard magnitudes as a standard. A colon (:) designates a DM visual magnitude from the *Henry Draper Catalogue*. For a variable star either the maximum magnitude or the maximum and minimum are given. For a double star the magnitude of the measured component is marked with a dagger (†). The column headed "M," which begins with the F dwarfs, gives the visual absolute magnitude from Mount Wilson[5].

The spectra in Table 3 are from different sources. The O to B5 stars were taken from Plaskett and Pearce,[6] supplemented by the lists of Be and cB stars of P. W. Merrill[7] and

[4] *Mt. W. Contr.*, No. 485, p. 34; *Ap. J.*, **79**, 41, 1934.

[5] *Mt. W. Contr.*, Nos. 244, 262, 511, 668; *Ap. J.*, **56**, 242, 1922; **57**, 294, 1923; **81**, 187, 1935; **96**, 344, 1942.

[6] *Pub. Dom. Ap. Obs.*, **5**, 99, 1931.

[7] *Mt. W. Contr.*, Nos. 471, 512, 576, 682; *Ap. J.*, **78**, 87, 1933; **81**, 351, 1935; **86**, 274, 1937; **98**, 153, 1943.

TABLE 3

COLORS OF 238 STARS

HD	Name	Z	m	Spec.	U	V	B	G	R	I	V−I	Obs.
					O Stars							
14633		o	7.3	O8	−2.27	−1.17	−0.53	−0.03	+0.57	+1.38	−2.55	4
214680	10 Lac	o	4.91	O9s	−2.26	−1.16	− .53	− .05	+ .58	+1.33	−2.49	5
1337		i	6.12	O8n	−2.11	−1.07	− .46	− .05	+ .51	+1.14	−2.21	1
198846*	Y Cyg	i	7.1	O9nn	−1.96	−0.98	− .44	− .05	+ .49	+1.14	−2.12	4
188209		i	5.51	O8s	−2.02	− .99	− .44	− .05	+ .48	+1.09	−2.08	2
203064	68 Cyg	i	5.06	O8nn	−1.93	− .91	− .36	− .04	+ .40	+0.91	−1.82	2
24912	ξ Per	i	4.05	O7n	−1.85	− .89	− .36	− .03	+ .40	+ .91	−1.80	1
199579		i	6.01	O6	−1.77	− .84	− .35	− .03	+ .38	+ .86	−1.70	1
209975	19 Cep	i	5.17	O9	−1.73	− .81	− .34	− .04	+ .37	+ .81	−1.62	2
193322		i	5.82	O8	−1.64	− .75	− .31	− .04	+ .35	+ .82	−1.57	1
210839	λ Cep	i	5.19	O6nf	−1.48	− .61	− .23	− .01	+ .24	+ .56	−1.17	1
207198		i	5.97	O9s	−1.31	− .55	− .18	− .02	+ .20	+ .48	−1.03	1
207538		i	7.03	O9ss	−1.22	− .47	− .15	− .03	+ .18	+ .50	−0.97	2
192639		i	7.02	O7f	−1.23	− .49	− .16	− .02	+ .18	+ .38	−0.87	1
192281		i	7.47	O5	−1.16	− .43	− .10	− .01	+ .12	+ .37	−0.80	2
193443		i	7.4	O9	−1.12	− .45	− .13	− .02	+ .15	+ .33	−0.78	2
193514		i	7.29	O8	−0.95	−0.35	−0.07	+0.01	+0.05	+0.13	−0.48	2
					B0 Stars							
36486	δ Ori	o	2.48	B0	−2.22	−1.15	−0.53	−0.05	+0.58	+1.37	−2.52	4
5394*	γ Cas	i	2.25	B0ne	−2.21	−1.17	− .55	− .05	+ .61	+1.33	−2.50	3
37742	ζ Ori	o	2.05	B0ne	−2.18	−1.11	− .51	− .04	+ .56	+1.32	−2.43	2
37128	ε Ori	o	1.75	cB0e	−2.12	−1.10	− .50	− .04	+ .54	+1.27	−2.37	2
186994*		?	7.3	B0	−1.99	−1.04	− .44	− .05	+ .48	+1.16	−2.20	3
204172	69 Cyg	?	5.84	B0	−2.04	−1.02	− .45	− .05	+ .49	+1.16	−2.18	3
184915	κ Aql	?	5.04	B0n	−1.61	−0.83	− .33	− .05	+ .38	+0.92	−1.75	1
209339		i	6.48	B0	−1.74	− .86	− .36	− .04	+ .39	+ .86	−1.72	1
10516	φ Per	?	4.19	B0ne	−1.88	− .91	− .36	− .00	+ .36	+ .80	−1.71	2
2905	κ Cas	i	4.24	cB0e	−1.64	− .77	− .30	− .04	+ .35	+ .73	−1.50	2
191201		i	7.12	B0	−1.53	− .71	− .25	− .03	+ .28	+ .76	−1.47	1
37022*	θ^1 Ori	o	.....	(B0)	−1.64	− .74	− .29	+ .02	+ .27	+ .56	−1.30	2
+35°3955		i	7.3	B0	−1.39	− .63	− .23	− .07	+ .30	+ .55	−1.18	1
206773		i	6.98	B0ne	−1.51	− .61	− .18	− .03	+ .21	+ .48	−1.09	1
213087	26 Cep	i	5.66	cB0	−1.19	− .55	− .15	− .03	+ .18	+ .52	−1.07	1
203374		i	6.64	B0ne	−1.33	− .53	− .17	− .01	+ .18	+ .43	−0.96	1
192422*		i	7.10	cB0	−0.99	− .37	− .06	− .01	+ .07	+ .10	−0.47	2
205196		i	7.36	cB0	−0.77	− .12	+ .02	+ .02	− .04	− .12	0.00	1
195592		i	7.15	cB0e	−0.14	+ .13	+ .18	+ .04	− .21	− .62	+0.75	3
194839		i	7.45	cB0e	+0.09	+ .34	+ .30	+ .01	− .31	−0.80	+1.14	3
166734*		i	8.8	B0e	+0.09	+ .40	+ .38	+ .05	− .43	−1.06	+1.46	3
169034*		i	8.6	cB0	+0.66	+0.63	+0.50	+0.05	−0.55	−1.38	+2.01	2
					B1 Stars							
205021*	β Cep	i	3.32	B1	−2.13	−1.17	−0.54	−0.07	+0.61	+1.36	−2.53	2
201819		?	6.40	B1n	−2.04	−1.07	− .47	− .05	+ .53	+1.24	−2.31	2
214993*	12 Lac	o	5.18	B1s	−1.97	−1.08	− .48	− .04	+ .52	+1.21	−2.29	4
218376	1 Cas	i	4.93	cB1	−1.88	−0.97	− .42	− .05	+ .47	+1.06	−2.03	2
198781		i	6.38	B1n	−1.67	− .87	− .35	− .04	+ .38	+0.85	−1.72	1
24398	ζ Per	i	2.91	cB1	−1.59	− .79	− .33	− .04	+ .37	+ .78	−1.57	1
205139		i	5.52	B1s	−1.57	− .73	− .29	− .01	+ .31	+ .75	−1.48	1
190919		i	7.30	cB1	−1.30	− .61	− .17	− .02	+ .20	+ .60	−1.21	1
218342		i	7.46	cB1	−1.11	− .42	− .12	+ .03	+ .08	+ .22	−0.64	1
199216		i	7.13	cB1	−0.87	− .35	− .03	− .03	+ .06	+ .25	−0.60	1
193237	P Cyg	i	4.88	B1eq	−1.10	− .40	− .08	+ .02	+ .06	+ .16	−0.56	2
203938		i	7.10	cB1	−0.78	− .33	− .07	− .01	+ .08	+ .15	−0.48	1
216411		i	7.16	cB1e	−0.72	− .17	− .03	+ .04	− .01	− .08	−0.09	2
169454		i	6.84	cB1e	+0.03	+0.28	+0.30	+0.02	−0.31	−0.76	+1.04	2

TABLE 3—*Continued*

HD	Name	Z	m	Spec.	U	V	B	G	R	I	V−I	Obs.
						B2 Stars						
24760	ϵ Per	i	2.96	B2	−2.12	−1.14	−0.53	−0.07	+0.60	+1.33	−2.47	1
188252		?	5.70	B2s	−1.96	−1.08	− .49	− .05	+ .54	+1.24	−2.32	1
157056*	θ Oph	i	3.37	B2	−1.92	−1.11	− .54	− .05	+ .60	+1.21	−2.32	1
217101		o	6.07	B2	−1.90	−1.05	− .50	− .05	+ .55	+1.21	−2.26	1
166182	102 Her	o	4.32	B2s	−1.77	−1.02	− .47	− .04	+ .51	+1.24	−2.26	2
193536		i	6.28	B2	−1.75	−1.03	− .49	− .06	+ .54	+1.17	−2.20	1
171871		o	7.39	B2s	−1.79	−1.07	− .44	− .02	+ .46	+1.08	−2.15	1
224572	σ Cas	i	4.93	B2n	−1.87	−1.01	− .45	− .05	+ .50	+1.11	−2.12	1
188439		?	6.15	B2nn	−1.92	−0.99	− .43	− .06	+ .49	+1.12	−2.11	1
184279		i	6.78	B2se	−1.62	− .85	− .37	− .05	+ .42	+0.84	−1.69	1
206165	9 Cep	i	4.78	cB2	−1.19	− .59	− .20	− .04	+ .25	+ .47	−1.06	1
197770		i	6.36	cB2	−1.08	− .53	− .18	− .03	+ .22	+ .44	−0.97	1
198478	55 Cyg	i	4.89	cB2e	−0.98	− .43	− .12	− .01	+ .12	+ .23	−0.66	2
193183		i	7.12	cB2	−0.88	− .38	− .08	− .02	+ .10	+ .22	−0.60	2
200857		i	7.16	cB2	−0.52	− .25	+ .01	− .03	+ .02	− .02	−0.23	1
194279		i	7.05	cB2	+0.20	+0.36	+0.34	+0.03	−0.37	−0.92	+1.28	2
						B3 Stars						
120315	η UMa	o	1.91	B3n	−1.80	−1.12	−0.52	−0.06	+0.58	+1.28	−2.40	2
194335		i	5.68	B3ne	−2.05	−1.11	− .50	− .06	+ .56	+1.22	−2.33	2
199081	57 Cyg	i	4.68	B3	−1.65	−1.06	− .50	− .05	+ .55	+1.20	−2.26	3
214168	8 Lac, A	o	5.83	B3ne	−1.94	−1.06	− .45	− .04	+ .49	+1.16	−2.22	1
200120	59 Cyg	i	4.86	B3ne	−2.00	−1.00	− .41	− .02	+ .43	+1.06	−2.06	2
212455*		i	8.0	cB3	−0.87	−0.47	−0.11	−0.03	+0.14	+0.25	−0.71	1
						B5–B9 Stars						
147394	τ Her	o	3.91	B7s	−1.64	−1.09	−0.50	−0.07	+0.57	+1.22	−2.31	2
34759	ρ Aur	i	5.12	B5n	−1.61	−1.07	− .48	− .06	+ .54	+1.22	−2.29	1
4727	ν And	o	4.42	B5s	−1.63	−1.07	− .50	− .05	+ .55	+1.16	−2.23	2
180163	η Lyr	?	4.46	B5s	−1.70	−1.06	− .47	− .05	+ .52	+1.14	−2.20	2
23338	19 Tau	o	4.37	B7n	−1.43	−1.01	− .48	− .05	+ .52	+1.11	−2.12	3
23302	17 Tau	o	3.81	B7n	−1.38	−1.03	− .49	− .05	+ .54	+1.08	−2.11	1
223640	108 Aqr	o	5.32	B9sp	−1.30	−0.98	− .47	− .05	+ .52	+1.13	−2.11	1
24504		i	5.34	B7n	−1.46	−0.98	− .45	− .06	+ .50	+1.08	−2.06	1
23324	18 Tau	o	5.63	B8n	−1.28	−0.98	− .46	− .06	+ .52	+1.08	−2.06	2
144206	υ Her	o	4.64	B8s	−1.26	−1.00	− .46	− .05	+ .52	+1.06	−2.06	2
188892	22 Cyg	i	4.87	B5s	−1.49	− .98	− .45	− .04	+ .49	+1.04	−2.02	2
1064		o	5.76	B9n	−1.05	− .93	− .45	− .05	+ .50	+1.09	−2.02	1
23753	26 Tau	o	5.51	B8nn	−1.26	−0.97	− .46	− .05	+ .50	+1.04	−2.01	1
23630	25 Tau	o	2.96	B7ne	−1.27	−1.00	− .45	− .05	+ .50	+1.01	−2.01	3
23480	23 Tau	o	4.25	B6n	−1.38	−0.96	− .46	− .03	+ .49	+1.03	−1.99	2
23408	20 Tau	o	4.02	B9s	−1.30	−0.96	− .46	− .05	+ .51	+1.02	−1.98	1
23850	27 Tau	o	3.80	B8n	−1.25	− .97	− .42	− .05	+ .47	+1.00	−1.97	2
183914	β Cyg, C	i	5.36	B9ne	−1.20	− .96	− .46	− .04	+ .50	+1.00	−1.96	2
222847	106 Aqr	o	5.26	B9n	−1.07	− .92	− .44	− .05	+ .49	+1.04	−1.96	1
216494	74 Aqr	o	5.89	B9s	−1.20	− .95	− .47	− .06	+ .54	+0.99	−1.94	1
23432	21 Tau	o	5.85	B8n	−1.13	− .92	− .44	− .06	+ .50	+1.02	−1.94	1
23441	22 Tau	o	6.46	B9n	−1.04	− .94	− .45	− .06	+ .50	+1.00	−1.94	1
23288	16 Tau	o	5.43	B7n	−1.24	− .93	− .44	− .05	+ .48	+0.98	−1.91	2
23862	28 Tau	o	5.18	B8nn	−0.89	− .93	− .44	− .05	+ .49	+ .96	−1.89	3
34085	β Ori	o	0.34	cB8e	−1.55	− .92	− .39	− .03	+ .42	+ .96	−1.88	2
19356*	β Per	o	2.3	B9n	−1.27	− .96	− .44	− .04	+ .47	+ .92	−1.88	2
222661	ω^2 Aqr	o	4.62	B9n	−0.93	− .89	− .44	− .06	+ .51	+ .99	−1.88	2
212710	NPS 2	o	5.38	B9	− .90	− .92	− .44	− .06	+ .49	+ .92	−1.84	2
218173		o	6.85	B9n	− .83	− .87	− .44	− .03	+ .47	+ .94	−1.81	1
157779*	ρ Her	o	4.14	B9	− .87	− .88	− .43	− .02	+ .46	+ .85	−1.73	1
199478*		i	5.76	cB8e	−0.76	−0.34	−0.06	−0.01	+0.07	+0.10	−0.44	2

TABLE 3—*Continued*

HD	Name	Z	*m*	Spec.	U	V	B	G	R	I	V−I	Obs.
					A0 Stars							
115735	21 CVn	o	5.13	A0.5s	−1.00	−0.93	−0.44	−0.06	+0.50	+1.04	−1.97	1
220020		o	7.8	A0n	−0.96	− .93	− .46	− .03	+ .49	+1.02	−1.95	1
225132	2 Cet	o	4.62	A0n	−0.98	− .97	− .45	− .04	+ .49	+0.95	−1.92	2
215766	69 Aqr	o	5.70	A0n	−1.03	− .89	− .44	− .05	+ .49	+ .96	−1.85	1
121409	86 UMa	o	5.65	A0n	−0.88	− .88	− .43	− .06	+ .49	+ .95	−1.83	1
128998		o	5.52	A0n	− .77	− .84	− .41	− .05	+ .47	+ .91	−1.75	1
218639		o	6.23	A0n	− .76	− .84	− .40	− .05	+ .46	+ .90	−1.74	1
219833		o	7.12	A0.5n	− .77	− .89	− .41	− .07	+ .48	+ .82	−1.71	1
156729	69 Her	o	4.80	A0n	− .76	− .82	− .40	− .02	+ .42	+ .84	−1.66	2
219659		o	6.36	A0n	− .74	− .79	− .38	− .01	+ .40	+ .82	−1.61	1
125162	λ Boo	o	4.26	A0.5n	− .64	− .75	− .37	− .06	+ .42	+ .83	−1.58	1
103483	65 UMa	o	6.46	A0.5n	−0.56	−0.72	−0.35	−0.06	+0.41	+0.71	−1.43	1
					A1–A3 Stars							
112413*	α^2 CVn	o	2.90	A1s	−1.32	−0.99	−0.48	−0.04	+0.52	+1.13	−2.12	5
143807	ι CrB	o	4.91	A1	−1.08	− .94	− .44	− .04	+ .48	+1.00	−1.94	2
172167	α Lyr	o	0.14	A1s	−0.81	− .92	− .44	− .04	+ .49	+0.93	−1.85	4
166205*	NPS 1	o	4.44	A2	− .72	− .85	− .40	− .05	+ .46	+ .88	−1.73	10
113865		o	6.44	A3n	− .80	− .82	− .41	− .04	+ .44	+ .89	−1.71	1
137422	γ UMi	o	3.14	A1n	− .59	− .82	− .38	− .03	+ .41	+ .72	−1.54	2
197345	α Cyg	i	1.33	cA2e	− .94	− .80	− .34	− .02	+ .36	+ .72	−1.52	2
192640	29 Cyg	i	4.98	A1.5n	− .62	− .64	− .30	− .03	+ .32	+ .66	−1.30	2
187642	α Aql	i	0.89	A1n	− .54	− .62	− .30	− .01	+ .31	+ .68	−1.30	4
166926*	NPS 4	o	5.86	A3p	− .49	− .60	− .29	− .04	+ .33	+ .68	−1.28	16
203280	α Cep	i	2.60	A3n	− .50	− .62	− .29	− .04	+ .33	+ .62	−1.24	2
66368	NPS 6	o	7.01	A3	− .49	− .65	− .31	− .01	+ .33	+ .58	−1.23	3
173649*	ζ Lyr, B	o	5.87	A3n	−0.48	−0.52	−0.23	−0.02	+0.25	+0.56	−1.08	3
					A5–A9 Stars							
5914	NPS 5	o	6.43	A5	−0.62	−0.76	−0.36	−0.04	+0.40	+0.80	−1.56	2
173648*	ζ Lyr, A	o	4.29	A9s	− .46	− .64	− .32	− .02	+ .34	+ .69	−1.33	3
127762	γ Boo	o	3.00	A5n	− .49	− .64	− .30	− .02	+ .32	+ .68	−1.32	2
10204		o	5.54	A9n	− .45	− .60	− .29	− .02	+ .32	+ .63	−1.23	1
211336*	ε Cep	i	4.23	A6n	− .47	− .53	− .24	− .03	+ .27	+ .54	−1.07	18
41074	39 Aur	?	5.90	A8n	− .45	− .49	− .21	− .04	+ .25	+ .49	−0.98	1
113139	78 UMa	o	4.89	A6n	− .46	− .42	− .16	− .02	+ .19	+ .44	−0.86	2
218753*	2 Cas	i	5.63	A9s	+ .02	− .48	− .18	− .01	+ .19	+ .25	−0.73	2
147365		o	5.54	A9n	− .49	− .37	− .14	.00	+ .14	+ .34	−0.71	1
164514*	−22°4510	i	7.28	cA6	+0.96	+0.39	+0.40	+0.06	−0.45	−1.44	+1.83	2

HD	Name	Z	*m*	Spec.	*M*	U	V	B	G	R	I	V−I	Obs.
					F Dwarfs								
14622		o	5.87	F2	+2.8	−0.50	−0.53	−0.23	−0.01	+0.24	+0.53	−1.06	1
432	β Cas	i	2.7†	F2	+2.2	− .38	− .47	− .20	− .02	+ .22	+ .50	−0.97	2
107192*	NPS 2s	o	6.28	F2	+3.0	− .51	− .49	− .20	− .02	+ .22	+ .46	− .95	2
107113	NPS 3s	o	6.33	F4	+3.2	− .48	− .36	− .13	− .02	+ .15	+ .34	− .70	6
118216		o	5.3†	F2	+2.7	− .39	− .38	− .14	− .01	+ .15	+ .24	− .62	2
198084		i	4.63	F9	+3.0	− .22	− .20	− .07	− .01	+ .08	+ .22	− .42	2
136064		o	5.23	F9	+3.1	− .20	− .20	− .07	.00	+ .07	+ .15	− .35	1
142373	χ Her	o	4.61	F7	+3.6	− .32	− .18	− .04	.00	+ .04	+ .13	− .31	2
6920	44 And	o	5.74	F7	+3.6	− .16	− .12	− .05	.00	+ .06	+ .10	− .22	1
111812	31 Com	o	5.07	F5	+2.3	−0.13	−0.07	−0.02	0.00	+0.01	+0.06	−0.13	2

TABLE 3—*Continued*

HD	Name	Z	m	Spec.	M	U	V	B	G	R	I	V−I	Obs.
							G Dwarfs						
114710	β Com	o	4.32	G0	+4.5	−0.26	−0.16	−0.06	−0.02	+0.08	+0.21	−0.37	2
16397		o	7.21	G0	+4.1	− .48	− .21	− .08	.00	+ .09	+ .10	− .31	1
109358	β CVn	o	4.32	G0	+4.2	− .25	− .14	− .04	− .01	+ .05	+ .16	− .30	2
10307		o	5.10	G0	+4.4	− .20	− .14	− .02	− .02	+ .05	+ .10	− .24	2
15830		o	7.55	G5	+5.3	− .24	− .08	− .05	.00	+ .06	+ .04	− .12	1
4406		o	7.60	G3	+4.0	− .07	− .05	− .01	− .05	+ .05	+ .06	− .11	1
111395		o	6.39	G6	+4.9	− .05	− .01	− .01	+ .01	− .01	+ .05	− .06	2
153344		o	7.04	G4	+4.7	+ .05	− .02	− .02	+ .02	.00	.00	− .02	1
152391		o	6.78	G9	+5.5	+0.04	+0.06	0.00	−0.01	0.00	−0.09	+0.15	1
							K and M Dwarfs						
154345		o	6.74	K0	+5.2	+0.05	+0.02	+0.02	+0.01	−0.02	+0.02	0.00	2
3651	54 Psc	o	6.08	K1	+5.9	+ .36	+ .20	+ .04	+ .01	− .05	− .12	+ .32	1
222935		o	8.9:	K2	+5.7	+ .37	+ .18	+ .04	+ .04	− .08	− .23	+ .41	1
166620		o	6.40	K2	+5.9	+ .51	+ .23	+ .10	+ .02	− .13	− .20	+ .43	2
3765		o	7.52	K5	+6.5	+ .66	+ .35	+ .11	+ .01	− .11	− .28	+ .63	2
202751		o	8.5:	K6	+6.8	+ .74	+ .34	+ .17	− .01	− .15	− .46	+ .80	1
128165		o	7.37	K5	+6.7	+0.96	+ .57	+ .18	+ .06	− .25	− .41	+0.98	2
151288*		o	8.2	M0	+8.7	.....	+ .90	+ .50	+ .04	− .53	− .98	+1.88	2
147379*		o	8.9:	M0	+8.7	.....	+0.98	+0.52	+0.06	−0.59	−1.23	+2.21	1
							F Giants						
221525*	NPS 3	o	5.62	F0	.....	−0.36	−0.60	−0.27	−0.05	+0.31	+0.57	−1.17	3
201601	γ Equ	o	4.76	cF1	−0.2	− .42	− .51	− .26	− .03	+ .30	+ .62	−1.13	2
163506	89 Her	o	5.48	cF5	−1.5	− .07	− .45	− .20	− .03	+ .22	+ .40	−0.85	2
195295	41 Cyg	i	4.09	cF4	−0.9	− .05	− .36	− .17	− .01	+ .17	+ .31	− .67	4
571	22 And	o	5.08	cF2	+0.2	− .11	− .37	− .14	+ .01	+ .14	+ .25	− .62	1
213306*	δ Cep	i	3.7	cF4	.....	+ .02	− .33	− .14	− .02	+ .15	+ .24	− .57	....
20902	α Per	i	1.90	cF4	−1.2	+ .09	− .28	− .11	− .02	+ .13	+ .21	− .49	5
8890*	NPS 1s	o	2.1	cF7	−2.2	+ .11	− .17	− .08	− .02	+ .09	+ .20	− .37	....
171635	45 Dra	o	4.95	cF8	−2.0	+ .28	− .09	− .04	− .01	+ .06	+ .12	− .21	2
31964*	ε Aur	i	3.3	cF2	−1.7	+ .12	− .21	− .05	.00	+ .05	− .01	− .20	1
194093*	γ Cyg	i	2.32	cF7	−2.1	+ .38	− .05	− .02	− .03	+ .04	+ .10	− .15	4
173638*		i	5.81	cF4	−0.5	+ .50	− .14	.00	− .01	+ .01	− .16	+ .02	3
193370*	35 Cyg	i	5.5†	cF5	−1.3	+ .40	− .01	+ .01	.00	− .01	− .07	+ .06	1
14662*		i	6.46	cF8	−1.9	+0.67	+ .17	+ .13	+ .01	− .14	− .35	+0.52	1
195593*	44 Cyg	i	6.30	cF5	−1.2	+1.04	+0.37	+0.27	0.00	−0.27	−0.69	+1.06	1
							G Giants						
204867	β Aqr	o	3.07	cG1	−2.5	+0.56	+0.18	+0.07	−0.01	−0.05	−0.09	+0.27	3
222574	104 Aqr	o	5.3†	cG1	−1.9	+ .57	+ .17	+ .08	− .02	− .07	− .10	+ .27	2
157910		o	6.48	G2	+0.3	+ .55	+ .24	+ .08	+ .01	− .10	− .19	+ .43	1
204075*	ζ Cap	o	4.2†	cG4	−1.3	+ .75	+ .39	+ .14	− .04	− .10	− .11	+ .50	2
16901	14 Per	o	5.58	cG0	−2.1	+ .73	+ .26	+ .13	− .01	− .13	− .24	+ .50	2
9270	η Psc	o	3.72	G3	+0.4	+ .62	+ .26	+ .08	− .01	− .08	− .25	+ .51	1
133208	β Boo	o	3.63	G5	+0.3	+ .80	+ .35	+ .15	− .01	− .14	− .21	+ .56	1
159181	β Dra	o	2.99	cG2	−1.7	+ .78	+ .33	+ .16	− .01	− .15	− .25	+ .58	2
192947	α^2 Cap	o	4.1†	G8	+0.3	+ .80	+ .33	+ .15	− .02	− .13	− .25	+ .58	3
209750	α Aqr	o	3.19	cG1	−2.2	+ .94	+ .39	+ .16	− .01	− .15	− .23	+ .62	2
135722	δ Boo	o	3.54	G4	+0.8	+0.77	+ .37	+ .16	.00	− .16	− .28	+ .65	1
187138*	NPS 4r	o	8.26	G9	.....	(+1.27)	+ .46	+ .22	− .02	− .20	− .31	+ .77	2
192876	α^1 Cap	o	4.55	cG5	−2.7	+1.03	+ .50	+ .21	− .01	− .20	− .40	+ .90	1
171779		o	5.42	G5	+0.4	+1.19	+ .49	+ .23	− .01	− .22	− .41	+0.90	1
206859	9 Peg	o	4.52	cG3	−1.3	+1.32	+ .62	+ .24	− .01	− .23	− .46	+1.08	2
20123*		i	5.29	cG2	−1.4	+1.09	+ .57	+ .29	.00	− .28	− .59	+1.16	1
217476*		i	5.48	cG3	−3.2	+1.53	+ .67	+ .39	+ .01	− .39	− .90	+1.57	1
224014*	ρ Cas	i	4.85	cG0	−3.0	+1.79	+0.86	+0.43	0.00	−0.43	−0.87	+1.73	1

TABLE 3—*Continued*

HD	Name	Z	*m*	Spec.	*M*	U	V	B	G	R	I	V−I	Obs.
					K Giants								
145328.....	τ CrB	o	4.94	K1	+1.3	+1.02	+0.43	+0.19	0.00	−0.19	−0.34	+0.77	2
112570.....	.....	o	6.22	K0	+1.8	+0.84	+ .43	+ .18	− .01	− .18	− .36	+0.79	2
125351.....	.....	o	5.1†	K1	+0.4	+1.36	+ .57	+ .24	− .02	− .22	− .41	+0.98	1
152601.....	23 Oph	i	5.35	K3	+0.2	+1.25	+ .52	+ .20	− .01	− .18	− .49	+1.01	1
183912*.....	β Cyg, AB	i	3.8†	(K0)	−0.7	+0.90	+ .57	+ .31	− .01	− .30	− .61	+1.18	2
163770.....	θ Her	o	3.99	cK1	−1.3	+2.04	+ .87	+ .35	− .02	− .32	− .63	+1.50	3
218356.....	56 Peg	o	4.98	cK0	−1.6	+1.76	+ .87	+ .39	.00	− .39	− .76	+1.63	2
214868*.....	11 Lac	o	4.64	K2	−0.1	+1.91	+0.88	+ .41	− .02	− .38	− .81	+1.69	1
114282*.....	NPS 3r	o	7.57	K2	.....	+2.44	+1.09	+ .48	− .02	− .46	− .91	+2.00	2
206778.....	ε Peg	o	2.54	cK0	−2.3	+2.51	+1.17	+ .49	− .01	− .47	− .90	+2.07	2
210745*.....	ζ Cep	i	3.62	cK5	−2.3	+2.58	+1.16	+ .49	− .02	− .47	−0.92	+2.08	3
192107.....	66 Aql	o	5.64	K5	−0.1	+1.98	+1.03	+ .51	.00	− .52	−1.08	+2.11	2
225212*.....	3 Cet	o	5.5†	cK5	−2.7	.....	+1.26	+ .54	− .01	− .53	−1.04	+2.30	2
29139.....	α Tau	i	1.06	K5	0.0	+2.63	+1.20	+ .54	+ .02	− .56	−1.18	+2.38	1
200905.....	ξ Cyg	i	4.2†	cK5	−2.0	+2.76	+1.28	+ .57	+ .01	− .58	−1.15	+2.43	1
196321.....	70 Aql	o	5.22	K5	−0.4	+2.61	+1.25	+0.53	+0.01	−0.53	−1.23	+2.48	1
					M Giants								
51802.....	NPS 1r	o	5.3	M0	−0.1	.....	+1.28	+0.63	+0.03	−0.66	−1.42	+2.70	3
213310.....	5 Lac	o	4.6	M0	−2.3	.....	+1.33	+ .66	+ .02	− .69	−1.42	+2.75	2
187076*.....	δ Sge	i	3.8	M2	−1.2	.....	+1.09	+ .62	+ .09	− .71	−1.71	+2.80	4
183030.....	NPS 2r	o	6.6	M1	−0.3	.....	+1.41	+ .70	+ .07	− .77	−1.76	+3.17	2
120933.....	.....	o	5.0	M2	−0.5	.....	+1.51	+ .69	+ .10	− .79	−1.85	+3.36	1
39801.....	α Ori	i	0.1–1.2	M2	−4.1	.....	+1.60	+ .77	+ .04	− .81	−1.78	+3.38	3
148478.....	α Sco	i	1.5†	M1	−3.7	.....	+1.55	+ .84	+ .04	− .87	−1.99	+3.54	2
209772.....	18 Cep	i	5.5	M5	0.0	.....	+1.34	+ .79	+ .12	− .91	−2.22	+3.56	2
132813.....	.....	o	4.9	M5	−0.3	.....	+1.37	+ .85	+ .12	− .97	−2.31	+3.68	1
214665.....	.....	i	5.5	M4	−0.4	.....	+1.43	+ .81	+ .13	−0.94	−2.25	+3.68	1
218634.....	57 Peg	o	5.4	M4	−1.1	.....	+1.33	+ .87	+ .15	−1.01	−2.42	+3.75	2
175588.....	δ^2 Lyr	o	4.5	M4	−1.6	.....	+1.46	+0.84	+ .11	−0.95	−2.30	+3.76	4
175865.....	R Lyr	o	4.0–4.5	M5	−1.1	.....	+1.48	+1.02	+ .15	−1.18	−2.84	+4.32	2
206936*.....	μ Cep	i	4.0–4.8	M2	−4.5	.....	.....	+1.18	− .01	−1.18	−2.47	.....	3
178770.....	.....	o	7.6	M6	−0.9	.....	.....	+1.13	+ .12	−1.25	−3.07	.....	1
148783.....	g Her	o	4.4–5.6	M6	−1.0	.....	.....	+1.29	+ .11	−1.40	−3.25	.....	2
144205.....	X Her	o	5.8–7.2	M6	−1.1	.....	.....	+1.47	+ .05	−1.52	−3.60	.....	1
182917.....	CH Cyg	o	6.4–7.4	M6	−1.4	.....	.....	+1.54	+ .01	−1.55	−3.78	.....	1
142143.....	ST Her	o	7.0–8.2	M7	−0.7	.....	.....	+1.93	− .14	−1.78	−4.19	.....	2
126327.....	RX Boo	o	7.0–9.2	M7–8e	−0.6	.....	.....	+2.27	−0.42	−1.85	−4.58	.....	1

NOTES TO TABLE 3

HD 5394	Magnitude and color variable
8890	Polaris, variable, colors at maximum
14662	Reddened
19356	Algol at maximum; colors change during eclipse
20123	Probably reddened
31964	Eclipsing variable, definitely reddened
37022	Four stars of Trapezium; combined color assumed equivalent to B0.
107192	Keenan calls this star an ordinary giant
112413	Variable, period 5.5 days; no large change in color noted
114282	Spectrum from Keenan; color of a supergiant
147379	Ultraviolet too faint to measure
151288	Ultraviolet too faint to measure
157779	Both components
164514	Strongly reddened. In Trifid nebula; see Seares and Hubble, *Mt. W. Contr.*, No. 187, pp. 10 and 15; *Ap. J.*, **52**, pp. 17 and 22, 1920. Spectrum cA6 from Adams and Joy, unpublished
166205	Standard star
166926	Standard star
169034	Variously classified, B0–B3; most strongly reddened star
173638	Reddened
173648–9	The brighter A9 component is definitely bluer than the fainter A3 component
183912	Spectrum and color composite
186994	Spectrum from HD only
187076	HD spectrum, Ma + A0; color also composite
187138	Spectrum from Keenan; ordinary giant. Ultraviolet poor but definitely weak
192422	Measures discordant
193370	Reddened
194093	Possibly not reddened

NOTES TO TABLE 3—*Continued*

195593	Strongly reddened
198846	Eclipsing variable; weak ultraviolet could be caused by a red companion
199478	Reddened
204075	Measures discordant
205021	Not tested for change of color in light-period of 4.6 hours
206936	Must be reddened
210745	If spectrum is as early as cK1, this star could be reddened
211336	Comparison star for δ Cephei; used also as secondary standard for color
212455	Strongly reddened
213306	Variable, colors at maximum; see J. Stebbins, *Mt. W. Contr.*, No. 704; *Ap. J.*, **101**, 47, 1945
214868	Possibly reddened; see 12 Lacertae under B1 stars
214993	No detectable change of color in light-period of 4.6 hours
217476	Reddened
218753	Weak ultraviolet has been confirmed
221525	Spectrum from Keenan
224014	Reddened
225212	Ultraviolet doubtful

of J. O'Keefe.[8] From B6 to M the classification is usually by Adams and Joy and others,[5] with additions of unpublished spectra kindly secured for us by Mr. A. H. Joy. The spectra for the North Polar Sequence are from P. C. Keenan.[9] Exceptions are marked in the notes.

The six colors from U to I are on the uniform system in magnitudes referred to the mean of blue, green, and red for each star; a plus sign (+) indicates that the color is relatively fainter than the mean. Because of the variability of the ultraviolet with the hydrogen absorption the difference V − I in the next to last column serves better than U − I as the over-all index for color in all spectral types, and the stars in each group are arranged according to that difference. The last column gives the number of observations, averaging about two per star; but about two-fifths of the stars have only one observation each.

II. COLORS BY SPECTRAL TYPES

In addition to the notes on individual stars in Table 3, we may consider each spectral type as a group. From the way the colors run down each column of the table, a discordant or peculiar star can be picked out, though too much should not be inferred from one observation alone. It is always possible, owing to variable extinction, that the ultraviolet or infrared should be off as much as 0.10 mag., but such cases must be rare for the mean of two or more observations. We note that the first, or bluest, star in the entire list is an O star, while the last, or reddest, star has the latest spectrum, M7–8.

Among the early-type stars from O to B3 we have found almost no clear-cut case of two stars with identical spectra but with different intrinsic colors. Even the slight variation in the three B0 stars in the Belt of Orion may be caused by differential absorption; the whole region of Orion is full of nebulosity. The color of P Cygni stands out among the B1 stars, but the spectrum of this star is anomalous. Otherwise the O's and B's, being nearly all in the zone of avoidance, simply show different degrees of space reddening, which was the basis on which they were selected in the first place.

For types B5 and later, the dispersion in color for a given spectrum becomes more apparent, although it is still possible that the dispersion may be as much in the spectral classification as in the color. About a dozen stars from B9 to M, practically all supergiants within the zone, are obviously reddened; but the difficulty in selecting proper nonreddened comparison stars prevents a study of the law of absorption comparable with that of the B stars.

O stars.—Only the first two stars in this group are outside the zone, and these apparently have normal colors; the others show various amounts of reddening which mask any progressive change in intrinsic color from O5 to O9. The smooth run of the colors down the list indicates that there are no large errors in the observations.

B0 stars.—Almost the only nonreddened B0 star in the summer sky is γ Cassiopeiae,

[8] *Ap. J.*, **94**, 353, 1941.

[9] *Ap. J.*, **91**, 113, 1940.

known to be variable in light and color; but we seem to have caught this star in the normal, or bluest, phase. The three stars δ, ϵ, and ζ Orionis were observed just before dawn in September, 1943, and again in 1944; and, as expected, they turned out to be among the bluest of their class. These three and θ^1 Orionis are discussed in Section IV. The colors of the B0's do not run as smoothly as those of the O's, but the discordances usually occur in cases of one observation.

The last two B0's stand out in any list of colors, HD 169034 having a color excess of 4.5 mag. on the V − I scale, or possibly 1.5 mag., International. Dr. R. Minkowski called our attention to the variable, RY Scuti, about one degree distant in the sky from HD 169034. Although the spectrum of this variable is weak in the shorter wave lengths, it is probably an early B. We compared these two stars differentially with the C_1 filters on one night and found RY Scuti to be of 10.0 visual magnitude and 0.01 mag. redder than HD 169034—practically the same. The three stars, HD 166734, HD 169034, and RY Scuti, are the most strongly reddened stars we have found in the entire sky.

B1 stars.—The two similar short-period variables, β Cephei and 12 Lacertae, are considered in the notes to Table 3. Though well out of the zone, 12 Lacertae appears to have a trace of reddening; and near-by 8 Lacertae, of spectrum B3, is likewise possibly colored. This evidence for a slight absorption in Lacerta is a possible delayed confirmation of the reddening of HD 216200 = 14 Lacertae, which stood out like a mistake among our "733 B Stars"[10] as the only star well outside the zone with color excess as large as $E_1 = +0.12$ mag. Since then we have found $E_1 = +0.13$ for HD 215227, which is 3° from 14 Lacertae toward the galactic equator.

The discordant case of P Cygni is discussed in Section IV. The jump in the colors between the last B1 star and the one preceding is merely a matter of selection; most of the stars discussed in the present paper culminate north of the zenith, and only a few were measured in the heavily obscured southern region near $l = 345°$.

B2–B3 stars.—The first star, ϵ Persei, though in the critical zone, seems to be near enough to us to miss the absorption; and θ Ophiuchi, observed only once at a low altitude, could possibly also be nearly normal. The first B3 star looks normal, and the others look slightly reddened. The last star, an eighth-magnitude supergiant in latitude $-2°$, was sure to be found reddened.

B5–B9 stars.—Most of these stars are outside the zone and, being nearer to us than the earlier-type stars of the same apparent magnitudes, show little evidence of reddening. As we go from B5 to later types, the hydrogen absorption increases, until in the A's the ultraviolet is usually fainter than the violet; but, as is to be expected, the ultraviolet is extra bright in the two c stars, β Orionis and HD 199478. The latter is obviously reddened.

A0 stars.—All but one of these were observed previously with the C_1 filters in an attempt to detect space reddening toward the poles of the galaxy.[11] The values of C_1 and V − I are well correlated, but the range in distance is not enough to determine a coefficient of space absorption from only a dozen stars.

A1–A3 stars.—The bright stars, α Lyrae and α Aquilae, measured through a 6-mag. wire screen, fit in well enough with the fainter stars of the same type, while α Cygni with a 3-mag. screen has the usual strong ultraviolet intensity of a c star. There is apparently no case of strong reddening in this group.

A5–A9 stars.—The colors progress in a way with advancing spectral type, but the A9's show a large dispersion. The anomalous ultraviolet magnitude of 2 Cassiopeiae was observed twice. The color excess of HD 164514, about 3 mag. in V − I, is exceeded by that of a number of the B stars.

F, G, K, and M dwarfs.—These stars may be discussed together; they were taken

[10] Stebbins and Huffer, *Pub. Washburn Obs.*, **15**, 237, 1934.

[11] Stebbins, Huffer, and Whitford, *Mt. W. Contr.*, No. 650; *Ap. J.*, **94**, 215, 1941.

mostly with the 100-inch telescope for comparison with the nebulae. There is little chance that reddening may be detected in any bright dwarf, the modulus $m - M$ being usually less than 3, or $r < 40$ parsecs. The progression of the colors is fairly uniform down the list, but there is some overlapping of the groups. The first F's are bluer than the last non-reddened A's. The last three F's, which average F6, are redder than the F9's before them; and they fit in at about G2 in the next group, giving as good evidence as we have of dispersion of the colors within the spectral types. The G's and K's scarcely overlap, nor do the K's and M's. The ultraviolet intensities of the two faint M stars were too weak to be measured.

F giants.—In the giants we can expect reddening of stars in low latitude, and perhaps differences between ordinary giants and supergiants. The F's in the list are practically all supergiants, owing to the well-known gap for ordinary giants in the Russell diagram. The colors run pretty smoothly from star to star; even the variables, δ Cephei and NPS 1s = Polaris, fit in well. Reddening seems to begin at ϵ Aurigae; γ Cygni may be normal; but the last four stars are all reddened.

G giants.—The reddening might begin at HD 20123 were it not for 9 Pegasi with about the same spectrum and color; but 9 Pegasi is outside the zone, and there is little other evidence of absorption near this star. The last two G giants, both in the zone, are undoubtedly reddened.

K giants.—Any slight reddening of the bright stars in the zone is hidden in the rapid change of the colors with advancing spectral type. There seems to be an absolute-magnitude effect in the early K's. Six giants with M fainter than 0.0 have colors midway between the supergiants and the dwarfs. This effect is shown in Figure 1.

M giants.—Of the twenty M stars in the list, eight are recognized variables, nine have been found with the photocell[12] to be either variable or suspicious, leaving three not sufficiently tested. We might as well call them all variable, particularly HD 178770, with its late spectrum, M6. The ultraviolet in a red star is usually too weak to measure; toward the end of the list the ultraviolet becomes 10 or 12 mag. fainter than the infrared. If mere faintness were all, the ultraviolet could be measured, but the leak of the strong infrared radiation through the ultraviolet filter may become fifty or one hundred times as intense as the ultraviolet we are trying to measure. Because of a lesser leak, the violet values for the last seven stars are also omitted; in fact, the violet becomes uncertain in all the M stars.

No space reddening in the M giants is evident until we get to μ Cephei, called the "garnet star" by William Herschel, who was probably not thinking of interstellar absorption when he noted the color. With modulus $m - M = 8.5$, $r = 500$ parsecs, $b = +4°.1$, μ Cephei undoubtedly shows space reddening and is, indeed, a doubly red star, although it still should not look as red to the eye as g Herculis and other stars later in the list.

All types.—In Figure 1 the values of V − I from Table 3 are plotted against spectral type. For the early stars, O to B5, the two bluest stars are used for each type, on the assumption that all the others are more or less reddened. Later than B5, stars in the zone that are clearly reddened or doubtful are omitted. From B6 to A6, if there are more than four stars to a type, the two highest and two lowest values are used; and after A6 all reliable stars are plotted. The scale of abscissae is doubled for the M's without an attempt to differentiate between the scales for dwarfs and giants in the interval K5–M0, as is done for the spectra.[13] The difference between ordinary giants and supergiants begins at about G5 and extends to K3. It will require several times as many stars in the region G5–M0 as have been used in this investigation to establish this absolute-magnitude effect satisfactorily.

[12] Stebbins and Huffer, *Pub. Washburn Obs.*, **15**, 147, 1930.

[13] Adams *et al.*, *Mt. W. Contr.*, No. 511, p. 7; *Ap. J.*, **81**, 193, 1935.

III. COLOR TEMPERATURES

With six colors we can compare the energy-curves of stars with those of a black body at different temperatures; but since we are pretty sure to get a temperature scale disagreeing with many others, we consider again the limitations, as well as the advantages, of the present method.

The wave lengths for the different colors are the effective means for the cell and filters referred to a source of uniform energy throughout the spectrum.[3] They are not the "mean effective wave lengths" of F. H. Seares[14] or the "isophotal wave lengths" of A. Brill,[15] which take into account the energy-curves of the stars, the differential extinction of the atmosphere for different spectral types, and the optical system of the telescope. Our col-

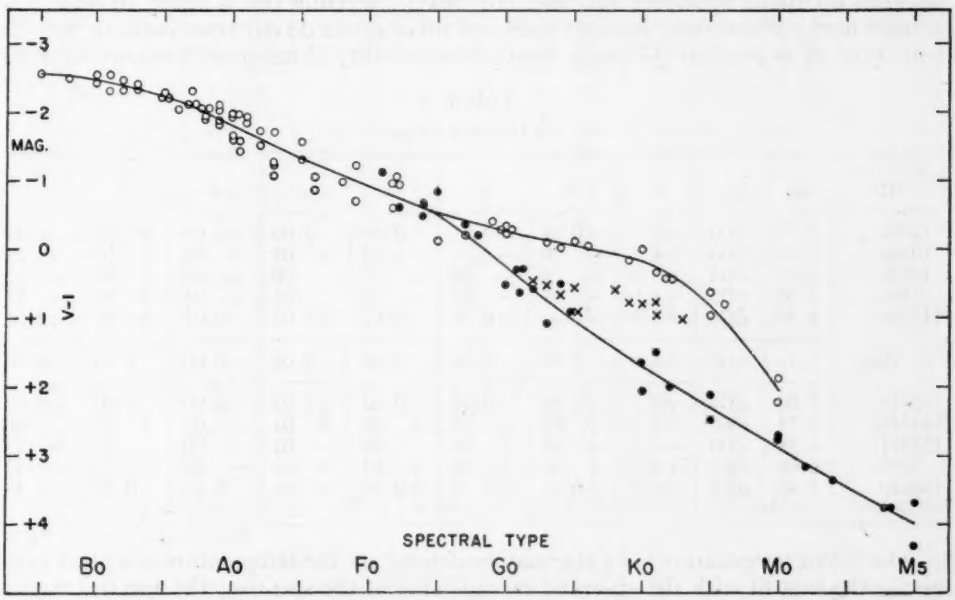

FIG. 1.—Color index V − I (λλ 4220–10,300 A) and spectral type. *Open circles*, main-sequence stars; *solid circles*, supergiants; *crosses*, ordinary giants with *M* fainter than 0.0 mag.

ors have the same characteristic as those of any other system not dealing with monochromatic radiation; the effective wave length depends upon the color of the star measured; but since the filters take in smaller spectral ranges than the ordinary photographic plate, the shift of the wave length with spectral type—for instance, in the violet—is less than half the shift of the wave length in a photographic magnitude.

As mentioned before, it is impractical to make a complete correction for atmospheric extinction for each star; even with the Mount Wilson sky, there are night-to-night variations which exceed the differential effects between stars on the same night. Hence, it seems best to go ahead using the same extinction for all stars as a first approximation and, if desired, apply mean corrections for each star later. The sensitivity-curve of the cell was determined through the regular window of the photometer, so that reflections from two aluminum mirrors are the only additional effects in the optical system.

Whatever may be the shortcomings of filters in isolating spectral regions, the photo-

[14] *Mt. W. Contr.*, No. 685, p. 28; *Ap. J.*, **98**, 329, 1943.

[15] *Veröff. d. U. Sternw. Berlin-Babelsberg*, **7**, Part V, 5, 1929.

cell will always repeat accurately the same response for the same radiation. The scale of magnitudes is apparently linear and essentially correct for all colors over the entire range of intensity. The variation of sensitivity available in the installation at any time is distributed as follows:

	Mag.
Wire screens	6
Galvanometer shunts, from 1/1 to 1/100	5
Galvanometer scale, deflections from 10 to 400 mm	4
Low to high resistance in circuit	2
Total	17

The extreme range has not been needed; but, for instance, the difference in the infrared between α Orionis, spectrum M2, and HD 14633, spectrum O8, is about 10 mag., and neither here nor elsewhere in other stars and other colors do our tests indicate that the scale runs off as much as 0.10 mag. from proportionality of response to energy received.

TABLE 4

STANDARD STARS

HD	m	Spec.	M	U	V	B	G	R	I	V−I
16397	7.21	dG0	+4.1	−0.48	−0.21	−0.08	0.00	+0.09	+0.10	−0.31
10307	5.10	dG0	+4.4	− .20	− .14	− .02	− .02	+ .05	+ .10	− .24
15830	7.55	dG5	+5.3	− .24	− .08	− .05	.00	+ .06	+ .04	− .12
4406	7.60	dG3	+4.0	− .07	− .05	− .01	− .05	+ .05	+ .06	− .11
111395	6.39	dG6	+4.9	−0.05	−0.01	−0.01	+0.01	−0.01	+0.05	−0.06
Mean	6.7	dG6	+5.0	0.00	0.00	0.00	0.00	0.00	0.00	0.00
153344	7.04	dG4	+4.7	+0.05	−0.02	−0.02	+0.02	0.00	0.00	−0.02
154345	6.74	dK0	+5.2	+ .05	+ .02	+ .02	+ .01	− .02	+ .02	.00
152391	6.78	dG9	+5.5	+ .04	+ .06	.00	− .01	.00	− .09	+ .15
3651	6.08	dK1	+5.9	+ .36	+ .20	+ .04	+ .01	− .05	− .12	+ .32
166620	6.40	dK2	+5.9	+0.51	+0.23	+0.10	+0.02	−0.13	−0.20	+0.43

The "color temperature" of a star may be defined as "the temperature of a black body giving the best fit with the observed energy-curve of the star over the spectral regions concerned." In the present case, when the intensities in six colors are plotted in magnitudes against $1/\lambda$, that temperature is selected which gives the best representation of the six points by the corresponding black-body curve, which is nearly a straight line. Practically, it turns out that a good fit serves as well as the best one, since the deviations from black-body radiation can be referred to any approximate curve.

The energy-curves and resulting temperatures for the stars here studied are, of course, affected by the absorption lines and bands in their spectra, just as color indices in the International and other photographic systems are likewise affected. Even in spectrophotometry, where clear spaces of continuous spectrum are measured, there can always be an undetected veil of general absorption over the surface of a star, and we come back to the question of what part of a star we mean when we speak of its temperature. The color temperature simply describes the over-all distribution of the energy as received outside our atmosphere.

Since all our measures were differential between stars or groups of stars, we began with arbitrary standards for color and temperature. For convenience of reference for the nebulae, ten stars of types dG0 to dK2 were selected; the average spectrum is dG6, which is assumed to correspond to a color temperature of 5500° K. Any change or improvement of the zero point can be readily introduced later. The colors of these stars are in Table 4. Although marked as standards, they are not better measured than others of

the list; the really standard stars are the intermediate ones, NPS 4 and NPS 1. After several good comparisons of a polar star with the ten standard stars are obtained, the polar star itself can serve as a standard. On any night the colors of each star observed are then referred to the original standards by way of the polar stars, thus controlling possible changes in the photocell or the extinction.

TABLE 5

BLACK-BODY COLORS

T_1	U	V	B	G	R	I	V−I
∞	−2.59	−1.47	−0.71	−0.04	+0.75	+1.61	−3.08
100,000°	−2.50	−1.42	− .69	− .04	+ .73	+1.55	−2.97
50,000	−2.40	−1.36	− .66	− .04	+ .70	+1.49	−2.85
30,000	−2.24	−1.28	− .62	− .04	+ .65	+1.40	−2.68
20,000	−2.04	−1.16	− .56	− .03	+ .59	+1.27	−2.43
15,000	−1.82	−1.04	− .50	− .03	+ .53	+1.13	−2.17
12,000	−1.58	−0.90	− .44	− .03	+ .46	+0.99	−1.89
10,000	−1.34	− .76	− .37	− .02	+ .39	+ .83	−1.60
9000	−1.16	− .66	− .32	− .02	+ .34	+ .73	−1.39
8000	−0.93	− .54	− .26	− .02	+ .28	+ .59	−1.13
7000	−0.64	− .38	− .18	− .01	+ .19	+ .41	−0.79
6500	−0.47	− .27	− .13	− .01	+ .14	+ .30	−0.57
6000	−0.26	− .15	− .07	.00	+ .08	+ .16	−0.31
5500	0.00	.00	.00	.00	.00	.00	0.00
5000	+0.30	+ .18	+ .09	+ .01	− .09	− .20	+0.38
4500	+0.69	+ .39	+ .19	+ .01	− .21	− .45	+0.84
4000	+1.16	+0.67	+ .33	+ .02	− .35	−0.76	+1.43
3500	+1.77	+1.02	+ .51	+ .03	− .54	−1.17	+2.19
3000	+2.57	+1.50	+0.74	+ .05	−0.79	−1.73	+3.23
2500	+3.71	+2.16	+1.07	+ .07	−1.14	−2.51	+4.67
2000	+5.45	+3.15	+1.57	+0.11	−1.67	−3.70	+6.85

In Table 5 the black-body colors for the six wave lengths concerned were computed from Planck's formula,

$$E_\lambda = \frac{c_1/\lambda^5}{e^{c_2/\lambda T} - 1},$$

where the constant c_1 and the units of the energy cancel out in the ratio of two values of E, and where λ is taken in centimeters, T in degrees absolute, and $c_2 = 1.435$ cm × degrees. For $T = \infty$ the ratio of the energies for two wave lengths, λ_1 and λ_2, becomes

$$\frac{E_1}{E_2} = \frac{\lambda_2^4}{\lambda_1^4}.$$

For each temperature the colors were referred in magnitude to the mean of the blue, green, and red and then to the corresponding colors for $T = 5500°$. The complete table is about five times as extensive as Table 5. The relative temperature of any star may be derived by a comparison of its colors with those of the table. In anticipation of the subsequent discussion, the temperatures on this scale are denoted by T_1.

In Table 6 the mean colors of stars grouped by types are compared with black-body colors from Table 5. For each type the first line gives the observed colors, and the second line the differences from the black-body colors at the stated temperature, taken in the sense, Observed *minus* Computed. Only those stars clearly free from space reddening were used, thus omitting all high-luminosity stars in the zone of absorption. Of course.

there is still the probability of a small reddening toward the galactic poles, and the final standards of any precise system of stellar colors will have to be based upon stars close to the sun, if they can be found.

TABLE 6

COLORS AND TEMPERATURES OF STARS BY SPECTRAL TYPES

Spectrum and T_1	U	V	B	G	R	I	V−I	Stars
O.....	−2.26	−1.16	−0.53	−0.04	+0.58	+1.36	−2.52	2
23,000°.....	−0.14	+0.05	+0.06	−0.01	−0.04	+0.04	+0.01	
B0.....	−2.20	−1.13	− .52	− .04	+ .57	+1.34	−2.47	2
21,000.....	−0.13	+0.05	+ .05	− .01	− .03	+0.05	0.00	
B5.....	−1.65	−1.07	− .48	− .05	+ .54	+1.17	−2.24	3
16,000.....	+0.23	0.00	+ .04	− .02	− .01	0.00	0.00	
A0.....	−0.86	−0.87	− .42	− .05	+ .47	+0.93	−1.80	5
11,300.....	+0.64	−0.01	.00	− .03	+ .03	−0.01	0.00	
dF2.....	−0.42	−0.47	− .19	− .02	+ .21	+0.43	−0.90	4
7300.....	+0.31	−0.03	+ .02	− .01	− .01	−0.04	+0.01	
dG0.....	−0.24	−0.16	− .05	− .01	+ .06	+0.12	−0.28	4
5950.....	0.00	−0.02	+ .01	− .01	− .01	−0.02	0.00	
dG6.....	.00	.00	.00	.00	.00	.00	.00	10
5500.....	.00	.00	.00	.00	.00	.00	.00	
dK1.....	+0.31	+0.15	+ .05	+ .01	− .07	−0.10	+0.25	3
5150.....	+0.10	+0.03	− .01	+ .01	− .01	+0.04	−0.01	
dK5.....	+0.81	+0.46	+ .14	+ .04	− .18	−0.34	+0.80	2
4550.....	+0.17	+0.09	− .04	+ .03	+ .02	+0.08	+0.01	
dM0.....	.....	+0.94	+ .51	+ .05	− .56	−1.10	+2.04	2
3590.....	.....	−0.01	+ .04	+ .02	− .06	−0.01	0.00	
cF3.....	−0.11	−0.39	− .18	− .02	+ .19	+0.36	−0.75	5
6900.....	+0.50	−0.03	− .01	− .01	+ .01	−0.03	0.00	
cG1.....	+0.72	+0.27	+ .12	− .01	− .11	−0.18	+0.45	5
4900.....	+0.35	+0.05	+ .01	− .02	.00	+0.06	−0.01	
cK1.....	+2.19	+1.00	+ .43	− .01	− .41	−0.80	+1.80	4
3750.....	+0.75	+0.16	+ .02	− .04	+ .03	+0.16	0.00	
gK5.....	.....	+1.18	+ .53	.00	− .53	−1.12	+2.30	3
3450.....	.....	+0.12	.00	− .04	+ .03	+0.10	+0.02	
gM1.....	.....	+1.38	+0.67	+ .06	−0.73	−1.61	+2.99	4
3100.....	.....	−0.01	−0.01	+ .01	0.00	−0.01	0.00	
gM6.....	.....	.....	+1.36	+0.07	−1.43	−3.42	.....	4
2130.....	.....	.....	−0.06	−0.03	+0.08	−0.08	.....	

In Figure 2 the comparisons in Table 6 are shown graphically, omitting several types as superfluous. For convenience, the temperature has been taken from the value of V − I in each case, giving agreement of the curves for the points for V and I in the

graph. In the main sequence the radiation of the ultraviolet is strong in B0; it decreases from B5 to A0, owing to hydrogen absorption, and is back to normal at dG0. In the giants the ultraviolet is weak from hydrogen absorption in cF3, but in the G and K giants

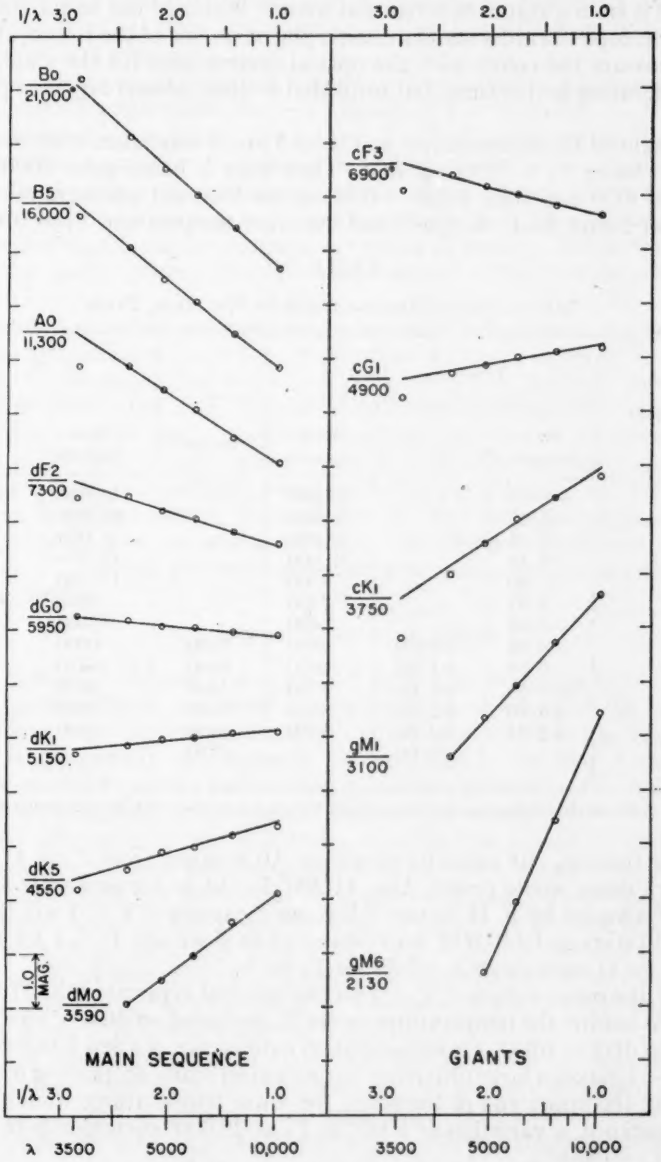

FIG. 2.—Colors and temperatures by spectral types

the weak ultraviolet simply conforms to the general curve of the deviations from a straight line. This curve of the deviations, suggested in the dwarf K's but conspicuous in the giant G's and K's, is apparently not present in the dwarf or giant M's, which, despite

the strong spectrum bands, give very good over-all agreement with black-body radiation. The measures of color index in the diagram range from U − I = −3.54 for B0 to B − I = +4.78 for gM6, or more than 8 mag.

The zero point of our temperature scale must remain preliminary until we have actually determined it from a standard terrestrial source. It should not be too difficult to turn the 60-inch telescope toward a standard lamp placed on one of the towers at Mount Wilson and to measure the colors with the optical system used for the stars. We hope to make this calibration in due time; but until that is done, almost any zero point will suffice.

The zero point of the temperatures in Tables 5 and 6 was taken from Russell, Dugan, and Stewart,[16] using $T_1 = 5500°$ for dG6. Their scale is based upon 6000° for the sun, with spectrum dG0 and color index +0.57 on the Harvard photographic-visual scale. However, if we follow G. P. Kuiper[17] and use color temperature $T_2 = 6700°$ and spectrum dG2 for the sun, our value for spectrum A0 is raised from $T_1 = 11{,}000°$ to $T_2 = 16{,}000°$, which many would prefer. Also, 11,200° for A5 on the new scale agrees with the value 11,000° adopted by F. H. Seares.[18] But our measures of V − I will then give $T_2 = 85{,}000°$ for B0 stars and 140,000° for O stars, while if we use U − I for the index, the value −3.62 for O stars exceeds −3.56 for $T_2 = \infty$.

TABLE 7

MEAN COLOR TEMPERATURES OF SPECTRAL TYPES

Spectrum*	V−I		T_1		T_2	
	Main Sequence	Giants	Main Sequence	Giants	Main Sequence	Giants
O	−2m52	.....	23,000°	.....	140,000°±	.....
B0	−2.47	.....	21,000	.....	85,000±	.....
B5	−2.24	.....	16,000	.....	34,000	.....
A0	−1.76	.....	11,000	.....	16,000	.....
A5	−1.30	.....	8700	.....	11,200	.....
F0	−0.92	.....	7300	.....	9000	.....
F5	−0.52	.....	6400	.....	7600	.....
G0	−0.28	+0m30	5950	5100°	6900	5780°
G5	−0.05	+1.00	5570	4360	6420	4830
K0	+0.16	+1.68	5280	3830	6020	4180
K5	+0.80	+2.30	4550	3440	5080	3730
M0	+2.04	+2.86	3590	3160	3900	3400
M5	.....	+4.00	.....	2710	.....	2880

* From O to B5 the classification can be taken as from Victoria;[8] from A0 to M5, as from Mount Wilson.[5]

In Table 7 the mean values of V − I for the spectral types are taken from the curves in Figure 2. As before, the temperatures under T_1 are based on dG6 = 5500°, while under T_2 they are on dG2 = 6700°. On either system a difference of a few hundredths of a magnitude in V − I makes a large difference in the hottest stars; or, putting it the other way, if we could fix the upper end of the scale, the lower temperatures would be well established. For instance, a variation of 1000° in T_1 at 25,000° corresponds in V − I to less than 50° at $T_1 = 6000°$.

Now that the relative temperature scales are established, we consider again the pos-

[16] *Astronomy*, p. 753, New York, 1927.

[17] *Ap. J.*, **88**, 461, 1938.

[18] *Mt. W. Contr.*, No. 685, p. 27; *Ap. J.*, **98**, 328, 1943.

sible systematic errors introduced by neglecting the shift of the effective wave lengths of the filters with the colors of the stars. First, as a sample, the mean wave lengths for the violet and infrared filters were computed for sources of 20,000° and 5000°, instead of for uniform energy throughout the spectrum. The change in $1/\lambda$ for 20,000° is from 2.37 to 2.40 for the violet and from 0.97 to 1.00 for the infrared. Similar small changes hold for 5000°. The net differential effect turns out to be less than 0.01 mag. in V − I between 20,000° and 5000° in T_1 in Table 7.

The effect of atmospheric extinction, treated in the same way, is to give only a slightly longer wave length for the violet filter—a change of $1/\lambda$ from 2.37 to 2.36—while the change in the infrared is negligible. The net result is that the computed T_1 is raised from 20,000° to 20,500° for an observed value of V − I for a star in the zenith.

The two reflections from the aluminum mirrors of the telescope have even less effect on the effective wave lengths than does the atmospheric extinction; so we conclude that there is no need of modifying the temperature scales at present. When the zero point is fixed and we are able to present absolute temperatures, further refinements can be discussed in detail.

The representation of the observed colors by black-body curves is practically independent of the adopted zero point for temperature. For each value of T_1 in Table 7 or Figure 2 there is a corresponding value of T_2 which will give the same computed colors, usually within less than 0.01 mag. The use of six colors has shown that the stars radiate so nearly like black bodies that the conventional color index from two colors gives a very good measure of the relative color temperature of a star. The determination of the effective temperature, which requires a knowledge of both the diameter and the total radiant energy of a star, is another matter. We are forced to leave our color temperatures without a definitive zero point. For the present we prefer the system T_1 to that of T_2 in Table 7, perhaps because T_1 does not give such extremely high values as T_2; but either choice will have to be changed.

IV. SPECIAL GROUPS OF STARS

The bluest stars.—The bluest O and early B stars may be compared with each other without the complication of the many absorption lines or bands of the later types. In Figure 3 are shown the deviations for some individual stars from black-body colors at $T_1 = 23{,}000°$, the necessary data being in Tables 3 and 5. The two O stars are almost certainly more than 500 parsecs distant, and in galactic latitude −17° their colors could be affected by an absorbing layer near the plane of the galaxy.

Likewise the differences in the three Orion stars may be caused by space reddening; all three of their spectra show the interstellar K line of calcium. As we go along the Belt eastward from δ Orionis, we get nearer to the Orion nebula, where the Trapezium is strongly reddened, although the measured order of color is δ, ζ, ϵ, not δ, ϵ, ζ, according to their positions. In terms of V − I we have $\epsilon - \delta = +0.15$; and for the Trapezium, $\theta^1 - \delta = +1.22$. With faint nebulosity over all the constellation we may assume that the differential absorption in the distance of 1°.4 between δ and ϵ could amount to one-eighth of that in the 5° between δ and the Trapezium.

It is a strange coincidence that δ Orionis, the first star with an observed interstellar spectrum line, should turn out to be the bluest B0 star we have measured. Therefore, in the O's and B0's we are suspicious of space reddening in the bluest stars in the whole sky. At present there seems to be no possibility of telling whether the small differences at the top of the color scale are caused by such reddening or by intrinsic differences in the stars themselves.

The two stars β Cephei and ϵ Persei stand out as the bluest of spectrum B1 and B2, respectively, but both are in the zone of avoidance. Their distances, probably less than 200 parsecs, are small for much absorption. The curves for these two stars are practically

the same; and, taken together, they both differ from the others in Figure 3, but the reason for the difference is not clear.

The Pleiades.—We have measures of a dozen bright stars of the Pleiades; but since some of them have been observed only once, they are grouped in pairs in Figure 3 and referred to $T_1 = 13{,}000°$. The spectra are from the latest unpublished results of Adams and Joy. We have found no clear-cut case of correlation between any two of the following properties: magnitude, spectrum, color, and hydrogen absorption in the ultraviolet. The hydrogen absorption and the color index, V − I, are both greater for the fainter stars; but the progression of these quantities is not uniform down the scale of brightness.

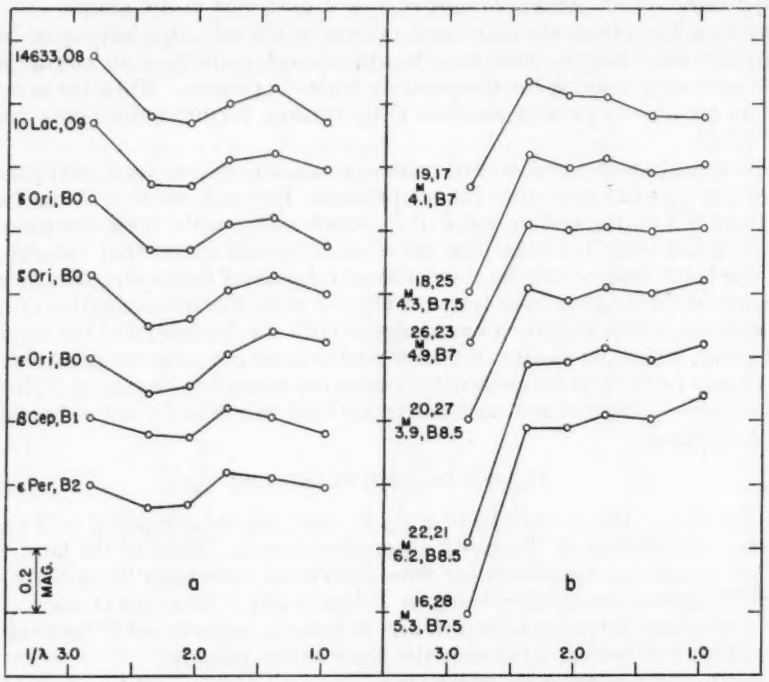

FIG. 3.—(*a*) Deviations of bluest stars from black-body colors at $T_1 = 23{,}000°$ K. (*b*) Deviations of Pleiades stars by pairs from black-body colors at $T_1 = 13{,}000°$. Each pair is identified by the Flamsteed numbers in Taurus.

Even in this closely related cluster of stars there seems to be a dispersion of each property with respect to any other.

Seares[19] has found a general color excess E_{int} of at least +0.10 for the Pleiades, which we do not seem to get in the bright stars. For fifteen other B5–B9 stars in Table 3 we find: average spectrum B7.9, V − I = −2.04, as against B7.7, V − I = −1.99 for twelve Pleiades. Allowing 0.02 for the difference in average spectrum, the color excess of the Pleiades in V − I becomes +0.07, or $E_{int} = +0.02$. Similarly, the six Pleiades previously measured among the 1332 B stars[20] give $E_1 = +0.01 \pm 0.006$ (p.e.), on a scale about half that of International. With the ever-present possibility of systematic errors, no great significance is given to these small figures; but since the scale of V − I is about

[19] *Mt. W. Ann. Rept., 1943–1944*, p. 8.

[20] Stebbins, Huffer, and Whitford, *Mt. W. Contr.*, No. 621, p. 10; *Ap. J.*, 91, 29, 1940.

three times the International scale, we could scarcely miss a color excess of 0.30 mag. The reasons for the disagreement are not clear.

Another matter to consider in both sides of Figure 3 is that the deviations there shown are not from an ideal black body; they are the differential deviations from a system where the mean of ten standard stars of average spectrum G6 is taken as a black body at 5500°. Pending an absolute calibration of the scale, we can use any star or group of stars for the standard. If we ignored the ultraviolet, we could make the run of the four colors, violet to red, smoother by raising the blue points by 0.02 mag. and lowering the green by 0.02 mag. each; the same improvement would also hold for the main-sequence stars from O to dGo in Table 6 and Figure 2. But the infrared would still run off from type to type. After all, it is still remarkable how closely we can represent the stars with their complicated spectra by simple black bodies.

P Cygni.—This well-known star with its peculiar spectrum and many bright lines might be expected to deviate in color from a normal B star. In the heavily obscured region, in latitude +0°.4, there must be considerable space reddening added to the intrinsic color of the star; and the best we can do is to estimate this selective absorption from

TABLE 8

COLORS OF P CYGNI

	HD	Spec.	U	V	B	G	R	I	U−I
Deviations from normal colors...	193443	O9	+1.14	+0.71	+0.40	+0.02	−0.43	−1.03	+2.17
	193183	cB2	+1.24	+ .76	+ .45	+ .05	− .50	−1.11	+2.35
Mean.....	.....	.....	+1.19	+ .74	+ .42	+ .04	− .46	−1.07	+2.26
Observed colors, P Cyg.....	193237	B1eq	−1.10	−0.40	− .08	+ .02	+ .06	+0.16	−1.26
True colors, P Cyg.	.....	.....	−2.29	−1.14	− .50	− .02	+ .52	+1.23	−3.52
Normal B1.....	.....	.....	−2.16	−1.15	− .53	− .06	+ .60	+1.35	−3.51
P Cyg−Normal B1	.....	.....	−0.13	+0.01	+0.03	+0.04	−0.08	−0.12	−0.01

near-by stars. Two such stars, HD 193183 and HD 193443, are, respectively, 0°.2 and 0°.3 distant from P Cygni.

In Table 8 the first two lines give the amount of the space absorption fo these stars, and the third line the mean. Subtracting the mean from the observed colors of P Cygni in the next line, we have the "true" colors of P Cygni. The normal B1 in the following line is the mean of δ Orionis, B0; β Cephei, B1; and ϵ Persei, B2. It seems best not to refer P Cygni to the variable β Cephei alone, the only apparently normal B1 star. The last line of the table gives the deviations of P Cygni from a normal star with the same absorption lines; these deviations are also shown in Figure 4. Ordinarily, the bright lines in a spectrum seem to have little effect upon the over-all distribution of energy measured through our filters, but in P Cygni the curve of the deviations showing extra strength in the ultraviolet and the infrared can presumably be traced in part to anomalies in the spectrum. Any other guess for the space reddening will give a similar curve for the colors of this star.

The Trapezium cluster of the Orion nebula.—The four components of θ^1 Orionis were measured together through a diaphragm of 41″ diameter; the corrections for the nebulous background were from 1 to 2 per cent of the intensities of the various colors. The average spectrum of the group may be taken as B0. In Table 9 is the comparison with the three stars of the Belt in the procedure followed for reddened stars. From the last two lines it is seen that the deviations of θ^1 Orionis from the $1/\lambda$ law are more than double the corresponding deviations of reddened B stars. (See also Fig. 4.) Except for the connection with the nebula we should not expect anomalous color in the Trapezium; but whether the comparison is made with the Belt stars or with any other standards, the result would be

the same. This is the only clear-cut case we have found of a wide difference from the average law of space reddening.

These results confirm the conclusion of Baade and Minkowski[21] that the selective absorption in the Trapezium region is different from that of reddened stars in general. Our deviations from the general law of reddening are qualitatively the same as theirs. Also, we find additional evidence for their suggestion that the Trapezium stars stand out from

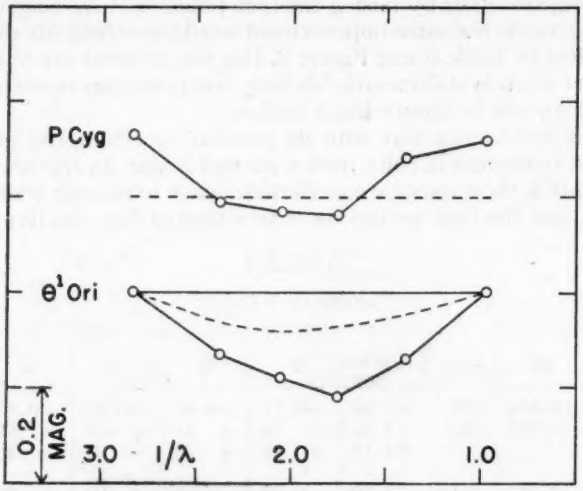

FIG. 4.—P Cygni: *open circles* are deviations from colors of a normal B1 star (*broken line*). θ^1 Orionis: *open circles* are deviations from normal law of space reddening (*broken line*) and from $1/\lambda$ law (*horizontal line*).

TABLE 9

COLORS OF THE TRAPEZIUM CLUSTER

	U	V	B	G	R	I	U−I
θ^1 Ori	−1.64	−0.74	−0.29	+0.02	+0.27	+0.56	−2.20
Mean, δ, ϵ, ζ Ori	−2.17	−1.12	− .51	− .04	+ .56	+1.32	−3.49
θ^1 − Mean	+0.53	+0.38	+ .22	+ .06	− .29	−0.76	+1.29
U − I = 1.00	+0.41	+ .29	+ .17	+ .05	− .22	−0.59	+1.00
$1/\lambda$ law	+0.41	+ .16	− .01	− .17	− .36	−0.59	+1.00
Difference, θ^1 Ori	0.00	+ .13	+ .18	+ .22	+ .14	0.00	.....
Difference, B stars	0.00	+0.06	+0.09	+0.08	+0.05	0.00	.....

a larger cluster because the optical properties of the absorbing interstellar material are modified to give greater transparency in the Trapezium region. There is plenty of opportunity in the whole constellation of Orion for work on differential colors of early-type stars, both in the apparently clear spaces and in the various nebulosities.

The North Polar Sequence.—The only direct connection we have with the International scale of color is through thirteen bright stars of the North Polar Sequence. In Table 10 these stars are listed in the order of V − I. The fifth column gives C_{int} by F. H. Seares;[22]

[21] *Mt. W. Contr.*, Nos. 571, 572; *Ap. J.*, **86**, 119, 123, 1937.

[22] *Mt. W. Contr.*, No. 701, p. 2; *Ap. J.*, **101**, 16, 1945.

the sixth, C_1 of the photoelectric system for B stars, previously unpublished. The other columns are self-explanatory.

In Table 11 the ratios of the different scales of color are brought together as we have them now. The respective values in column (2) were derived from the data of Table 10. The single value in column (3) is the ratio of the difference between the $1/\lambda$'s of V and I to the difference between the $1/\lambda$'s of C_1. The value in column (4) from 52 A stars north of declination $+80°$ is by Seares.[23] Column (5) gives an observed ratio from 69 reddened O and B stars;[3] column (6) the corresponding ratio computed from the derived law of space reddening.

TABLE 10

COLORS OF THE NORTH POLAR SEQUENCE

HD	NPS	m	Spec.	C_{int}	C_1	U	V	B	G	R	I	V−I
212710.....	2	5.38	B9	−0.11	−0.08	−0.90	−0.92	−0.44	−0.06	+0.49	+0.92	−1.84
166205.....	1	4.44	A2	+ .03	− .04	− .72	− .85	− .40	− .05	+ .46	+ .90	−1.73
5914.....	5	6.48	A5	+ .03	+ .01	− .62	− .76	− .36	− .04	+ .40	+ .80	−1.56
166926.....	4	5.86	A3p	+ .14	+ .07	− .49	− .60	− .29	− .04	+ .33	+ .68	−1.28
66368.....	6	7.01	A3	+ .06	+ .03	− .49	− .65	− .31	− .01	+ .33	+ .58	−1.23
221525.....	3	5.62	dF0	+ .18	+ .08	− .36	− .59	− .27	− .04	+ .30	+ .56	−1.15
107192.....	2s	6.28	dF2	+ .15	+ .13	− .51	− .49	− .20	− .02	+ .22	+ .46	−0.95
107113.....	3s	6.33	dF4	+ .23	+ .15	− .48	− .36	− .13	− .02	+ .15	+ .34	−0.70
8890.....	1s	2.12	cF7	+0.49	+ .30	+0.16	− .14	− .06	− .02	+ .08	+ .16	−0.30
187138.....	4r	8.26	gG9	+1.02	+ .67	+1.40	+0.46	+ .22	− .02	− .20	− .31	+0.77
114282.....	3r	7.57	gK2	+1.41	+0.98	+2.44	+1.09	+ .48	− .02	− .46	−0.91	+2.00
51802.....	1r	5.26	gM0	+1.53	+1.08	.....	+1.28	+ .63	+ .03	− .66	−1.42	+2.70
183030.....	2r	6.55	gM1	+1.57	+0.99	.....	+1.41	+0.70	+0.07	−0.77	−1.76	+3.17

TABLE 11

RATIOS OF COLOR SCALES

(1)	(2) Obs. 13 NPS Stars	(3) Comp. 1/λ Law	(4) Obs. 52 A Stars	(5) Obs. 69 O and B Stars	(6) Comp. Reddening Law
$(V-I)/C_1$.....	3.9	4.9	.....	6.5	6.4
$(V-I)/C_{int}$.....	2.7	.....	.....	.....	.....
C_{int}/C_1.....	1.5	.....	1.9	.....	.....

Table 11, with half the entries blank, indicates more what we should like to get than what we actually have. The only stars observed in common in the three systems, V − I, C_{int}, and C_1, are the bright polar stars, which are difficult to observe by photography; and, moreover, two of the red stars which carry much weight, NPS 1[12] and NPS 2, are probably variable in both light and color. We have measures of four other NPS stars; and from the total of seventeen we get $C_{int}/C_1 = 1.44 \pm 0.01$ (p.e.), which is near the value in the table. The 52 A stars give $C_{int}/C_1 = 1.90 \pm 0.10$ (p.e.). These stars, which range from B8 to A4, are affected by hydrogen absorption and have only a small dispersion in space reddening; but they give the same result as every other test we have made, namely, that the ratio of a long base-line color scale to the C_1 scale is greater for space

[23] *Mt. W. Contr.*, No. 684, p. 12; *Ap. J.*, 98, 272, 1943.

reddening than for differences of spectral type. The same effect in $(V - I)/C_1$ in columns (2) and (5) follows simply from the curve of the deviations from the $1/\lambda$ law, as shown in columns (3) and (6).

We have not attempted to compute theoretical ratios with C_{int}; these could be derived from the investigations of Seares,[24] but the International photographic magnitudes are affected by hydrogen absorption in the ultraviolet, which must be considered. Hence, we let the figures in Table 11 stand until we have more six-color observations of International stars and until someone has managed to get International colors of strongly reddened B stars. In the meantime we shall not go far wrong if we assume that the V − I scale is about 3 times the C_{int} scale for space reddening.

V. COMPARISON WITH OTHER COLOR SYSTEMS

The possibilities are endless for the comparison of the foregoing results with the color systems of other observers. As someone has put it, the six colors of a star give fifteen different color indices, which may be compared with each other as well as with still other independent color indices of various wave lengths, not to mention the classification and the details of the spectrum of the star. The present situation in stellar colorimetry is that there is no extended list of stars for intercomparisons by everybody. As mentioned previously, our stars were, in part, selected in somewhat the following fashion: F–M dwarfs as standards for nebulae; O–B3 stars for space reddening; B5–A9 stars to fill out the main sequence; F–M supergiants for further calibration; ordinary giants as convenient; the brightest stars of the North Polar Sequence; other special groups of stars as they fitted into the foregoing programs; first-magnitude stars like Vega, Betelgeuse, and others; and a few variable stars like δ Cephei, Polaris, and β Cephei, to be observed as opportunity offered. Obviously, any such list as the foregoing can scarcely serve as standard. The stars range from the zero magnitude to the ninth; they are all over the sky—in and out of the Milky Way, in obscured and unobscured regions. We probably wasted some time in measuring the late-type giant stars in low galactic latitude, since, on account of undetermined space reddening, the colors of such stars are not of particular significance. Nevertheless, we have enough stars in common with other lists to derive some interrelations, though where only two series are compared, it may be difficult to trace the causes for discrepancies. It is our purpose here not to give detailed studies but simply to comment on one or two other systems.

Greenwich gradients.—We have about forty-five stars in common with the Greenwich gradients.[25] The gradients were determined photographically with a spectrophotometer and refer to spectral regions apparently free from absorption lines. Their range of $1/\lambda$ is usually $2.34 - 1.58 = 0.76\ \mu^{-1}$; this is slightly less than our difference between violet and the mean of green and red, which gives $2.37 - 1.57 = 0.80\mu^{-1}$. When the gradients are reduced to our scale and compared, star by star, with our colors, the agreement is very good; there are no outstanding discordances, either for normal or for reddened stars.

The apparent discrepancy in gradients and our previous colors C_1 between normal and reddened stars has been discussed by Atkinson, Hunter, and Martin.[26] Their suggestion that the results of Elvey at Yerkes and ourselves at Madison may have been vitiated by focal diaphragms that cut out part of the shorter wave lengths can be discarded. It would, indeed, be extraordinary if for ten years we had kept on trying to measure stars through a hole too small to let the light through! That such was not the case is shown by several considerations: (1) The C_1 scale of the refractor at Madison agrees within 1 per cent with the scale of the reflectors at Mount Wilson, where there is no question of chromatic aberration. (2) The diameter of the extrafocal image of the Madison refractor for

[24] *Mt. W. Contr.*, No. 685; *Ap. J.*, **98**, 302, 1943.

[25] *M.N.*, **100**, 189, 1940.

[26] *M.N.*, **100**, 196, 1940.

4000 A is 2.0 mm; the diameters of diaphragms used were 2.7 and 4.0 mm. Similar clearance was made at Yerkes: 5-mm image with 8-mm diaphragm. (3) Measures were usually made with the smaller diaphragm in moonlight and the larger in a dark sky. Occasionally, alternate measures were made with the diaphragms for a check on the sky correction. (4) Tests were often made for guiding error by measuring a star in different parts of the field. Such tests are a matter of routine for any observer endowed with the slightest trace of curiosity. (5) The simplest check is to look at a bright star through a violet filter. The halo around Sirius appears, to the eye, to be considerably smaller than the 2 mm computed for 4000 A, because of longer wave lengths, up to 4500 A, transmitted by the filter.

There is such a thing as overproving a case; but at Yerkes[27] we could not ignore the aberrations even if we had wanted to, owing to the scale of things at the focus of the 40-inch objective. When the photometer was first installed, we found that with the visual focus at a convenient place in front of the cell-box the violet focus was some 10 cm farther back; and there was a tremendous guiding error, depending upon whether or not the small violet image actually hit the wire anode of the photocell. The difficulty was overcome by using a negative lens for the window of the box, thus expanding all images up to 1 or 2 cm on the surface of the cell. Also in the Yerkes instrument, with a second diagonal eyepiece in front of the focus, the diaphragm could be placed not at the visual focus but, if desired, near the circle of least confusion for the wave lengths concerned. We could do the same at Madison, but we did not have to.

No; what the Greenwich observers unearthed was, not a long-continued ridiculous blunder on our part, but simply a confirmation of the law of space reddening and of the effect[28] shown in the discussion of Table 11 of the present paper. Changes of spectral type follow closely the $1/\lambda$ law; changes of reddening deviate from that law.

The revised zero point of the Greenwich gradients gives about 12,700°[24] for an A0 star on the Mount Wilson classification, which is between our $T_1 = 11{,}000°$ and $T_2 = 16{,}000°$; but when the colors are compared differentially from star to star, there seem to be few cases of marked disagreement.

Spectrophotometry by John S. Hall.[29]—The work most nearly like ours is that by Hall on sixty-seven bright stars with a photocell at the Sproul and Amherst observatories. By means of a grating over the telescope objective and slits at the focus, he could isolate spectral regions about 485 A in extent from 4560 A to 10,300 A, or from the mean of our violet and blue to the same infrared. Unless the performance of a photocell is an illusion, we ought to get very good agreement between his colors and ours.

Hall's measures are referred to the mean of A0 stars, since he was not bothered by the ultraviolet. We have therefore referred our colors to the mean of ten A0's and then compared them graphically with his measures. There are eighteen stars in common, all of third magnitude or brighter; and six of these from the Sproul data are shown as samples in Figure 5. No attempt was made to pick out the best cases. The worst divergence comes in the infrared, where both series have less weight. The only star with even moderate reddening is ζ Persei, and we agree on that one. The star ϵ Pegasi shows the same divergence from a straight line that we found in other K giants. With our total of five regions against his thirteen, our measures naturally look a little smoother; but there is little evidence of systematic difference between the series. There are a dozen other stars which give about the same good agreement; and, all told, the comparison is quite satisfactory.

Other color indices.—After the comparison with Hall there is little point in going over different two-color systems of other observers, whether photoelectric or photographic.

[27] J. Stebbins, *Ap. J.*, **74**, 289, 1931.

[28] In private correspondence Dr. Y. Öhman, of the Stockholm Observatory, states that he has found the same effect.

[29] *Ap. J.*, **94**, 71, 1941.

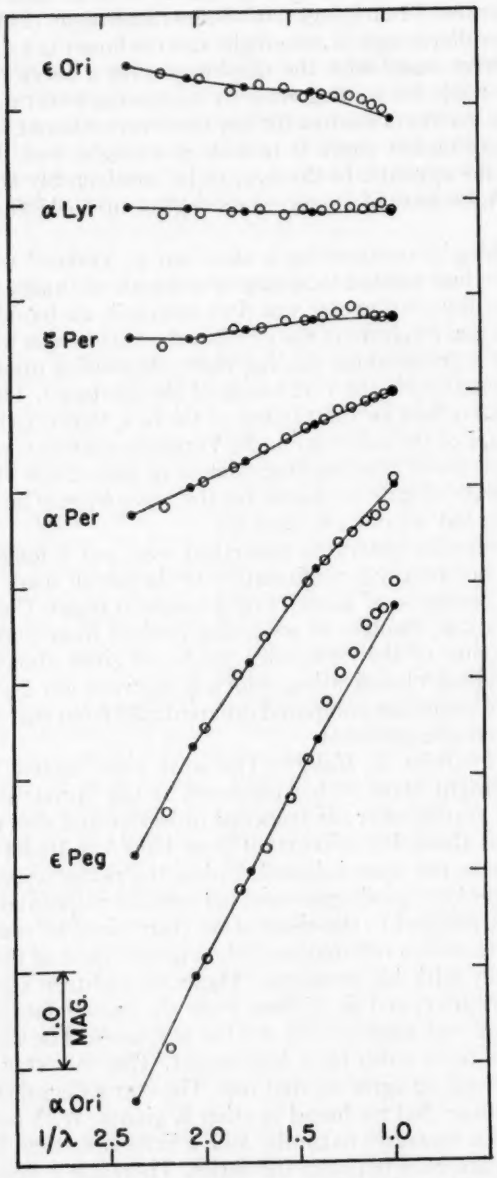

FIG. 5.—Comparison of five colors, violet to infrared (*solid circles*), with observations of John S. Hall (*open circles*).

Each time we get a new set of colors we cannot undertake to compare them with everything that has gone before; even the checking with our own previous work is troublesome enough. Such comparisons are usually made for a definite purpose; and for the present, at least, we are content to let the six colors stand for themselves.

VI. CONCLUDING REMARKS

In the hope that the results of the present investigation may be of value to others for one purpose or another, we give, at the risk of repetition, a few comments or words of caution.

First, too much weight should not be given to any star with only one observation. Although the measures are self-checking by the manner in which they were taken, it is always possible that an error in reading the galvanometer, an undiscovered mistake in the reductions, an unseen passing cloud in the sky, or a systematic variation of the extinction may remain undetected to the end. We believe that such cases are rare, but it may often be better to bunch several stars of the same color to minimize the accidental errors.

Next, beware of the colors of high-luminosity stars in low latitude or in the zone of avoidance. We are not at all sure that we have the pure colors of a single early-type star. If the sun is immersed in an absorbing layer, the optical path of, say, 500 parsecs to Orion at latitude $-17°$ can easily traverse enough interstellar material to give a detectable amount of reddening. Even at the galactic poles, where E. P. Hubble's[30] figure is 0.25 mag. for the photographic absorption, the selective absorption on our U − I scale should be nearly as much for distant stars. Perhaps a critical case is Spica (magnitude, 1.21; spectrum, B2; latitude, $+50°$), which may turn out to be as blue a star as can be found. We note that even Altair, at a measured distance of 5 parsecs, is too red for spectrum A1; but in this case, at least, we can feel sure that the colors are uncontaminated.

The spectra and absolute magnitudes quoted throughout this paper are not homogeneous. Even when they come from the same source, they are subject to continued revision and improvement. When Mr. Joy kindly helped to fill out the list by getting new spectra for us, we found in some cases that we could have estimated the spectral type and even the approximate absolute magnitude nearly well enough from our colors. From our point of view it would be a pleasant surprise if the spectra of the stars could be accurately classified from their colors, but there is no prospect of this development. Although the spectra may be simple functions of the masses, densities, and temperatures of the stars, the individual differences in the spectra are not imaginary; it may be, however, that the information derived from the colors, added to that from the line ratios, etc., may aid considerably in determining both spectral types and absolute magnitudes of near-by stars. For distant stars the colors are vitiated by space reddening.

The relative color temperatures we have given are to be taken with the same reservations as all other color temperatures of stars. Differentially they may be all right, but we cannot dodge the fact that the zero point of the temperature scale is not well determined. A good temperature for any one of our stars will fix all the rest of them. When we get around to determining the zero point by comparison with a terrestrial source like a standard lamp, we should plan to use not fewer than three such lamps—all calibrated, if possible, for different temperatures. There is no use of doing a halfway job in this determination. In the meantime the field is open to anyone else, as it has been for half a century, though there is something to be said for fixing the top of the temperature scale by theoretical considerations.

The photometry in six colors has naturally raised more problems than it has solved. In undertaking further work we could complete the measures of insufficiently observed stars, but little would come out of that effort. Neither should we expect much from addi-

[30] *Mt. W. Contr.*, No. 485, p. 44; *Ap. J.*, **79**, 51, 1934.

tional stars of types already well represented in the sequence. The absolute-magnitude effect in dwarfs, giants, and supergiants around spectrum K0 presents an attractive problem. The possibilities in variable stars are endless. Besides the light-curves for δ Cephei[31] already published, we have the six light-curves for Polaris; but because of the small variation of this star, it seems best to do them over again in another year—an hour or two on each of four good nights should be sufficient. Quite by accident, we once caught Algol almost exactly at minimum, when naturally the star was redder than normal. The combination of the colors at maximum and minimum with the dimensions of the apparent disks in the eclipsing system should give the colors and spectral type of the companion. We have carried through the calculations, but we do not believe the results; the computed colors of the companion do not fit a normal star. Presumably we were pushing the observations a little too far, and it is legitimate to suppress the results for the present.

Thus there are opportunities for many diversions, but we expect soon to return to the original problem of the colors of extragalactic nebulae.

This investigation has been supported in part by grants from the Observatory Council of the California Institute of Technology and from the Alumni Research Fund of the University of Wisconsin.

[31] J. Stebbins, *Mt. W. Contr.*, No. 704; *Ap. J.*, **101**, 47, 1945.

MEASUREMENTS IN THE SPECTRA OF U ORIONIS, R SERPENTIS, R AQUILAE, AND R CASSIOPEIAE*

PAUL W. MERRILL
Mount Wilson Observatory
Received July 10, 1945

ABSTRACT

This *Contribution* is the first of a series on the spectra of long-period variables observed with a dispersion of 10 A/mm. Tables 3 and 4 record data on the displacements of bright and dark lines which are more accurate than those previously available.

Comparison of the displacements of the dark lines of various metals shows that most of the residuals are within errors of measurement. Certain of the larger residuals are probably related to the behavior of lines of various excitation levels rather than to differential motions of various atoms. In U Ori, for example, among *Fe* I lines the mean displacement at E.P. 1.6 volts is about 3 km/sec greater than at E.P. 0.0 volts.

When the bright hydrogen lines are narrow, their displacements agree with those of other bright lines; when broad, they may have algebraically greater displacements. The *In* I line λ 4511 may be emitted by fluorescence, the exciting line being *Hδ*. Bright lines of *Fe* II and *Ti* II were observed in the spectrum of R Aql.

Discussion is largely postponed until additional data for other variables become available.

Some of the most interesting questions concerning the spectra of long-period variables refer to the structure and displacement of individual lines. Satisfactory answers to several such questions can be provided only by spectrograms with higher dispersion than that regularly employed in my previous survey (35–65 A/mm at *Hγ*). The few high-dispersion spectrograms of *o* Ceti obtained in the past by various observers[1] have already indicated rich possibilities. Recent improvements in photographic emulsions seemed to make this a strategic time for renewed observations.

Accordingly, half-a-dozen typical long-period variables of class Me were placed on the program for observation with the coudé spectrograph of the 100-inch telescope. About 60 spectrograms of the region *Hβ* to λ 3600 have now been obtained with the 32-inch camera, dispersion 10.3 A/mm, chiefly in the years 1943 and 1944. Most of them were taken on the experimental IIa-O emulsion developed by the Research Laboratory of the Eastman Kodak Company. This emulsion, which seems to exhibit little resemblance to the commercial II-O plate, is fast, fine-grained, with great latitude and low contrast; it yields excellent results on subjects of high intrinsic contrast, such as Me spectra with their numerous strong lines.

Data derived from a few spectrograms of each of the variables U Orionis, R Serpentis, R Aquilae, and R Cassiopeiae are recorded in the present *Contribution;* the somewhat longer series of plates of R Hydrae and R Leonis will be discussed in future *Contributions*. The photometric data in Tables 1 and 2 were kindly supplied by Mr. Leon Campbell of the Harvard Observatory.

ABSORPTION LINES

Outside the regions covered by titanium oxide bands, the spectra of these low-temperature stars are packed with lines of neutral metallic atoms, chiefly those arising from levels whose excitation potentials are less than 0.3 volts. Lines from higher levels, while not entirely absent, are of greatly reduced intensity in comparison with the spectrum of

* *Contributions from the Mount Wilson Observatory, Carnegie Institution of Washington,* No. 713.

[1] W. W. Campbell, *Ap. J.*, **9**, 31, 1899; W. S. Adams, *Mt. W. Contr.*, No. 638; *Ap. J.*, **93**, 11, 1941; A. H. Joy, unpublished.

the sun or of an ordinary laboratory arc. The only conspicuous lines of ionized elements are λ 3933, λ 3968 of *Ca* II, and λ 4077, λ 4216 of *Sr* II (see Pls. XXV and XXVI).

The data in Table 3 show that within narrow limits the displacements of lines of various elements agree. Most of the residuals are within errors of measurement. Lines of *Sr* II yield the same displacements as lines of neutral metals.

Certain of the larger residuals are probably related to the behavior of particular lines rather than to differential motions of various atoms. For example, the dependence of displacement on excitation potential, detected by W. S. Adams[2] in the spectrum of *o* Ceti, is exhibited by the iron lines in U Orionis and R Serpentis. The mean displacement at E.P. 1.6 volts is about 3 km/sec greater algebraically than that at 0.0 volts; it may be a function of phase in the light-cycle.

The weak potassium lines λ 4044, λ 4047 are sharp and well measurable. The mean residual, −3.3 km/sec, is greater than the error of measurement and is probably related to the similar but larger displacement of the red potassium lines in the spectrum of α

TABLE 1

PHOTOMETRIC DATA

Variable	Desig.	Spec.	Mean Max. Mag.	Mean Min. Mag.	Mean Period (Days)	$m-M$* (Days)	$(m-M)/P$
U Ori.....	054920a	M8e	6.6	11.9	372	228	0.61
R Ser.....	154615	M7e	6.8	13.3	357	268	.58
R Aql.....	190108	M7e	6.3	11.5	305†	173	.57
R Cas.....	235350	M7e	6.5	12.1	430	257	0.60

* $m-M$ is the interval from maximum to minimum light. It is regularly longer in Me variables than the interval from minimum to maximum.

† R Aql is one of the very few long-period variables to show a definite change of period. The value in the table—305 days—is that for the last twenty years; the average period for the whole time of observation is 322 days.

Herculis,[3] which, in turn, may be related to the core effect in lines of low excitation potential in the spectra of α Orionis and other M-type giants.[4] A tendency of λ 4044 to have a slightly greater negative displacement than λ 4047 requires further observation.

The negative residual of *Cr* is due in part to the three strong lines of E.P. 0.0 volts, λλ 4254, 4274, 4289, measured on some of the plates. The *Mn* line λ 4033.07 has a persistent negative residual (about −4 km/sec), probably because of a weak blended line on its shortward[5] edge. Another *Mn* line, λ 4035.73, has a large longward shift (about 7 km/sec) due to an unknown cause. The interesting behavior of these and other *Mn* lines will be studied in spectra of other long-period variables.

U Orionis.—During the interval from phase −38 days to phase −4 days, the brightness of the variable increased 2.2 mag. Nevertheless, changes in the dark-line spectrum were minor; most portions of the spectrum were nearly identical on the two dates (pls. Ce 3315, 3359). A few lines especially sensitive to the increase in temperature became weaker; notable examples are the narrow lines of potassium λ 4044, λ 4047, and the ex-

[2] *Mt. W. Contr.*, No. 638; *Ap. J.*, **93**, 11, 1941.

[3] P. W. Merrill, *Mt. W. Contr.*, No. 486; *Ap. J.*, **79**, 183, 1934.

[4] W. S. Adams, *Mt. W. Contr.*, No. 638, *Ap. J.*, **93**, 11, 1941, *Pub. A.S.P*, **57**, 95, 1945; Lyman Spitzer, Jr., *Mt. W. Contr.*, No. 619; *Ap. J.*, **90**, 494, 1939.

[5] "Shortward" and "longward" are suggested as abbreviations for the cumbersome expressions "toward shorter (or longer) wave lengths." The phrases "to the violet" and "to the red" are sometimes ambiguous.

PLATE XXV

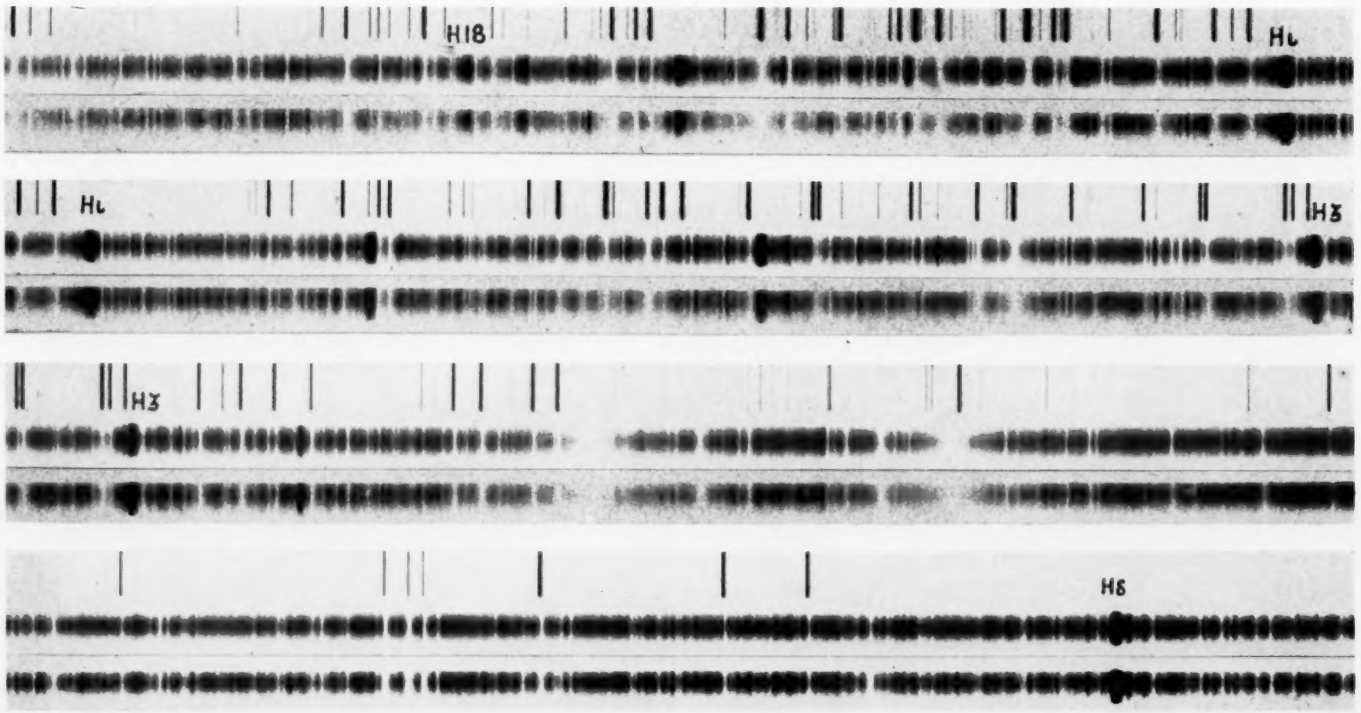

SPECTRA OF R AQUILAE AND R CASSIOPEIAE

Upper spectrum of each pair is of R Aql, May 18, 1943, phase, +5 days; lower is of R Cas, December 27, 1942, phase, +8 days

PLATE XXVI

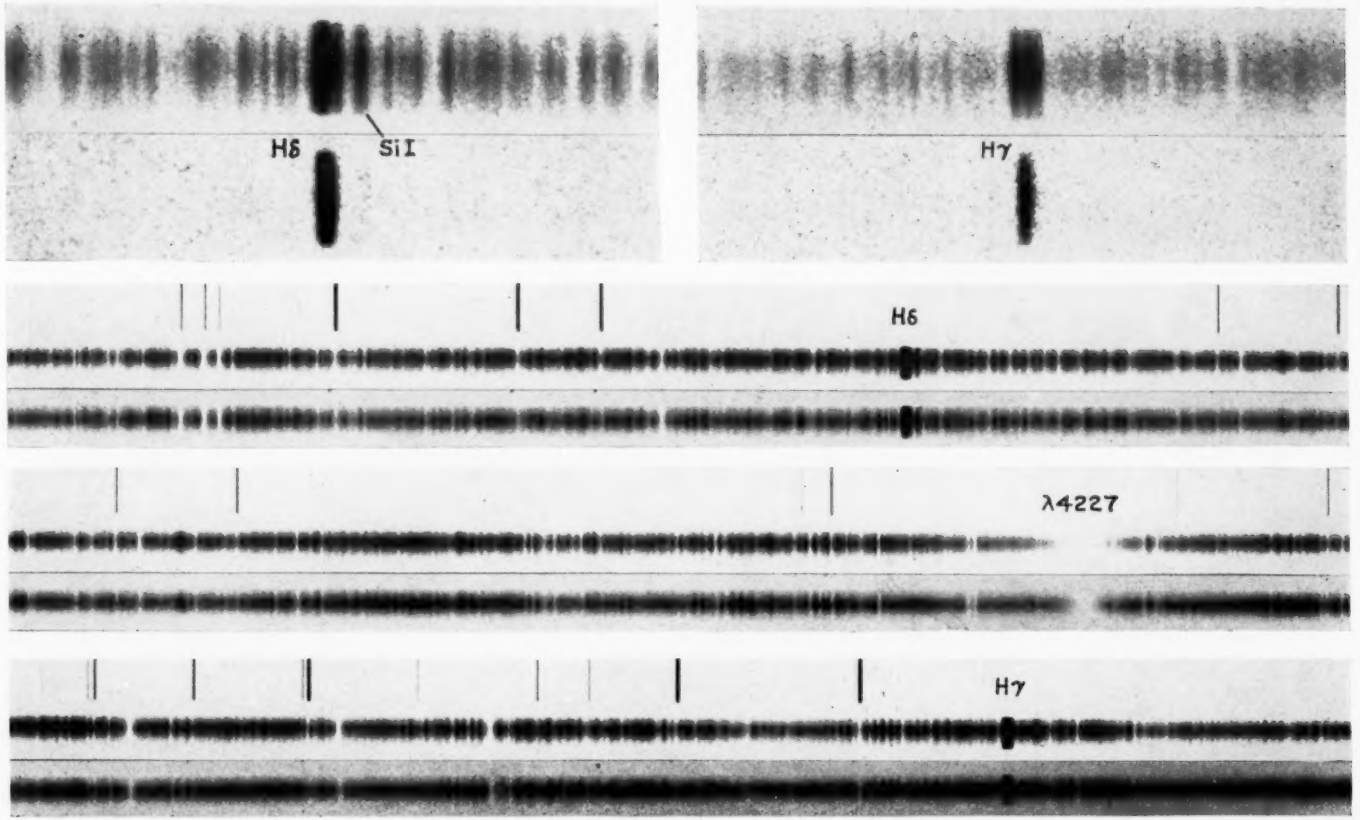

SPECTRA OF U ORIONIS AND R SERPENTIS

The greatly enlarged images of $H\gamma$ and $H\delta$ at the top are of U Ori: upper, December 12, 1943, phase, −38 days; lower, April 7, 1944, phase, +79 days.

Of the following spectra, the upper of each pair is of U Ori, January 16, 1944, phase, −3 days; the lower is of R Ser, August 4, 1944, phase, −15 days.

tremely broad line of calcium λ 4227. Changes in the titanium oxide bands were not marked.

R Serpentis.—The dark-line spectrum is much like that of U Orionis. The bands are stronger on Ce 3120, mag. 8.5, phase +3 days, taken in 1943, than on 3520, mag. 7.5, phase −18, taken in 1944; and a few minor differences may be noted in the atomic lines.

TABLE 2

JOURNAL OF OBSERVATIONS

Plate Ce	Date	JD 243	Mag.	Phase (Days)	Velocity from Abs. Lines*	
					Km/Sec	No. Lines
	U Orionis					
2956	1943 Feb. 24	0780	7.5	+40	.....	.....
3315	Dec. 12	1071	8.6	−38	−19.5	74
3359	1944 Jan. 15	1105	6.4	− 4	−20.2	90
3364	16	1106	6.4	− 3	.....	.....
3365	16	1106	6.4	− 3	−20.4	108
3383	Feb. 8	1129	6.9	+20	.....	.....
3386	9	1130	7.0	+21	.....	.....
3400	Apr. 7	1188	8.6	+79	.....	.....
	R Serpentis					
3115	1943 July 20	0926	8.5	+ 2	.....	.....
3120	21	0927	8.5	+ 3	+23.1	58
3520	1944 Aug. 1	1304	7.5	−18	+20.5	38
3534	4	1307	7.5	−15	+19.4	55
	R Aquilae					
3032	1943 May 18	0863	6.3	+ 5	+32.2	92
3058	June 9	0885	7.0	+27	+32.5	70
3060	10	0886	7.0	+28	.....	.....
3077	22	0898	7.6	+40	+30.6	31
3124	July 22	0928	8.5	+70	+32.5	21
	R Cassiopeiae					
2905	1942 Nov. 20	0684	7.0	−29	.....	.....
2937	Dec. 27	0721	6.6	+ 8	+21.4	58

* Measured velocity reduced to the sun.

R Aquilae.—The absorption-line spectrum indicates a slight decrease in temperature from phase +5, mag. 6.3, to phase +70, mag. 8.5.

R Cassiopeiae.—The absorption spectrum is much like that of the other stars, although differences in the relative intensities of certain lines can be detected.

−15 days.

EMISSION LINES

Detailed data concerning the displacement of various emission lines in Table 4 suggest numerous problems that can be discussed to better advantage with the more extensive data to be derived later from the spectra of other long-period variables. A few remarks may facilitate future comparisons with other stars.

TABLE 3

RELATIVE DISPLACEMENTS OF ABSORPTION LINES OF VARIOUS ELEMENTS
INDIVIDUAL *minus* ADOPTED (KM/SEC)

PLATE CE	*K*	*Sc*	*Ti*	*V*	*Cr*	*Mn*	*Fe*	*Co*	*Ni*	*Sr* II
	U Orionis									
3315	−2.8 2	+0.6 4	+0.6 12	−0.9 14	+0.1 2	−0.6 7	+0.8 11	−0.2 13	+0.6 3	+0.7 1
3359	−2.5 2	+ .6 7	− .3 19	.0 13	+ .4 4	− .8 8	+ .2 23	− .1 10	− .1 4	−1.6 2
3365	−1.5 2	+0.7 4	+0.6 21	−0.0 25	−0.2 9	+0.2 5	−0.5 34	+0.3 7	+0.9 6	+0.5 2
Mean	−2.3	+0.6	+0.3	−0.2	0.0	−0.5	−0.1	0.0	+0.5	−0.3
	R Serpentis									
3120	−5.7 1	+0.7 4	−0.4 10	−0.4 13	−3.1 6	−0.2 5	+0.2 16	+1.7 6	−1.3 2	−4.5 2
3520	−3.0 2	−0.6 2	.0 8	−2.1 5	−0.9 2	−1.5 6	+ .9 16	0.0 4	.....	−1.9 2
3534	−1.4 2	+1.4 4	−0.1 15	−0.6 9	−0.7 4	−2.0 2	+0.3 15	.....	+0.4 2	−3.2 2
Mean	−2.9	+0.7	−0.2	−0.8	−1.9	−1.1	+0.5	+1.0	−0.4	−3.2
	R Aquilae									
3032	.....	+0.7 5	+0.1 22	+0.1 17	−1.1 7	−0.5 3	+0.1 22	+0.5 5	−0.3 12	+1.2 2
3058	−3.4 2	+ .3 2	−0.5 15	−0.7 7	−2.5 5	0.0 2	+0.5 24	−0.8 4	0.0 9	+0.3 1
3077	−3.6 2	+ .2 2	−1.0 3	−1.5 4	−1.9 3	+0.6 3	+1.7 13	−1.3 6	.....	+1.4 1
3124	−5.7 2	−0.6 2	−0.8 4	−2.9 5	.....	+1.0 3	+2.1 9	+0.7 1	.....	+1.8 1
Mean	−4.2	+0.3	−0.3	−0.7	−1.7	+0.3	+0.8	−0.5	−0.2	+1.2
	R Cassiopeiae									
2937	−4.9 2	+1.3 2	−0.4 11	−0.6 13	0.0 3	−3.2 2	+0.1 16	−0.5 4	+1.3 5	+2.6 2
	All									
	−3.3	+0.5	−0.1	−0.5	−1.1	−0.6	+0.4	0.0	+0.2	−0.5

The minima within the bright hydrogen lines which give the appearance of separate emission components are visible on several plates (illustrated on Pl. XXV). Certain of these minima have been identified with absorption lines of atoms in the overlying reversing layer,[6] and it seems probable that others are formed in the same way. When the bright

[6] P. W. Merrill, *Pub. A.S.P.*, **57**, 178, 1945.

TABLE 4

DISPLACEMENTS OF BRIGHT LINES*
(Km/Sec)

Ce	*H*	*Si* I		*Fe* I		*Mg* I		
		λ3905	λ4103	λ3852	λ4202	λ3829	λ3832	λ3838
	U Orionis							
2956	−35.6	−37.4	.....	−34.4	−38.2	.....	−37.6	−36.0
3315	.....	−42.6	−38.4	.....	.....	.....	.....	.....
3359	−30.2	−42.2	−40.1	.....	.....	.....	.....	.....
3364	.....	−36.5	−38.0	.....	.....	.....	.....	.....
3365	−30.5	−37.1	−37.5	.....	.....	.....	.....	.....
3383	.....	−35.9	−36.8	−35.3	−38.0	(−44.0)	(−36.1)	(−33.8)
3386	−31.0	−35.3	−34.0	−32.1	−37.4	.....	(−41.0)	−35.5
3400	−33.5	.....	.....	−33.3	−34.6	.....	.....	.....
Mean	−32.1	−38.2	−37.4	−33.8	−37.0	.....	(−38.3)	(−35.1)
	R Serpentis							
3115	(− 2.1)	(+ 4.5)	+ 5.4	.....	.....	.....	.....	.....
3120	.....	(− 0.3)	+ 5.1	.....	.....	.....	.....	.....
3520	(+13.6)	(− 2.5)	(+ 0.9)	.....	.....	.....	.....	.....
3534	(+13.6)	(− 0.4)	(+ 0.7)	.....	.....	.....	.....	.....
Mean	.....	(+ 0.3)	(+ 3.0)	.....	.....	.....	.....	.....
	R Aquilae							
3032	+18.7	+20.7	.....	+19.9	+17.8	.....	+16.0	+21.5
3058	+21.8	+19.7	+24.5	+19.0	+19.9	+20.6	+12.0	+20.6
3060	+22.7	(+22.3)	.....	(+20.5)	.....	.....	.....	.....
3077	+20.2	+18.5	+20.9	+17.8	+18.4	+17.1	+14.0	+19.4
3124	+21.7	+23.7	+24.5	+24.9	+19.6	+21.1	+16.4	+22.6
Mean	+21.0	+21.0	+23.3	+20.4	+19.2	+19.6	+14.6	+21.0
	R Cassiopeiae							
2905	+ 9.1	− 0.3	+ 2.8	.....	.....	.....	.....	.....
2937	+ 7.2	− 0.9	+ 4.0	+ 5.6	(+ 2.0)	+ 2.6	+ 1.0	+ 6.5
Mean	+ 8.2	− 0.6	+ 3.4	.....	.....	.....	.....	.....

* Measured velocities reduced to the sun.

hydrogen lines are thus mutilated, it is not easy to determine their true displacements. Measurements of certain plates (Table 4) indicate longward displacements of a few km/sec with respect to the bright lines of other elements. As the phase advances after maximum, however, the bright lines become narrower, and the effects of overlying absorption tend to become less. When the lines are narrow, their displacements seem to agree with those of other bright lines. The same effect was noticed several years ago on spectrograms of lower dispersion. "The meager data suggest that large residuals tend to disappear after maximum and that especially narrow lines usually yield small residuals."[7]

The spectrum of U Orionis before maximum shows the division of the bright hydrogen lines exceptionally well (see Pl. XXVI). On Plate Ce3315 the bright *Hδ* line is strongly notched by a minimum whose wave length (on the assumption that the displacement is the same as that of numerous dark lines in the continuous spectrum) is 4101.80 A. The identification may be *In* I λ 4101.773. On this plate λ 4511, tentatively identified with *In* I by A. H. Joy[8] and others, appears as a sharp bright line of moderate intensity; on later plates the line is much weaker. These facts seem to constitute evidence that *Hδ* excites indium atoms to the upper level for the line λ 4511, as suggested by A. D. Thackeray.[9] It is hoped to discuss this problem in a future *Contribution* after measurements of the spectra of other long-period variables become available.

The wave length of the indium line identified with the minimum in *Hδ* differs but a few hundredths of an angstrom from the normal wave length of *Hδ* itself. The position of the minimum decidedly toward the longward edge of the bright line thus testifies to the well-known shortward displacement of the bright hydrogen lines with respect to the dark metallic lines. The displacement is also shown by the behavior of the *H* 16 line. This bright line, λ 3703.855, is divided almost centrally by the *V* I dark line λ 3703.584. The difference of the wave lengths, 0.271 A (22 km/sec), corresponds approximately to the relative shift of the bright lines.

The lines of *Ti* II λ 3685, λ 3759, λ 3761, measured in emission on two or three plates of R Aquilae, yield the same displacements as those of most other bright lines. Bright lines of *Fe* II, however, show a definite longward displacement as found by Joy[8] in the spectrum of *o* Ceti.

[7] P. W. Merrill, *Mt. W. Contr.*, No. 642; *Ap. J.*, **93**, 40, 1941.

[8] *Mt. W. Contr.*, No. 311; *Ap. J.*, **63**, 281, 1926.

[9] *Mt. W. Contr.*, No. 517; *Ap. J.*, **81**, 467, 1935.

IDENTIFICATION OF THE POST-MAXIMUM LINES IN THE SPECTRUM OF NOVA (RS) OPHIUCHI*

A. H. JOY AND P. SWINGS
Mount Wilson Observatory
Received August 6, 1945

ABSTRACT

Interest in the spectra of recurring novae has been aroused by the recent (fourth) outburst of Nova (T) Pyxidis. A review of the hitherto unpublished measures of the Mount Wilson spectrograms of Nova (RS) Ophiuchi obtained between September 2 and November 10, 1933, shows many plausible identifications of lines which were impossible earlier.

The atoms now identified, in addition to *H*, are: *He* I, *He* II, *C* III, [*N* II], *N* III, [*O* I], *O* III, [*O* III], [*Ne* III], [*Ne* IV], *Na* I, *Si* I, *Si* II, *Si* III, *Si* IV, [*S* II], [*S* III], [*A* V], [*A* X], [*A* XI], [*K* IV], [*K* V], [*Ca* V], [*Ca* VI], [*Ca* VII], [*Ca* XIII], [*Sc* VII], [*V* VIII], *Fe* II, [*Fe* II], [*Fe* IV], [*Fe* V], [*Fe* VI], [*Fe* VII], [*Fe* X], [*Fe* XI], [*Fe* XIV], [*Ni* XII], [*Kr* III]. Of these, [*A* XI] λ 6919, [*Ca* VII] λ 3688 (and possibly [*V* VIII] λ 3686), [*Sc* VII] λ 4823, and [*Kr* III] λ 6827 are identified for the first time.

Considerations of the physical conditions in the solar corona as compared with those in the recurrent novae indicate marked differences, the coronal strata not permitting radiation of forbidden lines in the lower stages of ionization such as are found in the novae.

The maximum of the second outburst of Nova (RS) Ophiuchi, which occurred about August 12, 1933, showed spectral characteristics similar to those of other "fast" novae. Bright lines of *H*, *He*, *Fe* II, *Ca* II, and *Na* I, attaining a total width of about 25 A for the strongest lines, were observed from August 16 to September 11.[1] These lines did not have the strong absorption components usually found at the violet edge of the chief lines of novae spectra at this phase, but, with sufficient dispersion, they showed a narrow dark line slightly displaced toward the violet from the center of the bright line.

Comparatively sharp nebular lines soon appeared and were first observed as follows: λ 4362 [*O* III] on August 18; λ 5006 [*O* III], λ 4640 *N* III, and λ 4686 *He* II on August 29; λ 3868 [*Ne* III], λ 3967 [*Ne* III], and λ 4959 [*O* III] on August 30; [*Fe* II] on September 11; and λ 4068 [*S* II] on October 1.

The coronal lines were first definitely identified[2] on a spectrogram taken on October 2, but it seems probable that λ 6374 was present as early as September 7, enhancing the strength of λ 6371 *Si* II above that of λ 6347 *Si* II. The lines λ 5303 and λ 6374, previously observed only in the solar corona, were strong on October 2 and changed only slightly in intensity until the end of the observing season on November 10, 1933. At the end of October, λ 5303 was of intensity comparable to that of *Hβ*, and λ 6374 was more than twice as strong as λ 5875 *He* I. By the beginning of the next observing season in March, 1934, the coronal lines had completely disappeared.

On the Mount Wilson spectrograms obtained between September 2 and November 10, 1933, after the first appearance of the nebular and coronal lines, a considerable number of lines was measured whose identity could not be recognized at that time. In the last few years our knowledge of the forbidden transitions has increased many fold, so that a new attempt to identify the lines which attained their greatest intensity some two months or more after the maximum of the nova now seems justified. The recent outburst of the recurrent Nova (T) Pyxidis and the satisfactory identification[3] of nearly all its emission lines add new interest to the problem.

* *Contributions from the Mount Wilson Observatory, Carnegie Institution of Washington*, No. 714.

[1] Adams and Joy, *Pub. A.S.P.*, **45**, 249, 1933; Wright and Neubauer, *Pub. A.S.P.*, **45**, 252, 1933.

[2] Adams and Joy, *Pub. A.S.P.*, **45**, 301, 1933.

[3] A. H. Joy, *Pub. A.S.P.*, **57**, 171, 1945. The unidentified line λ 7999 in T Pyxidis may possibly be the $a^6S_{3½}-a^6D_{4½}$ transition of [*Cr* II] whose predicted wave length is 8000.12.

TABLE 1

IDENTIFICATION OF EMISSION LINES IN RS OPHIUCHI

Observed λ	Intensity	Laboratory or Computed λ	Identification
3628	1	30.3	[Fe VI]
		34.3	He I
3656*	2	64.1	[Fe VI]
		52.0	He I
3688	1	88	[Ca VII]
		86	[V VIII]
3705*	2	05.0	He I
		02.8	O III
		03.4	O III
		07.2	O III
3760	4	59.9	[Fe VII]
		59.9	O III
3773	1	74.0	O III
3793	1	91.3	O III
3811	1	13.5	He II
3821	2	19.6	He I
3857	2	58.1	He II
3868	8	68.7	[Ne III]
		67.5	He I
3880	1	.....	.....
3902	1	95.4	[Fe V]:
		05.5	Si I
3938.3	1	38.3	Fe II
3968.0	10	67.5	[Ne III]
3987.5*	4	86.9	[Fe XI]
4026.4	5	26.2	He I
		25.6	He II
4070*	4	68.6	[S II]
		71.4	[Fe V]
4085*	2	86.3	[Ca XIII]
4095.9	4	97.3	N III
4120.8	1	20.8	He I
4143.3	2	43.8	He I
4176.8	1	77.2	[Fe II]
		78.8	Fe II
4199.8	3	99.9	He II
4230.4*	4	31.4	[Ni XII]
4233	3	33.2	Fe II
4243.3	2	43.6	[Fe II]
4258.7	1	58.2	Fe II
4275.2	1	76.9	[Fe II]
		73.3	Fe II
4286.6	3	87.4	[Fe II]
4303	0	03.2	Fe II
4359.1	1	58.4	[Fe II]
		59.3	[Fe II]
4362.6*	35	63.2	[O III]
4387.1	5	87.9	He I
4412.2	2	13.8	[Fe II]
4416.0	2	16.3	[Fe II]
		16.8	Fe II
4436.7	1	37.5	He I
4451.7	0	52.1	[Fe II]
4471.6	15	71.5	He I
		89.2	Fe II
4489.9	3	91.4	Fe II
		88.8	[Fe II]
4507.2	2	08.3	Fe II
4515	1	15.3	Fe II
		14.9	N III
		14.9	[Fe II]
4519.3	2	20.2	Fe II
4521.6	4	22.6	Fe II
		23.6	N III
4540.7	2	41.5	Fe II
		41.6	He II
4551.4	2	49.5	Fe II
		52.6	Si III
		55.9	Fe II
4575.4	0	76.3	Fe II
		74.8	Si III
4583.9	7	83.8	Fe II
4628	2	29.3	Fe II
4631.5	2	31.4	Si IV
		40.6	N III
4637.5	20	34.2	N III
		39.7	[Fe II]
4647	25	47.4	C III
4685.6	35	85.8	He II
4713.2	4	13.1	He I
4728.2	1	28.1	[Fe II]
		25.5	[Ne IV]
4813.6	0	14.6	[Fe II]
4823.2	1	23.5	[Sc VII]
4922.8	6	21.9	He I
		23.9	Fe II
4957.3*	1	58.9	[O III]
5005.7*	3	06.8	[O III]
5015.7	4	15.7	He I
5017	4	18.4	Fe II
5040.8	3	41.2	Si II
		41.2	[Fe IV]
5055.3	2	56.0	Si II
5156.8	0	58.3	[Fe VII]
5169.2	3	69.0	Fe II
5302.7*	6	02.9	[Fe XIV]
5411.1	4	11.6	He II
5533.6*	8	36	[A X]
		34.9	Fe II

TABLE 1—*Continued*

Observed λ	Intensity	Laboratory or Computed λ	Identification	Observed λ	Intensity	Laboratory or Computed λ	Identification
5592.3	0	92.4	*O* III	6248.5	2	47.6	*Fe* II
		87.2	[*Ca* VI]	6297.6*	1	00.0	[*O* I]
5753.0	4	55.0	[*N* II]	6316.0	3	16.6	[*K* V]
5772.6	1					10.2	[*S* III]
5876.2*	15	75.6	*He* I	6347.6*	6	47.1	*Si* II
				6370.9	8	71.4	*Si* II
5892.1*	2	90.0	*Na* I			63.9	[*O* I]
5898.6*	2	95.9	*Na* I	6374.9*	20	74.5	[*Fe* X]
5987.2*	1			6430.9	1	34.9	[*A* V]
6028.8*	2			6456.2	2	56.4	*Fe* II
6074.4	1			6518.0	2	16.1	*Fe* II
		85.5	[*Fe* VII]	6678.3	8	78.2	*He* I
6084.6	3	85.9	[*Ca* V]	6720.6	0	17.0	[*S* II]
		84.1	*Fe* II			31.3	[*S* II]
6104.6	5	02	[*K* IV]	6827.0	15	26.9	[*Kr* III]
6145.9	1	47.8	*Fe* II	6914*	3	19	[*A* XI]

λ	Remarks	λ	Remarks
3656	Wide	5876.2	D3
3705	Wide	5892.1	Violet comp. D1 and red comp. D2
3987.5	Corona		
4070	Wide	5898.6	D1 red comp.
4085	Corona	5987.2	Wide
4230.4	Corona	6028.8	Wide
4362.6	Wide band	6297.6	Wide
4957.3	N2	6347.6	Wide
5005.7	N1	6374.9	Corona
5302.7	Corona	6914	Wide
5533.6	Corona		

Table 1 is a list of the measured wave lengths and the approximate relative intensities of the lines. The possible identifications and the laboratory or computed wave lengths are in the third and fourth columns, the most probable identification or the largest contributor to a blend being given first.

The observed wave lengths are corrected for the earth's orbital motion but not for the radial velocity of the star itself. The hydrogen lines are present in considerable strength but have not been included in the table.

The measured wave lengths are compiled from the results from 12 spectrograms. The lines of wave length shorter than λ 3850 occur on a single spectrogram (dispersion 160 A/mm at K) obtained on October 27. The longer wave lengths are derived from several plates with dispersions of from 40 to 120 A/mm at $H\gamma$.

Most of the unblended bright lines are comparatively sharp and easily measured on good plates, but wave lengths cannot be measured closer than a few angstrom units with the dispersion employed.

NEW IDENTIFICATIONS

1. [*A* XI].—The line observed at λ 6914 is probably the [*A* XI] transition $^3P_1 - {}^3P_2$, whose wave length was estimated by Edlén[4] at λ 6919 with an uncertainty of a few angstrom units. Other lines falling in the same neighborhood—λ 6911.05 [*Ni* II], λ 6906.1

[4] *Zs. f. Ap.*, **22**, 30, 1942; *Ap. J.*, **98**, 127, 1943.

[*Cr* IV], and λ 6915.6 [*Cr* IV]—cannot be important contributors. Moreover, the [*A* X] line λ 5536 is fairly strong, making the identification of [*A* XI] quite probable.

2. [*Kr* III].—The strong line observed at λ 6827 (shown midway between the two extreme right-hand comparison lines in Plate IX*e* in the *Publications of the Astronomical Society of the Pacific*, **57**, facing p. 173, 1945) agrees in wave length with the strongest member of the forbidden transition $^3P - {}^1D$ of *Kr* III, and no other identification seems possible. The only other [*Kr* III] line λ 9902.2 is four times weaker than λ 6827. In the relatively cool layers where atoms may be in the doubly ionized state, the low excitation potential of 1.81 volts of [*Kr* III] favors the intensity of the [*Kr* III] line relative to other forbidden lines, such as those of [*Ne* III] (E.P., 3.19 volts). Thus the identification of [*Kr* III] appears entirely satisfactory, and this conclusion is supported by the identification of the strong line λ 5536 with [*A* X] and the line λ 6914 with [*A* XI]. The identification of argon and krypton lines indicates that conditions are favorable for the emission of these lines, as well as for neon lines which have previously been found in a wide variety of celestial sources.

The $^3P - {}^1D_2$ λ 5846.3 [*Xe* III] line of the heavier noble gas has been observed in the Orion nebula, but in RS Ophiuchi the emission is extremely weak, if present.

3. [*Sc* VII], [*Ca* VII], and [*V* VIII].—As far as we know, RS Ophiuchi is the first object in which the λ 4823 [*Sc* VII] line and the blend of [*Ca* VII] and [*V* VIII] at λ 3688 have been observed; λ 3686.3 is the strongest [*V* VIII] line; λ 3688 [*Ca* VII] is a $^1D - {}^1S$ transition of relatively high probability.

PHYSICAL CONSIDERATIONS

A comparison of the intensities of the [*Fe* X] and [*Fe* XIV] lines shows that the excitation in the layers of RS Ophiuchi, where the lines of highly ionized atoms originate, is definitely lower than in most regions of the solar corona, where the coronal lines are emitted. RS Ophiuchi reveals several stages of ionization of iron and other atoms lower than X. This indicates that the physical conditions in this star differ radically from those in the solar corona, where no trace of *Fe* atoms with ionization lower than that of [*Fe* X] is found. On the sun the physical conditions in the layers intermediate between the [*Fe* X] regions and the chromosphere do not permit ions such as *Fe* VII to emit their forbidden lines. This absence of [*Fe* VII] lines is essentially the result of de-excitation by collisions of ions in the metastable state. The transition probabilities of the strongest [*Fe* VII] lines are 0.47 sec^{-1} and 0.37 sec^{-1}, but the higher ionization stages have much greater values, 69 sec^{-1} for [*Fe* X], 60 for [*Fe* XIV], and 106 for [*A* X]. Hence there is little possibility of [*Fe* VII] emission in the denser regions of the deep inner corona. In RS Ophiuchi, however, the stratification must be radically different from that in the sun, and those regions of the star's atmosphere of intermediate ionization, rich in ions such as *Fe* VII, must have a density sufficiently low to permit the emission of the forbidden lines.

Stratification of a type similar to that of RS Ophiuchi is found in the recurring Nova (T) Pyxidis and perhaps should be looked for at certain times in other novae. The relative intensities of [*Fe* X] lines with respect to those of [*Fe* XIV] show that, in the regions where the coronal lines are emitted, the ionization is higher in T Pyxidis than in RS Ophiuchi, while lower density of the layers emitting [*Fe* VII] is probably the reason that the intensity of [*Fe* VII] relative to [*Fe* X] and [*Fe* XIV] is greater in T Pyxidis than in RS Ophiuchi.

We are greatly indebted to Dr. W. S. Adams for his kind co-operation in allowing us to make use of his spectrograms and measurements in this study.

THE SPECTRUM OF NOVA PUPPIS 1942*

ROSCOE F. SANFORD
Mount Wilson Observatory
Received August 23, 1945

ABSTRACT

Sixty-five spectrograms of Nova Puppis 1942 were obtained between November 11, 1942, and November 28, 1944.

Emission lines.—Table 2 gives the observed emission lines and their identifications. Figure 1 shows the elements in the order of appearance of their emission lines and the intervals over which these emission lines were observed. The velocity of expansion of the atmosphere reached a maximum of no less than 1150 km/sec on November 17, 1942, whereas its value in 1944 dropped to 615 km/sec.

Radial velocities.—The mean radial velocity of the nova derived from bisections of the emission lines on plates after November 28, 1942, is +36.8 ± 2.1 km/sec. Eleven maxima in emission lines have been measured on spectrograms taken with a dispersion of 10 A/mm in and after April, 1943. The more pronounced maxima appear to have changed very slowly, if at all, between April, 1943, and November, 1944. A radial velocity of +66 km/sec results from assuming symmetry in the maxima of the broad emission lines. Although +36.8 km/sec seems the more satisfactory value for the radial velocity, it will be well to await the appearance of nebular structure about the nova to form a final decision.

Interstellar lines.—The interstellar velocity from coudé spectrograms is +23.4 km/sec from H λ 3933 and K λ 3968 *Ca* II, λ 4226 *Ca* I, and λ 4300 *CH*. That from D2 λ 5890 and D1 λ 5896 *Na* I is +23.9 km/sec. Weak components of H and K give velocities of +43.2 and +57.5 km/sec, respectively. The total absorption of interstellar K is 0.57 A. The interstellar *Ca* I line λ 4226 has a total absorption of about 1½ per cent of that of the interstellar K line of *Ca* II. The companion lines of H and K are about 5 per cent as strong as the primary lines.

Absolute magnitude.—Both the interstellar velocity and the total absorption give substantially the same distance (1460 parsecs) for the nova. This distance, however, leads to an absolute magnitude slightly brighter than −10, which is between the accepted luminosity of the brightest galactic novae and that of the faintest supernovae. Although this value may be too high, there can be little doubt that Nova Puppis belongs with the brighter galactic novae.

Nova Puppis was discovered on November 10, 1942, when its magnitude was about 0.7. It attained its maximum magnitude, 0.35, on November 11.5. Thereafter, its rapid decline was approximately as shown in the accompanying tabulation.

	Date (U.T.)	Mag.		Date (U.T.)	Mag.
1942	Nov. 10.....	0.7	1942	Nov. 27.0.....	5.0
	11.5.....	0.35		Dec. 9.5.....	6.0
	13.5.....	1.0	1943	Jan. 11.5.....	7.0
	15.6.....	2.0		Oct. 15.5.....	9.0
	17.8.....	3.0	1944	Dec. 1.....	10.0
	21.8.....	4.0			

Nova Puppis is one of the four brightest novae to be discovered in the last three hundred years and also one of those for which both magnitude and spectrum changes are most rapid. This *Contribution* gives an account of the spectrum and its changes as revealed by spectrograms taken at Mount Wilson.

Observations.—Sixty-five spectrograms of Nova Puppis 1942 were obtained with the 100-inch reflector at the Mount Wilson Observatory during the interval from November 11.5, 1942, to November 28.5, 1944, U.T. Spectrograms were photographed frequently during November and December, 1942, while the nova was fading rapidly from its maximum brightness. Thereafter, observations were made at greater intervals. All the spectrograms are listed in Table 1, together with dates, spectral regions, and dispersions.

General description of the spectrum.—The spectrum of Nova Puppis 1942, when first ob-

* *Contributions from the Mount Wilson Observatory, Carnegie Institution of Washington*, No. 715.

served at Mount Wilson on November 11.5, 1942, was characterized by broad emission lines bordered on the violet by absorption. The emission lines were relatively weak, but accompanying absorption was at first moderately well defined, although it soon became vague. By the end of 2 weeks the spectrum consisted primarily of emission lines threaded upon a very weak continuous spectrum; thereafter, these lines stood out more and more from the background of continuous spectrum.

TABLE 1

JOURNAL OF OBSERVATIONS

Plate*	Date (U.T.)	Spectral Region	Plate*	Date (U.T.)	Spectral Region
E647	1942 Nov. 11.43	$H\beta$ –$H\alpha$	E689	1942 Nov. 18.55	K –λ 5000
648	.46	$H\beta$ –$H\alpha$	690	.57	H 14–λ 5000
649	.48	$H\beta$ –$H\alpha$	691	26.46	$H\zeta$ –λ 5000
650	.50	K –$H\delta$	692	.49	$H\beta$ –λ 7000
651	.53	H 12–$H\beta$	693	.51	D –λ 6700
652	.54	H 12–$H\beta$	698	27.5	$H\gamma$ –$H\beta$
Ce2902	12.45	λ 5200–λ 7000	699	.5	$H\alpha$ only
2903	.51	K –λ 4900	702	28.42	H –λ 5000
2904	.54	K –λ 4900	703	.47	$H\delta$ –λ 6700
E655	13.43	$H\beta$ –λ 7000	704	.50	$H\delta$ –λ 6700
656	.44	$H\beta$ –λ 7000	G1789	29.46	λ 6300–λ 8600
657	.47	D –λ 7000	1792	30.43	$H\gamma$ –$H\alpha$
658	.48	$H\alpha$ –λ 7000	E708	Dec. 6.40	$H\beta$ –$H\alpha$
659	.49	H 10–λ 4583	709	.44	$H\delta$ –λ 5000
660	.50	H 15–λ 4583	G1795	19.40	$H\beta$ –$H\alpha$
663	14.48	$H\alpha$ –λ 7000	1796	.47	$H\delta$ –$H\beta$
664	.50	K –λ 5000	1805	20.47	$H\beta$ –$H\alpha$
667	15.43	D –λ 7000	E744	1943 Jan. 14.41	$H\zeta$ –λ 5000
668	.44	D –λ 7000	745	.45	$H\beta$ –λ 6700
669	.47	K –λ 5000	G1809	19.34	$H\gamma$ –$H\alpha$
670	.50	K –λ 4583	1810	.40	λ 7000–λ 8600
671	16.46	K –λ 5000	1816	Feb. 15.31	$H\gamma$ –λ 6678
672	.49	K –λ 5000	1820	Mar. 19.23	$H\gamma$ –λ 6678
673	.52	$H\delta$ –$H\alpha$	Ce3004	Apr. 19.17	$H\gamma$ –N1
674	.56	$H\beta$ –λ 7000	E1014	Nov. 3.51	$H\zeta$ –λ 5000
678	17.46	$H\beta$ –λ 7000	1024	9.48	λ 3868–λ 6700
679	.48	K –λ 7000	1025	9.5	λ 3868–λ 6700
680	.50	H 10–λ 5000	Ce3265	10.51	$H\gamma$ –N1
681	.52	H 14–λ 5000	E1264	1944 Oct. 26.51	$H\gamma$ –$H\alpha$
685	18.48	K –λ 5000	1265	26.55	λ 3868–λ 5000
686	.50	$H\beta$ –λ 7000	1269	28.52	N1 and N2
687	.52	K –λ 7000	1295	Nov 28.54	$H\delta$ –λ5000
688	.53	$H\beta$ –λ 7000			

* All spectrograms of the E series are prismatic and have a dispersion at $H\gamma$ of 34 A/mm, except E744, 745, and 1295 (65 A/mm); E1024, 1264, and 1265 (111 A/mm); and E1014 (222 A/mm). Spectrograms of the Ce and G series have been obtained with plane gratings. Ce2902 has a dispersion of 5.9 A/mm; Ce2903 and 2904, 2.9 A/mm; Ce3005 and 3265, 10 A/mm. All G spectrograms have a dispersion of 65 A/mm except G1789 and 1810 (110 A/mm), and G1805 (33 A/mm).

The emission lines appeared, at first, to have broad flat tops of even density. By November 15, 1942, however, a weak rift was barely discernible near their centers. On November 18 this was still central but could be seen more easily, its width being fully one-half that of the entire emission line. By November 26 the rift broke into several components, which on December 6 became so strong that the emission lines were almost completely cut in two, even though strongly exposed. This division of emission lines remained about the same through March 19, 1943, according to spectrograms of moderate dispersion taken up to that time. On April 19, 1943, a coudé spectrogram, Ce3004, dispersion 10 A/mm, recorded several emission lines, all of which showed numerous maxima.

PLATE XXVII

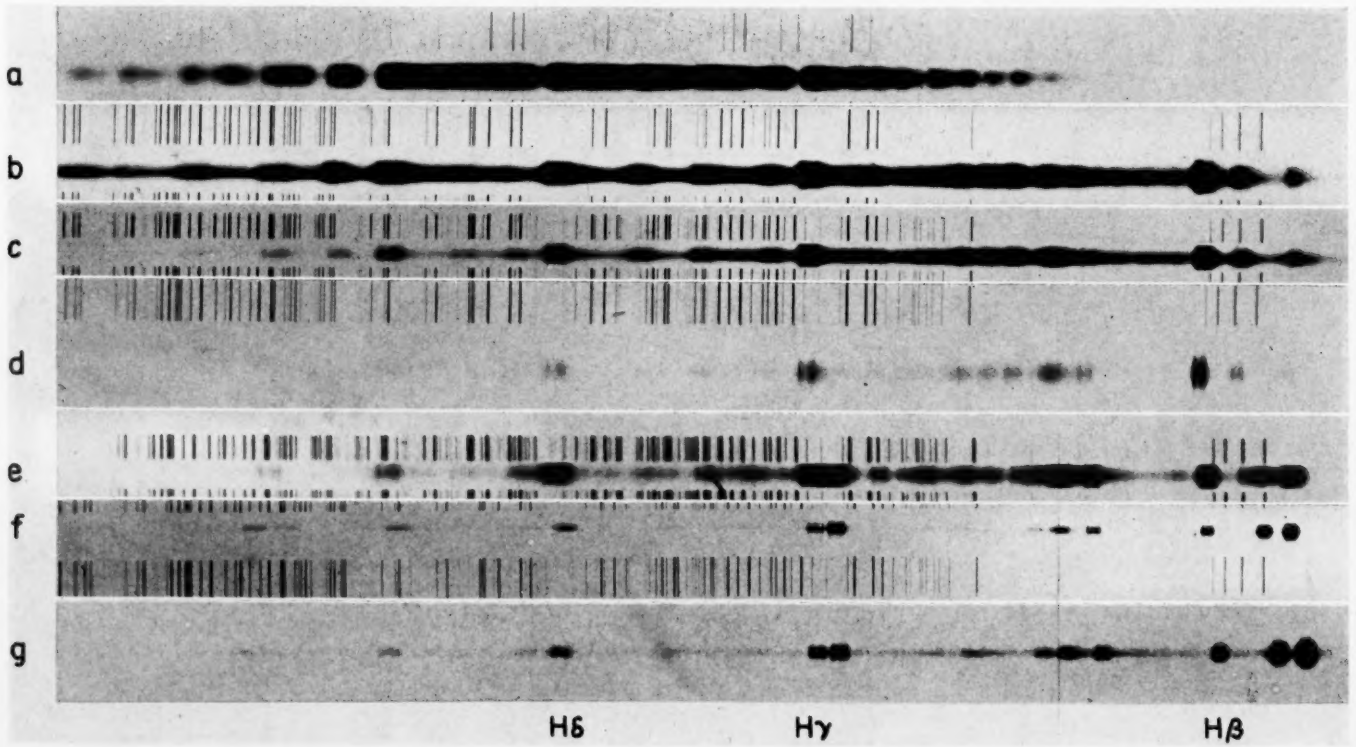

SPECTROGRAMS OF NOVA PUPPIS, BLUE-VIOLET REGION

a) E652, 1942 Nov. 11.54, mag. 0.4
b) E681, Nov. 17.52, mag. 2.8
c) E691, Nov. 26.46, mag. 4.8
d) E709, Dec. 6.44, mag. 6.0
e) E744, 1943 Jan. 14.41, mag. 6.9
f) E1025, Nov. 9.5, mag. 9.0
g) E1265, 1944 Oct. 26.55, mag. 10.0.

PLATE XXVIII

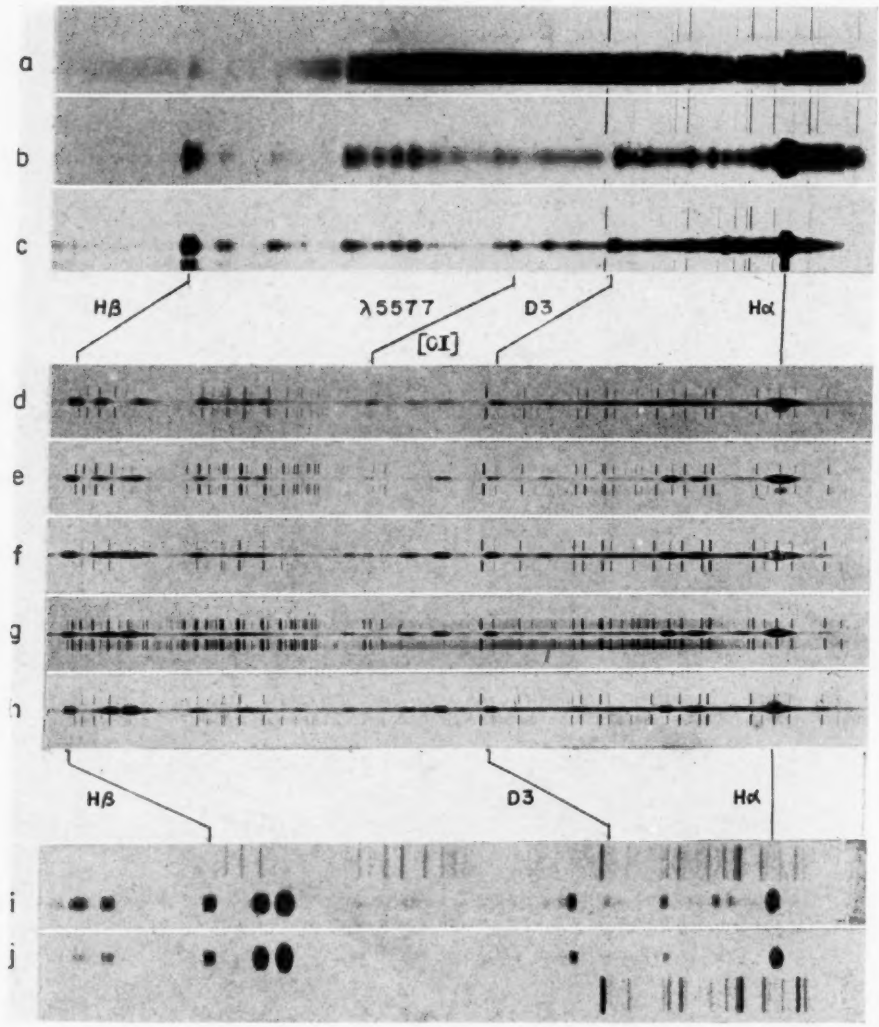

SPECTROGRAMS OF NOVA PUPPIS, REGION *Hα* TO *Hβ*

a) E649, 1942 Nov. 11.48, mag. 0.4
b) E674, Nov. 16.56, mag. 2.4
c) E692, Nov. 26.49, mag. 4.8
d) G1792, Nov. 30.43, mag. 5.5
e) G1795, Dec. 19.40, mag. 6.4
f) G1809, 1943 Jan. 19.34, mag. 6.9
g) G1816, Feb. 15.31, mag. .1
h) G1820, Mar. 19.23, mag. 7.5
i) E1024, Nov. 9.48, mag. 9.0
j) E1295, 1944 Nov. 28.54, mag. 10.0

PLATE XXIX

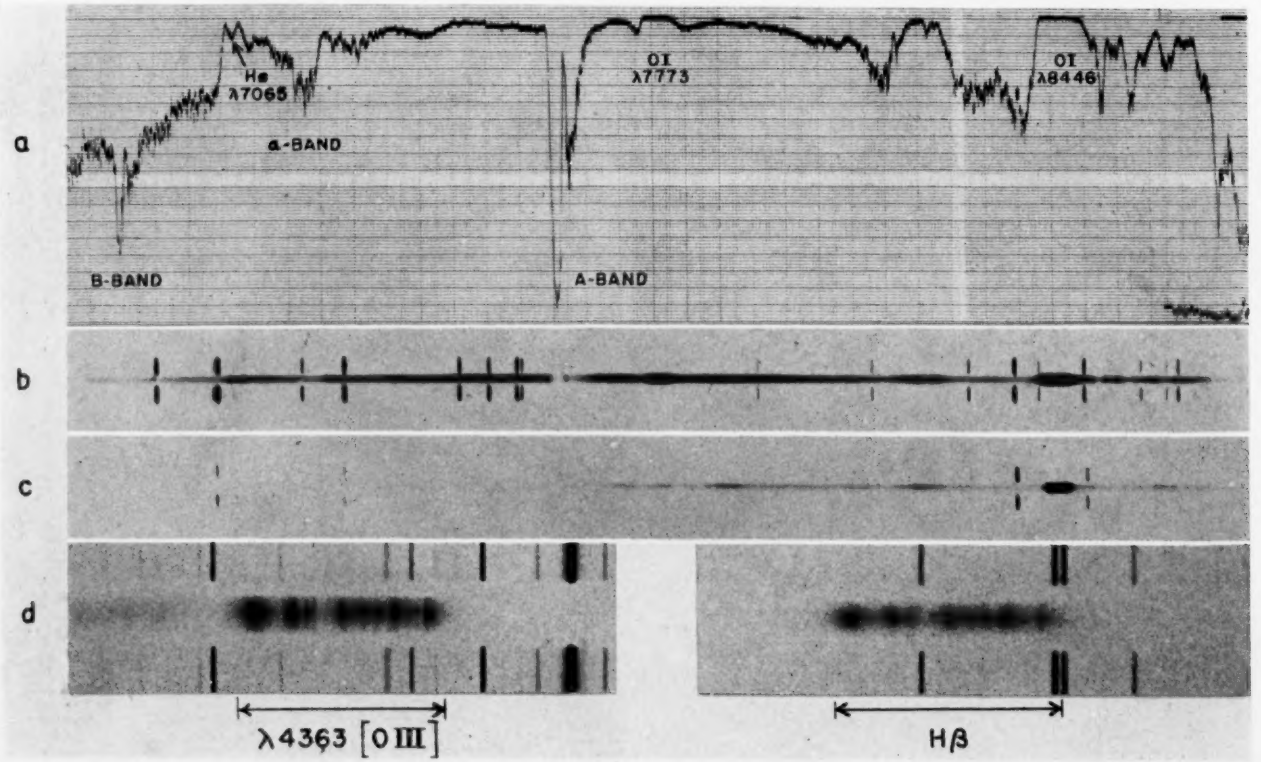

INFRARED REGION OF THE SPECTRUM OF NOVA PUPPIS, λλ 7000–8600

a) Microphotometer tracing of Plate G1789; *b*) G1789, 1942 Nov. 29; *c*) G1810, 1943 Jan. 19; *d*) enlargements (×20) of the lines λ 4363 *O* III and *Hβ* from Ce3265, 1943, Nov. 10, showing their numerous maxima.

UNIV. OF MICH.

These maxima persisted with minor changes through November, 1944. Plate XXVII illustrates the development of the nova's photographic spectrum with moderate and low dispersion between November, 1942, and November, 1944, the visual region being displayed by the spectrograms reproduced in Plate XXVIII. In Plate XXIX, *d*, are shown the numerous maxima in the emission lines λ 4363 [*O* III] and *Hβ* for November, 1943.

Identification and duration of emission lines.—Measures of representative spectrograms from Table 1 served to identify most of the emission lines which were not hopelessly entangled with one another and made it possible to follow their development. Wave lengths of emission lines have been obtained either by taking means of the values for their edges or for the two maxima into which the lines are sometimes divided or by bisecting their centers. Where lines were closely packed or overlapping, it was sometimes necessary to infer a wave length from partial data, supplemented with the complete data of well-isolated lines. Table 2 gives the measured wave length of all the emission lines, together with laboratory wave lengths and identifications for most of them. The wave lengths have been corrected for the earth's orbital motion but not for the velocity of the nova. Dates are given at the foot of the table for a few lines that appear but once or twice. Lines with wave lengths greater than λ 7000 were observed only on November 29, 1942, and January 18, 1943 (Pl. XXIX *a*, *b*, and *c*).

Figure 1 shows roughly the time intervals over which emission lines of the elements have been observed. The elements are in the order in which they first show lines. Various stages of ionization of each element come one after another in the order of their appearance. The logarithmic time scale is used in order to provide sufficient spread in the beginning when changes were rapid and to compress the end of the observing interval when changes were very slow. The logarithmic scale is at the top of the diagram. A rough idea of the calendar is provided by a few dates at the bottom.

Because of the great range in effective exposure produced by winter observing conditions, it is difficult to estimate when the emission lines of a given element attain their absolute maximum strength; estimates of time of maximum have, therefore, not been attempted.

The line λ 4363 [*O* III] was as strong as *Hγ* by December 5, 1942, growing rapidly stronger thereafter; λ 5007 [*O* III] became equal to *Hβ* between January 14 and February 15, 1943; and λ 4959 [*O* III] and *Hβ* were about equal on the latter date. All three [*O* III] lines continued to increase relatively to hydrogen lines, at least to November, 1944.

The line λ 4686 *He* II was probably stronger relative to *Hβ* in November, 1944, than at any previous date.

The line λ 5755 [*N* II] was outstanding by February 15, 1943, and remained so through November 28, 1944. It appears most nearly equal to *Hα* in November, 1943. The lines of *N* III maintained a nearly flat maximum between January and November, 1943, and then weakened decidedly by November, 1944.

Emission lines of *Ca* II, *Na* I, and *Si* II were the first to disappear, with *O* I and *C* II next.

One clear-cut line, λ 6004, as yet not identified, was present in the short interval between December 20, 1942, and February 15, 1943.

One of the latest lines to appear, λ 4605.04 ± 0.06, seems to belong to the same stage of the nova's development as the [*O* III] lines. This wave length must be reduced by at least one-half angstrom on account of the nova's radial velocity (as will appear presently). The measured line has been identified with a line of *N* V with a calculated wave length of λ 4603.2. An objection to this identification is that another *N* V line, about one-half as strong as λ 4603.2, should be present at λ 4620, and none has been certainly observed. Since blending would render identification of the fainter line difficult, failure to find it is not considered a serious objection to the identification of λ 4605.04 with *N* V.

Expanding atmosphere.—It is generally accepted that a nova has an atmosphere expanding rapidly more or less evenly in all directions. The emission lines of a nova are

TABLE 2

EMISSION LINES IN NOVA PUPPIS 1942

λ		Ident.	λ		Ident.
Obs.	Tab.		Obs.	Tab.	
3869	3868.7	[*Ne* III]	5413	5411.6	*He* II
3889	3889.1	*Hζ*	5427	5425.3	*Fe* VI?
				5428.6	*Fe* VI?
3933	3933.7	*Ca* II K	5534	5534.8	*Fe* II
3970	3970.1	*Hε*	5578	5577.4	[*O* I]
4028	4026.2	*He* I	5618	5615.8	[*Ca* VII]?
4061	.....	?*	5667	5666.6	*N* II
4071	4068.6	[*S* II]	5680	5679.6	*N* II, *Fe* VI?
	4076.2	[*S* II]	5720	5720.9	[*Fe* VII]?‡
4099	4097.3	*N* III	5756	5754.8	[*N* II]
4102	4101.8	*Hδ*	5804	5801.5	*C* IV?
4176	4173.5	*Fe* II		5812.1	*C* IV?
	4178.9	*Fe* II	5876	5875.6	*He* I, D3
4200	4199.9	*He* II	5898	5890	*Na* I, D2
4233	4233.2	*Fe* II		5896	*Na* I, D1
4244	4244.0	[*Fe* II]	5942	5933.4	[*Mn* VI]
4267	4267.2	*C* II		5945.1	[*Cr* III]
4276	4276.8	[*Fe* II]	5993	5991.4	*Fe* II
4289	4287.3	[*Fe* II]	6004	.....	?
4302	4296.6	*Fe* II	6087	6085.5	[*Fe* VII]
	4303.2	*Fe* II	6106	6101.1	*K* IV?
4341	4340.5	*Hγ*	6155	6156.4	*O* I
4364	4363.2	[*O* III]	6162	6158.2	*O* I
4416	many	*Fe* II, [*Fe* II], *O* II	6200	.....	?§
4447	4447.0	*N* II	6245	6242.5	*N* II
4472	4471.5	*He* I		6247.6	*Fe* II
4518	several	*Fe* II	6301	6300.2	[*O* I]
4551	4549.5	*Fe* II	6344	6347.1	*Si* II
	4555.9	*Fe* II	6364	6363.9	[*O* I]
4586	4583.3	*Fe* II	6372	6371.4	*Si* II
4605	.....	*N* V	6376	.....	[*Fe* X]
4630	4629.3	*Fe* II	6454	6454.1	*O* I
4637	4634.2	*N* III	6459	6456.1	*O* I
	4640.6	*N* III	6482	6483.9	*N* II
4686	4685.8	*He* II	6516	6516.1	*Fe* II
4729	4728.1	[*Fe* II]	6549	6548.4	[*N* II]
4766	.....	?†	6562	6562.8	*Hα*
4815	4814.6	[*Fe* II]	6584	6583.9	[*N* II]
4862	4861.3	*Hβ*	6621	.....	?
4925	4923.9	*Fe* II	6679	6678.1	*He* I
4960	4959.5	[*O* III]	6725	6717–31	[*S* II]
5009	5006.8	[*O* III]	7066	7065.2	*He* I
5019	5015.7	*He* I	7114	7112–15	*C* II?
	5018.4	*Fe* II	7219 to 7891	.....	‖
5058	.....	?	7772	7771–75	*O* I
5169	5169.0	*Fe* II	7891	7891.9	[*Fe* XI]?
5197	5197.6	*Fe* II	8216	8214	*N* I
5235	5234.6	*Fe* II	8450	8446	*O* I
5266	5264.8	*Fe* II	8496	8502	*P* 16
5276	5273.4	[*Fe* II]	8543	8545	*P* 15
	5276.0	*Fe* II	8600	8598	*P* 14
5291	5291	*O* VI	8660	8665	*P* 13
5317	5316.6	*Fe* II			
5334	5333.7	[*Fe* II]			
5365	5362.1	*Fe* II			
5377	5376.5	[*Fe* II]			

* November 18, 1942, only.
† November 26, 1942, only.
‡ March 20, 1943, only.
§ February 15 and March 19, 1943, only.
‖ Overlapping emission mutilated by atmospheric lines.

greatly widened by the Doppler shifts produced by this expansion. Atoms directly in front of the star will provide velocities of approach equal to the velocity of expansion, and those directly behind the star, velocities of recession of the same numerical value.

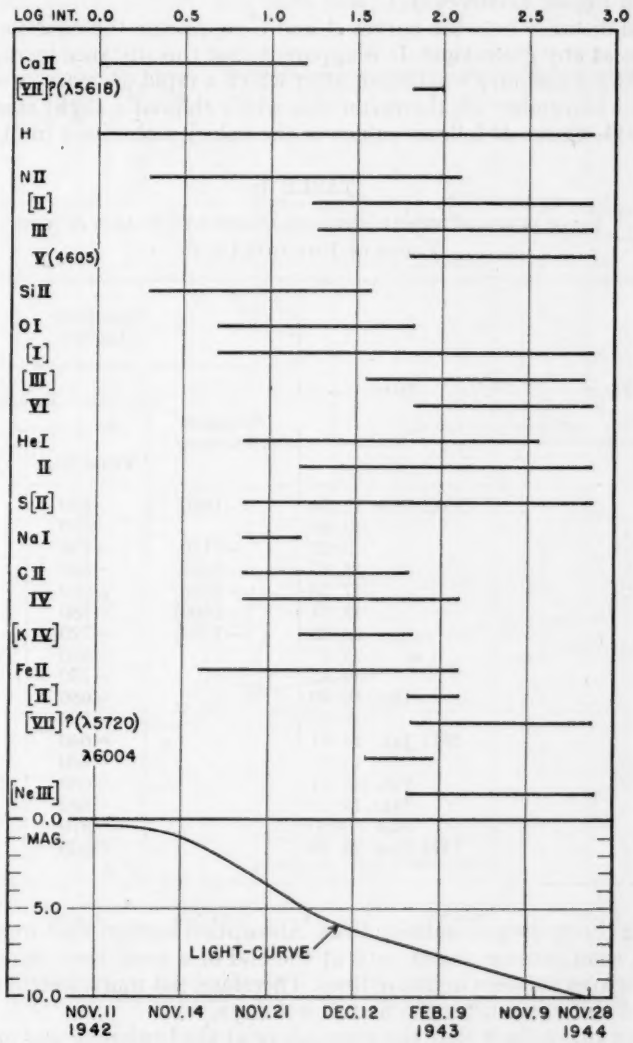

FIG. 1.—Horizontal lines show the duration of the spectral emission lines for the different elements. Different stages of ionization are arranged vertically in the time order of their appearance. The abscissae, at the top, are logarithms of time intervals from 1942 Nov. 10.5. A few calendar dates appear at the bottom.

Intermediate velocities will be filled in by other parts of the atmosphere. If the atmosphere is of the order of size of the photosphere, much of it will stand in front of or immediately behind the photosphere. Then absorption takes place in front and obscuration behind, and the velocity extremes of the wide emission lines are not a measure of the

velocity of expansion. As the shelf expands, the edges of the emission lines will yield more and more nearly the velocity of expansion.

Table 3 contains velocities derived from the edges of the emission lines and from the centers of what appear to be absorption borders to the emission lines. The values have been plotted in Figure 2, curves *A*, *C*, and *D*.

The vertical distance between curves *A* and *C* represents the emission-line widths of permitted lines at any given time. It is apparent that this distance increased during the first week following the nova's outburst, after which a rapid decrease in width set in and continued until November 28; thereafter this width showed a slight steady decrease to November, 1944. Curve *D* follows values of the velocity obtained from the absorption

TABLE 3

VELOCITIES OF THE ABSORPTION COMPONENTS AND OF THE EDGES OF EMISSION LINES

PLATE	DATE	VELOCITIES (KM/SEC)		
		Absorption (Hydrogen)	Emission	
			Violet Edge	Red Edge
E652	1942 Nov. 11.54	−1010	−690	+ 950
659	13.49	.....	−710	+1090
660	13.50	−1120	−750	+1060
669	15.47	−1350	−840	+1120
680	17.50	−1310	−910	+1190
690	18.57	(−1400)	−780	+1140
691	26.46	(−1290)	−720	+ 840
703	28.47	.....	−680	+ 770
G1792	30.43	.....	−730	+ 790
1795	Dec. 19.40	.....	−650	+ 740
1796	19.47	.....	−750	+ 810
E744	1943 Jan. 14.41	.....	−640	+ 720
G1809	19.34	.....	−630	+ 690
1816	Feb. 15.31	.....	−680	+ 740
1820	Mar. 19.23	.....	−680	+ 730
E1025	Nov. 9.50	.....	−570	+ 670
1295	1944 Nov. 28.54	.....	−640	+ 680

lines bordering the hydrogen emission lines. Absorption borders that were fairly well defined, at first, soon became vague until at the end of a week they could not be distinguished from spaces between emission lines. Therefore, not much weight should be given to the trend of this curve after the first 3 or 4 days.

It seems safe to conclude that the atmosphere at the beginning was expanding at the rate of 1000 km/sec, as shown by the absorption-line velocity at that time. Both emission-line width and absorption-line velocities point to a steady increase in the velocity of expansion that at the end of a week cannot be less than 1160 km/sec, judged by line-widths, and may be as much as 1350 km/sec if derived from absorption-line velocities.

This high velocity was not, however, maintained but declined rapidly to about 750 km/sec by November 28, 1942, and thereafter very slowly to a velocity of about 615 km/sec in November, 1944.

The radial velocity.—Curve *B*, Figure 2, is a plot of the radial velocity of the middle of the emission lines, i.e., the mean of curves *A* and *C*. After November 28, 1942, this is

nearly a straight line at velocity +30 to +40 km/sec and should give the radial velocity of the nova, provided the emission lines arise from a reasonably complete expanding atmosphere. Measures of radial velocity obtained by bisecting emission lines on nine spectrograms after November 28, 1942, gave the mean value +36.8 ±2.1 km/sec. Curve *B* is therefore in substantial accord (as it should be), except before November 28. But this

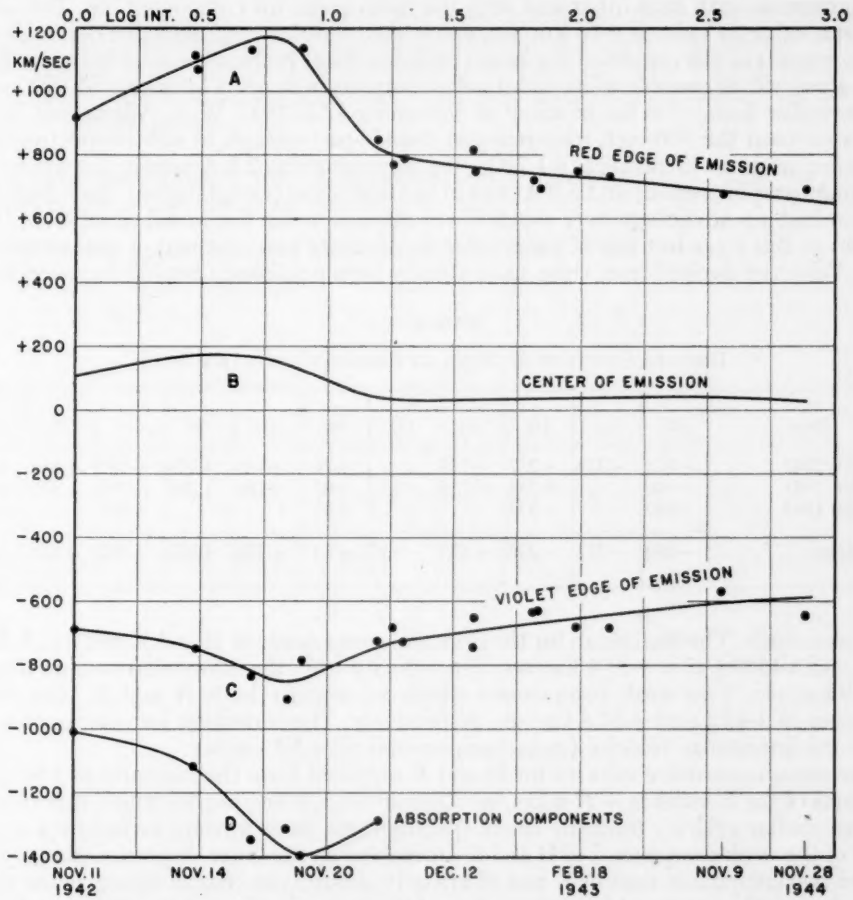

FIG. 2.—Plots of the Doppler displacements of the red edges: *A*, the centers; *B*, the violet edges; *C*, emission lines; *D*, Doppler displacements of the absorption borders of emission lines.

part of the curve could be explained by the finite width of the absorption-line borders during this stage. In other words, the amount by which curve *B* exceeds the radial velocity, +36.8 km/sec, might be taken as a measure of the effective half-width of absorption lines. It would be of the order of 80 km/sec.

In connection with the nova's radial velocity, it is convenient to discuss the velocity displacements of the numerous maxima into which the lines became divided in and after April, 1943. These maxima are seen best on two coudé spectrograms with a dispersion of 10 A/mm. Table 4 gives the measured Doppler displacements of these maxima on the two spectrograms Ce3004, April 19, 1943, and Ce3265, November 10, 1943, as well as

the measures on a very weak spectrogram of lower dispersion obtained on November 28, 1944.

If it is assumed that jets of matter are always shot out in diametrically opposite directions, mean values of properly selected pairs of maxima should provide a way of obtaining the radial velocity of the nova. One-half the sums of the mean values of components (1) and (11), of (2) and (10), of (3) and (9), of (4) and (8), and of (5) and (7) are all in fair agreement with each other and with the mean value for component (6). The overall mean value by pairs is +66 km/sec, exceeding by 30 km/sec the value derived from measurements of the centers of the broad emission lines. Perhaps a choice between these two values will be possible when and if nebular structure appears later around this nova.

Interstellar lines.—On the morning of November 12.5, 1942, W. S. Adams and M. L. Humason used the 100-inch telescope and coudé spectrograph to obtain spectrograms extending from the ultraviolet to λ 7000; the dispersion was 2.9 A/mm in the second order (photographic region) and 5.9 A/mm in the first order (visual region). Such high dispersion had no advantage over much lower dispersion for the broad absorption lines present at this stage but was of great value for accurate measurement of the interstellar lines. Velocities derived from them have already been published.[1] Second measures have

TABLE 4

DOPPLER SHIFTS OF MAXIMA IN EMISSION LINES (KM/SEC)

Date	(1)	(2)	(3)	(4)	(5)	(6)	(7)	(8)	(9)	(10)	(11)
Apr. 20, 1943.....	−461	−354	−237	−132	.....	+79	+185	+259	+379	+453	+569
Nov. 10, 1943.....	−460	.....	−238	−134	−33	+62	+186	+266	+365	+470	+574
Nov. 28, 1944.....	−442	.....	−232	.....	.....	+81	.....	.....	+401	.....	+566
Mean.....	−454	−354	−236	−133	−33	+74	+186	+262	+382	+462	+570

now been made. The final mean for the principal components of H and K of *Ca* II, λ 4226 *Ca* I, and λ 4300 *CH* is +23.4 km/sec. The velocity from the interstellar sodium lines is +23.9 km/sec. Two weak components which accompany both H and K give mean velocities of +43.2 and +57.5 km/sec, respectively. The correction for solar motion reduces the interstellar velocity (main components) to +5.5 km/sec.

The mean interstellar velocity for H and K obtained from the measures of five spectrograms of the E series is +27.6 km/sec. The amount, 4 km/sec, by which this exceeds the interstellar velocity from the coudé spectrograms, finds a ready explanation as the effect of the weak components of H and K unresolved on the lower-dispersion plates.

The two companion lines of K and H are only about 5 per cent as strong as the main components. The measured total absorption of the integrated interstellar K lines is 0.6 A. It was not possible to derive the total absorption for the interstellar D2 and D1 of *Na* I because of the extreme contrast shown by these lines on a very strongly exposed Eastman IV-F emulsion, although they were extremely good for micrometer measurement.

The interstellar line λ 4226 *Ca* I was found to have a total absorption of 0.009 A or approximately 1½ per cent that of the integrated interstellar K line of *Ca* II.

Absolute magnitude.—The distance for Nova Puppis 1942 corresponding to a total absorption of 0.6 A for K is 1500 parsecs if based on the relation between distance and total absorption of the interstellar K line found for B stars.[2] This agrees well with the

[1] Humason and Sanford, *Pub. A.S.P.*, **54**, 256, 1942.

[2] R. F. Sanford, *Mt. W. Contr.*, No. 573; *Ap. J.*, **86**, 141, 1937.

distance of 1420 parsecs derived from the residual interstellar velocity of +5.5 km/sec, on the assumption that differential galactic rotation amounts to 0.0177 km/sec/psc.[3]

A distance of 1460 parsecs gives a visual absolute magnitude slightly more luminous than −10 for the maximum apparent brightness of 0.35 mag. derived by E. Pettit.[4] The luminosity would thus be about midway between the accepted luminosity of the brighter galactic novae and that of the fainter supernovae. There are objections to both methods used to obtain the distance of the nova given above; possibly the computed distance is too great. However, there can be little doubt that Nova Puppis 1942 belongs with the bright galactic novae; for, as H. F. Weaver has pointed out, Nova Puppis "follows the pattern set by the fast novae in general,"[5] and fast novae are the brighter of the two classes of galactic novae.

I wish to thank Messrs. Adams, Humason, and Joy for permission to use the numerous spectrograms they obtained during 1942.

[3] R. E. Wilson, *Mt. W. Contr.*, No. 631; *Ap. J.*, **92**, 189, 1940.

[4] *Pub. A.S.P.*, **54**, 259, 1942.

[5] *Ap. J.*, **99**, 280, 1944.

REGRESSION LINES AND THE FUNCTIONAL RELATION. II*

CHARLIER'S FORMULAE FOR A MOVING CLUSTER

FREDERICK H. SEARES[1]
Mount Wilson Observatory
Received August 17, 1945

ABSTRACT

Whenever two or more coefficients of an observation equation (counting the absolute term as a coefficient) depend on measured quantities, the coefficients of the normal equations used to determine the unknown quantities will include the squares of the errors of observation. If the squares of the percentage errors of measurement are not negligible, the solution for the unknowns will be systematically affected by regression error. This error can be eliminated only by sufficiently increasing the precision of measurement or by correcting the coefficients of the normal equations. In practice, correction of the coefficients is often necessary.

The formulae for the functional coefficient of a linear relation derived in *Mt. W. Contr.* No. 698 are extended in the present article to the solution of Charlier's equations for the convergent of the motions of a moving star cluster. Application of the formulae to the Taurus cluster shows that neglect of the regression error leads to a distance for the cluster that is too small by about 7 per cent (different for other clusters).

Solutions by Merriman and by Hertzsprung for a linear equation involving constant weights that have recently come to light are shown to be a special case of the general solution given in *Mt. W. Contr.* No. 698. Equations (45) of the present article correct an error in the weights given in the original discussion.

I. CHARLIER'S FORMULAE

It seems not to have been noted that, as commonly used, Charlier's formulae for the distance of a moving cluster lead to a systematic error in the convergent of the proper motions and hence also to an error in the distance. The error, which arises from a hidden regression effect, may vary between wide limits. For the Taurus cluster the distance thus computed appears to be too small by about 7 per cent.

The observation equation,[2] to be applied to each member of the cluster, is

$$a'x - c'y + b' = 0 , \tag{1}$$

where

$$x = \cot A , \qquad y = \frac{\tan D}{\sin A} , \tag{2}$$

A and D being the right ascension and the declination of the convergent. The coefficients a', b', and c', functions of the position of the star and its proper motions, are defined by

$$a' = \mu_1' A_1 - \mu_2' A_2 , \qquad b' = \mu_1' B_1 + \mu_2' B_2 , \qquad c' = \mu_1' C \tag{3}$$

$$\left.\begin{aligned} A_1 &= \cos \alpha \sin \delta , & B_1 &= \sin \alpha \sin \delta , & C &= \cos \delta , \\ A_2 &= \sin \alpha , & B_2 &= \cos \alpha , \end{aligned}\right\} \tag{4}$$

$$\mu_1' = \mu_\alpha \cos \delta , \qquad \mu_2' = \mu_\delta . \tag{5}$$

* *Contributions from the Mount Wilson Observatory, Carnegie Institution of Washington*, No. 716.

[1] Research associate, Carnegie Institution of Washington.

[2] C. V. L. Charlier, *Lund Medd.*, Ser. II, No. 14, 1916. See also N. H. Rasmuson, *ibid.*, No. 26, 1921. To simplify the comparison given in Section IV, W. M. Smart's form of the equation (*M.N.*, 99, 168, 1939) has been used.

The coefficients of the normal equations used for the derivation of x and y are

$$\left.\begin{aligned} &[a'a'], -[a'c'], \quad [a'b'], \\ &-[a'c'], \quad [c'c'], -[b'c']. \end{aligned}\right\} \tag{6}$$

The point of significance for the present discussion is that the observed motions occur in a', b', and c', and hence also in the normal coefficients, whose values are affected systematically by the squares of the errors of measurement. If μ_1 and μ_2 are the true motions and e_1 and e_2 their respective errors, then

$$\mu_1' = \mu_1 + e_1\,, \qquad \mu_2' = \mu_2 + e_2\,; \tag{7}$$

and for the true coefficients of equation (1) we may write

$$a = \mu_1 A_1 - \mu_2 A_2\,, \qquad b = \mu_1 B_1 + \mu_2 B_2\,, \qquad c = \mu_1 C\,. \tag{8}$$

Combining formulae (3), (7), and (8), we obtain

$$\left.\begin{aligned} a' &= a + e_1 A_1 - e_2 A_2\,, \\ b' &= b + e_1 B_1 + e_2 B_2\,, \\ c' &= c + e_1 C\,. \end{aligned}\right\} \tag{9}$$

The errors e_1 and e_2 are not correlated with each other, nor with a, b, and c. Hence, if equations (9) be multiplied together and summed to form the normal coefficients (6), the terms involving e_1, e_2, and e_1e_2 will, for the most part, cancel; but not so those containing e_1^2 and e_2^2. We thus find

$$\left.\begin{aligned} [a'a'] &= [aa] + [e_1^2 A_1^2] + [e_2^2 A_2^2]\,, \\ [a'c'] &= [ac] + [e_1^2 A_1 C]\,, \\ [a'b'] &= [ab] + [e_1^2 A_1 B_1] - [e_2^2 A_2 B_2]\,. \\ [c'c'] &= [cc] + [e_1^2 C^2]\,, \\ [b'c'] &= [bc] + [e_1^2 B_1 C]\,. \end{aligned}\right\} \tag{10}$$

Only for $[a'b']$ is there a partial cancellation of e^2 terms.

Formulae (9) are rigorous; formulae (10), however, are not wholly exact, owing to the incomplete cancellation of the first-power terms in e_1 and e_2. But if $[aa]$, etc., be computed from (10), the residual errors will be only accidental in character, whereas those affecting $[a'a']$, etc., are both accidental and systematic—systematic in the sense that no increase in the observational data (by including more stars in the solution, for example) will ever bring $[a'a']$, etc., closer to the truth than the limits set by the corrective terms on the right of formulae (10). If the precision of measurement is high, the corrective terms may be negligible; if not negligible, then the solution should be made with $[aa]$, etc. In practice, the matter seems never to have been examined; and, so far as I am aware, the uncorrected coefficients have been used without question.

The error thus introduced into the values of x and y is a regression effect in two unknowns, fundamentally the same as that for a single unknown discussed in *Mt. W. Contr.* No. 698.[3] We digress from the application of equations (10) for a moment to trace this connection.

[3] *Ap. J.*, **100**, 255, 1944.

II. NATURE OF THE REGRESSION EFFECT

The matter may be clarified by partially expanding one of the uncorrected normal coefficients, say $[a'a']$. At the same time, we introduce throughout the factor p, the weight of an individual observation equation.[4] From the first of formulae (10) we thus find

$$[paa] = a_1 + a_2 - 2[p\mu'_1\mu'_2 A_1 A_2]\,. \tag{11}$$

where

$$\left.\begin{aligned} a_1 &= [p\mu'^2_1 A_1^2] - [pe_1^2 A_1^2]\,, \\ a_2 &= [p\mu'^2_2 A_2^2] - [pe_2^2 A_2^2]\,. \end{aligned}\right\} \tag{12}$$

Since the last term in equation (11) includes neither e_1^2 nor e_2^2, it contributes nothing to the regression effect and for the moment is of no further concern. The terms a_1 and a_2 are alike in form, and we need examine only the generalized expression

$$a = [p\mu'^2 A^2] - [pe^2 A^2]\,. \tag{13}$$

Since the angular separation of cluster stars is usually small, the variation in A will be small. But in any event, the product sums in a may be decomposed into series of partial sums such that the changes in A for any partial sum are negligible. We thus obtain

$$\left.\begin{aligned} a = {} & [p\mu'^2 A^2]_1 + [p\mu'^2 A^2]_2 + \ldots . \\ & - [pe^2 A^2]_1 - [pe^2 A^2]_2 - \ldots . \end{aligned}\right\} \tag{14}$$

For each pair of partial sums we now write

$$[p\mu'^2] = [p]\,\sigma_w^2\,, \qquad [pe^2] = [p]\,\epsilon_w^2\,. \tag{15}$$

Equation (14) thus becomes

$$a = [p\mu'^2 A^2]_1 R_1 + [p\mu'^2 A^2]_2 R_2 + \ldots . \tag{16}$$

where, since the A's may be treated as constants, the R's have the general form

$$R = 1 - \frac{\epsilon_w^2}{\sigma_w^2}\,. \tag{17}$$

From equations (15) it appears that σ_w is the weighted mean dispersion in μ' and ϵ_w the weighted mean error of measurement for μ'.

The bracket coefficients of the R's in equation (16) include all the components of $[pa'a']$ that require correction for regression error. The R's provide the correction and hence appropriately may be called "regression factors." The term ϵ_w^2/σ_w^2 may be called the "fractional regression error."

The other coefficients of equations (10) lead to the same general result. All the terms affected by regression error can be corrected by factors of the form defined by equation (17). The regression factors need not always be calculated; but, in any case, they are illuminating as to the mechanism of regression. They have already appeared as a characteristic feature of the formulae in *Mt. W. Contr.* No. 698[3] and thus provide the connection between the present discussion and the much simpler relations for a single unknown.

Formulae for a single unknown.—In equation (1) the unknowns are x and y. In the original discussion, however, x and y designated the measured quantities, the unknown being B, the functional coefficient connecting the true values of x and y. Because of this confusing interchange of symbols, we derive here some of the formulae for a single unknown, using the method and the notation of this paper.

[4] The more exact definition of p and its derivation are given in Sec. III.

The observation equation is

$$b' = a'X \,. \tag{18}$$

where a' and b' are measured quantities with errors e_a and e_b and weights p_a and p_b. Freed from regression error, a' and b' become a and b, respectively. The first regression coefficient x and the functional coefficient X are then given by

$$x = \frac{[pa'b']}{[pa'a']}, \qquad X = \frac{[pab]}{[paa]}, \tag{19}$$

where p, the weight of the residual

$$v = b' - a'X \,. \tag{20}$$

is (see Sec. III)

$$p = \frac{p_a p_b}{p_a + p_b X^2}. \tag{21}$$

The equivalent of the foregoing formulae (10)–(16) is simply the two relations

$$[pab] = [pa'b'], \qquad [paa] = [pa'a']R_a \,. \tag{22}$$

where the regression factor R_a is of the usual form, equation (17). Then from formulae (19) and (22)

$$X = \frac{x}{R_a}. \tag{23}$$

For a single unknown, R_a thus appears not only in the expression for $[paa]$ but also explicitly in the equation for X. It may be calculated from

$$R_a = 1 - \frac{[pe_a^2]}{[pa^2]} = 1 - \left[\frac{p}{p_a}\right]\frac{\epsilon_{oa}^2}{[pa^2]}, \tag{24}$$

where ϵ_{oa} is the mean error in a for $p_a = 1$.

Equations (23) and (24) correspond to the relations for the first regression line in group (20*).[5] A mistake is to be noted, however, in the weights of the original formulae. Each of equations (17*) involves both e_x and e_y. Hence in passing from equations (16*), which are correct, to (17*), p_y and p_x must be replaced, respectively, by the weights of the residuals

$$v_y = y - Bx \,, \qquad v_x = x - \frac{1}{B}y \,, \tag{25}$$

that is, by

$$P_y = \frac{p_x p_y}{p_x + p_y B^2}, \qquad P_x = \frac{p_x p_y}{p_y + p_x B^2}. \tag{26}$$

The corresponding changes in equations (18*)–(21*) are obvious but may be checked against the corrected formulae, equations (45), which are required for the comparison in Section V.

The solution starting directly from the observation equations

$$y = Bx \,, \qquad x = \frac{1}{B}y \,,$$

and the residuals v_y and v_x, as illustrated by formulae (18)–(23), is simpler than the original development and, because of the weighting, a safer approach to the problem. We now return to the application of equations (10).

[5] The asterisk indicates formulae in the original discussion, *Mt. W. Contr.*, No. 698; *Ap. J.*, **100**, 255, 1944.

III. CORRECTION OF THE NORMAL COEFFICIENTS

In the present problem the regression factors are concealed in the complex structure of the coefficients, and nothing is to be gained by their calculation. Approximate values of $\epsilon_1^2/\mu_1'^2$ and $\epsilon_2^2/\mu_2'^2$ are useful as an indication of the percentage amount of the regression error, but the actual solution of the problem is obtained by computing the corrective terms in equations (10). Inserting the weight p and writing the mean error ϵ for each of the actual errors e, we have for the corrected coefficients

$$\left.\begin{aligned}
[paa] &= [pa'a'] - [p\epsilon_1^2 A_1^2] - [p\epsilon_2^2 A_2^2]\,,\\
[pac] &= [pa'c'] - [p\epsilon_1^2 A_1 C]\,,\\
[pab] &= [pa'b'] - [p\epsilon_1^2 A_1 B_1] + [p\epsilon_2^2 A_2 B_2]\,,\\
[pcc] &= [pc'c'] - [p\epsilon_1^2 C^2]\,,\\
[pbc] &= [pb'c'] - [p\epsilon_1^2 B_1 C]\,,
\end{aligned}\right\} \tag{27}$$

where all the quantities on the right except p are given by equations (3)–(5).

As for p, the so-called "weight" of the observation equation, its significance becomes clear by noting that the least-squares criterion requires a minimum in $[pv^2]$, where v is the residual obtained by substituting the computed values of x and y into equation (1). Hence p is the weight of

$$v = a'x_c - c'y_c + b'\,. \tag{28}$$

The general expression for the mean error of a function $F(x, y, \ldots.)$ is

$$\epsilon_F = \left[\left(\frac{dF}{dx}\right)^2\epsilon_x^2 + \left(\frac{dF}{dy}\right)^2\epsilon_y^2 + \ldots.\right]^{1/2}. \tag{29}$$

Identifying F with v, and x and y with the observed motions, which are included in a', b', and c', we obtain

$$\epsilon_v^2 = \left(\frac{dv}{d\mu_1'}\right)^2\epsilon_1^2 + \left(\frac{dv}{d\mu_2'}\right)^2\epsilon_2^2\,, \tag{30}$$

in which

$$\left.\begin{aligned}
\frac{dv}{d\mu_1'} &= x_c A_1 - y_c C + B_1\,,\\
\frac{dv}{d\mu_2'} &= -x_c A_2 + B_2\,.
\end{aligned}\right\} \tag{31}$$

Then, finally, for the required weight,

$$p = \frac{\epsilon_o^2}{\epsilon_v^2}\,, \tag{32}$$

where ϵ_o, the mean error of v for $p = 1$, is so chosen that the values of p are of convenient size.

Since p is required to two significant figures at most, approximate values of x and y, which can always be found in advance of the final solution, will answer for the calculation of equations (31). Further, since the variations in A_1, B_1, etc., are small, the derivatives of v may be tabulated for three or four equally spaced values of α and of δ. An otherwise burdensome calculation thus becomes a simple matter, the resulting values of p being superior to any estimated weights.

If the range in p proves to be large, the data may, with advantage, be segregated into two or more groups such that the variation in weight within the groups remains moder-

ate. Separate solutions for x and y from the different groups can then be combined in accordance with their respective weights.

Remarks on the solution.—An important step in the foregoing procedure requires justification. It concerns a question that arises even when the corrective terms in equations (27) are negligible. The criterion accepted for the solution is a minimum in $[pv^2]$, where v is defined by equation (28) for the present problem or by one of the forms (20) or (25) when there is but a single unknown. These v's, however, are not the residuals with which least-squares theory is primarily concerned. Since a', b', and c' are all observed quantities, the residual v is a composite of three others, V_a, V_b, and V_c, which represent the deviations of a', b', and c' from their respective adjusted values. Geometrically, we are concerned with a surface. Corresponding to the observed point (a', b', c'), an adjusted point (a_1, b_1, c_1) lies on the surface, defined by the computed values of x and y such that

$$a_1x_c - c_1y_c + b_1 = 0 .$$

The co-ordinates of (a', b', c') relative to (a_1, b_1, c_1) are the residuals V_a, V_b, and V_c. Fundamentally, the least-squares problem is to find values of x_c and y_c that will make

$$S = \Sigma (p_aV_a^2 + p_bV_b^2 + p_cV_c^2)$$

a minimum. It can be proved, however, that the necessary and sufficient condition is a minimum in

$$S_v = [p\,v^2]$$

where v is the residual of equation (28).

For a single parameter connecting two measured quantities the proof may be obtained without difficulty from the geometrical relations involved. The only precaution to be noted is an equalization of the precision in the two co-ordinates (a', b' for eq. [20]; x, y for eq. [25]). For example, we use with x, not y itself, but $y' = ky$, where $k^2 = p_y/p_x$. We then find $S = S_v$; hence a minimum in S_v implies a minimum in S. For more complicated problems the proof follows from the generalized normal equations of W. E. Deming.[6]

It need scarcely be remarked that the principle underlying the foregoing solution is of general application. Whenever measured quantities occur in two or more coefficients (including the absolute term as such) of an observation equation, the squares of the errors of measurement will appear, implicitly if not explicitly, in the normal equations. Then, if the regression errors ϵ_x^2/σ_x^2, ϵ_y^2/σ_y^2, ..., are large enough to affect the solution for the parameters, the coefficients of the normals may be corrected by some method equivalent to that used here, and must be so corrected if the functional relationship is to be obtained free from systematic error. If the errors are involved implicitly, a transformation of the observation equation may be necessary. An illustration is afforded by Bohlin's formulae[7] for a moving cluster. The observation equation is

$$x \cos A' + y \sin A' + \tan D' = 0 ,$$

[6] *Phil. Mag.*, **11**, 146, 1931; **17**, 804, 1934; **19**, 389, 1935. These important results are also now available in *Statistical Adjustment of Data* (New York, 1943), especially chaps. iv and viii. A single general development provides for the minimization of the weighted squares of the residuals for any function, involving any number of measured quantities and parameters, either or both of which may be subject to supplementary conditions. For problems of the type here considered the generalized normal equations reduce to a group whose weights are p (W in Deming's notation), where p corresponds to the mean error derived from equation (29), as in the text. Hence, generally, a minimum in S_v implies a minimum in S. Deming's treatment is of unusual mathematical interest because of its generality; and it supplies an important extension of the classical theory, which, aside from problems involving conditioned observations, is concerned only with adjustments based on a single measured quantity. Deming supposes, however, that the squares of the errors of measurement are everywhere negligible. In other words, he considers only problems in which the regression effect is inappreciable.

[7] Rasmuson, *op. cit.*

where A' and D' are the right ascension and declination of the poles of the great circles along which the stars are moving. Here the coefficients obviously depend on the motions, but not explicitly. An explicit expression is easily found by a transformation of the coefficients, but Bohlin's equation then becomes that of Charlier.

Finally, it will be noted that regression error—and a good deal of computing—can sometimes be avoided by a judicious combination of the observational data. For example, if the stars of a cluster are numerous (the principle of application is general, but it is convenient to illustrate it by the problem already discussed), the motions of a group of neighboring stars may be combined into mean values, which will then be treated as the motions of a single star. For groups of 9 or 10 stars the mean errors of observation will then be one-third, and the regression errors one-ninth, those occurring in the detailed solution.

IV. APPLICATION OF EQUATIONS (27) TO THE TAURUS CLUSTER

For the Taurus cluster, chosen to illustrate the use of the formulae, the fractional regression error ϵ^2/σ^2 averages about 0.2 per cent for μ_1' and 1.8 per cent for μ_2'. These are small quantities; but since the geometrical conditions indicate an inherent uncertainty in the solution for x and y, the figures are sufficient to put one on guard. The investigation of the cluster by Smart[8] provides the data for a test calculation.

Smart has used two lists: A, 42 stars, and B, 30 stars, the errors for B averaging a little more than twice those for A. Ordinarily, it would be advisable to solve for x and y from each of these groups and combine the results. But since we are concerned only with an exploratory calculation to determine the order of the regression effect on the convergent and on the distance of the cluster, the 72 stars are used in a single group. Further, we adopt Smart's estimated weights for the individual stars instead of the more accurate values given by equations (30)–(32). As a final simplification, we disregard all variations in A_1, A_2, B_1, B_2, and C and use values found from equations (4) for the center of the cluster.

Writing now

$$[p\epsilon_1^2] = E_1 , \qquad [p\epsilon_2^2] = E_2 \tag{33}$$

and denoting the correction to $[pa'a']$ by (aa), etc., we obtain from equations (27)

$$\left.\begin{aligned}
(aa) &= -E_1A_1^2 - E_2A_2^2 &&= -1573.2 ,\\
(ac) &= -E_1A_1C &&= -\ 236.7 ,\\
(ab) &= -E_1A_1B_1 + E_2A_2B_2 &&= +\ 619.1 ,\\
(cc) &= -E_1C^2 &&= -2008.7 ,\\
(bc) &= -E_1B_1C &&= -\ 536.1 .
\end{aligned}\right\} \tag{34}$$

These values of the corrections depend on the following details:

Center of cluster, $\alpha\ 4^h24^m42^s$, $\delta\ +16°16'$

$\log A_1\ 9.05365$, $\log B_1\ 9.40864$, $\log C\ 9.98226$

$\log A_2\ 9.96132$, $\log B_2\ 9.60632$.

For Smart's calculation the proper motions are expressed in units of $0''.001$. The values of E_1 and E_2, referred to the same unit, were obtained from the tabulated probable er-

[8] *Op. cit.* Dr. Ralph E. Wilson calls my attention to the fact that the probable errors of $\mu_\alpha \cos\delta$ listed by Smart in his Tables I and II are erroneous. The values given by Boss's *General Catalogue*, which require no reduction, have been used for the following calculation.

rors, giving log $E_1 = 3.33839$, log $E_2 = 3.26637$. Since $p = 111.5$, equations (33) give for the weighted mean errors of the proper motions

$$\epsilon_1 = \pm 0''.0044 , \qquad \epsilon_2 = \pm 0''.0041 .$$

The motions themselves average $0''.110$ and $-0''.030$, respectively. The regression errors ϵ^2/σ^2 are therefore about 0.0016 and 0.0184, as already quoted.

The normal coefficients for Smart's solution (all taken as positive to agree with the signs in equations [27]) are

$$183{,}135.7 \qquad 426{,}651.2 \qquad 66{,}980.2$$

$$1{,}182{,}151.2 \qquad 182{,}988.5$$

Adding to these quantities the corrections from equations (34) and noting the algebraic signs shown in formulae (6), we obtain the corrected normal equations

$$+181{,}562.5x \quad -426{,}414.5y \quad +67{,}599.3 = 0 .$$

$$-426{,}414.5x + 1{,}180{,}142.5y - 182{,}452.4 = 0$$

whence

$$\log x = 8.784810_n , \qquad \log y = 9.122503 .$$

Equations (2) then give for the convergent

$$A = 93°29' , \qquad D = +7°32' . \tag{35}$$

Smart's values are 91°50′ and +8°9′, with probable errors of ±0°.66 and ±0°.26, respectively. The changes produced by the systematic corrections are +1°.65 and −0°.62, about 2.5 times Smart's probable errors for the uncorrected solution.

The parallax of an individual star is given by

$$V = \rho \sec \lambda . \tag{36}$$

$$\cos \lambda = \sin \delta \sin D + \cos \delta \cos D \cos (A - \alpha) . \tag{37}$$

$$\pi = \frac{k\mu}{V \sin \lambda} , \tag{38}$$

where V is the stream velocity, ρ the radial velocity, both in kilometers per second, λ the angular distance of the star from the convergent, μ the total proper motion, and $k = 4.738$ km/sec. Since we need only the change in Smart's parallaxes produced by the change in the convergent, we combine equations (36) and (38), whence

$$\pi = \pi_S \frac{\tan \lambda_S}{\tan \lambda} , \tag{39}$$

the subscript S referring to Smart's data. Calculating the λ's for the center of the cluster, we find the average result

$$\pi = 0.927 \pi_S . \tag{40}$$

Because of the simplifications used in the calculations, this equation is not to be regarded as a new determination of the distance of the cluster; it is, instead, an approximate evaluation of the regression effect, which thus appears to be of the order of 7 per cent.

Equation (38) shows that the distance of the cluster depends, in effect, on the mean of the total proper motions. Although not here of practical significance, it is worth re-

membering that the mean total motion also contributes a small systematic error. Since the total motion is computed from μ_1' and μ_2', it includes the errors $e_1^2/2$ and $e_2^2/2$, which do not cancel when the mean total motion is formed. The effect on the distance is small, however, in comparison with that arising from the accidental uncertainty in the position of the convergent, which enters through λ.

V. THE FORMULAE OF MERRIMAN AND HERTZSPRUNG FOR A SINGLE UNKNOWN

Shortly after the appearance of *Mt. W. Contr.* No. 698 Professor Raymond T. Birge of the University of California kindly called my attention to an equation by Mansfield Merriman[9] for the functional coefficient in a linear relation involving two measured quantities. Merriman's equation is

$$S^2 - \left(S_2 - \frac{p}{S_1}\right) S - p = 0 , \tag{41}$$

where S is the required functional coefficient connecting x and y, both of which are affected by errors of observation, S_1 and S_2 are the slopes of the regression lines, and p is the weight of each x, the weights of the y's being unity throughout.

Recently I have found that Hertzsprung[10] has also given a solution, which may be written

$$\tan^2\theta + \frac{[x^2] - [y'^2]}{[xy']} \tan\theta - 1 = 0 , \qquad S = \frac{\tan\theta}{k} , \tag{42}$$

where S again is the functional coefficient. Hertzsprung, who also presupposes constant weights, equalizes the mean errors in the x and y co-ordinates by introducing

$$y' = ky , \qquad k = \frac{\epsilon_x}{\epsilon_y} = \sqrt{\frac{p_y}{p_x}} . \tag{43}$$

He then determines a line of slope $\tan\theta$, such that the deviations of the points (x, y') from the line satisfy the least-squares criterion. The condition is $[x''y''] = 0$, x'' and y'' being measured along and perpendicular to the line; that is,

$$x'' = x\cos\theta + y'\sin\theta , \qquad y'' = -x\sin\theta + y'\cos\theta . \tag{44}$$

The quadratic for $\tan\theta$ then follows without difficulty.

The general solution from *Mt. W. Contr.* No. 698 (with corrected weights; see p. 369 above) is

$$\left.\begin{aligned}
&P_x = \frac{p_x p_y}{p_y + p_x B^2} , \qquad P_y = \frac{p_x p_y}{p_x + p_y B^2} , \\
&b_x = s_1 = \frac{[P_y xy]}{[P_y x^2]} , \qquad b_y = \frac{1}{s_2} = \frac{[P_x xy]}{[P_x y^2]} , \\
&R_x = 1 - \left[\frac{P_y}{p_x}\right] \frac{\epsilon_{ox}^2}{[P_y x^2]} , \qquad R_y = 1 - \left[\frac{P_x}{p_y}\right] \frac{\epsilon_{oy}^2}{[P_x y^2]} , \\
&B_x = \frac{s_1}{R_x} , \qquad \frac{1}{B_y} = \frac{1}{s_2 R_y} , \qquad B^2 = B_x B_y = s_1 s_2 \frac{R_y}{R_x} .
\end{aligned}\right\} \tag{45}$$

[9] *Method of Least Squares*, 8th ed., p. 127, New York, 1911. For the development of the equation the reader is referred to *Rept. U.S. Coast and Geodetic Surv., 1890*, p. 687.

[10] *Annalen, Sterrewacht te Leiden*, **14**, Part I, 5, 1922.

P_x, P_y are the weights of the residuals v_x, v_y defined by equations (25); b_x, b_y the regression coefficients; s_1, s_2 the slopes of the first and second regression lines; R_x, R_y the corresponding regression factors; and B the least-squares value of the functional coefficient whose true value satisfies the relation $y = Bx$ for true values of x and y.

Formally, $B_x = B_y = B$; in practice, B_x and B_y differ slightly, both numerically and in weight. Since from equation (29) $\epsilon^2(B_y) = B_y^4\,\epsilon^2(1/B_y)$, we find from

$$\epsilon^2(B_x) = \frac{[P_y v_y^2]}{(n-1)\,R_x\,[P_y x^2]}$$

and the similar expression for $\epsilon^2(1/B_y)$, after some reductions,

$$\frac{p(B_y)}{p(B_x)} = \frac{\epsilon^2(B_x)}{\epsilon^2(B_y)} = \frac{[P_y v_y^2]}{[P_x v_x^2]}\,\frac{[P_x xy]}{[P_y xy]}\,\frac{B_x}{B_y^3}. \tag{46}$$

To form the weighted product in $B^2 = B_x B_y$, we use

$$(Q_x + Q_y)\log B = Q_x \log B_x + Q_y \log B_y\,,$$

where the Q's are the respective weights of the logarithmic factors. Then, since in general $p(\log a) = (\mathrm{Mod}\ a)^2 p(a)$,

$$\frac{Q_y}{Q_x} = \frac{B_y^2 p(B_y)}{B_x^2 p(B_x)} = \frac{[P_y v_y^2]}{[P_x v_x^2]}\,\frac{[P_x xy]}{[P_y xy]}\,\frac{1}{B_x B_y}. \tag{47}$$

For comparison with equations (41) and (42), we require, not the general solution, formulae (45)–(47), but the simpler relations for constant values of p_x and of p_y. Both P_x and P_y are then constants, and

$$s_1 = \frac{[xy]}{[x^2]}, \qquad \frac{1}{s_2} = \frac{[xy]}{[y^2]}, \qquad R_x = 1 - \frac{\epsilon_x^2}{\sigma_x^2}, \qquad R_y = 1 - \frac{\epsilon_y^2}{\sigma_y^2}. \tag{48}$$

The remaining formulae for constant weights are the same as those of the last line of group (45). Finally, since $[v_y^2] = B^2[v_x^2]$, the weights of B_x and B_y, by equation (46), are formally equal.

It is now easy to compare the equations of Hertzsprung and Merriman with this solution. Since $S = B$ and $y' = ky$, formulae (42) give

$$k^2B^2 + \left(\frac{1}{k\,s_1} - k\,s_2\right) kB - 1 = 0\,. \tag{49}$$

By equations (43), $k^2 = p_y/p_x$, and since Merriman's assignment of weights is $p_x = p$, $p_y = 1$, equation (49) reduces to equation (41). The formulae of Hertzsprung and Merriman are therefore identical.

Introducing now $s_1 = B_x R_x$ and $s_2 = B_y/R_y$ into equation (49), we obtain

$$k^2B^2\left(1 - \frac{1}{R_y}\right) - \left(1 - \frac{1}{R_x}\right) = 0\,.$$

Substituting $k = \epsilon_x/\epsilon_y$ and the values of $R_y - 1$ and $R_x - 1$ from formulae (48), and noting also from (48) that $\sigma_y^2/\sigma_x^2 = s_1 s_2$, we find

$$B^2 = s_1 s_2 \frac{R_y}{R_x}, \tag{50}$$

the same as the last of equations (45). The Merriman-Hertzsprung equation is therefore equivalent to the solution of *Mt. W. Contr.* No. 698 for $p_x = \text{const.}$, $p_y = \text{const.}$

If this equation is to be used, it may be put in a form more convenient for logarithmic calculation by restoring $\tan\theta = kB$ in formula (49) and then introducing the angle 2θ. We thus find

$$\cot 2\theta = \frac{1}{2}\left(\frac{1}{k\,s_1} - k\,s_2\right), \qquad B = \frac{1}{k}\tan\theta\,. \tag{51}$$

For constant weights, equation (50) may advantageously be used in the form

$$B^2 = \frac{\sigma_y^2 - \epsilon_y^2}{\sigma_x^2 - \epsilon_x^2}. \tag{52}$$

The formulae of this section presuppose an observation equation of the form $y = Bx$. If, however, the observed quantities are X and Y, connected by

$$Y = A + BX\,,$$

we write $y = Y - \overline{Y}$ and $x = X - \overline{X}$, which eliminates A. Having found B, we then obtain the second parameter from

$$A = \frac{\Sigma P_y\,(Y - BX)}{\Sigma P_y}\,,$$

where P_y is the same as the weight of the residual $v_y = y - Bx$.

UNIV. OF MICH.

PLATE XXX

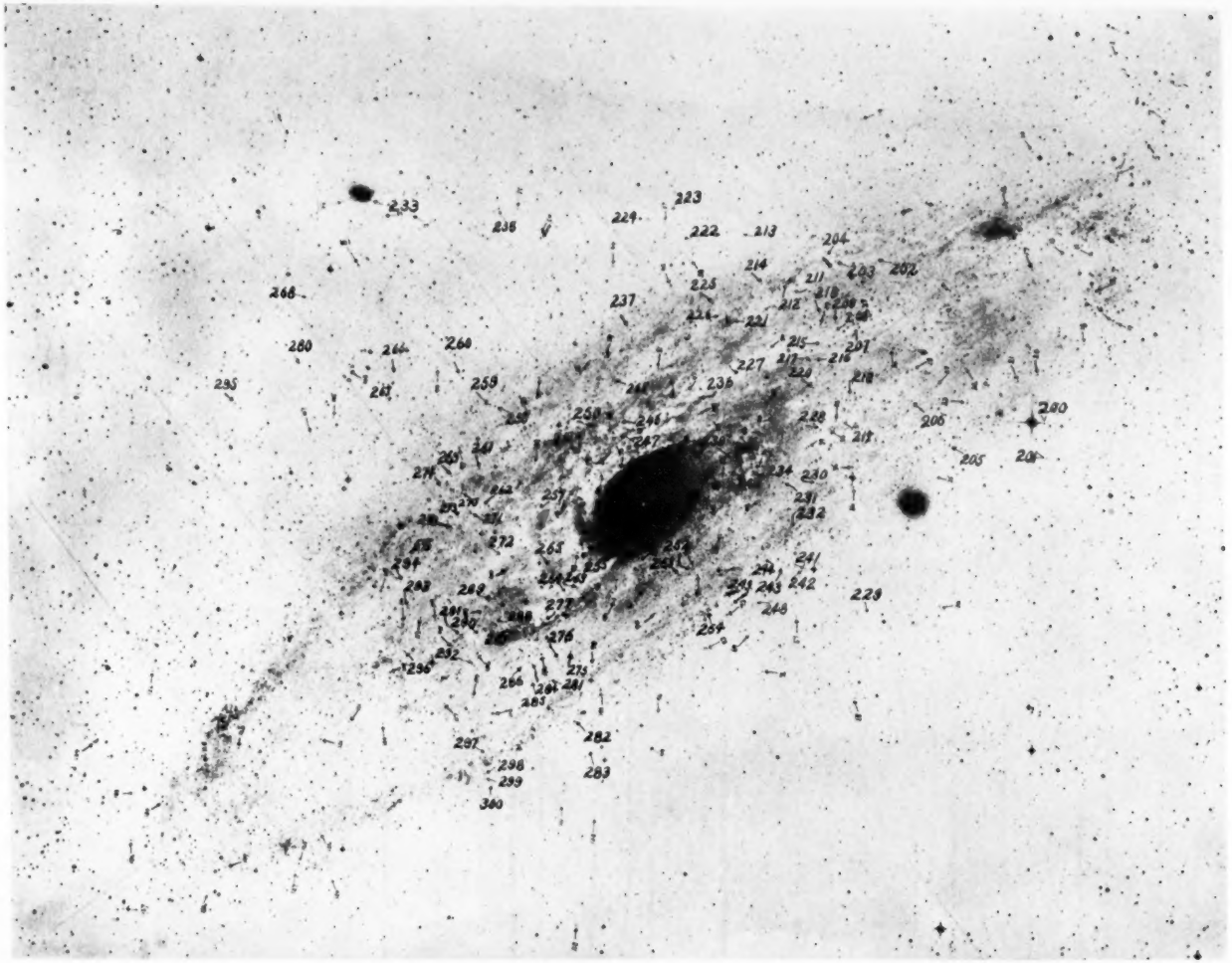

NEBULOUS OBJECTS IN M31 FOUND BY BAADE AT THE MOUNT WILSON OBSERVATORY (NOS. 200–300)

The other objects indicated by arrows are nebulous objects found earlier by Hubble.

Nebulous Objects in M31 Found by Baade at the Mount Wilson Observatory (Nos. 200–300)
The other objects indicated by arrows are nebulous objects found earlier by Hubble.

NEBULOUS OBJECTS IN THE ANDROMEDA NEBULA

C. K. Seyfert and J. J. Nassau

Warner and Swasey Observatory of the Case School of Applied Science
Received July 18, 1945

ABSTRACT

Photographic magnitudes have been obtained for 212 of the 249 nebulous objects in M31 found by Hubble and Baade and provisionally classified by them as globular clusters. Hubble's original estimates of the magnitudes of 148 of these objects are systematically too bright by 0.3 mag. The mean absolute magnitude of all the nebulous objects in M31 is approximately −5.0, or 2.5 mag. fainter than typical globular clusters in our galactic system. Since the nebulous objects are probably not single stars, the stellar luminosity distribution in M31 derived in a previous paper must be modified at the brightest end. With this revision the star counts in M31 reveal no stars belonging to the nebula which are brighter than 16.5 apparent magnitude or −5.8 absolute magnitude.

In 1932, Edwin Hubble[1] published a list of 148 nebulous objects in and near Messier 31 which he provisonally classified as globular clusters. A recent letter from Walter Baade to the writers indicated that Baade has found approximately one hundred additional nebulous objects in M31 within the magnitude range covered by Hubble. Since both Hubble and Baade believe that these objects are probably clusters rather than individual nebulous stars, a revision of the luminosity distribution published by the present writers in a previous paper[2] seems desirable, particularly in view of Baade's new material.

THE MAGNITUDES

Identification of the nebulous objects was accomplished by reference to Hubble's paper and by means of a marked photograph which Dr. Baade kindly sent to us (Pl. XXX). This latter print provided identification of those objects found by Baade and, in addition, furnished positive identifications of most of those found previously by Hubble.

The magnitude sequence near M31 established in the authors' earlier paper[2] was used as standard, and the magnitude of each object was determined by reference to that sequence, a graduated scale of star images being employed for that purpose. The magnitude estimates were made from the two photographic plates previously used for the star counts in M31. The images of most of the objects provisionally classified as clusters appear stellar on our plates, and hence their integrated magnitudes may be determined with considerable certainty. Most of the magnitudes are means from the two plates, and each plate was measured twice. The probable error of a single observation is ±0.09 mag. The final magnitudes are listed in Table 1. The numbers from 1 to 140 and I to VIII are from Hubble's list. Numbers from 200 to 300 refer to objects found by Baade.

Figure 1 is a plot of the present magnitudes against those determined by Hubble. A systematic difference between the two lists is clearly indicated, our magnitudes being fainter by 0.3 mag. Baade[3] also found a systematic correction to Hubble's photometric measures in M31. The correction which Baade finds varies from +0.35 mag. at 18.3 mag. to +0.63 mag. at magnitude 20.00. Since we were not able to determine magnitudes for 24 of Hubble's objects because of their faintness or proximity to the nucleus of M31 or NGC 205, we have adopted Hubble's magnitudes increased by 0.3 mag. for these objects. The magnitudes so obtained are inclosed in parentheses in Table 1.

[1] *Ap. J.*, **76**, 44, 1932.

[2] Seyfert and Nassau, *Ap. J.*, **101**, 179, 1945.

[3] *Ap. J.*, **100**, 137, 1945.

TABLE 1

PHOTOGRAPHIC MAGNITUDES OF NEBULOUS OBJECTS IN M31

Cluster No.	m_{pg}	Cluster No.	m_{pg}	Cluster No.	m_{pg}
1	17.81	51	18.16:	101	15.64
2	17.19	52	(17.8)	102	16.16
3	17.50	53	(17.2)	103	17.61
4	16.21	54	17.42	104	18.22
5	16.38	55	16.22	105	17.14
6	17.80	56	(16.9)	106	15.94
7	16.75	57	16.89	107	17.48
8	17.15	58	17.24	108	17.10
9	17.45	59	17.37	109	17.40
10	17.29	60	(17.4)	110	17.52
11	18.38	61	(16.9)	111	17.36
12	15.00	62	(15.7)	112	15.82
13	17.74	63	18.01	113	17.78
14	17.21	64	15.68	114	17.10
15	17.28	65	17.27	115	16.30
16	16.57	66	(17.3)	116	16.57
17	17.66	67	(16.8)	117	17.34
18	17.55	68	17.63	118	16.51
19	16.16	69	17.37	119	17.33
20	17.26	70	(15.3)	120	17.08
21	16.94	71	(17.1)	121	16.40
22	17.47	72	17.71	122	17.52
23	15.69	73	16.18	123	17.61
24	17.57	74	17.03	124	17.76
25	18.20	75	(15.9)	125	16.49
26	16.37	76	16.11	126	16.98
27	16.42	77	(16.9)	127	17.77
28	17.79	78	17.52:	128	17.38:
29	17.45	79	17.12	129	17.46
30	17.08	80	16.94:	130	16.86
31	17.66	81	(15.8)	131	17.25
32	17.34	82	17.44	132	17.51
33	16.82	83	17.00	133	17.35
34	16.89	84	17.85:	134	16.70
35	16.41	85	18.16:	135	18.16:
36	16.94	86	(16.2)	136	17.18
37	17.12	87	16.36	137	17.19
38	16.94	88	(16.8)	138	(17.3)
39	17.13	89	(16.3)	139	17.61
40	17.64	90	16.55	140	(15.8)
41	17.43	91	(16.1)	I	17.24
42	15.26	92	16.31	II	17.12
43	17.67	93	(15.7)	III	15.84
44	15.91	94	16.43	IV	(18.5)±
45	17.12	95	15.90	V	(18.3)±
				VI	(18.6)±
46	17.64:	96	17.67	VII	(17.9)
47	17.86	97	16.42	VIII	16.83
48	17.16	98	17.17		
49	17.06	99	16.19	200	17.38
50	17.22	100	16.21		

TABLE 1—*Continued*

Cluster No.	m_{pg}	Cluster No.	m_{pg}	Cluster No.	m_{pg}
201	17.26	236	18.09:	271	16.94
202	.....	237	18.15	272	.....
203	17.86	238	17.94	273	17.90
204	18.32	239	17.48	274	17.88:
205	17.18	240	17.49	275	16.65
206	17.70	241	17.42	276	18.07
207	18.28	242	17.93	277	17.48
208	18.09	243	18.00	278	17.46
209	17.31	244	18.36:	279	17.44:
210	17.51	245	17.87	280	17.77
211	17.51	246	17.55	281	17.41
212	17.92:	247	18.16	282	15.18
213	17.84	248	17.99	283	17.83
214	17.93:	249	16.67	284	17.19
215	17.92	250	17.80	285	.....
216	.....	251	17.58:	286	17.64
217	.....	252	17.10	287	18.09
218	17.85	253	18.12:	288	.....
219	18.08	254	15.56:	289	17.65
220	.....	255	17.10:	290	18.26:
221	17.91	256	17.64::	291	18.14:
222	.....	257	18.36::	292	17.82
223	18.33:	258	16.61	293	17.78
224	17.30	259	17.32	294	18.40::
225	17.88	260	17.33	295	16.66
226	18.36:	261	17.68	296	.....
227	17.31	262	17.72	297	17.18
228	.....	263	17.64	298	.....
229	18.10	264	18.28:	299	17.08
230	17.26	265	18.03	300	17.75
231	16.09	266	18.02		
232	.....	267	17.70		
233	.....	268	17.36		
234	17.67	269	17.81		
235	17.88	270	17.61		

LUMINOSITY DISTRIBUTION OF THE NEBULOUS OBJECTS

The luminosity distribution of the 236 nebulous objects for which magnitudes are available is given in Table 2. On the average, the apparent magnitude of the nebulous objects is close to 17.3. This corresponds to −5.0 abs. mag. if we adopt 22.3 for the apparent modulus of M31.

According to Shapley,[4] the mean absolute magnitude of 30 globular clusters in our galactic system is −7.5. Hence the objects which have been provisionally classed as globular clusters in M31 are, on the average, 2.5 mag. fainter than the globular clusters in the Milky Way. Even the *brightest* nebulous object in M31 has an absolute magnitude of only −7.3, or fainter than the average in our system. This discrepancy throws some doubt on the classification of these nebulous objects as globular clusters.

[4] *Proc. Natl. Acad.*, **30**, 61, 1944.

LUMINOSITY DISTRIBUTION OF THE STARS IN M31

Since these nebulous objects are probably not single stars, we may correct the luminosity distribution of stars in M31, which was published recently.[2] The distribution of stars in M31 corrected for these nebulous objects is given in Table 3. We note from this

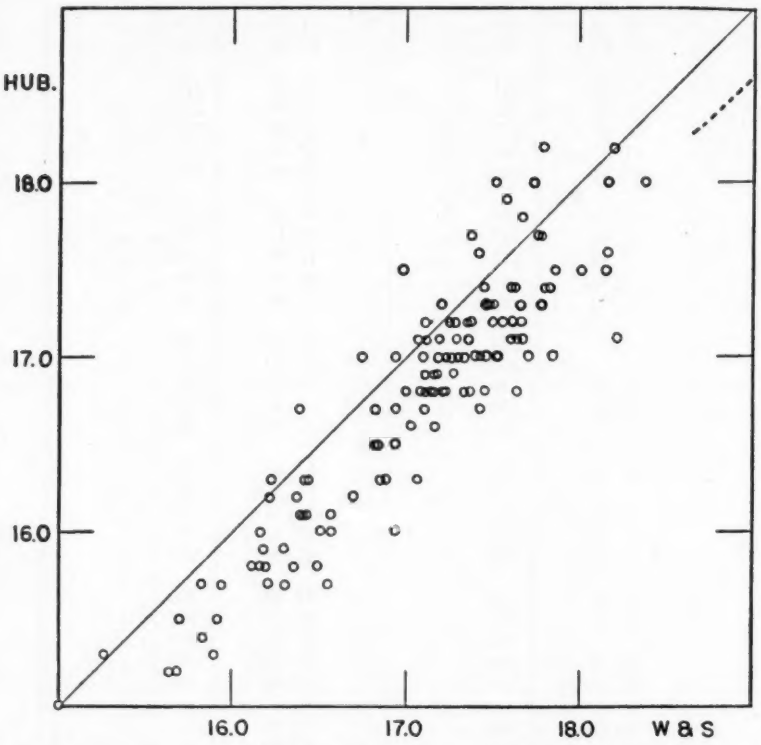

FIG. 1.—Plot of magnitudes of nebulous objects in M31 as determined at the Warner and Swasey Observatory (*abscissae*) and by Hubble (*ordinates*). The dotted line at the upper right indicates Baade's correction to Hubble's magnitudes of stars in M31.

TABLE 2

LUMINOSITY DISTRIBUTION OF NEBULOUS OBJECTS IN AND NEAR M31

App. mag.	15.00 to 15.49	15.50 to 15.99	16.00 to 16.49	16.50 to 16.99	17.00 to 17.49	17.50 to 17.99	18.00 to 18.49	18.50 to 18.60
No. of objects	4	14	23	26	73	64	30	2

table that the counts show no stars brighter than −5.8 in the main body and none brighter than −5.3 in the boundary region. Our value for the upper limit of luminosity of stars in M31 (−5.8) agrees closely with the corresponding value found earlier by Hubble.[5] We

[5] *Ap. J.*, **69**, 103, 1929.

also note here that allowance for the nebulous objects in M31 does not change the boundary of M31 as outlined by the star counts but reduces the total number of stars in M31 brighter than −3.8 abs. mag. from 2564 to 2364.

The data for M31 in Table 4 of our earlier paper[2] must also be modified, as shown in Table 4 of this paper. Table 4 is an interpolation table, which gives the logarithms of the

TABLE 3

THE DISTRIBUTION OF STARS IN M31

Absolute Magnitude	No. of Stars in Main Body	No. of Stars in Boundary	Total No. of M31 Stars
−6.3 to −5.8	.....	.....	.....
−5.8 to −5.3	56	.....	56
−5.3 to −4.8	183	97	280
−4.8 to −4.3	440	268	708
−4.3 to −3.8	774	546	1320
−6.3 to −3.8	1453	911	2364

TABLE 4

LOGARITHM OF NUMBER OF STARS IN M31 AT EACH HALF-INTEGRAL VALUE OF ABSOLUTE MAGNITUDE

Absolute Magnitude	M31 Stars (Total)	M31 Stars (Main Body)	M31 Stars (Boundary)
−6.5 to −6.0	.....	.....	.....
−6.0 to −5.5	1.3:	1.3:	.....
−5.5 to −5.0	2.23	2.09	1.7:
−5.0 to −4.5	2.71	2.50	2.29
−4.5 to −4.0	3.02	2.80	2.62
−4.0 to −3.5	3.25:	3.0:	2.9:

total number of stars in M31 between given limits of absolute magnitude. Any additional discoveries of nebulous objects will not appreciably change Tables 3 and 4 because such new objects are bound to be fainter ones, for the most part, and their effect on the star counts will be correspondingly small.

We are grateful to Dr. Baade for his kindness in allowing us to use his material in advance of publication.

RADIAL VELOCITIES AND SPECTRAL CLASSES FOR SOME STARS OF LARGE PROPER MOTION

W. J. LUYTEN
University of Minnesota
Received September 20, 1945

ABSTRACT

Radial velocities and spectral types are given for 14 faint stars of large proper motion. Spectral types alone are given for 8 proper-motion stars.

Through the kindness of Dr. Otto Struve, the author was permitted to use the 82-inch McDonald telescope for a short period in January, 1945. Observations were made with two different spectrographs, viz., with the 1-prism quartz spectrograph and $f/1$ Schmidt camera on stars of large parallax for radial-velocity estimates, and with the A-spectrograph on very faint proper-motion stars and suspected white dwarfs for the determination of spectral class.

Owing to the short time available, only one plate could be taken for each star; since the dispersion with the $f/1$ Schmidt camera is such that at λ 4200 a displacement of 1μ corresponds to a velocity of 21 km/sec and since in general only λ 4227 was well measurable in these late-type dwarfs, it is evident that the results obtained constitute only the roughest estimate. Yet it would seem of some value to publish these provisional results, since few, if any, observations of stars of this faintness are now in progress at other observatories. For the red dwarfs the radial-velocity plates were measured relative to the standard star, Boss 1237, for which the Mount Wilson velocity of +46 km/sec was adopted; for the white stars some A-type standards were kindly lent us by Dr. Frank K. Edmondson, of Indiana University. All plates were measured by Miss Helen Hughes; from the internal discordances of repeated measures a mean error of ±12 km/sec is indicated. The values adopted for the radial velocities, which have been rounded off to the nearest 5 km/sec, are given in Table 1.

For the two white stars, Co−32°5613 and L 1038-14, Popper has published values of +54 and −51, respectively.[1] For BD−18°359 two plates were obtained, giving velocities of +10 and −80 km/sec, respectively. Judging from the internal discordances, this difference should be real; but further observations will be required to settle the matter.

The spectrum of R 986 shows $H\delta$, H-$H\epsilon$, K, and $H\zeta$ as strong emission lines, while there are some further indications of emission in the region of λ 3734 and λ 3745, close to the *Fe* I lines at λλ 3720, 3737, and 3745. Since emission lines are often associated with double stars, it seemed to be of interest to ascertain whether this star might be an eclipsing binary. Twelve plates taken by Dr. P. D. Jose at the Steward Observatory at Tucson do not, however, give any indication of variability, the photographic magnitude of the star remaining constant at 13.28.

Spectrograms were likewise obtained for the three white dwarfs o_2 Eri B, L 1244-26, and the star at $\alpha = 6^h40^m.9$, $\delta = +37°39'$. The spectra of all three stars are similar in that the hydrogen lines are broad and shallow, but the second of the three appears to have a higher temperature than the other two. This is in agreement with the fact that Jose and the writer found this star to have a color index of −0.4.[2] Following the suggestion made by the writer,[3] these spectra might therefore be classified as DA, DB, and DA, respectively. Owing to the character of the lines, no radial-velocity measurements were made.

[1] *A.P. J.*, **95**, 308, 1942. [2] *Ap. J.*, **99**, 244, 1944. [3] *Ap. J.*, **101**, 131, 1945.

The spectrum of Co−32°5613, which has been classified by Kuiper as wA or of the o_2 Eri B type, appears entirely different with the present dispersion; its lines are fairly sharp and almost resemble those of an ordinary A or B9 star. Yet the star has an apparent magnitude of 11.6, and a proper motion of 1″.66 in 322°. Hence, using a radial velocity of about +50 km/sec, we find that, referred to the usual Θ-II-Z galactic system of velocities, with axes directed toward $l = 55°$, $b = 0°$ (Θ); $l = 325°$, $b = 0°$ (II); and $b = 90°$ (Z), the velocity components along the Z- and Θ-axes will be small, and nearly the entire motion will consist of a large negative II-component, i.e., directed toward $l = 145°$. Nearly all "high-velocity" stars, such as Kapteyn's star, have large positive II-components, and the largest negative values rarely exceed −150 km/sec numerically. Adopting this as an upper limit would yield a minimum value of 0″.050 for the parallax, or +10.1 for the absolute magnitude. There seems to be little doubt, therefore, that the star must have a density of the order of 10^4 or more, virtually the same as that for an

TABLE 1

RADIAL VELOCITIES AND SPECTRAL TYPES

STAR	POSITION FOR 1900		PHOTOGR. MAG.	SP.	V (KM/SEC)
	α	δ			
LDS 1A	0h06m1	−21° 17′	12.4	F0	− 85
Co−32°5613	8 37.7	−32 37	11.6	A:	+ 65
L 1038-14	9 35.6	+ 1 29	10.7	A5	− 45
R 555	1 46.8	−11 17	12.4	M4	0
BD−18°359	2 00.1	−18 06	10.8	M0	− 35:
R 556	2 38.4	+25 06	12.3	M4	+ 65
CPD−48°376	3 31.8	−48 46	10.1	K5	+ 65
R 986	7 03.3	+38 43	13.6	M5e	− 25
CPD−45°3978	9 40.7	−45 17	11.9	M2	+ 60
Grw+79°3888	11 41.3	+79 14	12.3	M4	−130
R 128	11 42.7	+ 1 23	12.6	M5	− 20
R 690	12 18.4	+64 35	12.9	M4	+ 60
R 486 A	13 23.2	− 1 50	12.0	M4	+ 10
L 1194-26	13 24.4	+11 59	13.0	M5	+ 40

ordinary white dwarf. Yet its spectrum appears entirely different. It may perhaps be mentioned that there seems to be a faint suspicion of emission in the region of the K line.

For the fainter stars, spectra were taken with the A-spectrograph, with a dispersion of 370 A/mm, from $H\beta$ to $H\delta$, on 103a-O emulsion for the white stars and Agfa Super Pan Press for the red stars. The classification of these spectra is given in Table 2.

The color indices of the components of LDS 1 have been determined by Jose and the writer at Tucson,[4] as has that of L 580-71 (still unpublished). All three stars appear to be too faint to be ordinary main-sequence dwarfs and may be "intermediates."

For the star L 232-29 a special effort had to be made to obtain a spectrogram, since this star lies within 6′ of the declination limit of the telescope and is, even when on the meridian, only 5° above the physical horizon of Mount Locke; accordingly, the slit had to be placed in declination, to avoid the effects of atmospheric dispersion. The writer has previously suggested[5] that the star should have a large parallax, even though the value as measured at Lembang is 0″.000, and it was hoped to obtain some indication of absolute magnitude from the spectrum. While the plate shows a spectrum which appears

[4] *Harvard Ann. Card*, No. 712, 1945.

[5] *Harvard Bull.*, No. 916, 1942.

very similar to that of an ordinary, rather early, M dwarf, it is too underexposed and shows insufficient detail to permit an estimate of the absolute magnitude.

The star LDS 275 is the only binary now known for which both components are white dwarfs. Owing to bad seeing at the low altitude of the star, it was not possible to obtain the spectra of the components separately. Since no lines are visible, the spectrum should probably be classified as DC. The proper motion of L 1820-21 was found by Mr. James L. Artig with the blink microscope at Minnesota.

The pair L 1405-40/41 was announced as a red-white binary by Jose and the writer;[6] the lines in the spectrum of the brighter component appear sharper than those in white

TABLE 2

SPECTRAL TYPES

STAR	POSITION FOR 1900		PHOTOGR. MAG.	μ	Sp.
	α	δ			
LDS 1A	0^h06^m1	$-21°17'$	12.4	0".25	F
LDS 1B	0 06.1	−21 17	14.8	0.25	G
L 580-71	1 01.1	−28 10	15.1	0.27	F–G
L 232-29	5 05.9	−53 10	13.4	1.16	M2:
LDS 275 AB	9 32.9	−36 54	14.2	0.36	DC
L 1820-21	9 40.9	+60 44	13.5	0.86	M2
L 1405-40	11 45.1	+25 52	15.4	0.20	DA
L 1405-41	11 45.1	+25 52	16.2	0.20	M2:

dwarfs of the o_2 Eri B type; in view of the physical connection between the two stars there can be little doubt, however, that the absolute magnitude of the white star is at least +11.

In conclusion it is a pleasure to express the writer's indebtedness to Dr. Otto Struve, who not only gave permission to use the 82-inch telescope almost exclusively for the present observations for several nights but who also bore a very considerable share of the burden of the actual observing.

MINNEAPOLIS, MINNESOTA
August 16, 1945

[6] *Harvard Ann. Card*, No. 691, 1944.

A THEORETICAL DISCUSSION OF THE CONTINUOUS SPECTRUM OF THE SUN

GUIDO MÜNCH[1]
Yerkes Observatory
Received August 25, 1945

ABSTRACT

The observational data relating to the various aspects of the intensity distribution in the continuous spectrum of the sun is examined in the light of recent developments in the theory of radiative equilibrium. It is shown that the intensity distribution in the continuous spectrum at the center of the solar disk, the distribution in the different wave lengths of the emergent monochromatic fluxes, and the law of darkening in the different wave lengths can all be accounted for, within the limitations of the theory, in terms of a single dependence of the continuous absorption coefficient with wave length (see Fig. 1). Further, the required variation of the absorption coefficient in the visual and in the near infrared regions of the spectrum receives a satisfactory explanation in terms of the continuous absorption coefficient of the negative ion of hydrogen.

1. *Introduction.*—In a recent paper S. Chandrasekhar[2] has rediscussed the problem of radiative transfer in an atmosphere in local thermodynamical equilibrium and has shown that a formula for the temperature distribution of the form

$$T^4 = \tfrac{3}{4} T_e^4 (\tau + q[\tau]) \tag{1}$$

where T_e denotes the effective temperature and $q(\tau)$ a certain monotonic increasing function of the optical depth τ, is valid also for a nongray atmosphere (in a second approximation) if the mean absorption coefficient $\bar{\kappa}$, in terms of which τ has to be measured, is defined as a straight average of the monochromatic absorption coefficient κ_ν, weighted according to the net flux $F_\nu^{(1)}$ of radiation of frequency ν in a gray atmosphere, and if, further, $\kappa_\lambda/\bar{\kappa}$ is independent of depth. Accordingly, it would appear that, under the stated conditions, the emergent intensity $I_\lambda(\vartheta)$ at the wave length λ and in a direction inclined to the normal by an angle ϑ will be given by

$$I_\lambda(\vartheta) = \int_0^\infty B_\lambda(T_\tau)\, e^{-\kappa_\lambda \tau \sec\vartheta/\bar{\kappa}} \frac{\kappa_\lambda}{\bar{\kappa}} \sec\vartheta\, d\tau\,, \tag{2}$$

where $B_\lambda(T_\tau)$ denotes the Planck function for the temperature T_τ prevailing at the depth τ.

The use of equation (2) for the discussion of the continuous spectrum of the sun and the stars has been well known since Milne's classical paper on "Radiative Equilibrium."[3] The method, as applied to the sun, has been to derive $\kappa_\lambda/\bar{\kappa}$ such that equations (1) and (2) together predict the correct intensity distribution in the continuous spectrum. More particularly, attention has been concentrated on two features of this distribution: first, on the intensity distribution in the continuous spectrum as observed at the center of the solar disk and, second, on the law of darkening in the different wave lengths. In this manner two independent determinations of the dependence of the continuous absorption coefficient on the wave length can be made. This is the principle underlying the discussions of Milne,[3] Unsöld and Maue,[4] and Mulders.[5] But these same discussions seemed to indi-

[1] Fellow of the John Simon Guggenheim Memorial Foundation at the Yerkes Observatory.

[2] *Ap. J.*, **101**, 328, 1945.

[3] *Phil. Trans. R. Soc.*, A, **223**, 201–255, 1922.

[4] *Zs. f. Ap.*, **5**, 1, 1932.

[5] *Zs. f. Ap.*, **11**, 132, 1935.

cate that the two determinations of $\kappa_\lambda/\bar{\kappa}$ were in poor agreement. In trying to examine the origin of this disagreement, it appeared that it might be profitable to re-examine the whole problem on the revised basic theory of Chandrasekhar and with a view to correlating the derived variation of $\kappa_\lambda/\bar{\kappa}$ with the known sources of opacity in the solar atmosphere.

2. *The determination of $\kappa_\lambda/\bar{\kappa}$ from the intensity distribution of the continuous spectrum at the center of the solar disk.*—At the center of the disk the intensity distribution will be given by

$$I_\lambda(0) = \int_0^\infty B_\lambda(T_\tau)\, e^{-\kappa_\lambda \tau/\bar{\kappa}} \frac{\kappa_\lambda}{\bar{\kappa}}\, d\tau\,, \tag{3}$$

and the determination of $\kappa_\lambda/\bar{\kappa}$ according to this formula requires a knowledge of $I_\lambda(0)$. For the sun this quantity has been derived by Mulders,[6] who has made special allowances for the energy in the continuous spectrum which has been lost in the absorption lines. Mulders' values were graphically smoothed out, and the specific intensities derived in this manner are given for various wave lengths in Table 1. These values were used in our

TABLE 1

$\kappa_\lambda/\bar{\kappa}$ DERIVED FROM THE INTENSITIES IN THE CENTER OF THE DISK

λA	$I_\lambda(0)\times10^{-13}$ (Ergs/Cm²/Sec)	$\kappa_\lambda/\bar{\kappa}$	λA	$I_\lambda(0)\times10^{-13}$ (Ergs/Cm²/Sec)	$\kappa_\lambda/\bar{\kappa}$
3000	15.0	1.34	6500	29.1	0.82
3230	16.8	1.41	6702	27.6	0.83
3400	19.2	1.38	7000	25.6	0.84
3737	31.7	0.94	7500	22.0	0.86
3800	36.9	0.80	8000	19.0	0.98
3900	42.0	0.72	8500	16.7	1.00
4000	44.0	0.67	8580	16.4	1.02
4265	46.2	0.65	9000	14.3	1.12
4500	45.4	0.66	9500	12.8	1.09
5000	41.6	0.72	10000	11.7	1.03
5062	41.1	0.72	10080	11.5	0.99
5500	37.6	0.73	10500	10.7	0.91
5955	33.7	0.77	11000	9.7	0.79
6000	33.1	0.78			

further discussion.

In deriving κ_λ/κ according to equation (3), the temperature distribution was assumed to be given by its solution in the "first approximation," namely,

$$T^4 = \tfrac{3}{4}T_e^4(\tau+\tfrac{2}{3}) = \sqrt{3}T_0^4(\tau+\tfrac{2}{3})\,. \tag{4}$$

It will be noticed that in equation (4) we have used the Hopf-Bronstein relation between the boundary and the effective temperatures. For the temperature distribution given by equation (4) the emergent intensity $I_\lambda(0)$ at the center of the disk can be expressed in the form

$$I_\lambda(0) = 2hc^2\left(\frac{2^{1/4}}{3^{1/8}}\frac{k}{hc}\right)^5 T_0^5\, f(\gamma, p)\,, \tag{5}$$

where

$$\gamma = \frac{3^{1/8}}{2^{1/4}}\frac{hc}{k\lambda T_0} \quad \text{and} \quad p = \frac{3}{2}\frac{\bar{\kappa}}{\kappa_\lambda} \tag{6}$$

[6] Dissertation, Utrecht, 1934.

and

$$f(\gamma, p) = \gamma^5 \int_0^\infty \frac{e^{-t}}{e^{\gamma(1+pt)^{-1/4}} - 1}\, dt \tag{7}$$

is the function which has been tabulated by Milne[7] and Lindblad for various values of the arguments. (In equations [5] and [6] h, c, and k have their usual meanings.)

For the effective temperature T_e of the sun the value 5740° K was adopted, which is the value derived by Milne[8] and Minnaert[9] in their reductions of Abbot's measures to the absolute scale.[10] With this value of T_e the boundary temperature T_0 is 4656° K, and equation (5) reduces to

$$I_\lambda(0) = 5.057 \times 10^{12} f(\gamma, p). \tag{8}$$

With the intensities given in Table 1 and with the tables of the function $f(\gamma, p)$ provided by Milne and Lindblad it is a simple matter to derive $\kappa_\lambda/\bar{\kappa}$ for the various wave lengths.

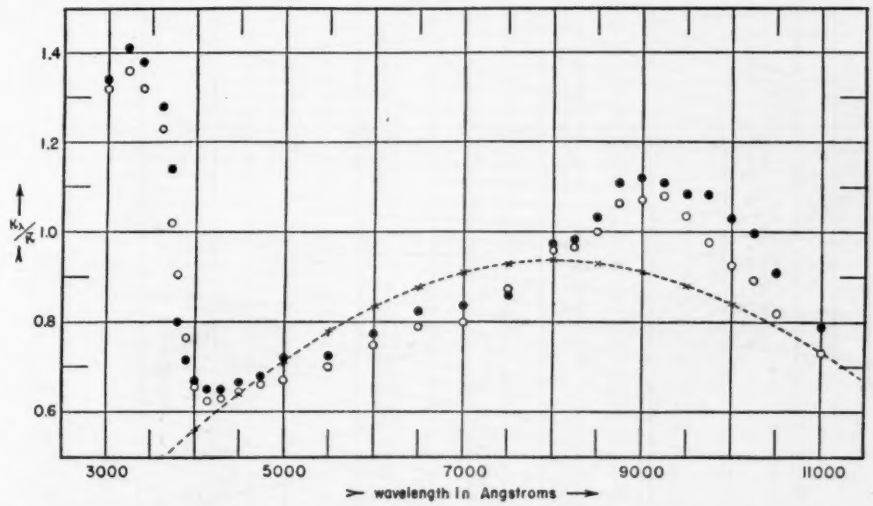

FIG. 1.—The dependence of κ_λ/κ on wave length. The solid circles represent values obtained from the intensities in the center of the solar disk; the open circles, those obtained from the monochromatic fluxes. The dotted line is the absorption of H^- computed on the assumption that this ion is the only source of opacity between 4000 A and 16,000 A.

The results are given in Table 1 and are further illustrated in Figure 1. The dependence of the continuous absorption on wave length which we have derived is in general agreement with that found earlier by Milne and Mulders. However, it differs in details from the earlier determinations for the following reasons. In Milne's discussion the effect of the absorption lines on the observed continuous spectrum was not allowed for, while in Mulders' discussion a boundary temperature, T_0, allowing for the so-called "blanketing effect," was used. On this latter point, reference may be made to a recent paper by Unsöld,[11] who has questioned the use of a blanketing theory in this form.

[7] *Op. cit.*, Appen. I.

[8] *Ibid.*, Appen. II.

[9] *B.A.N.*, **51**, 75, 1924.

[10] It should, perhaps, be mentioned in this context that Mulders' discussion (from which the values of $I_\lambda(0)$ given in Table 1 have been taken) is also based on these same measures of Abbot.

[11] *Zs. f. Ap.*, **22**, 356, 1943.

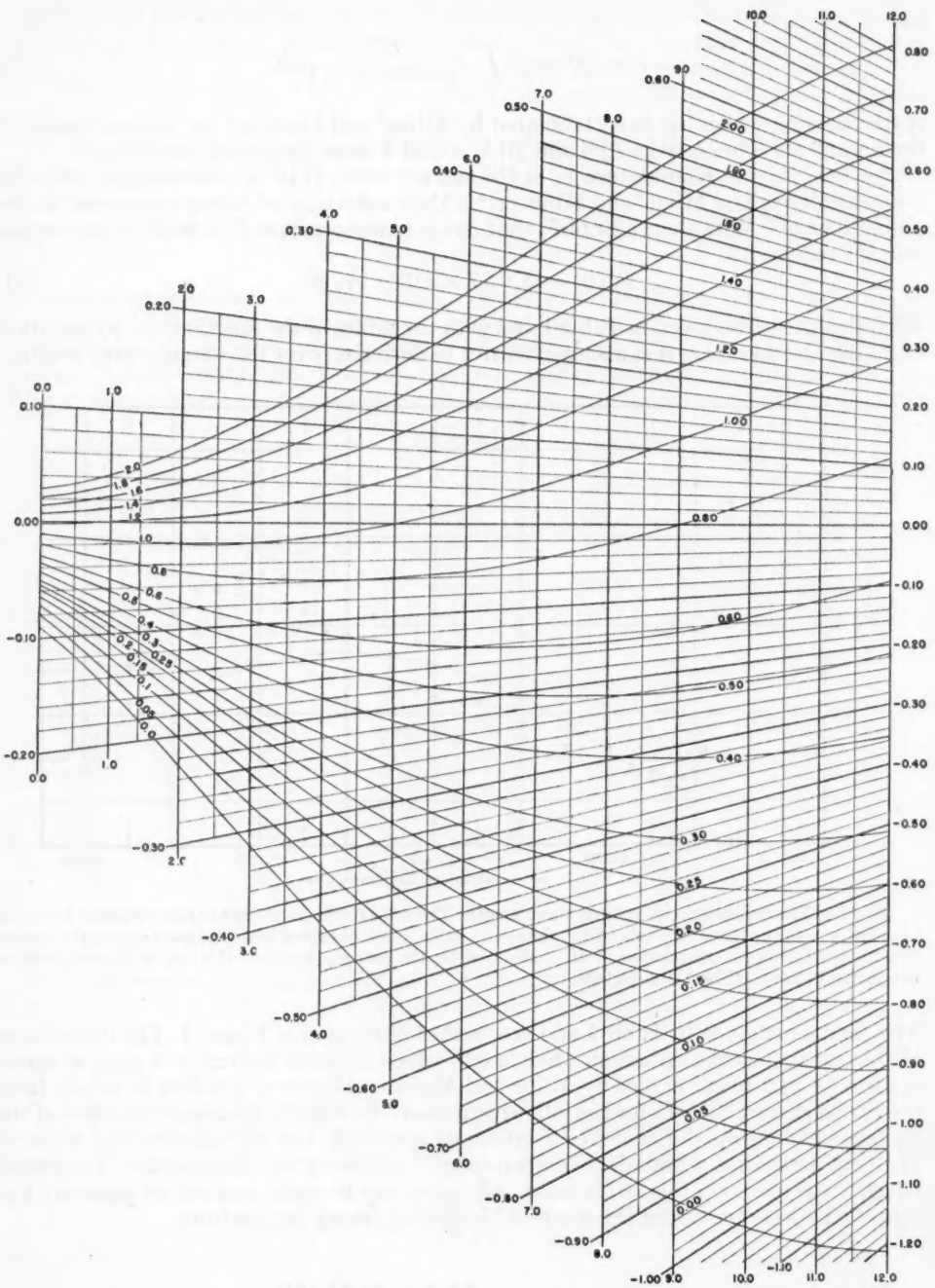

FIG. 2.—Graphical representation of Burkhardt's table (*Zs. f. Ap.*, **13**, 56, 1936). Every point of the region represented corresponds to one set of values (a, $\log F_\lambda(0)/B_\lambda(T_e)$, $\bar{\kappa}/\kappa_\lambda$). The vertical straight lines are the loci of constant a; the diagonal straight lines, the loci of constant $F_\lambda(0)/B_\lambda(T_e)$; and the curves themselves are the loci of constant $\bar{\kappa}/\kappa_\lambda$.

3. *The determination of $\kappa_\lambda/\bar{\kappa}$ from the intensity distribution in the emergent flux.*—A determination of $\kappa_\lambda/\bar{\kappa}$ can also be made from the intensity distribution in the emergent flux. For on the assumptions under which equation (1) for the temperature distribution may be expected to be approximately valid for a nongray atmosphere, it is true that[12]

$$F_\lambda(0) = 2\int_0^\infty B_\lambda(T_\tau)\, E_2\left(\frac{\kappa_\lambda}{\bar{\kappa}}\tau\right)\frac{\kappa_\lambda}{\bar{\kappa}}\, d\tau\,, \tag{9}$$

where

$$E_2(x) = \int_1^\infty \frac{e^{-xw}}{w^2}\, dw\,. \tag{10}$$

Equation (9) can be expressed alternatively in the form

$$\log\frac{F_\lambda(0)}{B_\lambda(T_e)} = \log\left\{2(e^\alpha - 1)\int_0^\infty \frac{E_2(\kappa_\lambda\tau/\bar{\kappa})}{e^{\alpha[3/4(\tau+q[\tau])]^{-1/4}} - 1}\,\frac{\kappa_\lambda}{\bar{\kappa}}\, d\tau\right\}, \tag{11}$$

where

$$\alpha = \frac{hc}{k\lambda T_e}\,. \tag{12}$$

The expression on the right-hand side of (11) has been evaluated by Burkhardt[13] for various values of $\kappa_\lambda/\bar{\kappa}$ and α. It was found that, in practice, the use of Burkhardt's tables

TABLE 2

$\kappa_\lambda/\bar{\kappa}$ DERIVED FROM THE MONOCHROMATIC FLUXES

λA	$F_\lambda(0)\times10^{-13}$ (Ergs/Cm²/Sec)	$\kappa_\lambda/\bar{\kappa}$	λA	$F_\lambda(0)\times10^{-13}$ (Ergs/Cm²/Sec)	$\kappa_\lambda/\bar{\kappa}$
3000	9.9	1.32	6500	24.3	0.79
3230	11.7	1.36	7000	21.3	0.80
3400	13.6	1.32	7500	18.4	0.87
3737	20.3	1.02	8000	15.9	0.96
3800	23.4	0.91	8500	14.0	1.00
3900	28.5	0.76	9000	12.2	1.07
4000	32.6	0.66	9500	11.0	1.04
4500	34.2	0.64	10000	10.2	0.93
5000	32.2	0.67	10500	9.5	0.82
5500	29.9	0.70	11000	8.8	0.73
6000	27.2	0.75			

is enormously facilitated by plotting them in the manner of Figure 2. With this plot, graphical interpolation, giving sufficient accuracy, is possible with considerable ease.

To determine $\kappa_\lambda/\bar{\kappa}$, according to equation (11), we require, of course, a knowledge of $F_\lambda(0)$ for various wave lengths. These follow also from Mulders' discussion and have been tabulated by Unsöld.[14] The values of $F_\lambda(0)$ used in the present discussion are those given in Table 2; these were obtained by graphical interpolation from those given by Unsöld. It may be pointed out in this connection that the observational determination of $F_\lambda(0)$ follows from a more direct and straightforward procedure than does $I_\lambda(0)$ (see § 4, below) and is, accordingly, more trustworthy.

With the values of $F_\lambda(0)$ given in Table 2 and with the plot of Figure 2, $\kappa_\lambda/\bar{\kappa}$ was de-

[12] Cf. E. A. Milne, *Handb. d. Ap.*, **3**, Part I, 147–155, Berlin: Springer, 1930.

[13] *Zs. f. Ap.*, **13**, 56, 1936.

[14] *Physik der Sternatmosphären*, Tables 7 and 8, pp. 38–39, Berlin: Springer, 1938.

rived for various wave lengths. The results are given in Table 2. For comparison with the values derived from the intensities in the center, the determination of κ_λ/κ from the monochromatic fluxes is also plotted in Figure 1. The agreement between the two determinations is seen to be very satisfactory, indeed; and it clearly implies that the same variation of the absorption coefficient with wave length is adequate (within limits) for accounting both for the law of darkening and for the intensity distribution over the different wave lengths (see § 4, below). Finally, we may draw attention to the fact that observational data relating to the monochromatic fluxes are available up to wave length λ 23,480 A. But, unfortunately, Burkhardt's table is not extensive enough to use this data for the evaluation of κ_λ/κ in these regions of the spectrum. However, the indications are that $\kappa_\lambda/\bar{\kappa}$ has a deep minimum at about λ 16,000 A.

4. *The darkening in the different wave lengths.*—We shall begin our discussion of this phenomenon by briefly recapitulating the procedure which is followed in the observational determination of the quantities $I_\lambda(0)$ and $F_\lambda(0)$ in absolute measure. Essentially what the observations give directly are the quantities $f_\lambda = c_1 F_\lambda(0)$ and $i_\lambda = c_2 I_\lambda(0)$, where c_1 and c_2 are certain scale factors to be determined, and the function

$$\phi_\lambda(\vartheta) = \frac{i_\lambda(\vartheta)}{i_\lambda(0)} = \frac{I_\lambda(\vartheta)}{I_\lambda(0)}. \tag{13}$$

In other words, the intensities at the center and the monochromatic fluxes are known in different units, and the law of darkening is also known. The constant c_1 is determined from the condition

$$\frac{1}{c_1}\int_0^\infty f_\lambda d\lambda = \int_0^\infty F_\lambda(0)\, d\lambda = F; \tag{14}$$

and as F is simply related to the solar constant, the unit in which f_λ measures the monochromatic fluxes is determinate.

The constant c_2 is next determined from the condition

$$\frac{2}{c_2}\int_0^{\pi/2} i_\lambda(0)\,\phi_\lambda(\vartheta)\sin\vartheta\cos\vartheta d\vartheta = F_\lambda. \tag{15}$$

It is now apparent that the substantial agreement between the two determinations of $\kappa_\lambda/\bar{\kappa}$, from the intensities at the center of the disk and from the fluxes, must mean that the same dependence of the absorption coefficient on wave length accounts for the law of darkening satisfactorily. That this is actually the case can be shown by evaluating $I_\lambda(\vartheta)$ according to equation (2), using the same values of $\kappa_\lambda/\bar{\kappa}$ as has been derived from the intensity distribution at the center of the disk. To do this we re-write equation (2) in a form analogous to (8). We have

$$I_\lambda(\vartheta) = 5.057\times 10^{12} f\left(\gamma, \frac{3}{2}\frac{\bar{\kappa}}{\kappa_\lambda}\cos\vartheta\right). \tag{16}$$

Using this formula and the Milne-Lindblad tabulation of the function $f(\gamma, p)$, $I_\lambda(\vartheta)/I_\lambda(0)$ was evaluated for various wave lengths. The results are exhibited in Figure 3, together with the darkening observations as collected by Unsöld.[15] It is seen that, as expected, the agreement between the observed and the computed darkening is quite good. However, there are systematic differences, in the sense that toward the limb there is observationally less contrast than computed. But it should be pointed out that the foundations both of the theory and of observations, in so far as they refer to the extreme limb, are not so secure. On the observational side, the photometric problem is one of exceptional complex-

[15] *Ibid.*, pp. 34–35. Tables 3 and 4.

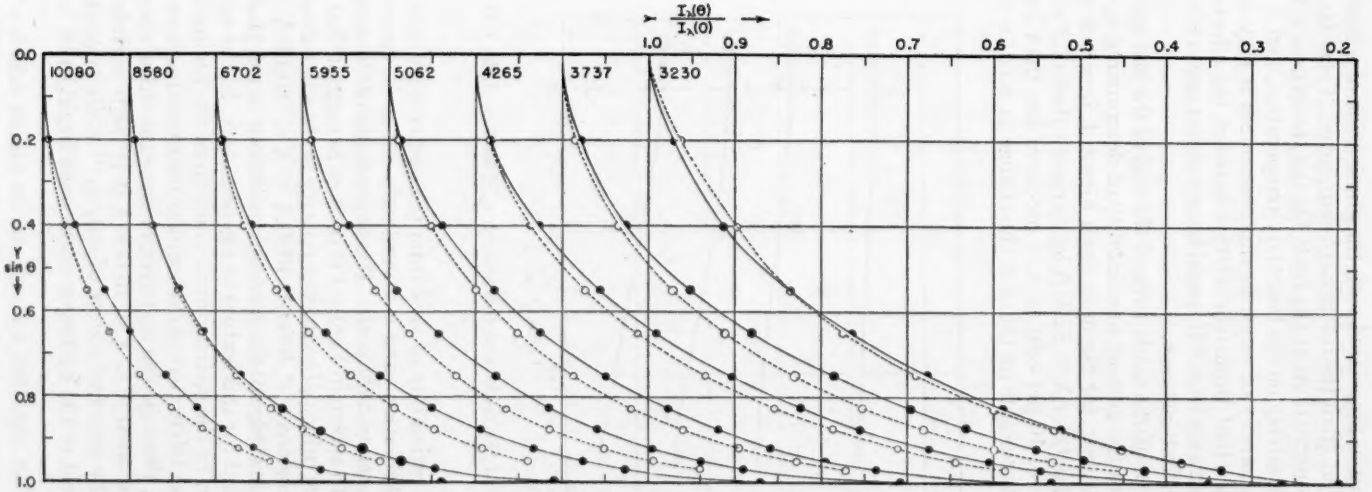

FIG. 3.—Comparison of the observed and computed darkening. Open circles are observational values; solid circles, the theoretical ones. The scale of the abscissae is displaced 0.10 to the left at each wave length considered.

ity, in view of the difficulties associated with the elimination of scattering not only from the earth's atmosphere but from the instruments employed. These factors become major sources of error for the observations at the limb. On the theoretical side the intensities at the limb depend very sensitively on the boundary temperature, and it is well known that this can be affected in a variety of ways. In this connection it may be noted that, for a nongray atmosphere, the Hopf-Bronstein relation between the effective and the boundary temperatures is not strictly true.[16] It would be of interest to examine the consequences of this correction in the first instance.

With reference to the remarks made toward the end of the last paragraph, we should draw further attention to the general unreliability of determining $\kappa_\lambda/\bar{\kappa}$ from the law of darkening alone. This is clear, for example, from Figure 4, in which we have illustrated the darkening function $\phi_\lambda(\vartheta)$ for $\lambda = 3230$ A for various values of ϑ as a function of $\kappa_\lambda/\bar{\kappa}$. It is seen that a change of 10 per cent in $\kappa_\lambda/\bar{\kappa}$ produces less than 2 per cent change in $\phi_\lambda(\vartheta)$ at the limb; at other points on the disk the change in $\phi_\lambda(\vartheta)$ is much less. It would

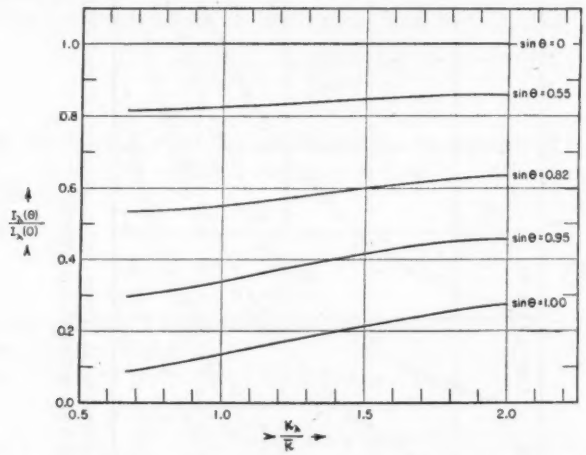

FIG. 4.—The dependence of the darkening function on $\kappa_\lambda/\bar{\kappa}$ for $\lambda = 3230$ A at different points of the solar disk.

therefore seem that the estimation of $\kappa_\lambda/\bar{\kappa}$ from the center-limb contrast is particularly sensitive to errors in observations and is accordingly not to be recommended.

5. *The continuous absorption coefficient.*—The dependence of the continuous absorption coefficient on wave length shown in Figure 1 is such as to suggest that we should perhaps distinguish between three principal sources of opacity in the solar atmosphere, contributing, respectively, in the regions $\lambda < 4000$ A, 4000 A $< \lambda <$ 16,000 A, and $\lambda >$ 16,000 A. And from our present knowledge of the physical conditions in the photosphere of the sun it is not difficult to account for this feature in a general way. In the region to the violet of 4000 A, the contribution to the opacity must come from the photoelectric ionization of the "metals." It is further likely that, on account of the excessive crowding of the absorption lines in this region, there is also an effective increase of the continuous absorption coefficient. In the region 4000 A $< \lambda <$ 16,000 A it is fairly certain that the negative hydrogen ions provide the principal source of opacity,[17] while beyond 16,000 A the free-free transitions in the field of the hydrogen atom must begin to be important.

[16] Cf. Chandrasekhar, *op. cit.*, eqs. (109) and (119), for the relation valid in a higher approximation.

[17] Wildt, *Ap. J.*, **89**, 295, 1939. Also B. Strömgren, *Festschrift für Elis Strömgren*, p. 218, Copenhagen, 1940.

By considering the continuous absorption in the region 4000 A$< \lambda <$ 16,000 A in greater detail, it is possible to make a more specific comparison with the physical theory. Chandrasekhar[18] has recently made what appears to be a fairly definitive evaluation of

TABLE 3

THE MEAN ABSORPTION COEFFICIENT OF H^-

τ	0.0	0.2	0.5	1.0	2.0
$\bar{\kappa}(H^-)\times 10^{17}$ cm^{-2}	2.82	2.90	2.94	2.89	2.76

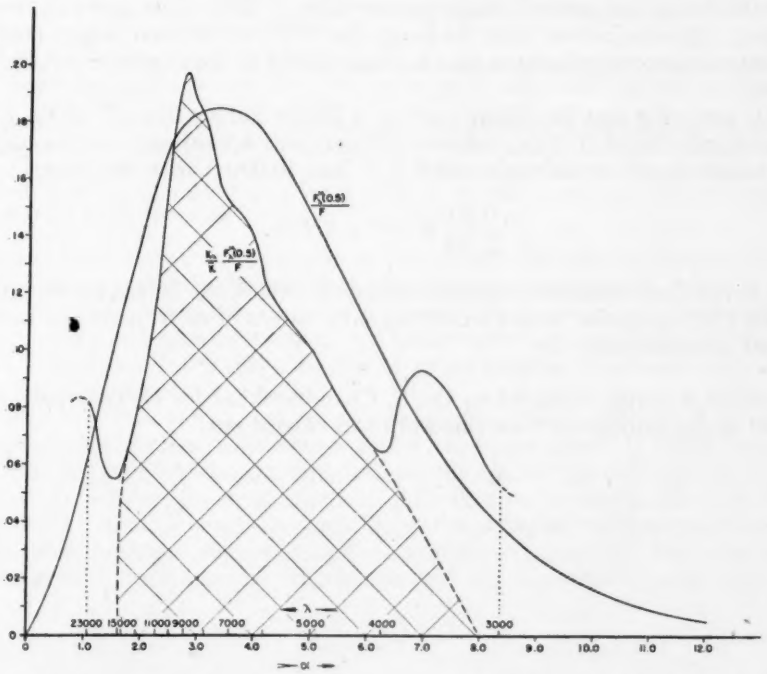

FIG. 5.—The net monochromatic flux $F_\lambda^{(1)}$ in units of F at $\tau = 0.5$ and $\kappa_\lambda F_\lambda^{(1)}/\bar{\kappa}$. The shaded portion is assumed to be the contribution of absorption by H^- to the integral $\int \kappa_\lambda F_\lambda^{(1)}/\bar{\kappa}$. (The abcissae is $\alpha = hc/k\lambda T_e$.)

the continuous absorption coefficient $\kappa_\lambda(H^-)$ of the negative hydrogen ion. Using these values, we can evaluate the mean absorption coefficient $\kappa(H^-)$ arising from this source, according to the formula[19]

$$\bar{\kappa}\,(H^-;\,\tau) = \frac{1}{F}\int_0^\infty \kappa_\lambda\,(H^-)\,F_\lambda^{(1)}\,(\tau)\,d\lambda\,, \qquad (17)$$

[18] *Ap. J.*, **102**, 395, 1945.

[19] S. Chandrasekhar, *Ap. J.*, **101**, 328, eq. (42), 1945.

where $F_\lambda^{(1)}(\tau)$ denotes the monochromatic flux at wave length λ and depth τ. By using for $F_\lambda^{(1)}(\tau)$ the values tabulated in Chandrasekhar's paper, $\kappa(H^-)$ was evaluated at various depths. The results are summarized in Table 3, where it is seen that the dependence of $\kappa(H^-)$ on the depth is very slight. The assumption of the constancy of $\kappa_\lambda/\bar{\kappa}$ arising from this source can therefore be justified. It would further appear that averaging κ_λ with $F_a^{(1)}(\tau = 0.5)$ ($a = h\nu/kT$) would be sufficient. Using the mean of our two determinations of $\kappa_\lambda/\bar{\kappa}$, we have plotted the quantity $\kappa_\lambda F_\lambda^{(1)}(\tau = 0.5)/\bar{\kappa}$ in Figure 5. Now the theory would require that

$$\frac{1}{F}\int_0^\infty \frac{\kappa_\lambda F_\lambda^{(1)}}{\bar{\kappa}}\, d\lambda = 1\,. \tag{18}$$

Actually, the evaluation of the integral on the left-hand side between $\lambda = 3000$ A and $\lambda = 23{,}000$ A yields the value 0.76. Considering that this evaluation does not include the contribution of the spectral region to the violet of 3000 A, we find this result to be satisfactory. The requirement that the integral over the entire wave-length range should equal unity would seem to suggest that $\kappa_\lambda/\bar{\kappa}$ has values in the neighborhood of 2 far into the violet.

Finally, assuming that the shaded portion in Figure 5 arises from H^- alone, it is found that the contribution of H^- to κ amounts to 61 per cent. Accordingly, we can compare the derived values of $\kappa_\lambda/\bar{\kappa}$ in the region $4000\text{ A} < \lambda < 16{,}000\text{ A}$ with the values

$$\frac{0.61}{2.94} \times 10^{17}\kappa_\lambda(H^-)\,. \tag{19}$$

Figure 1 shows the comparison between both sets of values, the dotted curve representing expression (19) computed with Chandrasekhar's values of $\kappa_\lambda(H^-)$. As one can see, the agreement is satisfactory.

The writer is deeply indebted to Dr. S. Chandrasekhar for his constant encouragement and advice during the time this work was carried out.

ON THE CONTINUOUS ABSORPTION COEFFICIENT OF THE NEGATIVE HYDROGEN ION. II

S. CHANDRASEKHAR
Yerkes Observatory
Received September 13, 1945

ABSTRACT

In this paper the continuous absorption coefficient of the negative hydrogen ion, determined in an earlier paper (*Ap. J.*, **102**, 223, 1945) in terms of the matrix elements of the momentum operator, is further improved to take into account the effect of the static field of the hydrogen atom on the motion of the ejected electron. It is shown that for wave functions for the ground state of H^- of the forms generally considered, the formula for the absorption cross-section can be reduced to the form

$$\kappa = \frac{3.7062}{k(k^2+0.05512)}\left|\int_0^\infty W_2(r)\chi_1(r)dr\right|^2 \times 10^{-18}\ \text{cm}^2,$$

where k denotes the momentum of the ejected electron in atomic units, $W_2(r)$ a certain weight function which can be tabulated, and $\chi_1(r)$ the radial part of a p-spherical wave in the Hartree field of a hydrogen atom which tends to unit amplitude at infinity.

The absorption cross-sections of H^- have been evaluated according to the foregoing formula for various wave lengths. It is found that the new values are larger than those obtained with a plane-wave representation of the outgoing electron by about 5 per cent in the visual and the near infrared regions. The new absorption-curve places the maximum at about λ 8500 A; at this wave length the atomic absorption coefficient has the value 4.52×10^{-17} cm^2.

1. *Introduction.*—In an earlier paper[1] it was shown that the continuous absorption coefficient of the negative hydrogen ion is most reliably determined in terms of the matrix elements of the momentum operator. However, in the actual evaluation of the absorption cross-sections by this method, the plane-wave approximation for the ejected electron was used (see I, eq. [15]). In this paper we propose to consider certain refinements in this direction.

2. *Formulae for the evaluation of the continuous absorption coefficient of* H^- *using the wave functions of an electron in the Hartree field of a hydrogen atom.*—It would seem that, if we abandon the plane-wave approximation[2] for the ejected electron, the next simplest thing to do will be to use the wave functions of an electron moving in the static field of a hydrogen atom.[3] In other words, it would appear that in the "next approximation" we use for the wave functions Ψ_c describing the continuous states of H^- that of a hydrogen atom in its ground state, together with an electron moving in the Hartree field,

$$-\left(\frac{1}{r}+1\right)e^{-2r}. \qquad (1)^4$$

On this approximation Ψ_c will have the form

$$\Psi_c = \frac{1}{\sqrt{2\pi}}\{e^{-r_2}\phi(r_1) + e^{-r_1}\phi(r_2)\}, \qquad (2)$$

where $\phi(r)$ satisfies the wave equation

$$\nabla^2\phi + \left[k^2 + 2\left(1+\frac{1}{r}\right)e^{-2r}\right]\phi = 0 \qquad (3)$$

[1] S. Chandrasekhar, *Ap. J.*, **102**, 223, 1945. This paper will be referred to as "I."

[2] First suggested in this connection by H. S. W. Massey and D. R. Bates, *Ap. J.*, **91**, 202, 1940.

[3] A. Wheeler and R. Wildt, *Ap. J.*, **95**, 281, 1942; also S. Chandrasekhar, *Ap. J.*, **100**, 176, 1944.

[4] In writing this equation, we have adopted the atomic system of units. These units will be used in all our formal developments.

and tends asymptotically at infinity to a plane wave of unit amplitude along some chosen direction. If this direction, in which the ejected electron moves at infinity, be chosen as the polar axis of a spherical system of co-ordinates, the requirement is that

$$\phi(r) \to e^{ikr\cos\vartheta} \qquad \text{as} \qquad r \to \infty . \tag{4}$$

On the other hand, since

$$\left.\begin{aligned} e^{ikr\cos\vartheta} &= \left(\frac{\pi}{2kr}\right)^{1/2} \sum_{l=0}^{\infty} i^l (2l+1) P_l(\cos\vartheta) J_{l+1/2}(kr) \\ &\to \sum_{l=0}^{\infty} \frac{i^l (2l+1)}{kr} P_l(\cos\vartheta) \cos(kr - \tfrac{1}{2}l\pi - \tfrac{1}{2}\pi) , \end{aligned}\right\} \tag{5}$$

it is evident that the solution for ϕ appropriate to our problem is

$$\phi = \sum_{l=0}^{\infty} \frac{i^l (2l+1)}{kr} P_l(\cos\vartheta)\, \chi_l(r) . \tag{6}$$

where the radial function $\chi_l(r)$ is a solution of the equation

$$\frac{d^2\chi_l}{dr^2} + \left\{k^2 - \frac{l(l+1)}{r^2} + 2\left(1+\frac{1}{r}\right)e^{-2r}\right\}\chi_l = 0 , \tag{7}$$

which tends to a pure sinusoidal wave of unit amplitude at infinity.

Thus, on our present approximation, the wave function can be expressed in the form (cf. I, eq. [33])

$$\left.\begin{aligned} \Psi_c = \frac{1}{\sqrt{2\pi}} \Big\{ & e^{-r_2} \sum_{l=0}^{\infty} \frac{i^l (2l+1)}{kr_1} P_l(\mu_1)\, \chi_l(r_1; k) \\ & + e^{-r_1} \sum_{l=0}^{\infty} \frac{i^l (2l+1)}{kr_2} P_l(\mu_2)\, \chi_l(r_2; k) \Big\} , \end{aligned}\right\} \tag{8}$$

where we have used μ_1 and μ_2 to denote $\cos\vartheta_1$ and $\cos\vartheta_2$, respectively.

For the evaluation of the absorption cross-sections according to formula II of paper I, we need the quantity

$$\left(\frac{\partial}{\partial z_1} + \frac{\partial}{\partial z_2}\right)\Psi_c . \tag{9}$$

For Ψ_c given by equation (8) it can be readily shown that

$$\left.\begin{aligned} \left(\frac{\partial}{\partial z_1} + \frac{\partial}{\partial z_2}\right)\Psi_c = \frac{1}{\sqrt{2\pi}} \Big[& -\mu_1 e^{-r_1} \sum_{l=0}^{\infty} \frac{i^l (2l+1)}{kr_2} P_l(\mu_2)\, \chi_l(r_2) \\ & - \mu_2 e^{-r_2} \sum_{l=0}^{\infty} \frac{i^l (2l+1)}{kr_1} P_l(\mu_1)\, \chi_l(r_1) \\ & + e^{-r_1} \sum_{l=0}^{\infty} \frac{i^l}{k} \{ l P_{l-1}(\mu_2)\, S_l(r_2) + (l+1) P_{l+1}(\mu_2)\, T_l(r_2) \} \\ & + e^{-r_2} \sum_{l=0}^{\infty} \frac{i^l}{k} \{ l P_{l-1}(\mu_1)\, S_l(r_1) + (l+1) P_{l+1}(\mu_1)\, T_l(r_1) \} \Big] , \end{aligned}\right\} \tag{10}$$

where

$$S_l(r) = \frac{\partial}{\partial r}\left(\frac{\chi_l}{r}\right) + (l+1)\frac{\chi_l}{r^2} \tag{11}$$

and

$$T_l(r) = \frac{\partial}{\partial r}\left(\frac{\chi_l}{r}\right) - l\frac{\chi_l}{r^2}. \tag{12}$$

For a wave function of the ground state of the form I, equation (3), we find after some lengthy but straightforward calculations that

$$\left.\begin{aligned}\int \Psi_d \left(\frac{\partial}{\partial z_1}+\frac{\partial}{\partial z_2}\right)\Psi_c d\tau \\ = -\frac{(2048\pi^3)^{1/2}\mathfrak{N}i}{k(1+a)^3}\left\{\int_0^\infty dr S_1(r)\left[e^{-ar}\sum_{j=0}^{7} s_j r^{j+1} + e^{-(1+2a)r}\sum_{j=0}^{+1}\sigma_j r^{j+1}\right]\right. \\ \left. - \int_0^\infty dr \chi_1(r)\left[e^{-ar}\sum_{j=-1}^{6} l_j r^j + e^{-(1+2a)r}\sum_{j=-1}^{+1}\lambda_j r^j\right]\right\},\end{aligned}\right\} \tag{13}$$

where s_j, σ_j, l_j, and λ_j have the same meanings as in I, equations (29)-(32). After some further reductions, equation (13) can be simplified to the form

$$\int \Psi_d \left(\frac{\partial}{\partial z_1}+\frac{\partial}{\partial z_2}\right)\Psi_c d\tau = -\frac{(2048\pi^3)^{1/2}\mathfrak{N}i}{k(1+a)^3}\int_0^\infty W_2(r)\,\chi_1(r)\,dr, \tag{14}$$

where

$$\left.\begin{aligned}W_2(r) = e^{-ar}\sum_{j=-1}^{7}[a s_j - j s_{j+1} - l_j]\, r^j \\ + e^{-(1+2a)r}\sum_{j=-1}^{+1}[(1+2a)\sigma_j - j\sigma_{j+1} - \lambda_j]\, r^j,\end{aligned}\right\} \tag{15}$$

with the understanding that

$$s_{-1} = s_8 = \sigma_{-1} = \sigma_2 = l_7 = 0. \tag{16}$$

Formula II (paper I) for the absorption cross-section now becomes

$$\kappa = 2.725\times 10^{-19}\,\frac{2048\pi^3\mathfrak{N}^2}{(1+a)^6 k\,(k^2+2I)}\left|\int_0^\infty W_2(r)\,\chi_1(r)\,dr\right|^2. \tag{17}$$

Inserting the numerical values for the various constants in equations (15) and (17), we find:

$$\left.\begin{aligned}W_2(r) = e^{-0.707735r}(0.1573261 r^{-1} + 0.2686713 + 0.9780967 r \\ - 0.2397504 r^2 + 0.06594301 r^3 - 0.006107001 r^4 + 0.0008050248 r^5 \\ - 0.00007231322 r^6 + 0.000004366322 r^7) - e^{-2.415470r}(0.1573261 r^{-1} \\ + 0.5373426 + 0.2294096 r)\end{aligned}\right\} \tag{18}$$

and

$$\kappa = \frac{3.7062}{\kappa(k^2+0.055118)}\left|\int_0^\infty W_2(r)\,\chi_1(r)\,dr\right|^2 \times 10^{-18}\ \mathrm{cm}^2. \tag{II$_1$}$$

For the purposes of evaluating the absorption cross-sections according to the foregoing formulae, it is convenient to have a fairly extensive table of the "weight function," $W_2(r)$. This is provided in Table 1.

TABLE 1

THE WEIGHT FUNCTION $W_2(r)$

r	$W_2(r)$	r	$W_2(r)$	r	$W_2(r)$	r	$W_2(r)$
0	0	4.4	0.18818	8.8	0.05010	16.4	0.00676
0.1	0.12932	4.5	.18220	8.9	.04872	16.6	.00638
0.2	.23292	4.6	.17644	9.0	.04738	16.8	.00601
0.3	.31486	4.7	.17089	9.1	.04609	17.0	.00567
0.4	.37865	4.8	.16554	9.2	.04484	17.2	.00530
0.5	.42731	4.9	.16039	9.3	.04363	17.4	.00502
0.6	.46340	5.0	.15541	9.4	.04245	17.6	.00473
0.7	.48911	5.1	.15061	9.5	.04132	17.8	.00443
0.8	.50628	5.2	.14598	9.6	.04021	18.0	.00417
0.9	.51649	5.3	.14150	9.7	.03915	18.2	.00391
1.0	.52105	5.4	.13718	9.8	.03811	18.4	.00366
1.1	.52106	5.5	.13300	9.9	.03711	18.6	.00342
1.2	.51744	5.6	.12896	10.0	.03614	18.8	.00321
1.3	.51097	5.7	.12506	10.2	.03428	19.0	.00302
1.4	.50229	5.8	.12128	10.4	.03253	19.2	.00281
1.5	.49192	5.9	.11763	10.6	.03089	19.4	.00264
1.6	.48030	6.0	.11409	10.8	.02934	19.6	.00246
1.7	.46778	6.1	.11067	11.0	.02787	19.8	.00230
1.8	.45467	6.2	.10736	11.2	.02649	20.0	.00214
1.9	.44118	6.3	.10415	11.4	.02518	20.2	.00200
2.0	.42753	6.4	.10105	11.6	.02394	20.4	.00187
2.1	.41384	6.5	.09804	11.8	.02277	20.6	.00174
2.2	.40026	6.6	.09514	12.0	.02165	20.8	.00162
2.3	.38686	6.7	.09232	12.2	.02059	21.0	.00151
2.4	.37373	6.8	.08959	12.4	.01959	21.2	.00140
2.5	.36090	6.9	.08695	12.6	.01863	21.4	.00130
2.6	.34844	7.0	.08440	12.8	.01771	21.6	.00121
2.7	.33635	7.1	.08192	13.0	.01684	21.8	.00112
2.8	.32465	7.2	.07952	13.2	.01601	22.0	.00104
2.9	.31338	7.3	.07720	13.4	.01522	22.2	.00097
3.0	.30250	7.4	.07496	13.6	.01446	22.4	.00090
3.1	.29204	7.5	.07278	13.8	.01373	22.6	.00083
3.2	.28197	7.6	.07068	14.0	.01304	22.8	.00077
3.3	.27230	7.7	.06864	14.2	.01239	23.0	.00071
3.4	.26301	7.8	.06666	14.4	.01175	23.2	.00066
3.5	.25410	7.9	.06475	14.6	.01115	23.4	.00061
3.6	.24553	8.0	.06291	14.8	.01057	23.6	.00056
3.7	.23732	8.1	.06112	15.0	.01001	23.8	.00052
3.8	.22943	8.2	.05938	15.2	.00949	24.0	.00048
3.9	.22185	8.3	.05771	15.4	.00899	24.2	.00044
4.0	.21457	8.4	.05608	15.6	.00849	24.4	.00041
4.1	.20758	8.5	.05451	15.8	.00803	24.6	.00038
4.2	.20086	8.6	.05299	16.0	.00758	24.8	.00035
4.3	0.19440	8.7	0.05152	16.2	0.00715	25.0	0.00032

In an analogous manner it is found that, under the same assumptions, formulae I and III of paper I become

$$\kappa = 9.266\,\frac{k^2+0.055118}{k}\left|\int_0^\infty W_1(r)\,\chi_1(r)\,dr\right|^2\times 10^{-19}\ \text{cm}^2 \qquad (\text{I}_1)$$

and

$$\kappa = 1.4825 \frac{1}{k\,(k^2+0.055118)^3}\left|\int_0^\infty W_3(r)\,\chi_1(r)\,dr\right|^2 \times 10^{-17}\ \text{cm}^2\ , \qquad (\text{III}_1)$$

where

$$\left.\begin{aligned} W_1(r) &= e^{-0.707735r}(0.7810175r + 1.0260897r^2 - 0.107743r^3 \\ &+ 0.0748147r^4 - 0.00432587r^5 + 0.000771209r^6 - 0.0000547250r^7 \\ &+ 0.00000616943r^8) - e^{-2.415407r}(0.7810175r + 1.333771r^2 \\ &\qquad + 1.138864r^3 + 0.3241463r^4) \end{aligned}\right\} \qquad (19)$$

and

$$\left.\begin{aligned} W_3(r) &= e^{-0.707735r}(0.3796213r^{-2} + 1.0311631r^{-1} - 0.1091749 \\ &- 0.00361463r + 0.00176560r^2 + 0.000847872r^3 - 0.0000857360r^4 \\ &+ 0.00001105546r^5 - 0.000001669208r^6 - 0.07846795r^4 \\ &\times Ei[1.707735r]) - e^{-2.415470r}(0.3796213r^{-2} + 0.1944878r^{-1} \\ &\qquad + 0.0553556 - 0.03151090r + 0.02690613r^2 - 0.04594855r^3)\,. \end{aligned}\right\} \qquad (20)$$

A brief table of the function $W_1(r)$ has been given in an earlier paper.[5] We now provide a similar tabulation of the function $W_3(r)$ (see Table 2). In Figure 1 we have further illus-

TABLE 2

THE WEIGHT FUNCTION $W_3(r)$

r	$W_3(r)$	r	$W_3(r)$	r	$W_3(r)$	r	$W_3(r)$
0.....	∞	0.6.....	1.408	1.4.....	0.293	3.5.....	0.021
0.1.....	13.49	0.7.....	1.100	1.6.....	.215	4.0.....	.013
.2.....	6.13	0.8.....	0.879	1.8.....	.160	4.5.....	.009
.3.....	3.721	0.9.....	0.713	2.0.....	.121	5.0.....	.006
.4.....	2.526	1.0.....	0.586	2.5.....	.064	5.5.....	0.004
0.5.....	1.853	1.2.....	0.408	3.0.....	0.036		

trated the dependence of the functions W_1, W_2, and W_3 on r. It is seen that the three weight functions are of entirely different orders of magnitude at large distances; it is in terms of these differences that the remarks made in paper I, §§ 2 and 5, have to be understood.

3. *The continuous absorption coefficient of* H^- *evaluated according to formula* (II_1).—The evaluation of the absorption cross-sections according to formula (II_1) requires a knowledge of the p-spherical waves $\chi_1(r)$ of an electron in the Hartree field of a hydrogen atom. The writer has at his disposal a large number of tables of these functions for various values of k^2 in the range $1.75 \geq k^2 > 0$.[6] Using these tables and the table of the weight function $W_2(r)$, we have evaluated the absorption cross-sections according to formula (II_1) by straightforward numerical quadratures. The results of these integrations are given in Table 3.

[5] S. Chandrasekhar, *Ap. J.*, **100**, 176, 1944 (Table 1).

[6] These tables were computed by Mrs. Frances H. Breen and the writer. It is hoped to publish these (and similar tables of the s-waves, which have also been completed) in the near future.

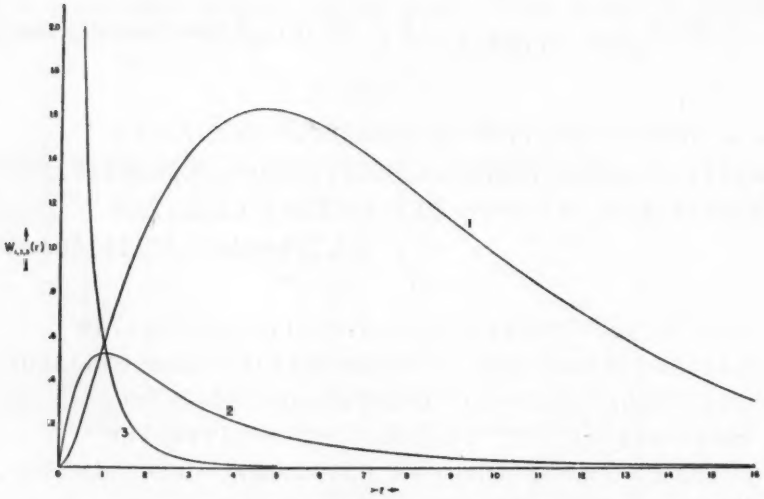

FIG. 1.—A comparison of the weight functions $W_1(r)$ (curve 1), $W_2(r)$ (curve 2), and $W_3(r)$ (curve 3), which occur in the formulae (I_1, II_1, and III_1) for the absorption cross-sections of H^- in terms of the matrix elements of the dipole moment, momentum, and acceleration, respectively.

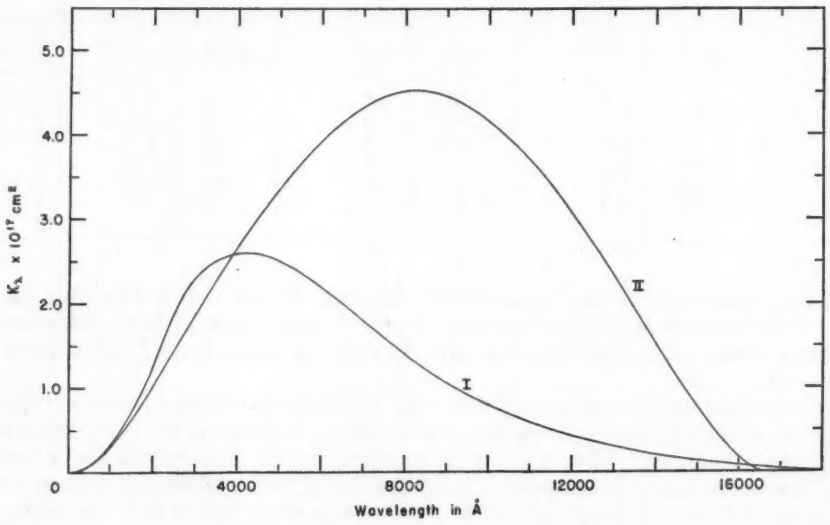

FIG. 2.—A comparison of the continuous absorption coefficient of H^- as determined by Massey and Bates (curve *I*) with the determination of the present paper (curve *II*).

It is seen that our present values differ from those obtained earlier on the plane-wave representation of the ejected electron by about 5 per cent in the entire spectral range of astrophysical interest. The maximum is, however, not appreciably shifted and is at the same place (λ 8500 A); here the atomic absorption coefficient has the value 4.52×10^{-17} cm.^{2} In view of the many determinations of the continuous absorption coefficient of H^- that have been made, it is perhaps of interest to compare the first of these determinations by Massey and Bates with that of the present paper. This is done in Figure 2.

TABLE 3

THE CONTINUOUS ABSORPTION COEFFICIENT OF H^- COMPUTED ACCORDING TO FORMULA (II_1)

k^2	λ(A)	$\kappa_\lambda \times 10^{17}$ Cm^2	k^2	λ(A)	$\kappa_\lambda \times 10^{17}$ Cm^2	k^2	λ(A)	$\kappa_\lambda \times 10^{17}$ Cm^2
1.75	505	0.0657	0.175	3960	2.62	0.055	8275	4.52
0.80	1066	0.333	.150	4443	2.97	.050	8669	4.50
0.50	1642	0.740	.125	5059	3.39	.045	9102	4.44
0.35	2249	1.231	.100	5875	3.87	.035	10,111	4.13
0.25	2987	1.84	.090	6280	4.06	.020	12,131	2.96
0.20	3572	2.32	0.070	7283	4.41	0.010	13,994	1.50

It is again a pleasure to record my indebtedness to Mrs. Frances H. Breen for valuable assistance with the numerical work.

THE RADIATIVE EQUILIBRIUM OF AN EXPANDING PLANETARY NEBULA

I. RADIATION PRESSURE IN LYMAN-α

S. CHANDRASEKHAR
Yerkes Observatory
Received September 16, 1945

ABSTRACT

In this paper the problem of the radiative equilibrium in Lyman-α of a differentially expanding planetary nebula is formulated *de novo*. Particular attention has been given to the formulation of the boundary conditions. It is shown that the transfer problem reduces to a novel boundary-value problem in hyperbolic partial differential equations. Explicit solutions have been found for the case in which the line absorption coefficient $\sigma(\nu)$ has a rectangular form. On the basis of the solutions obtained, the question of the radiation pressure in Lyman-α has been re-examined. It is shown that when the Doppler shift due to the difference in velocities between the inner and the outer boundaries of the nebula exceeds the line width $2\Delta\nu$ of $\sigma(\nu)$ by a factor $2\sqrt{3}$, the nebula can be divided into three parts: an inner, a central, and an outer part. In the central part the radiation pressure in Lyman-α is of the same order as that in the continuum, while in the inner and the outer parts it is not inappreciable. The bearing of this manner in which the radiation pressure in Lyman-α operates in an expanding atmosphere on the dynamics of a planetary nebula and also on other astrophysical problems is briefly indicated.

1. *Introduction.*—As is well known on Zanstra's theory[1] of nebular luminosity, the hydrogen emission in a planetary nebula is traced to the conversion in the nebula of the incident ultraviolet radiation of the central star beyond the head of the Lyman series into radiation principally in the Lyman and the Balmer series. More specifically, if the optical thickness of the nebula for the ultraviolet radiation[2] is sufficiently large, this conversion will be so nearly complete that for every ultraviolet quantum in the incident starlight, the nebula will emit a quantum in the first member of the Lyman series, namely, Lyman-α. This conversion of the radiation arises from the fact that, whenever an ultraviolet quantum is scattered, there is only a probability p of order $\frac{1}{2}$ that it will be re-emitted as such.[3] And on the occasions when the ultraviolet quantum is not re-emitted, a chain of absorptions and emissions takes place which so rapidly leads to the emission of a Lyman-α quantum that we may almost say that every time an ultraviolet quantum is scattered, there is a definite probability $(1-p) \sim \frac{1}{2}$ that a Lyman-α quantum is emitted.[4] The theory of radiative transfer of the ultraviolet radiation through the nebula has been developed along these lines by Ambarzumian and others[5] and shows that the conversion of the ultraviolet radiation into line radiation is so far advanced through most of the nebula that, if nothing else intervened, the nebula would be subject to enormous radiation pressure because the absorption coefficient in Lyman-α is several thousand times larger than in the continuum. The magnitude of the radiation pressure which may thus act on the nebula is so large that it will seriously endanger its permanence even over relatively limited periods of time. The consequences of this radiation pressure in Lyman-α

[1] *Ap. J.*, **65**, 50, 1927; *Pub. Dom. Ap. Obs.*, **4**, 209, 1931.

[2] In this paper we shall use the term "ultraviolet radiation" to denote all radiation beyond the head of the Lyman series.

[3] G. Cillié, *M.N.*, **92**, 820, 1932; **96**, 777, 1936.

[4] Cf. V. A. Ambarzumian, *M.N.*, **93**, 50, 1932; also *Bull. de l'Obs. centr. à Poulkovo*, **13**, No. 14, 3, 1933.

[5] *Ibid.* More accurate solutions of the transfer problem have been given by S. Chandrasekhar, *Zs. f. Ap.*, **9**, 266, 1935; *Ap. J.*, **100**, 76, 1944; and C. U. Cesco, S. Chandrasekhar, and J. Sahade, *Ap. J.*, **101**, 320, 1945.

acting on the nebula are, indeed, such as to lead one to re-examine whether some factor has not been overlooked, which, when properly allowed for, will cut down the radiation pressure. In this connection, Zanstra[6] has suggested that the very likely presence of differential motions in the nebula may very effectively reduce the radiation pressure which may act on the nebula. Unfortunately, Zanstra's particular considerations relating to this problem are vitiated by the use of an equation of transfer which, to put it bluntly, is incorrect under the circumstances envisaged. However, it appears that the methods which have been recently developed to treat an analogous problem in theory of the formation of absorption lines in a moving atmosphere[7] are sufficiently general to enable one to solve the problem of radiative transfer in an expanding nebula. In this paper we therefore propose to study the problem of an expanding planetary nebula, particularly with a view to estimating the selective radiation pressure in Lyman-α. In later papers it is our intention to extend the methods of this investigation to the consideration of a variety of related questions.

2. *The equation of transfer for Lyman-α radiation and its approximate forms.*—As was first pointed out by E. A. Milne,[8] in studying the transfer of radiation in a planetary nebula we can ignore the curvature of the layers except when formulating the boundary conditions. We shall accordingly consider the atmosphere as stratified in parallel planes in which all properties are assumed to be constant over the planes z = constant. Let $\rho(z)$ denote the density of the scattering material (neutral hydrogen atoms in our present context) at height z, and $w(z)$ the velocity of the material at the same height assumed parallel to the z-direction. Further, let $\sigma(\nu)$ denote the mass-scattering coefficient in Lyman-α for the frequency ν as judged by an observer at rest with respect to the material. We shall suppose that $\sigma(\nu)$ differs appreciably from zero only in a small range of ν. However, it is in the essence of the problem that the half-width of $\sigma(\nu)$ is of the same order as the Doppler shifts in frequency caused by the differential motions in the nebula. This last circumstance makes the change of frequency on scattering the only optical effect of the motion $w(z)$ which has any importance and allows us to ignore all such effects as aberration, etc.

In writing down the equation of transfer for the problem of an expanding nebula, it is especially important that we be careful in referring all the frequencies to some chosen fixed observer. As will become apparent when we come to formulating our boundary conditions (§3), it is most convenient to choose our fixed observer as at rest with respect to the central star. Let $I(\nu, z, \vartheta)$ then denote the specific intensity of the radiation at height z inclined at angle ϑ to the positive normal and in the frequency ν as judged by our fixed observer. This radiation will appear to an observer at rest with respect to the material at z as having a frequency

$$\nu\left(1-\frac{w}{c}\cos\vartheta\right). \tag{1}$$

It will accordingly be scattered as such in all directions with a scattering coefficient of

$$\sigma\left(\nu\left[1-\frac{w}{c}\cos\vartheta\right]\right). \tag{2}$$

The equation of transfer will accordingly take the form

$$\cos\vartheta\,\frac{\partial I(\nu, z, \vartheta)}{\rho\,\partial z} = -\sigma\left(\nu\left[1-\frac{w}{c}\cos\vartheta\right]\right) I(\nu, z, \vartheta) + j(\nu, z, \vartheta), \tag{3}$$

[6] *M.N.* **95**, 16, 1934.

[7] S. Chandrasekhar, *Rev. Mod. Phys.*, **17**, 138, 1945. This paper will be referred to as "Moving Atmospheres."

[8] *Zs. f. Ap.*, **1**, 98, 1930.

where $j(\nu, z, \vartheta)$ denotes the emission per unit time and per unit solid angle in the frequency ν and in the direction ϑ. This emission will consist of two parts: that derived from the scattering of the radiation of appropriate frequencies from other directions into the direction considered and that derived from the conversion of the ultraviolet radiation at z into Lyman-α. The former is given by (cf. "Moving Atmospheres," eq. [5])

$$\tfrac{1}{2}\sigma\left(\nu\left[1-\frac{w}{c}\cos\vartheta\right]\right)\int_0^\pi I\left(\nu\left[1-\frac{w}{c}\cos\vartheta+\frac{w}{c}\cos\chi\right], z, \chi\right)\sin\chi d\chi\,. \quad (4)$$

As for the latter, it will depend, among other things, on the probability $(1-p)$ with which an ultraviolet quantum is converted into a Lyman-α quantum on scattering and on the source function characteristic of the ultraviolet radiation. Thus, if πS_c denotes the flux of ultraviolet radiation incident per unit area of the inner boundary of the planetary nebula, the source function for the ultraviolet radiation is (cf. the references in n. 5),

$$p\left\{\frac{1}{2}\int_0^\pi I_c\sin\vartheta d\vartheta+\tfrac{1}{4}S_c e^{-(\tau_1-\tau)}\right\}, \quad (5)$$

where I_c denotes the intensity of the diffuse ultraviolet light, τ the optical depth for the ultraviolet radiation measured from the outer boundary inward, and τ_1 the total optical thickness of the nebula (also in ultraviolet light). To find the emission in Lyman-α at frequency ν, consider the number of ultraviolet quanta absorbed in a slab of material of unit cross-section and height dz at z. This is clearly given by

$$\frac{1}{h\nu_c}\{J_c(\tau)+\tfrac{1}{4}S_c e^{-(\tau_1-\tau)}\}\kappa_c\rho dz\,, \quad (6)$$

where κ_c denotes the absorption coefficient in the continuum, ν_c a suitably averaged frequency to represent the ultraviolet radiation, and

$$J_c=\frac{1}{2}\int_0^\pi I_c\sin\vartheta d\vartheta\,. \quad (7)$$

Since a Lyman-α quantum is emitted with a probability $(1-p)$ every time an ultraviolet quantum is scattered, the total energy emitted per unit time in Lyman-α (i.e., integrated over all the frequencies in the line) by the slab of material considered is

$$(1-p)\frac{\nu_0}{\nu_c}\{J_c(\tau)+\tfrac{1}{4}S_c e^{-(\tau_1-\tau)}\}\kappa_c\rho dz\,, \quad (8)$$

where ν_0 denotes the frequency of Lyman-α. The fraction of the energy (8) which will appear in the frequency ν, as judged by the fixed observer, is

$$\frac{\sigma\left(\nu\left[1-\frac{w}{c}\cos\vartheta\right]\right)}{\int_0^\infty\sigma(\nu)\,d\nu}. \quad (9)$$

Hence the contribution to the emission $j(\nu, z, \vartheta)$ by the conversion of the ultraviolet radiation is

$$(1-p)\frac{\nu_0}{\nu_c}\frac{\kappa_c}{2\sigma_0\Delta\nu}\{J_c(\tau)+\tfrac{1}{4}S_c e^{-(\tau_1-\tau)}\}\sigma\left(\nu\left[1-\frac{w}{c}\cos\vartheta\right]\right), \quad (10)$$

where we have written

$$2\sigma_0\Delta\nu=\int_0^\infty\sigma(\nu)\,d\nu\,. \quad (11)$$

The equation of transfer for the radiation of frequency ν (as judged by the fixed observer) can accordingly be written in the form

$$\left.\begin{aligned}\mu\frac{\partial I(\nu,\mu,z)}{\rho\partial z} &= -\sigma\left(\nu\left[1-\frac{w}{c}\mu\right]\right)\Big\{I(\nu,\mu,z)\\ &\quad -\frac{1}{2}\int_{-1}^{+1} I\left(\nu\left[1-\frac{w}{c}\mu+\frac{w}{c}\mu'\right],z,\mu'\right)d\mu'-\tfrac{1}{2}E(z)\Big\},\end{aligned}\right\} \tag{12}$$

where, for the sake of brevity, we have written

$$E(z) = (1-p)\frac{\nu_0}{\nu_c}\frac{\kappa_c}{\sigma_0\Delta\nu}\{J_c(\tau)+\tfrac{1}{4}S_c e^{-(\tau_1-\tau)}\}\,. \tag{13}$$

Further, in equation (12) we have written μ and μ' for $\cos\vartheta$ and $\cos\chi$, respectively.

In solving the equation of transfer (12), we shall adopt the method of approximation which has recently been developed in connection with the various problems of radiative transfer in the theory of stellar atmospheres.[9] In this method we replace the integrals which appear in the equation of transfer by sums according to Gauss's formula for numerical quadratures and replace the integrodifferential equation by a system of linear equations. Thus, considering equation (12), we replace it in the nth approximation by the system of $2n$ equations,

$$\left.\begin{aligned}\mu_i\frac{\partial I_i(\nu,z)}{\rho\partial z} &= -\sigma\left(\nu\left[1-\frac{w}{c}\mu_i\right]\right)\Big\{I_i(\nu,z)\\ &\quad -\tfrac{1}{2}\Sigma a_j I_j\left(\nu\left[1-\frac{w}{c}\mu_i+\frac{w}{c}\mu_j\right],z\right)-\tfrac{1}{2}E(z)\Big\} \qquad (i=\pm1,\ldots,\pm n),\end{aligned}\right\} \tag{14}$$

where the μ_i's ($i=\pm1,\ldots,\pm n$) are the zeros of the Legendre polynomial $P_{2n}(\mu)$ and the a_i's are the appropriate Gaussian weights. Further, in equation (14) we have written $I_i(\nu,z)$ for $I(\nu,z,\mu_i)$.

At this stage one further simplification of equation (14) is possible. In evaluating the Doppler shifts we need not distinguish between

$$\nu\left(1-\frac{w}{c}\mu\right) \quad \text{and} \quad \nu-\nu_0\frac{w}{c}\mu\,, \tag{15}$$

where ν_0 denotes the frequency of the center of the line. We may therefore replace equation (14) by the simpler one,

$$\left.\begin{aligned}\mu_i\frac{\partial I_i(\nu,z)}{\rho\partial z} &= -\sigma\left(\nu-\nu_0\frac{w}{c}\mu_i\right)\Big\{I_i(\nu,z)\\ &\quad -\tfrac{1}{2}\Sigma a_j I_j\left(\nu-\nu_0\frac{w}{c}\mu_i+\nu_0\frac{w}{c}\mu_j,z\right)-\tfrac{1}{2}E(z)\Big\} \qquad (i=\pm1,\ldots,\pm n).\end{aligned}\right\} \tag{16}$$

As in "Moving Atmospheres," instead of considering the intensities I_i ($i=\pm1,\ldots,\pm n$) for some fixed frequency ν, we shall consider them for the frequencies

$$\nu_i=\nu+\nu_0\frac{w}{c}\mu_i \qquad (i=\pm1,\ldots,\pm n)\,. \tag{17}$$

which are functions of z. If we now let

$$I_i(\nu_i,z)=\psi_i(\nu,z) \qquad (i=\pm1,\ldots,\pm n)\,, \tag{18}$$

[9] S. Chandrasekhar, *Ap. J.*, **100**, 76, 117, 1944; **101**, 95, 328, 348, 1945 (see particularly the first of these papers).

the differential equations for the ψ_i's become (cf. "Moving Atmospheres," eq. [16])

$$\mu_i \frac{\partial \psi_i}{\partial z} - \mu_i^2 \frac{\nu_0}{c} \frac{dw}{dz} \frac{\partial \psi_i}{\partial \nu} = -\rho\sigma(\nu)\ (\psi_i - \tfrac{1}{2}\Sigma a_j \psi_j - \tfrac{1}{2}E)\,. \tag{19}$$

In our subsequent work we shall restrict ourselves to the first approximation. In this approximation

$$\mu_1 = -\mu_{-1} = \frac{1}{\sqrt{3}} \qquad \text{and} \qquad a_1 = a_{-1} = 1\,, \tag{20}$$

and equations (16) and (19) become

$$\mu_1 \frac{\partial I_{+1}(\nu, z)}{\rho \partial z} = -\tfrac{1}{2}\sigma\left(\nu - \nu_0 \frac{w}{c}\mu_1\right)\left[I_{+1}(\nu, z) - I_{-1}\left(\nu - 2\nu_0 \frac{w}{c}\mu_1, z\right) - E(z) \right], \tag{21}$$

$$\mu_1 \frac{\partial I_{-1}(\nu, z)}{\rho \partial z} = +\tfrac{1}{2}\sigma\left(\nu + \nu_0 \frac{w}{c}\mu_1\right)\left[I_{-1}(\nu, z) - I_{+1}\left(\nu + 2\nu_0 \frac{w}{c}\mu_1, z\right) - E(z) \right], \tag{22}$$

and

$$\mu_1 \frac{\partial \psi_{+1}}{\partial z} - \mu_1^2 \frac{\nu_0}{c} \frac{dw}{dz} \frac{\partial \psi_{+1}}{\partial \nu} = -\tfrac{1}{2}\rho\sigma(\nu)\ (\psi_{+1} - \psi_{-1} - E)\,, \tag{23}$$

$$\mu_1 \frac{\partial \psi_{-1}}{\partial z} + \mu_1^2 \frac{\nu_0}{c} \frac{dw}{dz} \frac{\partial \psi_{-1}}{\partial \nu} = +\tfrac{1}{2}\rho\sigma(\nu)\ (\psi_{-1} - \psi_{+1} - E)\,, \tag{24}$$

where it may be recalled that

$$\psi_{+1}(\nu, z) = I_{+1}\left(\nu + \mu_1 \nu_0 \frac{w}{c}, z\right) \qquad \text{and} \qquad \psi_{-1}(\nu, z) = I_{-1}\left(\nu - \mu_1 \nu_0 \frac{w}{c}, z\right). \tag{25}$$

3. *The reduction to a boundary-value problem for the case $\sigma(\nu)$ = constant for $\nu_0 - \Delta\nu \leqslant \nu \leqslant \nu_0 + \Delta\nu$ and zero outside this interval and for a linear increase of* w *with the optical depth.*—In this paper we shall consider the problem of the expanding nebula for the case

$$\left.\begin{aligned} \sigma(\nu) &= \sigma_0 = \text{constant for } \nu_0 - \Delta\nu \leqslant \nu \leqslant \nu_0 + \Delta\nu \\ &= 0 \quad \text{otherwise}\,, \end{aligned}\right\} \tag{26}$$

and

$$\frac{1}{\rho}\frac{dw}{dz} = \text{constant}\,. \tag{27}$$

Further, we shall restrict ourselves to the first approximation.

When $\sigma(\nu)$ has the form (26), some care is required in the formulation of the boundary conditions; for, according to equations (21) and (22),

$$\frac{\partial I_{+1}}{\partial z} \neq 0 \qquad \text{only if} \qquad \nu_0 - \Delta\nu + \mu_1\nu_0 \frac{w}{c} \leqslant \nu \leqslant \nu_0 + \Delta\nu + \mu_1\nu_0 \frac{w}{c}\,, \tag{28}$$

and

$$\frac{\partial I_{-1}}{\partial z} \neq 0 \qquad \text{only if} \qquad \nu_0 - \Delta\nu - \mu_1\nu_0 \frac{w}{c} \leqslant \nu \leqslant \nu_0 + \Delta\nu - \mu_1\nu_0 \frac{w}{c}\,. \tag{29}$$

Accordingly, in the (ν, w)-plane the lines

$$\nu = \nu_0 - \Delta\nu + \mu_1\nu_0 \frac{w}{c} \qquad \text{and} \qquad \nu = \nu_0 + \Delta\nu + \mu_1\nu_0 \frac{w}{c} \tag{30}$$

delimit the regions in which I_{+1} is different from a constant from the regions in which it is a constant for varying z. The situation is further clarified in Figure 1, where AD and BC represent the lines (30). Similarly, the lines (AF and BE in Fig. 1)

$$\nu = \nu_0 - \Delta\nu - \mu_1 \nu_0 \frac{w}{c} \qquad \text{and} \qquad \nu = \nu_0 + \Delta\nu - \mu_1 \nu_0 \frac{w}{c} \tag{31}$$

delimit the regions in which I_{-1} is different from a constant from the regions in which it is a constant for varying z.

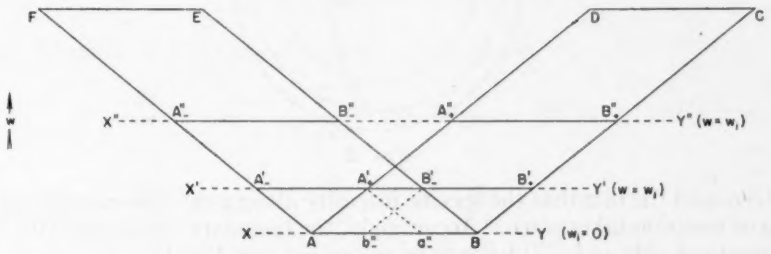

FIG. 1

In formulating the boundary conditions we must allow for the possibility that the inner boundary of the nebula may itself have a motion relative to our fixed observer, who, it will be remembered, is assumed to be at rest only with respect to the central star. Let w_i then denote the velocity of the nebula at its inner boundary. From Figure 1 it is apparent that we will have to distinguish three cases:

$$\left.\begin{aligned} &\text{case I:} \quad w_i = 0\,, \\ &\text{case II:} \quad \nu_0 - \Delta\nu + \mu_1 \nu_0 \frac{w_i}{c} < \nu_0\,, \\ &\text{case III:} \quad \nu_0 - \Delta\nu + \mu_1 \nu_0 \frac{w_i}{c} \gtrless \nu_0\,. \end{aligned}\right\} \tag{32}$$

These cases are, however, more conveniently distinguished in terms of the Doppler shift, $2D\nu^{(i)}$, due to the velocity w_i:

$$2D\nu^{(i)} = \nu_0 \frac{w_i}{c}\,. \tag{33}$$

We have

$$\left.\begin{aligned} &\text{case I:} \quad D\nu^{(i)} = 0\,, \\ &\text{case II:} \quad 0 < D\nu^{(i)} < \frac{\Delta\nu}{2\mu_1} = \frac{\sqrt{3}}{2}\Delta\nu\,, \\ &\text{case III:} \quad D\nu^{(i)} \gtrless \frac{\Delta\nu}{2\mu_1} = \frac{\sqrt{3}}{2}\Delta\nu\,. \end{aligned}\right\} \tag{34}$$

These three cases correspond to situations in which the inner boundary of the nebula is at XY, $X'Y'$, or $X''Y''$, respectively, as shown in Figure 1.

Now the physical boundary conditions which have to be translated into mathematical terms are, first, that there is no radiation incident on the nebula from the outside and, second, that

$$I^*(\nu, \vartheta) = I^*(\nu, \pi - \vartheta) \tag{35}$$

whenever $I^*(\nu, \vartheta)$ refers to the intensity of a ray which, as judged by the fixed observer at the central star, has not suffered any change by absorptions or emissions by the intervening medium (see Fig. 2). This latter boundary condition arises from the geometry of

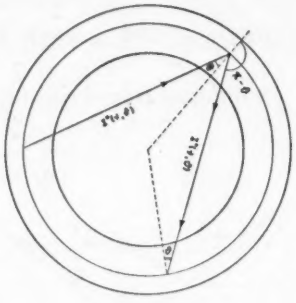

FIG. 2

the problem and the fact that the specific intensity along a ray does not change if no absorption or emission takes place.[10] Accordingly, the boundary conditions with respect to which equations (21) and (22) have to be solved are (see Fig. 1):

$$\text{case I} \quad \left\{ \begin{aligned} I_{-1}(\nu) &= 0 \ \text{along} \quad BE \quad \text{and} \quad EF\,, \\ I_{+1}(\nu) &= 0 \ \text{along} \quad BC\,, \\ I_{+1}(\nu) &= I_{-1}(\nu) \ \text{along} \quad AB\,; \end{aligned} \right\} \tag{36}$$

$$\text{case II} \quad \left\{ \begin{aligned} I_{-1}(\nu) &= 0 \ \text{along} \quad B'_{-}E \quad \text{and} \quad EF \\ I_{+1}(\nu) &= 0 \ \text{along} \quad B'_{-}B'_{+} \quad \text{and} \quad B'_{+_1}C\,, \\ I_{+1}(\nu) &= I_{-1}(\nu) \ \text{along} \quad A'_{+}B'_{-}\,; \end{aligned} \right\} \tag{37}$$

and

$$\text{case III} \quad \left\{ \begin{aligned} I_{-1}(\nu) &= 0 \ \text{along} \quad B''_{-}E \quad \text{and} \quad EF\,, \\ I_{+1}(\nu) &= 0 \ \text{along} \quad A''_{+}B''_{+} \quad \text{and} \quad B''_{+}C\,. \end{aligned} \right\} \tag{38}$$

When expressed for the intensities ψ_{+1} and ψ_{-1}, the foregoing boundary conditions become

$$\left. \begin{aligned} \psi_{-1}(\nu, z_1) &= 0 \quad \text{for} \quad \nu_0 - \Delta\nu \leqslant \nu \leqslant \nu_0 + \Delta\nu\,, \\ \psi_{-1}(\nu_0 + \Delta\nu, z) &= 0 \quad \text{for} \quad 0 \leqslant z \leqslant z_1\,. \\ \psi_{+1}(\nu_0 + \Delta\nu, z) &= 0 \quad \text{for} \quad 0 \leqslant z \leqslant z_1\,. \end{aligned} \right\} \tag{39}$$

for all three cases, while

$$\psi_{-1}(\nu, 0) = \psi_{+1}(\nu, 0) \quad \text{in case I}\,. \tag{40}$$

$$\left. \begin{aligned} &\psi_{+1}(\nu, 0) = 0 \quad \text{for} \quad \nu_0 + \Delta\nu - 4D\nu^{(i)}\mu_1 \leqslant \nu \leqslant \nu_0 + \Delta\nu\,, \\ &\psi_{+1}(\nu, 0) = \psi_{-1}(\nu + 4D\nu^{(i)}\mu_1, 0) \quad \text{for} \quad \nu_0 - \Delta\nu \leqslant \nu < \nu_0 + \Delta\nu - 4D\nu^{(i)}\mu_1 \end{aligned} \right\} \text{in case II}\,. \tag{41}$$

and

$$\psi_{+1}(\nu, 0) = 0 \quad \text{for} \quad \nu_0 - \Delta\nu \leqslant \nu \leqslant \nu_0 + \Delta\nu \quad \text{in case III}\,. \tag{42}$$

In the forgoing equations, $z = 0$ refers to the inner boundary of the nebula, while $z = z_1$ refers to the outer boundary.

[10] Cf. Milne, *op. cit.* (n. 8.)

We shall now transform equations (23) and (24) to forms more convenient for their solution.

Let t denote the optical depth of the atmosphere measured from the outer boundary inward in terms of σ_0. Then

$$dt = -\rho\sigma_0 dz\,. \tag{43}$$

It is, however, more convenient to use the variable

$$x = \frac{1}{2\mu_1}t = \frac{\sqrt{3}}{2}t \tag{44}$$

instead of t. In terms of x, equations (23) and 24) become

$$\frac{\partial\psi_{+1}}{\partial x} - \mu_1\frac{\nu_0}{c}\frac{dw}{dx}\frac{\partial\psi_{+1}}{d\nu} = \psi_{+1} - \psi_{-1} - E(x)\,, \tag{45}$$

and

$$\frac{\partial\psi_{-1}}{\partial x} + \mu_1\frac{\nu_0}{c}\frac{dw}{dx}\frac{\partial\psi_{-1}}{\partial\nu} = \psi_{+1} - \psi_{-1} + E(x)\,. \tag{46}$$

Now the assumption (27) concerning the variation of w clearly implies that the velocity is a linear function of x. Accordingly, we may write

$$w = w_1 - (w_1 - w_i)\frac{x}{x_1}\,, \tag{47}$$

where w_1 and w_i denote the velocities at the outer ($x = 0$) and the inner ($x = x_1$) boundaries of the planetary nebula, respectively. As in "Moving Atmospheres," we shall express the difference in velocities between the inner and the outer boundaries of the nebula in terms of a *Doppler width*, $D\nu$, according to

$$2\,D\nu = \frac{\nu_0}{c}(w_1 - w_i)\,. \tag{48}$$

With these definitions,

$$\mu_1\frac{\nu_0}{c}\frac{dw}{dx} = -2\mu_1\frac{D\nu}{x_1} = -\frac{4}{3}\frac{D\nu}{t_1}\,. \tag{49}$$

Equations (45) and (46) become

$$\frac{\partial\psi_{+1}}{\partial x} + 2\mu_1\frac{D\nu}{x_1}\frac{\partial\psi_{+1}}{\partial\nu} = \psi_{+1} - \psi_{-1} - E(x) \tag{50}$$

and

$$\frac{\partial\psi_{-1}}{\partial x} - 2\mu_1\frac{D\nu}{x_1}\frac{\partial\psi_{-1}}{\partial\nu} = \psi_{+1} - \psi_{-1} + E(x)\,. \tag{51}$$

We now introduce the variable y, defined by

$$(\nu_0 + \Delta\nu) - \nu = 2\mu_1\frac{D\nu}{x_1}\,y\,; \tag{52}$$

y therefore measures the frequency shifts from the violet edge of $\sigma(\nu)$ (as they enter the intensities ψ_{+1} and ψ_{-1}) in units of

$$2\mu_1\frac{D\nu}{x_1}\,. \tag{53}$$

Equations (50) and (51) simplify to the forms

$$\frac{\partial \psi_{+1}}{\partial x} - \frac{\partial \psi_{+1}}{\partial y} = \psi_{+1} - \psi_{-1} - E(x) \tag{54}$$

and

$$\frac{\partial \psi_{-1}}{\partial x} + \frac{\partial \psi_{-1}}{\partial y} = \psi_{+1} - \psi_{-1} + E(x)\,. \tag{55}$$

The range of the variables x and y in which the solution has to be sought is (cf. eq. [52])

$$0 \leqslant x \leqslant x_1 \quad \text{and} \quad 0 \leqslant y \leqslant y_1 = \frac{1}{\mu_1}\frac{\Delta\nu}{D\nu}\, x_1\,; \tag{56}$$

and the boundary conditions with respect to which equations (54) and (55) have to be solved are (see Fig. 3):

$$\left.\begin{aligned} \psi_{-1} = 0 \quad &\text{on} \quad CD: \quad x = 0 \quad \text{and} \quad 0 \leqslant y \leqslant y_1\,, \\ = 0 \quad &\text{on} \quad CB: \quad y = 0 \quad \text{and} \quad 0 \leqslant x \leqslant x_1\,, \\ \psi_{+1} = 0 \quad &\text{on} \quad CB: \quad y = 0 \quad \text{and} \quad 0 \leqslant x \leqslant x_1 \end{aligned}\right\} \text{in all three cases}\,; \tag{57}$$

and on BA

$$\psi_{+1} = \psi_{-1} \quad \text{for} \quad x = x_1 \quad \text{and} \quad 0 \leqslant y \leqslant y_1 \quad \text{(case I)}\,. \tag{58}$$

$$\left.\begin{aligned} \psi_{+1}(y, x_1) &= 0 \quad \text{for} \quad 0 \leqslant y \leqslant y^* = 2\,\frac{D\nu^{(i)}}{D\nu}\, x_1\,, \\ \psi_{+1}(y, x_1) &= \psi_{-1}(y - y^*, x_1) \quad \text{for} \quad y^* < y \leqslant y_1 \end{aligned}\right\} \text{(case II)}\,. \tag{59}$$

and

$$\psi_{+1} = 0 \quad \text{for} \quad x = x_1 \quad \text{and} \quad 0 \leqslant y \leqslant y_1 \quad \text{(case III)}\,. \tag{60}$$

It is convenient to introduce one further transformation of the variable. Let

$$\psi_{+1} = e^{-\nu} F \quad \text{and} \quad \psi_{-1} = e^{-\nu} G\,. \tag{61}$$

Equations (54) and (55) become

$$\frac{\partial F}{\partial x} - \frac{\partial F}{\partial y} = -G - e^{\nu} E(x) \tag{62}$$

and

$$\frac{\partial G}{\partial x} + \frac{\partial G}{\partial y} = +F + e^{\nu} E(x)\,. \tag{63}$$

The corresponding boundary conditions follow from equations (57)-(60). Thus,

$$\left.\begin{aligned} G = 0 \quad &\text{on} \quad CD: \quad x = 0 \quad \text{and} \quad 0 \leqslant y \leqslant y_1 \\ = 0 \quad &\text{on} \quad CB: \quad y = 0 \quad \text{and} \quad 0 \leqslant x \leqslant x_1\,, \\ F = 0 \quad &\text{on} \quad CB: \quad y = 0 \quad \text{and} \quad 0 \leqslant x \leqslant x_1 \end{aligned}\right\} \text{in all three cases}\,; \tag{64}$$

and on BA

$$F = G \quad \text{for} \quad x = x_1 \quad \text{and} \quad 0 \leqslant y \leqslant y_1 \quad \text{(case I)}\,. \tag{65}$$

$$\left.\begin{aligned} F(y, x_1) &= 0 \quad \text{for} \quad 0 \leqslant y \leqslant y^*\,. \\ F(y, x_1) &= e^{+\nu^*} G(y - y^*, x_1) \quad \text{for} \quad y^* < y \leqslant y_1 \end{aligned}\right\} \text{(case II)}\,. \tag{66}$$

and

$$F = 0 \quad \text{for} \quad x = x_1 \quad \text{and} \quad 0 \leqslant y \leqslant y_1 \quad \text{(case III)}\,. \tag{67}$$

Finally, we may note that $E(x)$ can be written in the form (cf. eq. [13])

$$E(x) = \frac{1}{2\mu_1}(1-p)\frac{\nu_0}{\nu_c \Delta\nu}\,\alpha\{J_c(\alpha x) + \tfrac{1}{4}S_c e^{-\tau_1} e^{\alpha x}\}. \tag{68}$$

where

$$\alpha x = \tau \quad \text{and} \quad \alpha = 2\mu_1 \frac{\kappa_c}{\sigma_0}. \tag{69}$$

The quantity α introduced in equation (68) is essentially the ratio of the absorption coefficients in the continuum and in the line; this ratio is generally of the order of 10^{-4}, so that, if the need should arise, we may treat this as a small quantity. However, it should be remembered that the optical depth t_1 in Lyman-α, under the circumstances of our problem, is so large that $\alpha t_1 (= \tau_1)$ is of the order of unity.

4. *The solution of the boundary-value problem for the case* p = 0.—Before we can proceed with the solution of the boundary-value problem formulated in the preceding section, it is necessary for us to have an expression for the density of the diffuse ultraviolet radiation. This is given by the theory of radiative transfer of the ultraviolet radiation, and in a first approximation the solution for J_c has the form[11]

$$J_c(\tau) = A e^{-\lambda\tau} + B e^{+\lambda\tau} + \frac{3p}{4(2-3p)} S_c e^{-(\tau_1 - \tau)}, \tag{70}$$

where A and B are certain constants and $\lambda^2 = 3(1-p)$. While the solution of the boundary-value problem with this general form for $J_c(\tau)$ is entirely feasible, we shall be avoiding a great deal of formal complexity without losing, at the same time, any of the essential features of the problem by considering the case $p = 0$. Indeed, it is known that the flux in the diffuse ultraviolet radiation is generally so small that the case $p = 0$ provides ample accuracy for most problems. Moreover, since in this investigation our prime interest is to evaluate the selective radiation pressure in Lyman-α, we shall not be restricting our treatment in any essential way if we put $p = 0$. It is evident that, when this is the case,

$$J_c(\tau) \equiv 0 \qquad (p = 0). \tag{71}$$

The expression for $E(x)$ now reduces to (cf. eq. [68])

$$E(x) = \left(\frac{\nu_0}{8\mu_1 \nu_c \Delta\nu} S_c e^{-\tau_1}\right) \alpha e^{\alpha x}; \tag{72}$$

and equations (62) and (63) become

$$\frac{\partial F}{\partial x} - \frac{\partial F}{\partial y} = -G - Q\alpha e^{\alpha x + y} \tag{73}$$

and

$$\frac{\partial G}{\partial x} + \frac{\partial G}{\partial y} = +F + Q\alpha e^{\alpha x + y}, \tag{74}$$

where we have written

$$Q = \frac{\nu_0}{8\mu_1 \nu_c \Delta\nu} S_c e^{-\tau_1}. \tag{75}$$

Equations (73) and (74) are nonhomogeneous. But they can be reduced to homogeneous forms, since a particular integral is readily found. Thus

$$F = -Q\frac{2+\alpha}{\alpha} e^{\alpha x + y} \quad \text{and} \quad G = -Q\frac{2-\alpha}{\alpha} e^{\alpha x + y} \tag{76}$$

[11] Cf. S. Chandrasekhar, *Zs. f. Ap.*, **9**, 266, 1935 (see eqs. [24] and [28]).

are seen to satisfy equations (73) and (74). We accordingly write

$$F = Q\left(f - \frac{2+a}{a}\, e^{ax+y}\right) \tag{77}$$

and

$$G = Q\left(g - \frac{2-a}{a}\, e^{ax+y}\right) \tag{78}$$

and obtain for f and g the homogeneous equations

$$\frac{\partial f}{\partial x} - \frac{\partial f}{\partial y} = -g\,. \tag{79}$$

and

$$\frac{\partial g}{\partial x} + \frac{\partial g}{\partial y} = +f\,. \tag{80}$$

The boundary conditions with respect to which the foregoing equations have to be solved are (cf. eqs. [64]-[67] and [77] and [78]):

$$\left.\begin{aligned} &g = \frac{2-a}{a}\, e^{y} \quad \text{on} \quad CD\colon x = 0 \quad \text{and} \quad 0 \leqslant y \leqslant y_1\,, \\ &f = \frac{2+a}{a}\, e^{ax} \quad \text{and} \quad g = \frac{2-a}{a}\, e^{ax} \quad \text{on} \quad CB\colon y = 0 \quad \text{and} \quad 0 \leqslant x \leqslant x_1\,, \end{aligned}\right\} \tag{81}$$

in all three cases, and on AB ($x = x_1$ and $0 \leqslant y \leqslant y_1$)

$$f = g + 2e^{ax_1+y} \qquad \text{(case I)}\,. \tag{82}$$

and

$$f = \frac{2+a}{a}\, e^{ax_1+y} \qquad \text{(case III)}\,. \tag{83}$$

For case II there is a similar boundary condition on AB. But as we shall not be obtaining explicitly the solution for this case, we shall not continue to write down the boundary conditions for this case.

Eliminating g between equations (79) and (80), we obtain

$$\frac{\partial^2 f}{\partial x^2} - \frac{\partial^2 f}{\partial y^2} + f = 0\,. \tag{84}$$

We require to solve this hyperbolic equation with the boundary conditions (cf. eqs. [79]-[83])

$$\left.\begin{aligned} &f = \frac{2+a}{a}\, e^{ax}\,, \qquad \frac{\partial f}{\partial x} = (2+a)\, e^{ax}\,, \qquad \text{and} \qquad \frac{\partial f}{\partial y} = \frac{a^2+a+2}{a}\, e^{ax} \\ &\qquad\qquad \text{on} \quad BC\colon y = 0 \quad \text{and} \quad 0 \leqslant x \leqslant x_1\,. \\ &\frac{\partial f}{\partial x} = \frac{\partial f}{\partial y} - \frac{2-a}{a}\, e^{y} \quad \text{on} \quad CD\colon x = 0 \quad \text{and} \quad 0 \leqslant y \leqslant y_1\,, \end{aligned}\right\} \tag{85}$$

in all three cases, and on AB ($x = x_1$ and $0 \leqslant y \leqslant y_1$)

$$f + \frac{\partial f}{\partial x} - \frac{\partial f}{\partial y} = 2e^{ax_1+y} \qquad \text{(case I)}\,. \tag{86}$$

and

$$f = \frac{2+a}{a}\, e^{ax_1+y} \qquad \text{(case III)}\,. \tag{87}$$

The solution to the boundary-value problem we have just formulated can be carried out in a manner quite analogous to that which was followed in the solution of a similar boundary-value problem in "Moving Atmospheres." Briefly, the method consists in applying Green's theorem to contours which are, in parts, the characteristics $x-\xi = \pm(y-\eta)$, passing through suitably selected points (ξ, η) and with the further choice of the Riemann function $v(x, y; \xi, \eta)$ for the solution of the adjoint equation.[12]

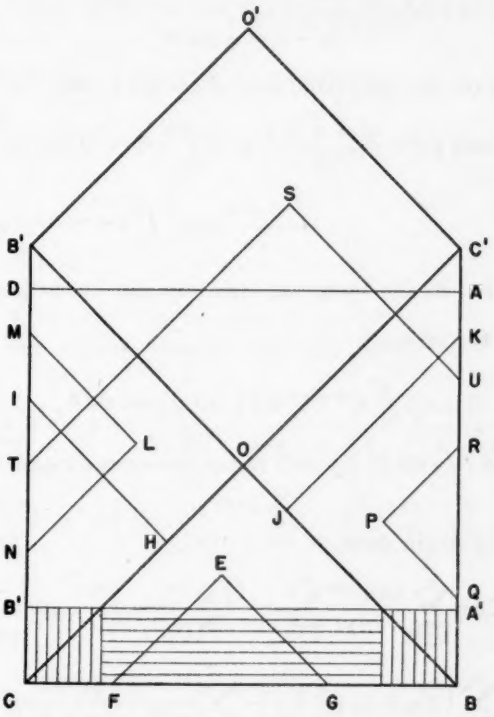

FIG. 3

a) The solution in the region OCB.—Let the characteristic $x = y$ through C intersect AB at C' and the characteristic $x_1 - x = y$ through B intersect CD at B'. Further, let CC' and BB' intersect at O (see Fig. 3).

Now, since the function and its derivatives are specified along CB, the solution in the region OCB (including the sides OC and OB) can be found directly by Riemann's method. Thus, applying Green's theorem to a contour such as $EFGE$ where EF and EG are the characteristics through $E = (\xi, \eta)$, we find that

$$f(\xi, \eta) = \frac{2+a}{a} e^{a\xi} \cosh a\eta - \frac{1}{2}\int_{\xi-\eta}^{\xi+\eta} \left(f \frac{\partial v}{\partial y} - v \frac{\partial f}{\partial y} \right)_{y=0} dx . \qquad (88)$$

The Reimann function appropriate for the contour $EFGE$ is

$$v(x, y; \xi, \eta) = I_0([(y-\eta)^2 - (x-\xi)^2]^{\frac{1}{2}}) . \qquad (89)$$

[12] A more detailed description of the method will be found in "Moving Atmospheres," § 5.

Using this v in equation (88) and substituting also for f and $\partial f/\partial y$ according to equation (85), we find

$$\left.\begin{aligned} f(\xi,\eta) = \frac{2+a}{a}\, e^{a\xi}\cosh a\eta + \frac{a^2+a+2}{2a}\int_{\xi-\eta}^{\xi+\eta} e^{ax} I_0\left(\left[\eta^2-(x-\xi)^2\right]^{\frac{1}{2}}\right) dx \\ + \frac{2+a}{2a}\,\eta\int_{\xi-\eta}^{\xi+\eta} e^{ax}\,\frac{I_1\left(\left[\eta^2-(x-\xi)^2\right]^{\frac{1}{2}}\right)}{\left[\eta^2-(x-\xi)^2\right]^{\frac{1}{2}}}\, dx . \end{aligned}\right\} \tag{90}$$

Putting

$$x-\xi = \eta\cos\vartheta \tag{91}$$

into the two integrals on the right-hand side of equation (90), we obtain

$$\left.\begin{aligned} f(\xi,\eta) = \frac{2+a}{a}\, e^{a\xi}\cosh a\eta + \frac{a^2+a+2}{2a}\,\eta\, e^{a\xi}\int_0^{\pi} e^{a\eta\cos\vartheta} I_0(\eta\sin\vartheta)\sin\vartheta\, d\vartheta \\ + \frac{2+a}{2a}\,\eta\, e^{a\xi}\int_0^{\pi} e^{a\eta\cos\vartheta} I_1(\eta\sin\vartheta)\, d\vartheta . \end{aligned}\right\} \tag{92}$$

The integrals occurring in the foregoing equation can be evaluated in the following manner:

Considering, first, the integral

$$a\eta\int_0^{\pi} e^{a\eta\cos\vartheta} I_0(\eta\sin\vartheta)\sin\vartheta\, d\vartheta , \tag{93}$$

we replace $e^{a\eta\cos\vartheta}$ and $I_0(\eta\sin\vartheta)$ by their respective series expansions and integrate term by term. We find

$$\left.\begin{aligned} a\eta\int_0^{\pi} e^{a\eta\cos\vartheta} I_0(\eta\sin\vartheta)\sin\vartheta\, d\vartheta \\ = 2a\eta\sum_{n=0}^{\infty}\frac{(a\eta)^{2n}}{(2n)!}\sum_{m=0}^{\infty}\frac{(\frac{1}{2}\eta)^{2m}}{m!\Gamma(m+1)}\int_0^{\pi/2}\cos^{2n}\vartheta\sin^{2m+1}\vartheta\, d\vartheta \\ = \sum_{n=0}^{\infty}\Gamma(n+\tfrac{1}{2})\frac{(a\eta)^{2n+1}}{(2n)!}\sum_{m=0}^{\infty}\frac{(\frac{1}{2}\eta)^{2m}}{m!\Gamma(m+n+\frac{3}{2})} \\ = \sum_{n=0}^{\infty}\Gamma(n+\tfrac{1}{2})\frac{(2a^2\eta)^{n+\frac{1}{2}}}{(2n)!}\sum_{m=0}^{\infty}\frac{(\frac{1}{2}\eta)^{2m+n+\frac{1}{2}}}{m!\Gamma(m+n+\frac{3}{2})} \\ = \sum_{n=0}^{\infty}\Gamma(n+\tfrac{1}{2})\frac{(2a^2\eta)^{n+\frac{1}{2}}}{(2n)!}\, I_{n+\frac{1}{2}}(\eta) \\ = (2\pi\eta)^{\frac{1}{2}} a\sum_{n=0}^{\infty}(\tfrac{1}{2}a^2\eta)^n\frac{1}{n!}\, I_{n+\frac{1}{2}}(\eta) . \end{aligned}\right\} \tag{94}$$

But

$$I_\nu\{\eta\sqrt{(1+a^2)}\} = (1+a^2)^{\frac{1}{2}\nu}\sum_{n=0}^{\infty}(\tfrac{1}{2}a^2\eta)^n\frac{1}{n!}\, I_{\nu+n}(\eta) . \tag{95}$$ [13]

[13] This formula can be established by following the method used by G. N. Watson in his *Theory of Bessel Functions*, p. 141, Cambridge University Press, 1944, in proving a similar relation involving the Bessel functions with real arguments.

The last summation which occurs in equation (94) is therefore a special case of equation (95). We have

$$\sum_{n=0}^{\infty} (\tfrac{1}{2}a^2\eta)^n \frac{1}{n!} I_{n+\frac{1}{2}}(\eta) = \frac{1}{(1+a^2)^{1/4}} I_{\frac{1}{2}}\{\eta\sqrt{(1+a^2)}\}. \tag{96}$$

Hence,

$$\eta\int_0^{\pi} e^{a\eta\cos\vartheta} I_0(\eta\sin\vartheta)\sin\vartheta\, d\vartheta = \frac{(2\pi\eta)^{\frac{1}{2}}}{(1+a^2)^{1/4}} I_{\frac{1}{2}}\{\eta\sqrt{(1+a^2)}\}; \tag{97}$$

or, substituting the explicit expression for $I_{\frac{1}{2}}$, we have

$$\eta\int_0^{\pi} e^{a\eta\cos\vartheta} I_0(\eta\sin\vartheta)\sin\vartheta\, d\vartheta = \frac{2}{\sqrt{(1+a^2)}}\sinh\{\eta\sqrt{(1+a^2)}\}. \tag{98}$$

Similarly,

$$\left.\begin{aligned}
&a\eta\int_0^{\pi} e^{a\eta\cos\vartheta} I_1(\eta\sin\vartheta)\, d\vartheta \\
&\quad = 2\sum_{n=0}^{\infty}\frac{(a\eta)^{2n+1}}{(2n)!}\sum_{m=0}^{\infty}\frac{(\frac{1}{2}\eta)^{2m+1}}{m!\Gamma(m+2)}\int_0^{\pi/2}\cos^{2n}\vartheta\sin^{2m+1}\vartheta\, d\vartheta \\
&\quad = \sum_{n=0}^{\infty}\Gamma(n+\tfrac{1}{2})\frac{(a\eta)^{2n+1}}{(2n)!}\sum_{m=0}^{\infty}\frac{(\frac{1}{2}\eta)^{2m+1}}{(m+1)!\Gamma(m+n+\frac{3}{2})} \\
&\quad = \sum_{n=0}^{\infty}\Gamma(n+\tfrac{1}{2})\frac{(2a^2\eta)^{n+\frac{1}{2}}}{(2n)!}\sum_{m=1}^{\infty}\frac{(\frac{1}{2}\eta)^{2m+n-\frac{1}{2}}}{m!\Gamma(m+n+\frac{1}{2})} \\
&\quad = \sum_{n=0}^{\infty}\Gamma(n+\tfrac{1}{2})\frac{(2a^2\eta)^{n+\frac{1}{2}}}{(2n)!}\left[I_{n-\frac{1}{2}}(\eta) - \frac{(\frac{1}{2}\eta)^{n-\frac{1}{2}}}{\Gamma(n+\frac{1}{2})}\right] \\
&\quad = a(2\pi\eta)^{\frac{1}{2}}\sum_{n=0}^{\infty}(\tfrac{1}{2}a^2\eta)^n\frac{1}{n!}I_{n-\frac{1}{2}}(\eta) - 2a\sum_{n=0}^{\infty}\frac{(a\eta)^{2n}}{(2n)!} \\
&\quad = a(2\pi\eta)^{\frac{1}{2}}(1+a^2)^{1/4}I_{-\frac{1}{2}}\{\eta\sqrt{(1+a^2)}\} - 2a\cosh a\eta.
\end{aligned}\right\} \tag{99}$$

Hence,

$$\eta\int_0^{\pi} e^{a\eta\cos\vartheta} I_1(\eta\sin\vartheta)\, d\vartheta = 2\cosh\{\eta\sqrt{(1+a^2)}\} - 2\cosh a\eta. \tag{100}$$

Substituting from equations (98) and (100) in equation (92), we obtain

$$\left.\begin{aligned}
f(\xi,\eta) = \frac{1}{a}e^{a\xi}\Big[&\frac{a^2+a+2}{\sqrt{(1+a^2)}}\sinh\{\eta\sqrt{(1+a^2)}\} \\
&+ (2+a)\cosh\{\eta\sqrt{(1+a^2)}\}\Big].
\end{aligned}\right\} \tag{101}$$

This solves explicitly for f in the region OCB. With this solution for f, g can also be found in this region; for (cf. eq. [79])

$$g(\xi,\eta) = -\frac{\partial f}{\partial\xi} + \frac{\partial f}{\partial\eta}, \tag{102}$$

and equation (101) yields

$$g(\xi, \eta) = \frac{1}{a} e^{a\xi} \left[\frac{a^2 - a + 2}{\sqrt{(1+a^2)}} \sinh \{ \eta \sqrt{(1+a^2)} \} + (2-a) \cosh \{ \eta \sqrt{(1+a^2)} \} \right]. \tag{103}$$

The corresponding solutions for ψ_{+1} and ψ_{-1} are readily found. We have

$$\psi_{+1} = \frac{Q}{a} e^{ax-y} \left[\frac{a^2 + a + 2}{\sqrt{(1+a^2)}} \sinh \{ y \sqrt{(1+a^2)} \} + (2+a) \cosh \{ y \sqrt{(1+a^2)} \} - (2+a)\, e^{y} \right] \tag{104}$$

and

$$\psi_{-1} = \frac{Q}{a} e^{ax-y} \left[\frac{a^2 - a + 2}{\sqrt{(1+a^2)}} \sinh \{ y \sqrt{(1+a^2)} \} + (2-a) \cosh \{ y \sqrt{(1+a^2)} \} - (2-a)\, e^{y} \right]. \tag{105}$$

b) The integral equation which insures the continuity of the solution along CO.—Along *CD* neither the function nor its derivatives are known: only a relation between them is given (cf. eq. [85]). But our knowledge of the solution along *CO* and the requirement that the solution be continuous along this line suffice to determine $f(0, y)$ as the solution of an integral equation of Volterra's type. To obtain this integral equation we apply Green's theorem to a contour such as *CIHI*, where $H = (\eta, \eta)$ is a point on *OC* and *HI* is the characteristic $\eta - x = y - \eta$ through H. We find

$$2f(\eta, \eta) = f(0, 2\eta) + \frac{2+a}{a} + \int_0^{2\eta} \left(v \frac{\partial f}{\partial x} - f \frac{\partial v}{\partial x} \right)_{x=0} dy. \tag{106}$$

On the other hand, since (cf. eq. [85])

$$\frac{\partial f}{\partial x} = \frac{\partial f}{\partial y} - \frac{2-a}{a} e^{y} \tag{107}$$

along *CD*, we have

$$2f(\eta, \eta) = f(0, 2\eta) + \frac{2+a}{a} - \frac{2-a}{a} \int_0^{2\eta} e^{y} [v]_{x=0}\, dy + \int_0^{2\eta} \left(v \frac{\partial f}{\partial y} \right)_{x=0} dy - \int_0^{2\eta} f(0, y) \left(\frac{\partial v}{\partial x} \right)_{x=0} dy. \tag{108}$$

Integrating by parts the second of the three integrals occurring on the right-hand side of equation (108) and remembering that the Riemann function for this problem is always unity along the characteristics, we find that

$$2f(\eta, \eta) = 2f(0, 2\eta) - \frac{2-a}{a} \int_0^{2\eta} e^{y} [v]_{x=0}\, dy - \int_0^{2\eta} f(0, y) \left(\frac{\partial v}{\partial x} + \frac{\partial v}{\partial y} \right)_{x=0} dy. \tag{109}$$

The Riemann function appropriate for our present contour is

$$v(x, y; \xi, \eta) = J_0 ([(\eta - x)^2 - (y - \eta)^2]^{\frac{1}{2}}). \tag{110}$$

With this choice of v, equation (109) reduces to the form

$$\left.\begin{aligned} f(\eta, \eta) = f(0, 2\eta) &- \frac{2-a}{2a}\,\eta e^{\eta}\int_0^{\pi} e^{\eta\cos\vartheta} J_0(\eta\sin\vartheta)\sin\vartheta\, d\vartheta \\ &- \frac{1}{2}\int_0^{2\eta} f(0, y)\, J_1\left(\left[\eta^2-(y-\eta)^2\right]^{\frac{1}{2}}\right)\frac{y\,dy}{\left[\eta^2-(y-\eta)^2\right]^{\frac{1}{2}}}. \end{aligned}\right\} \tag{111}$$

The definite integral on the right-hand side of equation (111) can be evaluated. We have

$$\left.\begin{aligned} \eta\int_0^{\pi} e^{\eta\cos\vartheta} J_0(\eta\sin\vartheta)\sin\vartheta\, d\vartheta &= \sum_{n=0}^{\infty}\frac{\eta^{2n+1}}{(2n)!}\sum_{m=0}^{\infty}(-1)^m\frac{(\frac{1}{2}\eta)^{2m}}{m!\Gamma(m+1)}\int_0^{\pi/2}\cos^{2n}\vartheta\sin^{2m+1}\vartheta\, d\vartheta \\ &= \sum_{n=0}^{\infty}\Gamma(n+\tfrac{1}{2})\frac{\eta^{2n+1}}{(2n)!}\sum_{m=0}^{\infty}(-1)^m\frac{(\frac{1}{2}\eta)^{2m}}{m!\Gamma(m+n+\frac{3}{2})} \\ &= \sum_{n=0}^{\infty}\Gamma(n+\tfrac{1}{2})\frac{(2\eta)^{n+\frac{1}{2}}}{(2n)!}\sum_{m=0}^{\infty}(-1)^m\frac{(\frac{1}{2}\eta)^{2m+n+\frac{1}{2}}}{m!\Gamma(m+n+\frac{3}{2})} \\ &= (2\pi\eta)^{\frac{1}{2}}\sum_{n=0}^{\infty}(\tfrac{1}{2}\eta)^n\frac{1}{n!}J_{n+\frac{1}{2}}(\eta) \\ &= (2\pi\eta)^{\frac{1}{2}}\frac{(\frac{1}{2}\eta)^{\frac{1}{2}}}{\Gamma(1+\frac{1}{2})} = 2\eta. \end{aligned}\right\} \tag{112}$$

Equation (111) thus becomes

$$\left.\begin{aligned} &\frac{1}{a}\,e^{a\eta}\left[\frac{a^2+a+2}{\sqrt{(1+a^2)}}\sinh\{\eta\sqrt{(1+a^2)}\}+(2+a)\cosh\{\eta\sqrt{(1+a^2)}\}\right] \\ &\quad+\frac{2-a}{a}\,\eta e^{\eta} = f(0, 2\eta) - \frac{1}{2}\int_0^{2\eta} f(0, y)\frac{J_1\left(\left[\eta^2-(y-\eta)^2\right]^{\frac{1}{2}}\right)}{\left[\eta^2-(y-\eta)^2\right]^{\frac{1}{2}}}\,y\,dy, \end{aligned}\right\} \tag{113}$$

where we have also substituted for $f(\eta, \eta)$ according to equation (101).

It is now seen that the right-hand side of equation (113) is simply the derivative of

$$\frac{1}{2}\int_0^{2\eta} f(0, y)\, J_0\left(\left[\eta^2-(y-\eta)^2\right]^{\frac{1}{2}}\right) dy \tag{114}$$

with respect to η. We can accordingly reduce equation (113) to an integral equation of Volterra's type. To perform this reduction we need only know the integral of the left-hand side of equation (113). We thus find that

$$\left.\begin{aligned} &\frac{1}{a}\,e^{a\eta}\left[(2-a)\cosh\{\eta\sqrt{(1+a^2)}\}+\frac{a^2-a+2}{\sqrt{(1+a^2)}}\sinh\{\eta\sqrt{(1+a^2)}\}\right] \\ &\quad+\frac{2-a}{a}(\eta-1)\,e^{\eta} = \frac{1}{2}\int_0^{2\eta} f(0, y)\, J_0\left(\left[\eta^2-(y-\eta)^2\right]^{\frac{1}{2}}\right) dy, \end{aligned}\right\} \tag{115}$$

which is the required equation for $f(0, y)$.

c) The solution of the integral equation (115).—To solve equation (115) we apply a Laplace transformation to this equation, i.e., we multiply both sides of the equation by $e^{-s\eta}$ and integrate over η from 0 to ∞. The right-hand side then becomes (cf. "Moving Atmospheres," eqs. [90]–[95])

$$\frac{1}{2s}\int_0^\infty f(0, y) \exp[-y(s+s^{-1})/2]\, dy, \tag{116}$$

while the evaluation of the Laplace transform of the left-hand side requires only elementary integrals. We find

$$\left.\begin{aligned}\frac{1}{a}\left[\frac{(2-a)(s-a)}{(s-a)^2-(1+a^2)}+\frac{a^2-a+2}{(s-a)^2-(1+a^2)}\right]+\frac{(2-a)(2-s)}{a(s-1)^2}\\ =\frac{1}{2s}\int_0^\infty f(0, y) \exp[-y(s+s^{-1})/2]\, dy.\end{aligned}\right\} \tag{117}$$

We can re-write the foregoing equation in the form

$$\left.\begin{aligned}\frac{2(s+1)-a(s+3)+2a^2}{a(s^2-2sa-1)}+\frac{(2-a)(2-s)}{a(s-1)^2}\\ =\frac{1}{2s}\int_0^\infty f(0, y) \exp[-y(s+s^{-1})/2]\, dy.\end{aligned}\right\} \tag{118}$$

If we now let

$$s+s^{-1}=2u \tag{119}$$

or, equivalently,

$$s=u+\sqrt{(u^2-1)}, \tag{120}$$

equation (118) provides the simple Laplace transform of $f(0, y)$, and the solution can, in principle, be found. However, since a is a small quantity of the order of 10^{-4}, the solution in the form of a series expansion in a will suffice for most purposes. Accordingly, we expand the left-hand side of equation (118) in powers of a. We thus obtain

$$\left.\begin{aligned}\frac{2+a}{a}\frac{2s}{(s-1)^2}+a\frac{4s}{(s-1)^3}+O(a^2)\\ =\int_0^\infty f(0, y) \exp[-y(s+s^{-1})/2]\, dy.\end{aligned}\right\} \tag{121}$$

With the substitutions (119) and (120), equation (121) becomes

$$\left.\begin{aligned}\frac{2+a}{a}\frac{1}{u-1}+\frac{2a}{(u-1)^{3/2}[\sqrt{(u+1)}+\sqrt{(u-1)}]}+O(a^2)\\ =\int_0^\infty f(0, y)\, e^{-yu}dy.\end{aligned}\right\} \tag{122}$$

Now the inverse Laplace transform of the first term on the left-hand side of equation (122) is

$$\frac{2+a}{a}e^y; \tag{123}$$

while writing the second term in the form

$$a\left[\frac{1}{(u^2-1)^{\frac{1}{2}}}+\frac{2}{(u-1)^{3/2}(u+1)^{\frac{1}{2}}}-\frac{1}{u-1}\right], \tag{124}$$

we see that its inverse Laplace transform is

$$a\{I_0(y)+2y[I_0(y)+I_1(y)]-e^y\}. \tag{125}$$

Hence,

$$f(0, y)=\frac{2+a}{a}e^y+a\{I_0(y)+2y[I_0(y)+I_1(y)]-e^y\}+O(a^2). \tag{126}$$

The corresponding solution for $\psi_{+1}(0, y)$ is

$$\left.\begin{aligned}\psi_{+1}(0, y)=Qae^{-y}\{I_0(y)+2y[I_0(y)+I_1(y)]-e^y\}+O(a^2)\\ (0\leqslant y\leqslant x_1),\end{aligned}\right\} \tag{127}$$

while $\psi_{-1}(0, y)$, of course, vanishes along this line, as required by the boundary conditions.

d) The integral equation insuring the continuity of the solution along OB *and its solution (case I).*—Applying, next, Green's theorem to a contour such as $JKBJ$, where $J=(x_1-\eta, \eta)$ is a point on OB, and JK is the characteristic $x-x_1+\eta=y-\eta$ through J, we find in the usual manner that

$$2f(x_1-\eta, \eta)=\frac{2+a}{a}e^{ax_1}+f(x_1, 2\eta)-\int_0^{2\eta}\left(v\frac{\partial f}{\partial x}-f\frac{\partial v}{\partial x}\right)_{x=x_1}dy. \tag{128}$$

In case I,

$$\frac{\partial f}{\partial x}=-f+\frac{\partial f}{\partial y}+2e^{ax_1+y} \tag{129}$$

along AB (cf. eq. [86]). Using this in equation (128), we find, after some minor reductions, that

$$\left.\begin{aligned}f(x_1-\eta, \eta)=\frac{2+a}{a}e^{ax_1}-e^{ax_1}\int_0^{2\eta}e^y[v]_{x=x_1}dy\\ +\frac{1}{2}\int_0^{2\eta}f(x_1, y)\left(v+\frac{\partial v}{\partial x}+\frac{\partial v}{\partial y}\right)_{x=x_1}dy.\end{aligned}\right\} \tag{130}$$

The Riemann function appropriate to our present contour is

$$v(x, y; x_1-\eta, \eta)=J_0([(x-x_1+\eta)^2-(y-\eta)^2]^{\frac{1}{2}}). \tag{131}$$

With v given by equation (131), equation (130) becomes

$$\left.\begin{aligned}f(x_1-\eta, \eta)=\frac{2+a}{a}e^{ax_1}-\eta e^{ax_1+\eta}\int_0^{\pi}e^{\eta\cos\vartheta}J_0(\eta\sin\vartheta)\sin\vartheta d\vartheta\\ +\frac{1}{2}\int_0^{2\eta}f(x_1, y)J_0([\eta^2-(y-\eta)^2]^{\frac{1}{2}})dy\\ -\frac{1}{2}\int_0^{2\eta}f(x_1, y)J_1([\eta^2-(y-\eta)^2]^{\frac{1}{2}})\frac{2\eta-y}{[\eta^2-(y-\eta)^2]^{\frac{1}{2}}}dy.\end{aligned}\right\} \tag{132}$$

But (cf. eq. [112])

$$\int_0^{\pi}e^{\eta\cos\vartheta}J_0(\eta\sin\vartheta)\sin\vartheta d\vartheta=2. \tag{133}$$

Using this result in equation (132) and substituting also for $f(x_1 - \eta, \eta)$ according to equation (101), we obtain

$$\left.\begin{aligned}\frac{1}{a}e^{a(x_1-\eta)}\left[\frac{a^2+a+2}{\sqrt{(1+a^2)}}\sinh\{\eta\sqrt{(1+a^2)}\}+(2+a)\cosh\{\eta\sqrt{(1+a^2)}\}\right]\\ -\frac{2+a}{a}e^{ax_1}+2\eta e^{ax_1+\eta}=\frac{1}{2}\int_0^{2\eta}f(x_1,y)J_0([\eta^2-(y-\eta)^2]^{\frac{1}{2}})\,dy\\ -\frac{1}{2}\int_0^{2\eta}\frac{f(x_1,y)}{y}J_1\{\sqrt{(2\eta y-y^2)}\}\sqrt{(2\eta y-y^2)}\,dy,\end{aligned}\right\}\quad(134)$$

which is again an integral equation of Volterra's type for $f(x_1, y)$.

To solve equation (134) we apply, as before, a Laplace transformation to this equation. We find (cf. eq. [116])

$$\left.\begin{aligned}\frac{1}{a}e^{ax_1}\left[\frac{a^2+a+2}{(s+a)^2-(1+a^2)}+\frac{(2+a)(s+a)}{(s+a)^2-(1+a^2)}\right]-\frac{1}{a}e^{ax_1}\frac{2+a}{s}\\ +\frac{2e^{ax_1}}{(s-1)^2}=\frac{1}{2s}\int_0^{\infty}f(x_1,y)\exp[-y(s+s^{-1})/2]\,dy\\ -\frac{1}{2}\int_0^{\infty}d\eta\,e^{-s\eta}\int_0^{2\eta}\frac{f(x_1,y)}{y}J_1\{\sqrt{(2\eta y-y^2)}\}\sqrt{(2\eta y-y^2)}\,dy.\end{aligned}\right\}\quad(135)$$

Inverting the order of the integration in the double integral in equation (135) and introducing the variable

$$2\eta y - y^2 = t^2 \qquad (136)$$

we find that it reduces to

$$\int_0^{\infty}\frac{dy}{y^2}f(x_1,y)\,e^{-sy/2}\int_0^{\infty}dt\,t^2J_1(t)\,e^{-st^2/2y}. \qquad (137)$$

But the integral over t in (137) has the value[14]

$$\left(\frac{y}{s}\right)^2 e^{-y/2s}. \qquad (138)$$

Accordingly, the

$$\left.\begin{aligned}\text{Laplace transform of}\int_0^{2\eta}\frac{f(x_1,y)}{y}J_1\{\sqrt{(2\eta y-y^2)}\}\sqrt{(2\eta y-y^2)}\,dy\\ =\frac{1}{s^2}\int_0^{\infty}f(x_1,y)\exp[-y(s+s^{-1})/2]\,dy,\end{aligned}\right\}\quad(139)$$

and equation (135) becomes

$$\left.\begin{aligned}\frac{1}{a}e^{ax_1}\left[\frac{2(s+1)+a(s+3)+2a^2}{s^2+2sa-1}-\frac{2+a}{s}+\frac{2a}{(s-1)^2}\right]\\ =\frac{s-1}{2s^2}\int_0^{\infty}f(x_1,y)\exp[-y(s+s^{-1})/2]\,dy.\end{aligned}\right\}\quad(140)$$

With the substitution of equation (119) and (120) in equation (140), we shall obtain the Laplace transform of $f(x_1, y)$, and the solution beomes determinate. But again, as in

[14] Cf. Watson, *op. cit.*, p. 394, eq. (4).

the preceding subsection, we shall content ourselves with finding a solution in the form of a series expansion in a. Thus, expanding the left-hand side of equation (140) in powers of a and after some rearranging of the terms, we find

$$\left.\begin{aligned}\frac{2}{a}\,e^{ax_1}\left[\frac{(2+a)\,s}{(s-1)^2}+2a^2\,\frac{s^2}{(s-1)^4}+O(a^3)\right]\\ =\int_0^\infty f(x_1, y)\exp\left[-y(s+s^{-1})/2\right]dy\,.\end{aligned}\right\}\quad(141)$$

In terms of the variable u defined as in equation (119) or equation (120), the foregoing equation reduces to

$$e^{ax_1}\left[\frac{2+a}{a}\,\frac{1}{(u-1)}+\frac{a}{(u-1)^2}+O(a^2)\right]=\int_0^\infty f(x_1, y)\,e^{-yu}dy\,. \quad (142)$$

Hence,

$$f(x_1, y)=\frac{2+a}{a}\,e^{ax_1+y}+a\,y\,e^{ax_1+y}+O(a^2)\,. \quad (143)$$

The corresponding solutions for ψ_{+1} and ψ_{-1} are (cf. eq. [58])

$$\psi_{+1}(x_1, y)=Qa\,y\,e^{ax_1}+O(a^2) \quad (144)$$

and

$$\psi_{-1}(x_1, y)=Qa\,y\,e^{ax_1}+O(a^2)\,. \quad (145)$$

e) The integral equation insuring the continuity of the solution along OB *and its solution (case III).*—In case III the boundary condition specified along AB is that (cf. eq. [87])

$$f=\frac{2+a}{a}\,e^{ax_1+y}, \quad (146)$$

and we require to find $(\partial f/\partial x)_{x=x_1}$. The solution proceeds along lines now familiar. Equation (128), which is valid also under our present conditions, gives

$$\left.\begin{aligned}2f(x_1-\eta, \eta)=\frac{2+a}{a}\,e^{ax_1}(1+e^{2\eta})+\frac{2+a}{a}\,e^{ax_1}\int_0^{2\eta}e^{y}\left(\frac{\partial v}{\partial x}\right)_{x=x_1}dy\\ -\int_0^{2\eta}\left(v\,\frac{\partial f}{\partial x}\right)_{x=x_1}dy\,.\end{aligned}\right\}\quad(147)$$

The Riemann function is the same as in case I and is given in equation (131). Using this in equation (147), we find after some minor transformations that

$$\left.\begin{aligned}2f(x_1-\eta, \eta)=\frac{2+a}{a}\,e^{ax_1}(1+e^{2\eta})-\frac{2+a}{a}\,\eta\,e^{ax_1+\eta}\int_0^{\pi}e^{\eta\cos\vartheta}J_1(\sin\vartheta)\,d\vartheta\\ -\int_0^{2\eta}\left(\frac{\partial f}{\partial x}\right)_{x=x_1}J_0\left(\left[\eta^2-(y-\eta)^2\right]^{\frac{1}{2}}\right)dy\,.\end{aligned}\right\}\quad(148)$$

But (cf. "Moving Atmospheres," eqs. [105] and [106])

$$\eta\int_0^{\pi}e^{\eta\cos\vartheta}J_1(\eta\sin\vartheta)\,d\vartheta=2(\cosh\eta-1)\,. \quad (149)$$

Using this result in equation (148) and substituting also for $f(x_1 - \eta, \eta)$ according to equation (101), we obtain

$$\left.\begin{aligned}\frac{2+a}{a}e^{ax_1+\eta}-\frac{1}{a}\,e^{a(x_1-\eta)}\left[\frac{a^2+a+2}{\sqrt{(1+a^2)}}\sinh\{\eta\sqrt{(1+a^2)}\}+(2+a)\right.\right.\\ \left.\left.\times\cosh\{\eta\sqrt{(1+a^2)}\}\right]=\frac{1}{2}\int_0^{2\eta}\left(\frac{\partial f}{\partial x}\right)_{x=x_1}J_0\left([\eta^2-(y-\eta)^2]^{\frac{1}{2}}\right)dy\,.\end{aligned}\right\}\quad(150)$$

This is the required Volterra integral equation for $(\partial f/\partial x)_{x=x_1}$.

The solution of the integral equation (150) proceeds as in the other cases. We apply a Laplace transformation to the equation and obtain

$$\left.\begin{aligned}\frac{1}{a}\,e^{ax_1}\left[\frac{2+a}{s-1}-\frac{2(s+1)+a(s+3)+2a^2}{s^2+2sa-1}\right]\\ =\frac{1}{2s}\int_0^{\infty}\left(\frac{\partial f}{\partial x}\right)_{x=x_1}\exp\left[-y(s+s^{-1})/2\right]dy\,.\end{aligned}\right\}\quad(151)$$

And again, as in the earlier cases, we shall obtain a solution of this equation in the form of a series expansion in a by expanding the left-hand side of the equation in powers of a. We thus find

$$\left.\begin{aligned}e^{ax_1}\left[\frac{4s}{(s-1)^2}-a\,\frac{4s}{(s-1)^3}+O(a^2)\right]\\ =\int_0^{\infty}\left(\frac{\partial f}{\partial x}\right)_{x=x_1}\exp\left[-y(s+s^{-1})/2\right]dy\,.\end{aligned}\right\}\quad(152)$$

With the substitutions (119) and (120), equation (152) becomes

$$\left.\begin{aligned}e^{ax_1}\left[\frac{2}{u-1}-\frac{2a}{(u-1)^{3/2}\left[\sqrt{(u+1)}+\sqrt{(u-1)}\right]}+O(a^2)\right]\\ =\int_0^{\infty}\left(\frac{\partial f}{\partial x}\right)_{x=x_1}e^{-yu}dy\,.\end{aligned}\right\}\quad(153)$$

Equation (153) is seen to be similar in form to equation (122). We can accordingly write (cf. eqs. [124] and [125])

$$\left(\frac{\partial f}{\partial x}\right)_{x=x_1}=2e^{ax_1+y}-ae^{ax_1}\{I_0(y)+2y[I_0(y)+I_1(y)]-e^y\}+O(a^2)\,.\quad(154)$$

Since (cf. eq. [146])

$$\left(\frac{\partial f}{\partial y}\right)_{x=x_1}=\frac{2+a}{a}\,e^{ax_1+y},\quad(155)$$

we have

$$\left.\begin{aligned}g(x_1,y)=\frac{2-a}{a}\,e^{ax_1+y}+ae^{ax_1}\{I_0(y)+2y[I_0(y)+I_1(y)]\\ -e^y\}+O(a^2)\,.\end{aligned}\right\}\quad(156)$$

The corresponding solution for $\psi_{-1}(x_1, y)$ is

$$\left.\begin{aligned}\psi_{-1}(x_1,y)=Qae^{ax_1-y}\{I_0(y)+2y[I_0(y)+I_1(y)]-e^y\}+O(a^2)\\ (0\leqslant y\leqslant x_1)\,,\end{aligned}\right\}\quad(157)$$

while $\psi_{+1}(x_1, y)$ vanishes in accordance with the boundary conditions.

f) The solution in the region O′B′COBC′O′ *and its further continuation.*—With the determination of f along CB' and f and its derivatives along BC', our knowledge of the

function and its derivatives along $B'CBC'$ is complete, and the solution in the region $O'B'COBC'O'$ becomes determinate; for, as in Riemann's method, by applying Green's theorem to contours such as $LMNL$, $PQRP$, $STCBUS$, we can find the solution in the regions $OB'C$, OBC', and $O'B'OC'$. It is seen how a knowledge of the function along COB, together with the boundary conditions on CB' and BC', enables us to determine f in the region $O'B'COBC'O'$, including the sides $B'O'$ and $O'C'$. It is now apparent that, in the same way, we can utilize our present knowledge of the function along $B'O'C'$ to extend the solution still further. We shall not, however, consider these further extensions of the solution in this paper but content ourselves with the solution which has been completed in the first square, $B'CBC'$. According to equation (56), this will suffice to determine the radiation field in all cases in which the ratio $D\nu:\Delta\nu$ exceeds $\sqrt{3}$.

5. *Formulae for the radiation pressure in an expanding atmosphere.*—Consider a slab of material of unit cross-section and height dz. The normal force acting on this slab due to the absorption of radiation is

$$\frac{1}{c}\,2\pi\rho dz\int_0^\infty d\nu\sigma(\nu)\int_0^\pi d\vartheta I\left(\nu+\nu_0\frac{w}{c}\cos\vartheta,\ z,\ \vartheta\right)\cos\vartheta\sin\vartheta\,, \tag{158}$$

since the radiation in the direction ϑ, which will appear to our fixed observer as having a frequency $\nu+\nu_0(w/c)\cos\vartheta$, will be judged by an observer at rest with respect to the material as having a frequency ν: it will accordingly be absorbed only as such.

The pressure Π exerted by the radiation is therefore given by

$$\Pi(z)=\frac{1}{c}\,2\pi\rho\int_0^\infty d\nu\sigma(\nu)\int_{-1}^{+1}d\mu I\left(\nu+\nu_0\frac{w}{c}\mu,\ z,\ \mu\right)\mu\,. \tag{159}$$

Equation (159) is perfectly general. We shall now consider certain alternative forms of this equation suitable under various conditions and approximations.

First, replacing the integral over μ in equation (159) by a sum according to Gauss's formula for numerical quadratures, we obtain

$$\Pi(z)=\frac{1}{c}\,2\pi\rho\int_0^\infty\sigma(\nu)\sum_i a_i\mu_i I_i\left(\nu+\nu_0\frac{w}{c}\mu_i,\ z\right)d\nu\,. \tag{160}$$

The intensities which appear in equation (160) are exactly the intensities $\psi_i(\nu, z)$ as we have defined them in equations (17) and (18). We may therefore write

$$\Pi(z)=\frac{1}{c}\,2\pi\rho\int_0^\infty\sigma(\nu)\sum_i a_i\mu_i\psi_i(\nu,\ z)\,d\nu\,. \tag{161}$$

In the first approximation, equation (160) reduces to

$$\Pi(z)=\frac{1}{c}\,2\pi\mu_1\rho\int_0^\infty\sigma(\nu)\,[\psi_{+1}(\nu,\ z)-\psi_{-1}(\nu,\ z)]\,d\nu \qquad \left(\mu_1=\frac{1}{\sqrt{3}}\right), \tag{162}$$

an equation which has an obvious physical interpretation.

For the particular form (26) for $\sigma(\nu)$, equation (162) further simplifies to

$$\Pi(z)=\frac{1}{c}\,2\pi\mu_1\rho\sigma_0\int_{\nu_0-\Delta\nu}^{\nu_0+\Delta\nu}[\psi_{+1}(\nu,\ z)-\psi_{-1}(\nu,\ z)]\,d\nu\,, \tag{163}$$

or, expressing ν in the unit (53), we have

$$\Pi(x)=\frac{1}{c}\,4\pi\mu_1^2\frac{D\nu}{x_1}\,\rho\sigma_0\int_0^{y_1}[\psi_{+1}(x,\ y)-\psi_{-1}(x,\ y)]\,dy\,. \tag{164}$$

On the other hand, since (cf. eq. [44])

$$x_1 = \frac{1}{2\mu_1} t_1 , \tag{165}$$

where t_1 is the optical depth of the atmosphere in σ_0, we can re-write equation (164) in the form

$$\Pi(x) = \frac{1}{c} 8\pi\mu_1^3 D\nu \frac{\rho\sigma_0}{t_1} \int_0^{y_1} [\psi_{+1}(x, y) - \psi_{-1}(x, y)] \, dy . \tag{166}$$

For the particular model considered in this paper,

$$\frac{\rho\sigma_0}{t_1} = \frac{\rho\kappa_c}{\tau_1} , \tag{167}$$

where κ_c and τ_1 refer to the ultraviolet continuum. Hence, in this case we may also write

$$\Pi(x) = \frac{1}{c} 8\pi\mu_1^3 D\nu \frac{\rho\kappa_c}{\tau_1} \int_0^{y_1} [\psi_{+1}(x \;\; y) - \psi_{-1}(x \;\; y)] \, dy . \tag{168}$$

6. *The radiation pressure in Lyman-α in an expanding planetary nebula.*—With the solution of the transfer problem completed in the preceding sections, we are now in a

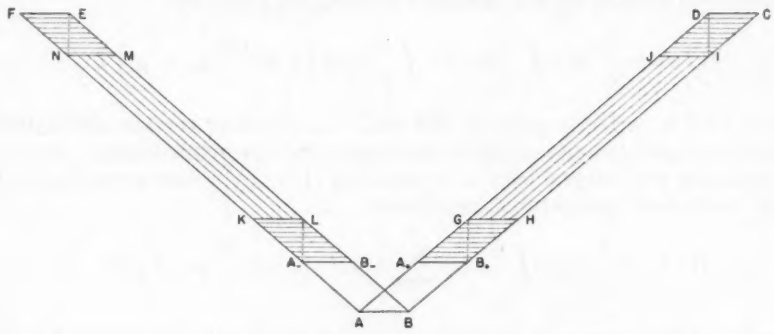

FIG. 4

position to answer the question raised in the introductory section, namely, as to how effective differential expansion can be in reducing the magnitude of the radiation pressure in Lyman-α which will otherwise act. As we shall presently see, the case of greatest interest in this connection arises when

$$D\nu > \frac{2}{\mu_1} \Delta\nu \tag{169}$$

or, alternatively, when (cf. eq. [56])

$$y_1 < \tfrac{1}{2} x_1 . \tag{170}$$

When (170) is the case, for

$$y_1 \leqslant x \leqslant x_1 - y_1 , \tag{171}$$

the solution for the radiation field is known explicitly and is given by equations (104) and (105) (see Figs. 3 and 4, where the regions so defined are indicated). The range (171) for x corresponds to the range

$$\frac{y_1}{x_1} \leqslant \frac{t}{t_1} \leqslant 1 - \frac{y_1}{x_1} \tag{172}$$

for the optical depth t. Since (cf. eq. [56])

$$\frac{y_1}{x_1}=\frac{1}{\mu_1}\frac{\Delta\nu}{D\nu}, \tag{173}$$

we can re-write (172) in the form

$$t_1\frac{1}{\mu_1}\frac{\Delta\nu}{D\nu}\leqslant t\leqslant t_1\left(1-\frac{1}{\mu_1}\frac{\Delta\nu}{D\nu}\right). \tag{174}$$

We shall refer to the part of the nebula included in the range of optical depths specified by (174) as the *central part* of the nebula. Similarly, we shall refer to the parts included in

$$0<t<t_1\frac{1}{\mu_1}\frac{\Delta\nu}{D\nu} \tag{175}$$

and

$$t_1\left(1-\frac{1}{\mu_1}\frac{\Delta\nu}{D\nu}\right)<t<t_1 \tag{176}$$

as the *outer* and the *inner* parts of the nebula, respectively. It should be emphasized at this point that this distinction between the outer, central, and inner parts of a nebula applies only to those cases in which the Doppler width, $2D\nu$, exceeds the line width, $2\Delta\nu$, by a factor $2\sqrt{3}$.

We shall now show how the selective radiation pressure in the central part of a nebula can be estimated. From equations (104) and (105) we find that

$$\left.\begin{aligned}\psi_{+1}-\psi_{-1}=2Qe^{ax}\Big[&\frac{e^{-y}}{\sqrt{(1+a^2)}}\sinh\{y\sqrt{(1+a^2)}\}\\&+e^{+y}\cosh\{y\sqrt{(1+a^2)}\}-1\Big];\end{aligned}\right\} \tag{177}$$

and, since we have assumed that $y_1<\frac{1}{2}x_1$, this solution is valid for the entire range of y for x in the range (171).

Now, according to equation (168), the radiation pressure in Lyman-α is related directly to the integral of $\psi_{+1}-\psi_{-1}$ over the line; and this can be readily found from the solution (177). We have

$$\left.\begin{aligned}\int_0^{y_1}(\psi_{+1}-\psi_{-1})\,dy=2Qe^{ax}\Big\{&\frac{e^{-y_1}}{a^2}\Big[2\cosh\{y_1\sqrt{(1+a^2)}\}\\&+\frac{2+a^2}{\sqrt{(1+a^2)}}\sinh\{y_1\sqrt{(1+a^2)}\}\Big]-\frac{2}{a^2}-y_1\Big\}\quad(y_1\leqslant x\leqslant x_1-y_1).\end{aligned}\right\} \tag{178}$$

Inserting this value in equation (168) and substituting also for Q according to equation (75), we obtain

$$\left.\begin{aligned}\Pi(x)=\left(\frac{\pi\rho\kappa_c}{c}\frac{\nu_0}{\nu_c}S_c\right)2\mu_1^2\frac{D\nu}{\Delta\nu}\frac{e^{-(\tau_1-\tau)}}{\tau_1}\Big\{&\frac{e^{-y_1}}{a^2}\Big[2\cosh\{y_1\sqrt{(1+a^2)}\}\\&+\frac{2+a^2}{\sqrt{(1+a^2)}}\sinh\{y_1\sqrt{(1+a^2)}\}\Big]-\frac{2}{a^2}-y_1\Big\},\end{aligned}\right\} \tag{179}$$

where we have further used the relation $ax=\tau$ (eq. [69]).

The full implications of equation (179) are best understood when we expand the quantity in braces in powers of a and retain the first nonvanishing term. We find in this manner that

$$\Pi = \left(\frac{\pi\rho\kappa_c}{c}\frac{\nu_0}{\nu_c}S_c\right) 2\mu_1^2 \frac{D\nu}{\Delta\nu}\frac{e^{-(\tau_1-\tau)}}{\tau_1}\left\{\frac{a^2}{4}[y_1^2 - y_1 + \tfrac{1}{2}(1-e^{-2y_1})] + O(a^4)\right\}. \quad (180)$$

A further simplification of this equation is possible. Since y_1 is a large quantity of the order of 10^3 or 10^4, we may write, to a sufficient accuracy,

$$\Pi = \left(\frac{\pi\rho\kappa_c}{c}\frac{\nu_0}{\nu_c}S_c\right)\tfrac{1}{2}\mu_1^2\frac{D\nu}{\Delta\nu}\frac{e^{-(\tau_1-\tau)}}{\tau_1}a^2y_1^2. \quad (181)$$

But (cf. eqs. [69] and [173])

$$a y_1 = \frac{1}{\mu_1}\frac{\Delta\nu}{D\nu}a x_1 = \frac{1}{\mu_1}\frac{\Delta\nu}{D\nu}\tau_1. \quad (182)$$

Equation (181) therefore reduces to

$$\Pi(x) = \left(\frac{\pi\rho\kappa_c}{c}\frac{\nu_0}{\nu_c}S_c\right)\frac{1}{2}\frac{\Delta\nu}{D\nu}\tau_1 e^{-(\tau_1-\tau)} \quad (y_1 \leqslant x \leqslant x_1 - y_1). \quad (183)$$

In other words, *in the central part of a nebula the radiation pressures due to Lyman-α and the Lyman continuum are of the same order of magnitude.*

Now for the case $p = 0$ (no re-emission in the Lyman continuum), the selective radiation pressure which will act in a static nebula can be readily written down. We must clearly have

$$\Pi_{\text{static}} = \left(\frac{\pi\rho\sigma_0}{c}\frac{\nu_0}{\nu_c}S_c\right)[1 - e^{-(\tau_1-\tau)}]. \quad (184)$$

From a comparison of equations (183) and (184) the remarkable result emerges that if a differential expansion to the extent required by equation (169) exists, then in the central part of the nebula the radiation pressure in Lyman-α is effectively cut down by a factor of the order of 10^4.

We cannot, of course, expect that the large reduction in the radiation pressure achieved in the central part will be maintained throughout the nebula. We should rather expect certain "edge effects." To investigate the nature of these edge effects in detail, we need the radiation field in regions where the solution can be found only by quadratures (cf. §4, subsec. *f*). However, we can estimate the radiation pressure acting on the outer and the inner boundaries of the nebula, and these might provide some indications.

At $\tau = 0$ the inward intensity $\psi_{-1}(0, y)$ vanishes, and the radiation pressure depends only on the integral of the outward intensity $\psi_{+1}(0, y)$ over the line. Using the solution (127) for $\psi_{+1}(0, y)$, we have, for the radiation pressure acting at $\tau = 0$,

$$\left.\begin{aligned}\Pi(0)\left(=\frac{\pi\rho\kappa_c}{c}\frac{\nu_0}{\nu_c}S_c\right)\mu_1^2\frac{D\nu}{\Delta\nu}\frac{e^{-\tau_1}}{\tau_1}\\ \times\left[a\int_0^{y_1}e^{-y}\{I_0(y) + 2y[I_0(y) + I_1(y)] - e^y\}dy + O(a^2)\right].\end{aligned}\right\} \quad (185)$$

It does not appear that the integrals over the Bessel functions occurring in equation (185) can be evaluated explicitly. However, its asymptotic value for large y_1 can be readily found. We have

$$\left.\begin{aligned}\int_0^{y_1}e^{-y}\{I_0(y) + 2y[I_0(y) + I_1(y)] - e^y\}dy\\ \rightarrow\frac{4}{(2\pi)^{\frac{1}{2}}}\int_0^{y_1}y^{\frac{1}{2}}dy = \frac{8}{3(2\pi)^{\frac{1}{2}}}y_1^{3/2}.\end{aligned}\right\} \quad (186)$$

Using this result in equation (185), we obtain

$$\text{II}(0) \simeq \left(\frac{\pi\rho\kappa_c}{c}\frac{\nu_0}{\nu_c}S_c\right)\frac{8}{3(2\pi a)^{\frac{1}{2}}}\mu_1^2\frac{D\nu}{\Delta\nu}\frac{e^{-\tau_1}}{\tau_1}(a y_1)^{3/2}. \qquad (187)$$

Substituting for ay_1 from equation (182), we finally have

$$\text{II}(0) \simeq \left(\frac{\pi\rho\kappa_c}{c}\frac{\nu_0}{\nu_c}S_c\right)\frac{8}{3}\left(\frac{\mu_1\tau_1}{2\pi a}\frac{\Delta\nu}{D\nu}\right)^{\frac{1}{2}}e^{-\tau_1}. \qquad (188)$$

Accordingly, at $\tau = 0$, the radiation pressure due to Lyman-α is cut down only by a factor of the order of $\sqrt{(D\nu/a\Delta\nu)}$. We may, therefore, expect that in the outer parts of a nebula the radiation pressure due to Lyman-α will be appreciable, though it is not likely to exceed the radiation pressure due to the Lyman continuum by any very large factor.

The radiation pressure acting at $\tau = \tau_1$ will depend on the boundary conditions here. If we suppose that the inner boundary is at rest with respect to the central star (case I), the radiation pressure at $\tau = \tau_1$ vanishes identically, simply in virtue of the boundary conditions. But this will not clearly be true of the rest of the inner part, and it is likely that a truer estimate of the radiation pressure which may act in these regions is to be found from that acting at $\tau = \tau_1$ in our case III. It will be recalled that this case arises when the Doppler shift, owing to the velocity at the inner boundary, exceeds the line width by a factor $\sqrt{3}/2$ (eq. [34]). When this happens, ψ_{+1} vanishes at $\tau = \tau_1$, but there is a net flux directed *inward* owing to the nonvanishing of ψ_{-1}. Since the solution (157) for $\psi_{-1}(x_1, y)$ in case III is similar in form to the solution (127) for $\psi_{+1}(0, y)$, we can at once write down (cf. eq. [188])

$$\text{II}(\tau_1) \simeq \left(\frac{\pi\rho\kappa_c}{c}\frac{\nu_0}{\nu_c}S_c\right)\frac{8}{3}\left(\frac{\mu_1\tau_1}{2\pi a}\frac{\Delta\nu}{D\nu}\right)^{\frac{1}{2}} \qquad \text{(case III)}. \qquad (189)$$

which has the same validity as equation (188). A comparison of equations (188) and (189) suggests that, in general, we may expect that the order of magnitude of the radiation pressure acting in the outer and the inner parts will be about the same.

We may summarize the results of our discussion so far in the following general terms.

In a static nebula, selective radiation pressure in Lyman-α is so large that we may expect a differential expansion to set in. This will have a tendency to reduce the magnitude of the radiation pressure acting. But the reduction, while it would set in only gradually, becomes suddenly very effective when the differential expansion present exceeds a certain critical value. On the basis of our calculations we expect reduction factors of the order of 10^4 over at least parts of the nebula when the Doppler shift due to the difference in velocities at the inner and outer voundaries exceeds the undisplaced line width by a factor of the order of 3.5. When this happens, the nebula may be divided into a central part and the edges. In the central part, selective radiation pressure is cut down effectively to zero, while at the edges it may still be appreciable.

An exact discussion of the dynamics of a planetary nebula, which will properly take into account the rather complex manner in which radiation pressure in Lyman-α acts, is likely to be a problem of considerable difficulty. But we may expect that a nebula, initially static, will "feel its way" to a state in which the parts we have described as central are fairly extensive; for such a state will have the character of quasi-stationariness, and dissipation, to the extent that it is present, will be confined only to the inner and the outer edges. We can expect such a quasi-stationary state to be reached, since the effectiveness with which selective radiation pressure acts is controlled very sensitively when the differential expansion has reached a certain stage.

7. *The role of radiation pressure in Lyman-α in other astrophysical problems.*—The

manner and effectiveness of operation of the radiation pressure in Lyman-α which we have described in the preceding section is likely to have a bearing on other astrophysical problems besides that of emission nebulae. Here we shall make reference to only two such groups of problems.

The first of these relates to the problem of gaseous shells surrounding Be stars. As Struve[15] has pointed out, the clue to the variety of questions which a study of these interesting stars raises is probably to be found in the manner in which the radiation pressure in Lyman-α acts on these shells. While a detailed discussion of these questions is beyond the scope of this investigation, we may refer particularly to the fact to which Struve has called attention, namely, that the atmospheres of these stars appear to consist of three separate layers: a normal reversing layer, a relatively stationary but extensive shell, and an extreme outer part which is expanding. This division of the atmosphere into three parts is strongly reminiscent of our own distinction of the inner, the central, and the outer parts of a planetary nebula. It is, moreover, not inconceivable that the very capriciousness of the phenomena exhibited by the Be stars is to be understood in terms of the extreme sensitiveness with which the effectiveness of the radiation pressure in Lyman-α is controlled by the extent of the differential expansion present.

A second group of problems to which we wish to make reference relates to the spheres of ionized hydrogen surrounding luminous early-type stars. As B. Strömgren[16] has particularly called attention, the conversion of the radiation in the Lyman continuum into radiation in Lyman-α (in the manner of Zanstra's theory) is a principal feature of this problem. We cannot, therefore, escape the conclusion that something of the sort which we expect to happen in a planetary nebula also happens in these ionized hydrogen regions. And it is interesting to speculate on the bearing of this, in turn, on the still larger problems of the interstellar clouds.

From the foregoing brief discussion it is apparent that the clue to the understanding of a great many astrophysical problems may lie in the very remarkable manner in which the radiation pressure in Lyman-α operates in an expanding atmosphere.

[15] *Ap. J.*, **95**, 134, 1942. The writer is indebted to Dr. O. Struve for illuminating discussions of these and other stellar spectroscopic problems.

[16] *Ap. J.*, **89**, 526, 1939.

CURVE OF GROWTH FOR δ CANIS MAJORIS*

HELEN R. STEEL[1]
Yerkes Observatory
Received August 10, 1945

ABSTRACT

A curve of growth for *Fe* I in δ Canis Majoris is plotted from O'Keefe's measures of the equivalent widths of 62 lines and from Menzel and Goldberg's solar log X'_0 values. The excitation temperature for *Fe* I is approximately 4400°. The value of v, obtained by superposition of the observational curve on the theoretical curve of growth, is 5.1 km/sec. Eye estimates of relative intensities of lines originating from normal and metastable levels are compared in δ Canis Majoris, the sun, and α Canis Minoris. No evidence of dilution is found, but the possibility of small dilution effects is not excluded.

The determination of the turbulent velocity in δ Canis Majoris, a highly luminous star, and a search for dilution effects should prove interesting. W. W. Morgan[2] gives F8 I*a* for the spectral type of δ Canis Majoris. The visual absolute magnitude[3] is about −7.0. Several years ago Dr. J. O'Keefe, then an assistant at the Yerkes Observatory, measured the equivalent widths of a number of lines in the spectrum of δ Canis Majoris. When he left for war research elsewhere, he gave the measures to Dr. O. Struve, who turned them over to me to determine the physical conditions in the atmosphere of this star. The next section contains a description of the observational material and Dr. O'Keefe's method of reduction.

OBSERVATIONAL DATA

For the intensity measures Dr. O'Keefe used plates taken by P. Swings and O. Struve with the coudé spectrograph of the McDonald Observatory. Photographs of parts of the spectrograms have been published in J. L. Greenstein's[4] article on α Carinae. The region λλ 3800–6700 is covered with considerable overlap by two settings of the prisms in the autocollimating prism train of the spectrograph. The measures in the region λλ 4100–4334 were from a 2-hour and 30-minute exposure taken on January 22, 1941, on Eastman I*a*-O emulsion. A 45-minute exposure taken on February 12, 1941, also with the "blue" setting of the prisms and on an Eastman I*a*-O plate, provided measures in the region λλ 4334–4620. Measures in the region λλ 4620–6520 were from a 4-hour exposure taken on January 27, 1941, with the "red" setting of the prisms. The plate for the "red" setting was an Eastman 103-F. The dispersion on the "blue" setting ranged from 2.5 to 4 A/mm; on the "red" setting, from 2.5 to 4 A/mm at $H\beta$ and about 15 A/mm at λ 6600.

A tube photometer equipped with blue, green, and red filters provided the calibrations for the spectrograms. The plates were traced, at a magnification of thirty times, with the Yerkes microphotometer.

Apparently no line was measured on tracings from more than one plate. Therefore we cannot estimate the size of systematic errors arising from instrumental, photographic, and development effects and from the characteristic curve, change of dispersion, and position assumed for the continuum. This is especially unfortunate, since appreciable

* *Contributions from the McDonald Observatory, University of Texas*, No. 113.

[1] National Research Fellow at the Yerkes Observatory in 1944.

[2] Morgan, Keenan, and Kellman, *Atlas of Stellar Spectra*, Chicago: University of Chicago Press, 1943.

[3] J. L. Greenstein, *Proc. Nat. Acad. Sci.*, **26**, 259, 1940.

[4] *Ap. J.*, **95**, 161, 1942.

systematic differences have been found[5] to exist between measures from plates of the "blue" setting and those of the "red," taken at about the same time and presumably under the same conditions as the spectrograms used by O'Keefe. Such systematic differences undoubtedly account for some of the scatter in the curve of growth for δ Canis Majoris.

For about 20 lines Dr. O'Keefe measured the areas and obtained the equivalent widths in millimeters on the tracing. Of those 20 lines, about one-third were in the blue, one-third in the green, and one-third in the red. Each color group contained strong, weak, and intermediate lines. Dr. O'Keefe tried a second method for the determination of the equivalent widths. With a ruler he prolonged the most nearly straight portion of the line contour on the tracings, on each side of the line center, until it met the continuum. Then he measured the width, D, between the points of intersection of the prolonged contour with the continuum. For each of the lines the product of $D \times I$, the intensity at the center of the line, was then plotted against the equivalent width in millimeters, obtained from the area of the original contour. Dr. O'Keefe found the two quantities to be proportional to

TABLE 1

EQUIVALENT WIDTHS OF *Fe* I LINES IN THE SPECTRUM OF δ CANIS MAJORIS

λ	$-\log W/\lambda$	λ	$-\log W/\lambda$	λ	$-\log W/\lambda$	λ	$-\log W/\lambda$
4147.68.....	4.00	5012.09.....	4.08	5405.79.....	4.02	6003.15.....	4.58
4157.78.....	4.11	5049.83.....	4.19	5434.56.....	4.17	6024.02.....	4.41
4175.66.....	3.94	5067.23.....	4.88	5445.06.....	4.06	6056.08.....	4.69
4199.97.....	4.59	5074.77.....	4.32	5497.51.....	4.14	6065.52.....	4.34
4210.38.....	3.95	5150.87.....	4.38	5506.84.....	4.27	6173.22.....	4.74
4404.77.....	4.19	5151.97.....	4.64	5554.92.....	4.54	6180.29.....	4.51
4476.05.....	4.10	5162.30.....	4.31	5569.56.....	4.32	6213.44.....	4.52
4733.58.....	4.61	5229.91.....	4.69	5572.91.....	4.26	6230.77.....	4.26
4772.80.....	4.54	5281.76.....	4.69	5576.09.....	4.57	6254.19.....	4.66
4787.89.....	5.60	5307.25.....	4.61	5615.64.....	4.10	6265.09.....	4.62
4903.30.....	4.15	5324.21.....	4.28	5624.66.....	4.24	6335.30.....	4.64
4907.80.....	4.75	5341.04.....	4.17	5678.87.....	4.69	6336.88.....	4.65
4919.01.....	3.98	5373.74.....	4.86	5705.97.....	4.52	6393.67.....	4.45
4946.39.....	4.46	5389.51.....	4.61	5731.81.....	4.67	6411.47.....	4.33
4950.20.....	4.84	5393.18.....	4.28	5859.75.....	4.76		
4966.09.....	4.44	5400.52.....	4.48	5976.76.....	4.76		

each other. He used the constant of proportionality and measures of D and I to determine the equivalent widths of additional lines. These additional lines were those which appeared on the tracing to be unblended and for which T. Dunham's[6] identifications for α Persei indicated no blending. The final values of the equivalent widths, W, were corrected for the magnification of the tracings and the dispersion of the spectrograms. Table 1 contains $-\log W/\lambda$ for 62 *Fe* I lines.

CURVE OF GROWTH AND DILUTION EFFECTS

By plotting $\log W/\lambda$ against factors proportional to the optical depth at the line center, X_0, we obtain an observational curve of growth. In this work Menzel and Goldberg's solar $\log X_0'$ values, with the Boltzmann factor added, were used. A curve of growth was plotted for an assumed excitation temperature of 4400°, and another curve for a temperature of 4000°. As there is a great deal of scatter in the curves of growth, it is difficult to determine the temperature with accuracy. The temperature probably is not greater than 4400°—certainly not by more than one or two hundred degrees, since

[5] H. R. Steel, *Ap. J.*, **102**, 43, 1945.

[6] *Contr. Princeton Obs.*, No. 9, 1929.

at a higher temperature there would be a displacement of the points for lines of high excitation potential relative to those for lower excitation potential lines. The points for lines of different excitation potentials appear to lie more nearly together along a curve in the 4400° than in the 4000° plot. The 4400° curve (Fig. 1) has therefore been adopted as the curve of growth for *Fe* I in δ Canis Majoris.

An excitation temperature of 4400° is of the order of the temperatures found for other F-type supergiants: i.e., 4900° for α Carinae,[4] F0; 4400° for α Persei,[5] F5; and 4400° for γ Cygni,[7] F8.

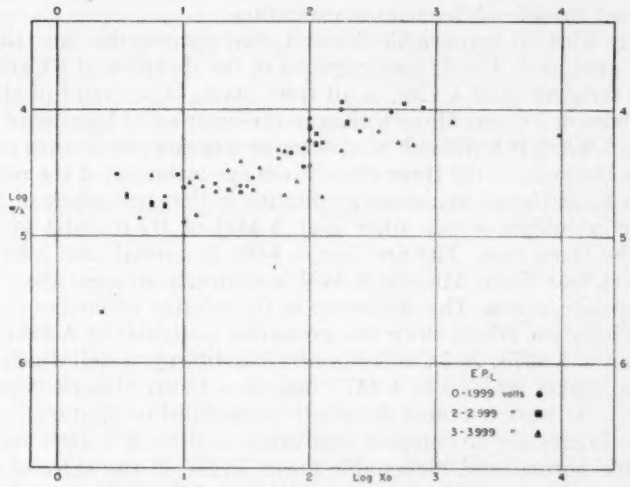

FIG. 1.—Curve of growth for *Fe* I in δ Canis Majoris

According to theory, we may plot $(W/\lambda)\ (c/v)$ as a function of X_0 and Z, where Z is given by

$$Z = \frac{\Gamma c}{\nu v}.$$

D. H. Menzel[8] has derived expressions for the three parts of the curve of growth, the 45°, the flat, and the damping portions. These portions may be joined to form a smooth theoretical curve of growth.

The vertical shift necessary for superposition of the observational on the theoretical curve determines c/v and, consequently, v. For δ Canis Majoris the velocity is 5.1 km/sec. Using the formula[9]

$$v_T^2 = v^2 - v_0^2$$

to remove[10] the thermal contribution to v, we obtain 4.9 km/sec for the turbulent velocity, v_T. The turbulent velocity of δ Canis Majoris is considerably larger than that of α Carinae[4] (v = 3.5 km/sec) and that of α Persei[5] (3.4 km/sec). The broad lines of δ Canis Majoris also lead one to expect a greater turbulent velocity than for α Carinae and α Persei.

[7] K. O. Wright, *Pub. A.A.S.*, **10**, 338, 1940.

[8] *Ap. J.*, **84**, 462, 1936.

[9] L. Goldberg, *Ap. J.*, **89**, 623, 1939.

[10] The thermal velocity, v_0, is that for G. Kuiper's value of the effective temperature (*Ap. J.*, **88**, 429, 1938).

As the points in Figure 1 do not cover the damping portion of the curve of growth, we cannot determine the damping constant.

The phenomenon of turbulence has been found[11] in supergiant atmospheres. It is interesting to investigate further the properties of the atmospheres of the very luminous stars. Dr. Struve suggested a search for dilution effects.

When radiation is diluted, lines originating from normal levels are weakened relative to lines originating from metastable levels.[12] For the investigation of dilution effects we select two *Fe* I lines: a normal line, λ 4260, and a metastable line, λ 4282. The lower excitation potentials of these lines are so nearly the same—2.4 and 2.2 volts, respectively—that we need not consider differences in excitation.

As standards with no appreciable dilution, two dwarfs, the sun (G0) and α Canis Minoris (F5), were used. Coudé spectrograms of the dwarfs and δ Canis Majoris show that λ 4260 is stronger than λ 4282 in all three stars. On account of the much greater widths of the lines in δ Canis Majoris than in the dwarfs and because of the closeness of another line to λ 4260, it is difficult to determine whether the intensity ratios of λ 4260 and λ 4282 are the same in the three stars. From eye estimates of the relative intensities it appears that λ 4260 is not weakened by dilution in the atmosphere of δ Canis Majoris.

The relative intensities of two other lines, λ 4481 of *Mg* II and λ 4473 of *Fe* II, were compared in the three stars. The first line, λ 4481, is normal; and λ 4473 has a metastable lower level. In α Canis Minoris, λ 4481 is definitely stronger than λ 4473, while in the sun the opposite is true. This difference in the relative intensities in the two stars is probably an excitation effect, since the excitation potential of λ 4481 is considerably higher than that of λ 4473. In δ Canis Majoris it is difficult to tell which line is stronger. That λ 4481 is weaker relative to λ 4473 than in α Canis Minoris is probably also an excitation effect. At least it cannot definitely be ascribed to dilution.

It would be interesting to compare equivalent widths of λ 4260 and λ 4282 and of other lines with normal and metastable lower levels, in the three stars, to establish definitely whether dilution effects are appreciable in δ Canis Majoris. From this examination by eye no definite evidence of dilution has been found; it seems probable, but not certain, that dilution effects are not present.

I wish to thank Dr. Struve for his suggestion of this investigation, and for the use of Dr. O'Keefe's measures.

[11] See, e.g., Struve and Elvey, *Ap. J.*, **79**, 409, 1934.

[12] Struve, *Proc. Amer. Phil. Soc.*, **81**, 211, 1939.

THE SPECTROSCOPIC ORBIT OF TU MONOCEROTIS*

ARMIN J. DEUTSCH
Yerkes and McDonald Observatories
Received August 16, 1945

ABSTRACT

From measures of 27 spectrograms of the eclipsing binary TU Monocerotis, it is found that the lines of *He* I give a velocity-curve from which the following elements can be derived: P (photometric) = 5.049 days; T = 0.210 days after primary minimum; K = 55 km/sec; γ = +20 km/sec; e = 0.2; ω = 115°; $a \sin i = 3.8 \times 10^6$ km; and $f(m)$ = 0.09. The hydrogen lines give velocities which scatter widely about the γ-axis of the *He* I velocity-curve but which do not themselves indicate orbital motion. The line *Ca* II K gives a velocity-curve which is 180° out of phase with *He* I and with about twice the amplitude. The K line exhibits pronounced changes in appearance, which are associated with the secondary eclipse. The spectra indicate a brighter secondary star than is compatible with Gaposchkin's photometric elements.

The brightness of the eclipsing binary TU Monocerotis was estimated on 548 Harvard plates by E. Hertzsprung.[1] He finds that

$$\text{Principal minimum} = \text{JD } 2420930.57 + 5.049011\ E.$$

The light-curve is of the Algol type, with no constant phase during minimum but "showing a minimum at the place of the secondary minimum and a maximum rather nearer to the secondary than to the primary minimum in accordance with a combined ellipticity and reflection effect."[1] The light-range is from $m_{pg} = 9.0$ to $m_{pg} = 10.9$.

S. Gaposchkin[2] concludes from Hertzsprung's light-curve that the depth of secondary minimum is 0.13 mag. and that primary minimum has a semiduration of $0^d.071 = 8^h.6 = 26°$. These figures are compatible with Hertzsprung's curve, although the semiduration may be considerably greater. Gaposchkin also gives the depth of primary minimum as 0.97 mag., which value is not compatible with Hertzsprung's curve. If Gaposchkin has used this value in his derivation of the photometric elements, they also must be inconsistent with Hertzsprung's observations. In any case, he finds that principal minimum occurs at a partial eclipse of the smaller, brighter star by the larger, fainter one, his values of the ratio k of radii being 0.90 and 0.85 for the undarkened and the darkened solutions, respectively. According to his solution, the brighter star is responsible for at least 94 per cent of the light of the system. Taking the type of the primary as B8, he then infers the type of the secondary to be late G. He finds the inclination $i = 80°$ in both solutions.

Twenty-eight spectrograms of TU Monocerotis were secured last winter at the McDonald Observatory with the Cassegrain quartz spectrograph and the 500-mm camera. All plates were taken on Eastman 103*a*-O emulsion; at maximum light the exposures ran about 40 minutes, but during principal minimum about 2 hours were required. The slit width was 0.075 mm. The dispersion is 55 A/mm at $H\gamma$. Plate XXXI exhibits spectrograms at five different phases; the last two were taken at principal minimum. Since the star was found to be faint at the times predicted by Hertzsprung's formula, the latter was used to calculate the phases. Phases are counted from principal minimum throughout this paper.

At phase 214°, the spectrum is seen to be typical of type B5, with *Ca* II K a little stronger than usual and with the helium lines less broad than is often the case. The hydrogen lines are heavily winged but are not unusually broad. The K line changes its character quite abruptly at 140° and again near 220°; within this interval of phase it is usually sharp and strong, although there may be slight changes in its appearance. At

* *Contributions from the McDonald Observatory, University of Texas*, No. 114.

[1] *B.A.N.*, **4**, 155, 1928.

[2] *Veröff. Berlin-Babelsberg*, Vol. **9**, Part V, 1932.

phases earlier than 140° and later than 220° the K line is broad and diffuse; on a few plates there is a suggestion that a sharp line is unsymmetrically superposed on a broad one. The lines of *He* I look wider at 300° than at 214°, as is apparent in Plate XXXI, and the lines seem a little shallower. Hydrogen may be similarly affected. These effects are probably synchronized with the variation of K, but they are smaller and are uncertain on many of the plates. Since the 28 spectrograms are distributed over five cycles, there is every reason to suppose that all these changes repeat themselves with the period of the light-variation.

TABLE 1

RADIAL VELOCITIES OF TU MONOCEROTIS

PLATE CQ	U.T.	PHASE	*H*		*He* I		*Ca* II
			R.V. (Km/Sec)	*N*	R.V. (Km/Sec)	*N*	R.V. (Km/Sec)
4330	1945 Jan. 12.408	4°	+34	2	.....	.....	.....
4226	1944 Dec. 23.267	8	− 1	4	.....	.....	+ 19
4308*	1945 Jan. 8.276	69	+31	5	− 47	6	+127
4335*	1945 Jan. 13.432	77	+12	5	− 16	5	+174
4291	1945 Jan. 3.341	77	+33	5	− 35	6	+151
4336	1945 Jan. 13.464	79	+28	4	− 11	4	+170
4244	1944 Dec. 24.288	80	+30	5	− 56	4	+146
4181	1944 Dec. 19.297	85	+69	2	− 9	4	+197
4312	1945 Jan. 9.259	139	+40	5	+ 40	6	+ 96
4293	1945 Jan. 4.253	142	+46	5	+ 14	5	+ 46
4340	1945 Jan. 14.391	145	+28	5	+ 2	5	+ 57
4341*	1945 Jan. 14.428	148	+ 6	5	− 26	5	+ 69
4315	1945 Jan. 9.459	153	+ 6	2	+ 16	4	.....
4196	1944 Dec. 20.295	155	+22	5	− 8	6	+ 63
4318*	1945 Jan. 10.272	211	+38	5	+ 24	5	− 8
4345	1945 Jan. 15.407	218	+38	2	+ 51	5	+ 7
4325	1945 Jan. 11.347	218	+29	5	+ 98	4	− 76
4207	1944 Dec. 21.235	222	+22	4	+ 58	6	.....
4324	1945 Jan. 11.281	283	+39	5	+ 67	5	−229
4301	1945 Jan. 6.314	290	+49	5	+105	6	− 74
4263	1944 Dec. 31.265	293	+21	4	+ 50	6	.....
4303	1945 Jan. 6.453	299	+24	5	+ 79	7	−175
4218	1944 Dec. 22.316	300	+62	5	+121	1	− 61
4146	1944 Dec. 17.350	306	+48	5	+ 40	5	− 28
4328	1945 Jan. 12.260	353	+35	5	− 6	3	− 9
4329	1945 Jan. 12.330	358	+26	2	.....	.....	+ 18
4306	1945 Jan. 7.290	358	+ 2	2	.....	.....	+ 58

* The plates were measured twice; the mean velocities are recorded.

The two lowermost spectra of Plate XXXI were secured during the partial phase of the principal eclipse. From these plates it is concluded that the secondary component is of type A5. The plates are necessarily weak, of course, but many of the stronger lines of *Fe* I and II, *Ti* II, *Sr* II, *Mg* II, etc., have been identified; some may be detected on the reproductions. *He* I is probably absent from both plates.

Twenty-seven of the spectrograms were measured for radial velocity; the other one was rejected because of excessive temperature-variation during exposure. On all 27 plates I measured as many as possible of the hydrogen lines γ, δ, ζ, η, and ϑ; $H\epsilon$ was avoided because of the blend with *Ca* II H. For each plate the mean radial velocity, reduced to the sun, from the number "*N*" of hydrogen lines measured, is given in Table 1 under "*H*." The average mean error of these velocities is 20 km/sec, which is unusually large, notwithstanding the breadth of the lines. The velocities given in Table 1 under "*He* I" comprise measures of the lines λλ 3820, 4009, 4026, 4121, 4144, 4388, and 4722;

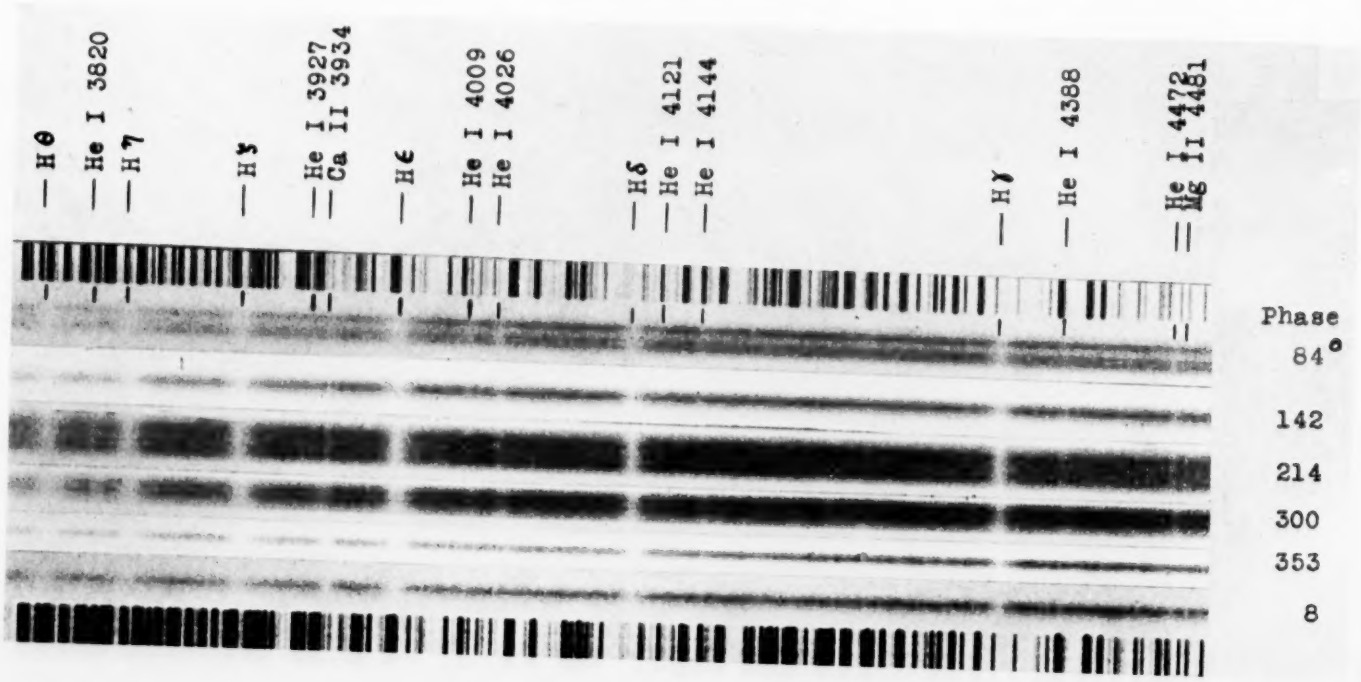

SPECTRA OF TU MONOCEROTIS

The phases are counted from principal minimum; the two lowermost spectra were taken during partial eclipse. Note the changes in the lines of *He* I and in *Ca* II K.

UNIV. OF MICH.

"*N*" again gives the number of lines measured. The mean error of these velocities is 30 km/sec, which is again unusually large. Under "*Ca* II" are given the velocities derived from the K line. Plates CQ 4308, 4335, 4341, and 4318 were measured twice; the two sets of measures were found to be in substantial agreement.

Figure 1 exhibits the velocity-curves derived from the lines of *He* I, *H*, and *Ca* II K, respectively. The plates are poorly distributed over the cycle because the period is so nearly equal to five days. The velocities are seen to scatter badly, as might have been expected from their large mean errors. The lines of *He* I indicate that it is the B5 star which is eclipsed at principal minimum. The velocities from the hydrogen lines scatter about the γ-axis of the *He* I curve, but they do not indicate orbital motion. The K line gives a velocity-curve which is 180° out of phase with that of *He* I and has two or three times the amplitude.

Using Hertzsprung's period, the following spectroscopic elements were derived by the Lehmann-Filhés method from the *He* I velocities:

$$P\,(\text{photometric}) = 5.049011 \text{ days}$$
$$T = 0.210 \text{ days after principal minimum} = 15°$$
$$K = 55 \text{ km/sec}$$
$$\gamma = +20 \text{ km/sec}$$
$$e = 0.2$$
$$\omega = 115°$$
$$a \sin i = 3.8 \times 10^6 \text{ km}$$
$$\frac{m_2^3}{(m_1 + m_2)^2} \sin^3 i = 0.09\ \odot$$

On the assumption that the K line is primarily due to the A5 star, the *Ca* II velocities were fitted with the complementary curve of semi-amplitude $K_2 = 125$ km/sec. This leads to the following results:

$$m_1 \sin^3 i = 2.3\odot\ , \qquad m_2 \sin^3 i = 1.0\odot\ , \qquad \frac{m_2}{m_1} = 0.43\ .$$

The paucity of plates and the very large scatter of the derived velocities render these elements provisional. In particular, no great weight should be attached to the derived value of the eccentricity. Taken at their face value, the K-line velocities would indicate that periastron is on the other side of the orbit; however, the distortion of the curve is in the direction to be expected if K is, in fact, a blend of the lines in the two components.

An attempt was made to derive velocities from the metallic lines which appear on the five spectrograms taken during principal minimum. To this end, all strong lines were measured which are relatively free from blends in the A2 dwarf ϵ Serpentis, according to the wave lengths for lines in that star as published by W. W. Morgan and Miss G. Farnsworth.[3] Table 2 gives the lines measured on each plate, together with the mean radial velocity indicated by those lines, the mean error of the velocity, and the residual O − C from the curve based on the above elements for the A5 star.

The behavior of the K line is most readily interpreted on the hypothesis that it is a blend of the lines in the two components. At maximum light, except in the interval 140°–220°, we apparently observe a blend of the sharp K line of the B5 star and the broad, somewhat shallower K line of the A5 star. The narrowing of the K line between phases 140° and 220° is then to be associated with the eclipse of the A star by the B star. The hydrogen lines must likewise be blended, which accounts for the difficulty in measuring them and for the absence of orbital variation in the velocities. The apparent narrowing of the helium lines during the secondary eclipse remains unexplained.

[3] *Ap. J.*, **76**, 299, 1932.

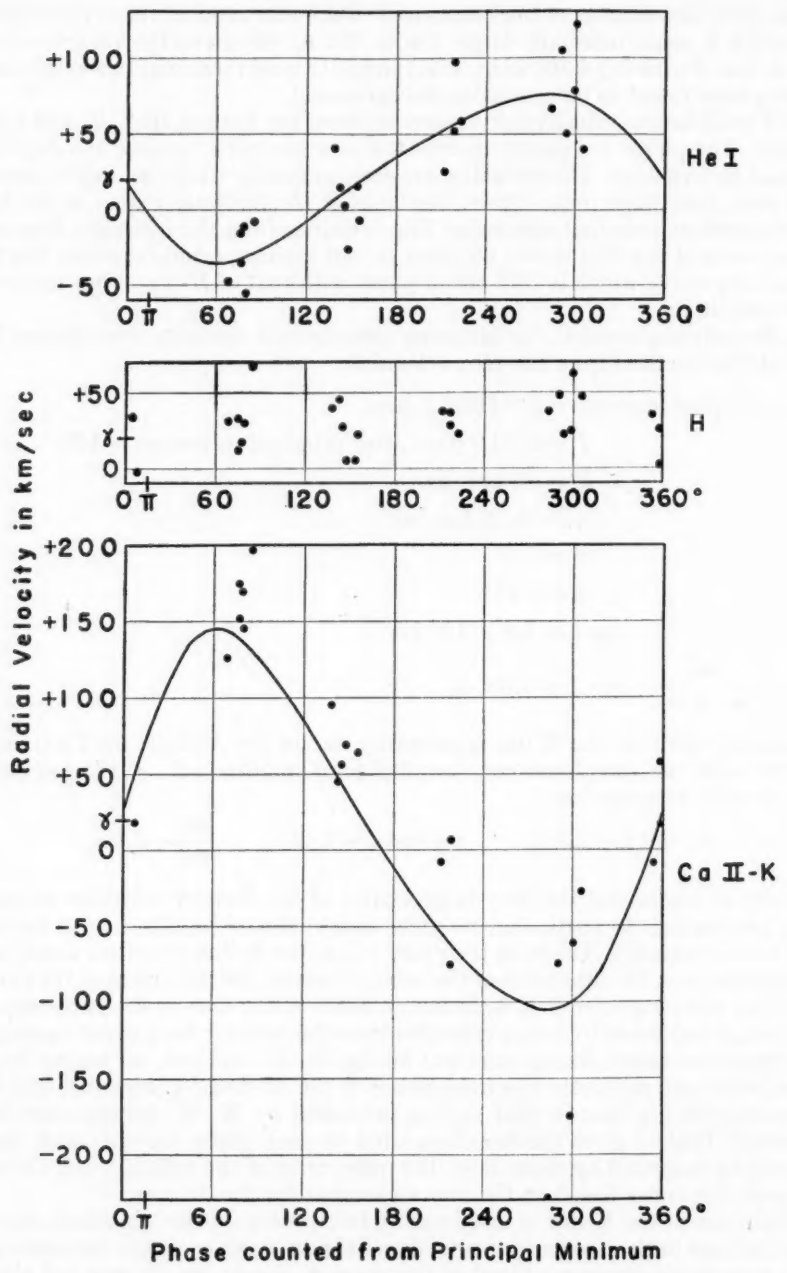

FIG. 1.—Radial velocities of TU Monocerotis. Each point represents a single plate

This hypothesis requires that the A star be comparable in brightness with the B star. Since more than half the light of the system is lost at principal minimum, the star which is eclipsed at principal minimum must be the brighter. If this star is the larger, then we must have, in the notation of Russell,

$$\frac{L_f}{L_b} = \frac{1-\lambda_s}{\alpha_0 - 1 + \lambda_s} \quad \text{and} \quad k^2 = \frac{1-\lambda_p}{\alpha_0 - 1 + \lambda_s};$$

if this star is the smaller, then

$$\frac{L_f}{L_b} = \frac{\alpha_0 - 1 + \lambda_p}{1-\lambda_p} \quad \text{and} \quad k^2 = \frac{1-\lambda_s}{\alpha_0 - 1 + \lambda_p}.$$

In the first case the light-ratio is greatest when α_0 is smallest. Since $k \leq 1$ by definition, the minimum of α_0 is $2 - (\lambda_p + \lambda_s)$. Therefore, the maximum light-ratio in this case is $L_f/L_p = (1 - \lambda_s)/(1 - \lambda_p) = 0.11$. In the second case the light-ratio is greatest when

TABLE 2

RADIAL VELOCITIES OF THE SECONDARY COMPONENT OF TU MONOCEROTIS

CQ Plate	Phase	Lines Measured	R.V. (Km/Sec)	M.E.	O − C
4328.....	353°	*Mn* I 4030.76, *Fe* I 4045.82, *Sr* II 4077.71, *Sr* II 4215.52	+ 6	30	+ 4
4306.....	358	*Fe* I 4260.49, *Fe* I 4325.79, *Y* II 4374.96, *Ti* II 4501.27	+15	32	− 3
4329.....	358	*Fe* I 4045.82, *Sr* II 4077.71, *Fe* I 4260.49, *Fe* II 4385.39, *Fe* II 4416.81, *Fe* II 4491.41	− 7	26	−25
4330	4	*Fe* I 4005.25, *Mn* I 4030.76, *Fe* II 4178.87, *Fe* I 4383.55	+60	19	+20
4226.....	8	*Fe* I 4325.77, *Y* II 4374.96, *Mg* II 4481.23(bl)	+40	8	−12

α_0 is largest, i.e., when the eclipse is total and $\alpha_0 = 1$. In this case, then, the maximum light-ratio is $L_f/L_b = \lambda_p/(1 - \lambda_p) = 0.21$.

Considerations of limb darkening may raise the maximum light-ratio to somewhat more than 0.21. The values of k and γ corresponding to this maximum light-ratio are 0.71 and 9.4, respectively. A ratio of surface brightnesses equal to 9.4 is in good agreement with that to be expected from the spectral types. It appears, then, that the system may comprise a normal B5 star of the main sequence and an A5 star larger by about one-half and fainter by about 1 mag. The relatively long duration of eclipse, however, would seem to require that the stars be larger than normal. Alternatively, the light-ratio can be sufficiently increased on the hypothesis that the B5 star is the larger only if the amplitude of primary minimum has been considerably overestimated and/or the amplitude of secondary minimum considerably underestimated. In any case, a difference in brightness of more than about 1 mag. is wholly incompatible with the spectroscopic phenomena. It is suggested that this system is worthy of further study, both spectroscopically and photometrically.

In conclusion, I wish to thank Drs. O. Struve, W. W. Morgan, J. L. Greenstein, W. A. Hiltner, and Jorge Sahade, all of whom have helped me in one way or another with this investigation.

THE SPECTRUM OF β CORONAE BOREALIS*

W. A. HILTNER†
Yerkes and McDonald Observatories
Received August 24, 1945

ABSTRACT

A high-dispersion spectrogram of β Coronae Borealis has been measured for wave lengths in the region λλ 3980–4638. The identifications show that *Cr* I, *Cr* II, *Fe* I, *Fe* II, *Mg* II, *Sr* II, *Ca* II, and *H* are very strong; *Ca* I, *Mg* I, *Ti* II, and *Ba* II are strong; *Mn* I and *Sc* II are moderately strong; *Si* II, *Mn* II, *Sc* I, *Ti* I, *V* II, *Co* I, *Ni* I, *Ni* II, *Sr* I, *Y* II, and *Zr* II are weak. The singly ionized rare earths are well represented; *Eu* II is very strong, *Ce* II and *Gd* II moderately strong, and all others weak when present.

Intensity tracings of the spectral region λλ 3987–4642 are given in Figures 1–13 and the profile of $H\gamma$ is given in Figure 14.

The star β Coronae Borealis (1900 $\alpha = 15^h23^m.7$, $\delta = +29°27'$, ptm. mag. 3.72, Sp. near F0[1]) is one of the few known bright stars with exceptionally strong europium lines. Neubauer[2] has investigated this star for variation in radial velocity with moderately high dispersion and has derived a period of 10.496 years with an amplitude of 18.18 km/sec. In addition, some evidence was presented for a shorter period (320.13 days, amplitude 2.8 km/sec) superimposed on the longer one. In connection with a general investigation of peculiar bright stars[3,4,5,6] at McDonald Observatory, a high dispersion spectrogram was obtained of β CrB and measured for wave lengths and intensities.

The coudé spectrograph[7] at the McDonald Observatory is of the Littrow type, with one $63\frac{1}{2}°$ prism and one $31\frac{3}{4}°$ prism, both of light flint glass. The diameter of the single lens is 127 mm, and its focal length is 2130 mm. The dispersion of the spectrograph at any given wave length varies with the setting of the prism of smaller angle. The usual blue setting is such that λ 4200 is central in the spectrograph. With this setting, the dispersion is 2.04 A/mm at λ 4000, 3.02 A/mm at λ 4250, and 4.15 A/mm at λ 4500. The photographic plates which have been employed in the spectrograph since October, 1942, are 10 inches long; and with the above setting of the second prism the region from λ 3930 to λ 4640 is obtained—all in excellent focus. Because of the short radius of curvature of the focal plane (0.6 meters), glass plates 0.6–0.7 mm in thickness, backed with a hard gelatin, must be used.

In October, 1942, a calibration device was installed in the coudé spectrograph. It consists of a linear wedge slit that can be inserted in place of the stellar slit, along with an appropriate illumination system. The length of the slit is 16 mm, and the maximum width is 4.0 mm. The range in intensity is approximately 50, but the true value is of secondary importance as long as the slit width varies linearly and the position of zero intensity is known. The illumination system consists of a No. 2 photoflood lamp and a

* *Contributions from the McDonald Observatory, University of Texas*, No. 115.

† The coudé spectrogram was obtained and the intensity tracings were made while the author was a Fellow of the National Research Council.

[1] Morgan, Keenan, and Kellman, *An Atlas of Stellar Spectra*, 1943.

[2] *Ap. J.*, **99**, 134, 1944.

[3] O. Struve and W. A. Hiltner, *Ap. J.*, **98**, 225, 1943.

[4] O. Struve and P. Swings, *Ap. J.*, **98**, 361, 1943.

[5] W. A. Hiltner, *Ap. J.*, **99**, 256, 1944.

[6] W. A. Hiltner and W. W. Morgan, *Ap. J.*, **99**, 318, 1944.

[7] G. Van Biesbroeck, *McDonald Observatory Contribution*, No. 1, p. 103, 1940.

PLATE XXXII

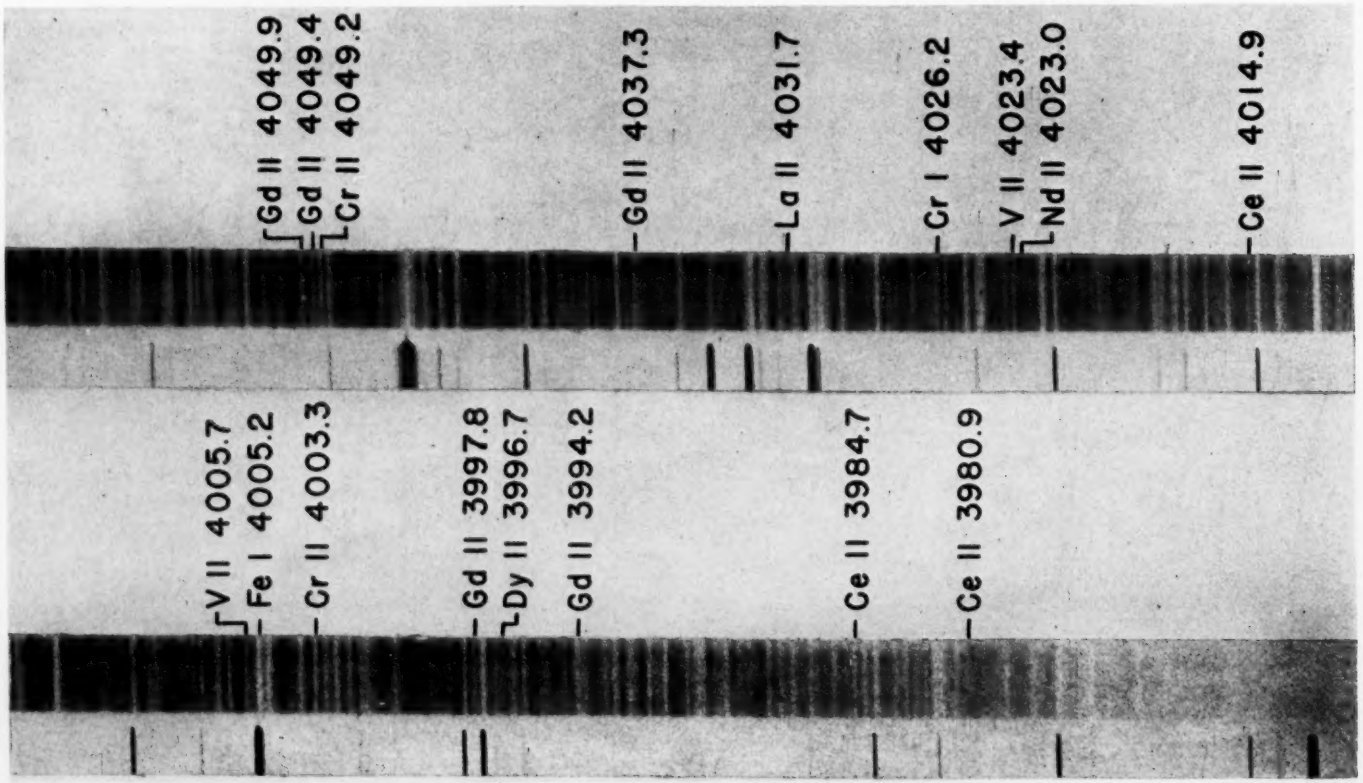

THE SPECTRUM OF β CORONAE BOREALIS

PLATE XXXIII

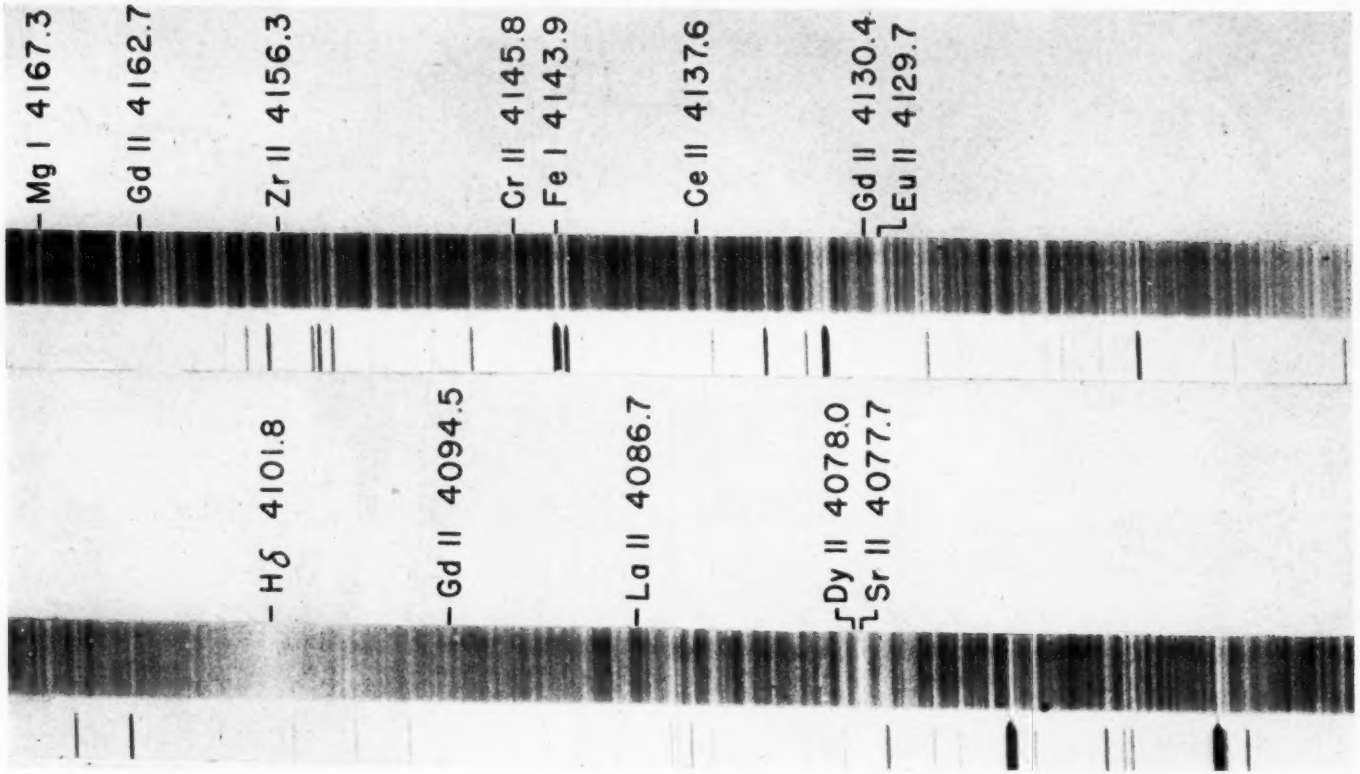

THE SPECTRUM OF β CORONAE BOREALIS

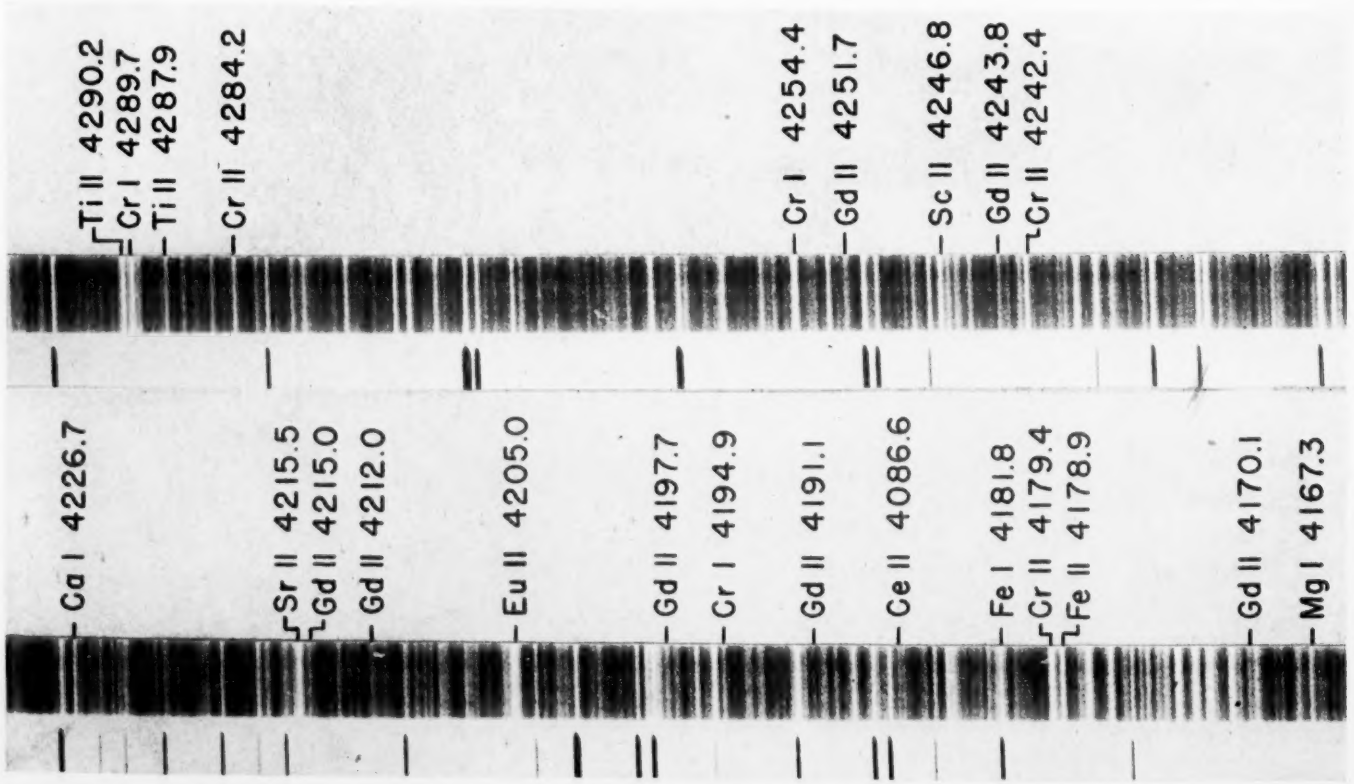

THE SPECTRUM OF β CORONAE BOREALIS

Sm II 4350.5
Ce II 4349.8
Hγ 4340.5
Gd II 4327.1
Gd II 4324.1
Sm II 4319.0
Gd II 4311.0
Gd II 4304.9
Ti II 4300.0
Gd II, 4296.1
Ti II 4443.8
Eu II 4435.6
Sm II 4434.3
Sm II 4424.3
Pr II 4408.8
Gd II 4406.7
Sc II 4374.5

PLATE XXXVI

THE SPECTRUM OF β CORONAE BOREALIS

UNIV. OF MICH.

filter to yield light of a color similar to that of the star under investigation. Since the width of the photographic plate is not sufficient to accommodate the calibration spectra (usually 3–5) as well as the stellar spectrum, the calibration spectra are exposed on separate plates taken from the same box. Normally, the stellar and calibration spectra are brush-developed together in D-76 for 20 minutes.

A spectrogram of β CrB of excellent quality was obtained on May 31, 1943, on Eastman 103a-O baked emulsion with an exposure time of 3^h52^m. The width of the spectrogram is 1.4 mm, a desirable width for general investigations on high-dispersion spectrograms. Reproduction of this spectrogram of β CrB is shown in Plates XXXII–XXXVI.

The spectrogram was measured for wave lengths in six sections, with a short-screw measuring engine commonly used by the author. Wave lengths were determined by the usual Hartmann method and then corrected for radial velocity and curvature of the spectral lines by using the stronger *Fe* I lines in the stellar spectrum. The wave lengths for these *Fe* I lines were taken from Burns and Walter.[8] The correction for radial velocity and curvature increased uniformly from 0.074 A at λ 4000 to 0.087 A at λ 4480, but it then decreased rapidly to 0.050 A at λ 4600.

The wave lengths, estimated intensities, and identifications of approximately 1560 lines in the region λλ 3980–4638 are recorded in Table 1. The first column of Table 1 gives the measured wave length, corrected for radial velocity and curvature. The accidental mean error of a spectral line of moderate intensity (4) is approximately 0.015 A. The estimated intensities are given in the second column. The following abbreviations are used: "n" = diffuse, "nn" = very diffuse, "v" = shaded to violet, and "r" = shaded to red. The estimated intensities are on a scale of 10. An intensity of zero indicates that some doubt exists as to the reality of the line, but only those lines measured in the reverse direction as well as in the direct are listed in the table. The identifications of the measured lines are given in the third column in Table 1. The identifications were first made independently of earlier investigations of stellar spectra and then compared with the investigation on α^2 CVn, a spectrum variable with strong lines of the singly ionized rare-earth elements, spectral class AOp, by Struve and Swings,[9] the investigation on α Car, a supergiant of intermediate luminosity, spectral class near F0, by Greenstein[10] and the investigation on β CrB with low dispersion by Morgan.[11] The laboratory material used for the identifications consisted of Miss Moore's multiplet table, considerable unpublished material loaned to me by O. Struve, King's numerous investigations on the spectra of the rare-earth elements, and the M.I.T. table of wave lengths.

Contrary to α^2 CV*n*, all lines in β CrB have the same radial velocity. This greatly facilitated the identification.

Table 2 contains a list of the stronger ($I \geq 2$) unidentified lines. The measured wave lengths, estimated intensities, and identifications in α^2 CVn given by Struve and Swings[12] are listed in the third, fourth, and fifth columns, respectively. The sixth column contains remarks concerning the reasons why the line was not similarly identified in β CrB. The seventh, eighth, and ninth columns contain the measured wave lengths, estimated intensities, and identifications in α Car given by Greenstein,[13] and the tenth column contains remarks as to why the line was not likewise identified in β CrB. It is evident that many of the unidentified lines are common to α^2 CVn and not to α Car. When the table is compared with the solar spectrum, it is seen that many of the unidentified lines in CrB are common to weak or moderately weak unidentified lines in the solar spectrum.

In addition to numerous neutral and singly ionized elements (*Cr* I, *Cr* II, *Fe* I, *Fe* II, *Mg* II, *Sr* II, *Ca* II, and *H* are very strong; *Ca* I, *Mg* I, *Ti* II, *Ba* II are strong; *Mn* I, and

[8] *Pub. Allegheny Obs.*, Vol. 6, No. 11, 1929.

[9] *Loc. cit.*

[10] *Ap. J.*, 95, 161, 1942.

[11] *Pub. Yerkes Obs.*, Vol. 7, Part III, 1935.

[12] *Loc. cit.*

[13] *Loc. cit.*

TABLE 1

LIST OF LINES IN THE SPECTRUM OF β CRB

λ	*I*	Identification	λ	*I*	Identification
3980.89	2	*Ce* II .90(100)	4000.24	0	*Fe* I .27(8)
3981.22	2	*Cr* II .24(5)	4000.47	4	*Fe* I .46(35), *Dy* II .45(800)
3981.74	5	*Fe* I .77(150), *Fe* II .61(pr)	4000.73	1n	*Ce* II .68(5)
3981.98	5	*Ti* II .01(3), *Dy* II .94(100)	4001.18	2n	*Gd* II .26(600)
3982.26	2	.....	4001.46	4	*Cr* I .44(200)
3982.61	3	*Y* II .60(150)	4001.68	3	*Fe* I .67(80)
3982.93	4	*Ce* II .90(60), *Gd* II .01(80)	4002.06	5	*Fe* II .07(2)
3983.28	4	*Cr* I .24(20)	4002.52	6	*Cr* II .48(5), *Fe* II .55(3)
3983.60	0	*Dy* II .66(150)	4002.91	5	(*V* II .94(80))
3983.94	6	*Cr* I .91(200), *Fe* I .96(200)	4003.27	6	*Cr* II .33(25)
3984.34	5	*Cr* I .34(80)	4003.78	7r	*Fe* I .77(30), *Ce* II .77(100), *Ti* I .81(50), *Gd* II .85(30), *Eu* II .71(12)
3984.68	4	*Ce* II .68(100)			
3984.97	1	.....			
3985.37	4	*Fe* I .39(125)	4004.12	1	*Fe* II .15(pr)
3985.66	1	.....	4004.61	1	*Eu* II .59(6), *Ce* II .58(12)
3985.96	1	*Mn* II .01(1)	4004.90	8	(*Fe* I .84(10)), (*Gd* II .94(150))
3986.17	4	*Fe* I .17(125)	4005.25	9	*Fe* I .25(250)
3986.42	1	*Ce* II .40(15)	4005.49	1	*Fe* I .48, *Tb* II .55(200)
3986.76	4	*Mg* I .73(15)	4005.71	3	*V* II .71(800)
3987.17	3	*Gd* II .21(600), *Mn* I .10(30)	4006.12	0	*Fe* I .16
3987.60	4	.....	4006.31	5	*Fe* I .32(60)
3987.92	0	.....	4006.70	6n	*Cr* II .75(1), *Fe* I .64(20), *Fe* I .76(7), *Pr* II .70(8)
3988.06	0	.....			
3988.25	2	*Eu* II .24(8)	4007.03	1	*Cr* II .04(pr)
3988.60	2	*La* II .52(500), *Eu* II .59(5)	4007.28	3	*Fe* I .27(80)
3989.03	5	*Sc* II .09(1)	4007.56	2	*Cr* II .56(2)
3989.28	1	*Gd* II .25(50)	4007.98	2n	.....
3989.47	1	*Ce* II .45(30)	4008.44	1	*Ce* II? .44(6)
3989.96	7nn	*Cr* I .99(80), *Fe* I .86(30), *Ti* I .76(150)	4008.70	0	*Pr* II .72(75)
			4008.91	4	*Gd* II .91(400), *Ti* I .94(80), *Eu* II .87(6), *Fe* I .87(5)
3990.40	4	*Fe* I .38(70)			
3990.72	0	*Ce* II .69(6)	4009.17	4	(*Gd* II .22(80))
3991.12	5	*Cr* I .12(200), *Zr* II .13(40)	4009.72	6	*Fe* I .72(120)
3991.38	1	*Ce* II .33(5), *Dy* II .33(40)	4010.16	3	.....
3991.69	4	*Cr* I .67(100)	4010.59	4r	.....
3992.17	2	*Cr* I .13(20)	4010.87	4	*Fe* I .95(2), *Fe* I .78(1)
3992.36	3	*Ce* II .39(125)	4011.38	1	*Fe* I .41(5)
3992.84	4	*Cr* I .83(150)	4011.68	2	*Eu* II .69(100), *Fe* I .72(2)
3993.16	2	*Gd* II .21(200)	4011.94	0	.....
3993.86	2	*Ce* II .82(200), *Mn* II .86(1), *Eu* II .93(15)	4012.13	1	*Nd* II .25(300), *Ce* II? .15(4)
			4012.46	10	*Cr* II .47(30), *Fe* II .47(1), *Ti* II .39(50), *Ce* II .39(300)
3994.16	4	*Gd* II .16(800), *Fe* I .12(25)			
3994.59	2	*Ce* II .58(6)	4012.85	2	*Eu* II .82(15), *Tb* II .84(40)
3994.78	1	*Nd* II .68(80), *Pr* II .82(200)	4013.16	1	*Nd* II .22(15)
3995.42	1	*Co* I .32(1000R)	4013.60	2	*Fe* I .64(8)
3995.99	4	*Fe* I .99(60), *Eu* II .98(10)	4013.82	4	*Fe* I .82(200), *Fe* I .80(80), *Gd* II .80(250)
3996.37	4n	*Gd* II .32(800), *Fe* II .36(pr)			
3996.78	1	*Dy* II .70(150)	4014.27	1	*Fe* I .27(3)
3997.00	2	*Fe* I .97(40)	4014.54	5r	*Fe* I .53(200), *Sc* II .53(20), *Cr* I .68(40)
3997.43	7	*Fe* I .40(300)			
3997.76	2	*Gd* II .76(300)	4014.92	2	*Ce* II .90(125)
3998.07	5	*Fe* I .06(150)	4015.19	1	*Dy* II .18(4)
3998.26	0	.....	4015.62	4	.....
3998.61	2n	*Ti* I .64(150)	4015.88	1	*Ce* II .88(20)
3998.91	2n	*Zr* II .98(30)	4016.10	1	.....
3999.24	2	*Ce* II .25(500), *Pr* II 19.(20)	4016.42	4	*Fe* I .43(15)
3999.68	2	*Cr* I .68(40)	4016.84	1	(*Pr* II .75(20))
3999.98	1	.....	4017.14	5	*Fe* I .16(80), *Fe* I .10(5)

TABLE 1—*Continued*

λ	*I*	Identification	λ	*I*	Identification
4017.52	6n	*Eu* II .58(100), *Ce* II .60(10), *Eu* II. 72(20)	4036.05	0	.....
4018.03	5	*Cr* II .96(3), *Mn* I .09(80)	4036.28	1	*Dy* II .34(15)
4018.29	6n	*Fe* I .27(50), *Cr* I .22(35), *Zr* II .38(10), *Eu* II .39(6)	4036.49	0	*Eu* II .55(20)
			4036.93	0	.....
			4037.15	0	*Eu* II .15(5)
4018.97	2n	(*Ce* II .05(15))	4037.34	3	*Gd* II .33(1500), *Cr* I .30(80)
4019.30	1	*Ce* II .27(4)	4037.64	1	*Ce* II .66(25)
4019.50	1	*Ce* II .47(6), *Dy* II .48(2)	4037.99	5	*Cr* II .03(25), *Gd* II .90(1200)
4019.70	0	*Eu* II .72(4)	4038.30	1	.....
4019.92	1	*Sm* II .98(80)	4038.79	2	(*Fe* I .82(2))
4020.28	2	.....	4039.10	3	*Cr* I .10(100)
4020.52	1	*Sc* I .40(50), *Fe* I .49(2)	4039.34	1	*Pr* II .36(30)
4020.90	1	*Co* I .90(500) *Nd* II .87(60)	4039.65	2	*Gd* II .67(100), *V* II .57(20)
4021.13	0	.....	4040.08	3nn	*Fe* I .09(1), *Fe* I .94(1), *Zr* II .24(4)
4021.40	1	*Nd* II .33(80)			
4021.64	0	*Fe* I .62(2)	4040.71	5	*Ce* II .76(300), *Fe* I .65(20)
4021.88	6	*Fe* I .87(200), *Ti* I .83(100), *Nd* II .80(60)	4041.30	5	*Mn* I .36(100), *Fe* I .29(5)
			4041.67	3	*Fe* II .64(pr), *Sm* II .68(200)
4022.35	7nn	*Cr* II .36(3), *Gd* II .33(300)	4042.16	2v	*Ce* II .14(6), *Cr* I .25(30), *Eu* II .02(15)
4022.75	1	*Fe* I .75(3), *Pr* II.75(15)			
4023.00	1	*Nd* II .00(600)	4042.60	3	*Ce* II .58(200)
4023.40	3	*V* II .39(600)	4042.79	2	*Gd* II .76(20), *Sm* II .72(200)
4023.72	2	*Sc* I .69(100)	4042.97	0	*Sm* II .91(250), *La* II .91(300)
4024.09	1	*Fe* I .10(8)	4043.45	1	.....
4024.56	7v	*Cr* I .58(20), *Fe* II .55(5), *Zr* II .45(5), *Ce* II .49(60), *Ti* I .58(80)	4043.69	1	*Cr* I .70(30)
			4043.96	6	*Fe* II .01(2), *Fe* I .91(25)
			4044.60	5	*Fe* I .61(70)
4024.74	6	*Fe* I .73(120)	4045.16	5	(*Fe* I .14(pr)), (*Gd* II .15(100))
4025.12	7	*Ti* II .14(25), *Cr* I .01(100)	4045.61	5	*Fe* I .60(pr), *Zr* II .63(15)
4025.46	1	.....	4045.83	9	*Fe* I .82(400)
4025.87	2	(*La* II .87(50))	4046.06	5	(*Fe* I .08(pr))
4026.19	2	*Cr* I .17(100)	4046.34	2	*Ce* II .34(100)
4027.08	3	*Cr* I .11(80), *Co* I .04(200)	4046.50	1	*Fe* I .46(1)
4027.40	1	.....	4046.82	4	*Fe* II .81(pr), *Cr* I .77(30), *Gd* II .84(150)
4027.69	2	*Ce* II .69(20)			
4027.97	2	*Cr* I .02(35)	4047.32	3	*Fe* I .31(3), *Ce* II .28(18)
4028.36	5•	*Ti* II .34(80), *Ce* II .41(150)	4047.75	3n	*Gd* II .81(100), *Sc* I .81(25)
4028.73	1	*Fe* I .77(2)	4048.03	2	*Cr* II .02(pr)
4029.26	1	.....	4048.36	1	*Ce* II .37(8)
4029.65	4n	*Fe* I .64(80), *Zr* II .68(20)	4048.62	1	*Gd* II .60(80), *Zr* II .67(30)
4030.23	3	*Fe* I .19(20)	4048.80	4	*Cr* I .79(80), *Mn* I .76(60), *Fe* II .83(3)
4030.45	6	*Fe* I .49(120), *Ti* I .51(80), *Cr* II .37(pr)	4049.11	4	*Cr* II .16(18)
			4049.41	3r	*Gd* II .43(1200), *Fe* I .33(10)
4030.79	6	*Mn* I .76(500), *Cr* II .68(3)	4049.83	4r	*Gd* II .86(2000), *La* II .08(200)
4031.20	1	*Fe* I .25(2), *Cr* II .13(2)	4050.64	3n	*Dy* II .58(100), *Fe* I .69(5)
4031.40	3	*Fe* II .46(1), *Ce* II .34(150), *Zr* II .35(1)	4051.32	3n	*Cr* I .34(35), *V* II .34(100), *Fe* II .21(pr)
4031.73	1	*La* II .72(300), (*Pr* II .76(50)), (*Nd* II .81(100))	4051.67	0	.....
			4051.96	7	*Cr* II .97(12), *Fe* I .91(10)
4031.98	3	*Fe* I .96(80)	4052.33	3	*Fe* I .30(2)
4032.56	5n	*Fe* I .64(80), *Fe* I .46(4), *Dy* II .48(50), *Pr* II .51(15)	4052.55	3	*Mn* .47(20)
			4052.74	2	*Fe* I .72(3), *Fe* I .66(3)
4032.99	7	*Fe* II .95(3), *Mn* I .07(400), *Tb* II .05(200)	4053.33	3	*Gd* II .29(1000), *Fe* I .27(6)
			4053.48	3	*Cr* II .45(1), *Ce* II .51(100)
4033.20	5	*Cr* I .26(30), *Mn* I .07(400)	4053.82	4	*Ti* II .84(25), *Fe* I .82
4033.70	2n	*Dy* II .67(10), *Eu* II .71(10)	4054.10	6	*Cr* II .18(8), *Fe* I .18(2)
4034.16	1	*Zr* II .10(5), *Cr* I .23(pr)	4054.48	1	.....
4034.52	3	*Mn* I .49(250)	4054.86	5	*Fe* I .88(25), *Fe* I .82(25)
4035.63	4	*V* II .63(400), *Fe* II .54(pr), *Mn* I .73(50)	4055.07	3	*Fe* I .04(40), *Ce* II .99(50)

TABLE 1—*Continued*

λ	*I*	Identification	λ	*I*	Identification
4055.53	1	*Mn* I .55(80)	4075.14	1	*Nd* II .12(60), *Nd* II .27(50)
4055.77	0		4075.64	3n	*Cr* II .63(pr), *Ce* II .71(150)
4056.08	4	*Cr* II .07(4), *Ti* II .20(8)	4075.94	4	*Cr* II .97(4), *Ce* II .86(125), *Fe* II .95(pr)
4056.33	2	*Fe* I .34			
4056.81	2n	*Cr* I .79(15)	4076.23	1	*Ce* II .24(12), *Fe* I .23(2)
4057.28	1	*Fe* I .34(20)	4076.64	4n	*Fe* I .64(80), *Fe* I .50(2)
4057.50	5	*Fe* II .46(2), *Mg* I .63(10)	4076.86	4	*Cr* II .87(3), *Fe* I .80(8)
4057.88	1		4077.10	0	*Cr* I .09(35), *Fe* II .16(3?)
4058.24	4	*Fe* I .23(80)	4077.49	4	*Cr* II .50(4), *Ce* II .48(75)
4058.79	5r	*Cr* I .77(80), *Fe* I .76(40), *Mn* I .94(80)	4077.73	7	*Sr* II .71(500)
			4077.98	0	*Dy* II .97(800)
4059.36	3	*Gd* II .37(80), *Eu* II .37(15)	4078.39	4	*Fe* I .36(80), *Gd* II .44(1200), *Ce* II .33(60), *Ti* I .47(125)
4059.72	3	*Fe* I .72(15)			
4060.21	1n	*Ti* I .26(60)	4078.56	1	
4060.48	1	*Ce* II .47(10)	4079.07	1	
4060.72	2	*Cr* II .77(pr)	4079.28	1	*Fe* I .25, *Mn* I .24(50)
4061.12	1n	*Nd* II .09(200)	4079.81	2n	*Fe* I .84(80), (*Pr* II .79(30))
4061.42	1		4080.26	2	*Fe* I .22(60), *Nd* II .23(50)
4061.85	2n	*Fe* II .79(1), *Mn* I .74(80), *Fe* I .96(3), *Cr* II .77(pr)	4080.52	1	*Ce* II .44(5)
			4080.82	0	*Fe* I .88(5)
4062.21	1	*Ce* II .23(60), *Eu* II .15(15)	4080.98	0	
4062.48	4	*Fe* I .44(120), *Gd* II .59(500)	4081.25	3	*Ce* II .22(150), *Cr* II .21(1)
4062.70	0	*Eu* II .65(15)	4081.54	1	
4062.94	1	*Ce* II .94(25)	4082.14	2	*Fe* I .12(10)
4063.31	5	*Fe* I .29(10), *Gd* II .39(1500)	4082.33	3	*Cr* II .30(10)
4063.62	9	*Fe* I .60(400), *Gd* II .59(200)	4082.98	1	*Mn* I .95(80)
4064.01	2	*Cr* II .05(pr), *Cr* II .94(pr)	4083.24	1	*Ce* II .24(200)
4064.38	1	*Ti* II .40(2), *Fe* I .45(2)	4083.65	4n	*Fe* I .76(15), *Fe* I .57(10), *Mn* II .67(pr), *Mn* I .64(80)
4064.59	0	*Sm* II .58(300)			
4064.86	0	*Ce* II .90(8)	4084.53	3r	*Fe* I .50(120), *Fe* II .58(pr)
4065.14	0	*Ti* I .10(80), *V* II .07(100)	4085.02	3	*Fe* I .02(80)
4065.40	1	*Fe* I .39(15)	4085.32	4n	*Fe* I .32(100), *Ce* II .25(100), *Gd* II .56(2000), *Eu* II .38(40)
4065.70	2	*Cr* I .72(80)			
4066.14	4	*Cr* II .16(pr)	4086.12	3	*Cr* II .14(8)
4066.58	4	*Fe* I .59(40)	4086.45	2	*Eu* II .42(8)
4066.98	6	*Fe* I .98(100), *Ni* II .05(30), *Cr* II .05(pr)	4086.78	1	*La* II .72(300)
			4087.14	4	*Fe* I .10(50), *Dy* II .21(25), *Pr* II .21(15)
4067.29	5	*Fe* I .28(80), *Ce* II .29(50)			
4067.96	6n	*Fe* I .99(150)	4087.33	4	*Fe* II .28(pr), *Ce* II .30(4)
4068.46	1		4087.63	4	*Cr* II .61(2), *Gd* II .69(200)
4068.85	1	*Ce* II .84(75)	4088.00	0	
4069.11	1		4088.30	0	
4069.60	1		4088.59	1	*Fe* I .57(7)
4070.00	2n	*Fe* II .02(pr), *Ce* II .09(15), *Fe* II .88(1)	4088.85	3r	*Cr* II .90(1), *Fe* II .76(pr), *Gd* II .81(10)
4070.36	2n	*Gd* II .29(600), *Gd* II .39(200), *Fe* I .28(2), *Mn* I .28(80)	4089.20	1	*Fe* I .23(10)
			4089.51	1	*Cr* II .49(2)
4070.82	5	*Fe* I .78(50), *Cr* II .90(10)	4089.81	1	*Ce* II .85(6)
4071.12	1	*Zr* II .09(4)	4090.08	1	*Fe* I .08(2)
4071.50	2	*Fe* I .52(1), *Eu* II .38(10)	4090.48	2n	*Zr* II .52(10)
4071.76	6	*Fe* I .74(300), *Ce* II .81(150)	4090.98	2	*Ce* II .95(6)
4072.02	0		4091.21	1	
4072.56	5	*Cr* II .56(4), *Fe* I .51(2)	4091.58	2	*Fe* I .56(8), *Dy* II .53(20)
4072.92	1		4091.87	1	*Dy* II .77(10)
4073.17	1	*Gd* II .20(400), *Dy* II .11(150)	4092.11	1	*Ce* II .09(10)
4073.49	1	*Ce* II .48(200), *Fe* II .45(8)	4092.28	1	*Fe* I .29(6), *Sm* II .27(400)
4073.76	4	*Gd* II .76(1500), *Fe* I .78(80)	4092.68	2	*Ca* I .67(15)
4074.14	1		4093.26	1	*Fe* II .24(0)
4074.38	0	*Fe* II .41(2?)	4093.64	0	
4074.77	4	*Fe* I .79(80)	4093.98	2	*Ce* II .96(30)

TABLE 1—*Continued*

λ	*I*	Identification	λ	*I*	Identification
4094.48	2	*Gd* II .48(300)	4117.83	1	*Fe* I .86(6)
4094.95	2	*Ca* I .94(15)	4117.96	1	.....
4095.28	1	(*Fe* I .27(0))	4118.18	1	*Ce* II .15(200)
4095.58	0	*Fe* I .65(2)	4118.55	5	*Fe* I .55(200), *Sm* II .55(400), (*Pr* II .48(200))
4095.95	3n	*Fe* I .98(80)			
4096.75	2n	*Eu* II .80(40), *Zr* II .63(4)	4118.94	3n	*Fe* I .90(2), *Ce* II .02(25), *Co* I .77(1000)
4097.11	2	*Fe* I .11(4), *Ca* II .12(1)			
4097.49	1	*Fe* II .51(1)	4119.42	3n	*Fe* II .53(pr), *Gd* II .38(80), *Dy* II .32(20)
4098.08	1	*Fe* I .18(100), *Cr* I .96(20)			
4098.55	3	*Ca* I .54(15), *Cr* II .44(8), *Gd* II .61(3000)	4119.85	3n	*Ce* II .78(20), *Ce* II .88(20)
			4120.22	2	*Fe* I .21(80)
4098.94	2	*Gd* II .90(400)	4120.58	1	*Cr* I .62(40)
4099.43	1n	.....	4120.81	2	*Ce* II .83(150)
4099.74	1n	*Ce* II .75(12)	4121.27	2	*Co* I .32(1000)
4100.46	0	.....	4121.54	1	.....
4101.77	10x	*Hδ* .75	4121.82	2	*Fe* I .81(100), *Cr* I .82(40)
4102.33	1	*Ce* II .36(18)	4122.16	1	*Cr* I .15(30)
4103.32	1	*Dy* II .31(600)	4122.61	8n	*Fe* II .64(4), *Fe* I .52(70)
4104.11	1	*Fe* I .13(100)	4122.96	1	*Gd* II .00(20), *Eu* II .94(5)
4104.43	1	*Ce* II .43(30), *Fe* I .47(0)	4123.27	1	*La* II .23(400), *Ce* II .23(5?)
4104.96	2	*Ce* II .00(50), *Fe* I .95(4), *Mn* II .01(2)	4123.45	1	*Ce* II .49(20?)
			4123.82	2	*Fe* I .76(80), *Ce* II .88(150)
4105.42	1n	.....	4124.54	1	*Eu* II .54(10)
4105.79	1	*Gd* II .79(15), *Eu* II .84(6)	4124.81	5	*Fe* II .79(1), (*Eu* II .89(12))
4106.19	1	*Fe* I .26(6), *Ce* II .13(30)	4125.45	1	*Ce* II? .44(6)
4106.46	0	*Fe* I .43(10)	4125.64	2	*Fe* I .62(80)
4106.89	1	*Ce* II .88(5d?)	4125.81	1	*Fe* I .89(25), *Mn* II .86(1)
4107.16	0	.....	4126.18	3	*Fe* I .19(80)
4107.47	3	*Fe* I .49(120), *Ce* II .42(200), *Sm* II .39(200)	4126.53	2	*Cr* I .52(100)
			4127.06	3	*Cr* II .08(3)
4107.83	1	*Eu* II .90(10), *Pr* II .76(10)	4127.33	1	*Ce* II .37(150), *Cr* I .28(20)
4108.28	1	*Ce* II .26(8)	4127.70	7r	*Fe* I .62(100), *Fe* I .81(25), (*Gd* II .72(25))
4108.53	2	*Ca* I .54(6)			
4108.78	0	.....	4128.09	6	*Si* II .05(8), *Mn* II .15(2)
4109.01	1	*Fe* I .06(12), *Nd* II .07(100)	4128.40	2	*Gd* II .39(10), *Cr* I .40(10)
4109.56	2v	*Cr* I .58(40), *Nd* II .46(200)	4128.76	3	*Fe* II .74(3), *Mn* II .87(pr)
4109.83	3	*Fe* I .80(120), *Ca* II .83(1)	4129.18	4	*Ti* II .15(pr), *Fe* I .19(5), *Sm* II .23(100)
4110.05	1	*Zr* II .05(3)			
4110.40	2	*Ce* II .38(60), *Gd* II .43(30)	4129.72	8nn	*Eu* II .70(5000)
4110.62	2	*Gd* II .60(150)	4130.39	2	*Gd* II .37(3000)
4110.97	4n	*Cr* II .00(18), *Cr* I .91(20), *Mn* I .90(80)	4130.74	2	*Ce* II .71(100), *Ba* II .66(50)
			4130.92	3	*Si* II .88(10)
4111.41	3	*Gd* II .44(500), *Cr* I .36(20), *Ce* II .40(60), *Dy* II .35(125)	4131.09	2	*Ce* II .10(100), *Fe* II .17(pr)
			4131.42	2	*Gd* II .48(200)
4111.86	2	*Fe* II .90(1), *Gd* II .74(100)	4132.05	7	*Fe* I .06(300)
4112.24	1	*Fe* I .32(6), *Eu* II .17(20)	4132.46	7	*Cr* II .44(7), *Gd* II .28(2000), *Fe* I .54(3)
4112.59	2	*Cr* II .59(1)			
4112.95	2	*Fe* I .97(70)	4132.92	4	*Fe* I .91(100)
4113.24	3	*Cr* II .24(5)	4133.83	5v	*Ce* II .80(500), *Fe* I .86(50)
4113.57	0	*Ce* II? .55(6)	4134.42	3	*Fe* I .43(10), *Fe* I .34(2)
4113.76	1	*Ce* II .73(30), *Gd* II .77(15)	4134.70	5	*Fe* I .69(150)
4114.17	1	*Ce* II .14(12)	4134.98	0n	*Eu* II .96(5)
4114.47	3	*Fe* I .45(80)	4135.10	1	*Sm* II .14(50)
4114.95	1	*Fe* I .96(10)	4135.45	1	*Ce* II .44(20), (*Nd* II .32(50))
4115.38	3	*Ce* II .38(150), *Gd* II .38(80)	4135.82	1n	*Cr* II .77(pr)
4115.91	1	*Fe* I .90	4136.56	2	*Fe* I .53(1n), *Eu* II .59(20)
4116.69	1	*Cr* II .66(2),	4137.00	5	*Fe* I .00(100), *Gd* II .10(500)
4116.98	1	*Ce* II .01(75), *Fe* I .96(1)	4137.44	3	*Fe* I .42(2)
4117.28	1	*Ce* II .29(20?)	4137.64	3	*Ce* II .64(400)
4117.58	1	*Ce* II .59(30)	4138.20	3	*Fe* II .21(pr)

TABLE 1—*Continued*

λ	*I*	Identification	λ	*I*	Identification
4138.40	4	*Fe* II .40(pr)	4157.13	0	.....
4138.79	1	.....	4157.32	0	.....
4139.07	2	.....	4157.79	5	*Fe* I .79(150)
4139.41	1	*Ce* II? .43(6)	4158.36	2	*Fe* II .44(pr)
4139.72	2	*Eu* II .67(15)	4158.80	5	*Fe* I .80(100)
4139.94	2	*Fe* I .94(40)	4159.17	5	(*Ce* II .04(50))
4140.45	4	*Gd* II .45(100), *Fe* I .41(1)	4159.70	0	.....
4140.73	1	*Ce* II .75(8)	4160.12	1	.....
4141.01	2	*Eu* II .02(25), *Gd* II .02(25)	4160.41	3	*Ti* II .37, *Eu* II .48(12)
4141.42	1	*Dy* II .52(40)	4160.69	0	*Co* II? .66
4141.79	3	*Fe* I .87(15), *Eu* II .72(40), *La* II .76(200)	4161.14	6	*Cr* II .05(2), *Fe* I .09(10), *Ce* II .14(50), *Ce* II .18(18?), *Zr* II .20(20)
4142.17	2	*Ni* I .18(2)			
4142.51	4	(*Ti* I .49(12)), (*Ce* II .40(150))	4161.49	6	*Ti* II .54(30), *Cr* II .56(pr)
4142.84	2	.....	4161.82	6	*Sr* II .80(30)
4143.11	0	*Dy* II .10(150), *Pr* II .14(150), *Fe* II .07(pr)	4162.25	1	*Eu* II .14(8)
			4162.71	3	*Gd* II .73(500)
4143.44	7	*Fe* I .42(200)	4163.06	2	.....
4143.88	8	*Fe* I .87(400)	4163.63	9	*Ti* II .65(150), *Cr* I .62(100)
4144.48	3	*Ce* II .49(10), *Tb* II .47(100), *Eu* II .51(8)	4164.06	1n	.....
			4164.53	1	.....
4145.01	4nn	*Ce* II .99(60), *Ti* I .05(15), *Eu* II .23(8), *Fe* I .20(1)	4164.78	1	.....
			4165.05	0	*Nd* II .04(5)
4145.50	0	.....	4165.53	6n	*Cr* I .52(80), *Ce* II .61(200), *Fe* I .42(12)
4145.78	6	*Cr* II .80(25)			
4146.32	4nn	*Cr* II .45(1), *Ce* II .23(75), *Eu* II .32(4), *Cr* II .50(pr)	4165.89	1	.....
			4166.25	1	*Ti* I .32(35)
4146.69	0	*Cr* I .70(25)	4166.66	2	*Fe* II .70(tr)
4146.92	0	.....	4166.88	2	*Ce* II .88(20)
4147.30	2	*Fe* I .35(2), *Eu* II .22(12)	4167.26	5	*Mg* I .28(6)
4147.68	4	*Fe* I .68(200)	4167.57	0	.....
4148.16	1	*Ce* II .16(15)	4167.87	5	*Fe* I .86(8), *Fe* I .96(10), *Ce* II .80(12?)
4148.44	1	*Eu* II .40(8)			
4148.66	0	.....	4168.65	2	*Fe* I .62(1n), *Fe* II .66(pr)
4148.90	1	*Ce* II .90(25)	4168.94	2	*Fe* I .95(10)
4149.19	1	*Zr* II .22(75)	4169.82	5v	*Cr* I .84(80), *Ce* II .88(30), *Fe* I .77(3), *Ce* II .77(12?)
4149.40	3	*Fe* I .37(100)			
4149.90	3n	*Ce* II .94(60), *Sm* II .83(200), *Fe* I .77(1)	4170.16	3	*Gd* II .11(150), *Cr* I .20(70)
			4170.59	3	*Cr* II .58(pr)
4150.26	3	*Fe* I .26(50), *Eu* II .31(8)	4170.99	7	*Fe* I .91(80), *Cr* II .86(1)
4150.60	1	*Gd* II .61(20)	4171.39	1	*Ce* II .39(18)
4150.98	6	*Cr* II .00(5), *Zr* II .97(10)	4171.69	1	*Fe* I .69
4151.19	0	*Eu* II .19(12)	4171.92	9	*Cr* II .92(3), *Ti* II .90(70)
4151.62	2	*Gd* II .63(30), *Eu* II .64(8), *Eu* II .52(20)	4172.12	4	*Fe* I .13(80)
			4172.65	9n	*Cr* II .60(2), *Fe* I .75(60), (*Eu* II .80(30))
4152.06	7n	*Ce* II .98(200), *Fe* I .17(70), *La* II .95(250), *Sm* II .21(200)	4173.49	10	*Fe* II .45(8), *Ti* II .55(40), (*Gd* II .56(100))
4152.81	2	*Cr* I .77(50), *La* II .78(100)			
4153.11	2	*Ce* II .13(12), *Cr* I .07(40), *Fe* II .98(pr)	4174.03	5n	*Ti* II .08(12), *Fe* I .94(50)
			4174.43	5	.....
4153.46	2	*Gd* II .51(125), *Eu* II .44(8)	4174.89	5	*Fe* I .92(100), *Cr* I .80(100)
4153.88	7	*Fe* I .91(120), *Cr* I .81(50)	4175.23	4	*Eu* II .16(12)
4154.07	0	*Fe* I .11(3)	4175.64	6	*Fe* I .64(100)
4154.49	5	*Fe* I .50(100)	4175.98	4	*Cr* I .94(40), *Fe* I .91(1), *Ce* II .08(12)
4154.82	6	*Fe* I .81(100), *Gd* II .86(250)			
4155.25	2	*Sm* II .22(100), *Sm* II .32(100)	4176.61	8	*Fe* I .57(100), *Mn* I .60(100), (*Eu* II .62(8))
4155.51	2	*Ce* II .53(6)			
4155.95	3	.....	4177.09	0	.....
4156.34	5	*Zr* II .24(15)	4177.63	9	*Fe* I .60(100), *Y* II .54(125), *Fe* II .70(pr), *Eu* II .57(15?)
4156.77	6	*Fe* I .80(100)			

TABLE 1—*Continued*

λ	*I*	Identification	λ	*I*	Identification
4178.07	3	*Sm* II .02(100), *Fe* I .05(3)	4198.06	5	.....
4178.41	1	*V* II .39(60)	4198.29	9	*Fe* I .31(250)
4178.87	10	*Fe* II .86(8)	4198.65	7	*Ce* II .67(75), *Ce* II .72(60), *Cr* I .52(100), *Fe* I .64(10)
4179.38	10	*Cr* II .43(12), *Cr* I .26(100)			
4179.93	1	*Cr* II .92(pr), *Zr* II .81(15), *Eu* II .88(8), *Sm* II .02(100)	4199.11	6	*Fe* I .10(300), *Cr* II .02(pr)
			4199.50	1	.....
4180.38	0	.....	4199.90	1	*Fe* I .98(1), *Tm* II .92(100)
4180.74	0	.....	4200.11	0	*Cr* I .10(80)
4181.11	2	*Ce* II .08(20), *Ti* II .17(pr)	4200.54	0	*Ti* II .40(pr)
4181.58	2	*Cr* II .50(1), *Fe* I .55(1)	4200.93	3	*Fe* I .93(80)
4181.77	8	*Fe* I .76(200)	4201.30	2	*Dy* II .37(10)
4181.96	3	.....	4202.04	7	*Fe* I .03(400)
4182.37	3	*Fe* I .39(80)	4202.48	2n	*Gd* II .52(80), *V* II .35(150)
4182.75	2	*Fe* II .69(pr)	4202.76	1	*Fe* I .76(10)
4183.12	1	*Fe* II .20(pr), *Fe* I .01(1n)	4202.91	2	*Ce* II .95(150)
4183.46	1	*V* II .44(250)	4203.33	0	.....
4183.99	6v	.....	4203.56	2	*Cr* I .59(100)
4184.31	6	*Ti* II .33(20), *Gd* II .25(2000), (*Lu* II .31(120))	4203.98	4	*Fe* I .99(200)
			4204.19	0	*V* II .20(2)
4184.91	6	*Fe* I .90(100)	4204.46	1	.....
4185.35	2	*Cr* I .34(30), *Ce* II .33(5?)	4204.99	10n	*Eu* II .05(6000), *Cr* II .83(pr), *Gd.* II .86(300), *V* II .08(250)
4185.55	1	*Cr* II .50(pr)			
4186.12	1	*Fe* I .12(100), *Cr* II .08(pr), *Ti* I .12(100)	4205.48	5n	*Fe* I .55(50), *Nd* II .60(40), *Eu* II .57(5), *Mn* II .37(pr)
4186.37	2	*Cr* I .36(50)	4205.86	1	*Zr* II .91(2), *Ti* II .92(pr)
4186.62	2	*Ce* II .60(600)	4206.29	1n	*Ca* II .21, *Mn* II .43(2)
4187.04	6	*Fe* I .04(250)	4206.85	2	*Fe* I .70(125), *Cr* I .90(80)
4187.32	1	*Ce* II .32(35?)	4207.13	2	*Fe* I .13(80)
4187.62	1	*Fe* I .59(3)	4207.36	3	*Cr* II .34(4)
4187.83	6	*Fe* I .80(200)	4207.83	1	.....
4188.10	1	*Gd* II .10(60), *Sm* II .13(200)	4208.33	3	*Cr* I .36(100), (*Gd* II .37(8))
4188.48	1	.....	4208.60	4	*Fe* I .62(100)
4188.74	6	.....	4209.09	3	*Cr* II .02(3), *Zr* II .99(30)
4189.19	0	*Ce* II .18(8)	4209.38	3	*Cr* I .37(100), *Ce* II .41(25)
4189.62	3	(*Pr* II .52(125))	4209.80	3n	*Cr* II .84(pr), *V* II .83(10)
4190.20	3	*Ti* II .24(1), *Cr* I .13(40), *V* II .40(15)	4210.34	4	*Fe* I .35(300), *Sm* II .35(150)
			4211.00	1	.....
4190.66	1	*Ce* II .63(30), *Cr* I .66(12), *Si* II .74(3), *Co* I .72(20)	4211.33	1	*Cr* I .35(100), *Eu* II .28(10), *Nd* II .29(40)
4191.06	2	*Gd* II .07(800)	4211.58	0	.....
4191.41	8	*Fe* I .44(200), *Cr* I .27(70), *Zr* II .50(6)	4211.96	3n	*Gd* II .00(800), *Zr* II .88(18)
			4212.66	2	*Cr* I .66(80), (*Nd* II .75(6))
4191.71	4	*Cr* I .75(50), *Fe* I .68(20)	4213.08	2	*Ce* II .04(15)
4192.10	1	*Ni* II .07(1)	4213.60	4	*Fe* I .65(100)
4192.46	1	(*La* II .35(100))	4214.03	2	*Ce* II .04(50)
4192.77	1	.....	4214.74	2	.....
4193.20	5	*Gd* II .15(60), *Ce* II .10(50)	4215.02	4	*Gd* II .02(600)
4193.69	4	*Cr* I .66(100)	4215.51	10	*Sr* II .52(400)
4193.86	4	*Ce* II .87(35?)	4215.78	3	*Cr* II .77(2), *Zr* II .76(1)
4194.44	0	*La* II .36(30)	4216.22	4n	*Fe* I .19(200), *Cr* I .36(60)
4194.94	4	*Cr* I .95(70)	4217.12	4	*Cr* II .07(1), *Gd* II .20(500)
4195.37	8	*Cr* II .41(10), *Fe* I .34(150), (*Gd* II .41(60)), (*Eu* II .36(10))	4217.57	6	*Fe* I .56(100), *Cr* I .63(150), *Ce* II .59(30), *La* II .56(200)
			4217.89	1	.....
4195.83	2n	*Gd* II .85(20), *Fe* I .62(25)	4218.22	1	*Ti* II .18(pr)
4196.23	5	*Fe* I .21(100), *Eu* II .18(15), *Ce* II .34(75)	4218.51	1	*Eu* II .45(6), *Dy* II .58(5)
			4219.37	6	*Fe* I .36(250), *Fe* I .42(5)
4196.56	1	*La* II .55(250)	4219.71	2	(*Pr* II .65(15))
4197.19	4n	*Cr* I .23(70), *Fe* I .10(2), *Gd* II .07(150)	4220.08	3	*Ca* II .13, *V* II .04(10), *Fe* I .05(1)
4197.63	4	*Gd* II .68(800), *Ce* II .67(6)	4220.34	1	*Fe* I .35(80)

TABLE 1—*Continued*

λ	*I*	Identification	λ	*I*	Identification
4220.64	1n	*Sm* II .64(200)	4241.71	1	.....
4221.20	1	*Eu* II .08(25), *Nd* II .33(80)	4242.07	1	*Tm* II .15(300)
4221.56	2	*Cr* I .57(80)	4242.38	9	*Cr* II .38(30), *Mg* II .47(4), *Mn* II .30(2)
4222.04	3	*Cr* II .00(1)			
4222.23	4	*Fe* I .22(200)	4242.76	5	(*Ce* II .73(15))
4222.64	4	*Ce* II .60(300), *Cr* I .73(100)	4243.37	3	*Fe* I .37(10)
4223.04	1	*Gd* II .02(60), (*Pr* II .99(150))	4243.83	4	*Gd* II .84(150)
4223.32	1	.....	4244.27	1	*Mn* II .25(1)
4223.83	0	*Eu* II .88(15)	4244.55	0	*Fe* II .53(pr)
4223.18	6	*Fe* I .18(200), *Cr* II .09(pr), *Zr* II .22(3)	4244.89	1	*Ni* II .80(1), *Cr* II .08(1)
			4245.31	4	*Fe* I .26(80)
4224.52	5	*Fe* I .52(60), *Cr* I .51(60)	4245.98	4	*Fe* I .09(80), *Ce* II .98(6)
4224.86	5	*Cr* II .85(20)	4246.43	4	*Cr* II .41(2)
4225.17	2	*Gd* II .15(100), *V* II .23(120)	4246.83	6	*Sc* II .83(500), *Cr* II .88(1)
4225.44	4	*Fe* I .46(80), *Sm* II .33(400), *Pr* II .34(150)	4247.44	5	*Fe* I .43(200), *Dy* II .36(20), *Nd* II .38(200)
4225.71	2	*Eu* II .68(8)	4247.89	1	*Eu* II .88(6), *Mn* II .95(1)
4225.97	2	*Fe* I .96(80)	4248.25	4	*Fe* I .23(150)
4226.42	2	*Fe* I .43(80)	4248.69	2	*Ce* II .67(200)
4226.74	8	*Ca* I .74(500), *Cr* I .76(125)	4249.05	1	(*Pr* II .08(10))
4227.40	9	*Fe* I .43(300), (*Eu* II .40(6))	4249.61	1n	(*Pr* II .48(15))
4227.75	2	*Ce* II .75(100), *Cr* I .73(1), *Nd* II .72(30)	4250.13	6	*Fe* I .13(250)
			4250.46	0	*Cr* I .51(1), (*Pr* II .40(20))
4228.28	1	*Ce* II .30(15), *Nd* II .20(8)	4250.80	9	*Fe* I .79(400)
4228.80	1	*Nd* II .84(2), *Ce* II? .83(5)	4251.40	1	(*Pr* II .48(20))
4229.45	3n	*Eu* II .33(12), *Eu* II .52(5)	4251.73	3n	*Gd* II .73(2000), *Mn* II .77(2)
4229.80	3	*Cr* II .82(1), *Fe* I .78(20), *Gd* II .80(200), *Sm* II. 70(300)	4252.19	1	*Cr* I .24(35), *Ti* II .05(pr)
			4252.63	6	*Cr* II .63(10)
4230.18	1	.....	4252.98	1	*Mn* II .02(2)
4230.52	2	*Cr* I .48(70), *Eu* II .63(12)	4253.36	2	*Gd* II .37(800), *Ce* II .37(50)
4231.06	1	*La* II .95(150), *Gd* II .03(5)	4253.64	1	*Gd* II .61(800)
4231.38	1	.....	4253.92	0	*Fe* I .93(2)
4231.71	0	*Ce* II .75(30), *Zr* II .64(8)	4254.38	10r	*Cr* I .35(5000)
4232.01	2n	*V* II .07(80), *Cr* I .22(70)	4254.95	1	*Fe* I .94(2)
4232.50	2	*Gd* II .47(40), *Eu* II .45(12), *Ce* II .57(20)	4255.46	3	*Fe* I .50(5), *Gd* I .41(15), *Gd* II .57(20)
4233.20	10v	*Fe* II .17(11), *Cr* II .25(10), *Cr* II .96(pr)	4255.80	1	*Ce* II .79(60)
			4256.14	3	*Cr* II .16(5)
4233.60	8	*Fe* I .61(250)	4256.37	0	*Sm* II .39(400), *Dy* II .32(80)
4234.00	1	.....	4256.75	2	*Cr* I .62(12), *Nd* II .82(8)
4234.21	1	*Ce* II .21(30), *V* II .23(7)	4257.13	1	*Ce* II .12(20)
4234.60	1n	*Sm* II .57(200), *V* II .55(40), *Ce* II .73(12)	4257.42	1	*Cr* I .37(35)
			4257.77	0	*Mn* I .66(100)
4235.22	2n	*Mn* I .27(100), *Mn* I .15(80)	4258.19	6r	*Fe* II .16(3), *Fe* I .33(60), *Zr* II .05(12), *Fe* II .35(pr)
4235.95	9	*Fe* I .94(300)			
4236.40	3	*Cr* II .33(pr), *Zr* II .56(5)	4259.16	2	*Cr* I .16(35), *Mn* II .26(2)
4236.79	1	*Sm* II .74(250)	4259.70	1	*Ce* II .75(15)
4237.17	2	*Fe* I .18(5)	4260.11	3	*Fe* I .01(15), *Fe* I .13(7)
4237.53	1	*Eu* II .51(40), *Sm* II .66(200)	4260.49	6	*Fe* I .48(400)
4238.01	4vn	*Fe* I .03(80), *Cr* I .71(70), *Eu* II .93(6)	4261.13	0	*Ce* II .16(18)
			4261.33	1	*Cr* I .35(125)
4238.81	9	*Fe* I .82(200), *Gd* II .78(500), *Cr* II .69(pr), *Mn* II .79(pr), *Eu* II .69(20)	4261.92	7	*Cr* II .91(20), *Gd* II .09(2500)
			4262.36	1	*Cr* I .36(30)
			4262.74	1	*Sm* II .68(300)
4239.37	1	*Cr* II .31(0), *Fe* I .37(2)	4263.14	4	*Cr* I .14(125), *Ti* I .13(125)
4239.81	6n	*Fe* I .85(40), *Mn* I .72(100), *Ce* II .91(200)	4263.43	1	*Ce* II .43(40?), *Cr* II .49(pr)
			4263.90	3	*Fe* II .90(1)
4240.41	2	*Ca* I .46(10), *Fe* I .37(30)	4264.27	3	*Fe* I .22(35), *Cr* II .18(pr), *Ce* II .37(10?)
4240.73	2	*Cr* I .70(200)			
4241.26	1n	*Gd* II .28(80), *Cr* I .19(10)	4264.73	3	*Fe* I .74(12)

TABLE 1—*Continued*

λ	*I*	Identification	λ	*I*	Identification
4265.27	3	*Fe* I .27(2)	4288.66	1	*Ce* II .67(30)
4265.71	1	.....	4288.98	1	*Fe* I .96(5), *Ti* I .07(125)
4265.98	2	*Mn* I .92(100)	4289.38	4	*Ca* I .37(35), *Ce* II .45(25)
4266.28	1	*Cr* II .23(pr)	4289.73	6r	*Cr* I .72(3000), *Ce* II .93(300)
4266.96	2	*Fe* I .97(70)			*Gd* II .88(80)
4267.32	1n	.....	4290.25	6r	*Ti* II .23(60)
4267.83	2	*Fe* I .83(125)	4290.89	1	*Fe* I .88(20), *Ti* I .93(70)
4268.28	1	*Ce* II .16(500)	4291.50	1n	*Fe* I .47(125)
4268.81	3n	*Fe* I .76(30), *Cr* II .93(1),	4291.94	1	*Cr* I .96(35), *Eu* II .95(5)
		Cr I .79(30), *Gd* II .73(150)	4292.26	1	*Fe* I .29(15), *Mn* II .25(2),
4269.27	4	*Cr* II .28(10)			*Sm* II .18(150)
4270.20	2	*Ce* II .19(60), *Eu* II .24(10),	4292.75	1n	*Gd* II .75(25), *Ce* II .77(4)
		Ti I .14(30)	4293.52	1	*Cr* I .56(50), *Pr* II .58(20)
4270.71	2	*Ce* II .72(50)	4294.11	6	*Fe* I .13(700), *Ti* II .12(80)
4271.15	4	*Fe* I .16(400)	4294.81	3n	*Sc* II .78(20)
4271.78	5	*Fe* I .76(1000)	4295.31	2	*Cr* II .37(pr)
4272.41	1n	*Ti* I .43(40)	4295.76	2	*Cr* I .76(125), *Ti* I .76(100)
4272.89	2	*Cr* I .90(40)	4296.05	3	*Gd* II .08(1000), *La* II .05(300)
4273.35	4	*Fe* II .32(3)	4296.60	6	*Fe* II .57(6), *Ce* II .68(200)
4273.74	1	.....	4297.14	2	*Gd* II .17(400), *Cr* I .05(100)
4274.02	1n	.....	4297.73	2	*Cr* I .74(125), *Pr* II .76(80)
4274.80	5v	*Cr* I .80(4000), *Ti* I .58(100)	4298.07	2	*Fe* I .04(100)
4275.56	5	*Cr* II .57(30)	4298.40	1	*Gd* II .43(30)
4275.99	1	*Eu* II .91(10)	4298.67	1	*Ti* I .66(125)
4276.32	1	*Ti* I .43(50), *Eu* II .20(30)	4299.16	6nn	*Fe* I .24(500), *Ca* I .00(30),
4276.68	1	*Fe* I .68(10)			*Ce* II .36(60), *Ce* II .09(5)
4277.35	1	*Zr* II .37(4)	4299.62	0	*Cr* I .72(100), *Ti* I .64(60)
4277.68	1	.....	4300.04	6	*Ti* II .05(100)
4278.17	4	*Fe* II .13(1), *Cr* II .10(1)	4300.26	0	*Ce* II .33(60), *Mn* II .22(1)
4278.83	2	*Ca* II .87(2), *Ce* II .87(20)	4300.53	1	*Cr* I .51(100), *Ti* I .56(125)
4279.17	1	.....	4300.86	1	*Ce* II .86(15), *Eu* II .84(5)
4279.50	2	*Fe* I .48(5)	4301.16	1•	*Cr* I .18(100), *V* II .18(40),
4279.90	0	*Fe* I .87(1), *Sc* II .95(1)			*Ti* I .09(150)
4280.15	0	*Ce* II .14(15)	4301.92	5	*Ti* II .93(50)
4280.42	4	*Gd* II .49(1500), *Eu* II .36(8),	4302.14	1	*Fe* I .19(50)
		Cr II .33(pr)	4302.54	4r	*Ca* I .54(50), *Cr* II .58(1)
4281.06	3	*Mn* I .10(100), *Cr* II .03(pr),	4303.18	5	*Fe* II .17(8)
		Sm II .01(100)	4303.54	1	*Nd* II .57(400), *Gd* II .47(25)
4281.53	1	*Ti* I .38(80)	4304.19	1n	*Gd* II .09(25)
4281.94	2	*Eu* II .92(8)	4304.57	0	*Fe* I .54(1)
4282.41	4	*Fe* I .41(600), (*Mn* II .50(3))	4304.86	1	*Gd* II .90(400)
4282.76	1	*Gd* II .79(50)	4305.18	1	*Ce* II .14(20)
4283.02	3	*Ca* I .02(40), *Cr* II .02(1)	4305.46	4	*Fe* I .46(100), *Sr* II .46(40),
4283.53	1	.....			*Cr* I .45(150)
4283.84	1	*Mn* II .81(1)	4305.80	1n	*Sc* II .72(20), *Ti* I .92(300),
4284.18	4	*Cr* II .21(20)			(*Pr* II .77(100))
4284.41	0	*Mn* II .42(0), *Nd* II .51(100)	4306.33	1	*Eu* II .38(4), (*Gd* I .34(1500))
4284.74	1	*Cr* I .74(40)	4306.73	1	*Ce* II .72(100)
4284.89	1	*Cr* I .90(15)	4306.91	2	*Cr* II .95(5)
4285.42	3v	*Fe* I .44(125), *Sm* II .50(200),	4307.85	7	*Fe* I .91(1000), *Ti* II .91(100),
		Ce II .37(30)			*Ca* I .75(45)
4285.88	1n	*Ti* I .01(100)	4308.23	0	*Gd* II .23(40)
4286.27	2	*Fe* II .31(1), *Cr* II .36(1)	4308.81	2	*Cr* II .82(2)
4286.48	1	*Zr* II .51(5)	4309.02	2	*Sm* II .01(200), *Fe* I .04(40)
4286.95	3	*Fe* I .99(10), *La* II .01(400),	4309.37	2	*Fe* I .38(125)
		Fe I .89(2)	4309.70	3	*Cr* II .75(3), *Y* II .63(50),
4287.47	0	*Ti* I .40(100)			*Ce* II .74(50)
4287.88	3	*Ti* II .88(30)	4310.38	1	*Fe* I .38(1), (*Ti* I .38(10))
4288.13	1	*Fe* I .15(50)	4310.65	1	*Ce* II .70(30)
4288.41	0	*Cr* I .38(15)	4311.00	1	*Gd* II .98(200)

TABLE 1—*Continued*

λ	*I*	Identification	λ	*I*	Identification
4311.61	1	.....	4338.69	0	*Fe* II .70(pr), *Nd* II .70(80), (*Pr* II .69(25))
4312.09	0	*Tb* II .09(8), *Zr* II .23(3)			
4312.53	1	*Mn* I .55(100)	4339.39	2	*Cr* I .45(300), *Ce* II .32(30)
4312.88	5	*Ti* II .87(100)	4340.50	10x	*H*γ .48
4313.59	1	*Ce* II? .60(10)	4341.36	2	*Ti* II .38(40), *Gd* II .28(600)
4314.07	4	*Sc* II .09(50)	4341.77	0	.....
4314.31	4	*Fe* II .29(4)	4342.22	2	*Gd* II .18(1500), *Fe* II .36(0)
4315.00	6	*Ti* II .98(20), *Fe* I .09(500)	4342.51	0	.....
4315.43	1	.....	4343.28	1	*Fe* I .27(20), *Cr* I .21(60)
4315.69	0	.....	4343.76	0	*Fe* I .71(12)
4316.02	1	*Gd* II .05(600)	4344.16	1	.....
4316.33	1	*Gd* II .27(150)	4344.44	4nn	*Ti* II .29(50), *Cr* I .51(400), *Gd* II .30(100), *Gd* II .49(40)
4316.82	2r	*Ti* II .80(35)			
4317.31	1	*Zr* II .32(12)	4344.95	0	*Ce* II .92(6)
4317.65	1	*Eu* II .67(8)	4345.22	0	.....
4318.12	2n	*Fe* II .22(0n)	4345.54	1	*Mn* II .60(pr)
4318.64	3	*Ca* I .66(60)	4345.96	2	*Ce* II .96(6)
4319.06	1	*Sm* II .94(500)	4346.55	3n	*Fe* I .56(50)
4319.62	1v	*Cr* I .64(100), *Fe* II .72(1n)	4346.88	2	*Cr* I .83(200)
4320.11	0	.....	4347.35	2	*Gd* II .31(400)
4320.47	0	.....	4347.78	2	*Sm* II .80(400), *Fe* I .84(5)
4320.76	5	*Sc* II .74(40), *Ce* II .72(60), *Cr* I .59(125)	4348.35	2n	*Mn* II .49(1), *Ce* II .19(4)
			4348.64	0	.....
4321.02	4	*Ti* II .96(40), *Gd* II .11(200)	4349.04	1	*Fe* I .95(8)
4321.27	1	*Fe* II .34(1n), *Cr* I .24(70)	4349.48	1	*Eu* II .49(2)
4321.72	1n	*Ti* I .66(70)	4349.86	2	*Ce* II .79(100)
4322.20	1	*Gd* II .20(125)	4350.48	1	*Sm* II .46(300)
4322.55	0	*La* II .51(150)	4350.99	2nn	*Ti* II .83(30), *Cr* I .05(100)
4322.85	1	*Ce* II .80(8)	4351.84	6r	*Fe* II .76(9), *Cr* I .77(300), *Mg* I .91(15), *Sm* II .10(200)
4323.18	1	*Sm* II .28(200)			
4323.49	1	*Pr* II .55(25), (*Zr* II .62(2))	4352.71	5r	*Fe* I .74(300), *Cr* II .68(pr), *Ce* II .72(75)
4324.08	2	*Gd* II .06(150)			
4325.03	4v	*Sc* II .00(50), *Cr* I .08(125)	4353.46	2	.....
4325.54	3	*Gd* II .57(200)	4354.00	2	*Cr* I .98(20), *Gd* II .06(40)
4325.78	5	*Fe* I .76(1000)	4354.38	1	*Fe* II .36(2), *La* II .44(200)
4326.66	3n	*Mn* II .71(3), *Fe* I .76(10)	4354.65	0	*Sc* II .62(60)
4327.09	3	*Gd* II .12(1500), *Fe* I .10(100)	4355.11	3	*Ca* I .10(50), *Eu* II .09(300)
4327.83	2	*Nd* II .93(30)	4355.36	2	.....
4328.11	1	.....	4355.94	1	.....
4328.90	2n	*Cr* II .91(pr), *Dy* II .90(20), *Sm* II .02(400)	4356.75	3n	*Cr* I .76(15), *Ce* II .75(10), (*Gd* II .74(10))
4329.91	0	.....	4357.13	1	.....
4330.23	5	*Ti* II .24(40)	4357.56	3	*Fe* II .57(4)
4330.63	5n	*Gd* II .61(600), *Ti* II .71(30), *Ce* II .45(30), *Eu* II .61(40)	4357.85	1	*Gd* II .87(10)
			4358.48	2	*Fe* I .50(70), *Dy* II .46(60)
4330.96	1	*Fe* I .96(5), *Gd* II .95(20)	4358.76	1	*Y* II .72(30)
4331.74	2	*Fe* II .53(3), *Ni* I .64(200)	4359.12	2	*Gd* II .15(40), (*Pr* II .11(15))
4331.94	1	.....	4359.63	4	*Cr* I .63(200), *Zr* II .74(10), *Gd* II .64(30)
4332.58	2nn	*Cr* I .57(125)			
4332.93	0	.....	4360.07	2n	*Cr* I .99(15), *Ce* II .16(25)
4333.24	0	*Zr* II .28(15)	4360.46	1	*Ti* I .48(60)
4333.74	0	*La* II .76(500)	4360.84	2	*Gd* II .92(250), *Sm* II .72(150)
4334.01	0	*Sm* II .15(400), (*Pr* II .91(100))	4361.29	2	*Fe* II .25(2)
4334.29	1	.....	4361.63	1	*Eu* II .57(8)
4334.74	2n	*Eu* II .75(12)	4362.04	1	*Sm* II .04(300), *Ni* II .10(1)
4335.41	2	.....	4362.47	2	.....
4336.21	2	*Ce* II .25(50)	4363.00	3	*Cr* II .93(3), *La* II .05(50)
4337.00	0	*Fe* I .05(400)	4363.45	2	*Mo* II .64(200)
4337.31	0	*Ti* II .26(1)	4364.12	2	*Gd* II .14(25), *Dy* II .28(40), *Nd* II .14(10)
4337.56	0	*Zr* II .63(5)			
4337.90	3	*Ti* II .92(125), *Ce* II .78(125)	4364.59	2v	*Ce* II .66(125), *La* II .66(100)

TABLE 1—*Continued*

λ	*I*	Identification	λ	*I*	Identification
4365.26	0	*Mn* II .29(1)	4390.53	2v	*Mg* II .59(10)
4365.56	0	.....	4390.98	5	*Fe* I .95(100), *Ti* II .03(25), *Gd* II .95(300), *Sm* II .86(600)
4366.00	0	.....			
4366.51	0	.....	4391.38	1	*Eu* II .37(10)
4366.97	1	*Ce* II .00(25)	4391.76	4	*Cr* I .77(50), *Ce* II .67(250)
4367.32	1	*Gd* II .31(15)	4392.59	1	.....
4367.62	5	*Ti* II .66(25), *Fe* I .58(100)	4393.20	1	*Ce* II .19(35)
4368.14	4v	*Cr* II .20(pr), *Fe* I .91(60), *Fe* II .26(1), *Sm* II .03(150)	4393.50	0	*Cr* I .53(5)
			4394.06	4	*Ti* II .06(15), (*Ti* I .92(60))
4368.60	0	*Nd* II .63(60)	4394.78	1	*Ce* II .78(30), *Gd* II .72(25)
4368.90	0	*Cr* I .91(5)	4395.04	7	*Ti* II .04(50)
4369.39	4	*Fe* II .40(2), *Eu* II .47(40)	4395.43	0	*Cr* I .42(15)
4369.76	4	*Fe* I .77(200), *Gd* II .77(500)	4395.84	4	*Ti* II .84(10)
4370.33	1	*Eu* II .34(20)	4396.55	2n	(*Ce* II .58(20))
4370.72	1	.....	4397.28	2n	.....
4370.97	0	*Zr* II .99(8)	4397.60	0	*Gd* II .51(300)
4371.28	3	*Cr* I .29(200)	4397.95	1	*Y* II .01(100)
4371.60	0	*Pr* II .61(40)	4398.29	1	*Ti* II .31(10)
4371.86	0	.....	4398.80	1	*Ce* II .79(20)
4372.32	3n	*Ce* II .40(35), *Fe* II .22(pr), *Eu* II .20(8)	4399.21	1	*Ce* II .20(60), *Eu* II .32(15)
			4399.78	5	*Ti* II .77(40)
4372.65	0	.....	4400.40	1	*Sc* II .36(150)
4373.20	2	*Cr* I .25(50), *Ce* II .22(25)	4400.65	0	.....
4373.56	3	*Fe* I .57(50)	4401.01	1	.....
4373.81	0	*Ce* II .82(50)	4401.32	2	*Fe* I .30(60)
4374.17	3	*Cr* I .16(50)	4401.55	1	*Ni* I .55(1000)
4374.47	3	*Sc* II .47(100)	4402.12	0n	.....
4374.85	4	*Ti* II .82(35), *Mn* I .95(150), *Y* II .94(300), *Dy* II .80(100)	4403.05	4n	(*Fe* II .88(2))
			4403.44	4	*Sm* II .36(100), *Zr* II .35(6)
4375.28	2	*Dy* II .32(50)	4404.10	1n	(*Ti* I .28(50))
4375.93	3	*Fe* I .93(500), *Ce* II .92(60)	4404.75	7	*Fe* I .75(1000)
4376.80	2	*Fe* I .78(7), *Cr* I .80(20)	4405.34	3n	*Eu* II .27(20)
4377.47	1n	*Cr* I .55(25)	4405.92	0	*Pr* II .85(80)
4377.82	0	*Mo* II .76(200)	4406.67	3	*Gd* II .67(400)
4378.42	1nn	*Cr* II .34(1), (*Sm* II .24(150))	4407.18	3n	*Eu* II .07(15), *Ce* II .28(40)
4379.04	1	.....	4407.72	4	*Ti* II .68(10), *Fe* I .72(100)
4379.68	1	*Zr* II .77(9), *Mn* II .74(1)	4408.33	3	*Fe* I .42(125), *Gd* II .25(400)
4380.11	1	.....	4408.82	1	*Pr* II .84(200)
4380.62	3n	*Gd* II .64(100)	4409.23	2	*Ti* II .22(8)
4381.10	3	*Cr* I .12(30)	4409.49	2	*Ti* II .52(10)
4381.76	1	*Mn* I .70(80), *Fe* II .79(pr)	4409.92	1	.....
4382.11	3	*Ce* II .17(200), *Gd* II .06(60)	4410.30	1	*Cr* I .31(25)
4382.53	1	*Cr* II .53(1)	4410.69	1	*Ce* II .64(30)
4382.72	1	*Fe* I .77(10), *Mn* I .63(80)	4411.07	4	*Ti* II .08(100)
4383.12	2	*Gd* II .12(150), *Eu* II .17(200)	4411.97	3	*Ti* II .94(12), *Mn* I .88(100)
4383.55	6	*Fe* I .55(1000)	4412.36	1	.....
4384.07	1	.....	4412.79	0	.....
4384.34	3	*Fe* II .33(pr)	4413.58	2	*Fe* II .60(0)
4384.68	1	*Mg* II .64(8)	4413.83	1	*Cr* I .87(25)
4384.95	1	*Cr* I .98(150)	4414.40	0	*Zr* II .54(5)
4385.36	6	*Fe* II .38(7)	4414.81	0	.....
4386.27	1	.....	4415.13	7	*Fe* I .12(600)
4386.82	5	*Ti* II .85(80)	4415.58	3	*Sc* II .56(25)
4387.48	2	*Cr* I .50(15)	4416.12	0	.....
4387.74	2	*Gd* II .67(300)	4416.84	8	*Fe* II .82(7)
4387.98	2	*Fe* I .90(150), *Ce* II .01(8)	4417.28	0	*Ti* I .28(80)
4388.40	2	*Fe* I .41(125)	4417.72	8	*Ti* II .72(40)
4389.11	2	*Fe* I .25(35)	4418.34	3	*Ti* II .34(10)
4389.70	1n	*Mn* .75(50)	4418.92	2n	*Gd* II .03(800), *Ce* II .78(200)
4390.26	1	.....	4419.34	0	.....

TABLE 1—*Continued*

λ	*I*	Identification	λ	*I*	Identification
4419.68	1	*Eu* II .66(8), (*Pr* II .67(30))	4448.25	1	.....
4420.27	1	.....	4449.31	2v	*Ce* II .33(200), *Ti* I .15(150)
4420.55	0	*Sm* II .53(200)	4449.63	2	*Fe* II .66(1n), *Dy* II .70(300)
4421.15	3n	*Sm* II .14(200), *Gd* II .24(200)	4450.47	6	*Ti* II .49(50)
4421.96	3	*Ti* II .96(6)	4450.81	2	*Ce* II .73(75), *Ti* I .90(150)
4422.56	5	*Fe* I .57(300), *Gd* II .55(20)	4451.56	4	*Fe* II .54(4), *Nd* II .57(400), *Mn* I .59(125)
4422.96	1	.....	4452.03	1	*Nd* II .98(50)
4423.24	3	*Ti* II .27(pr)	4452.60	2	.....
4423.71	1	*Ce* II .68(25)	4453.23	2	*Ti* I .32(150), (*V* II .35(30))
4424.26	3vr	*Sm* II .34(600), *Cr* I .28(25), *Gd* II .10(40)	4453.86	2nn	*Gd* II .93(60), *Ti* I .71(80)
4425.13	0	*Cr* I .13(15)	4454.37	3	*Fe* I .38(200)
4425.44	3	*Ca* I .45(100)	4454.78	6r	*Ca* I .80(200), *Zr* II .80(10), (*Fe* I .03(20))
Absorption 4426.0 to 4426.7	1	*Gd* II .15(80), *Eu* II .42(5)	4455.28	4	*Fe* II .26(3), *Ti* I .33(150)
			4455.86	5	*Ca* I .89(100), *Fe* II .85(pr)
			4456.68	4n	*Ti* II .65(10), *Ca* I .63(20)
			4457.43	1	*Ti* I .43(150), *Zr* II .42(8)
4427.20	5n	*Fe* I .31(500), *Ti* I .10(125)	4457.71	1	.....
4427.92	4v	*Ti* II .92(pr), *Mg* II .00(7), *Ce* II .92(6)	4458.13	2	*Fe* I .11(30)
			4458.54	2	*Sm* II .52(400), *Cr* I .54(50)
4428.44	4n	*Cr* I .52(25), (*Fe* I .55(1))	4459.16	5r	*Fe* I .12(400), *Ni* I .04(400), *Cr* I .36(20)
4429.27	3	*Ce* II .27(100), (*Pr* II .24(100))	4459.75	2	*Cr* I .76(25)
4430.05	4n	*Ce* II .00(8), *Cr* I .94(15), (*La* II .91(400))	4460.22	3	*Ce* II .21(400)
4430.46	4	*Cr* I .49(15)	4461.13	3	*Ce* II .14(50), *Zr* II .22(10)
4430.72	2	*Fe* I .62(200)	4461.42	4	(*Fe* I .38)
4431.35	1	*Sc* II .37(50)	4461.67	5	*Fe* I .65(300)
4431.66	1	*Fe* II .63(1n)	4462.00	5	*Mn* I .01(40), *Fe* I .97(4)
4432.16	2	*Cr* I .17(30), *Ti* II .09(tr)	4462.28	0	.....
4432.69	1	*Fe* I .57(6)	4462.75	1	*Cr* I .77(20)
4433.23	3	*Fe* I .22(150)	4463.36	4	*Ce* II .41(60), *Gd* II .25(80)
4433.79	3n	*Cr* II .84(1), *Fe* I .79(30), *Sm* II .88(300), *Mg* II .99(8), *Ti* I .00(100)	4463.83	1	.....
			4464.14	0	.....
			4464.46	5	*Ti* II .46(40)
4434.33	2	*Sm* II .32(400)	4464.67	3	(*Cr* I .68(15))
4434.96	4	*Ca* I .97(150)	4465.02	2	*Cr* II .00(1), *Eu* II .97(200)
4435.61	9	*Eu* II .56(5000), *Ca* I .69(100)	4465.36	2	*Cr* I .36(20)
4436.25	2n	*Gd* II .22(200), *Mn* I .35(80)	4465.74	3	*Cr* II .78(4), *Ti* I .81(100)
4436.95	2	*Fe* I .95(15)	4466.57	6	*Fe* I .55(500), *Gd* II .55(500)
4437.31	0	*Gd* II .45(8)	4467.15	3nn	*Gd* II .23(80), *Sm* II .34(500)
4437.61	1	*Ce* II .61(20)	4467.54	2	*Ce* II .54(30), *Cr* I .56(20)
4438.20	3n	*Gd* II .26(150), (*Gd* II .13(30)), (*Pr* II .18(20))	4468.02	2nn	*Dy* II .14(60), *Dy* II .89(20)
			4468.50	8	*Ti* II .50(150)
4439.24	1	*Fe* II .13(pr)	4469.29	4nn	*Fe* I .38(200), *Ti* II .16(1)
4439.92	0n	.....	4470.54	0	*Ni* I .49(15)
4440.44	0	*Zr* II .45(10), *Fe* I .48(1)	4470.86	4	*Ti* II .86(25)
4440.93	3r	*Ce* II .88(20)	4471.25	3	*Ce* II .24(200), *Gd* II .29(200), *Ti* I .24(100)
4441.72	4	*Ti* II .72(pr)			
4442.35	4	*Fe* I .34(400)	4471.69	1	*Eu* II .64(4)
4442.83	1	*Ce* II .72(50), (*Zr* II .99(25))	4472.09	0	.....
4443.21	3	*Fe* I .20(200)	4472.86	4n	*Fe* II .92(2), *Mn* I .79(100)
4443.79	8	*Ti* II .80(125), (*Ce* II .74(18))	4473.72	2	*Cr* I .78(25)
4444.55	6v	*Fe* II .56(1), *Ti* II .56(12), *Ce* II .40(60), *Ce* II .70(75)	4474.19	1	*Fe* II .19(0)
			4474.71	2n	(*Ti* I .85(80))
4445.30	0	*Fe* II .26(pr)	4475.33	2	*Cr* I .34(40)
4446.22	2	*Fe* II .25(1n)	4476.06	7	*Fe* I .02(500)
4446.50	2	*Gd* II .49(250)	4476.54	1	.....
4446.86	2	*Fe* I .84(10)	4477.04	1	*Cr* I .05(20)
4447.72	5	*Fe* I .72(200)	4477.55	0	.....

TABLE 1—*Continued*

λ	*I*	Identification	λ	*I*	Identification
4478.01	1	.....	4508.28	5	*Fe* II .28(8)
4478.74	3	*Gd* II .80(250), *Mn* II .74(1), *Sm* II .66(125)	4508.73	2	*Ce* II .73(5), *Eu* II .66(10)
			4509.15	3	*Ce* II .18(12), *Gd* II .08(50)
4479.38	4n	*Ce* II .36(50), *Ce* II .43(30)	4509.70	1	.....
4479.58	1	*Fe* I .61(15)	4510.08	1	*Pr* II .16(100)
4480.12	3	*Fe* I .15(10), (*Eu* II .11(10))	4510.40	1	*Gd* II .38(30)
4480.75	2	*Fe* II .69(1)	4510.89	1	.....
4481.23	8r	*Mg* II .34(100), *Mg* II .14(50), *Cr* II .49(1)	4511.80	5	*Cr* II .82(pr), *Sm* II .83(200)
			4512.36	0	*Ca* I .28(10)
4482.23	4	*Fe* I .17(150), *Fe* I .26(150)	4512.81	0	*Ti* I .74(100)
4482.75	4	*Fe* I .75(20), *Ti* I .69(40)	4513.46	0	.....
4483.05	0	.....	4514.21	2	*Fe* I .20
4483.36	3	*Gd* II .33(300)	4514.46	5	*Gd* II .50(200), *Cr* I .53(30)
4483.91	2	*Ce* II .90(100)	4515.33	5	*Fe* II .34(7)
4484.24	3	*Fe* I .22(125)	4515.80	3	.....
4484.78	1	*Ce* II .82(30)	4516.27	1	*Nd* II .35(30), *Fe* I .27(1)
4485.17	0	*Eu* II .15(100)	4516.64	1	*Cr* II .56(pr)
4485.64	3n	*Fe* I .68(50), *Zr* II .44(2)	4517.11	2	*Gd* II .10(30)
4486.38	1	*Gd* II .35(100)	4517.57	1	*Fe* I .54(30), (*Pr* II .60(40))
4486.90	3	*Ce* II .91(150)	4518.00	0	*Ti* I .03(100)
4487.53	0	.....	4518.34	3	.....
4488.32	5v	*Ti* II .32(125), *Eu* II .28(15)	4519.59	1	*Sm* II .63(200)
4488.86	0	*Fe* I .92(3)	4520.21	5	*Fe* II .24(7)
4489.16	7	*Fe* II .18(4), *Ti* I .09(100)	4521.14	3	*Cr* I .14(25), *Gd* II .30(100)
4489.46	0	*Fe* I .74(100), *Cr* I .47(25)	4521.98	2	*Gd* II .94(150)
4490.10	1	*Fe* I .08(40), *Mn* I .08(100)	4522.60	9	*Fe* II .63(19), *Eu* II .57(2000)
4490.72	3n	*Fe* I .76(40)	4523.04	1	*Ce* II .08(125), *Sm* II .04(150)
4491.40	4	*Fe* II .41(5)	4523.46	1	.....
4491.80	1	*Cr* I .85(50)	4523.88	1	*Gd* II .88(20), *Sm* II .91(250)
4492.31	2	*Cr* I .31(30)	4524.58	3n	*Ti* II .73(10)
4492.80	1	.....	4525.16	5vn	*Fe* I .15(100), *Ba* II .95(80), *La* II .31(100)
4493.54	4	*Ti* II .53(8), *Fe* II .58(1n)			
4494.10	1n	.....	4526.13	2	*Cr* I .11(20), *La* II .12(200)
4494.56	6	*Fe* I .57(400)	4526.46	4	*Cr* I .46(50), *Fe* II .58(1)
4494.90	1	*Gd* II .85(25)	4526.92	1	*Ca* I .94(100)
4495.45	2n	*Ti* II .43(pr), *Fe* II .52(pr), *Zr* II .44(3), *Ce* II .39(4)	4527.38	4	*Ce* II .35(200), *Ti* I .31(100)
			4527.91	0n	*Dy* II .78(30)
4495.93	0	*Eu* II .92(2)	4528.60	7	*Fe* I .62(600), *Ca* II .48(150), *V* II .51(300)
4496.19	1	*Ti* I .16(60)			
4496.87	5	*Cr* I .86(200), (*Zr* II .96(15))	4529.52	6	*Ti* II .46(40), *Fe* II .56(pr)
4497.84	1	*Ce* II .85(25)	4529.88	1	*Cr* I .86(25)
4498.30	1	*Gd* II .28(300)	4530.75	5	*Cr* I .74(150)
4498.79	1	*La* II .76(10), *Cr* I .73(30)	4531.17	3	*Fe* I .15(125)
4499.10	1	.....	4531.71	2	*Fe* I .63(8), *Tb* II .83(6)
4499.68	2n	*Fe* II .71(0)	4532.48	1	*Ce* II .50(6)
4500.29	3	*Eu* II .27(30)	4533.09	3n	*Ti* I .24(150)
4500.72	1	*Gd* II .64(20), *Gd* II .83(20)	4533.63	0	*Eu* II .63(5)
4501.26	6	*Ti* II .27(100)	4534.05	9	*Ti* II .97(150), *Fe* II .17(2)
4501.75	2	*Nd* II .82(50), *Cr* I .79(15)	4534.73	1	*Ti* I .79(100)
4502.15	1	*Mn* I .22(125)	4535.20	1	*Cr* I .14(50)
4502.58	1	*Fe* I .60(3)	4535.72	4	*Cr* I .72(125), *Ti* I .58(80)
4503.02	1n	*Cr* I .04(10)	4536.56	1	.....
4503.58	1	.....	4536.89	0	.....
4504.67	2nn	(*Cr* II .52(pr))	4537.91	1	*Sm* II .95(200)
4505.46	0	.....	4538.47	0	.....
4505.86	1	.....	4538.77	0	*Dy* II .76(20)
4506.33	2	*Gd* II .33(200)	4539.07	0	.....
4506.99	4n	*Fe* II .20(0), *Ti* II .74(pr), *Gd* II .93(60), *Cr* II .19(pr)	4539.65	8	*Cr* II .62(2), *Ce* II .75(200)
			4540.62	4	*Cr* I .50(40), *Cr* I .72(40)
4507.77	2	.....	4541.09	1	*Cr* I .07(30)

TABLE 1—*Continued*

λ	*I*	Identification	λ	*I*	Identification
4541.53	5	*Fe* II .52(4)	4575.82	1	.....
4542.62	1v	*Nd* II .60(60), *Cr* I .62(30), *Cr* II .77(pr)	4576.37	6	*Fe* II .33(4)
			4576.87	0	*Eu* II .93(10)
4542.91	0	.....	4577.58	1n	*Sm* II .69(250)
4543.69	1	*Cr* I .74(20)	4578.55	2	*Ca* I .56(80)
4544.05	2	*Ti* II .01(20), *Sm* II .95(250)	4579.41	2n	*Fe* II .52(1)
4544.63	2	*Cr* I .62(100), *Ti* I .69(150), *Cr* II .69(pr)	4580.05	4	*Cr* I .06(300), *Fe* II .05(1)
			4580.47	1	*Ti* II .46(5)
4545.14	2	*Ti* II .14(15)	4581.11	2	*Gd* II .09(200), *Cr* I .06(300)
4545.40	0	*Cr* I .34(25), *Cr* II .49(pr)	4581.49	3	*Ca* I .41(100), *Fe* I .52(60)
4545.91	3	*Cr* I .96(200)	4582.45	3	*Gd* II .53(400), *Gd* II .38(300), *Ce* II .50(50)
4546.64	2	*Cr* II .62(1)			
4546.92	0	*Ni* I .94(5)	4582.85	3	*Fe* II .84(3)
4547.26	1	*Eu* II .22(3)	4583.40	2	*Ti* II .44(10)
4547.86	2	*Fe* I .85(200)	4583.90	7r	*Fe* II .85(11)
4548.70	1	*Ti* I .76(125)	4584.82	2r	*Fe* I .83(8), *Sm* II .83(150)
4549.22	4	*Fe* II .21(4)	4585.89	2	*Ca* I .88(125)
4549.56	10r	*Ti* II .63(200), *Fe* II .47(10)	4586.17	2	*Cr* I .14(25)
4550.33	1	.....	4587.22	3	*Fe* I .13(12)
4550.82	3	*Fe* I .77(50), *Gd* II .95(150)	4588.23	7	*Cr* II .22(75)
4551.41	1r	*Gd* II .46(30), *Ce* II .30(20)	4588.69	0	*Gd* II .76(10)
4552.39	4	*Ti* I .45(150), *Ti* II .29(pr)	4589.29	0n	.....
4554.01	5	*Ba* II .04(200), *Zr* II .96(12)	4589.93	7	*Ti* II .95(100), *Cr* II .94(3)
4554.57	0	.....	4590.72	0	.....
4554.98	5	*Cr* II .03(20)	4591.16	0	.....
4555.47	0	*Ti* I .49(125)	4591.49	1	*Cr* I .39(200), *Cr* II .39(tr)
4556.02	5n	*Fe* II .90(8), *Fe* I .12(150)	4592.06	6	*Cr* II .06(20)
4556.99	0	.....	4592.61	2	*Fe* I .66(200)
4557.35	1	.....	4593.83	3n	*Ce* II .93(200)
4558.14	1	*Gd* II .08(250)	4594.46	0	*Nd* II .45(6)
4558.70	9	*Cr* II .66(100), *Cr* II .83(pr)	4595.46	3vnn	*Fe* II .68(pr), *Sm* II .29(250)
4559.33	0	*La* II .28(100)	4596.05	2	*Fe* I .06(10)
4560.21	2n	*Ce* II .28(125)	4596.34	0	.....
4560.96	2	*Ce* II .96(60)	4597.06	2vn	*Gd* II .98(400)
4561.49	2	.....	4597.95	3	*Gd* II .91(500), *Fe* I .13(50)
4562.37	2	*Ce* II .36(400)	4598.46	2	*Cr* I .44(20), *Fe* II .53(1n)
4563.22	3n	*Nd* II .22(40), *Cr* I .24(12), (*Pr* II .13(30))	4599.06	0	.....
			4599.83	1	*Fe* I .90(1)
4563.79	5	*Ti* II .77(200)	4600.11	2	*Cr* .10(20)
4564.27	2	*Cr* II .27(1)	4600.78	2	*Cr* I .75(150)
4564.78	2	*Fe* I .70(1), *Fe* I .83	4601.00	2	*Gd* II .05(500)
4565.44	1	.....	4601.40	1	*Fe* II .34(pr)
4565.77	6	*Cr* II .78(10), *Ce* II .85(50)	4601.96	2	*Zr* II .97(2), *Fe* I .01(20)
4566.55	0	.....	4602.94	2	*Fe* I .94(300)
4566.93	1	*Fe* I .88(1)	4603.38	0	.....
4567.44	0	.....	4603.87	0	.....
4568.04	0	.....	4604.44	1n	.....
4568.35	1	*Ti* II .31(8)	4604.94	1	*Ni* I .00(300)
4568.85	1	.....	4605.51	2	*Mn* I .36(150)
4569.62	3	*Cr* I .64(50)	4606.42	2	*Ce* II .40(50), *Sm* II .51(100)
4571.16	2	*Mg* I .15(20), *Cr* II .24(pr)	4607.31	1	*Sr* I .33(1000)
4571.72	2	*Cr* I .68(50)	4607.69	2	*Fe* I .65(50)
4572.00	7	*Ti* II .98(300)	4607.98	0	*Gd* II .03(40)
4572.26	2	*Ce* II .28(250)	4608.75	1	.....
4572.87	3	*Cr* II .83(pr)	4609.29	1	*Ti* II .27(pr)
4573.63	2n	*Cr* II .63(pr), *Eu* II .66(4)	4609.90	0	.....
4574.26	0	.....	4610.54	0	.....
4574.82	1	*Fe* I .72(12), *La* II .88(200)	4611.32	3	*Fe* I .29(200)
4575.10	1	*Cr* I .12(25)	4611.92	1	*Cr* I .97(15)
4575.52	1	.....	4612.49	0	.....

TABLE 1—*Continued*

λ	*I*	Identification	λ	*I*	Identification
4613.29	3n	*Fe* I .22(30), *Cr* I .37(150), *La* II .38(200)	4625.47	1	*Fe* II .55(tr)
4614.05	2n	.....	4626.08	3n	*Fe* II .91(1), *Cr* I .18(100)
4614.61	1	*Eu* II .63(6)	4626.83	1	*Fe* II .78(pr)
4614.90	1	.....	4627.57	1n	*Gd* II .66(40)
4615.55	1	*Sm* II .44(150), *Sm* II .69(300)	4628.22	2	*Ce* II .16(500)
4616.16	5	*Cr* I .14(300)	4628.83	1	*Fe* II .82(0n)
4616.64	6	*Cr* II .66(18)	4629.37	4	*Fe* II .33(7)
4617.34	0	*Ti* I .27(200), *Dy* II .27(30)	4630.22	1n	*Fe* I .13(10), *Sm* II .21(60)
4618.00	0	.....	4630.72	1n	.....
4618.82	6	*Cr* II .83(35)	4632.12	1v	*Fe* II .90(0n)
4619.43	4n	*Fe* I .30(100), *Cr* .55(50)	4632.87	1	*Fe* I .92(70)
4620.00	0	*Dy* II .04(60)	4633.27	0	*Cr* I .26(20)
4620.54	5	*Fe* II .51(3)	4633.70	0	*Eu* II .68(6)
4621.19	0	.....	4634.09	4	*Cr* II .09(25)
4621.59	0	*Cr* II .41(pr)	4634.76	1	*Fe* I .71
4621.93	2	*Cr* .96(50)	4635.34	3	*Fe* II .33(5)
4622.55	2r	*Cr* .49(30)	4635.85	0	*Fe* I .86(12)
4623.14	0	*Ti* I .10(125)	4636.33	1	*Ti* II .33(1)
4623.56	0	.....	4636.78	0	.....
4624.36	1n	*Cr* II .58(2)	4637.17	0	*Cr* I .18(20)
4625.05	2	*Fe* I .06(100), *Ce* II .91(60)	4637.57	2	*Fe* I .52(100)
			4638.04	3	*Fe* I .02(80)

Sc II are moderately strong; and *Si* II, *Mn* II, *Sc* I, *Ti* I, *V* II, *Co* I, *Ni* I, *Ni* II, *Sr* I, *Y* II, and *Sr* II are weak), the spectrum of β CrB contains many lines that can be identified with singly ionized rare earths. For example, the *Eu* II lines λλ 4129, 4205, 4435, and 4522 (blended with *Fe* II) are among the strongest lines in the spectrum. Other singly ionized rare earths are present; *Gd* II and *Ce* II are especially well represented. The evidence in regard to all the singly ionized rare earths is as follows:

La II	Weak, but present
Ce II	Moderately strong
Pr II	Probably present, but very weak
Nd II	Very weak, if present. May contribute to blends
Il II	Laboratory data not complete
Sm II	Present, but weak
Eu II	Very strong
Gd II	Moderately strong
Tb II	May contribute to blends
Dy II	Very weak, but present
Ho II	Probably not present
Er II	Laboratory data not complete
Tm II	May be present
Yb II	Probably not present, but *Yb* II spectrum not well represented in investigated region
Lu II	Probably not present

The presence of neutral rare earths has been investigated with negative results. The *Eu* I spectrum has two especially strong lines at λ 4594.03 and λ 4627.22, but neither one can be identified in β CrB. The spectrum of *Gd* I has an abundance of strong lines in the region under investigation, but again none of the lines can be identified with certainty in the spectrum of β CrB.

TABLE 2

UNIDENTIFIED LINES ($I \leq 2$)

β CrB		α² CVn				α Car			
λ	I	λ (Mean)	I	Identification	Reasons Why Not Similarly Identified in β CrB	λ	I	Identification	Reasons Why Not Similarly Identified in β CrB
3982.26...	2	3982.39	0–1	*Nd* II .36(20), *Pr* II .50(40)	Strong laboratory lines of *Nd* II and *Pr* II very weak if present	.....	.....	.....	
3987.60...	4	3987.68	0–4	*Nd* II .81(5), *Ho* II .55(3)	Strong laboratory lines of *Ho* II not present	3987.59...	6	.....	
4002.91...	5	4002.88	0–1	*V* II .94(80)	Too strong	4002.93...	4	*V* II .94(80)	Too strong
4004.90...	8	4004.78	0–2	*Gd* II .94(150)	Too strong	4004.89...	3	*Fe* I .84(10)	Too strong
4007.98...	2n	4008.02	1	(*Er* (II?) .97(57))		4007.97...	0	.....	
4009.17...	4	4009.24	0–2	*Gd* II .22(80)	Too strong	4009.17...	1–0	.....	
4010.16...	3	4010.09	1–2	*Dy* II .08(3)	Strong laboratory lines of *Dy* II very weak	.....	.....	.....	
4010.59...	4r	4010.65	0–1	*Mn* II .84(1)	Wave-length difference too great	4010.59...	1–0	*Fe* I .78(1)	*Fe* I .78 identified with 4010.87
4015.62...	4	.....	.....	.....		4015.60...	0v	.....	
4018.97...	2n	4019.09	0–2	*Tb* II .14(20)	Strong laboratory lines of *Tb* II very weak if present	.....	.....	.....	
4020.28...	2	.....	.....	.....		4020.26...	0	.....	
4045.16...	5	4045.32	0–2	*Ho* II .43(200), *Gd* II .15(100)	Too strong	4045.13...	1	*Fe* I .12(pr)	Too strong
4139.07...	2	.....	.....	.....		.....	.....	.....	
4142.84...	2	4142.73	0–1	.....		.....	.....	.....	
4155.95...	3	.....	.....	.....		.....	.....	.....	
4159.17...	5	4159.11	0–1	*Ce* II .03(50)	Too strong	4159.20...	2	.....	
4163.06...	2	.....	.....	.....		.....	.....	.....	
4174.43...	5	4174.51	0	.....		.....	.....	.....	
4181.96...	3	4181.98	0–2	.....		4181.95...	1–0	.....	

TABLE 2—*Continued*

CrB		α^2 CVn				α Car			
λ	*I*	λ (Mean)	*I*	Identification	Reasons Why Not Similarly Identified in β CrB	λ	*I*	Identification	Reasons Why Not Similarly Identified in β CrB
4183.99...	6v	.....	....	.....		4184.00...	2	.....	
4188.74...	6	4188.78	1–3	.....		4188.74...	2	.....	
4189.62...	3	.....	....	.....		4189.58...	1n	*Pr* II .52(125)	Too strong
4198.06...	5	4198.12	2–3	*Si* II .17(2)	Too strong	4198.11...	1	.....	
4214.74...	2	.....	....	.....		.....	....	.....	
4242.76...	5	4242.85	0–1	*Ce* II .72(15)	Too strong	.....	....	.....	
4335.41...	2	.....	....	.....		.....	....	.....	
4353.46...	2	4353.37	0–1	*Tb* II .19(50)	Strong laboratory line of *Tb* II very weak if present	4353.44...	0	.....	
4355.36...	2	4355.38	1–6	*Eu* II .09(300)	*Eu* II .09 identified with λ 4355.11	.....	....	.....	
4362.47...	2	.....	....	.....		.....	....	.....	
4396.55...	2n	4396.52	0–1	.....		.....	....	.....	
4397.28...	2n	.....	....	.....		.....	....	.....	
4403.05...	4n	.....	....	.....		.....	....	.....	
4452.60...	2	4452.55	0–2	(P II .44(150))	*P* II not present	.....	....	.....	
4461.42...	4	4461.30	0–3	*Zr* II .22(10)	Wave-length difference too great	4461.49...	8nn	*Zr* II .21(10), *Fe* I .65(8)	*Zr* II .21 identified with 4461.13 *Fe* I .65 identified with 4461.67
4464.67...	3	.....	....	.....		.....	....	.....	
4474.71...	2n	4474.86	0–1	*Ti* I .85(80)	Probably too strong	.....	....	.....	
4504.67...	2nn	.....	....	.....		.....	....	.....	
4507.77...	2	4507.52	0–1	.....		.....	....	.....	
4515.80...	3	4515.76	1–3	(*Tb* II .87(6))	*Tb* II very weak if present	.....	....	.....	
4518.34...	3	4518.28	0–2	(*Ti* I .03(100))	*Ti* I .03 identified with λ 4518.00	4518.35...	4	.....	
4561.49...	2	4561.55	1	(*Pr* II .46(6))	Too strong	.....	....	.....	
4614.05...	2n	.....	....	.....		.....	....	.....	

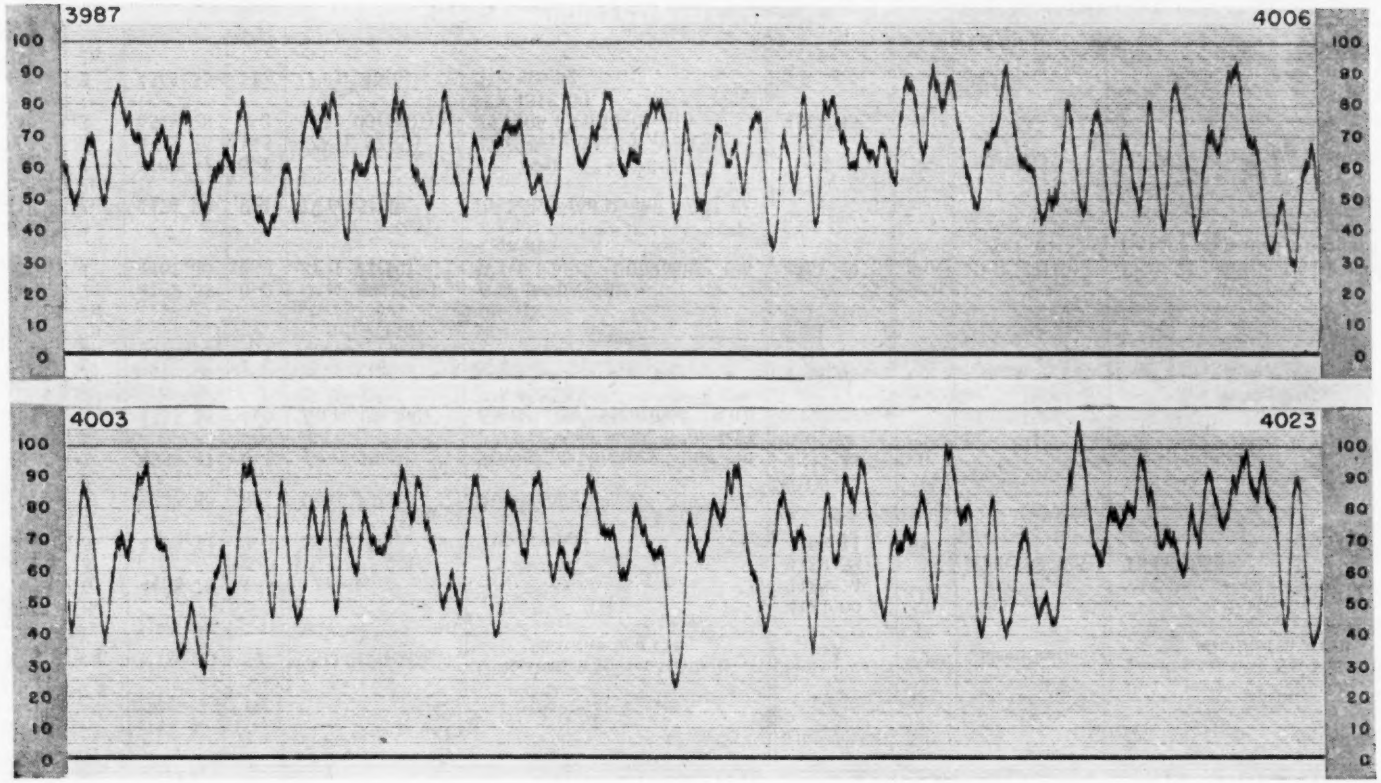

FIG. 1.—Intensity tracings of the spectrum of β Coronae Borealis

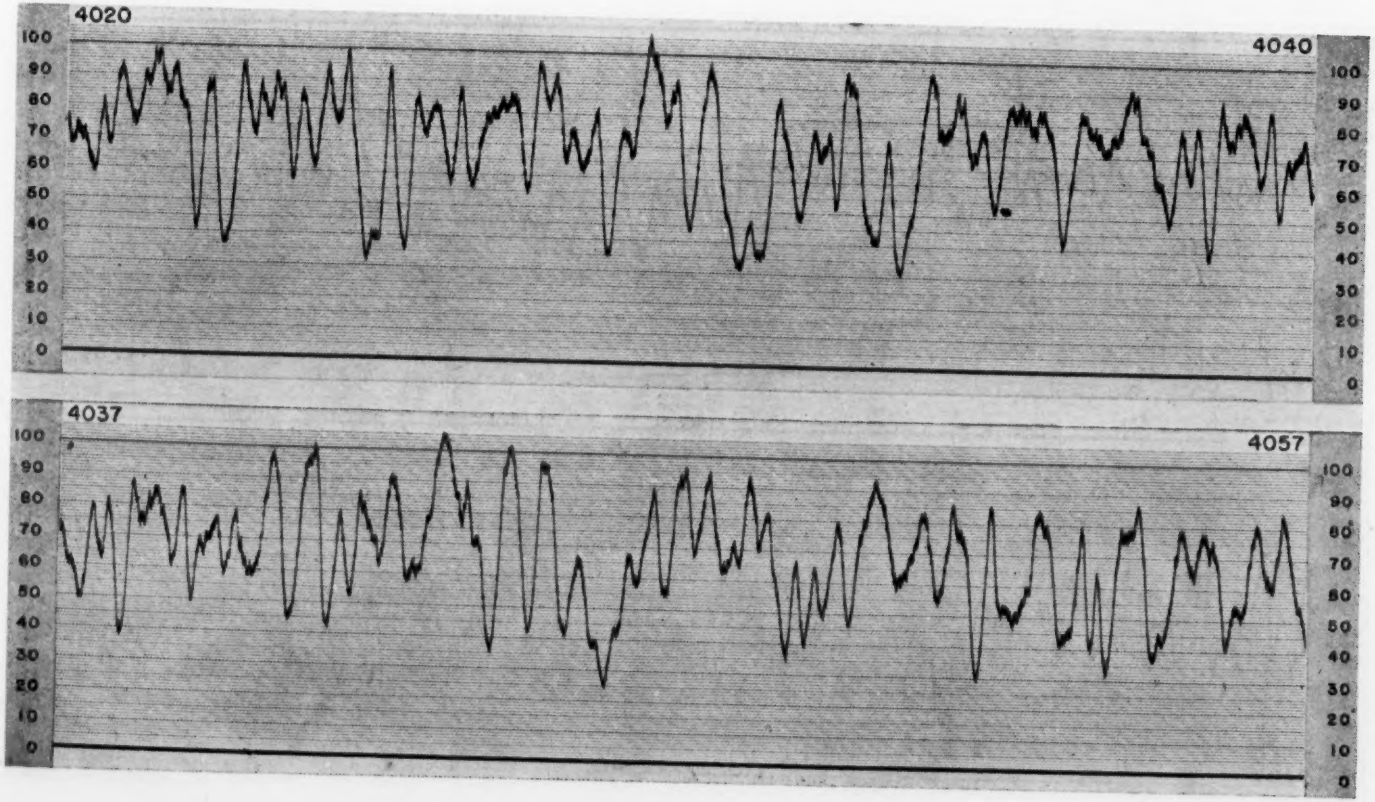

FIG. 2.—Intensity tracings of the spectrum of β Coronae Borealis

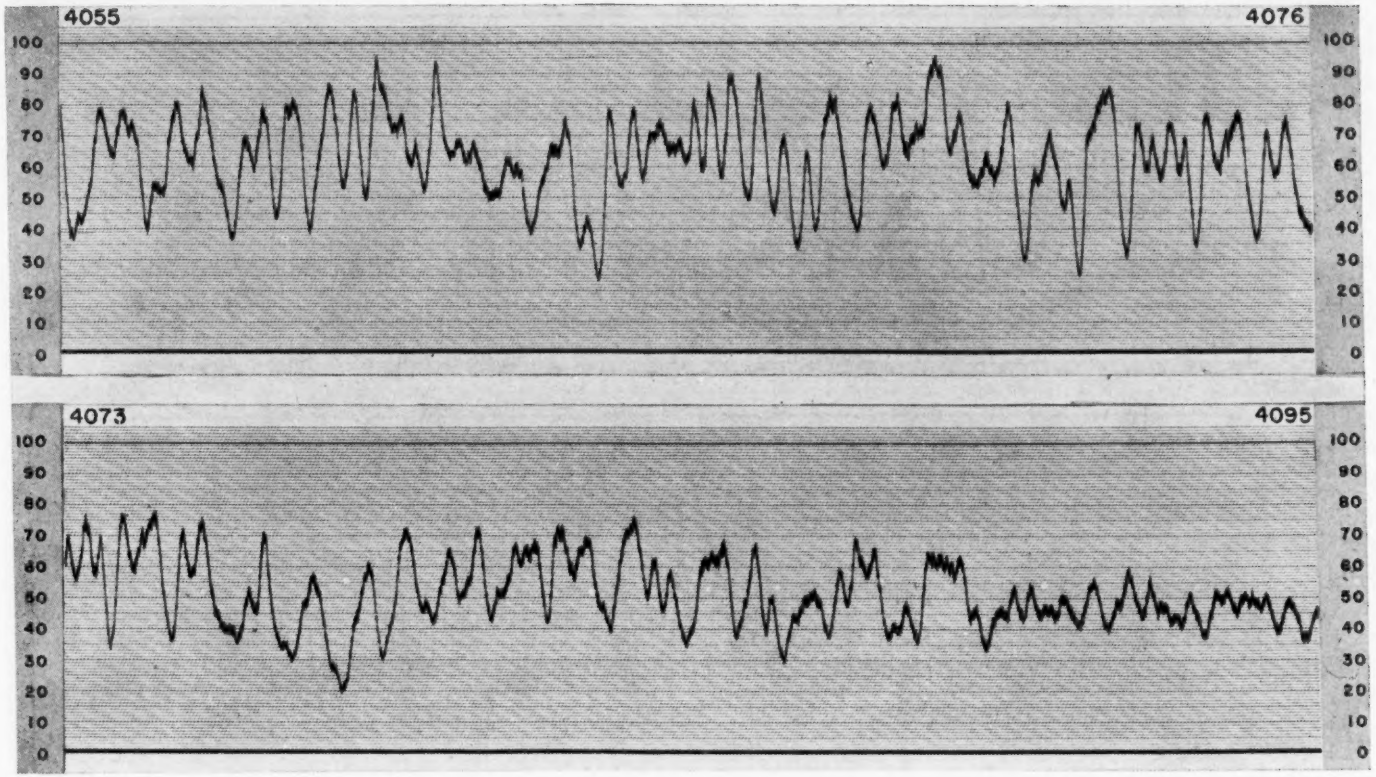

FIG. 3.—Intensity tracings of the spectrum of β Coronae Borealis

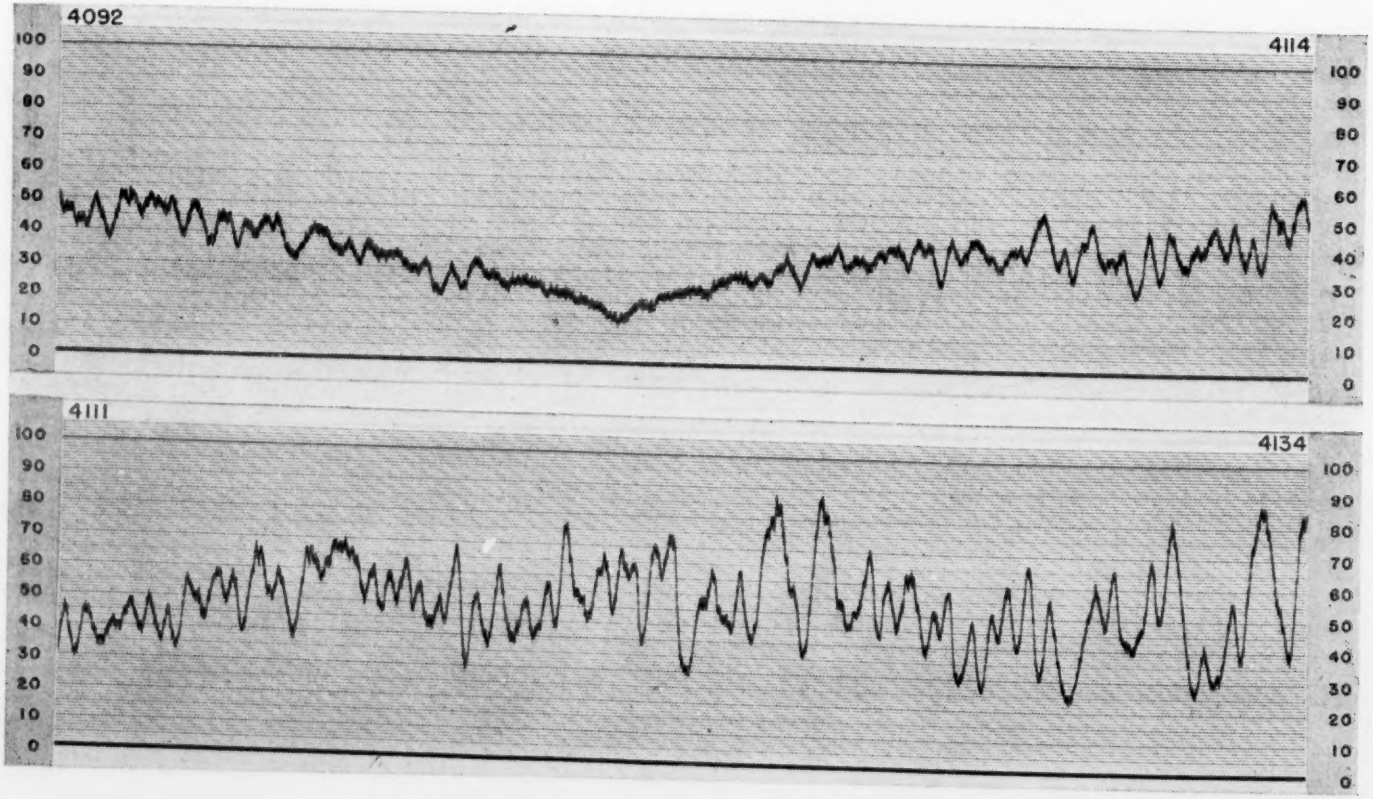

FIG. 4.—Intensity tracings of the spectrum of β Coronae Borealis

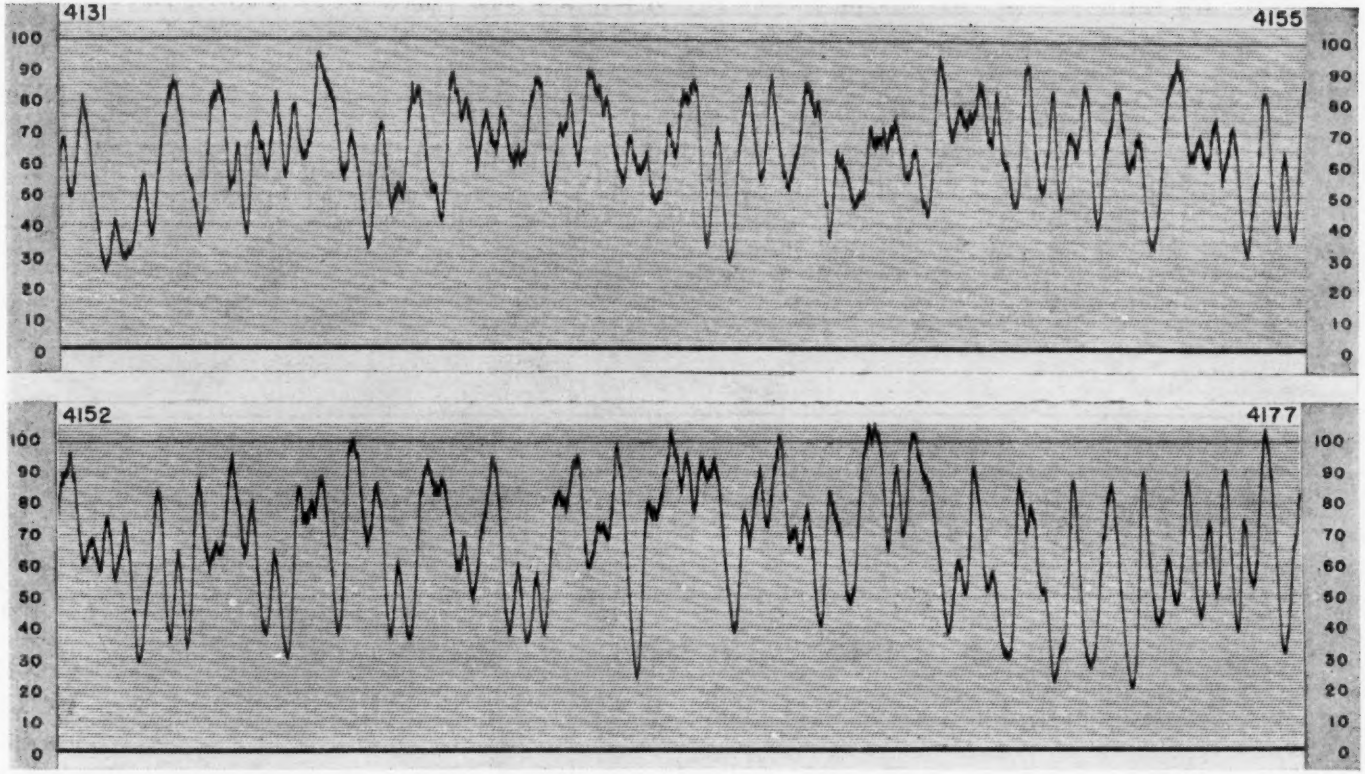

FIG. 5.—Intensity tracings of the spectrum of β Coronae Borealis

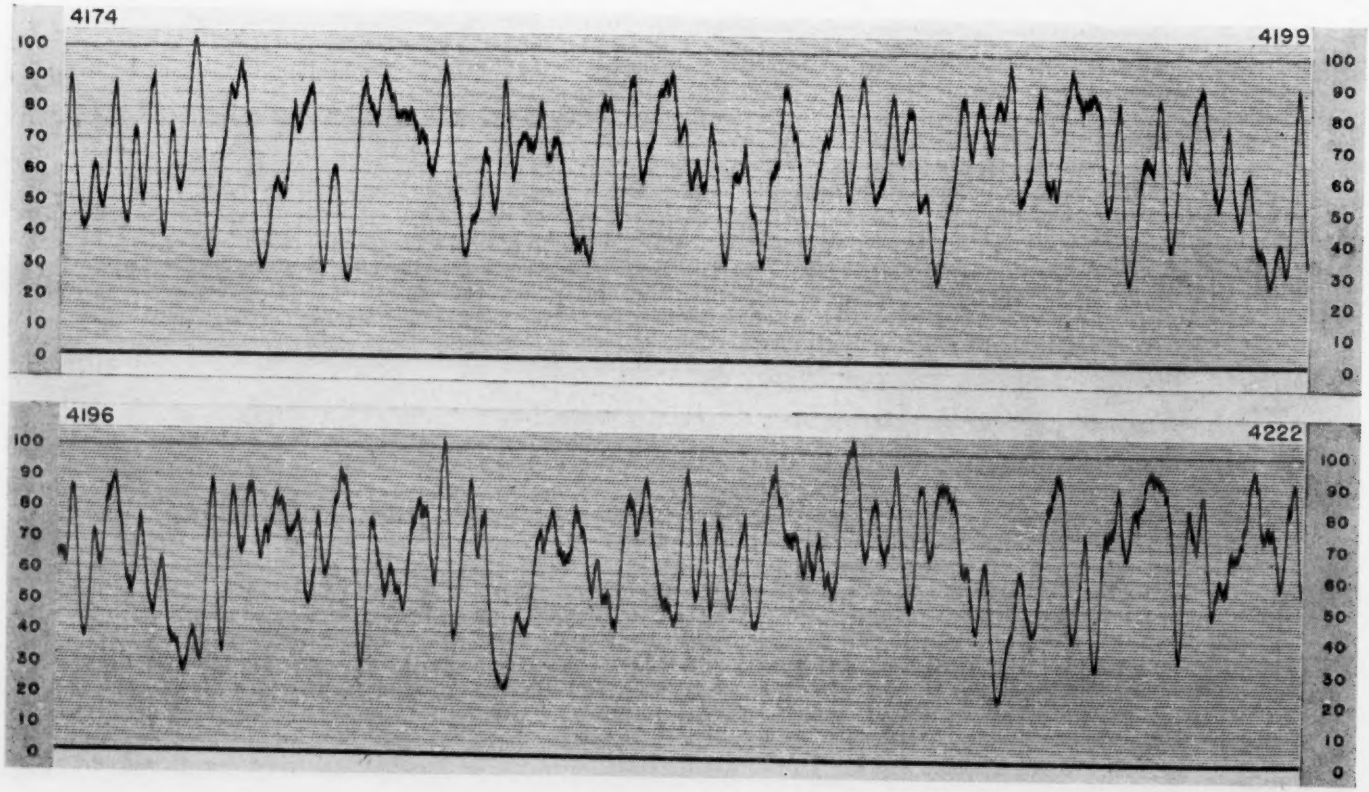

FIG. 6.—Intensity tracings of the spectrum of β Coronae Borealis

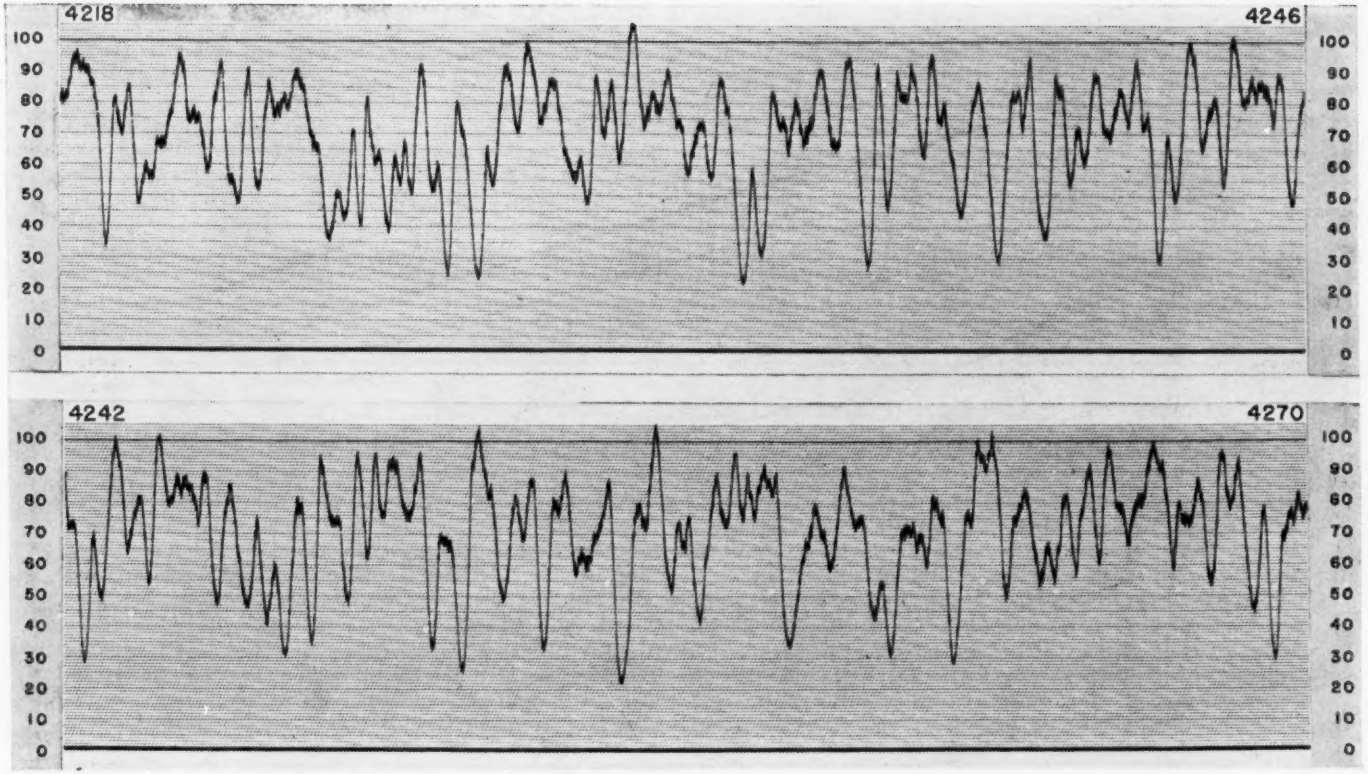

FIG. 7.—Intensity tracings of the spectrum of β Coronae Borealis

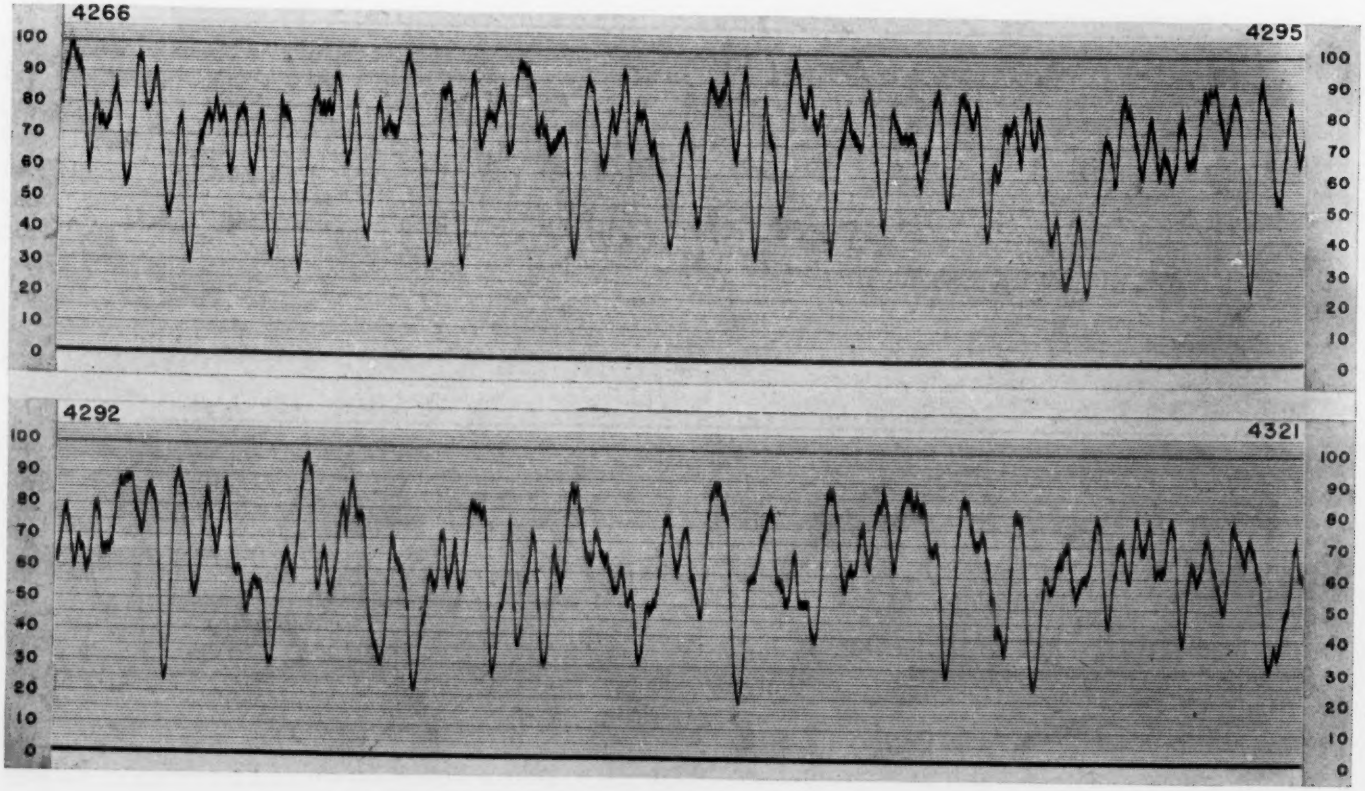

FIG. 8.—Intensity tracings of the spectrum of β Coronae Borealis

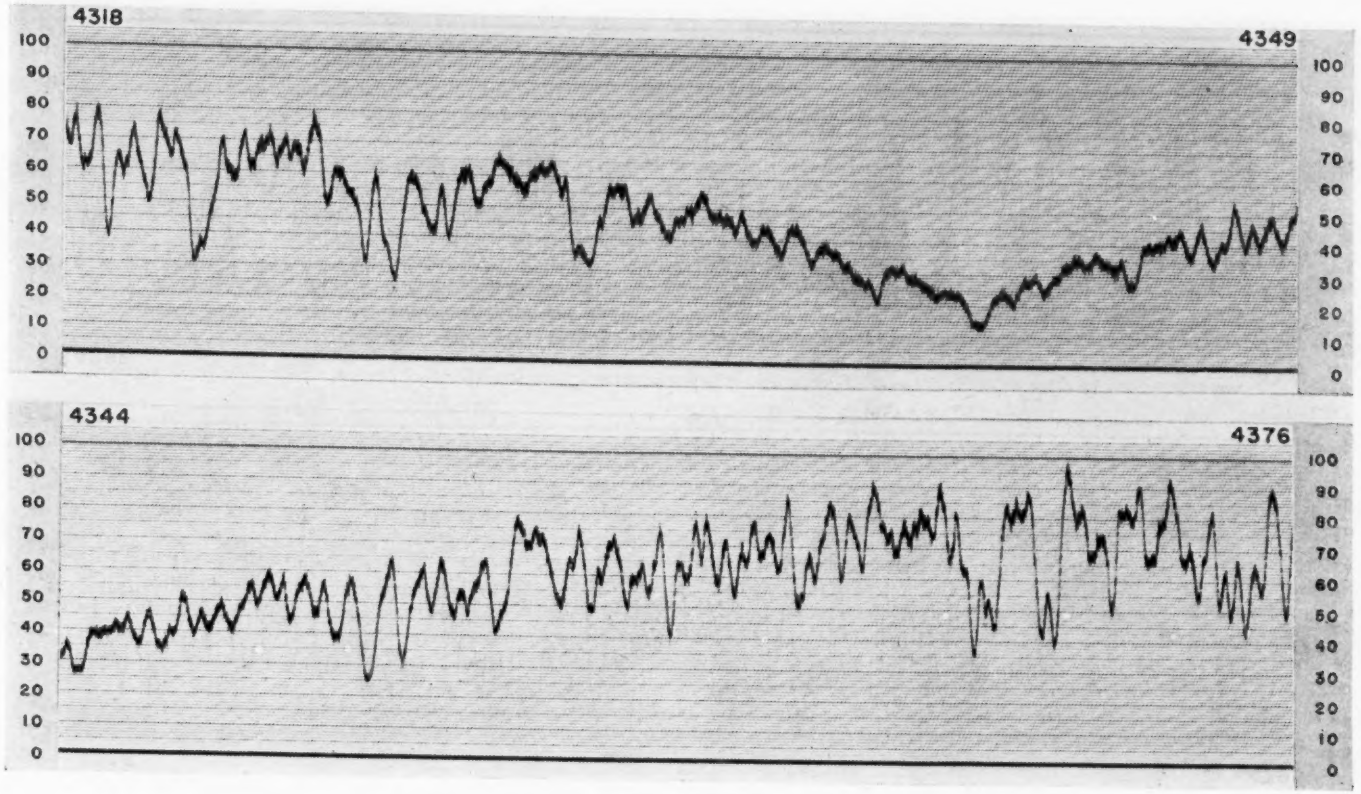

FIG. 9.—Intensity tracings of the spectrum of β Coronae Borealis

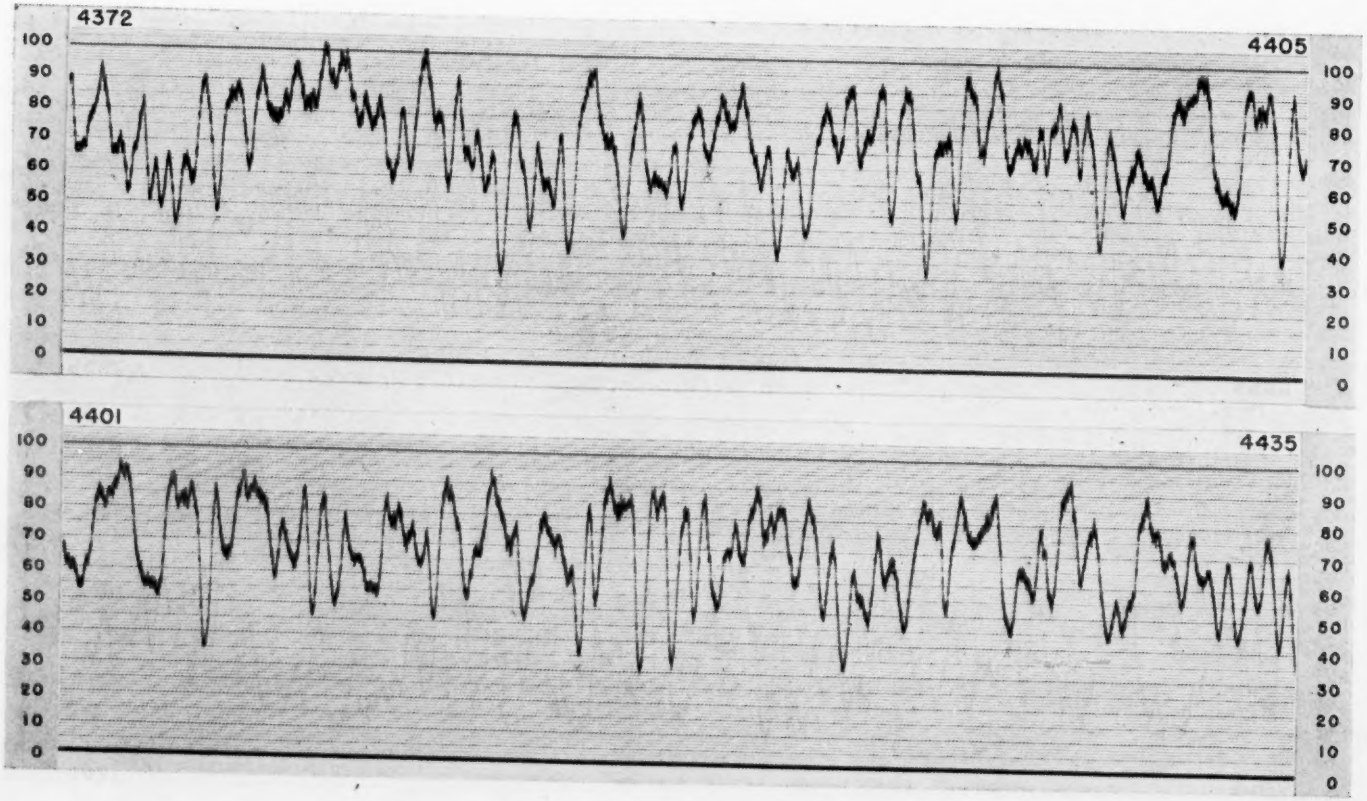

FIG. 10.—Intensity tracings of the spectrum of β Coronae Borealis

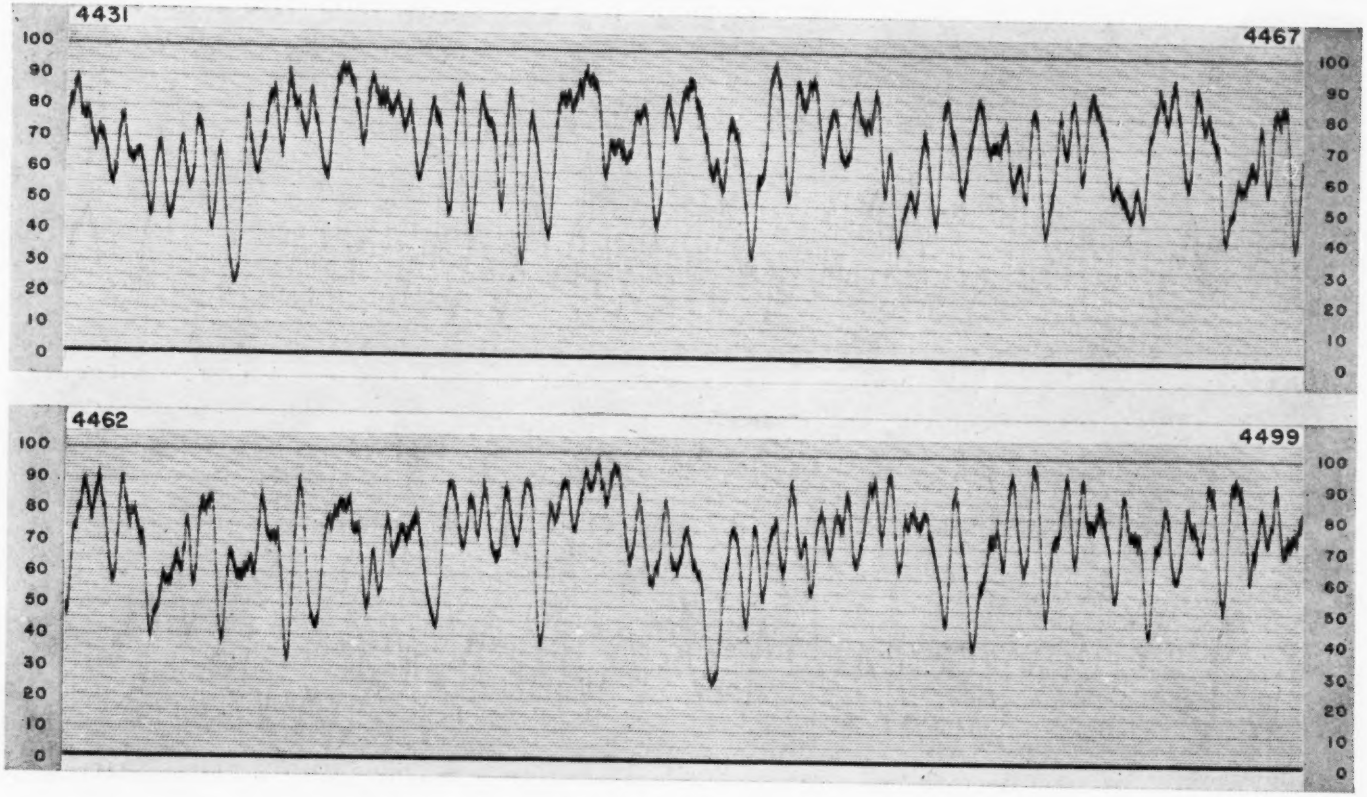

FIG. 1.—Intensity tracings of the spectrum of β Coronae Borealis

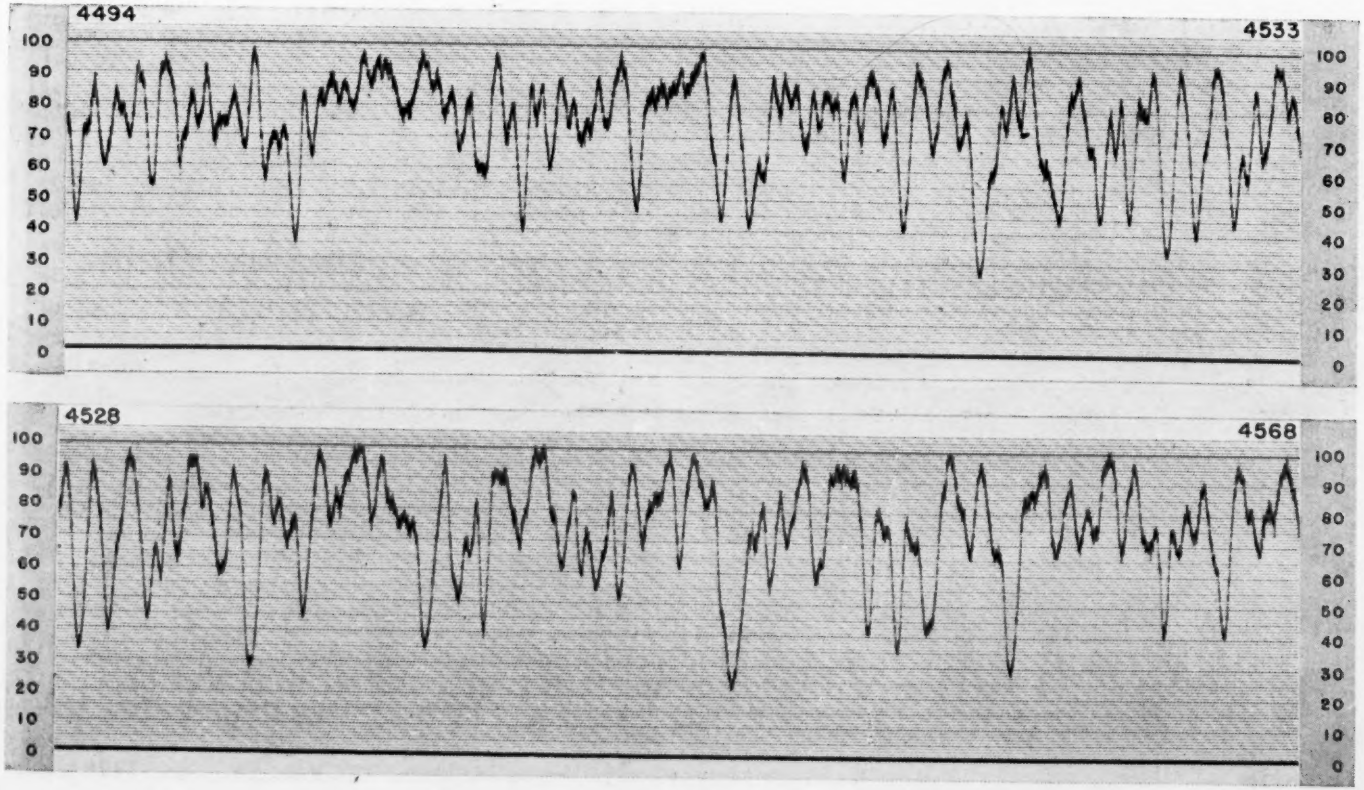

FIG. 12.—Intensity tracings of the spectrum of β Coronae Borealis

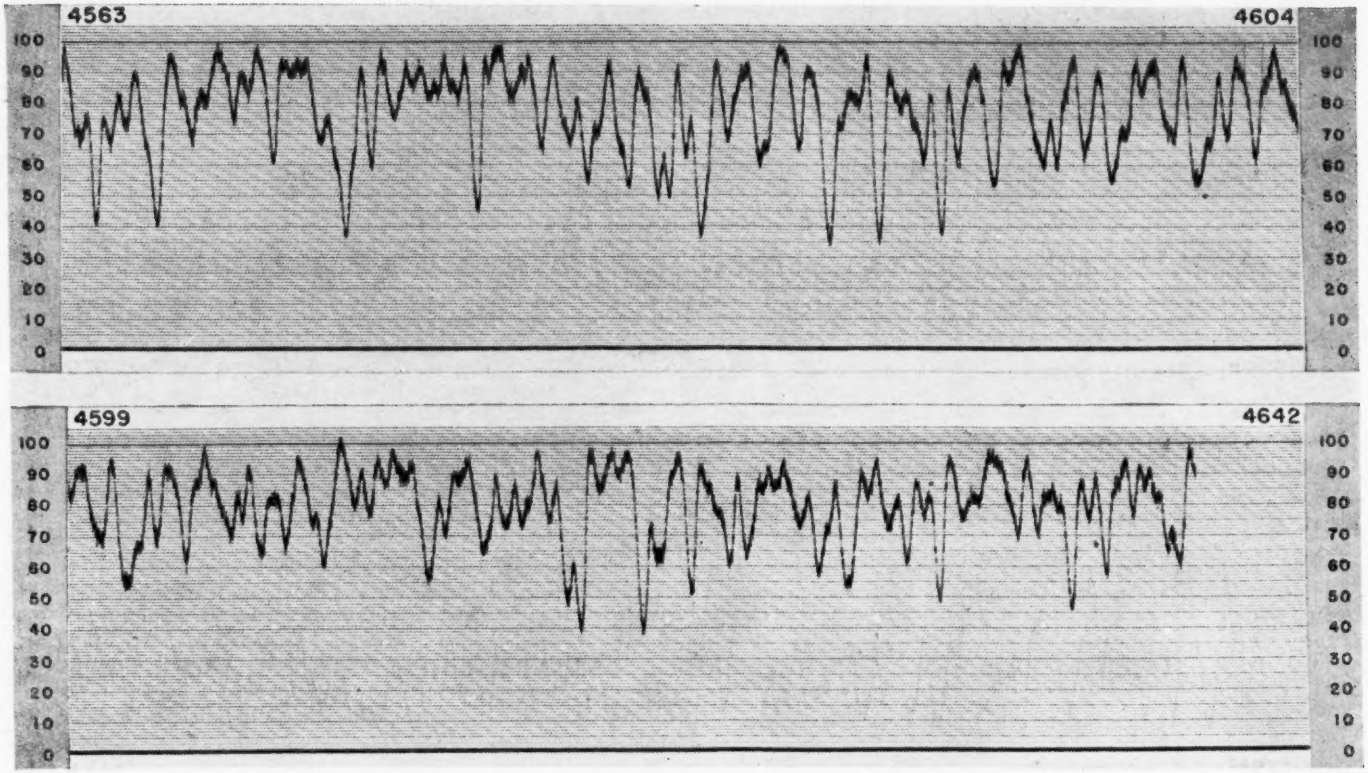

FIG. 13.—Intensity tracings of the spectrum of β Coronae Borealis

Previous to measuring the spectrogram for wave lengths, it was analyzed with the direct-intensity microphotometer[14] of the University of Michigan. The resulting tracings are shown in Figures 1–13. An attempt was made to place the apparent continuum at an intensity of 100, but this was difficult at the shorter wave lengths, where the continuum is poorly defined.

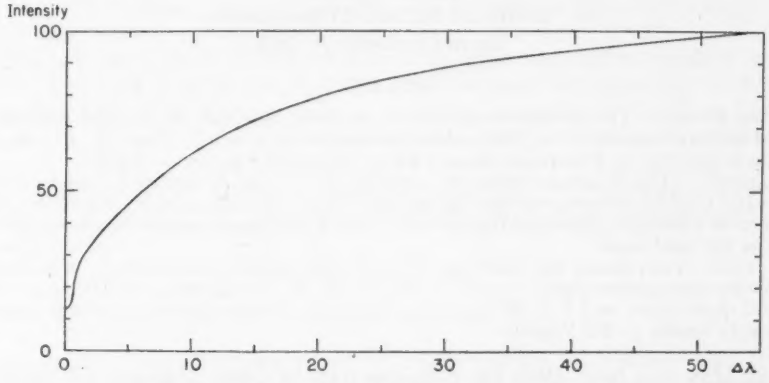

FIG. 14.—The profile of $H\gamma$ in β Coronae Borealis

Since it is not feasible to determine the profile of the broad hydrogen lines from the large-scale tracings, the profile of $H\gamma$ was determined from a small-scale tracing of the high-dispersion spectrogram. It is shown in Figure 14. The hydrogen lines in β CrB are much broader than in α Car.[15] The equivalent width of $H\gamma$ in β CrB is 18.3 A, in contrast to 7.5 A (as measured on coudé spectrograms) in α Car. The absolute magnitudes of β CrB and α Car are $+1.3$ and -3.8, respectively.

[14] Robley C. Williams and W. A. Hiltner, *Ap. J.*, **98**, 43, 1943.

[15] Greenstein, *op. cit.*, p. 193.

SPECTROGRAPHIC OBSERVATIONS OF THE ECLIPSING VARIABLES W URSAE MINORIS, XZ SAGITTARII, AND KO AQUILAE*

JORGE SAHADE
Yerkes and McDonald Observatories
Received September 10, 1945

ABSTRACT

W Ursae Minoris.—The primary component is of about type A3. The orbital elements from 29 McDonald spectrograms are: $P = 1.70116$ days (photometric); $\gamma = -17.9$ km/sec; $K = 86.6$ km/sec; $e = 0.09$; $\omega = 221°.6$; $T =$ Phase 0.611 days; $a \sin i = 2.0 \times 10^6$ km; $f(m) = 0.11 \odot$.

XZ Sagittarii.—This system is formed by a primary star of type A3 and by a secondary star of type late F or early G and is extremely interesting because of the small value of K ($\sim$11 km/sec), considering that the period is 3.3 days. The mass function is so small as to impose severe restrictions upon the mass ratio and/or the total mass.

KO Aquilae.—The primary star is of type A0 or A1. The orbital elements from 38 spectrograms are $P = 2.863844$ days (photometric); $\gamma = -2.7$ km/sec; $K = 37.8$ km/sec; $e = 0.02$; $\omega = 130°.9$; $T =$ Phase 0.372 days; $a \sin i = 1.5 \times 10^6$ km; $f(m) = 0.016 \odot$. As far as the mass ratio is concerned, this system is very similar to BD Virginis.

During May and June, 1945, the eclipsing stars W Ursae Minoris, XZ Sagittarii, and KO Aquilae were included in the spectrographic program of the 82-inch reflecting telescope of the McDonald Observatory. They were selected from Dugan's *Finding List*[1] in consideration of the shortness of the periods, the apparent brightness at maximum light, and the large difference in the depths of the two minima of light. Table 1 lists the

TABLE 1

THE PROGRAM

STAR	POSITION FOR 1945		PERIOD (IN DAYS)	CHAR.	MAGNITUDE			D	d	SP.	REMARKS
	α	δ			M	A_1	A_2				
W UMi.....	$16^h21^m.2$	$+86°\ 21'.6$	1.70116	A	8.61	1.12	0.17	9^h	0^h	A0	Good light-curve; br. star larger
XZ Sgr.....	18 18.7	−25 16.2	3.275537	A	8.5	2.8	.....	7	2.2	A2	Deep; total? Dense A?
KO Aql.....	18 44.6	+10 41.9	2.863844	A	8.15	1.13	0.08	9.1	1.0	A0	Shal. total; secondary?

periods, the photometric data, and the spectral types as they appear in Schneller's *Katalog und Ephemeriden veränderlicher Sterne für 1941*;[2] the remarks are from Dugan's list. A spectrographic orbit of W UMi has already been worked out by Joy and Dustheimer.[3] The star XZ Sgr was selected in order to find whether the spectrum at mid-eclipse shows emission lines like those of RW Per[4] and TT Hya[5]—stars which also have very deep principal minima.

* *Contributions from the McDonald Observatory, University of Texas*, No. 116.

[1] *Contr. Princeton U. Obs.*, No. 15, 1934. [2] *Kl. Veröff. Berlin-Babelsberg*, No. 22, 1940.

[3] *Ap. J.*, **81**, 479, 1935; *Mt. W. Contr.*, No. 521.

[4] O. Struve, *Ap. J.*, **102**, 89, 1945; *McD. Contr.*, No. 110.

[5] Wyse, *Lick Obs. Bull.*, No. 464, 1934; Sahade and Cesco, unpublished.

All the observations were made with the Cassegrain spectrograph. Most of the spectrograms were taken on glass plates of Eastman 103a-O emulsion, using two quartz prisms and a 500-mm camera, a combination which gives a linear dispersion of 55 A/mm at $H\gamma$. They are indicated with the designation "CQ" in the tables which list the measured radial velocities. A few other spectrograms, especially those taken at the principal minima of W UMi and XZ Sgr, were obtained on 103a-O film with two glass prisms and a 180-mm Schmidt camera, giving a dispersion of 76 A/mm at $H\gamma$. The films are marked "Gf/2" in the tables of radial velocities.

The exposure times in fair seeing, at maximum light, were approximately as follows: W UMi, 30 minutes on the plates; XZ Sgr, 45 minutes on the plates and 15 minutes on the films; KO Aql, 30 minutes on the plates and 10 minutes on the films. For the exposures with the 500-mm camera, except in one or two cases, a slit width of 0.075 mm was used; with the Schmidt camera this width was increased to 0.10 mm. During the interval of nearly 4 weeks in which the three stars were observed, 29 spectrograms were secured of W UMi, 27 of XZ Sgr, and 39 of KO Aql. Spectrograms at mid-eclipse were obtained in each case.

W URSAE MINORIS[6]

PHOTOMETRIC DATA

The variability of the star was discovered independently by Astbury[7] and Davidson[8] in 1913, and its provisional designation was 12.1913 and 23.1913. Both discoverers stated that the star is of the Algol type. Up to the present time, four determinations of the light-curve of W UMi have been published. The first was a photographic curve by Martin and Plummer,[9] who considered 1.701213 days as being the period and stated that "the whole variation is sensibly symmetrical, and a circular orbit may be assumed." A second determination was undertaken by McLaughlin,[10] who used the visual observations of Hassenstein.[11] McLaughlin was led to the conclusion that a different value should be adopted for the period, namely, 1.70116 days, and that reflection effect was present. This discussion was followed by one by M. Shapley and I. Woods,[12] based upon Harvard photographs; this new photographic light-curve "shows no evidence of ellipticity or of reflection." The last photometric study of W UMi is that of Dugan,[13] who gave for the epoch of minimum and the period the value

$$\text{JD } 2422813.6137 + 1.70116\,E$$

and for the magnitude at maximum and minima of light the values quoted by Schneller and repeated in Table 1 of this paper. Dugan's light-curve shows both reflection and ellipticity effects and the secondary minimum "clearly outlined at mid-period." All the photometric observations indicate that the more luminous body is the larger. There is no indication of the change of period suggested by Gadomski.[14]

THE SPECTRUM OF W UMI

The plates obtained at maximum light show only the spectrum of the primary star, which is about of type A3; the criterion for the classification was the relation ($H\epsilon$ + H)/K. The spectrogram secured at mid-eclipse still shows the spectrum of the primary

[6] BD+86°244 (8.7 mag.); HD 150265 (Sp. A0).

[7] *A.N.*, **194**, 414, 1913.

[8] *A.N.*, **195**, 416, 1913.

[9] *M.N.*, **78**, 644, 1918.

[10] *A.J.*, **36**, 113, 1926.

[11] *Potsdam Pub.*, **25**, Part IV, 17, 1925.

[12] *Harvard Bull.*, No. 844, 1927.

[13] *Contr. Princeton U. Obs.*, No. 10, p. 15, 1930. This paper gives the complete bibliography to 1930.

[14] *Circ. Obs. Cracovie*, No. 22, p. 14, 1926.

star because the eclipse is not total. This spectrum seems to be blended with a later A-type spectrum because the lines of *Ca* II K and *Ca* I 4226 look stronger than on the rest of the spectrograms taken with the same slit width; but the evidence is not conclusive, since the region of λ 3930 is not very well exposed and the metallic lines appear too faintly.

TABLE 2

STAR LINES USED FOR W URSAE MINORIS AND KO AQUILAE

Element	λ	Element	λ
Ca II	3933.67	*Hγ*	4340.47
Hδ	4101.74	*Mg* II	4481.23

TABLE 3

RADIAL VELOCITIES OF W URSAE MINORIS

Plate	Date (1945)	U.T.	Phase (in Days)	Radial Velocity (Km/Sec)
CQ 4395	May 23	4:34	0.286	− 85.4*
4396	23	5:17	0.316	−116.4
4397	23	5:53	0.341	−106.7
4398	23	6:32	0.368	−105.7
4520	June 9	10:00	0.501	−116.0
4521	9	10:28	0.520	−105.9
4522	9	10:54	0.538	−111.7
4419	May 25	6:47	0.719	− 54.5
4502	June 6	9:55	0.900	− 2.4
4385	May 22	6:21	1.062	+ 38.8
4386	22	6:54	1.085	+ 51.4
4561	June 15	4:34	1.171	+ 78.0
4476	3	9:56	1.303	+ 56.4
4407	May 24	5:52	1.340	+ 68.3
4436	29	8:42	1.355	+ 69.1
4408	24	6:24	1.363	+ 42.0
4409	24	6:50	1.381	+ 55.3
4437	29	9:20	1.381	+ 43.0
4531	June 10	10:46	1.533	+ 28.0
4493	5	9:48	1.596	+ 16.9
4494	5	10:35	1.629	+ 18.3
G*f*/2 5717	May 31	9:54	0.003	− 34.4
5722	June 7	5:59	0.035	− 69.2
5723	7	6:51	0.071	− 63.2
5724	7	7:34	0.101	− 60.1
5728	7	9:11	0.168	− 62.2
5729	7	9:34	0.184	− 72.6
5730	7	9:53	0.197	− 42.8
5734	12	6:32	1.655	+ 16.3

* This value is a mean of two measures.

THE RADIAL VELOCITIES

The radial velocities of W UMi at different phases were determined by measuring on each plate the lines listed in Table 2. The results are listed in Table 3 and plotted in Figure 1, which also shows the velocity-curve computed with the orbital elements shown in Table 4. These orbital elements have been derived by applying the Wilsing-Russell method. As a check of the computations, the method of Lehmann-Filhés was also applied, but the best representation of the present observations was given by the adopted values. The phases were determined by adopting Dugan's epoch of minimum and period.

Before computing the elements, the writer plotted, tentatively, the radial velocities obtained from the *Ca* II K line alone, but the trend of the velocity-curve was practically the same as the one of Figure 1, for which the mean radial velocities from all the measured lines were taken into account.

The observations we are discussing indicate a slight eccentricity of the orbit, which is in disagreement with the photometric observations and which depends largely upon the plates CQ 4419 (at phase 0.719 day) and CQ 4502 (at phase 0.900 day). Even though these two plates were not difficult to measure, the writer thought it advisable, after the computation of the orbit, to remeasure them so as to be certain of the values of these radial velocities. The new results were consistent with those obtained from the first measure-

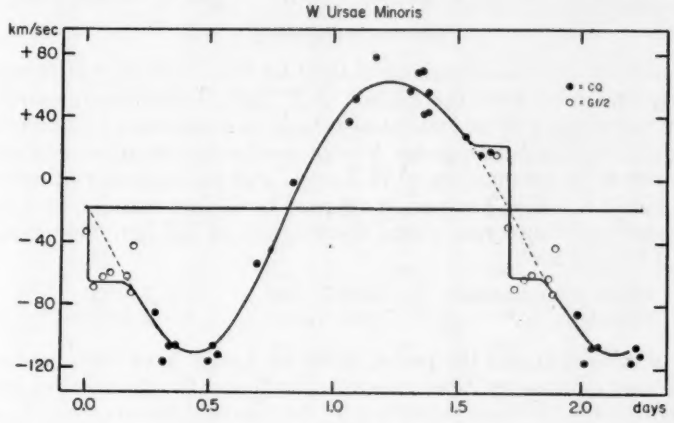

FIG. 1

TABLE 4

ORBITAL ELEMENTS OF W URSAE MINORIS

$P =$ 1.70116 days (assumed)	$T =$ Phase 0.611 days
$\gamma = -17.9$ km/sec	$a \sin i^* = 2.0 \times 10^6$ km
$K =$ 86.6 km/sec	$\frac{m_2^3 \sin^3 i}{(m_1 + m_2)^2} = 0.11 \odot$
$e =$ 0.09	
$\omega =$ 221°.6	

* According with Dugan's photometric solutions, $i \sim 83°$.

ment (-63.2 km/sec and $+4.4$ km/sec, respectively, in the second measure, against -54.5 km/sec and -2.4 km/sec, respectively, in the first measure). One might think that perhaps the *H* lines on these two plates are too broad to give reliable results and that one should take into account only the radial velocities obtained from the K line of *Ca* II, but even in that case the final results would be practically the same. The radial velocities from the *Ca* II K line alone are shown in the accompanying tabulation.

Plate	First Measure	Second Measure	Plate	First Measure	Second Measure
CQ 4419.....	−71.6 km/sec	−62.5 km/sec	CQ 4502.....	−2.6 km/sec	−4.7 km/sec

The spectrograms taken during the principal eclipse indicate a velocity of rotation of the A3 star of the order of 40 km/sec, the direction of rotation being the same as the direction of the orbital revolution.

In Joy and Dustheimer's determination of the spectrographic orbit of W UMi,[3] based upon eleven plates secured at the Mount Wilson Observatory, the authors assumed $e = 0$ and obtained the following elements:

$$\gamma = -7.7 \text{ km/sec} \qquad \frac{m_2^3 \sin^3 i}{(m_1 + m_2)^2} = 0.21 \odot$$
$$K = 105.5 \text{ km/sec}$$
$$a \sin i = 2.47 \times 10^6 \text{ km}$$

Joy and Dustheimer estimated that the spectral type of the primary star is A4n and that its absolute magnitude is +2.2.

XZ SAGITTARII[15]

PHOTOMETRIC DATA

This star was discovered to be variable in light by Miss Cannon,[16] at Harvard in 1908, and it was given the provisional designation of 32.1908. The communication of the discovery gave for the magnitude at maximum 8.9 and at minimum 11.2 and indicated that the star belongs to the Algol-type group. Visual observations made several years later by Zinner[17] indicated $M = 8.5$ mag., $m = 11.3$ mag., and no constancy of light during the eclipse, which lasted 0.3 day. The period adopted by Zinner was 3.2755 days.

In 1926, Lange[18] published new visual observations of XZ Sgr. The photometric elements obtained by him are:

Epoch of minimum = JD 2420311.519 $\qquad D = 7$ hours
Period = 3.275537 days $\qquad d = 2.2$ hours

The epoch of minimum and the period given by Lange have been confirmed by the observation of four minima by Zessewitsch,[19] who found the duration of totality to be 1.9 hours. A light-curve has been published by the Harvard Observatory,[20] and the period was stated to be 3.2755338 days.

THE SPECTRUM OF XZ SGR

At maximum light the spectrum is purely that of the primary star. The spectral type is A3, and the lines are sharp; the criterion for the classification was the relation ($H\epsilon$ + H)/K. With the purpose of obtaining one spectrogram of the secondary star, special care was taken to get an exposure during the total phase of the principal eclipse. According to the photometric elements, totality lasts about 2 hours, and, as the magnitude then would be 11.3, 2 hours would be the right exposure time for the Schmidt camera. The spectrogram obtained under the desired conditions was film G $f/2$ 5718, taken on the night of June 2, 1945 (U.T.). The mid-exposure corresponds to phase 3.2696 days, i.e., 6 minutes before mid-eclipse; the length of the exposure was 2^h03^m. However, the plate shows a spectrum which is composite, the spectrum of the secondary star being blended with the one corresponding to the primary star. Furthermore, at the beginning of the observation the star was very faint, but long before the predicted end of totality the writer noticed through one of the finders of the telescope that the star was becoming brighter. The obvious conclusion is that either the eclipse is partial or the length of the total phase is much less than the published one, since the epoch and the period published by Lange, which were adopted for the computation of the phases, seem to be correct.

The fact that the spectrum taken at mid-eclipse is blended and the lack of comparison spectra with the same dispersion make it difficult to give an accurate spectral type for the

[15] CD − 25°13054 (8.9 mag.) = HD 168710 (Sp. A2).

[16] *Harvard Circ.*, No. 137, 1908; *A.N.*, **179**, 7, 1908.

[17] *Astr. Abh.*, Vol. **4**, No. 3.

[18] *A.N.*, **228**, 71, 1926.

[19] *Astr. Circ., Acad. Sci. U.S.S.R.*, No. 18, p. 4, 1943.

[20] H. Shapley, *Rice Institute Pamphlet*, Vol. **18**, No. 2, 1931 (*Harvard Reprint*, No. 68).

PLATE XXXVII

UNIV. OF MICH.

secondary star. However, from the examination of the features of the spectrum, a late F or an early G type can be estimated. No emission lines are present in the spectrum of the secondary star.

THE RADIAL VELOCITIES

The only lines that could be measured were the K line of *Ca* II, $H\delta$, $H\gamma$, and *Mg* II 4481. A few metallic lines were also present but were not strong enough for measurement. When the means of the four lines were plotted against phase, the points were too badly

TABLE 5

RADIAL VELOCITIES OF XZ SAGITTARII

PLATE*	DATE (1945)	U.T.	PHASE (IN DAYS)	RADIAL VELOCITIES IN KM/SEC FROM	
				Ca II K	*Mg* II 4481
CQ 4519	June 9	9:09	0.484	− 6.3	− 5.2
4500	6	8:04	0.714	.....	−12.3
4501	6	8:56	0.750	−13.9	−32.5
4412	May 24	9:34	0.879	+25.3	−18.6
4413p	24	10:14	0.907	.....	+ 6.0
4477p	June 3	10:42	1.100	.....	+ 1.6
4549	13	9:12	1.208	−11.3	− 3.2
4526	10	7:16	1.406	− 3.4	+35.4
4586p	23	10:22	1.432	.....	− 4.2
4527	10	8:32	1.458	− 0.6	+27.2
4423	May 25	9:14	1.865	.....	+ 9.7
4424	25	9:52	1.892	+24.9	+ 9.6
4389	22	9:08	2.137	+ 5.0	+ 3.0
4390	22	9:56	2.170	− 1.2	+10.9
4537	June 11	9:10	2.485	+57.5	+30.6
4538	11	9:58	2.518	.....	−15.0
4508	8	6:36	2.653	+31.1	+11.7
4491	5	8:04	2.990	+47.7	−11.8
4492	5	8:48	3.021	+23.2	+ 8.9
G*f*/2 5719	June 2	9:58	0.069	−10.6	−18.2
5735	12	7:42	0.148	−18.9	+ 6.7
5736	12	8:16	0.172	− 3.7	+24.5
5715	May 30	10:56	0.385	.....	−51.7
5716	30	11:13	0.397	.....	− 5.6
5732	June 7	10:38	1.821	.....	+ 2.9
5745	17	7:53	1.880	+42.7	− 1.7
5718	2	8:10	3.270	.....	−18.0

* The letter "p" indicates a "poor plate."

scattered to give even a rough idea of the shape of the velocity-curve, although they suggested that we were dealing with a star with very small range in velocity. It was then thought advisable to take into account only the measures from the lines *Ca* II K and *Mg* II 4481, since they appear to be more reliable than the rest. The results from each of the two lines are listed in Table 5 and the means of them are plotted in Figure 2. The scattering is still quite large; nevertheless, the points give an indication of the trend of the velocity-curve and the order of magnitude of the amplitude.

Considering the principal eclipse to be total or nearly so, and assuming $A_2 = 0.1$ mag., the photometric elements indicate that $k \approx 1.0$ and that the ratio of the surface brightnesses is about 10. Hence, at full light, the spectrum of the primary star cannot be

noticeably blended with the spectrum of the secondary star. The case of partial eclipse would be even more unfavorable for the possibility of blending; therefore, we conclude that the small range in velocity which has been found must be real.

An attempt to draw a velocity-curve through the points (the value from the film G*f*/2 5715, at phase 0.385 day, was not taken into account) led to the elements in Table 6, which were obtained by applying the Wilsing-Russell method. They are quite uncer-

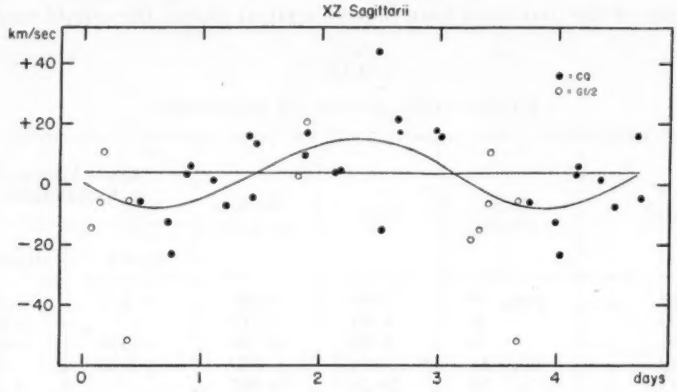

FIG. 2

TABLE 6

ORBITAL ELEMENTS OF XZ SAGITTARII

$P =$ 3.275537 days (assumed)	$T =$ Phase 0.2.7 days
$\gamma = +4.1$ km/sec	$a \sin i = 5.2 \times 10^5$ km
$K =$ 11.5 km/sec	$\frac{m_2^3 \sin^3 i}{(m_1 + m_2)^2} = 0.0005 \odot$
$e =$ 0.05	
$\omega = 132°.5$	

tain and are published only to show the results of the trial. Unfortunately, the photometric observations do not give any indication concerning the eccentricity, as no secondary minimum has been observed.

KO AQUILAE[21]

PHOTOMETRIC DATA

The variability of KO Aql was discovered at Sonneberg by Hoffmeister[22] in 1930, and the provisional designation given to the star was 302.1930. The discoverer stated that the new variable was of the Algol type. An approximate period of 2.9 days was first given by Zessewitsch,[23] and his value was improved successively by Plaut,[23] Szczyrbak,[24] Piegza,[25] and Pagaczewski,[26] who gave for the period the values 2.864, 2.8636, 2.86377, and 2.86385 days, respectively.

[21] BD+10°3655 (8.2 mag.) = AG Lpz I (8.5 mag.) = HD 173847 (Sp. A0). The star is included in Prager's *Bibliography of Variable Stars* (*Harvard Ann.*, No. 111, 1941). Proper motions of KO Aql were published three years ago by Kopal (*Harvard Bull.*, No. 916, 1942): $\mu_\alpha = +0''.012 \pm 0''.007$, $\mu_\delta = -0''.002 \pm 0''.007$.

[22] *A.N.*, **240**, 193, 1930.

[23] *A.N.*, **244**, 289, 1931.

[24] *Krakow Obs. International Suppl.*, No. 10, p. 44, 1932.

[25] *Krakow Obs. International Suppl.*, No. 12, p. 42, 1934.

[26] *Acta astr.*, Ser. c, **2**, 52, 1933.

The last photometric elements were derived by Lause,[27] and these are the ones which appear in Schneller's *Katalog* for 1941 and are quoted in Table 1. The latest value of the epoch of minimum and of the period are

$$\text{JD } 2426585.442\,(\pm 0.004) + 2.863844\,(\pm 0.000009)\,E$$

as published by Lause.[28]

TABLE 7

RADIAL VELOCITIES OF KO AQUILAE

PLATE	DATE (1945)	U.T.	PHASE (IN DAYS)	RADIAL VELOCITIES IN KM/SEC FROM	
				All Lines	*Ca* II K
CQ 4446	May 30	6:16	0.000	+ 9.6	+24.3
4431	27	9:37	0.004	− 4.3	+ 0.6
4432	27	10:22	0.035	.....	+15.8
4447	30	7:07	0.036	−11.5	− 6.3
4448	30	7:50	0.066	−17.6	+ 8.9
4490	June 5	7:20	0.317	−27.3	−11.5
4387	May 22	7:51	0.658	−37.8	−31.2
4388	22	8:22	0.679	−48.9	−25.2
4420	25	7:36	0.784	−37.9	−25.9
4421	25	8:07	0.805	−45.8	−26.0
4422	25	8:36	0.825	−42.8	−26.1
4559	June 14	10:49	0.871	−34.3	−36.7
4452	May 31	5:38	0.974	−25.1	−30.9
4574	June 17	10:26	0.991	−39.3	−25.7
4453	May 31	6:18	1.002	−24.1	−24.8
4575	June 17	10:50	1.008	−38.9	−34.9
4471	3	5:22	1.099	−18.3	−16.7
4472	3	5:55	1.122	−29.0	−25.9
4497	6	5:40	1.248	−41.2	−20.8
4498	6	6:34	1.285	− 2.9	− 8.7
4499	6	7:14	1.313	+ 3.9	+ 3.4
4516	9	7:11	1.447	−23.9	+ 8.3
4517	9	7:47	1.472	−12.2	− 0.8
4518	9	8:22	1.496	+ 0.2	+ 5.1
4455	1	6:56	2.028	+28.8	+32.7
4456	1	7:32	2.053	+32.3	+35.6
4457	1	8:00	2.072	+30.9	+23.4
4410	May 24	7:48	2.656	+21.2	+10.9
4411	24	8:45	2.695	+23.7	+ 3.8
4551	June 13	10:17	2.712	+22.7	+12.5
4445	May 30	5:33	2.834	− 2.8	+27.5
G*f*/2 5720	June 2	11:04	0.336	−22.5	−23.7
5738	12	10:30	1.721	+16.5	+32.1
5739	12	10:44	1.731	+17.7	+20.6
5740	12	10:56	1.739	+19.1	+16.8
5725	7	8:11	2.352	+46.2	+45.6
5726	7	8:23	2.361	+30.5	+41.8
5727	7	8:40	2.373	+25.3	+34.2
5731	7	10:17	2.440	+30.5	+30.1

[27] *A.N.*, **253**, 403, 1934.

[28] *A.N.*, **266**, 17, 1938.

THE SPECTRUM OF KO AQL

The spectrograms, taken outside principal eclipse, show the pure spectrum of the primary star, which is of type A0 or perhaps A1. In an effort to obtain a spectrogram of the secondary component of KO Aql, the plate CQ 4446 was exposed at the time of minimum predicted by the photometric elements. The exposure time was 60 minutes, and the mid-exposure corresponds to phase 0.0003 day. The spectrogram obtained is not later in type

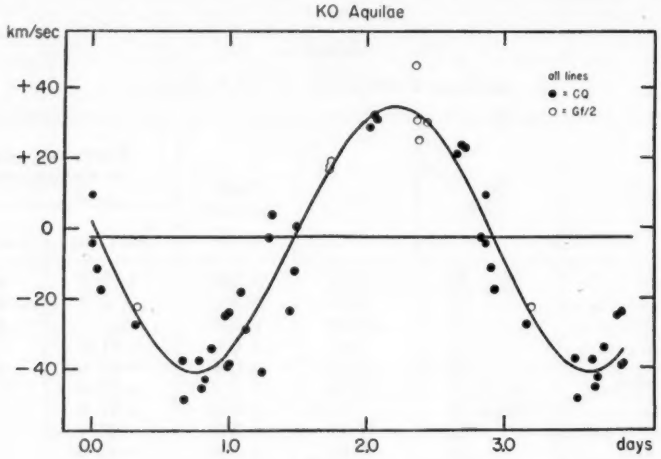

FIG. 3

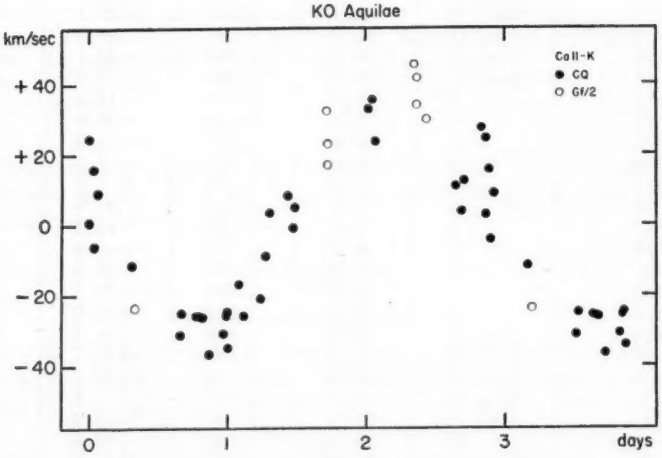

FIG. 4

than the ones obtained at maximum light; the lines look somewhat broader than usual, but this might be due to the quality of the spectrogram. It seems reasonable to conclude that the eclipse is only partial.

THE RADIAL VELOCITIES

The radial velocity from each spectrogram was obtained by measuring the lines listed in Table 2 and by taking the mean of the individual results. These mean values are listed

in Table 7 and are plotted in Figure 3. The phases were computed by adopting Lause's epoch of minimum and period. The radial velocities from the *Ca* II K line alone show less scatter, and they indicate an amplitude smaller by a few kilometers (Fig. 4), but there was no reason to disregard the measurements from the other lines; and the orbital elements were computed by applying the Wilsing-Russell method to the mean radial velocities from all lines. The orbital elements are shown in Table 8.

TABLE 8

ORBITAL ELEMENTS OF KO AQUILAE

$P =$ 2.863844 days (assumed)	$T =$ Phase 0.372 days
$\gamma = -$ 2.7 km/sec	$a \sin i = 1.5 \times 10^6$ km
$K =$ 37.8 km/sec	$\frac{m_2^3 \sin^3 i}{(m_1 + m_2)^2} = 0.016\odot$
$e =$ 0.02	
$\omega =$ 130°.9	

CONCLUSIONS

The most interesting of the three stars which we have just discussed is, undoubtedly, XZ Sgr. Its mass function is so small as to impose severe restrictions upon the mass ratio and/or the total mass. The spectra of the two components of XZ Sgr look quite normal. Hence we should be inclined to suppose that the masses are also normal. If we consider $m_2 = 1\odot$ (assuming $i \sim 90°$), then $\alpha = m_1/m_2 \sim 44$, and $m_1 \sim 44\odot$. If we consider, instead, $m_1 = 3\odot$, then $\alpha \sim 17$ and $m_2 \sim 0.16\odot$. We have accepted here the values of $f(m)$ indicated in Table 8, which cannot be very far from the truth. We conclude, then, that reasonable values of the masses would require a value of α between 15 and 45. This result is quite important, since it shows that the mass ratio in close systems can be greatly different from unity. In the study of BD Virginis[29] it was shown that, in that case, the value of α should be between 4 and 6; now we have a system for which α must be many times larger. The system of KO Aql is similar to BD Vir in mass ratio.

I am indebted to Dr. O. Struve for helpful discussions and advice. A few spectrograms were kindly secured for me by Dr. O. Struve. Miss Alice Johnson, Mrs. Martha Carlson, and Miss Gertrude Peterson helped in the reductions of the plates and in making the diagrams. The late Professor R. Prager of Harvard Observatory very kindly furnished some references to the literature of the three stars.

[29] Struve, Cesco, and Sahade, *Ap. J.*, **100**, 181, 1944; McD. Contr., No. 95.

THE PROBLEM OF U CORONAE BOREALIS, RS VULPECULAE, AND TV CASSIOPEIAE.*

J. SAHADE AND O. STRUVE
Yerkes and McDonald Observatories
Received September 11, 1945

ABSTRACT

At principal minimum the spectra of U CrB and RS Vul show faint lines of *Fe* I, *Fe* II, *Ca* I, and *Sr* II, suggesting that the types of the secondaries are about A2. This confirms the discrepancy between the photometric and the spectrographic types announced previously. The reflection effect cannot account for this discrepancy, but the existence of a peculiarity in the structure of the *H* lines of U CrB near maximum radial velocity suggests that a stream of gas similar to that previously observed in AU Mon may account for the otherwise unexplained early type of the secondary spectrum. If this should be true, the eclipse would be partial, and the true spectrum of the secondary would be unobservable; the metallic lines at minimum would then be attributed to the absorption of the light of the partly eclipsed primary by the atoms of the stream.

THE PROBLEM

In Wyse's study of the spectra of eclipsing binaries,[1] attention was called to the fact that the stars U Coronae Borealis, RS Vulpeculae, and TV Cassiopeiae present a discrepancy between the photometric and the spectrographic observations: the light-curves show large differences between the depths of the two minima of light; but J. S. Plaskett's spectrographic observations[2] indicate very similar, if not identical, spectral types for the two components of each of the three systems. Table 1 summarizes the relevant data.

TABLE 1

PHOTOMETRIC AND SPECTROGRAPHIC DATA

Star	A_1	A_2	Spectra	Star	A_1	A_2	Spectra
U CrB.....	1.02	0.00	B3+B3	TV Cas.....	1.05	0.09	A0+A0
RS Vul.....	0.73	0.08	B8+B9				

Most of Plaskett's spectrographic observations were made outside of the eclipses, and his conclusions concerning the spectral types were largely drawn from the measurements of double lines at maximum positive and negative velocities. Wyse believed that the discrepancies could perhaps be explained by the reflection effect, but the problem has thus far remained without an entirely satisfactory solution.

In a recent discussion of the astrophysical problems encountered in the study of spectroscopic binaries,[3] the need for reobserving these stars, especially at minimum light, has been stressed. Since Wyse's paper, a new set of spectrograms of U CrB has been obtained by Pearce,[4] whose results appear to confirm those of Plaskett, with the difference that he estimated the spectral type of the system as being B5 + B9. It is, however, not clear from Pearce's published account whether or not these estimates were obtained from

* *Contributions from the McDonald Observatory, University of Texas*, No. 117.

[1] *Lick Obs. Bull.*, No. 464, 1934.

[2] *Pub. Dom. Ap. Obs.*, **1**, 141, 187, 1922; **2**, 141, 1922.

[3] O. Struve, *Ap. J.*, **102**, 74, 1945; *McD. Contr.*, No. 110.

[4] *Pub. A.A.S.*, **8**, 219, 1936.

plates taken at minimum. In order to clarify the problem, the three stars were placed upon the observing program of the 82-inch reflecting telescope of the McDonald Observatory.

THE OBSERVATIONS

The observations were obtained during the months of May and June, 1945, with the combination of two quartz prisms and a 500-mm camera, which gives a linear dispersion of 40 A/mm at λ 3933. The exposures were made on Eastman 103a-O emulsion, and the slit width used was 0.05 mm. Only three plates of U CrB (CQ 4427, 4428, and 4429, at phases 0.018, 0.046, and 0.064 days, respectively) and five plates of TV Cas (CQ 4459, 4400, 4401, 4402, and 4458, at phases 0.020, 0.027, 0.061, 0.086, and 1.810 days, respectively) were taken with a wider slit, namely, 0.075 mm. At maximum light the exposure times were of the order of 35 minutes for U CrB, 20 minutes for RS Vul, and 25 minutes for TV Cas. We obtained 30 spectrograms of U CrB, 25 of RS Vul, and 17 of TV Cas.

U CORONAE BOREALIS[5]

PHOTOMETRIC DATA

This star was discovered to be variable in light by Winnecke[6] in 1869, and the first epoch of minimum was given by Chandler[7] in the form

$$\text{JD } 2404147.4434 + 3.4522269\,E - 0.000000021\,E^2 .$$

Later, Chandler concluded that the epoch of minimum is best represented[8] by

$$\text{JD } 2404147.396 + 3.452219\,E + 0.056 \sin (0.^{\circ}06\,E + 78^{\circ}) .$$

Since then there have been many photometric studies of U CrB;[9] the last of these is due to Dugan and Wright,[10] who concluded that there exists a small variation in the period and that

$$M_1 = 7.56 \text{ mag.}; \qquad A_1 = 1.36 \text{ mag.}; \qquad D = 0.46 \text{ day} .$$

They also state that "a careful study of the observations gives no conviction that there is sure evidence of a secondary minimum" and that "comparison of photographic and photovisual observations shows little change in color index of the variable from maximum to minimum and hence agrees with the spectrographic findings, namely, that the two components are much alike in spectral type." Dugan and Wright adopted the following elements:

$$\text{Principal minimum} = \text{JD } 2416747.964 + 3.45220416\,E ,$$

which they thought "will probably give fairly close predictions."

Schneller's *Katalog und Ephemeriden veränderlicher Sterne für 1941*[11] lists the following elements:

M_1 = 7.65 mag.	D = 12 hours
A_1 = 1.02 mag.	d = 0.9 hours
A_2 = ...	Minimum = JD 2404147.4297 + 3.4522008 E

[5] BD+32°2569 (var.) = HD 136175 (Sp. B8) ($\alpha = 15^h12^m17^s$; $\delta = +32^{\circ}10'.8$ [1855.0]).

[6] *A.N.*, **76**, 249, 1870. [7] *A.J.*, **9**, 97, 1889. [8] *Harvard Ann.*, **55**, 46, 1907.

[9] See bibliography in Prager's *Geschichte und Literatur des Lichtwechsels der veränderlichen Sterne*, **1**, 308, Berlin, 1934. Some of the authors did not find a second-order term in the expression for the epoch of minimum.

[10] *Contr. Princeton U. Obs.*, No. 19, p. 26, 1939.

[11] *Kl. Veröff. Berlin-Babelsberg*, No. 22, 1940.

The values for the epoch of minimum and the period are those of Hellerich,[12] disregarding the second-order term. We have adopted them in the computation of the phases, since they seem to agree very well with the spectroscopic observations.

THE SPECTRUM OF U CRB (PL. XXXVIII)

At maximum light the spectrum of U CrB is of type B5, but on the plates taken at phases 2.5695, 2.5952, 2.6258, 2.7367, and 2.7610 days, the lines $H\delta$ and $H\gamma$ look as though there is a sharp red component superimposed over a shallow violet component. (Notice the core having a sharp violet edge in $H\delta$ and $H\gamma$ at phase 2.626 on Pl. XXXVIII.)

The spectrogram obtained during the predicted total phase (mid-exposure at phase 0.0002 day; exposure time, 55 minutes) still shows the lines of the primary star; however, the B5 spectrum is blended with a spectrum of later type; hence the eclipse is probably only partial. The blending is indicated by the faint appearance of lines of *Fe* I, *Fe* II, *Ca* I, *Sr* II, etc., and by the strengthening of *Mg* II 4481 relative to *He* I 4471. The later-type spectrum, which may belong to the second component, is probably not later than

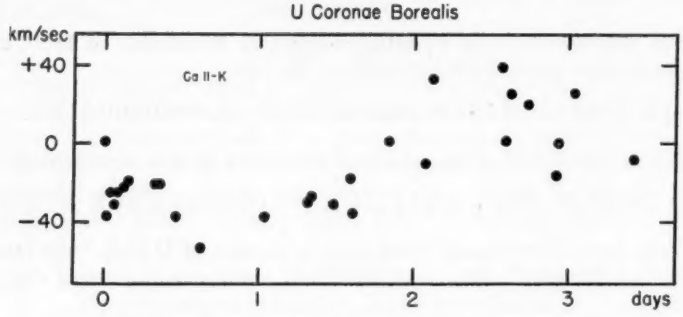

FIG. 1

A2, because there is no evidence of a broad K line underlying the K line of the spectrum of the primary star, and it is not much earlier than A2 because of the presence of *Ca* I and *Sr* II.

The spectrum belonging to the secondary star is so faint on our exposure taken at mid-eclipse that it can hardly be expected to show on our plates taken at maximum light. A careful inspection of the latter shows no convincing evidence of the presence of *Fe* I, *Ca* I, and *Sr* II. Nor can we detect any weak components of the lines of *He* I. On Plate XXXVIII the positions of the expected weak components of *He* I 4026 are indicated by markers. The peculiar structure of the *H* lines near maximum radial velocity could conceivably be attributed to a doubling of these lines. But it must be remembered that the strong *H* cores give larger velocities than the single *He* I lines; the latter, however, should be completely divided so that they are not vitiated by blending. We incline toward the idea that the structure of the *H* lines is not caused by the relative orbital motion of the two stars but is related to a phenomenon already observed in AU Monocerotis.[13] Our failure to observe the weak components at maximum and minimum radial velocity does not imply a criticism of the measurements by Plaskett and by Pearce. It is possible that with the larger dispersion of their spectrograph they could measure lines which remain invisible on our plates. Our observations at minimum light tend to reduce the discrepancy between photometric and spectrographic results, but by no means remove them. The spectral type of the secondary, as predicted from the light-curve, should be at least as late as G or K.

[12] *A.N.*, **220**, 331, 1924. [13] Sahade and Cesco, *Ap. J.*, **101**, 235, 1945; *McD. Contr.*, No. 106.

PLATE XXXVIII

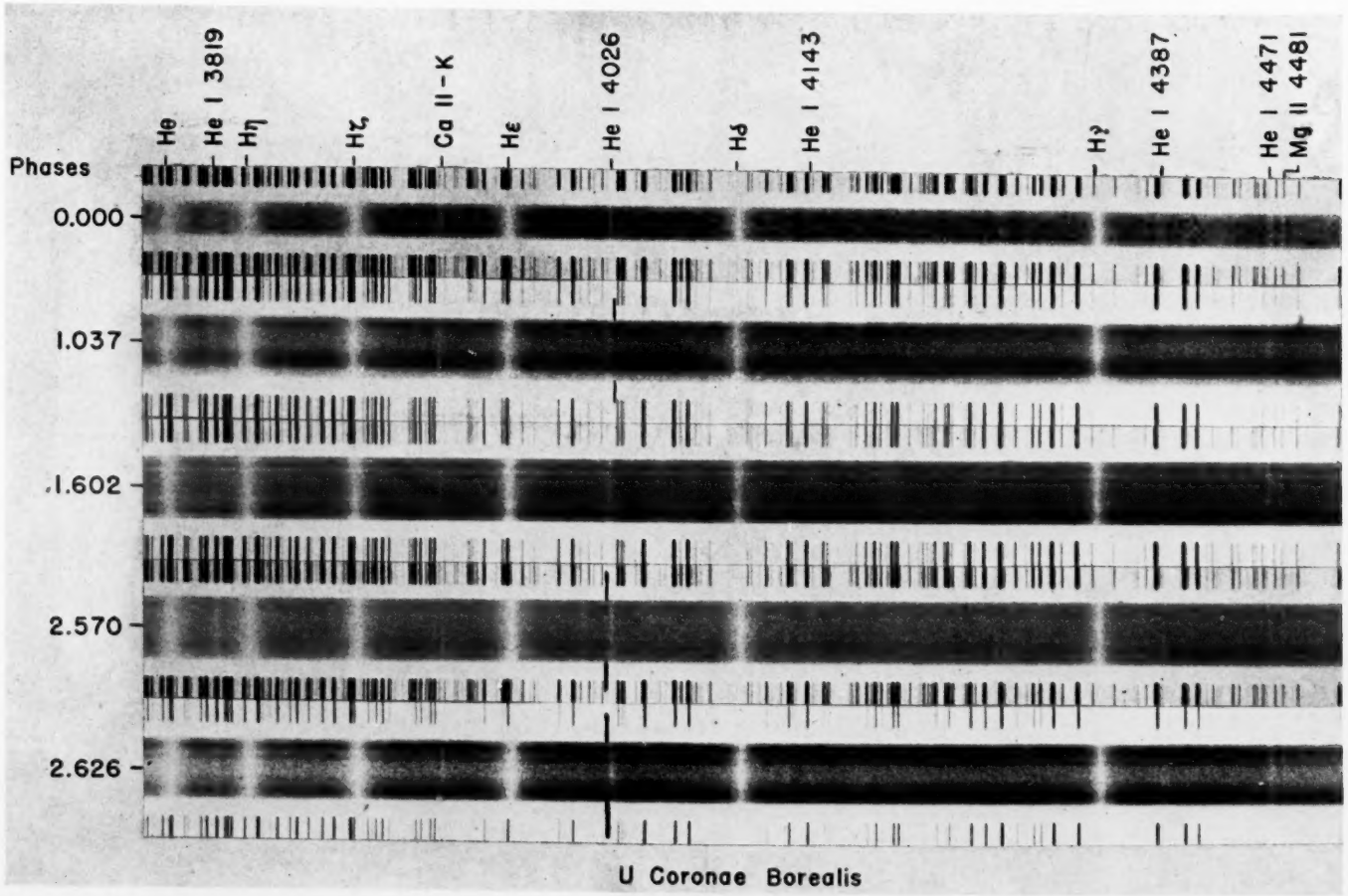

RADIAL VELOCITIES

The radial velocities from each spectrogram were determined by measuring the lines listed in Table 2. The radial velocities from the K line of *Ca* II (Fig. 1) indicate that the stellar line is blended with a K line from interstellar sources, a conclusion already reached by Pearce.[4] If we plot the means of the results from all lines except *Ca* II K against phase (Fig. 2), we find a set of points in the region of maximum positive velocity

TABLE 2

STAR LINES USED FOR U CORONAE BOREALIS AND RS VULPECULAE

H	*He* I	*Ca* II	*Mg* II
3797.90	3819.64	3933.67	4481.23
3835.39	4026.22		
3889.05	4143.76		
3970.08	4387.93		
4101.74	4471.51		
4340.47			

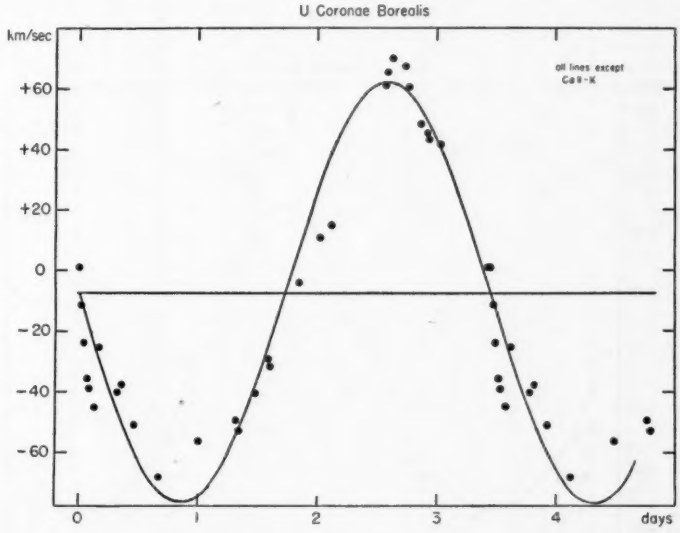

FIG. 2

which look suspicious. Hence we made separate plots for the *He* I lines and for the *H* lines (Figs. 3 and 4). The radial velocities from the *H* lines, as obtained from those plates on which $H\delta$ and $H\gamma$ look double, are systematically higher than those from the *He* I lines. Since the *He* I lines do not show anything unusual throughout the different phases, a graphical solution of the orbit by the Wilsing-Russell method was performed with the values for the radial velocities obtained from these lines (Table 3). The elements are shown in Table 4, and the corresponding velocity-curve has been drawn in Figures 3 and 4; in the latter the set of points which remains above the curve in the region of the maximum positive velocity suggests the existence of a stream of relatively cool gas—because

of the absence of *He* I—moving toward the B5 star. A similar conclusion had already been reached in the case of AU Monocerotis.

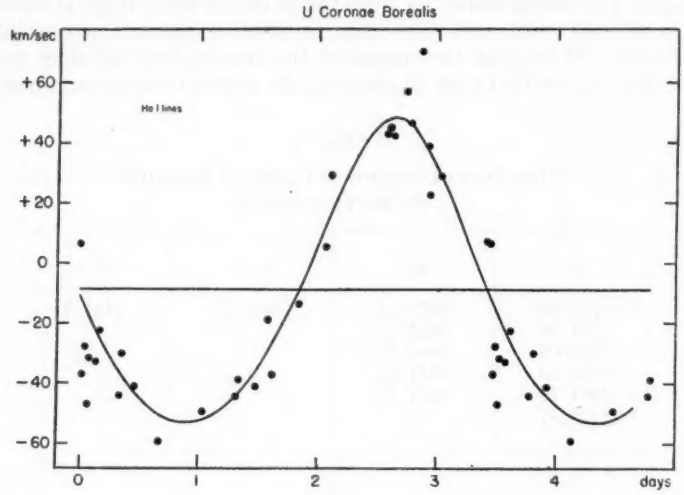

FIG. 3

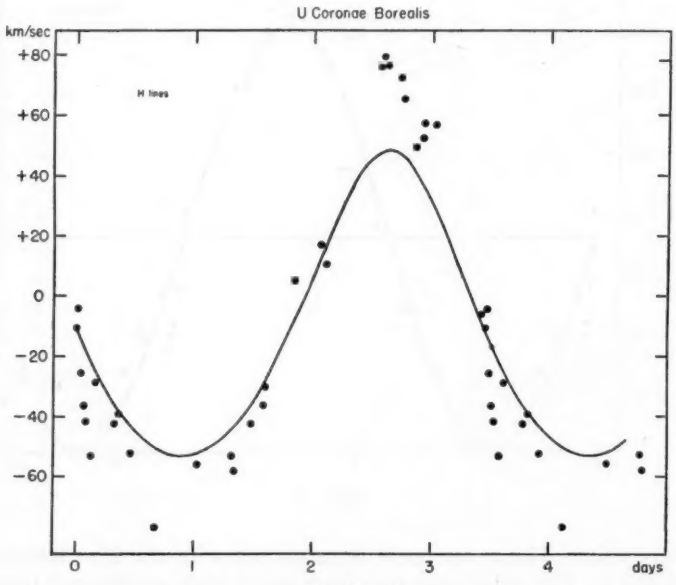

FIG. 4

In Figure 2 we have shown the velocity-curve according to Plaskett's orbital elements,[14] namely,

$P = 3.4522269$ days (assumed) $\quad \gamma = -7.5$ km/sec
$e = 0$ (assumed) $\quad K_1 = 69.5$ km/sec

[14] *Pub. Dom. Ap. Obs.*, 1, 187, 1922.

The elements derived by Pearce[4] resulted from a combination of his observations and those of Plaskett; they are as follows:

P = 3.4522008 days (assumed) e = 0.072
γ = −7.65 km/sec ω = 23°.8
K_1 = 80.1 km/sec T = JD 2425809.969

Both Plaskett and Pearce gave also the value of K_2 for the secondary star.

TABLE 3

RADIAL VELOCITIES OF U CORONAE BOREALIS

PLATE	DATE (1945)	U.T.	PHASE (IN DAYS)	NUMBER OF MEASURES	RADIAL VELOCITIES IN KM/SEC FROM			
					Ca II K	All Lines except *Ca* II K	*H*	*He* I
CQ 4470.....	June 3	4:30	0.000	1	+ 1.0	+ 0.9	−10.6	+ 6.4
4427.....	May 27	7:14	0.018	1	−37.0	−11.6	− 4.3	−37.1
4428.....	27	7:54	0.046	1	−24.8	−24.0	−25.7	−27.4
4429.....	27	8:20	0.064	1	−31.0	−35.9	−36.4	−47.1
4523.....	June 10	4:16	0.086	1	−25.1	−39.1	−41.7	−31.7
4524.....	10	5:16	0.128	1	−22.2	−45.3	−53.2	−32.8
4525.....	10	6:02	0.160	1	−19.1	−25.5	−28.6	−22.5
4405.....	May 24	3:49	0.328	1	−20.5	−40.2	−42.6	−44.3
4406.....	24	4:33	0.359	1	−20.6	−37.8	−39.3	−30.1
4451.....	31	4:52	0.468	1	−37.8	−51.1	−52.3	−41.3
4553.....	June 14	5:08	0.670	1	−53.5	−68.4	−77.0	−59.2
4532.....	11	3:05	1.037	1	−37.4	−56.4	−55.9	−49.4
4416.....	May 25	3:31	1.316	1	−29.9	−49.5	−52.8	−44.5
4417.....	25	4:09	1.342	1	−26.9	−52.8	−58.0	−38.8
4504.....	June 8	2:56	1.483	1	−30.6	−40.4	−42.3	−41.3
4507.....	8	5:35	1.593	1	−21.7	−29.3	−36.2	−19.0
4560.....	15	3:30	1.602	1	−35.4	−31.7	−30.1	−37.3
4384.....	May 22	5:25	1.847	1	+ 1.3	− 4.3	+ 5.2	−13.8
4540.....	June 12	3:53	2.070	1	−10.2	+10.7	+17.3	+ 5.4
4541.....	12	4:56	2.114	1	+33.2	+14.7	+10.8	+29.2
4513.....	9	5:01	2.570	2	+39.9	+61.2	+76.0	+43.0
4514.....	9	5:38	2.595	2	+ 1.0	+65.6	+79.2	+45.0
4515.....	9	6:22	2.626	2	+25.5	+70.0	+76.4	+42.6
4393.....	May 23	2:46	2.737	3	+20.5	+67.3	+72.4	+57.0
4394.....	23	3:21	2.761	2	.....	+60.5	+65.6	+46.6
4442.....	30	3:28	2.862	1	.....	+48.3	+49.5	+70.3
4444.....	30	4:53	2.921	1	−16.1	+45.4	+52.5	+38.7
4495.....	June 6	3:02	2.939	1	+ 0.4	+43.3	+57.3	+22.5
4542.....	13	2:56	3.030	1	+36.0	+41.8	+56.8	+28.9
4469.....	3	3:44	3.420	1	− 8.2	+ 0.8	− 6.0	+ 7.3

TABLE 4

ORBITAL ELEMENTS OF U CORONAE BOREALIS

P = 3.4522008 days (assumed) T = Phase 2.687 days
γ = −8.7 km/sec $a \sin i$ = 2.4×10^6 km
K = 50.8 km/sec $\dfrac{m_2^3 \sin^3 i}{(m_1 + m_2)^2}$ = 0.05 ⊙
e = 0.13
ω = 5°.8

RS VULPECULAE[15]

PHOTOMETRIC DATA

The variability of RS Vul in light was discovered by Astbury,[16] in 1908, and the provisional designation given to the star was 16.1908. Up to the present time there have been published four photometric solutions for RS Vul. The solution by H. Shapley,[17] based upon the observations of Nijland,[18] and the solution by Stewart,[19] based upon Maggini's observations,[20] led the authors to interpret the primary minimum as a total eclipse. The third solution is a photographic one by Baker,[21] who concluded that the principal eclipse is annular and central. Finally, the fourth solution is due to Dugan,[22] who stated in his discussion that the "primary minimum cannot be interpreted as a total eclipse" and who adopted a partial eclipse with $\alpha_0 = 0.636$. In Dugan's solution the secondary minimum "occurs a little later than one-half period after the primary."

Schneller's *Katalog* for 1941 lists the epoch of minimum and the period adopted by Dugan, namely,

$$\text{JD } 2420606.6226 + 4.477666\,E$$

and

$$M_1 = 6.90 \text{ mag.} \qquad D = 15.4 \text{ hours}$$
$$A_1 = 0.73 \text{ mag.} \qquad d = 0 \text{ hours}$$
$$A_2 = 0.08 \text{ mag.}$$

THE SPECTRUM OF RS VUL (PL. XXXIX)

The spectograms taken at the phases of maximum light show a spectrum of type B5. At mid-eclipse this spectrum is blended with one which may correspond to the secondary component of the system, a fact which agrees with Dugan's conclusion that the principal eclipse is partial. The spectrum of the secondary star is definitely later than the one which corresponds to the primary star, since at mid-eclipse some metallic lines appear faintly and the line *Mg* II 4481 becomes strengthened relative to *He* I 4471. The faint lines of the secondary include *Fe* I, *Fe* II, *Ca* I, and *Sr* II, all of which are invisible on our plates taken outside of eclipse. But, as in the case of U CrB, the line *Ca* II K is not greatly strengthened at mid-eclipse. Hence we again conclude that the spectral type of the secondary is probably not later than A2 and probably not much earlier than A2 because of the presence of *Fe* I, *Ca* I, and *Sr* II. Our plates taken near maximum and minimum of radial velocity show no duplicities in *He* I and *H*, but again we wish to emphasize that this does not disprove the Victoria observations. We agree with Plaskett in making the spectral type of the secondary considerably earlier than that which would have been predicted from the values of A_1 and A_2, but the discrepancy is somewhat less pronounced than had been believed previously.

RADIAL VELOCITIES

The radial velocities of RS Vul (Table 5) were determined by measuring the same stellar lines as in the case of U CrB, which are listed in Table 3. The values from the K line of *Ca* II, which are plotted in Figure 5, indicate that the stellar line is blended with an interstellar K line. The plot of the means of the individual results from the rest of the

[15] BD+22°3647 (7.5 mag.) = HD 180939 (Sp. B8) ($\alpha = 19^h\ 11^m30^s$; $\delta = +22°11'.0$ [1855.0]).

[16] *A.N.*, **178**, 367, 1908.

[17] *Contr. Princeton U. Obs.*, No. 3, 1915.

[18] *Ibid.*, p. 17.

[19] *Ap. J.*, **42**, 315, 1915.

[20] *A.N.*, **200**, 54, 1915.

[21] *Pub. U. Missouri Obs.*, No. 32, 1921.

[22] *Contr. Princeton U. Obs.*, No. 6, 1924.

PLATE XXXIX

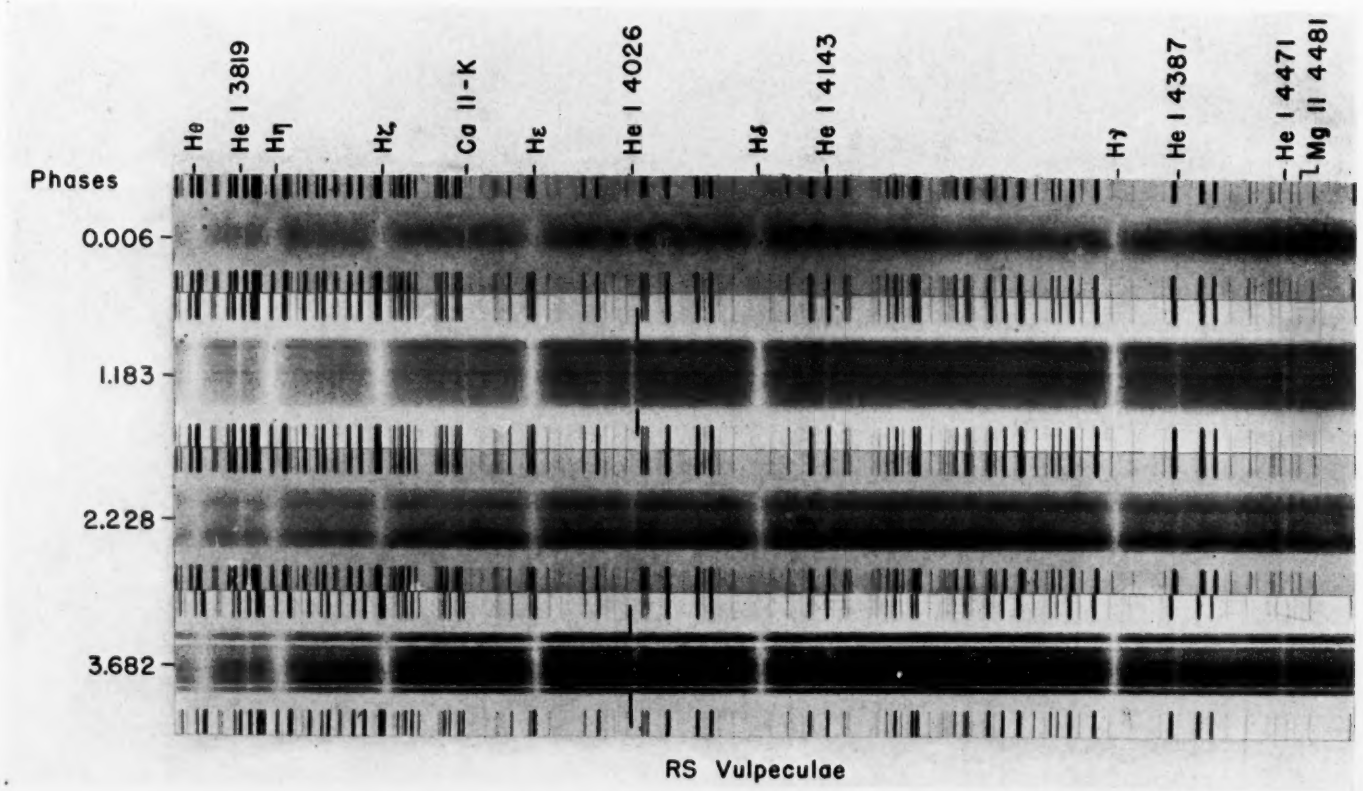

UNIV. OF MICH.

PLATE XL

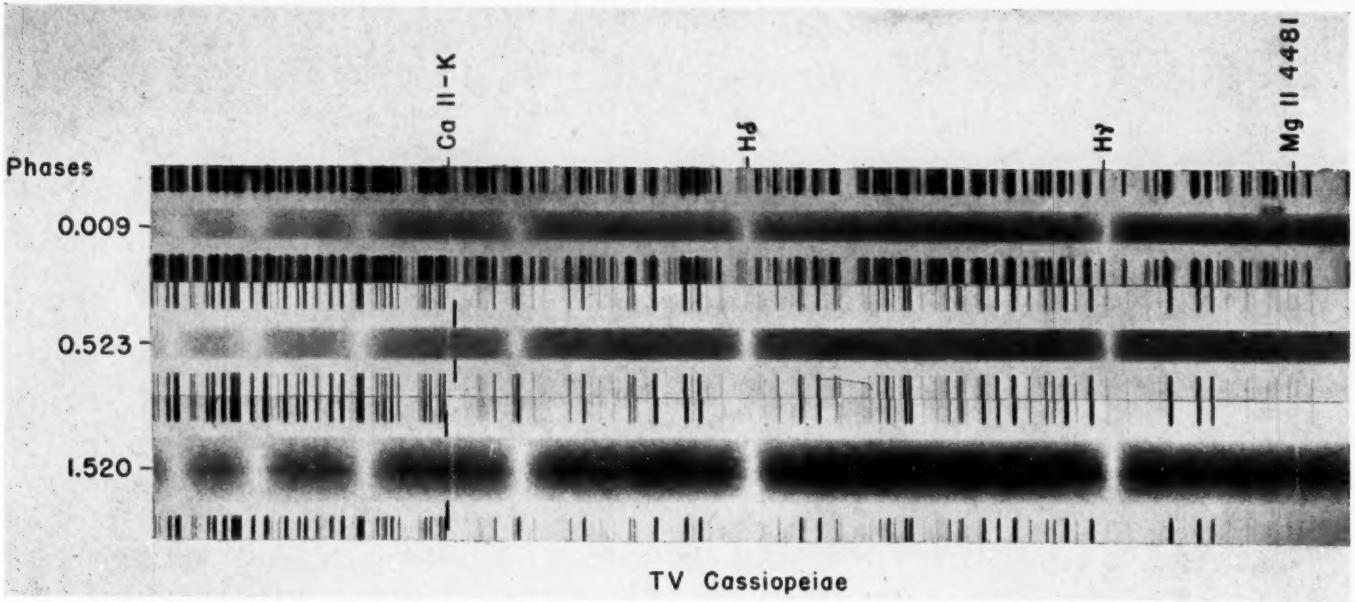

lines is shown in Figure 6, where we have drawn the velocity-curve which corresponds to Plaskett's elements[23] for the primary star, namely,

P = 4.477325 days (assumed)	γ = −22.04 km/sec
e = 0.053	ω = 236°.26
K = 54.98 km/sec	T = Phase 1.903 days

Our observations are fairly well represented by Plaskett's curve, after a slight change in the origin of the phases; our phases were computed with Dugan's elements.

TABLE 5

RADIAL VELOCITIES OF RS VULPECULAE

PLATE	DATE (1945)	U.T.	PHASE (IN DAYS)	RADIAL VELOCITIES IN KM/SEC FROM	
				Ca II K	All Lines except *Ca* II K
CQ 4435	May 28	6:58	0.020	+ 7.6	−18.8
4503	June 6	10:44	0.221	−25.6	−44.3
4414	May 24	11:02	0.667	−28.4	−71.1
4539	June 11	10:47	0.746	−36.3	−76.6
4438	May 29	10:00	1.146	−17.3	−77.7
4439	29	10:36	1.171	−35.7	−80.0
4440	29	11:09	1.194	−20.4	−71.4
4566	June 16	9:19	1.207	.....	−85.9
4567	16	9:41	1.222	− 1.0	−75.1
4425	May 25	10:34	1.648	−25.6	−66.2
4571	June 17	8:46	2.184	− 4.3	−20.2
4512	8	10:53	2.228	−20.1	−27.1
4550	13	9:50	2.706	− 3.2	+17.5
4580	22	9:26	2.734	+ 9.5	+15.1
4581	22	9:52	2.752	− 5.8	+18.9
4391	May 22	10:28	3.121	− 3.6	+39.0
4555	June 14	8:56	3.669	− 6.4	+26.4
4556	14	9:15	3.682	+ 8.8	+35.2
4557	14	9:42	3.701	− 6.5	+24.7
4585	23	9:35	3.740	+17.2	+24.1
4404	May 23	11:20	4.157	+ 8.3	−14.0
4528	June 10	9:23	4.165	− 8.4	+ 6.1
4529	10	9:38	4.176	− 5.4	−12.9
4530	10	9:57	4.189	− 5.4	− 1.1
4434	May 28	6:19	4.470	+ 4.7	−35.7

TV CASSIOPEIAE[24]

PHOTOMETRIC DATA

This star has been known as a variable since its discovery by Astbury,[25] in 1911, who suggested that it probably belongs to the Algol-type group. Its provisional designation was 45.1911.

H. Shapley[17] in his photometric solution based upon Nijland's observations,[26] which

[23] *Pub. Dom. Ap. Obs.*, **1**, 141, 1922.

[24] BD + 58°30 (7.3 mag.) = HD 1486 (Sp. B9) = AG Hels 205 (7.7 mag.) (α = 0^h 11^m 31^s; δ = + 58° 20′.0 [1855.0]). See Bibliography in Prager's *Geschichte und Literatur*, **1**, 221, Berlin, 1924.

[25] *A.N.*, **189**, 357, 1911; *Observatory*, **34**, 416, 1911.

[26] *Op. cit.*, p. 16.

showed no secondary minimum, considered the eclipse as partial, a conclusion which agrees with the observations by Van Biesbroeck and Casteels,[27] Lazzarino,[28] and others. Some years later, McDiarmid[29] found that there is a secondary minimum which "occurs 17 minutes before mid-period" and that the light-curve shows "a combined effect of reflection and ellipticity." The secondary minimum was also found by Jordan[30] to occur a little before mid-period.

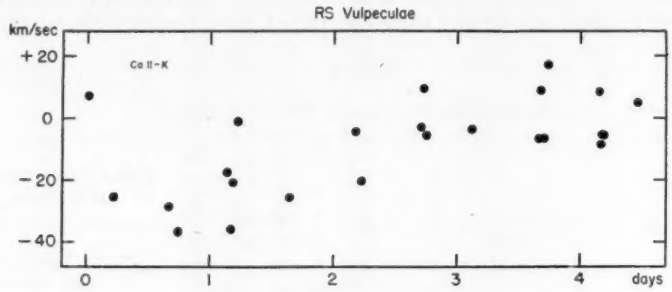

FIG. 5

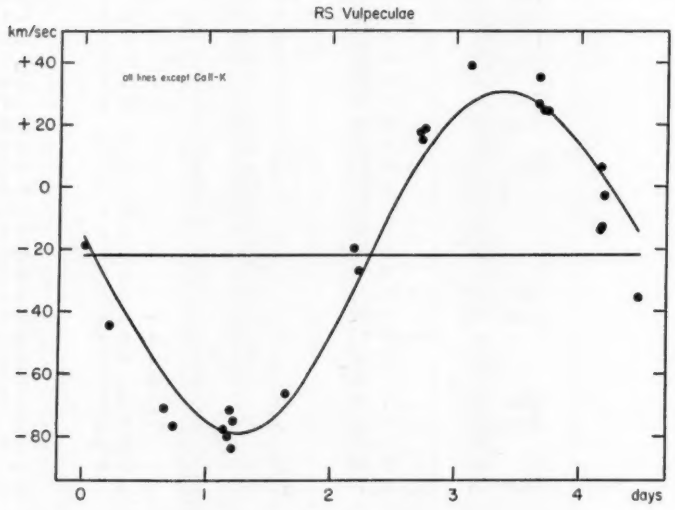

FIG. 6

Schneller's *Katalog* for 1941 gives the photometric elements derived by Hellerich,[31] namely,

$$\text{Minimum} = \text{JD } 2420117.7464 + 1.8126096\,E$$

and

$M_1 = 7.30$ mag. $\quad D = 8$ hours
$A_1 = 1.05$ mag. $\quad d = 0.4$ hours
$A_2 = 0.09$ mag.

Ellsworth[32] suggested a small variation in the period.

[27] *Ann. Obs. r. de Belgique*, **13**, 181, 1914.
[28] *A.N.*, **197**, 373, 1914.
[29] *Contr. Princeton U. Obs.*, No. 7, 1924.
[30] *Pub. Allegheny Obs.*, **7**, 184, 1929.
[31] *A.N.*, **221**, 241, 1924.
[32] *Gaz. astr.*, **17**, 119, 1930.

THE SPECTRUM OF TV CAS (PL. XL)

The spectrum of TV Cas obtained at maximum light is of type B9. In order to secure the spectrum of the secondary star, a plate was taken on the night of June 1, 1945, with mid-exposure at phase 1.8103 days, i.e., about 3 minutes before mid-eclipse as predicted by Hellerich's elements. Owing to weather conditions, the exposure time was 34 minutes, i.e., 10 minutes longer than the predicted duration of total phase. The spectrum obtained under these conditions does not look later in spectral type than the ones secured outside

TABLE 6

STAR LINES USED FOR TV CASSIOPEIAE

Element	λ	Element	λ
Ca II K	3933.67	*Hγ*	4340.47
Hδ	4101.74	*Mg* II	4481.23

TABLE 7

RADIAL VELOCITIES OF TV CASSIOPEIAE

Plate	Date (1945)	U.T.	Phase (in Days)	Radial Velocity in Km/Sec
CQ 4459	June 1	9:34	0.020	−48.4
4400	May 23	8:13	0.027	−45.8
4460	June 1	10:12	0.046	−47.0
4401	May 23	9:02	0.061	−52.3
4402	23	9:38	0.086	−31.1
4403	23	10:24	0.118	−51.9
4426	25	11:12	0.338	−66.5
4558	June 14	10:14	0.359	−83.1
4433	May 27	11:08	0.523	−79.4
4568	June 16	10:12	0.545	−55.9
4569	16	10:40	0.565	−86.4
4392	May 2	11:00	0.955	+20.2
4582	June 22	10:26	1.117	+52.2
4583	22	10:48	1.133	+32.7
4572	17	9:22	1.511	+72.0
4573	17	9:49	1.529	+57.6
4458	1	9:02	1.810	− 7.5

of eclipse. Probably the eclipse is partial, and the spectrum of the secondary star does not show. Our plates taken near maximum and minimum radial velocity do not show the doubling of *He* I and *H*.

RADIAL VELOCITIES

For the determination of the radial velocities the lines listed in Table 6 were measured. The results are shown in Table 7 and are plotted in Figure 7, where we have also drawn a velocity-curve according to Plaskett's elements[33] for the primary star, namely,

$$e = 0 \text{ (assumed)}, \qquad K = 87.92 \text{ km/sec}, \qquad \gamma = +0.54 \text{ km/sec}.$$

[33] *Pub. Dom. Ap. Obs.*, **2**, 141, 1922.

Our observations indicate an appreciable rotational disturbance, the direction of rotation being the same as the direction of the orbital revolution.

On our spectrograms the line *He* I 4026 is too faint for accurate measurement; however, an attempt to measure it with a low-power eyepiece indicates that the radial velocities follow the trend of the velocity-curve of the primary star.

CONCLUSIONS

The results of this investigation are as follows:

1. The spectral types of the visible components of U CrB and RS Vul at principal eclipse are both in the vicinity of A2, while the types predicted from the ratio of the surface brightnesses as given by the light-curves are at least as late as G. Because the reflection effect is absent at mid-eclipse, this interpretation must be abandoned to account for the discrepancy.

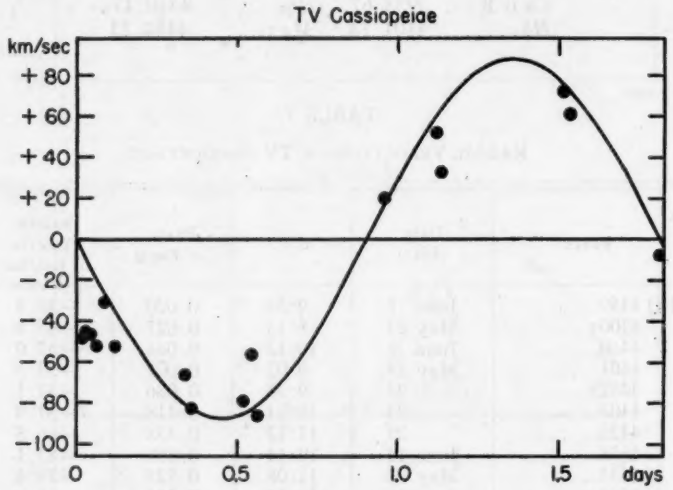

FIG. 7

2. We did not observe the metallic lines of the secondary at maximum light, and our plates do not show double lines of *He* I, etc., as were measured at Victoria. This may be due to the smaller dispersion of our spectrograph.[34] In the case of U CrB our smaller value of K_1 compared to the values obtained by Plaskett and by Pearce might mean that some effect of blending is present in our measures. On the other hand, the indicator lines showing where the secondary components should be, in Plates XXXVIII-XL, leave little doubt that the lines are absent on our spectrograms. The fact that the Victoria spectral types are earlier than ours is probably not significant. But if it were real, it would mean that only this small difference (and not the entire discrepancy between observed and predicted spectral types) can be due to the reflection effect.

3. In the case of U CrB, an anomaly in structure of the *H* lines near maximum radial velocity suggests the presence of a stream which is probably similar to the streams previously discovered in AU Mon, SX Cas, etc. The fact that the anomaly is not observed

[34] The dispersion used by us was adopted in order to secure satisfactory spectrograms with relatively short exposures, at the mid-eclipses.

at minimum radial velocity rules out the possibility that we are concerned with the fainter component of the binary. It is possible (but as yet not certain) that the discrepancy between photometric and spectrographic types may be due to the presence of this stream.[35]

4. The spectrum of TV Cas at principal minimum shows no departure from that observed at maximum light.

We are indebted to Miss Alice Johnson, Mrs. Martha Carlson, and Miss Gertrude Peterson for help in the reduction of the plates and in the making of the diagrams.

[35] However, it is somewhat disconcerting that the principal eclipses of all three stars are not very deep and may not even be total. In many other systems in which the absorption lines and the emission lines prove beyond doubt the existence of gaseous streams, the spectral types of the secondaries were observed to be those predicted by the ratios of the surface brightnesses. It is just barely possible that in U CrB and RS Vul the spectrum, even at mid-eclipse, gives no indication of the true light of the secondary star and that the observed spectrum is solely that of the primary star modified by the sharpening effect upon broad absorption lines of the rotational effect, and perhaps by other causes, such as stream of gas, tidal distortion, etc.

THE WOLF-RAYET SPECTROSCOPIC BINARY HD 168206*

W. A. HILTNER
Yerkes and McDonald Observatories
Received September 11, 1945

ABSTRACT

The Wolf-Rayet star HD 168206 is investigated as a spectroscopic binary. Its spectral class is WC7 +. Three emission bands, *He* II 4686, *C* III–IV 4652, and *C* IV 4441, and one absorption line, $H\gamma$, were measured for radial velocity. The period of the system is 29.675 days. The emission has a semi-amplitude of 165 km/sec. The hydrogen absorption varies oppositely to the emission, with a semi-amplitude of 55 km/sec, suggesting that the hydrogen lines have their origin in an early-type companion. The minimum masses are $M_{WR} \sin^3 i = 8.2 \odot$, and $M_B \sin^3 i = 24.8 \odot$.

The Wolf-Rayet star HD 168206[1] was recently announced[2] to be a spectroscopic binary on the basis of two spectrograms, one taken in July, 1941, and the other in June, 1944. The relative displacement of the blend of *C* III and *C* IV near λ 4652 was found to be approximately 250 km/sec. The spectrum of this star is WC7 +. The most pronounced feature of the spectrum is the above-mentioned blend. This band normally has a weak violet absorption edge. The bands *He* II 4686 and *C* IV 4441 are of moderate strength; but the rest of the spectrum in the ordinary photographic region shows only broad, weak emission bands, much too faint to be measured for radial velocity, except $H\gamma$, which is in absorption and can usually be measured without difficulty. In the ultraviolet region of the spectrum, higher members of the Balmer lines are observed in absorption. The spectrum is reproduced in Plate XLI.

Between February and August, 1945, 42 additional spectrograms were obtained with the 82-inch reflector of the McDonald Observatory. Three different arrangements of the Cassegrain spectrograph were used: the 500-mm camera with two quartz prisms (designated by "CQ") giving a dispersion of 69 A/mm at λ 4652; the $f/2$ Schmidt camera with two glass prisms ($f/2$ G), giving a dispersion of 100 A/mm at λ 4652; and the $f/2$ Schmidt camera with two quartz prisms ($f/2$ Q), giving a dispersion of 213 A/mm at λ 4652. Eastman 103a-O emulsion was generally used.

The spectrograms were measured in the usual fashion with settings made on the centers of the bands. When possible, *C* III–IV 4652, *He* II 4686, *C* IV 4441, and $H\gamma$ 4340 were measured; but a few of the spectrograms were underexposed so that only *C* III–IV 4652 could be measured. Also, $H\gamma$ could not be measured on the $f/2$ Q spectrograms. Only one of the spectrograms ($f/2$ Q 5711) taken with the quartz prisms is sufficiently well exposed in the ultraviolet to permit one to measure the higher members of the Balmer series. Table 1 gives the observed radial velocities. An arbitrary wave length of λ 4652.00 was adopted for the blend of *C* III and *C* IV. Consequently, the velocities for this band are listed in the table as "Velocity + *C*." The other lines are not blended, except $H\gamma$, which may be blended by an unknown amount with *He* II.

The velocity-curves for all the measured emission and absorption features are shown in Figures 1–4. The period adopted is 29.675 days. The zero-point in phase was arbitrarily assumed to be JD 2431543.10.

* *Contributions from the McDonald Observatory, University of Texas*, No. 118.

[1] $\alpha = 18^h13^m5$, $\delta = -11°40'$ (1900), Sp. 0a, mag. ptm. 8.9.

[2] W. A. Hiltner, *Ap. J.*, **101**, 356, 1945.

PLATE XLI

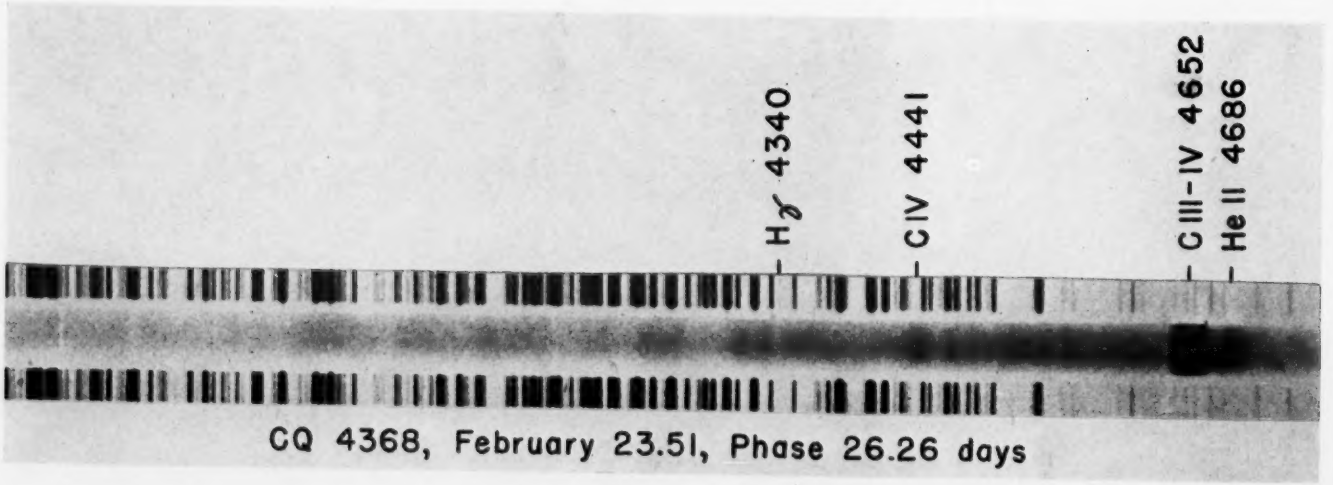

THE SPECTRUM OF HD 168206

UNIV. OF MICH.

In spite of the large scatter in the absorption velocities, the velocity-curve of $H\gamma$ is certainly opposite to the velocity-curves for the emission features, suggesting that the companion star is responsible for the hydrogen absorption in the spectrum.

The approximate orbital elements derived from the C III–IV blend and $H\gamma$ are as follows:

$P = 29.675$ days — $\gamma_{WR} = +45 + C$ km/sec
$e = 0.0$ (assumed) — $\gamma_B = +10$ km/sec
$K_{WR} = 165$ km/sec — $M_{WR} \sin^3 i = 8.2 \odot$
$K_B = 55$ km/sec — $M_B \sin^3 i = 24.8 \odot$

TABLE 1

RADIAL VELOCITIES OF HD 168206

Plate	Date, U.T.	Phase (in Days)	Velocity + C III–IV 4652 (Km/Sec)	Velocity He II 4685.81 (Km/Sec)	Velocity C IV 4441.81 (Km/Sec)	Velocity $H\gamma$ 4340.47 (Km/Sec)
CQ 895	1941 July 25.251	22.701	−111	.....	.....	.....
3271	1944 June 16.206	11.356	+194	.....	.....	.....
4358	1945 Feb. 22.521	25.271	−112	− 48	−121	− 38
4368	23.510	26.260	−112	+ 29	− 97	+ 54
4380	27.499	0.574	− 1	+ 39	−112	+ 10
f/2 G 5340	Mar. 2.480	3.555	+ 40	+ 51	+ 43	−100
5341	2.513	3.588	+ 46	+150	+ 37	+ 89
5395	6.490	7.565	+215	.....	.....	.....
5445	9.440	10.515	+209	+342	+229	− 40
5446	9.469	10.544	+164	+409	+128	− 40
5447	9.503	10.578	+242	+436	+162	− 93
5463	10.439	11.514	+196	+257	+190	− 40
5464	10.466	11.541	+132	+296	+184	+ 49
5465	10.489	11.564	+164	+460	+230	− 19
5466	10.506	11.581	+157	+422	+145	+ 12
5467	10.519	11.594	+125	+422	+145	− 77
5480	11.424	12.499	+132	+316	+ 45	− 41
5481	11.445	12.520	+125	+363	+101	− 83
5482	11.465	12.540	+145	+423	+160	+ 70
5483	11.481	12.556	+151	+343	+112	− 50
5484	11.496	12.571	+132	+389	+162	− 88
5485	11.509	12.584	+125	+363	+157	− 76
5486	11.520	12.595	+145	+376	+ 95	− 35
5500	12.510	13.585	+144	+407	+ 50	− 41
5501	12.519	13.594	+138	+264	+ 67	− 9
f/2 Q 5528	15.499	16.574	+127	+338	− 20	.....
5529	15.515	16.590	+ 59	.....	.....	.....
f/2 G 5661	26.502	27.577	− 36	+ 33	− 84	+ 44
5662	26.511	27.586	− 36	−120	−140	+ 29
f/2 Q 5711	Apr. 2.503	4.903	+149	+393	+ 76	.....
f/2 G 5752	July 18.318	22.693	− 76	+112	− 79	+114
5762	19.241	23.616	−140	− 14	− 56	+ 41
5775	20.181	24.556	−115	− 14	−209	+ 24
5801	22.202	26.577	−103	+ 5	−148	+ 97
5815	23.208	27.583	0	+ 51	−103	+ 86
5840	25.199	29.574	− 14	+ 96	−161	+127
5865	27.191	1.891	+ 44	+174	−110	+ 74
5887	29.176	3.876	+ 69	+ 94	− 72	+110
5979	Aug. 4.198	9.898	+266	+323	+189	+ 49
5996	5.174	10.874	+246	+455	+160	− 13
6026	7.161	12.861	+220	+408	+154	− 56
6041	9.293	14.993	+142	+315	+ 86	+ 47
6068	11.192	16.892	+ 96	+215	− 32	− 20
6106	14.215	19.915	− 86	+221	+ 6	+ 78

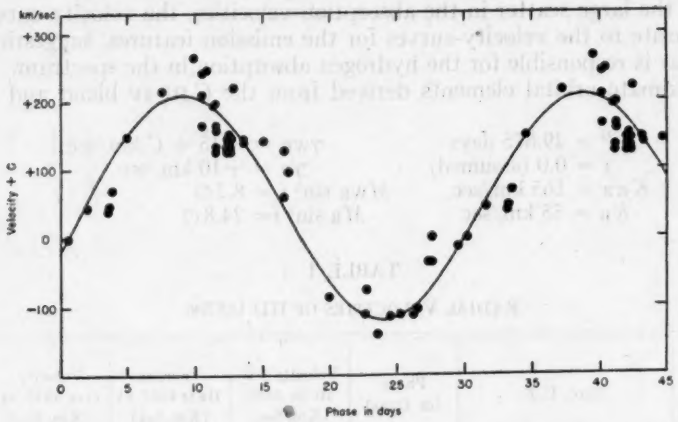

FIG. 1.—Velocity-curve from the *C* III and *C* IV blend near λ 4652

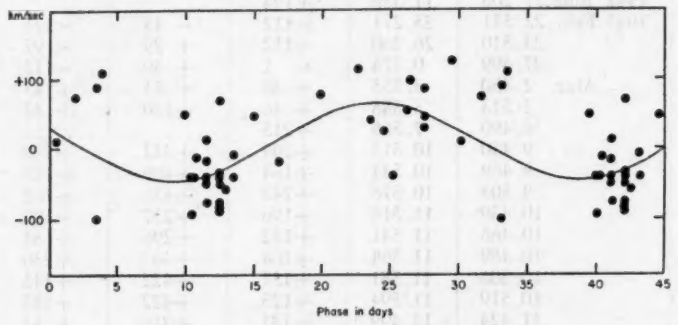

FIG. 2.—Velocity-curve from $H\gamma$ absorption

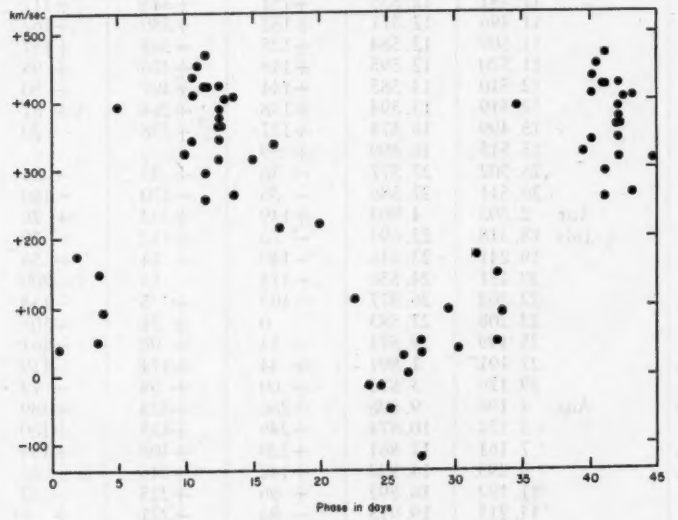

FIG. 3.—Velocity-curve from *He* II 4686

The other measured emission bands give similar orbital elements. The value of K, however, should be increased to approximately 195 km/sec in the case of *He* II 4686. Generally in Wolf-Rayet stars the *He* II 4686 band is displaced to the red with respect to other bands, and HD 168206 is no exception. The velocity of the system is + 200 km/sec for *He* II 4686, −10 km/sec for *C* IV 4441, and +10 km/sec for $H\gamma$ absorption. The last two are in good agreement, but it must be emphasized that the velocity of the system is not necessarily represented by either line.

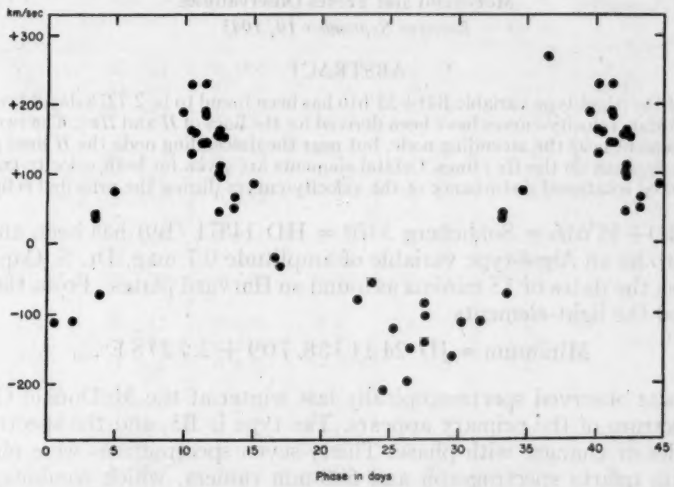

FIG. 4.—Velocity-curve from *C* IV 4441

The violet absorption edge of the *C* III and *C* IV blend varies in intensity. At phases near 4 days (plates *f*/2 G 5340, phase 3.55 days; *f*/2 G 5341, phase 3.59 days; *f*/2 Q 5711, phase 4.90 days; and *f*/2 G 5887, phase 3.88 days), when the Wolf-Rayet star is on the near side of the system, the absorption edge is unusually strong, but at other phases it is weak. It is significant that, in spite of the appreciable change in intensity of the violet absorption, the velocity-curve remains sensibly undistorted.

I wish to thank Dr. O. Struve for obtaining some of the spectrograms.

THE SPECTROSCOPIC ORBIT OF THE ECLIPSING VARIABLE BD+55°616*

ARMIN J. DEUTSCH
McDonald and Yerkes Observatories
Received September 19, 1945

ABSTRACT

The period of the Algol-type variable BD+55°616 has been found to be 2.7278 days. From 49 spectrograms of this B5 star, velocity-curves have been derived for the lines of *H* and *He* I. The two curves are in substantial agreement near the ascending node, but near the descending node the *H* lines give velocities somewhat nearer γ than do the *He* I lines. Orbital elements are given for both velocity-curves. There is evidence of marked rotational disturbance of the velocity-curves during the principal eclipse.

The star BD+55°616 = Sonneberg 3370 = HD 14871 (B9) has been announced by Hoffmeister[1] to be an Algol-type variable of amplitude 0.7 mag. Dr. S. Gaposchkin has kindly sent me the dates of 15 minima as found on Harvard plates. From these minima, I have derived the light-elements

$$\text{Minimum} = \text{JD } 2431358.709 + 2.7278\,E\,.$$

This star was observed spectroscopically last winter at the McDonald Observatory. Only the spectrum of the primary appears. The type is B5, and the spectrum exhibits no peculiarities or changes with phase. Thirty-seven spectrograms were obtained with the Cassegrain quartz spectrograph and 500-mm camera, which combination gives a dispersion of 55 A/mm at $H\gamma$. All plates were taken on Eastman 103a-O emulsion, the exposure time being about 10 minutes. The slit width was 0.075 mm. Dr. Struve also observed the star at the Cassegrain focus, using the $f/2$ Schmidt camera and the glass prism. This combination gives a dispersion of 75 A/mm at $H\gamma$. The exposures were about 5 minutes and were made on film coated with Eastman 103a-O emulsion. The slit width was 0.100 mm. Twelve such spectrograms were obtained and used.

Table 1 gives the radial velocities derived from these 49 spectrograms. The letter "Q" before the plate number indicates that the spectrogram was obtained with the 500-mm camera and quartz prism; the letter "G" that it was obtained with the Schmidt camera and glass prism. The period 2.7278 days was found to satisfy the velocities and was used in the calculation of the phases; these are counted from an arbitrary zero at JD 2431440.000. The lines measured were γ, δ, ζ, η, ϑ of hydrogen; $\lambda\lambda$ 3820, 4009, 4026, 4121, 4144, 4388, 4272 of *He* I; and *Ca* II K. Table 1 gives, under "*H*," the mean velocity from the hydrogen lines measured on each plate; under "*He* I," the mean velocity from the helium lines; and under "*Ca* II," the velocity from the K line. The average mean error of the *H* velocities is 15 km/sec; and of the *He* I velocities, 18 km/sec. Normal points were formed as indicated in the table, the spectrograms of smaller dispersion being given only half-weight.

The K line appears to be mainly interstellar. On one spectrogram, G4898, it appears double, the violet component being much the weaker of the two. There is a systematic difference between the velocity-curves from *H* and from *He* I (see Figs. 1 and 2). At and near the ascending node, the agreement between the two curves is not bad, but near the descending node *H* gives systematically smaller speeds of approach than does *He* I. There can be little doubt that the difference is real.

* *Contributions from the McDonald Observatory, University of Texas*, No. 119.

[1] A.N., Vol. **274**, No. 1, 1943.

TABLE 1

RADIAL VELOCITIES OF BD+55°616

PLATE	JD 2431400+	PHASE* (DAYS)	RADIAL VELOCITY (KM/SEC)			NORMAL POINTS		
						Phase* (Degrees)	Radial Velocity (Km/Sec)	
			H	*He* I	*Ca* II		*H*	*He* I
Q4203	45.524	0.068	+20	+ 11	−12	15	+ 4	+ 5
Q4252	53.769	0.129	− 6	+ 15	+14			
G4986	86.543	0.167	− 6	− 14	− 6			
Q4326	67.538	0.258	−13	− 22	0	36	−13	−12
Q4327	67.547	0.267	− 8	− 23	−15			
Q4314	64.845	0.293	−19	+ 10	−17			
G4888	78.549	0.357	+12	+ 14	− 2	52	−22	+ 4
Q4235	48.546	0.362	−46	+ 19	+46			
Q4292	59.538	0.442	−15	− 17	−16			
Q4342	70.542	0.534	+17	+ 54	−15	73	−11	−35
Q4343	70.552	0.544	−25	− 90	+18			
G4915	81.544	0.624	−38	−102	−20			
Q4295	59.842	0.746	−38	− 82	+ 8	109	−43	−85
Q4176	43.529	0.801	−23	− 68	− 2			
G4955	84.542	0.894	−62	− 91	− 6			
Q4254	54.535	0.895	−59	−104	−14			
Q4257	65.533	0.981	−56	−127	+19	138	−67	−107
Q4317	54.684	1.044	−59	−105	− 8			
Q4346	76.537	1.073	−71	− 98	−29			
Q4347	76.544	1.080	−81	− 98	+ 5			
Q4217	46.622	1.166	−70	− 97	−19	161	−76	−117
Q4279	57.590	1.222	−86	−115	−19			
Q4332	68.532	1.252	−73	−125	+24			
Q4333	68.542	1.262	−76	−131	+31			
G4890	79.543	1.351	−48	−102	−13	180	−48	− 94
G4891	79.550	1.358	−58	− 98	− 6			
Q4280	57.738	1.370	−44	− 88	− 1			
Q4296	60.537	1.441	−63	−118	−20	202	−46	− 89
Q4137	41.585	1.585	−27	− 66	−10			
G4927	82.543	1.623	−49	− 78	−10			
Q4307	63.547	1.723	−33	− 74	−14	236	−23	− 52
Q4189	44.538	1.810	−15	− 37	−18			
G4974	85.542	1.894	−18	− 36	−43			
Q4259	55.594	1.954	−18	− 7	− 9	262	−20	− 9
Q4322	66.543	1.997	−33	− 23	+ 6			
Q4194	44.725	1.997	− 9	+ 4	−22			
Q4262	55.694	2.054	− 7	+ 1	−22	274	− 8	+ 5
Q4369	77.542	2.078	− 8	+ 11	+ 1			
Q4350	77.552	2.088	− 9	+ 2	+16			

* The phase is zero at JD 2431440.000 + 2.7278 E.

TABLE 1—*Continued*

Plate	JD 2431400+	Phase* (Days)	Radial Velocity (Km/Sec)			Normal Points		
						Phase* (Degrees)	Radial Velocity (Km/Sec)	
			H	*He* I	*Ca* II		*H*	*He* I
Q4225	47.580	2.124	− 7	+ 3	+12	292	− 1	+ 2
G5016	88.546	2.170	− 9	− 22	−17			
Q4338	69.538	2.258	+10	+ 6	+ 6			
Q4339	69.545	2.265	− 1	+ 8	+ 3			
G4898	80.544	2.352	−26	+ 34	−16	316	+ 8	+ 25
G4899	80.547	2.355	+17	+ 18	− 6			
Q4300	61.547	2.451	+20	+ 24	−32			
G4845	83.543	2.623	+39	+ 16	−10	352	+22	+ 4
Q4168	42.640	2.640	+33	+ 4	+10			
Q4310	64.532	2.708	+ 2	− 3	− 5			

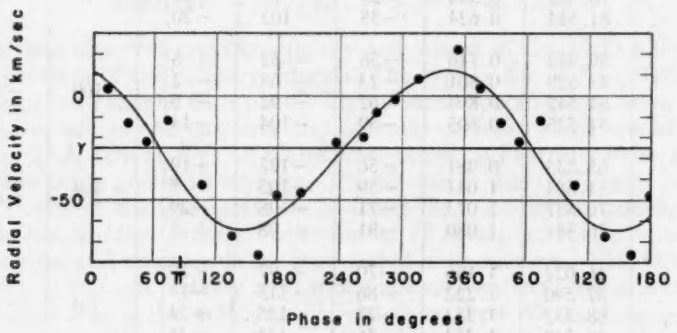

FIG. 1.—Velocity curve of BD + 55°616 from lines of *H*

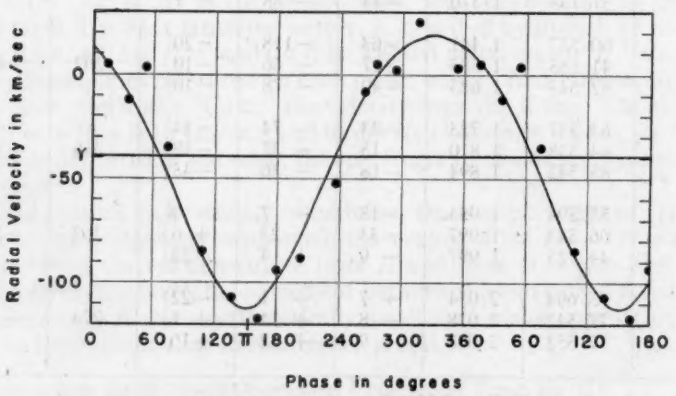

FIG. 2.—Velocity curve of BD + 55°616 from lines of *He* I

By the Wilsing-Russell method, orbital elements have been derived separately from the curves of *H* and *He* I. The results are as given in the accompanying tabulation. It is

	H	He I
P (photometric)	2.7278 days	2.7278 days
T	JD 2431440.660=87°	JD 2431441.152=152°
K	38.4 km/sec	65.6 km/sec
γ	−25.3 km/sec	−39.6 km/sec
e	0.09	0.11
ω	112°	182°
$a \sin i$	1.44×10^6 km	2.48×10^6 km
$m_2^3 \sin^3 i/(m_1+m_2)^2$	0.0150⊙	0.0795⊙

unknown which of these sets of elements, if either, represents the actual orbital motion. In view of the strength of the hydrogen lines, it is perhaps more likely that their velocity-curve is distorted, as it is known to be distorted in other systems. On the other hand, it is difficult to see what sort of model would produce distortion of the velocity-curve only in the half of the orbit centered at the descending node. Moreover, one would expect the disturbing streams of gas, if such be present, to make themselves known by producing changes in the appearance of the affected lines. As has already been remarked, none of the lines changes in appearance, and all look symmetrical at all phases.

Mention should be made of the highly discrepant velocities derived from plates Q4342 and Q4343, which were taken in quick succession. Both plates are of better-than-average quality. Since the light-elements predict an eclipse at phase 0.543 days, there can be little doubt that the discrepancy in the velocities is due to a rapidly changing rotation effect.

It is a pleasure to acknowledge here the assistance of Drs. O. Struve and S. Gaposchkin.

A SPECTROGRAPHIC STUDY OF 68 u HERCULIS

BURKE SMITH
Yerkes Observatory
Received July 27, 1945

ABSTRACT

A new determination of the orbital elements of 68 u Herculis has been made from 181 Yerkes spectrograms obtained in 1944. Lines of the secondary were measured on 123 spectrograms. The new values for γ and K differ slightly from the 1935 Yerkes results. There is a large increase in the value of ω as compared to the earlier results, but this is of doubtful significance, in view of the small value of e. Approximate synchronism between rotation and orbital revolution for the bright component is indicated. There is a discrepancy of the order of 10° between zero phase for the primary and secondary, as determined from the least-squares solution for the primary.

A spectrographic determination of the orbit of the eclipsing variable 68 u Herculis (HD 156663) was first published by R. H. Baker[1] in 1909. In 1939 Luyten, Struve, and Morgan[2] published a new determination of the orbit which indicated that no significant change had taken place in the orbital elements in the 27 years from 1908 to 1935, with the possible exception of a change in ω. However, the solution of the normal equations gave $e = 0.05$, while, according to photometric observations, $e \leq 0.01$.[3] It is known that

TABLE 1

STELLAR LINES USED FOR RADIAL-VELOCITY DETERMINATION

He I....4009.27	*C* II....4267.15	*Mg* II....4481.23
He I....4026.22	*Hγ* 4340.47	*Si* III....4552.62
Hδ 4101.74	*He* I....4387.93	*He* I 4713.20
He I....4143.76	*He* I....4471.51	

for small eccentricities the spectrographically determined values of e and ω have little significance.

In view of the recent interest in the discrepancies between spectrographic and photometric elements of certain eclipsing variables[4] it seemed worth while to compute an orbit based on more recent observations and with a greater number of spectrograms. The present study is the result of measurements of 181 spectrograms of this star, taken with the Bruce spectrograph (dispersion 30 A/mm at λ 4500), attached to the 40-inch Yerkes telescope, during the interval from January to September, 1944. Lines of the primary (bright) component are generally broad and hazy. The secondary (faint) component shows lines which are much fainter than those of the primary but are usually narrower, with the exception of *Mg* II 4481, which is occasionally of equal intensity and of similar appearance in both components. The secondary lines were measured on a total of 123 spectrograms.

The lines of both primary and secondary are difficult to measure for radial velocity. The hydrogen lines are especially difficult on account of their breadth and the overlapping of the lines of the two components. In the determination of the orbit the velocity of the hydrogen lines was accordingly omitted. Eleven stellar lines were selected for radial-velocity determination, and the wave lengths used are shown in Table 1. All these lines were measured at least once in the spectra of both components. *Si* III 4552 was measured on only 5 plates.

Table 2 shows the results of the radial-velocity measurements. As in the 1935 Yerkes

[1] *Pub. Allegheny Obs.*, **1**, 77, 1909. [2] *Pub. Yerkes Obs.*, **7**, Part 4, 18, 1939.

[3] Luyten, *Pub. Minn. Obs.*, **2**, 36, 1935. Martin, *B.A.N.*, **8**, 265, 1938.

[4] Struve, *Ap. J.*, **99**, 89 and 222, 1944; Kopal, *Ap. J.*, **99**, 239, 1944.

TABLE 2

RADIAL VELOCITIES OF 68 u HERCULIS

PLATE	1944 DATE (U.T.)	PHASE	PRIMARY				SECONDARY			
			He I, *C* II, *Mg* II, *Si* III		*H*		*He* I, *C* II, *Mg* II, *Si* III		*H*	
			V (Km/Sec)	No.	*V* (Km/Sec)	No.	*V* (Km/Sec)	No.	*V* (Km/Sec)	No.
(1)	(2)	(3)	(4)	(5)	(6)	(7)	(8)	(9)	(10)	(11)
13716	Sept. 25.671	1?8	+ 91.0	4	+115.5	2	−234.5	3	−235.5	1
13622	July 13.847	4.3	48.0	4	+ 24.9	2	363.4	2	295.8	1
13596	July 3.596	5.0	68.0	4	+ 41.5	2	279.4	2	294.6	2
13623	July 13.872	8.6	53.2	4	+ 40.0	2	280.5	3	.....	.....
13597	July 3.622	9.0	71.3	7	+ 52.6	2	264.9	1	.....	.....
13598	July 3.636	11.9	73.3	4	+ 38.7	2	240.3	2	179.4	1
13439	Feb. 4.912	12.2	80.5	7	+ 58.8	2	205.1	1	.....	.....
13574	July 1.596	13.7	73.6	5	+ 58.4	2	234.2	2	254.7	1
13599	July 3.666	17.3	63.5	6	+ 56.6	2	251.2	4	.....	.....
13575	July 1.621	18.4	72.1	6	+ 3.7	2	339.5	2	293.5	2
13440	Feb. 4.959	20.5	67.9	6	+ 64.4	2	159.1	2	.....	.....
13576	July 1.644	22.3	61.0	6	+ 54.3	2	322.1	1	.....	.....
13600	July 3.696	22.3	63.1	7	+ 42.0	2	224.3	2	183.0	1
13611	July 11.899	22.3	67.5	5	+ 52.4	2	258.7	2	.....	.....
13601	July 3.718	26.3	62.3	7	+ 60.3	2	219.8	1	204.1	1
13558	June 29.617	26.6	57.5	7	+ 49.7	2	308.3	3	211.1	1
13577	July 1.668	26.6	52.9	3	+ 60.8	2	221.1	3	.....	.....
13441	Feb. 4.040	28.1	62.4	6	+ 51.3	1	227.8	2	.....	.....
13602	July 3.738	29.9	50.7	8	+ 70.1	2	207.9	1	176.7	2
13578	July 1.698	31.7	60.8	5	+ 41.5	2	120.4	1	219.7	1
13559	June 29.655	33.1	45.5	6	+ 46.4	2	265.9	3	.....	.....
13603	July 3.758	33.5	48.5	5	+ 61.0	2	224.7	5	145.1	1
13579	July 1.722	36.0	59.5	5	+ 68.7	2	.....	.....	.....	.....
13604	July 3.778	36.7	61.7	6	+ 65.5	2	205.7	4	.....	.....
13580	July 1.746	40.3	47.3	4	+ 51.8	2	.....	.....	.....	.....
13605	July 3.800	40.7	47.6	7	+ 66.6	2	191.9	3	.....	.....
13560	June 29.701	41.4	46.4	5	+ 28.7	2	194.9	2	−236.7	2
13581	July 1.769	44.2	39.7	5	+ 54.3	2	134.8	1	.....	.....
13606	July 3.826	45.4	50.7	5	+ 46.6	2	.....	.....	.....	.....
13673	Aug. 5.648	46.1	44.8	4	+ 37.7	2	133.4	1	.....	.....
13561	June 29.737	47.5	43.4	4	+ 27.8	1	142.9	1	.....	.....
13582	July 1.793	48.2	47.1	4	+ 76.4	2	.....	.....	.....	.....
13607	July 3.851	49.7	49.5	5	+ 18.5	2	192.2	2	.....	.....
13583	July 1.817	52.6	49.9	4	+ 64.0	2	.....	.....	.....	.....
13562	June 29.771	53.6	28.2	6	− 1.4	2	190.8	2	.....	.....
13608	July 3.875	54.0	31.9	7	+ 20.2	2	.....	.....	.....	.....
13707	Sept. 9.560	54.0	53.5	7	+ 26.3	2	−207.9	2	.....	.....
13584	July 1.841	56.9	38.5	5	+ 55.5	2	.....	.....	.....	.....
13609	July 3.899	58.0	24.6	4	+ 22.0	1	.....	.....	.....	.....
13563	June 29.808	60.1	+ 25.3	6	+ 38.8	1	.....	.....	.....	.....

TABLE 2—*Continued*

Plate	1944 Date (U.T.)	Phase	Primary				Secondary			
			He I, *C* II, *Mg* II, *Si* III		*H*		*He* I, *C* II, *Mg* II, *Si* III		*H*	
			V (Km/Sec)	No.	*V* (Km/Sec)	No.	*V* (Km/Sec)	No.	*V* (Km/Sec)	No.
(1)	(2)	(3)	(4)	(5)	(6)	(7)	(8)	(9)	(10)	(11)
13708	Sept. 9.595	60?1	+ 29.5	7	+ 37.3	2	−117.0	2	.....	....
13585	July 1.867	61.6	+ 24.9	6	+ 30.7	2	.....	....	.....	....
13546	June 21.614	61.9	+ 29.9	4	+ 51.3	2	.....	....	.....	....
13709	Sept. 9.624	65.2	+ 37.6	6	+ 21.1	2	.....	....	.....	....
13586	July 1.896	66.6	+ 33.2	4	+ 13.9	2	.....	....	.....	....
13564	June 29.847	67.0	+ 39.4	7	+ 18.9	2	.....	....	.....	....
13547	June 21.649	68.1	+ 26.1	5	+ 20.0	2	.....	....	.....	....
13417	Jan. 23.941	70.9	+ 33.1	7	+ 52.1	2	.....	....	.....	....
13710	Sept. 9.659	71.3	+ 52.4	3	+ 47.8	2	.....	....	.....	....
13487	April 12.937	72.0	+ 23.2	5	+ 23.5	2	.....	....	.....	....
13565	June 29.891	74.5	+ 15.2	5	− 44.0	2	.....	....	.....	....
13548	June 21.702	77.4	+ 24.9	6	− 6.0	2	.....	....	.....	....
13549	June 21.728	81.8	− 5.0	5	− 19.5	2	.....	....	.....	....
13478	April 4.797	83.2	− 14.0	4	− 15.0	2	.....	....	.....	....
13550	June 21.762	87.8	− 15.6	5	− 18.0	2	.....	....	.....	....
13479	April 4.852	93.0	− 47.9	5	− 57.8	2	.....	....	.....	....
13551	June 21.795	93.7	− 57.8	5	− 30.9	2	.....	....	.....	....
13552	June 21.826	99.0	− 76.8	5	− 37.1	2	.....	....	.....	....
13476	April 2.846	100.8	− 55.3	7	− 30.8	2	+ 95.7	2	.....	....
13480	April 4.913	103.5	− 88.9	7	− 43.4	2	.....	....	.....	....
13553	June 21.856	104.4	− 71.1	4	− 34.6	2	+135.2	1	.....	....
13477	April 2.890	108.4	− 68.6	6	− 68.4	2	.....	....	.....	....
13554	June 21.888	109.7	− 63.2	4	− 66.3	2	+126.2	2	.....	....
13458	Feb. 19.842	112.8	− 65.6	7	− 47.1	2	.....	....	.....	....
13459	Feb. 19.892	121.2	− 84.4	7	− 97.4	2	+208.0	2	+178.1	2
13625	July 14.600	136.4	−101.8	8	− 85.1	2	+150.1	2	.....	....
13626	July 14.622	140.0	−106.1	6	−104.0	2	+180.4	2	215.8	1
13450	Feb. 13.891	148.0	−107.5	5	− 85.4	2	+211.9	1	.....	....
13628	July 14.683	150.8	−112.5	7	− 96.2	2	+243.5	3	277.3	1
13725	Sept. 26.538	154.1	−106.6	6	−112.3	2	.....	....	.....	....
13629	July 14.706	154.7	−118.1	6	− 95.7	2	+250.3	2	203.2	1
13630	July 14.728	158.7	−118.7	7	−132.0	2	+257.6	2	287.0	1
13523	June 1.658	159.1	− 81.3	5	− 45.1	1	+259.9	2	246.5	1
13726	Sept. 26.567	159.1	−114.2	6	− 91.6	1	+254.2	2	.....	....
13631	July 14.751	162.6	−108.8	7	− 86.1	2	+180.7	2	.....	....
13727	Sept. 26.596	164.2	− 96.3	6	−118.7	1	+255.6	3	.....	....
13514	May 30.652	167.0	−114.1	4	−115.7	1	+260.0	1	248.0	1
13524	June 1.708	167.7	−117.1	5	−114.2	1	+285.6	1	.....	....
13496	April 29.896	168.8	−126.6	5	− 99.0	2	+155.0	1	+228.3	1
13728	Sept. 26.626	169.4	− 96.6	6	−112.6	2	+296.2	2	.....	....

TABLE 2—*Continued*

Plate	1944 Date (U.T.)	Phase	Primary				Secondary			
			He I, *C* II, *Mg* II, *Si* III		*H*		*He* I, *C* II, *Mg* II, *Si* III		*H*	
			V (Km/Sec)	No.	*V* (Km/Sec)	No.	*V* (Km/Sec)	No.	*V* (Km/Sec)	No.
(1)	(2)	(3)	(4)	(5)	(6)	(7)	(8)	(9)	(10)	(11)
13633.....	July 14.798	171°0	−129.8	7	− 83.5	2	+216.3	4	+205.7	1
13634.....	July 14.820	174.9	118.2	5	86.6	2	284.6	3	360.6	1
13525.....	June 1.755	176.0	114.1	5	108.0	1	251.8	3	.....	....
13515.....	June 30.708	176.8	103.6	2	104.1	1	241.7	1	.....	....
13635.....	July 14.842	178.9	137.0	6	116.9	1	256.4	3	.....	....
13526.....	June 1.800	184.0	117.8	7	98.1	2	234.4	1	225.4	1
13587.....	July 2.601	190.0	116.5	5	115.6	2	217.2	2	.....	....
13527.....	June 1.852	193.0	112.7	3	153.1	1	.....	.....	209.4	1
13588.....	July 2.625	194.5	113.2	6	109.8	2	.....	.....	.....	....
13589.....	July 2.650	198.7	117.1	7	138.5	2	192.7	1	.....	....
13528.....	June 1.890	199.8	118.0	3	157.1	1	214.3	3	222.4	1
13516.....	May 30.845	201.0	94.7	4	109.7	1	218.8	1	145.3	1
13566.....	June 30.610	201.0	133.8	7	85.3	2	257.4	2	137.5	1
13590.....	July 2.678	203.9	119.4	6	96.5	2	171.5	3	.....	....
13567.....	June 30.649	207.8	115.3	6	137.2	2	227.8	2	.....	....
13591.....	July 2.717	210.6	129.8	5	113.0	2	171.2	2	.....	....
13592.....	July 2.746	215.7	109.4	6	120.4	2	116.2	2	.....	....
13432.....	Jan. 30.927	217.1	108.3	4	136.8	2	143.7	1	.....	....
13568.....	June 30.707	218.0	106.9	6	89.0	2	88.8	1	.....	....
13662.....	Aug. 4.588	220.3	95.1	7	90.0	2	147.5	2	118.6	1
13593.....	July 2.778	221.3	108.3	5	90.2	2	142.7	4	.....	....
13569.....	June 30.742	224.0	105.2	6	83.4	2	236.7	3	.....	....
13663.....	Aug. 4.617	225.2	103.3	5	73.7	2	137.3	1	.....	....
13594.....	July 2.814	227.5	100.8	7	47.9	2	158.1	2	.....	....
13664.....	Aug. 4.640	229.3	94.6	6	54.0	2	145.8	3	.....	....
13490.....	April 13.835	229.6	74.8	5	68.4	2	182.2	2	135.4	1
13570.....	June 30.781	230.8	77.3	7	63.1	2	125.8	2	.....	....
13665.....	Aug. 4.662	233.2	58.3	6	40.2	1	117.8	2	.....	....
13595.....	July 2.850	234.0	70.3	7	71.6	2	155.0	2	.....	....
13666.....	Aug. 4.684	237.0	65.8	6	41.6	1	125.1	3	.....	....
13571.....	June 30.817	237.2	78.5	8	80.2	2	.....	.....	.....	....
13697.....	Sept. 8.557	238.0	71.4	6	65.2	2	169.2	1	.....	....
13667.....	Aug. 4.706	241.0	48.3	6	71.4	1	.....	.....	.....	....
13698.....	Sept. 8.579	242.0	73.4	5	96.8	2	37.2	1	.....	....
13572.....	June 30.858	244.4	71.2	8	35.4	2	.....	.....	.....	....
13668.....	Aug. 4.728	245.0	54.8	6	53.4	1	85.9	1	.....	....
13537.....	June 20.610	245.4	50.2	4	82.3	2	135.1	1	+ 89.0	1
13699.....	Sept. 8.601	245.9	57.0	6	40.6	1	.....	.....	.....	....
13669.....	Aug. 4.753	249.0	59.0	3	89.6	1	129.1	1	.....	....
13700.....	Sept. 8.626	250.1	− 50.3	6	− 36.5	1	+ 40.5	1	.....	....

TABLE 2—*Continued*

Plate	1944 Date (U.T.)	Phase	Primary				Secondary			
			He I, *C* II, *Mg* II, *Si* III		*H*		*He* I, *C* II, *Mg* II, *Si* III		*H*	
			V (Km/Sec)	No.	*V* (Km/Sec)	No.	*V* (Km/Sec)	No.	*V* (Km/Sec)	No.
(1)	(2)	(3)	(4)	(5)	(6)	(7)	(8)	(9)	(10)	(11)
13573	June 30.894	250°.6	− 43.5	8	− 21.7	2	.....	.....	.....	.....
13538	June 20.644	251.6	− 46.5	6	− 34.8	2	+ 33.1	1	.....	.....
13701	Sept. 8.655	255.2	− 22.4	6	− 26.4	2	.....	.....	.....	.....
13539	June 20.644	257.2	− 46.4	4	− 25.6	2	.....	.....	.....	.....
13702	Sept. 8.683	260.2	− 38.5	6	+ 11.6	2	.....	.....	.....	.....
13540	June 20.713	263.4	− 32.5	5	− 41.7	2	.....	.....	.....	.....
13703	Sept. 8.713	265.3	− 26.0	5	− 26.1	2	.....	.....	.....	.....
13651	July 25.599	266.8	− 19.6	6	− 9.4	2	.....	.....	.....	.....
13541	June 20.756	271.0	− 17.2	5	− 18.4	2	.....	.....	.....	.....
13652	July 25.622	271.0	− 26.1	5	− 41.4	2	.....	.....	.....	.....
13640	July 23.595	275.0	− 33.6	6	− 22.3	2	.....	.....	.....	.....
13653	July 25.649	275.9	− 11.1	6	− 15.6	2	.....	.....	.....	.....
13542	June 20.794	278.0	+ 0.2	5	− 11.8	2	.....	.....	.....	.....
13641	July 23.617	279.0	+ 1.3	8	− 19.8	2	.....	.....	.....	.....
13654	July 25.672	279.6	− 13.7	7	− 43.1	2	.....	.....	.....	.....
13543	June 20.829	284.0	+ 21.3	7	− 0.7	1	−132.1	1	.....	.....
13642	July 23.645	284.0	− 22.3	6	− 40.9	2	−217.2	1	.....	.....
13655	July 25.694	284.0	− 18.1	5	− 9.2	2	−130.1	1	.....	.....
13684	Aug. 29.576	286.1	+ 10.2	5	− 5.9	1	−179.8	2	.....	.....
13656	July 25.716	287.1	+ 13.4	6	− 10.7	2	.....	.....	.....	.....
13643	July 23.669	288.0	+ 16.2	8	+ 15.6	2	.....	.....	.....	.....
13657	July 25.738	291.2	+ 4.8	6	− 23.7	1	−158.2	1	.....	.....
13544	June 20.872	291.5	+ 22.6	5	+ 4.1	1	.....	.....	.....	.....
13685	Aug. 29.608	291.6	+ 21.6	6	− 11.5	1	−136.7	1	.....	.....
13644	July 23.694	292.7	+ 10.6	5	− 4.0	2	.....	.....	.....	.....
13658	July 25.760	295.1	+ 28.5	5	+ 1.9	1	−122.1	1	.....	.....
13645	July 23.719	297.0	+ 9.7	8	+ 23.3	2	.....	.....	.....	.....
13686	Aug. 29.637	297.0	+ 23.3	5	+ 15.5	1	.....	.....	.....	.....
13646	July 23.744	301.2	+ 8.2	8	+ 9.0	2	−230.2	2	.....	.....
13687	Aug. 29.665	301.7	+ 27.9	6	− 12.2	1	−153.1	2	.....	.....
13674	Aug. 25.576	304.0	+ 22.9	6	+ 9.4	2	−192.2	2	.....	.....
13647	July 23.772	306.3	+ 35.4	6	+ 9.6	2	−301.3	1	.....	.....
13688	Aug. 29.694	306.8	+ 20.2	7	+ 17.4	2	−206.2	3	.....	.....
13501	April 30.686	307.5	+ 47.8	3	+ 62.3	1	.....	.....	.....	.....
13675	Aug. 25.608	309.6	+ 38.8	7	+ 50.6	2	−269.0	2	.....	.....
13637	July 15.592	310.3	+ 21.3	6	+ 1.7	2	.....	.....	.....	.....
13689	Aug. 29.722	311.8	+ 40.4	7	+ 47.2	1	−196.6	3	.....	.....
13676	Aug. 25.637	314.7	+ 39.1	6	+ 15.1	2	−289.1	2	.....	.....
13638	July 15.620	315.2	+ 18.0	7	+ 14.7	2	−260.8	3	.....	.....
13690	Aug. 29.753	317.0	+ 50.2	6	+ 56.9	1	−252.5	2	.....	.....

TABLE 2—*Continued*

Plate	1944 Date (U.T.)	Phase	Primary				Secondary			
			He I, *C* II *Mg* II, *Si* III		*H*		*He* I, *C* II, *Mg* II, *Si* III		*H*	
			V (Km/Sec)	No.	*V* (Km/Sec)	No.	*V* (Km/Sec)	No.	*V* (Km/Sec)	No.
(1)	(2)	(3)	(4)	(5)	(6)	(7)	(8)	(9)	(10)	(11)
13639.....	July 15.644	319°.4	+ 45.5	4	+ 4.1	1	−261.1	1	.....	....
13677.....	Aug. 25.668	320.0	42.5	6	+ 0.5	2	289.2	2	.....	....
13468.....	Mar. 24.856	323.0	74.2	5	+ 71.5	2	260.2	2	−211.2	1
13612.....	July 13.615	323.1	33.3	7	− 9.7	2	219.7	2	.....	....
13678.....	Aug. 25.701	325.8	48.1	8	+ 40.4	2	220.6	4	.....	....
13475.....	Mar. 26.932	327.3	56.1	5	+ 47.6	2	260.5	2	.....	....
13613.....	July 13.638	327.5	35.7	6	+ 28.7	2	.....	.....	208.1	1
13531.....	June 2.630	329.7	68.3	2	+ 54.9	1	229.0	2	.....	....
13610.....	July 11.613	331.9	58.6	6	+ 51.4	2	325.1	3	.....	....
13614.....	July 13.663	332.0	68.8	4	+ 45.2	2	177.5	1	221.2	1
13679.....	Aug. 25.738	332.5	62.4	4	+ 67.1	2	291.5	1	.....	....
13615.....	July 13.682	335.2	60.3	5	+ 33.6	2	211.8	4	123.5	1
13532.....	June 2.678	338.0	58.5	5	+ 32.2	2	.....	.....	.....	....
13616.....	July 13.704	339.0	59.1	6	+ 31.1	2	266.1	4	.....	....
13617.....	July 13.726	343.0	49.7	5	+ 56.0	2	263.4	2	.....	....
13618.....	July 13.749	347.0	47.5	6	+ 35.5	2	330.8	3	.....	....
13533.....	June 2.730	347.2	74.7	5	+ 60.7	2	286.6	3	.....	....
13619.....	July 13.771	351.0	49.2	7	+ 23.0	1	268.0	4	396.8	1
13620.....	July 13.793	354.4	53.8	6	+ 53.9	2	267.3	2	−289.9	1
13534.....	June 2.788	357.4	73.3	6	+105.0	1	244.2	3	.....	....
13621.....	July 13.820	359.1	+ 41.4	6	+ 48.5	2	−273.8	2	.....	....

study, the epoch of zero phase was taken one-quarter of a period (0.513 day) earlier than the principal light minimum, which was assumed to occur as given by Schneller for 1941:[5]

$$\text{Principal Minimum} = \text{JD } 2411431.384 + 2^{d}.0510280\,E.$$

So far as is known, this is the latest published determination of the light minimum and period. The phase (col. 3) is given in degrees. The principal eclipse should occur at or near phase 90°. The columns headed "*V*" and "No." give the mean velocities and numbers of lines measured. The velocities given in columns 4 and 8 were used in computing normal places and are plotted in Figure 1. The other columns are self-explanatory.

Two solutions for the orbital elements were derived, using Sterne's method[6] with preliminary circular elements. The value of O − C was determined for each spectrogram from the observed and calculated velocities, using circular elements; and O − C for each of the 15 normal places shown in Table 3 was computed by taking averages. No weight-

[5] *Kl. Veröff. Berlin-Babelsberg*, No. 22, 1939.

[6] *Proc. Nat. Acad. Sci.*, **27**, 175, 1941.

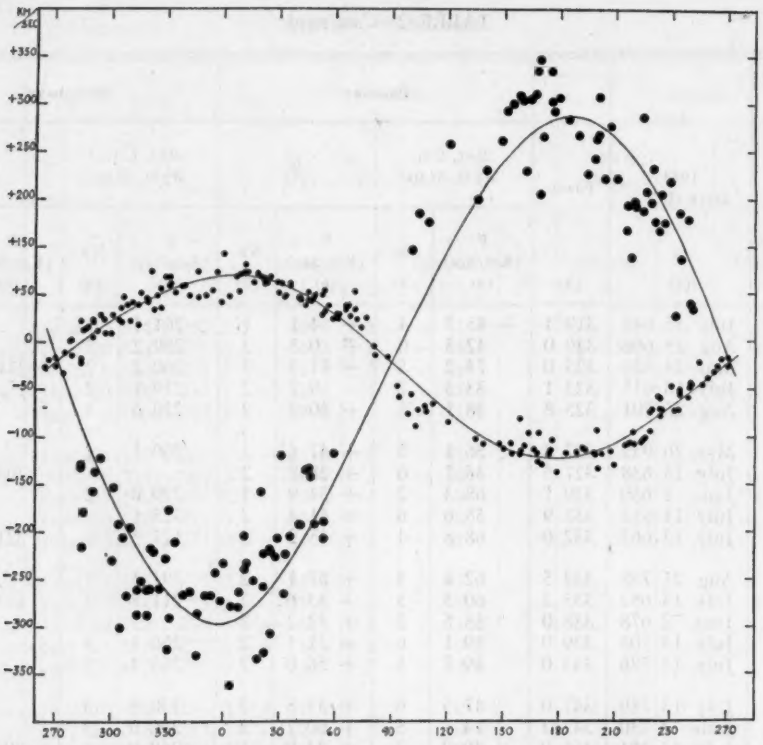

FIG. 1.—Velocity-curve of 68 u Herculis. Small circles are velocities of the primary; large circles, those of the secondary. Continuous curves are from Solution I, Table 4. Phase is given in degrees.

TABLE 3

NORMAL VELOCITIES—PRIMARY

No.	Limits of Phase	Mean Phase	No. of Plates	Mean Observed Vel. (Km/Sec)	(O−C) (Km/Sec)	
					Preliminary Solution	Solution I
1	1°8– 20°5	11°2	11	+ 69.3	+ 2.18	+ 1.3
2	22.3– 36.7	28.9	13	+ 58.0	+ 1.52	− 2.8
3	40.3– 54.0	47.5	13	+ 44.6	+ 8.02	+ 0.7
4	55.0– 77.4	66.1	15	+ 30.5	+20.31	+12.5
5	81.8–120.0	98.2	12	− 52.5	−10.43	−14.7
6	121.2–159.1	148.2	10	−105.5	+ 1.88	+ 4.8
7	162.6–184.0	171.8	12	−115.0	+ 5.78	+ 7.1
8	190.0–215.7	201.5	11	−116.2	− 2.75	− 4.5
9	217.1–238.0	228.2	15	− 87.9	− 0.30	− 4.2
10	241.0–257.2	248.1	12	− 51.9	+ 7.29	+ 3.8
11	260.2–279.6	271.4	11	− 19.7	+ 1.35	+ 0.7
12	284.0–297.0	289.9	13	+ 10.9	+ 1.77	+ 4.1
13	301.2–317.0	308.8	12	+ 30.5	− 5.53	− 1.2
14	319.4–332.5	326.5	11	+ 53.6	− 1.60	+ 3.3
15	335.2–359.1	347.1	10	+ 56.7	−10.50	− 7.6

TABLE 4

SOLUTIONS FOR ORBITAL ELEMENTS OF 68 u HERCULIS

ELEMENT	ALLEGHENY 1908 PLATES	YERKES 1935 PLATES	YERKES 1944 PLATES		
			Solution I	Solution II	Solution III
P	2^d0510	$2^d051028$	$2^d051028$	$2^d051028$	$2^d051028$
γ	-21.12	-30.5 ± 0.8	-24.6 ± 1.4	-22.7 ± 1.0	-20.9
K in km/sec	99.5 ± 1.0	99.6 ± 1.2	95.4 ± 1.9	93.8 ± 2.1	94.7 ± 1.0
e	0.053 ± 0.010	0.045 ± 0.012	0.050 ± 0.020	0.058 ± 0.014	0.053 ± 0.016
ω	$66^\circ.15\pm0^\circ.54$	$79^\circ\pm15^\circ$	$119^\circ\pm23^\circ$	$168^\circ\pm10^\circ$	$194^\circ\pm27^\circ$
T	1908, July 2.80	$77^\circ.4\pm14^\circ$	$119^\circ\pm23^\circ$	$170^\circ\pm10^\circ$	$198^\circ\pm28^\circ$
T_0	.....	$-1^\circ.6$	$-0^\circ.3\pm1^\circ.1$	$+1^\circ.9\pm1^\circ.1$	.....
No. of plates	65	38	181	154	154

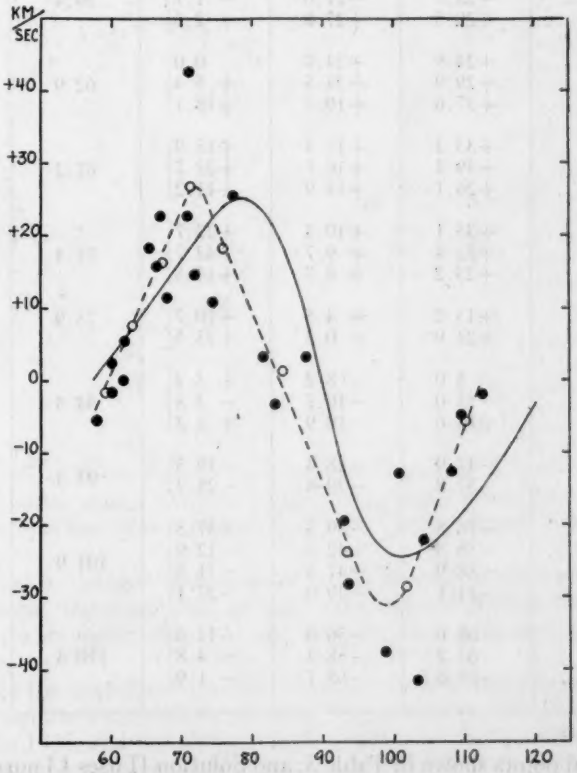

FIG. 2.—Filled circles, observed rotation velocities with reference to velocity-curve of primary; open circles, normal points. Dashed curve, rotational velocity from normal points; continuous curve, calculated rotational velocity, assuming synchronism. Phase given in degrees.

ing was applied because the number of plates is approximately the same for each normal place. The following preliminary elements were assumed:

$P = 2^{d}0510280$ $\quad e = 0$
$\gamma = -26.0$ km/sec $\quad \omega = 79°$
$K = 96.0$ km $\quad T_0 = -1^{d}6$

The values of γ and K were estimated from Figure 1, and ω and T_0 were taken from the 1935 Yerkes solution. The results of the two solutions are shown in Table 4. Solution I

TABLE 5

ROTATION EFFECT

PHASE	V_0 (KM/SEC)	V_C SOLUTION I (KM/SEC)	O−C (KM/SEC)	NORMAL PLACES	
				Phase	Km/Sec
58°0	+24.6	+30.0	− 5.4	59°4	− 1.5
60.1	+25.3	+27.0	− 1.7		
60.1	+29.5	+27.0	+ 2.5		
61.6	+24.9	+24.9	0.0	62.9	+ 7.8
61.9	+29.9	+24.5	+ 5.4		
65.2	+37.6	+19.5	+18.1		
66.6	+33.2	+17.3	+15.9	67.2	+16.6
67.0	+39.4	+16.7	+22.7		
68.1	+26.1	+14.9	+11.2		
70.9	+33.1	+10.4	+22.7	71.4	+26.6
71.3	+52.4	+ 9.7	+42.7		
72.0	+23.2	+ 8.7	+14.5		
74.5	+15.2	+ 4.5	+10.7	75.9	+18.1
77.4	+24.9	− 0.5	+25.4		
81.8	− 5.0	− 8.2	+ 3.2	84.3	+1.1
83.2	−14.0	−10.7	− 3.3		
87.8	−15.6	−18.9	+ 3.3		
93.0	−47.9	−28.4	−19.5	93.3	−23.8
93.7	−57.8	−29.6	−28.2		
99.0	−76.8	−39.3	−37.5	101.9	−28.5
100.8	−55.3	−42.4	−12.9		
103.5	−88.9	−47.4	−41.5		
104.4	−71.1	−49.0	−22.1		
108.4	−68.6	−56.0	−12.6	110.3	− 6.4
109.7	−63.2	−58.4	− 4.8		
112.8	−65.6	−63.7	− 1.9		

uses the 15 normal points shown in Table 3; and Solution II uses 13 normal points, omitting points 4 and 5, which correspond to the eclipse interval 55°–120°, in which the observed velocities are affected by the axial rotation of the primary. Table 4 also shows a third solution. Since there is a rather marked difference in the values of ω as obtained from Solutions I and II, Solution III was worked out as a check, with the same normal

points as Solution II, using Schlesinger's method[7] and preliminary elements from Solution I. Since the sum of the probable errors for ω in Solutions I and III is 50°, as compared to a difference of 75° between the two values for ω, the discrepancy does not seem to be serious, and the 1944 material appears to give an increased value of ω as compared to the 1935 material. Table 4 also shows the solutions published by Baker, using the Allegheny plates of 1908,[8] and by Luyten, Struve, and Morgan, using the Yerkes plates taken in 1935.

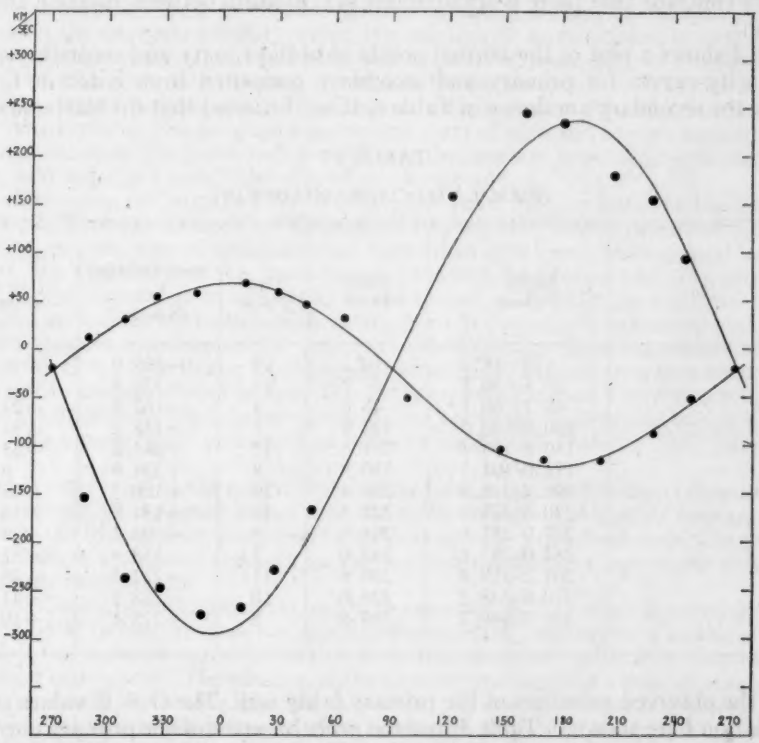

FIG. 3.—Small circles, normal points for primary; large circles, normal points for secondary. Continuous curves are from least-squares Solution I, Table 4. Phase is given in degrees.

The reason for the change in the values of γ and K between 1935 and 1944 is unknown. There is, of course, the possibility of large systematic errors; but the observations in these two years were made with the same instruments, and known errors were allowed for.

The answer to the question of possible synchronism between axial and orbital rotation was not clear from the Yerkes study of 1935. The present material is more extensive than that available in 1935, and the effect of axial rotation is clearly evident in Figure 1. Another computation has accordingly been made. There are 26 plates for the interval

[7] *Pub. Allegheny Obs.*, **1**, 33, 1908.

[8] Two additional solutions based on the Allegheny material of 1908 were published by Sterne (*Proc. Nat. Acad. Sci.*, **27**, 178 and 180, 1941) which are in close agreement with Baker's results except that ω was found equal to 85° and 93°. See also a solution by Luyten (*Pub. Minn. Obs.*, **2**, 35, 1935), who obtained ω equal to 83°.

55°–120°. If we assume, as in the 1935 study, that both stars are of the same size ($r = 3.2 \times 10^6$km), with uniformly illuminated disks and with $a = 10.2 \times 10^6$km, $i = 77°.6$, the calculated equatorial velocity of rotation for synchronism is around 106 km/sec. The excess ΔV, corresponding to synchronism, can then be found by numerical integration and is plotted in Figure 2 (continuous curve). The 1944 observations during eclipse were compared with the computed orbit, Solution I, and the 26 values of O − C were arranged in 9 normal places, as shown in Table 5 and plotted in Figure 2. The dashed curve in Figure 2 was drawn from these 9 normal points. Comparing the dashed and continuous curves, we conclude that there is approximate synchronism between rotation and orbital revolution.

Figure 3 shows a plot of the normal points of both primary and secondary, together with velocity-curves for primary and secondary computed from Solution I. Normal points for the secondary are shown in Table 6. It will be noted that the least-squares solu-

TABLE 6

NORMAL VELOCITIES—SECONDARY

No.	Limits of Phase	Mean Phase	No. of Plates	Mean Observed Vel. (Km/Sec)	O−C from Solution I (Km/Sec)
1	1°.8– 18°.4	10°.2	10	−268.9	+16
2	20.5– 36.7	27.7	13	−229.3	+21
3	40.7– 60.1	48.6	9	−167.3	+23
4	100.8–148.0	122.9	7	+158.2	+53
5	150.8–169.4	161.8	11	+245.3	+33
6	171.0–194.5	180.8	8	+234.9	0
7	198.7–218.0	207.4	10	+180.2	−38
8	220.3–234.0	227.5	10	+154.9	−15
9	237.0–251.6	244.8	8	+ 93.1	− 9
10	284.0–295.1	288.0	7	−153.8	−51
11	301.2–319.4	309.8	11	−237.5	−38
12	320.0–335.2	328.0	10	−248.5	+11
13	339.0–359.1	349.8	8	−275.1	+19

tion fits the observed velocities of the primary fairly well. The O − C values computed from Solution I are shown in Table 3, and the probable error of one primary normal point is ±4.4 km/sec. However, it is evident from Figure 3 and also from Figure 1 that the solution is not a good fit for the secondary points. If γ were made equal to about −15 km/sec and zero phase occurred about 10° earlier, the situation would be much improved. It is possible that the discrepancy is due to some unknown systematic errors, although a difference in phase of the order of 10° seems too great to be explained in this way, since both primary and secondary velocities were measured on the same plates. The 12 Yerkes 1935 observations of the secondary show a slight tendency in the same direction. There are only 9 measurements of secondary lines given in the Allegheny results published by Baker, but they are not inconsistent with the above results.

I wish to express my thanks to Dr. O. Struve for many helpful suggestions. I am also indebted to Dr. Struve, Messrs. G. Münch, J. W. Swensson, and A. J. Deutsch and Mrs. Margaret K. Krogdahl for obtaining the spectrograms and to Dr. Jorge Sahade for helpful discussions in connection with the least-squares solutions.

REVIEWS

A Multiplet Table of Astrophysical Interest (rev. ed.), Part I: *Table of Multiplets;* Part II: *Finding List.* By CHARLOTTE E. MOORE. ("Contributions from the Princeton University Observatory," No. 20 [1945].) Pp. xxxvi+110; iii+96.

Since 1933 one book could always be found on the desk or within reach in the office of any solar or stellar spectroscopist; the book was always worn out and patched up. It was the first edition of Miss Moore's multiplet table, probably the most helpful table for astrophysicists in recent years. The original table had not really been planned for publication. An extension of Russell's famous "List of Ultimate and Penultimate Lines of Astrophysical Interest,"[1] it had been prepared by Miss Moore in 1931 for her own use while working on the identification of atomic lines in the solar and sunspot spectra. Her manuscript was published in 1933 at the request of numerous colleagues; but the book was soon out of print, and, as a result of many laboratory investigations, it had become out of date for certain elements. When the need for a revision and extension became apparent, a program was planned at Princeton for the preparation of a revised edition. This program has required years of labor and has now been brought to a successful conclusion. The revised edition will save thousands of hours of labor to many astrophysicists, who will owe a great debt of gratitude to the author.

The work contains two parts: a *Table of Multiplets*, and a *Finding List* of all the lines in the multiplet table. Each part is again subdivided into two sections—one on permitted lines (more than 23,000 lines), the other on forbidden lines (more than 2550 lines). In its general layout the new edition has, over the first one, the great advantage of the *Finding List.* The need for the latter had indeed become quite imperative in the revised edition. In the multiplet table the multiplets for each spectrum of each element are listed in the order of increasing energy-level. Such an arrangement is undoubtedly of great use in identifying or discussing stellar lines, but it renders the search for a particular line somewhat laborious in the case of a complex spectrum. The *Finding List* answers this objection. This list is arranged in such a way that reference to the lines in the *Multiplet Table* is extremely easy. Work with the *Finding List* is even simplified by the use of a separate card containing an index to the *Revised Multiplet Table* (abbreviated *R.M.T.*).

The author makes the careful reservation that the book is intended for astrophysicists. From his own experience the reviewer knows that the tables will also be of great help to spectrochemists; and the Bibliography will be useful to them as well as to astronomers. The Introduction to the *Table* is a practical textbook on atomic spectra, and every user of the *R.M.T.* will find this feature most helpful.

Of necessity, some personal judgment had to be exercised by the author in selecting the material for her book. Indeed, her task was much harder than the preparation of a table of *Hauptlinien*, since it was desirable to reduce the lists to the minimum compatible with the present and future needs of astronomers. The selection of the material was based on a number of astronomical factors, especially the cosmic abundances and the physical conditions in astronomical objects. A good deal of personal judgment must necessarily be present, also, in rating the completeness of analysis from the standpoint of the astrophysicist, whose point of view is quite different from that of the physicist. For example, a laboratory spectroscopist may consider that his analysis of an atomic spectrum is satisfactorily completed if he has obtained all the essential terms of the atom by classifying lines in the far ultraviolet; but the astronomer will be satisfied only when he knows the transitions present in the astronomically observable region. The reviewer considers that selections of lines and ratings of completeness of analysis could not have been done with better judgment. In order to get a somewhat uniform notation out of the various papers, the author had to modify occasionally the term designations of the original publications, to an extent such that some authors may possibly not recognize their analyses! Actually, the matter of style of notation is still rather unsatisfactory in all publications.

Miss Moore's book illustrates clearly the serious situation which is at present facing astronomers who feel the need for progress in laboratory work on certain atoms. We certainly need better wave lengths (for example, even for atoms as common as *S* II, *Ca* I, and *Ca* II) and better intensities (even for *Na* I) in the case of many spectra which are considered well analyzed. In addition, many spectra have not yet been analyzed at all—as, for example: *Dy* I, *Dy* II, *Tb* I, *Tb* II, *Ho* I, *Ho* II, the doubly ionized rare earths, etc. The analysis of some others of great importance is still very incomplete, typical examples being *Mn* II, *Co* II, and many doubly

[1] *Mt. W. Contr.*, No. 286; *Ap. J.*, 61, 233, 1925.

ionized atoms. Few physicists feel inclined to undertake this kind of work. The reviewer feels more and more that the problem cannot be solved properly except in physical laboratories attached or closely related to astronomical institutions.

The long table of forbidden lines will no doubt be considered a useful innovation, although the limitations were even more difficult in this case than in the case of permitted lines. For the sake of uniformity the forbidden multiplets have been arranged in the same way as the permitted lines. The reviewer is not certain that an arrangement by the upper level, instead of the lower one, might not have been more adequate for the forbidden lines, which appear only in emission in astronomical spectra. When examining long tables, such as that of [*Ti* I], certain users may feel that their work might have been reduced if the multiplets had been listed according to the energy of the upper level; for example, assuming similar transition probabilities, the a^3F-a^5D multiplet of [*Ti* I] (upper level 3.6 v.) is certainly much weaker than a^5F-a^3G (upper level 1.9 v.), which comes later in the table. Happily, the large size of the pages makes the selection of the transitions according to the high levels comparatively easy.

In the Introduction the adjectives "nebular," "auroral," and "coronal" are used only in relation to the objects in which the corresponding lines originate. These adjectives have no relation, in the present book, to the types of forbidden transition which many astronomers also classify into nebular, auroral, and other types.

Some users may be surprised to find that several lines considered as predicted in this book are actually found in tables of wave lengths, such as the *M.I.T.* table. In such cases the laboratory data, for some reason, probably have been considered as still doubtful by the author. From the experience of the reviewer, the author's judgment can be trusted in such cases.

The author mentions that she has received information, help, and encouragement from many colleagues in this country and abroad. However, the reviewer suspects, also, that the author's work must very often have been hampered, since many of her separate lists of multiplets were on loan most of the time! On the other hand, this emphasizes the fact that the table was awaited by many with considerable interest.

The author plans the publication of additions and errata in the future. Some day the values in volts of the excitation potential may require slight changes, when the equivalent of the electron volt in cm^{-1} is better known. Miss Moore's *R.M.T.* leads to the hope that a few additional tables will also be published later, although they will be of more limited interest. For example, a table of transition probabilities of the forbidden lines should be published once the values for [*Fe* II], [*Fe* III], [*Fe* V], and a few other elements have been computed. In fact, tables of *f*-values will be desirable after the great improvements which are expected in this line of work have materialized. Some day an additional table of the strongest permitted and forbidden lines in the far ultraviolet, restricted to the elements of astrophysical interest, will also become imperative. The need for it is already felt at present by those who are studying the fluorescence and other excitation mechanisms in long-period variables, Wolf-Rayet or nova atmospheres, etc. It is also very likely that the postwar period will see great progress in our knowledge of astronomical spectra in the infrared region beyond the limits of photographic emulsions. The need will then arise for a table of infrared atomic lines.

The revised term tables from which Miss Moore calculated the excitation potentials are not published with the *R.M.T.*, and this will possibly be regretted. Most of the terms are found in the published papers on analysis, but some are not. It is the reviewer's hope that a revised edition of Miss Moore's table, "Term Designations for Excitation Potentials," will some day be published also. A table of configurations would also be useful.

A few ionization potentials not available to Miss Moore at the time of the publication may be mentioned here: *S* VIII 329; *S* XII 565; *A* X 477; *A* XI 539; *A* XIV 755; *K* VI 99; *Ca* VI 107; *Ca* VII 126; *Ca* XIII 726; and *Ca* XV 889. These values have been obtained from Dr. Bengt Edlén in Lund.

The author must be congratulated on her important contribution to astrophysical research. There is no doubt that her book will be used by many spectroscopists every day in the years to come, and this will be a well-deserved reward for the author. There is little likelihood that the information will soon become outdated for many atoms; occasional additions or errata such as planned by the author should easily take care of all possible changes or improvements.

P. SWINGS

Department of Astrophysics
University of Liége (Belgium)

INDEX TO VOLUME 102

INDEX TO SUBJECTS

Absorption Coefficient of the Negative Hydrogen Ion, On the Continuous. *S. Chandrasekhar* . . . 223

Absorption Coefficient of the Negative Hydrogen Ion. II. On the Continuous. *S. Chandrasekhar* . . . 395

Absorption in Four Small Dark Nebulae, A Study of General and Selective. *Laurence Garnett Stoddard* . . . 267

Andromeda Nebula, Nebulous Objects in the. *C. K. Seyfert and J. J. Nassau* . . . 377

KO Aquilae, Spectrographic Observations of the Eclipsing Variables W Ursae Minoris, XZ Sagittarii, and. *Jorge Sahade* . . . 470

QY Aquilae, The Photometric Orbit of. *Balfour S. Whitney* . . . 202

R Aquilae, and R Cassiopeiae, Measurements in the Spectra of U Orionis, R Serpentis. *Paul W. Merrill* . . . 347

Bethe's Law of Energy Generation, On the Internal Constitution of Stars of Small Masses According to. *N. R. Sen and U. R. Burman* . . . 208

BD+55°616, The Spectroscopic Orbit of the Eclipsing Variable. *Armin J. Deutsch* . . . 496

Binary HD 168206, The Wolf-Rayet Spectroscopic. *W. A. Hiltner* . . . 492

δ Canis Majoris, Curve of Growth for. *Helen R. Steel* . . . 429

Cape Magnitudes and the International System, The. *Frederick H. Seares and Mary C. Joyner* . . . 281

B Cassiopeiae as a Supernova of Type I. *W. Baade* . . . 309

R Cassiopeiae, Measurements in the Spectra of U Orionis, R Serpentis, R Aquilae, and. *Paul W. Merrill* . . . 347

TV Cassiopeiae, The Problem of U Coronae Borealis, RS Vulpeculae, and. *J. Sahade and O. Struve* . . . 480

WX Cephei, Spectroscopic Observations of the Eclipsing Variable. *Jorge Sahade and Carlos U. Cesco* . . . 128

Cepheid Variables, The Velocity-Curves of Seven. *Otto Struve* . . . 232

Charlier's Formulae for a Moving Cluster, Regression Lines and the Functional Relation. II. *Frederick H. Seares* . . . 366

Clusters NGC 5634 and NGC 6229, The Globular. *W. Baade* . . . 17

Co-albedo of the Moon, The. *Edison Pettit* . . . 14

Color Indices for Stars of Large Proper Motion. II. Preliminary. *Willem J. Luyten and Martin Dartayet* . . . 196

Colors of 238 Stars of Different Spectral Types, The. Six-Color Photometry of Stars. III. *Joel Stebbins and A. E. Whitford* . . . 318

Constitution of Stars of Small Masses According to Bethe's Law of Energy Generation, On the Internal. *N. R. Sen and U. R. Burman* . . . 208

Continuous Spectrum of the Sun, A Theoretical Discussion of the. *Guido Münch* . . . 385

Corona Taken during the Total Eclipse of the Sun on July 9, 1945, at Pine River, Manitoba, Canada, Photographs of the. *W. A. Hiltner and S. Chandrasekhar* 135

β Coronae Borealis, The Spectrum of. *W. A. Hiltner* 438

U Coronae Borealis, RS Vulpeculae, and TV Cassiopeiae, The Problem of. *J. Sahade and O. Struve* 480

Curve of Growth for δ Canis Majoris. *Helen R. Steel* 429

Curve of Growth for α Persei. *Helen R. Steel* 43

Density Gradients in the Anticenter Region of the Milky Way. *S. W. McCuskey* . . . 32

Eclipse of the Sun on July 9, 1945, at Pine River, Manitoba, Canada, Photographs of the Corona Taken during the Total. *W. A. Hiltner and S. Chandrasekhar* 135

Eclipsing Binaries, Intermediary Elements for. *Henry Norris Russell* 1

Eclipsing Variable BD+55°616, The Spectroscopic Orbit of the. *Armin J. Deutsch* . . 496

Eclipsing Variable WX Cephei, Spectroscopic Observations of the. *Jorge Sahade and Carlos U. Cesco* 128

Eclipsing Variables, Spectrographic Observations of Thirteen. *Otto Struve* 74

Eclipsing Variables W Ursae Minoris, XZ Sagittarii, and KO Aquilae, Spectrographic Observations of the. *Jorge Sahade* 470

HD 168206, The Wolf-Rayet Spectroscopic Binary. *W. A. Hiltner* 492

Helium Atom in Its Excited States. II. The Interaction of a Proton and a. *Margaret Kiess Krogdahl* 64

68 u Herculis, A Spectrographic Study of. *Burke Smith* 500

Magnitudes and the International System, The Cape. *Frederick H. Seares and Mary C. Joyner* 281

Milky Way, Density Gradients in the Anticenter Region of the. *S. W. McCuskey* . . . 32

TU Monocerotis, The Spectroscopic Orbit of. *Armin J. Deutsch* 433

Moon, The Co-albedo of the. *Edison Pettit* 14

Nebula, Nebulous Objects in the Andromeda. *C. K. Seyfert and J. J. Nassau* 377

Nebula, The Radiative Equilibrium of an Expanding Planetary. I. Radiation Pressure in Lyman-α. *S. Chandrasekhar* 402

Nebulae, Physical Processes in Gaseous. XVIII. The Chemical Composition of the Planetary Nebulae. *Lawrence H. Aller and Donald H. Menzel* 239

Nebulae, A Study of General and Selective Absorption in Four Small Dark. *Laurence Garnett Stoddard* 267

Negative Hydrogen Ion, On the Continuous Absorption Coefficient of the. *S. Chandrasekhar* 223

Negative Hydrogen Ion. II. On the Continuous Absorption Coefficient of the. *S. Chandrasekhar* 395

NGC 5634 and NGC 6229, The Globular Clusters. *W. Baade* 17

Nova (RS) Ophiuchi, Identification of the Post-maximum Lines in the Spectrum of. *A. H. Joy and P. Swings* 353

Nova Puppis 1942, The Spectrum of. *Roscoe F. Sanford* 357

Orbit of QY Aquilae, The Photometric. *Balfour S. Whitney* 202

Orbit of the Eclipsing Variable BD+55°616, The Spectroscopic. *Armin J. Deutsch* . . 496

Orbit of TU Monocerotis, The Spectroscopic. *Armin J. Deutsch* 433

Orion Stars, Note on the Suspected Gravitational Red Shift of the. *O. Struve* 137

U Orionis, R Serpentis, R Aquilae, and R Cassiopeiae, Measurements in the Spectra of. *Paul W. Merrill* 347

α Persei, Curve of Growth for. *Helen R. Steel* 43

Photometry of Stars, Six-Color. III. The Colors of 238 Stars of Different Spectral Types. *Joel Stebbins and A. E. Whitford* 318

Physical Processes in Gaseous Nebulae. XVIII. The Chemical Composition of the Planetary Nebulae. *Lawrence H. Aller and Donald H. Menzel.* 239

Pleiades Cluster, Investigations on Proper Motion. XXIV. Further Measures in the. *Adriaan van Maanen* 26

Proper Motion, Investigations on. XXIV. Further Measures in the Pleiades Cluster. *Adriaan van Maanen* 26

Proper Motion. II. Preliminary Color Indices for Stars of Large. *Willem J. Luyten and Martin Dartayet* 196

Proper Motion, Radial Velocities and Spectral Classes for Some Stars of Large. *W. J. Luyten* 382

Proton and a Helium Atom in Its Excited States. II. The Interaction of a *Margaret Kiess Krogdahl* 64

Pulsation of Gaseous Stars, On the Radial. *P. Ledoux* 143

Radial Velocities and Spectral Classes for Some Stars of Large Proper Motion. *W. J. Luyten* 382

Radiative Equilibrium of an Expanding Planetary Nebula, The. I. Radiation Pressure in Lyman-α. *S. Chandrasekhar* 402

Red Shift of the Orion Stars, Note on the Suspected Gravitational. *O. Struve* . . . 137

Regression Lines and the Functional Relation. II. Charlier's Formulae for a Moving Cluster. *Frederick H. Seares* 366

Reviews:

Annales de géophysique, Vol. 1, No. 1 (P. Swings) 138

Baker, James G., and George Z. Dimitroff. *Telescopes and Accessories* (Jesse L. Greenstein) 140

Dimitroff, George Z., and James G. Baker. *Telescopes and Accessories* (Jesse L. Greenstein) 140

Fessenkoff, V. G. *Cosmogony of the Solar System* (O. Struve) 264

Moore, Charlotte E. *A Multiplet Table of Astrophysical Interest* (rev. ed.), Part I: *Table of Multiplets;* Part II: *Finding List* (P. Swings) 511

XZ Sagittarii, and KO Aquilae, Spectrographic Observations of the Eclipsing Variables W Ursae Minoris. *Jorge Sahade* 470

R Serpentis, R Aquilae, and R Cassiopeiae, Measurements in the Spectra of U Orionis. *Paul W. Merrill* 347

Spectra of U Orionis, R Serpentis, R Aquilae, and R Cassiopeiae, Measurements in the. *Paul W. Merrill* . . . 347

Spectral Classes for Some Stars of Large Proper Motion, Radial Velocities and. *W. J. Luyten* . . . 382

Spectrographic Observations of the Eclipsing Variables W Ursae Minoris, XZ Sagittarii, and KO Aquilae. *Jorge Sahade* . . . 470

Spectrographic Observations of Thirteen Eclipsing Variables. *Otto Struve* . . . 74

Spectrographic Study of 68 u Herculis, A. *Burke Smith* . . . 500

Spectroscopic Binary HD 168206, The Wolf-Rayet. *W. A. Hiltner* . . . 492

Spectroscopic Observations of the Eclipsing Variable WX Cephei. *Jorge Sahade and Carlos U. Cesco* . . . 128

Spectroscopic Orbit of the Eclipsing Variable BD+55°616, The. *Armin J. Deutsch* . . . 496

Spectroscopic Orbit of TU Monocerotis, The. *Armin J. Deutsch* . . . 433

Spectrum of β Coronae Borealis, The. *W. A. Hiltner* . . . 438

Spectrum of Nova (RS) Ophiuchi, Identification of the Post-maximum Lines in the. *A. H. Joy and P. Swings* . . . 353

Spectrum of Nova Puppis 1942, The. *Roscoe F. Sanford* . . . 357

Stellar Model with a Gravitational Source of Energy, A. *Marjorie Hall Harrison* . . . 216

Sun, Chemical Compounds in the. *Harold D. Babcock* . . . 154

Sun, A Theoretical Discussion of the Continuous Spectrum of the. *Guido Münch* . . . 385

Sunspots, The Apparent Distribution of Preceding and Following. *W. Gleissberg* . . . 133

Supernova of Type I, B Cassiopeiae as a. *W. Baade* . . . 309

T Tauri Variable Stars. *Alfred H. Joy* . . . 168

W Ursae Minoris, XZ Sagittarii, and KO Aquilae, Spectrographic Observations of the Eclipsing Variables. *Jorge Sahade* . . . 470

Variable Stars, T Tauri. *Alfred H. Joy* . . . 168

Variables, The Velocity-Curves of Seven Cepheid. *Otto Struve* . . . 232

RS Vulpeculae, and TV Cassiopeiae, The Problem of U Coronae Borealis. *J. Sahade and O. Struve* . . . 480

Whitney's Paper, Comments on Captain. *Henry Norris Russell* . . . 207

Wolf-Rayet Spectroscopic Binary HD 168206, The. *W. A. Hiltner* . . . 492

INDEX TO AUTHORS

Aller, Lawrence H., and Donald H. Menzel. Physical Processes in Gaseous Nebulae. XVIII. The Chemical Composition of the Planetary Nebulae . . . 239

Baade, W. B Cassiopeiae as a Supernova of Type I . . . 309

Baade, W. The Globular Clusters NGC 5634 and NGC 6229 . . . 17

Babcock, Harold D. Chemical Compounds in the Sun . . . 154

Burman, U. R., and N. R. Sen. On the Internal Constitution of Stars of Small Masses According to Bethe's Law of Energy Generation . . . 208

CESCO, CARLOS U., and JORGE SAHADE. Spectroscopic Observations of the Eclipsing Variable WX Cephei 128

CHANDRASEKHAR, S. On the Continuous Absorption Coefficient of the Negative Hydrogen Ion 223

CHANDRASEKHAR, S. On the Continuous Absorption Coefficient of the Negative Hydrogen Ion. II 395

CHANDRASEKHAR, S. The Radiative Equilibrium of an Expanding Planetary Nebula. I. Radiation Pressure in Lyman-α 402

CHANDRASEKHAR, S., and W. A. HILTNER. Photographs of the Corona Taken during the Total Eclipse of the Sun on July 9, 1945, at Pine River, Manitoba, Canada 135

DARTAYET, MARTIN, and WILLEM J. LUYTEN. Preliminary Color Indices for Stars of Large Proper Motion. II 196

DEUTSCH, ARMIN J. The Spectroscopic Orbit of the Eclipsing Variable BD+55°616 . 496

DEUTSCH, ARMIN J. The Spectroscopic Orbit of TU Monocerotis 433

GLEISSBERG, W. The Apparent Distribution of Preceding and Following Sunspots . . 133

GREENSTEIN, JESSE L. Review of: *Telescopes and Accessories*, George Z. Dimitroff and James G. Baker 140

HARRISON, MARJORIE HALL. A Stellar Model with a Gravitational Source of Energy . . 216

HILTNER, W. A. The Spectrum of β Coronae Borealis 438

HILTNER, W. A. The Wolf-Rayet Spectroscopic Binary HD 168206 492

HILTNER, W. A., and S. CHANDRASEKHAR. Photographs of the Corona Taken during the Total Eclipse of the Sun on July 9, 1945, at Pine River, Manitoba, Canada . . . 135

JOY, ALFRED H. T Tauri Variable Stars 168

JOY, A. H., and P. SWINGS. Identification of the Post-maximum Lines in the Spectrum of Nova (RS) Ophiuchi 353

JOYNER, MARY C., and FREDERICK H. SEARES. The Cape Magnitudes and the International System 281

KROGDAHL, MARGARET KIESS. The Interaction of a Proton and a Helium Atom in Its Excited States. II 64

LEDOUX, P. On the Radial Pulsation of Gaseous Stars 143

LUYTEN, W. J. Radial Velocities and Spectral Classes for Some Stars of Large Proper Motion 382

LUYTEN, WILLEM J., and MARTIN DARTAYET. Preliminary Color Indices for Stars of Large Proper Motion. II 196

MCCUSKEY, S. W. Density Gradients in the Anticenter Region of the Milky Way . . 32

MENZEL, DONALD H., and LAWRENCE H. ALLER. Physical Processes in Gaseous Nebulae. XVIII. The Chemical Composition of the Planetary Nebulae 239

MERRILL, PAUL W. Measurements in the Spectra of U Orionis, R Serpentis, R Aquilae, and R Cassiopeiae 347

MÜNCH, GUIDO. A Theoretical Discussion of the Continuous Spectrum of the Sun . . 385

NASSAU, J. J., and C. K. SEYFERT. Nebulous Objects in the Andromeda Nebula . . . 377

PETTIT, EDISON. The Co-albedo of the Moon 14

RUSSELL, HENRY NORRIS. Comments on Captain Whitney's Paper 207

RUSSELL, HENRY NORRIS. Intermediary Elements for Eclipsing Binaries 1

SAHADE, JORGE. Spectrographic Observations of the Eclipsing Variables W Ursae Minoris, XZ Sagittarii, and KO Aquilae 470

SAHADE, JORGE, and CARLOS U. CESCO. Spectroscopic Observations of the Eclipsing Variable WX Cephei 128

SAHADE, J., and O. STRUVE. The Problem of U Coronae Borealis, RS Vulpeculae, and TV Cassiopeiae 480

SANFORD, ROSCOE F. The Spectrum of Nova Puppis 1942 357

SEARES, FREDERICK H. Regression Lines and the Functional Relation. II. Charlier's Formulae for a Moving Cluster 366

SEARES, FREDERICK H., and MARY C. JOYNER. The Cape Magnitudes and the International System 281

SEN, N. R., and U. R. BURMAN. On the Internal Constitution of Stars of Small Masses According to Bethe's Law of Energy Generation 208

SEYFERT, C. K., and J. J. NASSAU. Nebulous Objects in the Andromeda Nebula . . . 377

SMITH, BURKE. A Spectrographic Study of 68 u Herculis 500

STEBBINS, JOEL, and A. E. WHITFORD. Six-Color Photometry of Stars. III. The Colors of 238 Stars of Different Spectral Types 318

STEEL, HELEN R. Curve of Growth for δ Canis Majoris 429

STEEL, HELEN R. Curve of Growth for α Persei 43

STODDARD, LAURENCE GARNETT. A Study of General and Selective Absorption in Four Small Dark Nebulae 267

STRUVE, O. Note on the Suspected Gravitational Red Shift of the Orion Stars 137

STRUVE, OTTO. Spectrographic Observations of Thirteen Eclipsing Variables 74

STRUVE, OTTO. The Velocity-Curves of Seven Cepheid Variables 232

STRUVE, O. Review of: *Cosmogony of the Solar System*, V. G. Fessenkoff 264

STRUVE, O., and J. SAHADE. The Problem of U Coronae Borealis, RS Vulpeculae, and TV Cassiopeiae 480

SWINGS, P. Review of: *Annales de géophysique*, Vol. 1, No. 1 138

SWINGS, P., and A. H. JOY. Identification of the Post-maximum Lines in the Spectrum of Nova (RS) Ophiuchi 353

SWINGS, P. Review of: *A Multiplet Table of Astrophysical Interest* (rev. ed.), Part I: *Table of Multiplets;* Part II: *Finding List*, Charlotte E. Moore. 511

VAN MAANEN, ADRIAAN. Investigations on Proper Motion. XXIV. Further Measures in the Pleiades Cluster 26

WHITFORD, A. E., and JOEL STEBBINS. Six-Color Photometry of Stars. III. The Colors of 238 Stars of Different Spectral Types 318

WHITNEY, BALFOUR S. The Photometric Orbit of QY Aquilae 202

Astronomical

LANTERN SLIDES

Since 1903, the Yerkes Observatory of the University of Chicago has been reproducing in lantern slides, transparencies, and prints the original astronomical photographs made at Williams Bay.

The lantern slides are uniformly 4×3¼ inches in size. The frequent call for small sets of slides for school and lecture purposes has led to the preparation of a list of 100 representative slides (price $62.50), a catalogue of which may be obtained upon request to the University of Chicago Press, 5750 Ellis Avenue, Chicago.

Prints as well as slides can be furnished, and for many subjects window transparencies are also supplied.

For catalogue and further information write

The University of Chicago Press
5750 Ellis Avenue, Chicago, Ill.

POPULAR ASTRONOMY

A magazine now in its fiftieth year, devoted to the elementary aspects of Astronomy and allied sciences.

Published monthly, except July and September.

Yearly subscription rates: Domestic $4.00; Canadian $4.75 (including war tax); Foreign $4.50.

Address

POPULAR ASTRONOMY
CARLETON COLLEGE
NORTHFIELD, MINNESOTA, U.S.A.

What Are COSMIC RAYS?

By **PIERRE AUGER**

noted French physicist, discoverer of Auger showers and Auger effect in X-rays

TRANSLATED BY
MAURICE M. SHAPIRO

"The best that has yet appeared" for explaining cosmic rays to the general reader and to the physicist who wants a quick view of what has been done in this new field of specialization," says Professor ARTHUR H. COMPTON.

This book answers the question: "What are cosmic rays?" and traces the exciting adventures of their investigators from the discovery of cosmic rays to the latest stratospheric balloon flights.

$2.00

UNIVERSITY OF CHICAGO PRESS

In 1690, under the sign of "The Archimedes and Two Pairs of Golden Spectacles" on London's Ludgate Street, John Marshall invented the modern method of simultaneously grinding a number of lenses by cementing pieces of glass to a convex sphere and grinding them with a concave spherical tool.

One of the great opticians of the late 17th century, he stated, with more truth than modesty, in an advertisement published in 1693: "He hath also invented a double microscope, a pocket microscope, and a wheel perspective glass with a concave eye-lens fit for all weathers; these are more useful than any yet have been."

Today, modern methods of mass production of accurate optical instruments and parts are supplying scientists in Industry, Education, and the Armed Forces with the solution to important war-time problems. Some of these methods, such as the mass production of roof prisms, are the products of Perkin-Elmer research.

Soon, Perkin-Elmer, combining all its *pre-war* knowledge, experience and skill with the ideas and techniques of its war-time production methods, will bring welcome refinements to scientific optical instruments for *post-war* analysis, control, inspection, and observation.

WHAT PERKIN-ELMER MAKES

Perkin-Elmer serves the optical sciences that broaden man's horizons by supplying them with:

Custom-built optical instruments for industrial analysis, control, and inspection.

New optical devices to solve specific problems, such as the all-purpose infra-red spectrometer.

Special elements such as fine lenses, prisms, flats, photographic objectives, interferometer plates, retardation plates, Cornu prisms, Rochon prisms, Nicol prisms.

Perkin-Elmer is now 100% in war work, but after the war will resume manufacture of such peace-time products as Schmidt cameras, refracting and reflecting telescopes, equatorial mountings, oculars, direct-vision prisms, polarizing eye-pieces, and other equipment.

THE PERKIN-ELMER [illegible]
GLENBROOK